frontiers | Research Topics

Brain plasticity following sensory loss: From basic mechanisms to therapy

Edited by
Ron Kupers and Maurice Ptito

Published in
Frontiers in Neuroscience

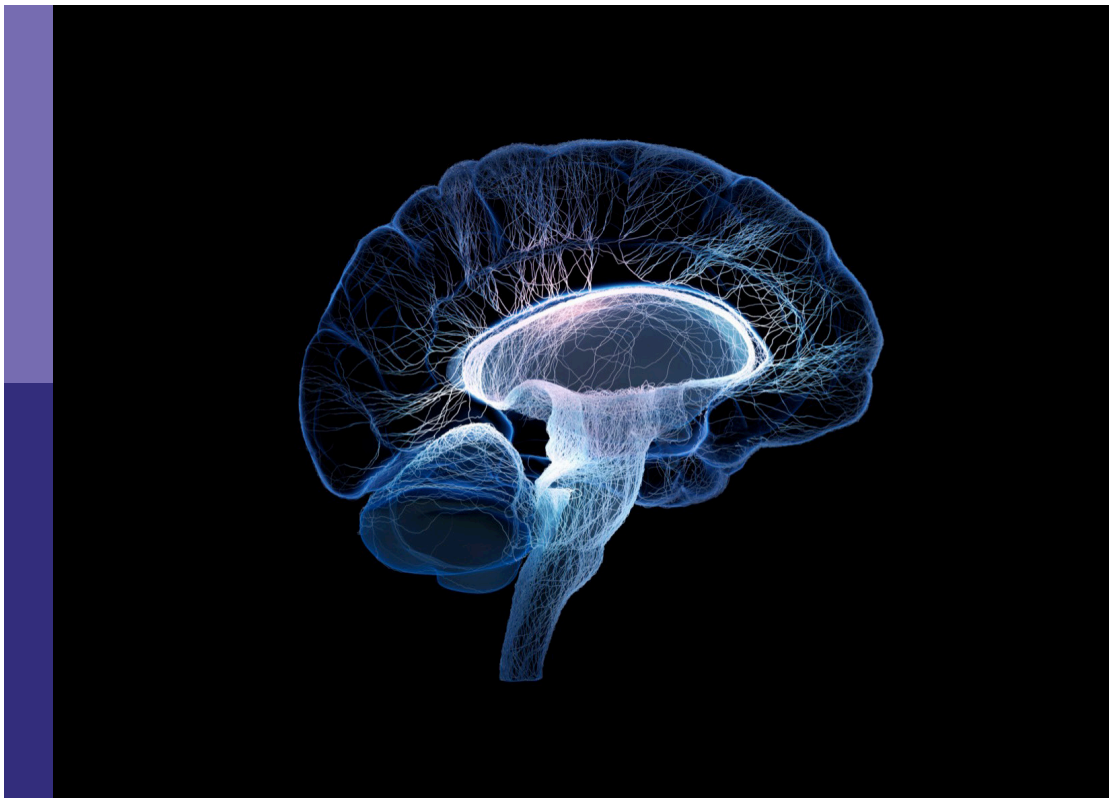

ISSN 1664-8714
ISBN 978-2-8325-4042-8
DOI 10.3389/978-2-8325-4042-8

About Frontiers

Frontiers is more than just an open access publisher of scholarly articles: it is a pioneering approach to the world of academia, radically improving the way scholarly research is managed. The grand vision of Frontiers is a world where all people have an equal opportunity to seek, share and generate knowledge. Frontiers provides immediate and permanent online open access to all its publications, but this alone is not enough to realize our grand goals.

Frontiers journal series

The Frontiers journal series is a multi-tier and interdisciplinary set of open-access, online journals, promising a paradigm shift from the current review, selection and dissemination processes in academic publishing. All Frontiers journals are driven by researchers for researchers; therefore, they constitute a service to the scholarly community. At the same time, the *Frontiers journal series* operates on a revolutionary invention, the tiered publishing system, initially addressing specific communities of scholars, and gradually climbing up to broader public understanding, thus serving the interests of the lay society, too.

Dedication to quality

Each Frontiers article is a landmark of the highest quality, thanks to genuinely collaborative interactions between authors and review editors, who include some of the world's best academicians. Research must be certified by peers before entering a stream of knowledge that may eventually reach the public - and shape society; therefore, Frontiers only applies the most rigorous and unbiased reviews. Frontiers revolutionizes research publishing by freely delivering the most outstanding research, evaluated with no bias from both the academic and social point of view. By applying the most advanced information technologies, Frontiers is catapulting scholarly publishing into a new generation.

What are Frontiers Research Topics?

Frontiers Research Topics are very popular trademarks of the *Frontiers journals series*: they are collections of at least ten articles, all centered on a particular subject. With their unique mix of varied contributions from Original Research to Review Articles, Frontiers Research Topics unify the most influential researchers, the latest key findings and historical advances in a hot research area.

Find out more on how to host your own Frontiers Research Topic or contribute to one as an author by contacting the Frontiers editorial office: frontiersin.org/about/contact

Brain plasticity following sensory loss: From basic mechanisms to therapy

Topic editors

Ron Kupers — University of Copenhagen, Denmark

Maurice Ptito — Montreal University, Canada

Citation

Kupers, R., Ptito, M., eds. (2023). *Brain plasticity following sensory loss: From basic mechanisms to therapy*. Lausanne: Frontiers Media SA.

doi: 10.3389/978-2-8325-4042-8

Table of contents

frontiers | Frontiers in Neuroscience

TYPE Editorial
PUBLISHED 17 November 2023
DOI 10.3389/fnins.2023.1331086

OPEN ACCESS

EDITED AND REVIEWED BY
Rufin VanRullen,
Centre National de la Recherche Scientifique (CNRS), France

*CORRESPONDENCE
Ron Kupers
kupers@sund.ku.dk

RECEIVED 31 October 2023
ACCEPTED 03 November 2023
PUBLISHED 17 November 2023

CITATION
Kupers R and Ptito M (2023) Editorial: Brain plasticity following sensory loss: from basic mechanisms to therapy.
Front. Neurosci. 17:1331086.
doi: 10.3389/fnins.2023.1331086

Editorial: Brain plasticity following sensory loss: from basic mechanisms to therapy

Ron Kupers[1,2]* and Maurice Ptito[2]

[1]Department of Neuroscience, Panum Institute, University of Copenhagen, Copenhagen, Denmark, [2]École d'optométrie, Université de Montréal, Montreal, QC, Canada

KEYWORDS

vision, audition, brain plasticity, brain imaging, somesthesis, cortex, rehabilitation

Editorial on the Research Topic
Brain plasticity following sensory loss: from basic mechanisms to therapy

There is now ample evidence that both congenital blindness (CB) and acquired or late-onset blindness (LB) trigger a myriad of brain neuroplastic changes. With the advent of modern non-invasive brain imaging techniques such as positron emission tomography (PET), (functional) magnetic resonance imaging (f)MRI, magnetoencephalography (MEG) and diffusion imaging, the scientific study of the mechanisms mediating brain plasticity following sensory loss has gathered momentum over the past decades. The first brain imaging studies focused largely on blindness and revealed that the visually deprived occipital cortex at rest is metabolically hyperactive. Ensuing studies showed that tactile input (e.g., Braille reading) and other forms of non-visual input activate the occipital cortex in CB and to a lesser extent also in LB subjects. Brain morphometric and diffusion imaging studies have further shed light on the associated brain structural changes. Although most of the initial work strongly focused on the absence of vision, later studies also dealt with brain plastic changes following loss of auditory input, and to a lesser extent following loss of smell, taste, and somatosensory input. With this Research Topic, we wanted to further our understanding of the mechanisms underlying brain plasticity following sensory loss, to highlight similarities and differences between sensory loss in different sensory domains (e.g., vision, audition and somesthesis), and to identify major challenges for novel avenues for therapeutic progress. Finally, studies of the sensory-deprived brain also help us to shed new light on normal brain development and function.

Therefore, this Research Topic of Frontiers in Neuroscience is timely and brings a collection of ground-breaking novel research on the effects of sensory loss on neuroplastic processes in humans and in animal models. We present nine original articles and two systematic reviews that will contribute to expand our knowledge of brain reorganization following sensory loss.

Description of the contents

The majority of the papers in this Research Topic deal with alterations in the visual system. Arend et al. report that blind individuals have changes in cortical gyrification, an anatomical measure that has not been previously reported in this context. The authors show an increase in gyrification in several brain areas of CB individuals and, importantly,

a negative correlation between gyrification and cortical thickness in several different cortical areas. The authors discuss the impact of their results in relation to brain development and plasticity. Yizhar et al. used fMRI to study the role of the extrastriate body area (EBA) in action-related functions in CB individuals. Their findings indicate that the absence of visual experience does not favorize the development of action-related responses in the EBA. Moreover, CB participants showed a decrease in functional connectivity of the EBA with sensorimotor cortices, whereas connectivity with perception-related visual occipital cortices remained high. The authors further demonstrated that action-related functions and connectivity of the visual cortex are dependent on visuomotor experience. Bleau et al. present a meta-analysis of the neural substrates of spatial processing and navigation in blind individuals through touch and audition. The meta-analysis reveals that most studies agree that CB individuals recruit the same neural pathways as sighted controls when processing non-visual spatial information. The meta-analysis further shows that the primary visual cortex and associative occipital areas are involved in visuo-spatial processing via cross-modal plasticity mechanisms. The authors discuss the results in terms of the *amodality* hypothesis of spatial representations. Arbel et al. present novel data on face recognition in CB individuals. The authors trained a group of CB participants to use a visual-to-auditory sensory substitution device to recognize faces, whereafter they participated in an fMRI study. The results showed activation of the fusiform gyrus and other face-responsive-regions of the ventral visual stream. The authors concluded that there is a predisposition for sensory-independent and computation-specific processing in specific cortical regions that is independent of previous perceptual experience and that is pertained following sensory deprivation. Nadvar et al. studied resting state functional connectivity (rsFC) of area V1 following sight restoration in patients with retinitis pigmentosa who were implanted with the Argus II retinal prosthesis which partially restores vision. The aim was to test whether sight restoration with this treatment would reverse, in full or partly, the plastic changes induced by the vision loss. Their results showed that the decrease in rsFC between V1 and the post-central gyrus in CB participants was partially reversed by vision restoration. The authors suggest that rsFC between the occipital and somatosensory cortices could provide a biomarker for functional plastic changes following vision recovery. Maimon et al. report on visual perception in a small but unique group of children who had undergone vision-restoring cataract removal surgery as part of the Himalayan Cataract Project. Some of the children in the study were born with cataracts and gained a sense of sight for the first time, whereas others suffered late-onset blindness in one eye alone. The authors discuss their findings in the context of Molyneux's problem, i.e., the ability to correlate vision with touch quickly following sight restoration in blind individuals, and Hubel and Wiesel's theory of critical periods.

Two papers relate to plasticity following auditory deprivation, one in humans and a second one in animals. Grégoire et al. performed a meta-analysis of the literature on brain plastic changes following hearing loss at birth or later in life. Hearing loss is a growing problem in modern Western societies due to an aging population. Moreover, knowledge of brain neuroplastic changes could help to understand some disappointing results with cochlear implants, and therefore could improve hearing rehabilitation. The literature research revealed that the most consistent finding in deaf individuals was a volumetric decrease in gray matter around the auditory cortex. In deaf children, an additional volumetric decrease was reported in both gray and white matter at the level of the visual cortex. Grégoire et al. further discuss the role of confounding factors that could affect brain plasticity in deaf individuals such as the use of sign language and hearing aids, and frequently observed associated vestibular dysfunction or neurocognitive impairments. Using kittens rendered deaf, Mitzetlfelt et al. investigated the stimulus-driven neural activity associated with visual localization. The researchers recorded visual evoked potentials (VEPs) in response to visual stimuli presented at various eccentricities in the visual field. Their results showed no significant changes in VEPs in deaf cats that could explain the previously observed behavioral advantage. The authors concluded that cross-modal plasticity in deafness does not play a major role in cortical processing of the peripheral visual field.

Two studies report on patient groups with either central or peripheral lesions. Araneda et al. used diffusion MRI to study changes in white matter (WM) architecture in the geniculo-striate pathway in 40 children with unilateral spastic cerebral palsy (USCP). The authors report several alterations in diffusion imaging parameters of the optic radiations on the lesional compared with the non-lesional hemisphere. Both the nature and the side of the lesion (left or right hemisphere) had an impact on the type and magnitude of the WM changes. In USCP with periventricular and right-hemispheric lesions, the diffusion imaging parameters correlated with the patients' visuospatial assessment. Dedry et al. studied three unique patients with unilateral vocal fold paralysis. The patients were followed for 1 year with multiparametric voice assessments and longitudinal fMRI during a sustained phonation task and rsfMRI. One patient received an augmentation injection in the paralyzed vocal fold. This patient showed a bilateral activation of the voice-related nuclei in the brainstem during sustained phonation. In addition, rsFC between the voice motor/sensory brainstem nuclei and other voice-related ROIs correlated with mean airflow measures in this patient. This observation supports the hypothesis that promoting proprioceptive feedback, by temporarily rehabilitating glottic closure, can enhance the neural recovery process.

Finally, the study by Vaessen et al. addressed the question whether there is an abstract representation of emotions in the brain that is shared across stimulus types (face, body, voice) and sensory origin (visual, auditory). Thereto, the authors studied fMRI responses to ecological types of emotion expressions of different types and modalities. Using multivariate statistical analyses, the authors showed that there is a specific brain organization for affective signals which depends on stimulus category and modality. These findings are consistent with the notion that emotion expressions conveyed by different stimulus types have different functional roles in triggering rapid adaptive behavior.

We hope that the papers presented in this Research Topic of Frontiers in Neuroscience will contribute to a better understanding of the mechanisms of cross-modal plasticity following different forms of sensory loss and of sensory substitution

and other restorative therapies that may lead to restoration of the lost functions.

Author contributions

RK: Conceptualization, Validation, Writing—original draft, Writing—review & editing, Project administration. MP: Project administration, Validation, Writing—original draft, Writing—review & editing.

Funding

The author(s) declare financial support was received for the research, authorship, and/or publication of this article. This work was supported by grants from the Canadian Institutes of Health Research (grant No. 451125).

Conflict of interest

The authors declare that the research was conducted in the absence of any commercial or financial relationships that could be construed as a potential conflict of interest.

Publisher's note

frontiers in Neuroscience

SYSTEMATIC REVIEW
published: 28 March 2022
doi: 10.3389/fnins.2022.850245

Brain Morphological Modifications in Congenital and Acquired Auditory Deprivation: A Systematic Review and Coordinate-Based Meta-Analysis

Anaïs Grégoire[1,2], Naïma Deggouj[1,2], Laurence Dricot[2], Monique Decat[1,2] and Ron Kupers[2,3,4]*

[1] Department of ENT, Cliniques Universitaires Saint-Luc, Brussels, Belgium, [2] Institute of NeuroScience (IoNS), UCLouvain, Brussels, Belgium, [3] Department of Neuroscience, Panum Institute, University of Copenhagen, Copenhagen, Denmark, [4] Ecole d'Optométrie, Université de Montréal, Montréal, QC, Canada

OPEN ACCESS

Edited by:
Elouise Alexandra Koops, Massachusetts General Hospital and Harvard Medical School, United States

Reviewed by:
Francesca Tinelli, IRCCS Stella Maris Foundation, Italy
Maria Bianca Amadeo, Italian Institute of Technology (IIT), Italy
Richard Charles Dowell, The University of Melbourne, Australia

***Correspondence:**
Anaïs Grégoire
anais.gregoire@saintluc.uclouvain.be

Specialty section:
This article was submitted to Perception Science, a section of the journal Frontiers in Neuroscience

Received: *07 January 2022*
Accepted: *01 March 2022*
Published: *28 March 2022*

Citation:
Grégoire A, Deggouj N, Dricot L, Decat M and Kupers R (2022) Brain Morphological Modifications in Congenital and Acquired Auditory Deprivation: A Systematic Review and Coordinate-Based Meta-Analysis. Front. Neurosci. 16:850245. doi: 10.3389/fnins.2022.850245

Neuroplasticity following deafness has been widely demonstrated in both humans and animals, but the anatomical substrate of these changes is not yet clear in human brain. However, it is of high importance since hearing loss is a growing problem due to aging population. Moreover, knowing these brain changes could help to understand some disappointing results with cochlear implant, and therefore could improve hearing rehabilitation. A systematic review and a coordinate-based meta-analysis were realized about the morphological brain changes highlighted by MRI in severe to profound hearing loss, congenital and acquired before or after language onset. 25 papers were included in our review, concerning more than 400 deaf subjects, most of them presenting prelingual deafness. The most consistent finding is a volumetric decrease in gray matter around bilateral auditory cortex. This change was confirmed by the coordinate-based meta-analysis which shows three converging clusters in this region. The visual areas of deaf children is also significantly impacted, with a decrease of the volume of both gray and white matters. Finally, deafness is responsible of a gray matter increase within the cerebellum, especially at the right side. These results are largely discussed and compared with those from deaf animal models and blind humans, which demonstrate for example a much more consistent gray matter decrease along their respective primary sensory pathway. In human deafness, a lot of other factors than deafness could interact on the brain plasticity. One of the most important is the use of sign language and its age of acquisition, which induce among others changes within the hand motor region and the visual cortex. But other confounding factors exist which have been too little considered in the current literature, such as the etiology of the hearing impairment, the speech-reading ability, the hearing aid use, the frequent associated vestibular

dysfunction or neurocognitive impairment. Another important weakness highlighted by this review concern the lack of papers about postlingual deafness, whereas it represents most of the deaf population. Further studies are needed to better understand these issues, and finally try to improve deafness rehabilitation.

Keywords: deafness/hearing loss, sign language (SL), neuroplasticity, brain morphology, cochlear implant, MRI, systematic review and meta-analysis

INTRODUCTION

Hearing Loss and Deafness

It is estimated that around 1.5 billion people worldwide experience some degree of hearing loss, which could grow to 2.5 billion by 2050 due to expected population growth and increased longevity (Geneva: World Health Organization, 2021). Although hearing loss can be congenital, affecting two in one thousand newborns, in the vast majority of the cases it is acquired later in life. Hearing impairment is characterized according to severity, ranging from mild to profound forms. The term of deafness is used in case of severe or profound hearing loss, with auditory thresholds greater than 70 dB HL (Hearing Level). Deafness is often classified into prelingual and postlingual, depending on whether its onset occurred before or after learning language, i.e., around the age of four. More than 50% of congenital hearing loss is genetic in origin (e.g., mutation of the connexin 26); other causes are complications at birth or in the neonatal period (birth asphyxia, low birth weight, and severe jaundice), certain infectious diseases (*in utero* infection by cytomegalovirus, rubella, or meningitis), chronic ear infections, ototoxic drugs (antibiotics like aminoglycosides, anti-tumor drugs like cisplatin), exposure to harmful noise levels (in a professional or recreational context), and ageing (Geneva: World Health Organization, 2021). The rate of moderate to severe (disabling) hearing loss increases exponentially with age in all regions of the world, rising from 15.4% among people aged in their 60s, to 58.2% among those aged more than 90 years (Geneva: World Health Organization, 2021). Recent studies on age-related hearing loss highlighted its association with enhanced risk of cognitive decline, depression and social isolation (Lin et al., 2013; Manrique-Huarte et al., 2016; Livingston et al., 2017; Maharani et al., 2019; Griffiths et al., 2020). Care and prevention, such as treatment of ear diseases, vaccination and limitation of the exposure to ototoxic drugs and noise, are essential to limit the negative consequences. The socio-economic impact of hearing loss can be substantial and depends on the severity and the age of onset of the hearing loss. Besides the direct medical costs, there are costs related to special education, vocational rehabilitation, and unemployment or lost productivity (Mohr et al., 2000; Keren et al., 2002; Shield, 2006). For example, Mohr et al. Mohr et al. (2000) estimated that in the United States, severe to profound postlingual hearing loss costs society $ 297.000 over the lifetime of an individual, and more than $ 1 million in case of prelingual deafness. Early intervention can significantly reduce these costs. A study comparing the lifetime societal costs of congenital deafness for a deaf child was estimated at $ 697.500 in case of normal language (due to early intervention), doubling to $ 1.126.300 in case of delayed language (Keren et al., 2002).

Early access to any type of hearing aids or sign language (SL) is therefore of utmost importance. In case of severe to profound deafness, especially if speech intelligibility with conventional hearing aids is poor (Zwolan et al., 2001), cochlear implant (CI) is the intervention of choice. A CI device consists of an internal part, with an electrode array placed directly in the cochlea, delivering electric stimulation to the branches of the auditory nerve, and an external part composed of a microphone and a speech processor (**Figure 1**). Most of the time, the CI allows oral language development in prelingual deafness, and functional hearing in postlingual deafness (Fulcher et al., 2012; Gaylor et al., 2013). According to estimates based on manufacturers' voluntary reports of registered devices to the United States Food and Drug Administration, 183.000 subjects have been implanted in the United States in 2019, of which a little more than a third were children. In case of prelingual deafness, CI implantation has to take place at least before the end of the language sensitive period to enable the normal development of auditory pathways (Ponton et al., 1996), and even before 9 months of age for optimum language development (Dettman et al., 2021). Despite significant improvement in mean speech scores after implantation (Gaylor et al., 2013), the variability of the outcomes is important, with speech discrimination in quiet conditions ranging from 0 to 100% (Lazard et al., 2012). The rate of poor performers varies from 10 to 50% depending on the definition used (Moberly et al., 2016). The reasons for poor CI success rates are unclear. For instance, a large multicentric study on 2,251 CI patients revealed that residual hearing, percentage of active electrodes, use of hearing aids during the period of profound hearing loss, and duration of moderate hearing loss only explain 20% of the variance (Lazard et al., 2012). Other studies reported that the remaining spiral ganglion cell count, representing the integrity of the peripheral auditory pathway, also does not explain the variance in speech perception (Fayad et al., 1991; Blamey et al., 1996). Thus, other factors must affect performance with a CI, such as the integrity of the central auditory pathways or already established brain plasticity (Sharma and Glick, 2016). Indeed, there is now ample evidence from both animal and human studies that the deprived

Abbreviations: CI, cochlear implant; DTI, diffusion tensor imaging; HG, Heschl's gyrus; IFOF, inferior-fronto-occipital fasciculus; PAC, primary auditory cortex; ROI, region of interest; SLF, superior longitudinal fasciculus; STG, superior temporal gyrus.

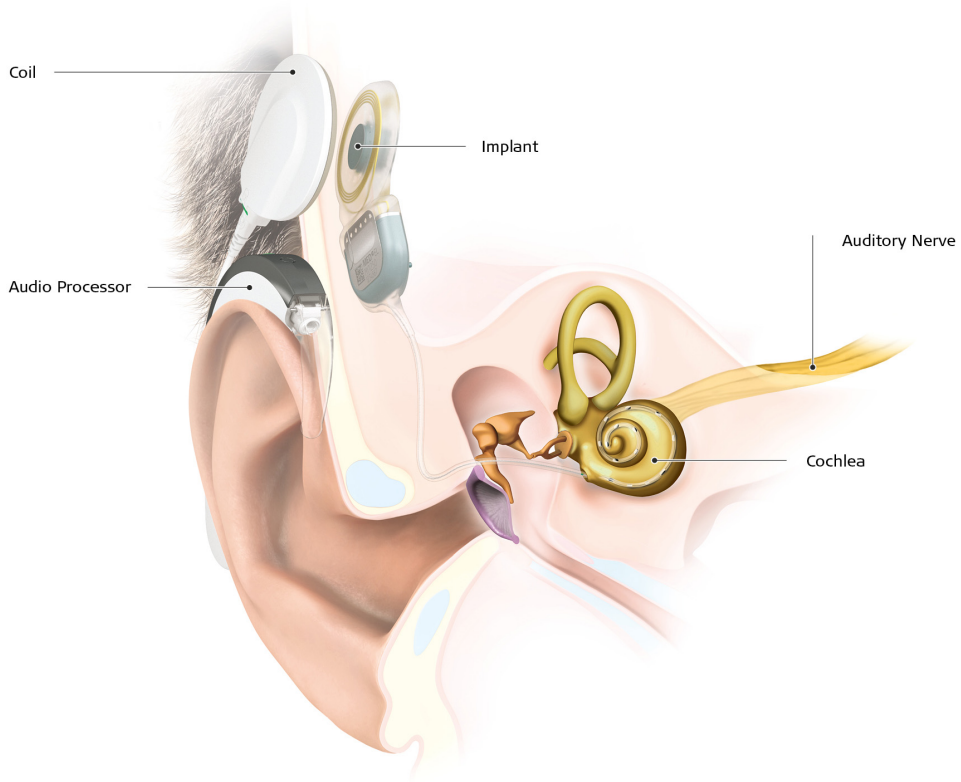

FIGURE 1 | Cochlear implant with its two main components. The external part, which is placed behind the ear, is composed of a microphone, an audio processor, a battery and a coil, kept in place in front of the internal part by a magnet. The internal part is placed during a surgical procedure under general anesthesia. The implant transmits the electrical stimulation to the fibers of the cochlear nerve through electrodes placed in the cochlea (from MED-EL© 2021).

auditory cortical areas process other sensory signals, like vision and touch (Petitto et al., 2000; Finney et al., 2001; Allman et al., 2009; Campbell and Sharma, 2014), a process referred to as cross-modal plasticity. Although cortical plasticity following loss of vision has been described in detail [see Kupers and Ptito (2014); for a review], there is a relative sparsity in studies on brain plastic changes following auditory loss. There is some evidence that structural and functional brain changes can impact rehabilitation with a CI (Lee et al., 2007; Lazard et al., 2013; Tan et al., 2015; Feng et al., 2018; Han et al., 2019; Wang et al., 2019; Sun et al., 2021). Furthering our understanding of brain plasticity and its structural substrate in deafness is therefore of utmost importance to improve therapeutic outcomes of CI therapy.

The aim of this systematic review and coordinate-based meta-analysis is to summarize the current knowledge on gray and white matter changes as revealed by structural MRI in subjects with severe to profound hearing loss. Plastic changes in deaf humans are compared with those in deaf animals and in human blind subjects. We end with some perspectives and further possible directions of investigation.

Animal Model of Deafness

Several animal models of deafness have been used to study neuroplastic changes following loss of audition. The most widely used animal model is the congenitally deaf white cat (Heid et al., 1998). These animals suffer from a genetic disease which means that 70 percent of them are born deaf. The auditory system of the cat is similar to that of humans in terms of auditory fields, gyrification and acoustic functions, making the deaf white cat a suitable model for studying congenital deafness (Kral and Lomber, 2015). Other animal models include transgenic mice (Kozel et al., 1998; Hunt et al., 2006), congenitally deaf dogs (Niparko and Finger, 1997), animals deafened at different ages by administration of ototoxic drugs (Hardie and Shepherd, 1999; Meredith and Allman, 2012), and gerbils deafened by aspiration of the content of the cochlea (Kitzes and Semple, 1985; Moore and Kitzes, 1985).

The modifications of the auditory pathways in animal models of deafness are discussed below according to structural or functional criteria.

Structural Changes in Animal Model of Deafness

Structural changes have been described at the different relays of the auditory pathway (**Figure 2**). Studies in neonatally deaf animals revealed that the cochlear nuclei, which form the first relay of the auditory pathway, are decreased in global volume, cell body size, and neuronal density (Hultcrantz et al., 1991;

Niparko and Finger, 1997; Butler and Lomber, 2013). The magnitude of these changes was correlated with the duration of hearing impairment, and thus also with age (Hardie and Shepherd, 1999). In contrast, no such changes were shown in animals with late-onset deafness (Tierney et al., 1997; Stakhovskaya et al., 2008). The next relay of the auditory pathway is the superior olivary complex, composed of three main nuclei surrounded by smaller periolivary nuclei. In animals with early-onset of deafness, the size and the number of neurons within the main olivary nuclei are decreased, and the tonotopy is disrupted [see Butler and Lomber (2013) for a review]. More rostrally, the volume of the inferior colliculi and their constituent neurons is decreased in animals with early-onset deafness, despite the fact that the total number of neurons remains globally stable [see Butler and Lomber (2013) for a review]. The thalamus has been very little studied in animal models of deafness, probably due to difficulty accessing the thalamic structures (Butler and Lomber, 2013). However, a study of thalamic projections to the primary auditory cortex A1 in neonatally deafened cats, using a retrograde tracer, showed that the labeling in the ventral division of the medial geniculate body did not differ between hearing and deafened animals (Stanton and Harrison, 2000).

At the level of the auditory cortex, studies in deaf cats showed an overall trend to a decrease in size, in particular in early-deaf cats (Lomber et al., 2019). In both early- and late-deaf cats, this global decrease was driven by a reduced volume of the primary auditory cortex (PAC), despite a conservation of its laminar structure (Hartmann et al., 1997). The secondary auditory areas also showed changes in size and of their borders with adjacent auditory, visual or somatosensory regions, which depended on the onset of deafness. For example, in early deaf cats compared to hearing cats, A2 was larger and the auditory field of the anterior ectosylvian sulcus (FAES) was smaller, whereas in late-deaf cats the posterior auditory field (PAF) was expanded (**Figure 3**) (Wong et al., 2014; Chabot et al., 2015). In congenitally deaf mice, the primary visual cortex was enlarged (Hunt et al., 2006).

Berger and co-workers compared the laminar organization of the auditory cortex in congenitally deaf and hearing cats. Although the auditory cortex preserved its six-layered cortical structure, the granular (IV) and infragranular (V–VI) layers were thinner in both A1 and the dorsal zone (DZ), which is part of the secondary auditory cortex (Berger et al., 2017). The thinner infragranular layers were explained by a combination of factors such as a reduction of the cell soma size, smaller dendritic trees, and reduced number and size of synaptic spines (Kral and Sharma, 2012; Berger et al., 2017). In contrast, there was no change in the global size of the supragranular layers (I to III), despite an increase in dendritic branching in A1 and the FAES in long-term neonatally deaf cats (Clemo et al., 2016, 2017).

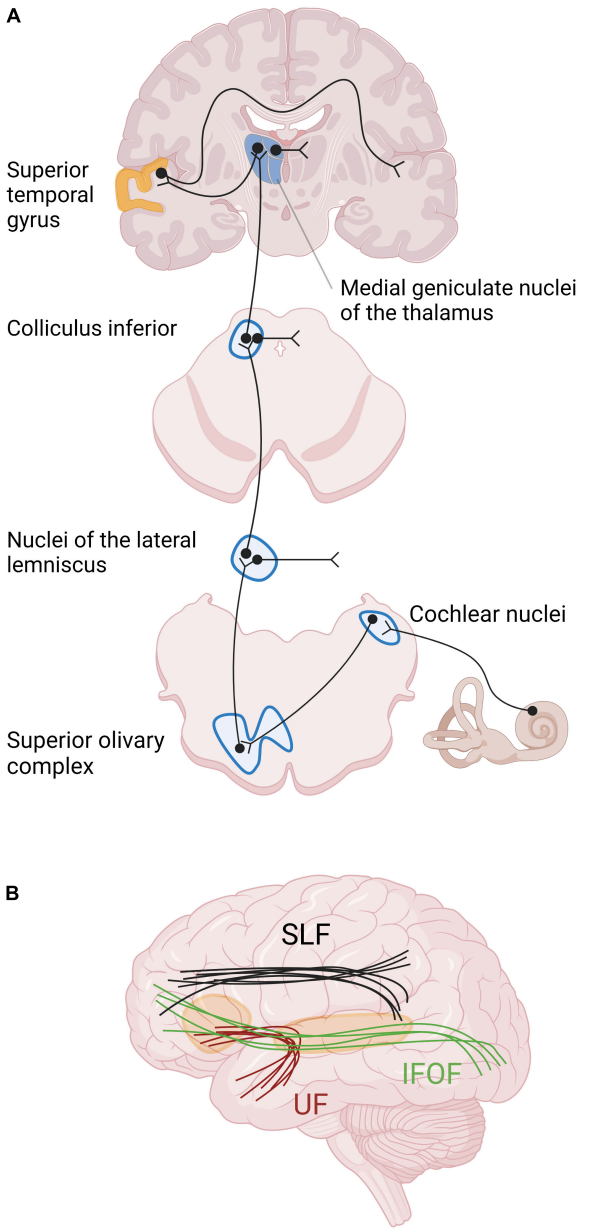

FIGURE 2 | Primary auditory pathway and main white matter tracts involved in auditory processing and language. **(A)** The relays of the auditory pathway are the cochlear nuclei, the superior olivary complex, the nuclei of the lateral lemniscus for some neurons, the inferior colliculus and the medial geniculate nucleus of the thalamus. The 8th cranial nerve finally reaches the auditory cortex in the superior temporal gyrus. The major part of the fibers from the cochlea cross the medial line at different levels of the neuraxis and arrive in contralateral auditory cortex. **(B)** The main intrahemispheric white matter bundles involved in auditory processing and language are the superior longitudinal fasciculus (SLF), the inferior fronto-occipital fasciculus (IFOF), and the uncinate fasciculus (UF), schematically represented here (Maffei et al., 2015).

Functional Changes in Animal Model of Deafness

Improved visual and tactile functions in both early- and late-deaf animals are well-documented (Rebillard and Pujol, 1977; Allman et al., 2009; Lomber et al., 2010; Meredith and Lomber, 2011). For example, congenitally deaf cats show better visual localization in the peripheral field and lower visual movement detection thresholds (Lomber et al., 2010). There is evidence that DZ and PAF play a significant role in these compensatory plastic

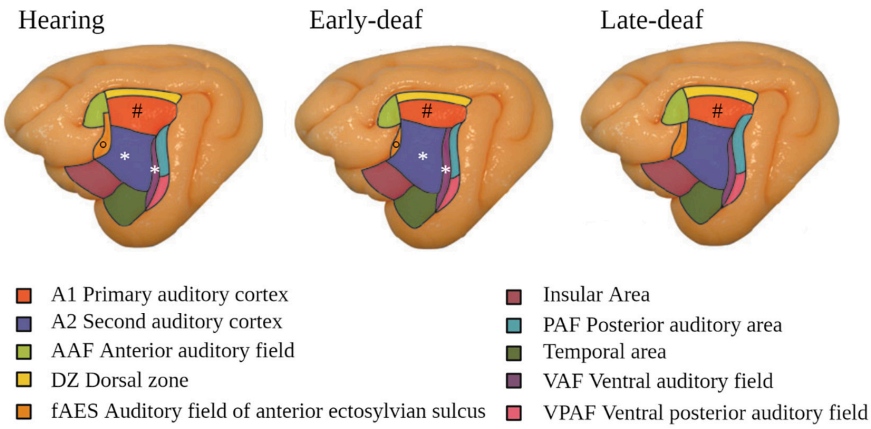

FIGURE 3 | Modifications in the auditory cortex in early- and late-deaf cats. Cytoarchitectonic study showing that A1 is reduced in both early- and late-deaf cats (#) compared to hearing cats. Additionally, in early-deaf cats, A2 and VAF are larger (*), whereas fAES is smaller compared to normal hearing cats (°). Data adapted from Wong et al. (2014) with permission of the author and publisher.

changes since inactivating these areas by local cooling makes thresholds return to normal (Lomber et al., 2010). Alterations in the response specificity of primary auditory cortical neurons have also been described (Hunt et al., 2006; Meredith and Lomber, 2011; Meredith et al., 2012): whereas more than 90% of neurons in A1 of normal hearing animals respond exclusively to auditory input, 68% of these neurons responded to unimodal somatosensory stimuli in congenitally deaf mice (Hunt et al., 2006). Plastic functional changes also take place in case of partial acquired hearing loss. For instance, Meredith et al. (2012) showed that the number of unimodal auditory neurons decreased from 65 to 31%, whereas neurons responding to different sensory modalities increased from 34 to 68% in partially hearing-impaired ferrets.

Local field potential recordings after intracochlear electrical stimulation showed that synaptic activity is preserved in the supragranular layers of the PAC in deaf cats, but is decreased in the infragranular layers (Klinke et al., 1999; Kral et al., 2000). This is in line with results from cytoarchitectural studies described above (Berger et al., 2017). The supragranular layers process bottom-up sensory-input, whereas the infragranular layers are the source of the outputs to the thalamic nuclei, the auditory midbrain and other brainstem structures (Schofield, 2009; Znamenskiy and Zador, 2013; Mellott et al., 2014). These layer-specific responses to electric cochlear stimulation suggest that the connections between the supra- and infragranular layers do not mature normally in congenitally deaf animals (Lomber et al., 2019).

Different mechanisms have been proposed to explain the above described functional and structural cortical changes. A first mechanism is the strengthening of existing cortico-cortical connections by the development of new synapses in the core and belt auditory cortex, both in early and late-onset deafness (Kok et al., 2014; Wong et al., 2015; Barone et al., 2016). For example, Wong et al. (2015) showed increased connections from visual and somatosensory areas to the anterior auditory field (AAF), as well as decreased connections from other auditory areas to AAF and PAF (Yusuf et al., 2021). These modifications were more pronounced in early-deaf compared to late-deaf cats. Together with A1, the AAF forms the core of the auditory cortex. Other authors reported an increase in projection strength from secondary visual areas (area 7 and region of the suprasylvian sulcus) to the secondary auditory area DZ in both early and late deaf cats (Kok et al., 2014; Barone et al., 2016). A second possible mechanism underlying cortical plasticity is the formation of new cortico-cortical connections. Although one study reported new projections to DZ from visual areas 19/20 and the multimodal areas of the anterior ectosylvian sulcus and the orbito-frontal region (Barone et al., 2013), there are no other reports in support of such a mechanism (Cardin et al., 2020). Finally, it has been suggested that cross-modal plastic changes are mediated by changes at the level of the brainstem (Allman et al., 2009; Butler et al., 2017). Although inputs from the somatosensory system to the dorsal cochlear nucleus and the inferior colliculus have been demonstrated in normal hearing animals (Aitkin et al., 1981; Shore et al., 2000; Kanold and Young, 2001; Shore and Zhou, 2006), these are enhanced after hearing loss, and their response thresholds are decreased (Shore et al., 2008; Meredith and Allman, 2012).

To summarize, there is ample evidence for a reduction of the size or the number of neurons at different levels of the auditory pathways and in the PAC, especially in case of early deafness. However, the global pattern of thalamo-cortical and cortico-cortical connections seems mainly preserved, with some strengthening but very few *de novo* connections. The responsiveness of PAC neurons to non-auditory sensory inputs may underlie the improved tactile and visual skills in deaf animals.

Structural Brain Modifications in Human Deafness

Enhancement of non-auditory sensory skills has also been reported in human deafness. For example, improved visual

functions have been described in congenitally deaf individuals, including distinguishing emotional facial expressions and local facial features, peripheral visual field tasks and attention to the peripheral visual field (Neville and Lawson, 1987a; McCullough and Emmorey, 1997; Arnold and Murray, 1998; Bavelier et al., 2000; Hauthal et al., 2013; Almeida et al., 2015). Activation of auditory areas has been demonstrated in response to somatosensory or visual stimuli, including sign language, in congenitally and acquired deaf humans, even in those presenting only a moderate hearing loss (Petitto et al., 2000; Finney et al., 2001, 2003; Levänen and Hamdorf, 2001; Schürmann et al., 2006; Campbell and Sharma, 2014). In line with results obtained in congenital blindness, the deprived auditory cortex becomes also involved in higher-order cognitive functions such as working memory and language (Buchsbaum et al., 2015; Ding et al., 2015; Cardin et al., 2020). In accordance with results from animal models of deafness (Diamond and Weinberger, 1984; Kral et al., 2003; Lomber et al., 2010; Meredith et al., 2011) and blindness (Rauschecker and Korte, 1993; Yaka et al., 1999), the higher-order auditory areas seem to have a higher capacity for plastic reorganization than the primary area (Kral, 2007; Butler and Lomber, 2013; Cardin et al., 2013, 2016, 2020). However, the structural basis underlying this functional plasticity remains an issue of debate (Lomber et al., 2019). A post-mortem histological study in subjects who suffered from profound deafness revealed that the cell bodies in the cochlear nuclei were larger at the side of the least affected ear (Chao et al., 2002).

In order to improve our understanding of the structural correlates of deafness associated functional plasticity, we conducted a systematic review and coordinate-based meta-analysis of the anatomical MRI studies conducted in subjects with severe to profound hearing loss.

METHODS

Search Strategy and Paper Selection

We performed a systematic review of the literature on studies published in English language peer-reviewed journals and comparing gray matter (GM)/white matter (WM) volume, cortical thickness, and cortical curvature between severe to profound deaf and normal hearing subjects. We followed the PRISMA guidelines (Page et al., 2021). The search was conducted in June 2020, using PubMed and Embase, with the MeSH search terms "magnetic resonance imaging" AND "deafness", the Emtree search terms "nuclear magnetic resonance imaging" AND "hearing impairment" OR "morphometry" AND "hearing impairment" and the key search terms "magnetic resonance imaging," "MRI," "morphometry," "cortex volume," "deaf," and "deafness." We screened all titles and abstracts and excluded studies of unilateral hearing loss, central hearing loss, tinnitus, and studies without a normal hearing control group. We built a chart collecting for each study the data about (1) meta-study information (e.g., authors and year of publication), (2) characteristics of the population (e.g., age, deafness and language characteristics, use of hearing aids, and handedness), (3) neuroimaging methods (e.g., region of interest or whole brain analysis, manual or voxel-based morphometry), technical information related to MRI and image acquisition (e.g., magnetic field strength, pulse sequences, and image resolution), (4) and significant results, if possible corrected for multiple comparisons. We encoded significant differences of global or regional brain volumes, GM and WM volumes, cortical thickness and curvature, specifying the hemisphere affected. When available, the MNI (Montreal Neurological Institute) or Talairach stereotactic coordinates were noted and reported on MRI for visualization. Since the size of the brain area affected by the change in volume or thickness was only rarely reported, it was not taken into account. This review has not been registered.

We classified the papers using the Oxford Center for Evidence-based Medicine (OCEBM) levels of evidence (Howick et al., 2011). Level 1 corresponds to systematic review, level 2 to randomized trials, level 3 to cohort studies and non-randomized controlled trial, and level 4 to case-series and case-control studies. We evaluated the quality of the included studies using the Newcastle-Ottawa quality assessment Scale (NOS) (Wells et al., 2000). In this scale, each study is judged on eight items, categorized into three groups: the selection of the study groups; the comparability of the groups, and the ascertainment of the exposure. The highest quality studies are awarded up to nine stars. The NOS is the most widely used instrument to assess quality of case-control and cohort studies (Luchini et al., 2017). However, some authors complained about a low inter-rater agreement (Hartling et al., 2013).

Activation Likelihood Estimation Meta-Analysis

We also performed an Activation Likelihood Estimation (ALE) meta-analysis of the literature of structural changes in deafness, based on the reported stereotactic coordinates. ALE was initially developed for meta-analysis of functional data (Turkeltaub et al., 2002), but the current version, GingerALE Version 3.0.2, has been adapted for brain structural analysis as well (Eickhoff et al., 2009). This technique gives a probabilistic localization of overlapping foci from different studies. The foci are transformed in spatial probability distributions centered at the given coordinates, with a width based on empirical estimates of spatial uncertainty due to the inter-subject and inter-template variability. It is important to note that this analysis does not take into account the extent of the reported brain modifications. The ALE results are finally compared with the null-distribution of the random spatial association between studies, resulting in a random-effect inference (Eickhoff et al., 2012).

To be included, the studies have to use Voxel-Based Morphometry (VBM), to provide the coordinates of the peaks in MNI or Talairach space, and to give significant results after correction for multiple comparisons. All the coordinates were transformed in MNI space, using SPM in GingerALE. Two datasets were built, the first one with the coordinates of the peaks where deaf subjects showed greater volume than the normal hearing control subjects, and the other one with the peaks where deaf subjects showed lower volume than their controls. For the paper from Olulade et al. (2014), which compared

four subgroups depending on the level of hearing (normal or profoundly impaired) and the type of language (oral or SL), we chose to only include the coordinates of peaks from the comparison deaf versus normal hearing SL users in order to avoid potential changes related to SL use. As recommended by Eickhoff et al. (2012), we applied to output images thresholds of $p < 0{,}01$ (cluster forming threshold) and 0,05 for cluster-level family-wise-error (FWE) with 1,000 thresholding permutations.

RESULTS

A total of 555 studies were identified and screened from all database searching (see **Figure 4** for flowchart PRISMA). Of these, 528 papers were excluded based on their title or abstract, mostly because their subjects did not present severe or profound bilateral hearing loss, or no anatomical MRI was included, or for a lack of a normal hearing control group. From the 27 remaining papers, 25 were finally included in the narrative systematic review, and nine in the coordinate-based meta-analysis. However, a recent tenth study was included in the meta-analysis to enhance statistical power (McCullough and Emmorey, 2021). All papers concerned case-control studies with an OCEBM level of evidence of 4 and are of good quality according to the Newcastle-Ottawa quality assessment Scale.

Demographics and Global Overview

In total, 427 deaf individuals and 539 normal hearing controls were included (see **Supplementary Table 1** for demographic characteristics). Of these, 110 were deaf children, 184 normal hearing children, 317 deaf adults, and 355 normal hearing adults. Several studies shared partially or totally the same population, but they focused on different regions of interest (ROIs) or used various methods (**Supplementary Table 1**). The age of the participants ranged from a few months until 70 years (mean age 24.5 years $\pm$ 1.7 SD). Seven studies focused on a pediatric population. Of these, two studies included toddlers from 8 to 38 months (Smith et al., 2011; Feng et al., 2018), one included children from 1 to 9 years (Shiohama et al., 2019), one included children from 5 to 14 years (Shi et al., 2016); three studies used the same population of children and adolescents from 10 to 18 years (Li J. et al., 2012; Li et al., 2013, 2015). Thirteen studies included participants with profound deafness (hearing loss over 90 dB), five included participants with severe to profound deafness (>70 dB). Seven studies had a mixture of patients with moderate hearing loss and severe to profound deafness (>50 dB HL) (Emmorey et al., 2003; Allen et al., 2008, 2013; Smith et al., 2011; Feng et al., 2018; Qi et al., 2019; Shiohama et al., 2019). For the study by Shiohama et al. (2019), we only took into account the group of children with severe to profound hearing loss, excluding those with mild to moderate hearing loss. In 24 out of 25 publications, only congenitally or prelingually deaf subjects were studied, most of them using SL as main language. Only one study included both pre- and postlingually deaf subjects (Kim et al., 2014). In most studies, deaf and hearing groups were matched for age, sex and handedness. Most studies excluded left-handed subjects, which increases population homogeneity but may induce selection bias. Cases presenting with additional neurological disease and brain malformation were excluded. Very little information is provided about the exact etiology of deafness (see **Supplementary Table 1**). The deaf and control groups are difficult to match in terms of level of education, since congenitally deaf people often do not have access to traditional education. However, some studies matched their groups for IQ (Olulade et al., 2014; Kumar and Mishra, 2018), linguistic proficiency (Penhune et al., 2003) or socio-economic status (Feng et al., 2018). **Supplementary Table 1** provides information about the demographic and main findings of the included papers.

Changes in Gray Matter

Figure 5 summarizes the significant brain modifications together with their stereotactic coordinates. The main GM and cortical thickness modifications were found in the visual cortex, extending from the occipital lobe to the fusiform gyrus of the temporal lobe, especially in the pediatric deaf population. Decrease of GM volume or in cortical thickness in deaf babies and children were found in right or left superior occipital gyri (Li J. et al., 2012; Feng et al., 2018), left middle and inferior occipital gyri (Shiohama et al., 2019), left lingual gyrus (Feng et al., 2018), and left fusiform gyrus (Li J. et al., 2012). Three other studies failed to detect GM changes among these visual areas in deaf children (Smith et al., 2011; Li et al., 2015; Shi et al., 2016). GM changes in the visual areas were more inconsistent in the adult deaf population, with half of the studies describing an increase or a decrease in GM. For example, a study of nine prelingually deaf adults, focusing on purported changes in the early visual cortex, did not find any differences in this area (Fine et al., 2005), whereas other studies reported a GM volume increase in the calcarine sulcus (Allen et al., 2013) or fusiform gyrus (Kumar and Mishra, 2018). Still others reported a GM volume reduction in both fusiform gyri (Olulade et al., 2014; Qi et al., 2019) and in the right middle occipital gyrus (Qi et al., 2019). Finally, one study reported a decrease in cortical thickness in the calcarine sulcus of prelingually deaf adults (Smittenaar et al., 2016). The age of SL acquisition may have an influence on the GM volume in the visual cortex. Pénicaud et al. (2013) showed that GM volume is decreased in left primary (V1) and secondary (V2) visual areas, and also in the left dorsal visual association areas (V3a/V7) in late SL learners (acquisition between 11 and 14 years), whereas it is increased in deaf adults with SL acquisition before 3 years old. These authors did not find differences between deaf and hearing subjects when all deaf subjects were analyzed together.

Modifications of GM in the temporal lobe were present in only five out of 19 studies. In deaf babies, one study reported a GM volume increase in the anterior part of Heschl's gyrus (HG) (Smith et al., 2011); in deaf adults, GM increases were found in bilateral superior temporal gyrus (STG) (Leporé et al., 2010a) or exclusively in the right STG extending posteriorly to the planum temporale (Emmorey et al., 2003), and in inferior temporal gyrus (Kumar and Mishra, 2018). In contrast, one study in deaf babies reported a reduction in GM density in bilateral STG and HG (Feng et al., 2018).

There are also reports of GM changes outside the occipital and temporal brain areas. Three studies in deaf adults reported

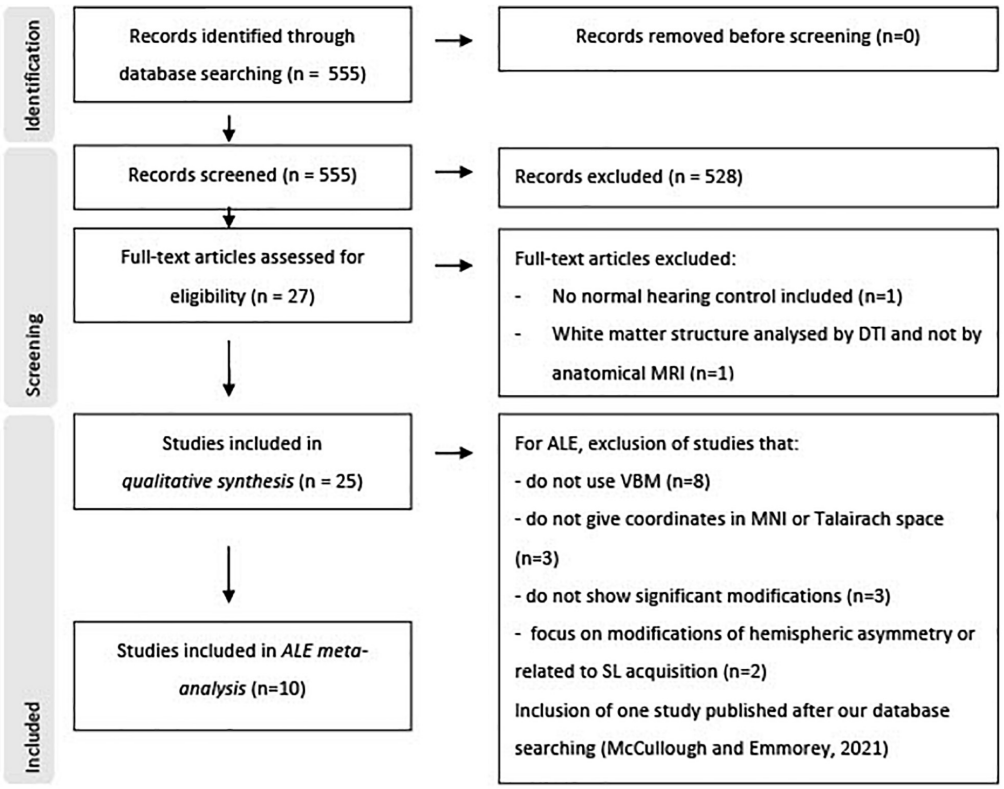

FIGURE 4 | Study flowchart according to PRISMA 2020.

increased GM volume in the bilateral (Allen et al., 2013; Kumar and Mishra, 2018) or left (Leporé et al., 2010a) inferior frontal gyrus, a brain area which is involved in language production. One study showed a reduction of GM cortical thickness of the left middle frontal gyrus in adolescents (Li et al., 2013); three others reported an increase of GM volume in adults either in both middle frontal gyri (Kumar and Mishra, 2018) or only at the right side (Leporé et al., 2010a; Olulade et al., 2014). One study in deaf babies reported a decrease in GM volume in the right supramarginal gyrus, an area which is part of the somatosensory association cortex (Feng et al., 2018). Three studies reported a GM volume increase in the precentral gyrus, more precisely within the left motor hand region (Leporé et al., 2010a; Li J. et al., 2012; Kumar and Mishra, 2018), likely due to the hand movements during SL production. The use of SL was also associated with a GM increase in different parts of the frontal gyri, especially the bilateral middle frontal, right medial frontal and right inferior frontal gyri (Olulade et al., 2014).

The GM modifications were also found in the precuneus, which is part of the parietal lobe and that plays a role, among others, in the integration of multisensory information. The modifications varied with age, deaf babies showing a GM decrease in the left precuneus (Feng et al., 2018), and deaf adolescents a cortical thickness increase of the right precuneus (Li et al., 2013). The use of SL was associated with a GM increase in the right precuneus (Olulade et al., 2014). Contradictory findings were also reported for the insula, with some studies reporting an increased GM volume in left posterior insula in congenitally deaf adults compared to hearing signers and non-signers (Allen et al., 2008), and other studies reporting a GM decrease in bilateral insula in deaf compared to hearing signers (Olulade et al., 2014). The GM decrease in the right insula seemed related to the use of SL in the congenitally deaf, rather than to deafness *per se* (Olulade et al., 2014). The limbic lobe was affected, with two studies describing a GM decrease in the right cingulate gyrus in deaf babies (Feng et al., 2018) and deaf adults (Olulade et al., 2014), and one study reporting an increase in cortical thickness in the left posterior cingulate gyrus in deaf adolescents (Li et al., 2013). Again, the use of SL, and not deafness, seemed to account for the GM increase in the left cingulate gyrus (Olulade et al., 2014).

Several studies reported increases in GM volume in the cerebellum, either at the right side (Leporé et al., 2010a; Li et al., 2013; Kumar and Mishra, 2018), but sometimes also bilaterally (Hribar et al., 2014) (see **Figure 6** for cerebellar anatomy). More specifically, these GM increases occurred in the crus I and II, also called superior and inferior semi-lunar lobules (Hribar et al., 2014; Kumar and Mishra, 2018), in right lobules IX and X (Leporé et al., 2010a) and in right lobules IV and V (Li et al., 2013). Interestingly, this GM increase was less pronounced in participants with long-term use of hearing aids (Li et al., 2013). One study in deaf adults reported a GM decrease in the left crus II and in left lobule VIII (Olulade et al., 2014).

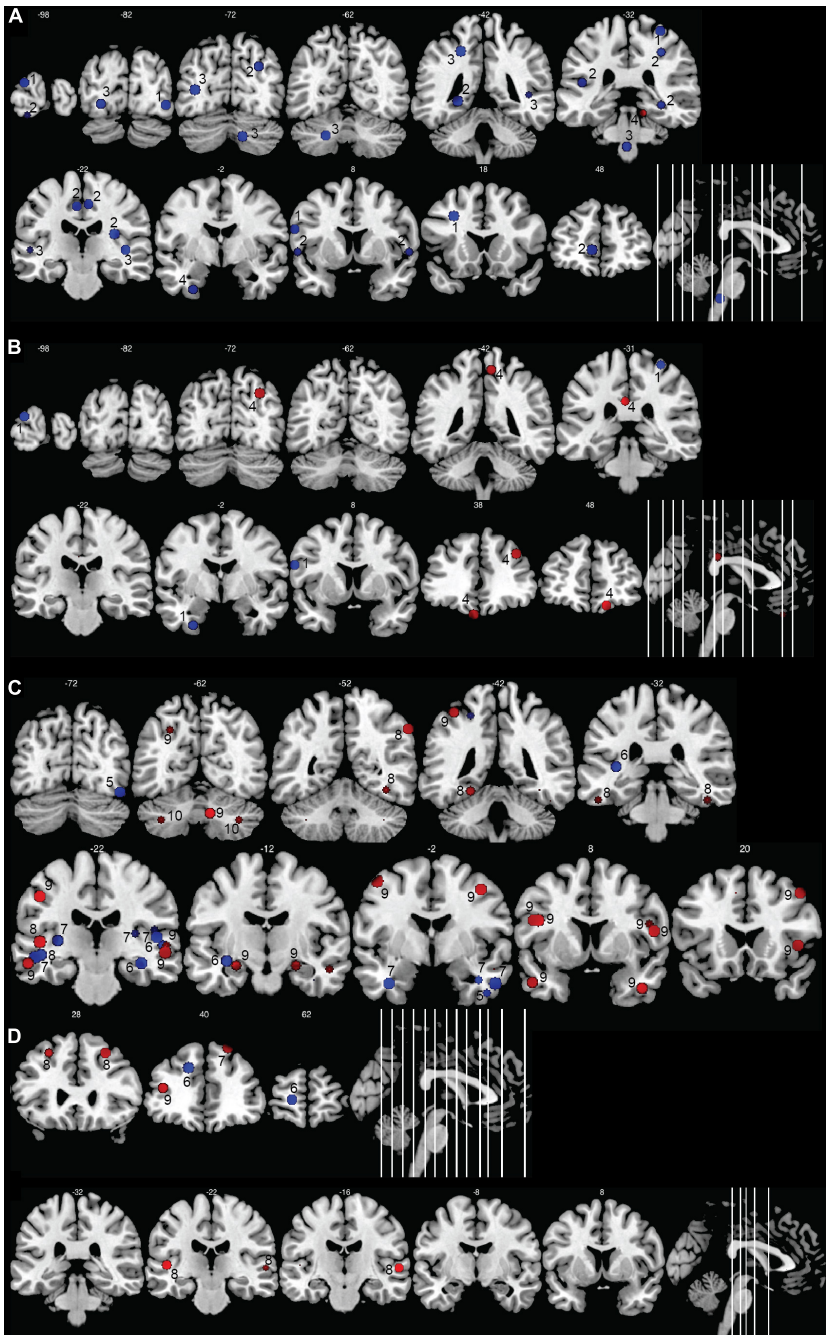

FIGURE 5 | Morphometric changes in the human deaf brain. Increases in GM or WM volume in the deaf compared to hearing controls are shown in red, decreases in blue. **(A)** GM and WM volume in deaf children; **(B)** cortical thickness in deaf children; **(C)** GM and WM volume in deaf adults; **(D)** cortical thickness in deaf adults. The image shows the peak (or center) of the areas with modifications in volume or cortical thickness; cluster volumes are not indicated. Some spheres appear smaller because they are shown on slices which are not positioned at the center of the spheres. Right hemisphere is shown on the right of the images. The numbers on top of the slices show the *y*-coordinates of the coronal slices in MNI space. The numbers inside the slices correspond to the studies from which the coordinates are taken. 1: Li J. et al. (2012); 2: Feng et al. (2018); 3: Smith et al. (2011); 4: Li et al. (2013); 5: Qi et al. (2019); 6: Kim et al. (2009); 7: Olulade et al. (2014); 8: Kumar and Mishra (2018); 9: Leporé et al. (2010a); 10: Hribar et al. (2014).

Finally, Amaral et al. (2016) showed that the right thalamus, right lateral geniculate nucleus and right inferior colliculus are larger than their left counterparts in congenitally deaf subjects, suggesting that these subcortical structures participate in the rerouting of visual information to the right auditory cortex.

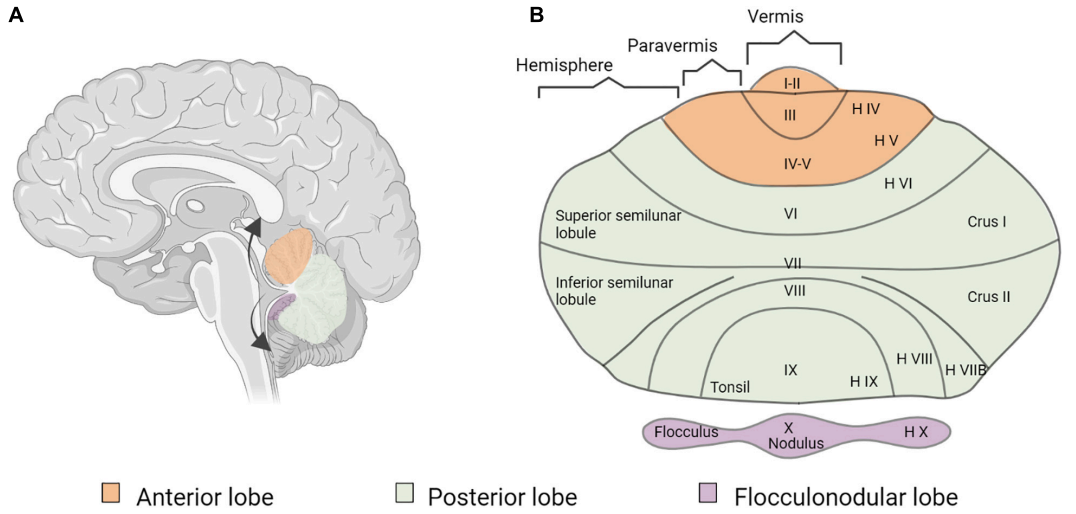

FIGURE 6 | Cerebellar anatomy. **(A)** Sagittal section of the human brain and cerebellum. The arrows show the way the cerebellum is unfolded. **(B)** Flatmap representation of the unfolded cerebellum, using both the classification of Larsell (1952) and the classical nomenclature of the human cerebellum (Malacarne, 1791; Reil, 1808; Burdach, 1829).

In summary, the most frequent morphometric change is a decrease in GM in visual areas of the deaf pediatric population. Changes in the visual cortex in deaf adults and in auditory regions are less frequent and less consistent. Increases in GM have also been described in the cerebellum, especially at the right side, and in the hand region of the precentral gyrus.

Changes in White Matter

Several studies reported decreases in WM in the temporal lobe in deaf adults and children. Seven studies reported WM decreases in the STG, either at the left side (Shibata, 2007; Olulade et al., 2014) or bilaterally (Emmorey et al., 2003; Kim et al., 2009; Smith et al., 2011; Feng et al., 2018; Kumar and Mishra, 2018). As for HG, three studies reported a left-lateralized decrease in WM (Shibata, 2007; Hribar et al., 2014; Olulade et al., 2014), whereas one study reported a bilateral decrease in WM (Emmorey et al., 2003). One other study reported a WM decrease within the anterior part of HG (Smith et al., 2011). In contrast, one study described increased WM volume around HG (Leporé et al., 2010a).

In deaf babies, WM decreases were described in the occipital lobe, either bilaterally (Feng et al., 2018) or in the left hemisphere only (Smith et al., 2011). A study in deaf adolescents reported a selective WM decrease in the right inferior occipital gyrus (Li J. et al., 2012).

Two studies described WM decreases in the left superior frontal gyrus (Kim et al., 2009) or in left middle frontal gyrus (Kim et al., 2009; Li J. et al., 2012) in deaf adolescents and adults. One study reported a WM increase in the left precentral gyrus and the right inferior frontal gyrus that was associated with the use of SL (Olulade et al., 2014). Deaf compared to hearing signers had a bilateral decrease in WM in the insula (Olulade et al., 2014). One other study reported a WM increase in the right insula in deaf and hearing signers (Allen et al., 2008).

Three studies reported a WM decrease within the cerebellum. In deaf babies, this WM reduction was either global (Feng et al., 2018), or limited to the region surrounding the crus II and lobule IX bilaterally (Smith et al., 2011). In deaf adults, this WM decrease covered the anterior lobe of the left cerebellum, and was just below statistical significance when corrected for multiple comparisons (Shibata, 2007).

A few studies also examined changes in long-range WM fiber tracts. One study in congenitally deaf adults reported a decrease of WM volume in the left superior longitudinal fasciculus (SLF) and left uncinate fasciculi (Meyer et al., 2007), but the effect disappeared after correction for multiple comparisons. Finally, two studies that focused on interhemispheric connections of the corpus callosum failed to show differences related to deafness (Kara et al., 2006; Leporé et al., 2010a).

In summary, the main modifications in WM in deaf individuals occurred in the temporal lobes, and more specifically around the STG which hosts the auditory cortex.

Changes in Cortical Curvature

Only two studies investigated changes in cortical curvature in the auditory cortex. One study reported a steeper slope of the posterior Sylvian fissure (Meyer et al., 2014), whereas the second study failed to find an effect (Penhune et al., 2003).

Results of the Activation Likelihood Estimation Meta-Analysis

Ten studies met the inclusion criteria for ALE, including the recent study of McCullough and Emmorey, for a total of 239 deaf subjects (68 children and 171 adults) compared to 289 normal hearing controls (82 children and 207 adults). All deaf participants except 30 presented with prelingual onset of deafness. The first dataset that we built gathers the coordinates of the peaks where deaf subjects showed greater volume than

the normal hearing control subjects. They concern 30 foci from five studies (Leporé et al., 2010a; Hribar et al., 2014; Olulade et al., 2014; Kumar and Mishra, 2018; McCullough and Emmorey, 2021). The second dataset consists of 47 foci of lower volume in deaf, from eight studies (Kim et al., 2009; Smith et al., 2011; Li J. et al., 2012; Olulade et al., 2014; Feng et al., 2018; Kumar and Mishra, 2018; Qi et al., 2019; McCullough and Emmorey, 2021). Despite a relatively low number of studies, the meta-analysis highlights significant convergence in three clusters where deaf individuals have lower volume than their normal hearing controls. There is no cluster of increased volume in deaf subjects (**Figure 7** and **Table 1**). Two clusters are located in the left hemisphere and one in the right. The clusters are mainly situated within the WM of both STG, including the HG, and the adjacent middle temporal gyrus and insula, and involve Brodmann Areas 13 (insula), 22 (posterior part of the STG, hosting Wernicke's area in the left hemisphere) and 41 (anterior part of the HG, hosting the PAC). However, this coordinate-based meta-analysis has some potential biases. First, as mentioned above, only ten papers were included due to missing coordinates, whereas it is recommended to have at least 20 studies (Eickhoff et al., 2016). Second, the mix of pediatric and adult study cohorts, and to a lesser degree the mix of pre- and postlingual deafness, may increase heterogeneity of the results. Finally, the ALE methodology does not take into consideration the extent of the brain modification, leading to a lack of accuracy.

DISCUSSION

Structural Brain Changes in Human Deafness

Overview of the Results

The three most consistent findings in deaf subjects derived from our review are (1) a volumetric decrease in WM in auditory cortex; (2) a volumetric decrease in GM and WM in visual cortex, particularly in babies and children; and (3) a GM increase in the right cerebellum. Cortical thickness and curvature have been studied sparsely in comparison with GM and WM volume, making it difficult to draw firm conclusions with respect to these measures.

Unlike a recent meta-analysis (Manno et al., 2021), we have chosen to focus exclusively on severe and profound congenital and acquired hearing loss, excluding other degrees of hearing impairment. A large part of the published studies focused on plastic changes in early deaf subjects, i.e., congenital and acquired prelingual deafness, for whom SL is typically the primary language. On the contrary, most studies on postlingual deafness include elderly people with only mild to moderate age-related hearing loss (Manno et al., 2021).

Impact of the Language

As most prelingually deaf adults use SL as their only language, the comparison with normal hearing subjects can introduce some bias due to the difficulty in distinguishing the effects of deafness from those of SL (Cardin et al., 2013). Only a few studies from our literature review dealt with this issue by including an extra control group of normal-hearing individuals who were fluent in SL (Fine et al., 2005; Allen et al., 2008, 2013; Olulade et al., 2014; McCullough and Emmorey, 2021). These studies revealed that SL use *per se* induces brain modifications, especially in the hand motor region, and in regions involved in visual processing of faces and hands during SL comprehension (see in subsequent sections for more details). Furthermore, the age of SL acquisition also plays a central role in brain morphology, corroborating the idea of a critical period of language acquisition, such as for the development of the auditory brain. For example, the lack of early SL access in case of deafness is responsible for a GM decrease within the occipital lobe (Pénicaud et al., 2013) and for microstructural alterations of the arcuate fasciculus (AF), which is part of the AF-SLF complex (Cheng et al., 2019). The AF-SLF complex, whose anatomical classification is still debated, is involved in language processing, as well as the inferior fronto-occipital fasciculus (IFOF) and the uncinate fasciculus (**Figure 2**). More specifically, the IFOF and uncinate fasciculus belong to the ventral language pathway which plays a critical role in semantic language processing, goal-oriented behavior, and visual task switching (Conner et al., 2018). On the other hand, the AF-SLF complex is part of the dorsal language pathway that is involved in syntax and speech repetition (Dick et al., 2014). This dorsal pathway also participates in the visuospatial attention network, and could more largely be involved in attentional control across multiple sensory modalities (Chechlacz et al., 2013). The alteration of the AF-SLF complex in late SL learners could explain the abnormal development of neuro-linguistic structures in the brain, affecting especially grammar and second language acquisition (Skotara et al., 2012). Indeed, a first language acquired in infancy facilitates the learning of a second language, independently of the modality of the first or second language (oral or signed) (Mayberry et al., 2002). This highlights the great importance of providing language tools to deaf babies to enable the development of related WM tracts and facilitating potential further adaptation to another language modality, for example after CI rehabilitation. Moreover, the lack of language access is responsible for impaired cognitive and socioemotional development (Cheng and Mayberry, 2019), causing cognitive delays, mental health difficulties and lower quality of life (Hall, 2017).

In summary, the modality of the language and its age of acquisition have an important impact on brain structure and function. Indeed, exposure to any language at a young age allows the normal development of the "language brain," especially its white matter bundles. This highlights the importance of hearing screening to be able to rapidly offer language, either oral after cochlear implantation or visual. Moreover, further studies are needed to explore the role of oral and visual language, e.g., SL and speech reading, on brain anatomy and CI rehabilitation.

Structural Changes in Auditory Brain Areas

The most conspicuous change was a decrease of WM density within the STG, which hosts the auditory cortex and part of Wernicke's speech area, in both children and adults. This finding is highlighted by the ALE meta-analysis that showed three clusters of decreased density in the deaf brain, mainly in WM,

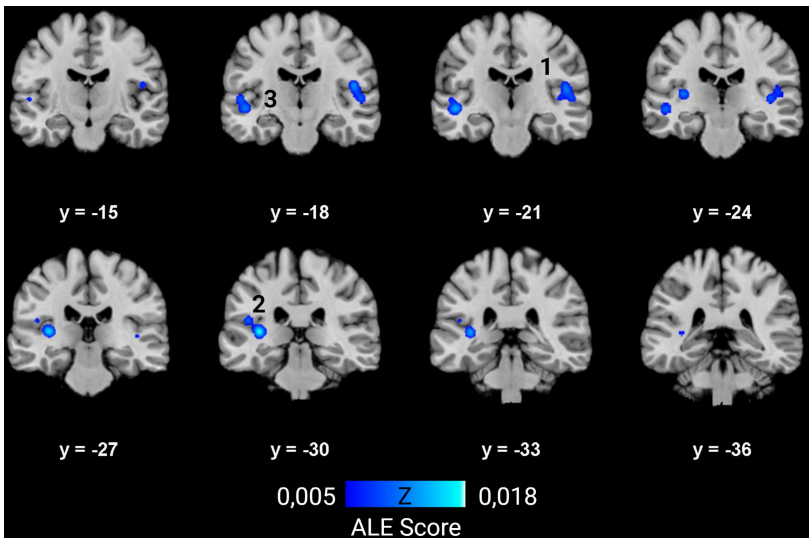

FIGURE 7 | ALE meta-analysis of changes in GM and WM density in the deaf brain. Right hemisphere is shown on the right in the images. The numbers on top of the slices show the *y*-coordinates of the coronal slices in MNI space. Three clusters of decreased volume in deaf were found significant, and none of increased volume ($p < 0.01$, cluster-level family-wise error $p < 0,05$). They are situated in both STG and adjacent middle temporal gyrus and insula, and involve mainly WM. The numbers correspond to those indicated in **Table 1**.

TABLE 1 | Characteristics of the clusters from the ALE meta-analysis showing decreased volume in deaf subjects.

Clusters	Location	Tissue type	Related BA (relative weight)	Coordinates of the center (MNI)			Size (mm^3)	Contributing studies
				x-	*y-*	*z-*		
1	R insula, STG, HG	52% WM	13 (26%), 41 (9%), 22 (7%)	49	−20	8	2152	Kim et al., 2009; Smith et al., 2011; Olulade et al., 2014; Kumar and Mishra, 2018
2	L STG, HG	75% WM	41 (16%), 13 (3%)	−37	−29	8	2016	Kim et al., 2009; Olulade et al., 2014; Feng et al., 2018; McCullough and Emmorey, 2021
3	L STG, MTG	71% WM	22 (21%), 13 (4%)	−50	−20	−4,5	1552	Smith et al., 2011; Olulade et al., 2014; Kumar and Mishra, 2018

MNI coordinates, P < 0.05 cluster-level FWE. BA, Brodmann area; R, right; L, left; STG, superior temporal gyrus; HG, Heschl's gyrus; MTG, middle temporal gyrus; WM, white matter.

around the STG and insula. The results for GM modifications were more ambiguous. The temporal lobe in prelingually deaf adults exhibited an increase of GM density in the STG, especially in the right hemisphere, and bilaterally in the inferior temporal gyrus. In children, the results were inconsistent, some reporting increases and others decreases in GM in STG. A recent study conducted in a large cohort of 94 postlingually deaf adults, not included in the ALE analysis because of lack of MNI coordinates, found a global GM decrease in the superior, middle and inferior temporal cortices (Sun et al., 2021). This study further showed an interaction between GM changes and duration of deafness: the decrease in the middle temporal cortices was found exclusively in participants who had been deaf for more than 10 years, whereas the decrease in the superior temporal cortices was limited to participants who had been deaf for less than 10 years. In addition to demonstrating that neuroplastic changes in postlingually deaf subjects evolve with duration of deafness, authors found correlation between specific GM modifications and speech comprehension after CI rehabilitation.

The WM decrease combined with the GM increase in prelingually deaf subjects suggests that early lack of auditory stimulation interferes with normal cortical GM and WM maturation in PAC, resulting in less myelination, fewer fibers projecting to and from auditory cortices, increased and inadequate axonal pruning, and incomplete neuronal migration (Emmorey et al., 2003; Penhune et al., 2003; Smith et al., 2011; Kumar and Mishra, 2018). Diffusion Tensor Imaging (DTI) studies confirmed the alteration of WM around the STG in prelingually [see Hribar et al. (2020) for reviews] and postlingually deaf subjects (Li Y. et al., 2012). More generally, the different relays of the auditory pathways of early deaf demonstrated a decrease in fractional anisotropy (Miao et al., 2013; Hribar et al., 2014; Huang et al., 2015; Wu et al., 2016; Karns et al., 2017) [see Tarabichi et al. (2018) for a review], which is

deleterious for CI rehabilitation (Wu et al., 2009; Chang et al., 2012; Huang et al., 2015). In congenitally deaf teenagers and adults, decreases in FA were also found in the IFOF, SLF and uncinate fasciculus (Kim et al., 2009; Miao et al., 2013; Hribar et al., 2014) [see Simon et al. (2020) for a review], although to a lesser extent. No such changes have been demonstrated in pediatric or postlingually deaf individuals. Interestingly, a recent study found that early language acquisition, whether oral or signed, enabled the normal development of the different WM bundles involved in language, whereas microstructural WM alteration were found within the AF-SLF complex in congenitally deaf adults with late SL acquisition (Cheng et al., 2019). Taken together, the modifications of these WM bundles could be due to oral language deprivation, to SL, or even to early language deprivation in case of delayed diagnosis of deafness. Furthermore, the alteration of the AF-SLF complex may be linked to deficits in executive functions, for instance memory and attention, demonstrated in deaf children and adults (Kronenberger et al., 2014; Kramer et al., 2018).

Structural Changes in the Frontal Lobe

Structural changes have been reported in the inferior frontal gyrus, involved in linguistic and cognitive functions such as text reading, speech production and working memory (Friederici and Gierhan, 2013), and also in other parts of the frontal lobe dealing with cognitive functions or hand movements. However, SL use seems to play a central role in the brain modifications of the frontal lobe, and further research with respect to this issue is needed. The GM increase in the inferior frontal gyri could be due to increased demand for deciphering oral language through print and lip-reading, and to increased reliance on visual working memory processes in the prelingually deaf (Allen et al., 2013). On the other hand, the volume and microstructure of the WM was altered in the inferior, middle and superior frontal gyri, as confirmed by some DTI studies (Chang et al., 2012; Zheng et al., 2017). This is in line with the alteration of SLF and IFOF, as discussed above. On the contrary, SL rather induces WM volume increase in the left precentral and right inferior frontal gyrus (Olulade et al., 2014).

Surprisingly, a recent meta-regression study (Manno et al., 2021) concludes that deaf subjects present a GM decrease in the frontal lobe, which is in contradiction with our results and those from other reviews (Hribar et al., 2020; Simon et al., 2020).

Structural Changes in the Visual Areas

The occipital cortex is the brain area with the second most structural modifications related to deafness. Especially in babies and children, decreases in GM volume and thickness, and to a lesser extent in WM volume, were observed in primary, secondary and high-level visual areas. The results in deaf adults are less consistent, perhaps due to differences in the age of acquisition of SL. Indeed, as discussed above, prelingually deaf adults with late SL acquisition present a GM decrease in primary, secondary and higher order visual association areas, whereas those with early SL acquisition have increased GM within these areas (Pénicaud et al., 2013). The important role of SL is corroborated by a recent study showing that lifelong signing experience is associated with a reduction in cortical thickness in the right occipital lobe and with an expansion in the surface area of the left occipital lobes (McCullough and Emmorey, 2021). This study also reported an expansion of the surface of the left anterior temporal lobe in SL users. All these changes were attributed to the high demands of processing and integration of visual information from the face and hands during SL comprehension. The well-documented enhanced peripheral vision of deaf subjects could also play a role in the modifications in the occipital lobe (Neville and Lawson, 1987b). However, enhanced peripheral vision may have a negative effect on central visual attention and may be responsible for increased distractibility in a central visual task with peripheral distractors (Quittner et al., 2004; Bavelier et al., 2006).

The results for the fusiform area are inconsistent, some authors reporting a GM density increase or decrease, others a cortical thickness decrease (Li J. et al., 2012; Olulade et al., 2014; Kumar and Mishra, 2018; Qi et al., 2019), and still others reporting no changes. The fusiform gyrus is a high-level visual area involved in face perception, object recognition and reading (Çukur et al., 2013; Weiner and Zilles, 2016). A DTI study showed that a decrease in GM or cortical thickness of the fusiform gyrus is associated with alterations in the IFOF (see above) and the inferior longitudinal fasciculus (Qi et al., 2019). Indeed, the inferior longitudinal fasciculus is involved in object recognition and face perception (Wang et al., 2020). The fact that the fusiform gyrus shows more GM decreases in the left compared to the right hemisphere could be explained by the stronger reliance on phonology and the increased engagement of the right hemisphere in visual word processing in deaf readers (Emmorey and Lee, 2021). On the other hand, Kumar and co-workers showed a GM increase in the fusiform and inferior temporal gyri which they attributed to a stronger reliance on ventral and higher visual processing in deaf individuals (Kumar and Mishra, 2018). Finally, the GM increase in the right lateral geniculate nucleus could be due to the stronger reliance on visual information in deaf subjects, which will also be processed in the right auditory cortex (Finney et al., 2001; Almeida et al., 2015; Amaral et al., 2016).

Structural Changes in the Cerebellum

Prelingual deafness induces anatomical changes within the cerebellum, especially a GM increase mostly at the right side in crus I and II, lobules IV–V and IX–X (Leporé et al., 2010a; Li et al., 2013; Hribar et al., 2014; Kumar and Mishra, 2018), and a GM decrease in the left crus II and lobule VIII (Olulade et al., 2014). The WM volume was decreased in deaf babies, especially around the crus II and the cerebellar tonsils or lobules IX bilaterally (Smith et al., 2011; Feng et al., 2018).

The cerebellum is best known for its role in motor control and planning. The sensorimotor cerebellum is located in anterior lobules III to V, and in lobules VI and VIII; it is functionally connected with the contralateral cerebral sensorimotor cortices (Stoodley and Schmahmann, 2009; Buckner et al., 2011). Since the hand is represented in lobule V (Grodd et al., 2001), the GM increase in this area could be explained by increased demands in fine motor coordination of hand movements during SL.

The cerebellum also controls balance and posture by integrating vestibular and sensorimotor inputs. In particular, vermal lobule IX, lobule X (flocculus and nodulus), and vermal lobules I and II (lingula) receive afferents from the vestibule (Stoodley and Schmahmann, 2009). Therefore, vestibular dysfunction could also induce neuroplastic changes in the cerebellum of deaf subjects. It is important to notice that more than 50% of congenitally deaf subject present some vestibular dysfunction (Kaga et al., 2008). This is not surprising since the cochlear and vestibular organs share anatomical, histological and physiological similarities (Cushing et al., 2013).

Finally, the cerebellum is also involved in many cognitive processes such as verbal working memory, phonological storage, sound and speech recognition, attention, spatial tasks, visual perception of motion, speed and direction, and affective regulation (Ivry and Diener, 1991; Middleton and Strick, 1994; Glickstein, 2007; Sens and De Almeida, 2007; Grimaldi and Manto, 2012; Mariën et al., 2014; McLachlan and Wilson, 2017). Some of these higher-level tasks, such as language and working memory, activate the right posterolateral lobe, which has increased GM in prelingually deaf (Stoodley and Schmahmann, 2009; Li et al., 2013). In addition to its role in spoken language, the cerebellum is even more strongly involved in the production and comprehension of SL (Kassubek et al., 2004; Sakai et al., 2005). Taken together, the cause of the changes in cerebellar GM and WM could be multifactorial, and be related to SL production and comprehension, modified cerebellar auditory and vestibular processing, deficits in memory and attention, stronger reliance on higher cognitive tasks such as deciphering spoken language through lip-reading, the use of visual cues for emotion recognition (Baumann and Mattingley, 2012) or visual working memory.

Structural Changes in the Insula

The reported volumetric changes in the insula vary considerably and range from a GM increase in the posterior left insula (Allen et al., 2008) to an overall bilateral GM decrease (Olulade et al., 2014). A recent study reported a GM decrease in the right insula in postlingual deafness (Sun et al., 2021), a finding which was confirmed in a meta-analysis and meta-regression study (Manno et al., 2021). Conflicting results were also reported for the insular WM, going from a bilateral decrease in deaf compared to normal hearing signers (Olulade et al., 2014) to a WM increase in the right insula in SL users (comparison between deaf and normal hearing signers, and normal hearing non-signers) (Allen et al., 2008). This suggests that deafness and SL exert different effects on the insula.

It has been hypothesized that the strong reliance of deaf individuals on lip-reading and articulatory-based representations of speech could impact the structure and the function of the insula (Allen et al., 2008). For instance, fMRI studies highlight an enhanced connectivity between the insula and auditory cortex or superior parietal gyrus, which could support the increased reliance on cross-modal integration in deaf subjects (Ding et al., 2016; Li et al., 2016). Moreover, deaf subjects show enhanced recruitment of the insula and thalamus during verbal memory tasks (Bavelier et al., 2008).

Negative Results

One third of the studies did not find any significant modifications in brain anatomy. Several hypotheses can be put forward to explain these negative findings. First, more than half of the included studies have a sample size of less than 20 subjects per group, resulting in low statistical power (Smith et al., 2011; Kim et al., 2014; Li et al., 2015). This is particularly the case for VBM whole brain analysis that requires larger numbers of subjects in order to reach statistical significance (Shibata, 2007). In line with this, studies that have shown GM changes in the temporal lobe were among those with the most participants. Second, the use of an univariate approach (e.g., measure of volume) instead of a multivariate one (e.g., measure of cortical thickness, surface, density, and curvature) reduces the chances to detect modifications, as they focus on one specific characteristic of brain tissue only (Kim et al., 2014; Ratnanather, 2020). Third, morphometric analyses like VBM and tensor-based morphometry (TBM) allow only evaluation of macrostructural alterations, whereas diffusion imaging enables to detect microstructural changes in WM. For example, in case of early deafness, only four out of 17 VBM studies found WM decrease in the STG, compared to 80% of studies using DTI (Simon et al., 2020).

Comparison With Animal Model of Deafness

Brain modifications in deafness have been more consistently reported in animal studies than in human studies. Some similar changes have been described in both animal and human studies. For instance, at the level of the cochlear nuclei, a decrease in the size of the cell bodies has been reported in histological studies in both animals and humans (Hultcrantz et al., 1991; Niparko and Finger, 1997; Hardie and Shepherd, 1999; Chao et al., 2002). MRI studies in deaf humans reported a decrease of WM density in the STG which is in line with a volumetric reduction of the infragranular cell layers of the auditory cortex in deaf animals, where the efferent fibers derive from. At the level of the visual cortex, GM volumetric decreases in V1 were consistently reported in deaf animals and in deaf human babies but not in prelingually deaf adults, possibly due to the use of sign-language. On the other hand, in contrast to animal studies, studies in human deaf individuals failed to find a global atrophy of the PAC. This could be due to the use of non-invasive imaging techniques in human studies which are less specific and suffer from a poorer spatial resolution (Moerel et al., 2014) compared to cytoarchitectonic methods used in animal studies. Although recent studies using ultrahigh-field (7 Tesla) multi-modal brain imaging techniques and novel methods for intersubject alignment have led to better probabilistic atlases of the human auditory cortex (Gulban et al., 2020), the exact delimitation of the boundaries of the human auditory cortex is still unresolved (Hackett et al., 2001; da Costa et al., 2011; Moerel et al., 2014). Another potential explanation for the lack of cortical atrophy in the STG in human studies is the use of visual-based SL instead of speech, which allows to maintain the language function of

some specific areas (Neville et al., 1998; Anderson et al., 2017; Cardin et al., 2020).

Comparison With Visual Deprivation

Brain structural and functional changes following loss of vision have been studied in far greater detail than those following auditory deprivation [see Kupers and Ptito (2014) for a review]. These studies highlighted that the deprived visual cortex becomes sensitive to other sensory modalities, including, tactile, auditory and olfactory inputs, leading to superior skills in some perceptual tasks (Bavelier and Neville, 2002; Burton et al., 2003, 2004; Chebat et al., 2007b; Renier et al., 2014; Araneda et al., 2016). These functional changes are accompanied with vast structural changes, including GM volume reductions in the different relays of the visual pathways, such as the superior colliculus, lateral geniculate nucleus, posterior pulvinar, primary and secondary visual cortices (Noppeney et al., 2005; Shimony et al., 2006; Pan et al., 2007; Ptito et al., 2008; Jiang et al., 2015; Cecchetti et al., 2016; Touj et al., 2021). The reductions in GM volume in visual areas could be the result of deprivation-related disuse (Noppeney et al., 2005; Voss et al., 2014). Reductions in WM of the visual tracts were reported in the optic nerve, optic chiasm and optic tract (Noppeney et al., 2005; Shimony et al., 2006; Pan et al., 2007; Ptito et al., 2008, 2021; Bridge et al., 2009; Leporé et al., 2010b; Tomaiuolo et al., 2014), the posterior part of the corpus callosum (Tomaiuolo et al., 2014) and the anterior commissure (Cavaliere et al., 2020). Several studies also reported increased cortical thickness of the primary visual cortex in early-blind subjects (Bridge et al., 2009; Jiang et al., 2009; Voss and Zatorre, 2012; Qin et al., 2013), which might be explained by a reduction of synaptic pruning due to lack of visual experience (Huttenlocher, 1984; Park et al., 2009; Kupers and Ptito, 2014; Anurova et al., 2015).

Some GM volume increases were also demonstrated outside the visual areas, for example in hippocampus (Chebat et al., 2007a; Fortin et al., 2008), sensorimotor areas (Jiang et al., 2015), the olfactory bulb, olfactory nucleus and piriform cortex (Rombaux et al., 2010; Touj et al., 2021), amygdala (Touj et al., 2021), and right inferior parietal cortex (Bauer et al., 2017). On the other hand, no studies showed structural changes in the auditory cortex of blind individuals (Noppeney et al., 2005; Pan et al., 2007; Ptito et al., 2008), except one which found a decrease in cortical thickness (Park et al., 2009).

Several hypotheses can be put forward to explain why structural changes are less prominent in case of deafness. A first explanation is that the visual system takes a much more prominent role in the human brain compared to audition. An estimated 30–40% of the cortical mantle is devoted to processing visual information, compared to only 8% for audition (Wandell et al., 2007). A second explanation is that studies investigating congenital blindness nearly all exclude individuals with residual vision, including light perception. This is in sharp contrast with studies on (congenital) deafness which uses a less stringent criterion, defining deafness in case of severe or profound hearing loss with auditory thresholds greater than 70 dB HL. In other words, these individuals still have remaining auditory capacities, although very limited. In this sense, deafness is more reminiscent to the categories of "low vision" or "legally blind," i.e., individuals with a visual acuity of 20/200 or less in the best eye, while wearing corrective glasses or contacts. Another hypothesis is that the potential structural modifications in the STG due to auditory deprivation are limited because this area continues to process language in the visual modality (Neville et al., 1998; Anderson et al., 2017; Cardin et al., 2020). Finally, there is ample anatomical and physiological evidence that auditory processing is strongly modulated by visual and somatosensory input (Bizley et al., 2007; Kayser et al., 2008; Smiley and Falchier, 2009; Banks et al., 2011; Ro et al., 2013; Meredith and Allman, 2015). The integration of auditory with visual and somatosensory input takes place at each level of the ascending auditory pathway, including the cochlear nucleus, inferior colliculus, medial geniculate body and the auditory cortex [for review: Wu et al. (2015)]. Therefore, the important multisensory input to auditory brain structures may explain why auditory brain areas are less affected by auditory deprivation.

Limitations and Perspectives

The included papers suffer from some limitations which should be considered in future investigations. First, the included papers attributed the reported brain modifications to deafness, omitting the possibility that other factors which can interact with cerebral morphology, such as etiology of the deafness (e.g., genetic, infectious, and due to medication), SL and hearing aids use, vestibular dysfunction, neurocognitive skills, etc. For example, the use of hearing aids may by itself induce functional and structural brain changes in auditory and language-related areas, the associative regions and the cerebellum (Li et al., 2013; Pereira-Jorge et al., 2018). Second, the exclusive reliance on non-oral communication in the prelingually deaf makes it difficult to match the deaf and control populations in terms of psychosocial and socio-economic variables. Indeed, most tools used for intellectual evaluation are based on oral communication, and moreover deaf subjects have less opportunities of professional training and inclusion. Third, some of the sample sizes are low which reduces the statistical power. Finally, whereas various metrics can be taken in morphometric analyses, such as volume, surface, cortical thickness, and curvature, most of the papers focused on an univariate approach. Although these metrics are interrelated (f.i., cortical volume is the product of cortical surface and thickness), they measure different aspects of the same cerebral region; the measure of cortical thickness and surface independently provides the best appreciation of the brain modifications (Ratnanather, 2020).

This review has also its proper limitations. First, the existing literature meeting our inclusion criteria concerned almost exclusively studies in prelingually deaf subjects, at the detriment of the postlingually deaf population. The study of prelingually deaf population presents some advantages linked to the homogeneity of this population with respect to the age of onset of deafness, the severity of the hearing loss, and the use of SL as primary language in absence of effective hearing aids. Mild to moderate hearing loss in the aging population has been more frequently studied, but studies of severe to profound hearing loss are lacking. This is more surprising since this population

is larger than the prelingually deaf population (Ratnanather, 2020), and will continue to grow due to an aging population. In this specific group, the frequent association with dementia or tinnitus should also not be forgotten. A second limitation of our review is the choice to concentrate on macrostructural brain modifications using 3D-T1-weighted MRI. Indeed, diffusion imaging provides more qualitative and quantitative information about WM microstructure. A third limitation relates to the absence of well-established anatomical limits of functional regions; these can differ from one brain atlas to another. Inter-individual variability in brain anatomy can also complicate the comparisons. For instance, in case of duplicated HG, authors considered that the PAC was situated on the most anterior gyri, while it has since been demonstrated that it spans both divisions of HG (da Costa et al., 2011). When hand-drawn ROIs are used, the delineation of anatomical areas is also susceptible to be biased by assumptions of what form the ROI should have (Shibata, 2007; Li J. et al., 2012). The use of stereotactic coordinates is certainly the most accurate method, and these one should be shared in the papers.

This review demonstrates that severe to profound prelingually deafness is responsible of structural brain modifications mainly but not limited to the temporal lobe. Our results are also of clear clinical interest, since brain plastic changes can facilitate, or complicate, CI auditory rehabilitation [for example Feng et al. (2018) or Sun et al. (2021)]. In contrast, regions unaffected by deafness, such as the fronto-parietal network and dorsal lateral or medial prefrontal cortex, showed a high predictive power. Another example where brain plasticity can predict CI outcome concerns lip-reading abilities. The use of lipreading, instead of written language, allows to maintain phonological representations and left hemispheric language specialization, which further increase speech comprehension (Lazard and Giraud, 2017). This teaches us that lip-reading must be encouraged in the deaf population. It would be very interesting to correlate this finding with structural or functional brain imaging. Finally, diffusion and functional imaging can also give some predictive factors of the speech outcomes with a CI. For example, preoperative inferior colliculus FA values correlate positively with postoperative auditory performance in deaf children (Wang et al., 2019). These examples highlight the potential contribution of pre-operative MRI to CI professionals as a clinical outcome prediction tool. It can also guide clinicians to adapt their strategy of care, for example by training lip-reading to avoid maladaptive plasticity.

CONCLUSION

Severe to profound deafness induces modifications of both brain GM and WM characteristics. The major modifications are a WM decrease around the auditory cortex, the occipital lobe and the cerebellum, a GM decrease in the occipital lobe of the deaf pediatric population, and a GM increase of the right cerebellum. Different measures (volume, surface, curvature, and cortical thickness) and methods (VBM, TBM, and DTI) should be combined to create a more comprehensive view of the brain modifications. Deaf subjects must be better categorized to dissociate brain changes due to deafness from those of sign language use, age of SL acquisition, lip-reading abilities, etiology of deafness, use of hearing aids, and vestibular dysfunction. More attention needs to be paid to structural changes in postlingual deafness which affects the vast majority of the deaf and aging population in western countries.

DATA AVAILABILITY STATEMENT

The original contributions presented in the study are included in the article/**Supplementary Material**, further inquiries can be directed to the corresponding author.

AUTHOR CONTRIBUTIONS

AG did the literature review and wrote the first draft of the manuscript. AG, ND, and RK wrote the final version of the manuscript. All authors contributed to conception and design of the study, manuscript revision, read, and approved the submitted version.

FUNDING

This literature review is part of a research project supported by the "Fund for Clinical Research" of the Academic Hospital of Saint-Luc in Brussels and the Rotary Club Mechelen, in Belgium.

ACKNOWLEDGMENTS

Figures 2, **3**, and **6** were created with BioRender.com.

SUPPLEMENTARY MATERIAL

The Supplementary Material for this article can be found online at: https://www.frontiersin.org/articles/10.3389/fnins.2022.850245/full#supplementary-material

REFERENCES

Aitkin, L., Kenyon, C., and Philpott, P. (1981). The representation of the auditory and somatosensory systems in the external nucleus of the cat inferior colliculus. *J. Comp. Neurol.* 196, 25–40. doi: 10.1002/cne.901960104

Allen, J. S., Emmorey, K., Bruss, J., and Damasio, H. (2008). Morphology of the insula in relation to hearing status and sign language experience. *J. Neurosci.* 28, 11900–11905. doi: 10.1523/JNEUROSCI.3141-08.2008

Allen, J. S., Emmorey, K., Bruss, J., and Damasio, H. (2013). Neuroanatomical differences in visual, motor, and language cortices between congenitally deaf

signers, hearing signers, and hearing non-signers. *Front. Neuroanat.* 7:26. doi: 10.3389/fnana.2013.00026

Allman, B. L., Keniston, L. P., and Meredith, M. A. (2009). Adult deafness induces somatosensory conversion of ferret auditory cortex. *Proc. Natl. Acad. Sci. U.S.A.* 106, 5925–5930. doi: 10.1073/pnas.0809483106

Almeida, J., He, D., Chen, Q., Mahon, B. Z., Zhang, F., Gonçalves, ÓF., et al. (2015). Decoding visual location from neural patterns in the auditory cortex of the congenitally deaf. *Psychol. Sci.* 26, 1771–1782. doi: 10.1177/0956797615598970

Amaral, L., Ganho-Ávila, A., Osório, A., Soares, M. J., He, D., Chen, Q., et al. (2016). Hemispheric asymmetries in subcortical visual and auditory relay structures in congenital deafness. *Eur. J. Neurosci.* 44, 2334–2339. doi: 10.1111/ejn.13340

Anderson, C. A., Lazard, D. S., and Hartley, D. E. H. (2017). Plasticity in bilateral superior temporal cortex: effects of deafness and cochlear implantation on auditory and visual speech processing. *Hear. Res.* 343, 138–149. doi: 10.1016/j.heares.2016.07.013

Anurova, I., Renier, L. A., De Volder, A. G., Carlson, S., and Rauschecker, J. P. (2015). Relationship between cortical thickness and functional activation in the early blind. *Cereb. Cortex* 25, 2035–2048. doi: 10.1093/cercor/bhu009

Araneda, R., Renier, L. A., Rombaux, P., Cuevas, I., and De Volder, A. G. (2016). Cortical plasticity and olfactory function in early blindness. *Front. Syst. Neurosci.* 10:75. doi: 10.3389/fnsys.2016.00075

Arnold, P., and Murray, C. (1998). Memory for faces and objects by deaf and hearing signers and hearing nonsigners. *J. Psycholinguist. Res.* 27, 481–497. doi: 10.1023/A:1023277220438

Banks, M. I., Uhlrich, D. J., Smith, P. H., Krause, B. M., and Manning, K. A. (2011). Descending projections from extrastriate visual cortex modulate responses of cells in primary auditory cortex. *Cereb. Cortex* 21, 2620–2638. doi: 10.1093/cercor/bhr048

Barone, P., Chambaudie, L., Strelnikov, K., Fraysse, B., Marx, M., Belin, P., et al. (2016). Crossmodal interactions during non-linguistic auditory processing in cochlear-implanted deaf patients. *Cortex* 83, 259–270. doi: 10.1016/j.cortex.2016.08.005

Barone, P., Lacassagne, L., and Kral, A. (2013). Reorganization of the connectivity of cortical field DZ in congenitally deaf cat. *PLoS One* 8:e60093. doi: 10.1371/journal.pone.0060093

Bauer, C. M., Hirsch, G. V., Zajac, L., Koo, B. B., Collignon, O., and Merabet, L. B. (2017). Multimodal MR-imaging reveals large-scale structural and functional connectivity changes in profound early blindness. *PLoS One* 12:e0173064. doi: 10.1371/journal.pone.0173064

Baumann, O., and Mattingley, J. B. (2012). Functional topography of primary emotion processing in the human cerebellum. *Neuroimage* 61, 805–811. doi: 10.1016/j.neuroimage.2012.03.044

Bavelier, D., Dye, M. W. G., and Hauser, P. C. (2006). Do deaf people see better? *Trends Cogn. Sci.* 10, 512–518. doi: 10.1016/j.tics.2006.09.006.Do

Bavelier, D., and Neville, H. J. (2002). Cross-modal plasticity: where and how? *Nat. Rev. Neurosci.* 3, 443–452. doi: 10.1038/nrn848

Bavelier, D., Newman, A. J., Mukherjee, M., Hauser, P., Kemeny, S., Braun, A., et al. (2008). Encoding, rehearsal, and recall in signers and speakers: shared network but differential engagement. *Cereb. Cortex* 18, 2263–2274. doi: 10.1093/cercor/bhm248

Bavelier, D., Tomann, A., Hutton, C., Mitchell, T., Corina, D., Liu, G., et al. (2000). Visual attention to the periphery is enhanced in congenitally deaf individuals. *J. Neurosci.* 20:RC93. doi: 10.1523/JNEUROSCI.20-17-j0001.2000

Berger, C., Kühne, D., Scheper, V., and Kral, A. (2017). Congenital deafness affects deep layers in primary and secondary auditory cortex. *J. Comp. Neurol.* 525, 3110–3125. doi: 10.1002/cne.24267

Bizley, J. K., Nodal, F. R., Bajo, V. M., Nelken, I., and King, A. J. (2007). Physiological and anatomical evidence for multisensory interactions in auditory cortex. *Cereb. Cortex* 17, 2172–2189. doi: 10.1093/cercor/bhl128

Blamey, P., Arndt, P., Bergeron, F., Bredberg, G., Brimacombe, J., Facer, G., et al. (1996). Factors affecting auditory performances of postlinguistically deaf adults using cochlear implants. *Audiol. Neuro Otol.* 1, 293–306. doi: 10.1159/000259212

Bridge, H., Cowey, A., Ragge, N., and Watkins, K. (2009). Imaging studies in congenital anophthalmia reveal preservation of brain architecture in "visual" cortex. *Brain* 132, 3467–3480. doi: 10.1093/brain/awp279

Buchsbaum, B., Pickell, B., Love, T., Hatrak, M., Bellugi, U., and Hickok, G. (2015). Neural substrates for verbal working memory in deaf signers: fMRI study and lesion case report. *Brain Lang.* 95, 265–272. doi: 10.1016/j.bandl.2005.01.009

Buckner, R. L., Krienen, F. M., Castellanos, A., Diaz, J. C., and Thomas Yeo, B. T. (2011). The organization of the human cerebellum estimated by intrinsic functional connectivity. *J. Neurophysiol.* 106, 2322–2345. doi: 10.1152/jn.00339.2011.-The

Burdach, K. (1829). *Vom Baue und Leben des Gehirns*. Leipzig: Dyk.

Burton, H., Diamond, J. B., and McDermott, K. B. (2003). Dissociating cortical regions activated by semantic and phonological tasks: a fMRI study in blind and sighted people. *J. Neurophysiol.* 90, 1965–1982. doi: 10.1152/jn.00279.2003

Burton, H., Sinclair, R. J., and McLaren, D. G. (2004). Cortical activity to vibrotactile stimulation: an fMRI study in blind and sighted individuals. *Hum. Brain Mapp.* 23, 210–228. doi: 10.1002/hbm.20064

Butler, B. E., and Lomber, S. G. (2013). Functional and structural changes throughout the auditory system following congenital and early-onset deafness: implications for hearing restoration. *Front. Syst. Neurosci.* 7:92. doi: 10.3389/fnsys.2013.00092

Butler, B. E., Meredith, M. A., and Lomber, S. G. (2017). Editorial introduction: special issue on plasticity following hearing loss and deafness. *Hear. Res.* 343, 1–3. doi: 10.1016/j.heares.2016.10.014

Campbell, J., and Sharma, A. (2014). Cross-modal re-organization in adults with early stage hearing loss. *PLoS One* 9:e90594. doi: 10.1371/journal.pone.0090594

Cardin, V., Grin, K., Vinogradova, V., and Manini, B. (2020). Crossmodal reorganisation in deafness: mechanisms for functional preservation and functional change. *Neurosci. Biobehav. Rev.* 113, 227–237. doi: 10.1016/j.neubiorev.2020.03.019

Cardin, V., Orfanidou, E., Rönnberg, J., Capek, C. M., Rudner, M., and Woll, B. (2013). Dissociating cognitive and sensory neural plasticity in human superior temporal cortex. *Nat. Commun.* 4:1473. doi: 10.1038/ncomms2463

Cardin, V., Smittenaar, R. C., Orfanidou, E., Rönnberg, J., Capek, C. M., Rudner, M., et al. (2016). Differential activity in Heschl's gyrus between deaf and hearing individuals is due to auditory deprivation rather than language modality. *Neuroimage* 124, 96–106. doi: 10.1016/j.neuroimage.2015.08.073

Cavaliere, C., Aiello, M., Soddu, A., Laureys, S., Reislev, N. L., Ptito, M., et al. (2020). Organization of the commissural fiber system in congenital and late-onset blindness. *Neuroimage Clin.* 25:102133. doi: 10.1016/j.nicl.2019.102133

Cecchetti, L., Ricciardi, E., Handjaras, G., Kupers, R., Ptito, M., and Pietrini, P. (2016). Congenital blindness affects diencephalic but not mesencephalic structures in the human brain. *Brain Struct. Funct.* 221, 1465–1480. doi: 10.1007/s00429-014-0984-5

Chabot, N., Butler, B. E., and Lomber, S. G. (2015). Differential modification of cortical and thalamic projections to cat primary auditory cortex following early- and late-onset deafness. *J. Comp. Neurol.* 523, 2297–2320. doi: 10.1002/cne.23790

Chang, Y., Lee, H.-R., Paik, J.-S., Lee, K.-Y., and Lee, S.-H. (2012). Voxel-wise analysis of diffusion tensor imaging for clinical outcome of cochlear implantation: retrospective study. *Clin. Exp. Otorhinolaryngol.* 5, S37–S42. doi: 10.3342/ceo.2012.5.S1.S37

Chao, T. K., Burgess, B. J., Eddington, D. K., and Nadol, J. B. (2002). Morphometric changes in the cochlear nucleus in patients who had undergone cochlear implantation for bilateral profound deafness. *Hear. Res.* 174, 196–205. doi: 10.1016/S0378-5955(02)00694-9

Chebat, D. R., Chen, J. K., Schneider, F., Ptito, A., Kupers, R., and Ptito, M. (2007a). Alterations in right posterior hippocampus in early blind individuals. *Neuroreport* 18, 329–333. doi: 10.1097/WNR.0b013e32802b70f8

Chebat, D. R., Rainville, C., Kupers, R., and Ptito, M. (2007b). Tactile-'visual' acuity of the tongue in early blind individuals. *Neuroreport* 18, 1901–1904. doi: 10.1097/WNR.0b013e3282f2a63

Chechlacz, M., Rotshtein, P., Hansen, P. C., Deb, S., Riddoch, M. J., and Humphreys, G. W. (2013). The central role of the temporo-parietal junction and the superior longitudinal fasciculus in supporting multi-item competition: evidence from lesion-symptom mapping of extinction. *Cortex* 49, 487–506. doi: 10.1016/j.cortex.2011.11.008

Cheng, Q., and Mayberry, R. I. (2019). Acquiring a first language in adolescence: the case of basic word order in American Sign Language. *J. Child Lang.* 46, 214–240. doi: 10.1017/S0305000918000417

Cheng, Q., Roth, A., Halgren, E., and Mayberry, R. I. (2019). Effects of early language deprivation on brain connectivity: language pathways in deaf native and late first-language learners of American Sign Language. *Front. Hum. Neurosci.* 13:320. doi: 10.3389/fnhum.2019.00320

Clemo, H. R., Lomber, S. G., and Meredith, M. A. (2016). Synaptic basis for cross-modal plasticity: enhanced supragranular dendritic spine density in anterior ectosylvian auditory cortex of the early deaf cat. *Cereb. Cortex* 26, 1365–1376. doi: 10.1093/cercor/bhu225

Clemo, H. R., Lomber, S. G., and Meredith, M. A. (2017). Synaptic distribution and plasticity in primary auditory cortex (A1) exhibits laminar and cell-specific changes in the deaf. *Hear. Res.* 353, 122–134. doi: 10.1016/j.heares.2017.06.009

Conner, A. K., Briggs, R. G., Sali, G., Rahimi, M., Baker, C. M., Burks, J. D., et al. (2018). A connectomic atlas of the human cerebrum-chapter 13: tractographic description of the inferior fronto-occipital fasciculus. *Oper. Neurosurg. (Hagerstown, Md.)* 15, S436–S443. doi: 10.1093/ons/opy267

Çukur, T., Huth, A. G., Nishimoto, S., and Gallant, J. L. (2013). Functional subdomains within human FFA. *J. Neurosci.* 33, 16748–16766. doi: 10.1523/JNEUROSCI.1259-13.2013

Cushing, S. L., Gordon, K. A., Rutka, J. A., James, A. L., and Papsin, B. C. (2013). Vestibular end-organ dysfunction in children with sensorineural hearing loss and cochlear implants: an expanded cohort and etiologic assessment. *Otol. Neurotol.* 34, 422–428. doi: 10.1097/MAO.0b013e31827b4ba0

da Costa, S., van der Zwaag, W., Marques, J. P., Frackowiak, R. S. J., Clarke, S., and Saenz, M. (2011). Human primary auditory cortex follows the shape of Heschl's Gyrus. *J. Neurosci.* 31, 14067–14075. doi: 10.1523/JNEUROSCI.2000-11.2011

Dettman, S., Choo, D., Au, A., Luu, A., and Dowell, R. (2021). Speech perception and language outcomes for infants receiving cochlear implants before or after 9 months of age: use of category-based aggregation of data in an unselected pediatric cohort. *J. Speech Lang. Hear. Res.* 64, 1023–1039. doi: 10.1044/2020_JSLHR-20-00228

Diamond, D., and Weinberger, N. (1984). Physiological plasticity of single neurons in auditory cortex of the cat during acquisition of the pupillary conditioned response: II. Secondary field (AII). *Behav. Neurosci.* 98, 189–210. doi: 10.1037/0735-7044.98.2.189

Dick, A., Bernal, B., and Tremblay, P. (2014). The language connectome: new pathways, new concepts. *Neuroscientist* 20, 453–467. doi: 10.1177/1073858413513502

Ding, H., Ming, D., Wan, B., Li, Q., Qin, W., and Yu, C. (2016). Enhanced spontaneous functional connectivity of the superior temporal gyrus in early deafness. *Sci. Rep.* 6:23239. doi: 10.1038/srep23239

Ding, H., Qin, W., Liang, M., Ming, D., Wan, B., Li, Q., et al. (2015). Cross-modal activation of auditory regions during visuo-spatial working memory in early deafness. *Brain* 138, 2750–2765. doi: 10.1093/brain/awv165

Eickhoff, S. B., Bzdok, D., Laird, A. R., Kurth, F., and Fox, P. T. (2012). Activation likelihood estimation meta-analysis revisited. *Neuroimage* 59, 2349–2361. doi: 10.1016/j.neuroimage.2011.09.017

Eickhoff, S. B., Laird, A. R., Grefkes, C., Wang, L. E., Zilles, K., and Fox, P. T. (2009). Coordinate-based activation likelihood estimation meta-analysis of neuroimaging data: a random-effects approach based on empirical estimates of spatial uncertainty. *Hum. Brain Mapp.* 30, 2907–2926. doi: 10.1002/hbm.20718

Eickhoff, S. B., Nichols, T. E., Laird, A. R., Hoffstaedter, F., Amunts, K., Fox, P. T., et al. (2016). Behavior, sensitivity, and power of activation likelihood estimation characterized by massive empirical simulation. *Neuroimage* 137, 70–85. doi: 10.1016/j.neuroimage.2016.04.072

Emmorey, K., Allen, J. S., Bruss, J., Schenker, N., and Damasio, H. (2003). A morphometric analysis of auditory brain regions in congenitally deaf adults. *Proc. Natl. Acad. Sci. U.S.A.* 100, 10049–10054. doi: 10.1073/pnas.1730169100

Emmorey, K., and Lee, B. (2021). The neurocognitive basis of skilled reading in prelingually and profoundly deaf adults. *Lang. Linguist. Compass* 15, e12407. doi: 10.1111/lnc3.12407

Fayad, J., Linthicum, F. Jr., Otto, S., Galey, F., and House, W. (1991). Cochlear implants: histopathologic findings related to performance in 16 human temporal bones. *Ann. Otol. Rhinol. Laryngol.* 100, 807–811. doi: 10.1177/000348949110001004

Feng, G., Ingvalson, E. M., Grieco-Calub, T. M., Roberts, M. Y., Ryan, M. E., Birmingham, P., et al. (2018). Neural preservation underlies speech improvement from auditory deprivation in young cochlear implant recipients. *Proc. Natl. Acad. Sci. U.S.A.* 115, 1022–1031. doi: 10.1073/pnas.1717603115

Fine, I., Finney, E. M., Boynton, G. M., and Dobkins, K. R. (2005). Comparing the effects of auditory deprivation and sign language within the auditory and visual cortex. *J. Cogn. Neurosci.* 17, 1621–1637. doi: 10.1162/089892905774597173

Finney, E. M., Clementz, B. A., Hickok, G., and Dobkins, K. R. (2003). Visual stimuli activate auditory cortex in deaf subjects: evidence from MEG. *Neuroreport* 14, 1425–1427. doi: 10.1097/00001756-200308060-00004

Finney, E. M., Fine, I., and Dobkins, K. R. (2001). Visual stimuli activate auditory cortex in the deaf. *Nat. Neurosci.* 4, 1171–1173. doi: 10.1038/nn763

Fortin, M., Voss, P., Lord, C., Lassonde, M., Pruessner, J., Saint-Amour, D., et al. (2008). Wayfinding in the blind: larger hippocampal volume and supranormal spatial navigation. *Brain* 131, 2995–3005. doi: 10.1093/brain/awn250

Friederici, A. D., and Gierhan, S. M. E. (2013). The language network. *Curr. Opin. Neurobiol.* 23, 250–254. doi: 10.1016/j.conb.2012.10.002

Fulcher, A., Purcell, A. A., Baker, E., and Munro, N. (2012). Listen up: children with early identified hearing loss achieve age-appropriate speech/language outcomes by 3years-of-age. *Int. J. Pediatr. Otorhinolaryngol.* 76, 1785–1794. doi: 10.1016/j.ijporl.2012.09.001

Gaylor, J. M., Raman, G., Chung, M., Lee, J., Rao, M., Lau, J., et al. (2013). Cochlear implantation in adults: a systematic review and meta-analysis. *JAMA Otolaryngol. Head Neck Surg.* 139, 265–272. doi: 10.1001/jamaoto.2013.1744

Glickstein, M. (2007). What does the cerebellum really do? *Curr. Biol.* 17, 824–827. doi: 10.1016/j.cub.2007.08.009

Griffiths, T. D., Lad, M., Kumar, S., Holmes, E., McMurray, B., Maguire, E. A., et al. (2020). How can hearing loss cause dementia? *Neuron* 108, 401–412. doi: 10.1016/j.neuron.2020.08.003

Grimaldi, G., and Manto, M. (2012). Topography of cerebellar deficits in humans. *Cerebellum* 11, 336–351. doi: 10.1007/s12311-011-0247-4

Grodd, W., Hülsmann, E., Lotze, M., Wildgruber, D., and Erb, M. (2001). Sensorimotor mapping of the human cerebellum: fMRI evidence of somatotopic organization. *Hum. Brain Mapp.* 13, 55–73. doi: 10.1002/hbm.1025

Gulban, O. F., Goebel, R., Moerel, M., Zachlod, D., Mohlberg, H., Amunts, K., et al. (2020). Improving a probabilistic cytoarchitectonic atlas of auditory cortex using a novel method for inter-individual alignment. *Elife* 9:e56963. doi: 10.7554/ELIFE.56963

Hackett, T. A., Preuss, T. M., and Kaas, J. H. (2001). Architectonic identification of the core region in auditory cortex of macaques, chimpanzees, and humans. *J. Comp. Neurol.* 441, 197–222. doi: 10.1002/cne.1407

Hall, W. C. (2017). What you don't know can hurt you: the risk of language deprivation by impairing sign language development in deaf children. *Matern. Child Health J.* 21, 961–965. doi: 10.1007/s10995-017-2287-y

Han, J. H., Lee, H. J., Kang, H., Oh, S. H., and Lee, D. S. (2019). Brain plasticity can predict the cochlear implant outcome in adult-onset deafness. *Front. Hum. Neurosci.* 13:38. doi: 10.3389/fnhum.2019.00038

Hardie, N. A., and Shepherd, R. K. (1999). Sensorineural hearing loss during development: morphological and physiological response of the cochlea and auditory brainstem. *Hear. Res.* 128, 147–165. doi: 10.1016/S0378-5955(98)00209-3

Hartling, L., Milne, A., Hamm, M. P., Vandermeer, B., Ansari, M., Tsertsvadze, A., et al. (2013). Testing the Newcastle Ottawa Scale showed low reliability between individual reviewers. *J. Clin. Epidemiol.* 66, 982–993. doi: 10.1016/j.jclinepi.2013.03.003

Hartmann, R., Shepherd, R., Heid, S., and Klinke, R. (1997). Response of the primary auditory cortex to electrical stimulation of the auditory nerve in the congenitally deaf white cat. *Hear Res.* 112, 115–133. doi: 10.1016/s0378-5955(97)00114-7

Hauthal, N., Sandmann, P., Debener, S., and Thome, J. D. (2013). Visual movement perception in deaf and hearing individuals. *Adv. Cogn. Psychol.* 9, 53–61. doi: 10.2478/V10053-008-0131-Z

Heid, S., Hartmann, R., and Klinke, R. (1998). A model for prelingual deafness, the congenitally deaf white cat – population statistics and degenerative changes. *Hear. Res.* 115, 101–112. doi: 10.1016/S0378-5955(97)00182-2

Howick, J., Chalmers, I., Glasziou, P., Greenhalgh, T., Heneghan, C., Liberati, A., et al. (2011). *The Oxford 2011 Levels of Evidence*. Oxford: Centre Evidence-Based Medicine.

Hribar, M., Šuput, D., Battelino, S., and Vovk, A. (2020). Review article: structural brain alterations in prelingually deaf. *Neuroimage* 220:117042. doi: 10.1016/j.neuroimage.2020.117042

Hribar, M., Šuput, D., Carvalho, A. A., Battelino, S., and Vovk, A. (2014). Structural alterations of brain grey and white matter in early deaf adults. *Hear. Res.* 318, 1–10. doi: 10.1016/j.heares.2014.09.008

Huang, L., Zheng, W., Wu, C., Wei, X., Wu, X., Wang, Y., et al. (2015). Diffusion tensor imaging of the auditory neural pathway for clinical outcome of cochlear implantation in pediatric congenital sensorineural hearing loss patients. *PLoS One* 10:e0140643. doi: 10.1371/journal.pone.0140643

Hultcrantz, M., Snyder, R., Rebscher, S., and Leake, P. (1991). Effects of neonatal deafening and chronic intracochlear electrical stimulation on the cochlear nucleus in cats. *Hear. Res.* 54, 272–280. doi: 10.1016/0378-5955(91)90121-O

Hunt, D. L., Yamoah, E. N., and Krubitzer, L. (2006). Multisensory plasticity in congenitally deaf mice: how are cortical areas functionally specified? *Neuroscience* 139, 1507–1524. doi: 10.1016/j.neuroscience.2006.01.023

Huttenlocher, P. R. (1984). Synapse elimination and plasticity in developing human cerebral cortex. *Am. J. Ment. Defic.* 88, 488–496.

Ivry, R., and Diener, H. (1991). Impaired velocity perception in patients with lesions of the cerebellum. *J. Cogn. Neurosci.* 3, 355–366. doi: 10.1162/jocn.1991.3.4.355

Jiang, A., Tian, J., Li, R., Liu, Y., Jiang, T., Qin, W., et al. (2015). Alterations of regional spontaneous brain activity and gray matter volume in the blind. *Neural Plast.* 2015:141950. doi: 10.1155/2015/141950

Jiang, J., Zhu, W., Shi, F., Liu, Y., Li, J., Qin, W., et al. (2009). Thick visual cortex in the early blind. *J. Neurosci.* 29, 2205–2211. doi: 10.1523/JNEUROSCI.5451-08.2009

Kaga, K., Shinjo, Y., Jin, Y., and Takegoshi, H. (2008). Vestibular failure in children with congenital deafness. *Int. J. Audiol.* 47, 590–599. doi: 10.1080/14992020802331222

Kanold, P. O., and Young, E. D. (2001). Proprioceptive information from the pinna provides somatosensory input to cat dorsal cochlear nucleus. *J. Neurosci.* 21, 7848–7858. doi: 10.1523/jneurosci.21-19-07848.2001

Kara, A., Hakan Ozturk, A., Kurtoglu, Z., Umit Talas, D., Aktekin, M., Saygili, M., et al. (2006). Morphometric comparison of the human corpus callosum in deaf and hearing subjects: an MRI study. *J. Neuroradiol.* 33, 158–163. doi: 10.1016/S0150-9861(06)77253-4

Karns, C. M., Stevens, C., Dow, M. W., Schorr, E. M., and Neville, H. J. (2017). Atypical white-matter microstructure in congenitally deaf adults: a region of interest and tractography study using diffusion-tensor imaging. *Hear. Res.* 343, 72–82. doi: 10.1016/j.heares.2016.07.008

Kassubek, J., Hickok, G., and Erhard, P. (2004). Involvement of classical anterior and posterior language areas in sign language production, as investigated by 4 T functional magnetic resonance imaging. *Neurosci. Lett.* 364, 168–172. doi: 10.1016/J.NEULET.2004.04.088

Kayser, C., Petkov, C. I., and Logothetis, N. K. (2008). Visual modulation of neurons in auditory cortex. *Cereb. Cortex* 18, 1560–1574. doi: 10.1093/cercor/bhm187

Keren, R., Helfand, M., Homer, C., McPhillips, H., and Lieu, T. (2002). Projected cost-effectiveness of statewide universal newborn hearing screening. *Pediatrics* 110, 855–865. doi: 10.1097/00004703-200304000-00023

Kim, D. J., Park, S. Y., Kim, J., Lee, D. H., and Park, H. J. (2009). Alterations of white matter diffusion anisotropy in early deafness. *Neuroreport* 20, 1032–1036. doi: 10.1097/WNR.0b013e32832e0cdd

Kim, E., Kang, H., Lee, H., Lee, H. J., Suh, M. W., Song, J. J., et al. (2014). Morphological brain network assessed using graph theory and network filtration in deaf adults. *Hear. Res.* 315, 88–98. doi: 10.1016/j.heares.2014.06.007

Kitzes, L. M., and Semple, M. N. (1985). Single-unit responses in the inferior colliculus: effects of neonatal unilateral cochlear ablation. *J. Neurophysiol.* 53, 1483–1500. doi: 10.1152/jn.1985.53.6.1483

Klinke, R., Kral, A., Heid, S., Tillein, J., Hartmann, R., Klinke, R., et al. (1999). Recruitment of the auditory cortex in congenitally deaf cats by long-term cochlear electrostimulation. *Science* 285, 1729–1733. doi: 10.1126/science.285.5434.1729

Kok, M. A., Chabot, N., and Lomber, S. G. (2014). Cross-modal reorganization of cortical afferents to dorsal auditory cortex following early- and late-onset deafness. *J. Comp. Neurol.* 522, 654–675. doi: 10.1002/cne.23439

Kozel, P. J., Friedman, R. A., Erway, L. C., Yamoah, E. N., Liu, L. H., Riddle, T., et al. (1998). Balance and hearing deficits in mice with a null mutation in the gene encoding plasma membrane Ca^{2+}-ATPase isoform 2. *J. Biol. Chem.* 273, 18693–18696. doi: 10.1074/jbc.273.30.18693

Kral, A. (2007). Unimodal and cross-modal plasticity in the "deaf" auditory cortex. *Int. J. Audiol.* 46, 479–493. doi: 10.1080/14992020701383027

Kral, A., Hartmann, R., Tillein, J., Heid, S., and Klinke, R. (2000). Congenital auditory deprivation reduces synaptic activity within the auditory cortex in a layer-specific manner. *Cereb. Cortex* 10, 714–726. doi: 10.1093/cercor/10.7.714

Kral, A., and Lomber, S. G. (2015). Deaf white cats. *Curr. Biol.* 25, R351–R353. doi: 10.1016/j.cub.2015.02.040

Kral, A., Schröder, J. H., Klinke, R., and Engel, A. K. (2003). Absence of cross-modal reorganization in the primary auditory cortex of congenitally deaf cats. *Exp. Brain Res.* 153, 605–613. doi: 10.1007/s00221-003-1609-z

Kral, A., and Sharma, A. (2012). Developmental neuroplasticity after cochlear implantation. *Trends Neurosci.* 35, 111–122. doi: 10.1016/j.tins.2011.09.004

Kramer, S., Vasil, K. J., Adunka, O. F., Pisoni, D. B., and Moberly, A. C. (2018). Cognitive functions in adult cochlear implant users, cochlear implant candidates, and normal-hearing listeners. *Laryngoscope Investig. Otolaryngol.* 3, 304–310. doi: 10.1002/lio2.172

Kronenberger, W., Beer, J., Castellanos, I., Pisoni, D., and Miyamoto, R. (2014). Neurocognitive risk in children with cochlear implants. *JAMA Otolaryngol. Head Neck Surg.* 140, 608–615. doi: 10.1001/jamaoto.2014.757

Kumar, U., and Mishra, M. (2018). Pattern of neural divergence in adults with prelingual deafness: based on structural brain analysis. *Brain Res.* 1701, 58–63. doi: 10.1016/j.brainres.2018.07.021

Kupers, R., and Ptito, M. (2014). Compensatory plasticity and cross-modal reorganization following early visual deprivation. *Neurosci. Biobehav. Rev.* 41, 36–52. doi: 10.1016/j.neubiorev.2013.08.001

Larsell, O. (1952). The morphogenesis and adult pattern of the lobules and fissures of the cerebellum of the white rat. *J. Comp. Neurol.* 97, 281–356. doi: 10.1002/cne.900970204

Lazard, D. S., and Giraud, A. L. (2017). Faster phonological processing and right occipito-temporal coupling in deaf adults signal poor cochlear implant outcome. *Nat. Commun.* 8:14872. doi: 10.1038/ncomms14872

Lazard, D. S., Lee, H. J., Truy, E., and Giraud, A. L. (2013). Bilateral reorganization of posterior temporal cortices in post-lingual deafness and its relation to cochlear implant outcome. *Hum. Brain Mapp.* 34, 1208–1219. doi: 10.1002/hbm.21504

Lazard, D. S., Vincent, C., Venail, F., van de Heyning, P., Truy, E., Sterkers, O., et al. (2012). Pre-, Per- and postoperative factors affecting performance of postlinguistically deaf adults using cochlear implants: a new conceptual model over time. *PLoS One* 7:e48739. doi: 10.1371/journal.pone.0048739

Lee, H. J., Giraud, A. L., Kang, E., Oh, S. H., Kang, H., Kim, C. S., et al. (2007). Cortical activity at rest predicts cochlear implantation outcome. *Cereb. Cortex* 17, 909–917. doi: 10.1093/cercor/bhl001

Leporé, N., Vachon, P., Lepore, F., Chou, Y. Y., Voss, P., Brun, C., et al. (2010a). 3D mapping of brain differences in native signing congenitally and prelingually deaf subjects. *Hum. Brain Mapp.* 31, 970–978. doi: 10.1002/hbm.20910

Leporé, N., Voss, P., Lepore, F., Chou, Y. Y., Fortin, M., Gougoux, F., et al. (2010b). Brain structure changes visualized in early- and late-onset blind subjects. *Neuroimage* 49, 134–140. doi: 10.1016/j.neuroimage.2009.07.048

Levänen, S., and Hamdorf, D. (2001). Feeling vibrations: enhanced tactile sensitivity in congenitally deaf humans. *Neurosci. Lett.* 301, 75–77. doi: 10.1016/S0304-3940(01)01597-X

Li, J., Li, W., Xian, J., Li, Y., Liu, Z., Liu, S., et al. (2012). Cortical thickness analysis and optimized voxel-based morphometry in children and adolescents with prelingually profound sensorineural hearing loss. *Brain Res.* 1430, 35–42. doi: 10.1016/j.brainres.2011.09.057

Li, W., Li, J., Wang, J., Zhou, P., Wang, Z., Xian, J., et al. (2016). Functional reorganizations of brain network in prelingually deaf adolescents. *Neural Plast.* 2016:9849087. doi: 10.1155/2016/9849087

Li, W., Li, J., Wang, Z., Li, Y., Liu, Z., Yan, F., et al. (2015). Grey matter connectivity within and between auditory, language and visual systems in prelingually deaf adolescents. *Restor. Neurol. Neurosci.* 33, 279–290. doi: 10.3233/RNN-140437

Li, W., Li, J., Xian, J., Lv, B., Li, M., Wang, C., et al. (2013). Alterations of grey matter asymmetries in adolescents with prelingual deafness: a combined VBM and cortical thickness analysis. *Restor. Neurol. Neurosci.* 31, 1–17. doi: 10.3233/RNN-2012-120269

Li, Y., Ding, G., Booth, J. R., Huang, R., Lv, Y., Zang, Y., et al. (2012). Sensitive period for white-matter connectivity of superior temporal cortex in deaf people. *Hum. Brain Mapp.* 33, 349–359. doi: 10.1002/hbm.21215

Lin, F. R., Yaffe, K., Xia, J., Xue, Q. L., Harris, T. B., Purchase-Helzner, E., et al. (2013). Hearing loss and cognitive decline in older adults. *JAMA Intern. Med.* 173, 293–299. doi: 10.1001/jamainternmed.2013.1868

Livingston, G., Sommerlad, A., Orgeta, V., Costafreda, S. G., Huntley, J., Ames, D., et al. (2017). Dementia prevention, intervention, and care. *Lancet* 390, 2673–2734. doi: 10.1016/S0140-6736(17)31363-6

Lomber, S. G., Butler, B. E., Glick, H., and Sharma, A. (2019). "Crossmodal neuroplasticity in deafness: evidence from animal models and clinical populations," in *Multisensory Perception: From Laboratory to Clinic*, eds K. Sathian and V. S. Ramachandran (London: Academic Press), 343–370. doi: 10.1016/B978-0-12-812492-5.00016-4

Lomber, S. G., Meredith, M. A., and Kral, A. (2010). Cross-modal plasticity in specific auditory cortices underlies visual compensations in the deaf. *Nat. Neurosci.* 13, 1421–1427. doi: 10.1038/nn.2653

Luchini, C., Stubbs, B., Solmi, M., and Veronese, N. (2017). Assessing the quality of studies in meta-analyses: advantages and limitations of the Newcastle Ottawa Scale. *World J. Meta Anal.* 5, 80–84. doi: 10.13105/wjma.v5.i4.80

Maffei, C., Soria, G., Prats-Galino, A., and Catani, M. (2015). "Imaging white-matter pathways of the auditory system with diffusion imaging tractography," in *Handbook of Clinical Neurology*, eds M. J. Aminoff, F. Boller, and D. F. Swaab (Amsterdam: Elsevier), 277–288. doi: 10.1016/B978-0-444-62630-1.00016-0

Maharani, A., Pendleton, N., and Leroi, I. (2019). Hearing impairment, loneliness, social isolation, and cognitive function: longitudinal analysis using English longitudinal study on ageing. *Am. J. Geriatr. Psychiatry* 27, 1348–1356. doi: 10.1016/j.jagp.2019.07.010

Malacarne, M. (1791). *Sulla Neuro-Encefalotomia. Lettere Anatomico-Fisiologiche di Vincenzo Malacarne e Carlo Bonnet.* Pavia: Stamperia del monastero di San Salvadore.

Manno, F. A. M., Rodríguez-Cruces, R., Kumar, R., Ratnanather, J. T., and Lau, C. (2021). Hearing loss impacts gray and white matter across the lifespan: systematic review, meta-analysis and meta-regression. *Neuroimage* 231:117826. doi: 10.1016/j.neuroimage.2021.117826

Manrique-Huarte, R., Calavia, D., Irujo, A. H., Girón, L., and Manrique-Rodríguez, M. (2016). Treatment for hearing loss among the elderly: auditory outcomes and impact on quality of life. *Audiol. Neurotol.* 21, 29–35. doi: 10.1159/000448352

Mariën, P., Ackermann, H., Adamaszek, M., Barwood, C. H. S., Beaton, A., Desmond, J., et al. (2014). Consensus paper: language and the cerebellum: an ongoing enigma. *Cerebellum* 13, 386–410. doi: 10.1007/s12311-013-0540-5

Mayberry, R. I., Lock, E., and Kazmi, H. (2002). Linguistic ability and early language exposure. *Nature* 417:38. doi: 10.1038/417038a

McCullough, S., and Emmorey, K. (1997). Face processing by deaf ASL signers: evidence for expertise in distinguishing local features. *J. Deaf Stud. Deaf Educ.* 2, 212–222. doi: 10.1093/oxfordjournals.deafed.a014327

McCullough, S., and Emmorey, K. (2021). Effects of deafness and sign language experience on the human brain: voxel-based and surface-based morphometry. *Lang. Cogn. Neurosci.* 36, 422–439. doi: 10.1080/23273798.2020.1854793

McLachlan, N. M., and Wilson, S. J. (2017). The contribution of brainstem and cerebellar pathways to auditory recognition. *Front. Psychol.* 8:265. doi: 10.3389/fpsyg.2017.00265

Mellott, J. G., Bickford, M. E., and Schofield, B. R. (2014). Descending projections from auditory cortex to excitatory and inhibitory cells in the nucleus of the brachium of the inferior colliculus. *Front. Syst. Neurosci.* 8:188. doi: 10.3389/fnsys.2014.00188

Meredith, M., Keniston, L., and Allman, B. (2012). Multisensory dysfunction accompanies crossmodal plasticity following adult hearing impairment. *Neuroscience* 214, 136–148. doi: 10.1016/j.neuroscience.2012.04.001

Meredith, M., and Lomber, S. (2011). Somatosensory and visual crossmodal plasticity in the anterior auditory field of early-deaf cats. *Hear. Res.* 280, 38–47. doi: 10.1016/j.heares.2011.02.004

Meredith, M. A., and Allman, B. L. (2012). Early hearing-impairment results in crossmodal reorganization of ferret core auditory cortex. *Neural Plast.* 2012:601591. doi: 10.1155/2012/601591

Meredith, M. A., and Allman, B. L. (2015). Single-unit analysis of somatosensory processing in core auditory cortex of hearing ferrets. *Eur. J. Neurosci.* 41, 689–698.

Meredith, M. A., Kryklywy, J., McMillan, A. J., Malhotra, S., Lum-Tai, R., and Lomber, S. G. (2011). Crossmodal reorganization in the early deaf switches sensory, but not behavioral roles of auditory cortex. *Proc. Natl. Acad. Sci. U.S.A.* 108, 8856–8861. doi: 10.1073/pnas.1018519108

Meyer, M., Liem, F., Hirsiger, S., Jäncke, L., and Hänggi, J. (2014). Cortical surface area and cortical thickness demonstrate differential structural asymmetry in auditory-related areas of the human cortex. *Cereb. Cortex* 24, 2541–2552. doi: 10.1093/cercor/bht094

Meyer, M., Toepel, U., Keller, J., Nussbaumer, D., Zysset, S., and Friederici, A. D. (2007). Neuroplasticity of sign language: implications from structural and functional brain imaging. *Restor. Neurol. Neurosci.* 25, 335–351.

Miao, W., Li, J., Tang, M., Xian, J., Li, W., Liu, Z., et al. (2013). Altered white matter integrity in adolescents with prelingual deafness: a high-resolution tract-based spatial statistics imaging study. *Am. J. Neuroradiol.* 34, 1264–1270. doi: 10.3174/ajnr.A3370

Middleton, F., and Strick, P. (1994). Anatomical evidence for cerebellar and basal ganglia involvement in higher cognitive function. *Science* 266, 458–461. doi: 10.1126/science.7939688

Moberly, A. C., Bates, C., Harris, M. S., and Pisoni, D. B. (2016). The enigma of poor performance by adults with cochlear implants. *Otol. Neurotol.* 37, 1522–1528. doi: 10.1097/MAO.0000000000001211

Moerel, M., De Martino, F., and Formisano, E. (2014). An anatomical and functional topography of human auditory cortical areas. *Front. Neurosci.* 8:225. doi: 10.3389/fnins.2014.00225

Mohr, P., Feldman, J., Dunbar, J., McConkey-Robbins, A., Niparko, J., Rittenhouse, R., et al. (2000). The societal costs of severe to profound hearing loss in the United States. *Int. J. Technol. Asses. Heal. Care* 16, 1120–1135. doi: 10.1017/s0266462300103162

Moore, D. R., and Kitzes, L. M. (1985). Projections from the cochlear nucleus to the inferior colliculus in normal and neonatally cochlea-ablated gerbils. *J. Camp. Neurol.* 240, 180–195. doi: 10.1002/cne.902400208

Neville, H. J., and Lawson, D. (1987a). Attention to central and peripheral visual space in a movement detection task: an event-related potential and behavioral study. I. Normal hearing adults. *Brain Res.* 405, 253–267. doi: 10.1016/0006-8993(87)90295-2

Neville, H. J., and Lawson, D. (1987b). Attention to central and peripheral visual space in a movement detection task: an event related potential and behavioral study. II. Congenitally deaf adults. *Brain Res.* 405, 268–283. doi: 10.1016/0006-8993(87)90296-4

Neville, H. J., Bavelier, D., Corina, D., Rauschecker, J., Karni, A., Lalwani, A., et al. (1998). Cerebral organization for language in deaf and hearing subjects: biological constraints and effects of experience. *Proc. Natl. Acad. Sci. U.S.A.* 95, 922–929. doi: 10.1073/pnas.95.3.922

Niparko, J. K., and Finger, P. A. (1997). Cochlear nucleus cell size changes in the dalmatian: model of congenital deafness. *Otolaryngol. Head Neck Surg.* 117, 229–235. doi: 10.1016/S0194-5998(97)70179-7

Noppeney, U., Friston, K. J., Ashburner, J., Frackowiak, R., and Price, C. J. (2005). Early visual deprivation induces structural plasticity in gray and white matter. *Curr. Biol.* 15, R488–R490. doi: 10.1016/j.cub.2005.06.053

Olulade, O. A., Koo, D. S., Lasasso, C. J., and Eden, G. F. (2014). Neuroanatomical profiles of deafness in the context of native language experience. *J. Neurosci.* 34, 5613–5620. doi: 10.1523/JNEUROSCI.3700-13.2014

Page, M. J., McKenzie, J. E., Bossuyt, P. M., Boutron, I., Hoffmann, T. C., Mulrow, C. D., et al. (2021). The PRISMA 2020 statement: an updated guideline for reporting systematic reviews. *BMJ* 372:n71. doi: 10.1136/BMJ.N71

Pan, W. J., Wu, G., Li, C. X., Lin, F., Sun, J., and Lei, H. (2007). Progressive atrophy in the optic pathway and visual cortex of early blind Chinese adults: a voxel-based morphometry magnetic resonance imaging study. *Neuroimage* 37, 212–220. doi: 10.1016/j.neuroimage.2007.05.014

Park, H. J., Lee, J. D., Kim, E. Y., Park, B., Oh, M. K., Lee, S. C., et al. (2009). Morphological alterations in the congenital blind based on the analysis of cortical thickness and surface area. *Neuroimage* 47, 98–106. doi: 10.1016/j.neuroimage.2009.03.076

Penhune, V. B., Cismaru, R., Dorsaint-Pierre, R., Petitto, L. A., and Zatorre, R. J. (2003). The morphometry of auditory cortex in the congenitally deaf measured using MRI. *Neuroimage* 20, 1215–1225. doi: 10.1016/S1053-8119(03)00373-2

Pénicaud, S., Klein, D., Zatorre, R. J., Chen, J. K., Witcher, P., Hyde, K., et al. (2013). Structural brain changes linked to delayed first language acquisition in congenitally deaf individuals. *Neuroimage* 66, 42–49. doi: 10.1016/j.neuroimage.2012.09.076

Pereira-Jorge, M. R., Andrade, K. C., Palhano-Fontes, F. X., Diniz, P. R. B., Sturzbecher, M., Santos, A. C., et al. (2018). Anatomical and functional MRI changes after one year of auditory rehabilitation with hearing aids. *Neural Plast.* 2018:9303674. doi: 10.1155/2018/9303674

Petitto, L. A., Zatorre, R. J., Gauna, K., Nikelski, E. J., Dostie, D., and Evans, A. C. (2000). Speech-like cerebral activity in profoundly deaf people processing signed languages: implications for the neural basis of human language. *Proc. Natl. Acad. Sci. U.S.A.* 97, 13961–13966. doi: 10.1073/pnas.97.25.13961

Ponton, C. W., Don, M., Eggermont, J. J., Waring, M. D., and Masuda, A. (1996). Maturation of human cortical auditory function: differences between normal-hearing children and children with cochlear implants. *Ear Hear.* 17, 430–437. doi: 10.1097/00003446-199610000-00009

Ptito, M., Paré, S., Dricot, L., Cavaliere, C., Tomaiuolo, F., and Kupers, R. (2021). A quantitative analysis of the retinofugal projections in congenital and late-onset blindness. *Neuroimage Clin.* 32:102809. doi: 10.1016/j.nicl.2021.102809

Ptito, M., Schneider, F. C. G., Paulson, O. B., and Kupers, R. (2008). Alterations of the visual pathways in congenital blindness. *Exp. Brain Res.* 187, 41–49. doi: 10.1007/s00221-008-1273-4

Qi, R., Su, L., Zou, L., Yang, J., and Zheng, S. (2019). Altered gray matter volume and white matter integrity in sensorineural hearing loss patients: a VBM and TBSS study. *Otol. Neurotol.* 40, e569–e574. doi: 10.1097/MAO.0000000000002273

Qin, W., Liu, Y., Jiang, T., and Yu, C. (2013). The development of visual areas depends differently on visual experience. *PLoS One* 8:e53784. doi: 10.1371/journal.pone.0053784

Quittner, A., Leibach, P., and Marciel, K. (2004). The impact of cochlear implants on young deaf children: new methods to assess cognitive and behavioral development. *Arch. Otolaryngol. Head Neck Surg* 130, 547–554. doi: 10.1001/archotol.130.5.547

Ratnanather, J. T. (2020). Structural neuroimaging of the altered brain stemming from pediatric and adolescent hearing loss—scientific and clinical challenges. *Wiley Rev. Syst. Biol. Med.* 12:e1469.

Rauschecker, J. P., and Korte, M. (1993). Auditory compensation for early blindness in cat cerebral cortex. *J. Neurosci.* 13, 4538–4548. doi: 10.1523/jneurosci.13-10-04538.1993

Rebillard, G., and Pujol, R. (1977). Enhancement of visual responses on the primary auditory cortex of the cat after an early destruction of cochlear receptors. *Brain Res.* 129, 162–164. doi: 10.1016/0006-8993(77)90980-5

Reil, J. (1808). Fragmente über die bildung des kleinen gehirns im menschen. *Arch. Physiol.* 8, 1–58.

Renier, L., De Volder, A. G., and Rauschecker, J. P. (2014). Cortical plasticity and preserved function in early blindness. *Neurosci. Biobehav. Rev.* 41, 53–63. doi: 10.1016/j.neubiorev.2013.01.025

Ro, T., Ellmore, T. M., and Beauchamp, M. S. (2013). A neural link between feeling and hearing. *Cereb. Cortex* 23, 1724–1730. doi: 10.1093/cercor/bhs166

Rombaux, P., Huart, C., De Volder, A. G., Cuevas, I., Renier, L., Duprez, T., et al. (2010). Increased olfactory bulb volume and olfactory function in early blind subjects. *Neuroreport* 21, 1069–1073. doi: 10.1097/WNR.0b013e32833fcb8a

Sakai, K. L., Tatsuno, Y., Suzuki, K., Kimura, H., and Ichida, Y. (2005). Sign and speech: amodal commonality in left hemisphere dominance for comprehension of sentences. *Brain* 128, 1407–1417. doi: 10.1093/brain/awh465

Schofield, B. R. (2009). Projections to the inferior colliculus from layer VI cells of auditory cortex. *Neuroscience* 159, 246–258. doi: 10.1016/j.neuroscience.2008.11.013

Schürmann, M., Caetano, G., Hlushchuk, Y., Jousmäki, V., and Hari, R. (2006). Touch activates human auditory cortex. *Neuroimage* 30, 1325–1331. doi: 10.1016/j.neuroimage.2005.11.020

Sens, P. M., and De Almeida, C. I. R. (2007). Participation of the cerebellum in auditory processing. *Braz. J. Otorhinolaryngol.* 73, 266–270. doi: 10.1016/s1808-8694(15)31076-4

Sharma, A., and Glick, H. (2016). Cross-modal re-organization in clinical populations with hearing loss. *Brain Sci.* 6, 4. doi: 10.3390/brainsci6010004

Shi, B., Yang, L. Z., Liu, Y., Zhao, S. L., Wang, Y., Gu, F., et al. (2016). Early-onset hearing loss reorganizes the visual and auditory network in children without cochlear implantation. *Neuroreport* 27, 197–202. doi: 10.1097/WNR.0000000000000524

Shibata, D. K. (2007). Differences in brain structure in deaf persons on MR imaging studied with voxel-based morphometry. *Am. J. Neuroradiol.* 28, 243–249.

Shield, B. (2006). *Evaluation of the Social and Economic Costs of Hearing Impairment: A Report for Hear-it*. London: London South Bank University.

Shimony, J. S., Burton, H., Epstein, A. A., McLaren, D. G., Sun, S. W., and Snyder, A. Z. (2006). Diffusion tensor imaging reveals white matter reorganization in early blind humans. *Cereb. Cortex* 16, 1653–1661. doi: 10.1093/cercor/bhj102

Shiohama, T., McDavid, J., Levman, J., and Takahashi, E. (2019). The left lateral occipital cortex exhibits decreased thickness in children with sensorineural hearing loss. *Int. J. Dev. Neurosci.* 76, 34–40. doi: 10.1016/j.ijdevneu.2019.05.009

Shore, S. E., Koehler, S., Oldakowski, M., Hughes, L., and Syed, S. (2008). Dorsal cochlear nucleus responses to somatosensory stimulation are enhanced after noise-induced hearing loss. *Eur. J. Neurosci.* 27, 155–168. doi: 10.1111/j.1460-9568.2007.05983.x

Shore, S. E., Vass, Z., Wys, N. L., and Altschuler, R. A. (2000). Trigeminal ganglion innervates the auditory brainstem. *J. Comp. Neurol.* 419, 271–285. doi: 10.1002/(SICI)1096-9861(20000410)419:3<271::AID-CNE1>3.0.CO;2-M

Shore, S. E., and Zhou, J. (2006). Somatosensory influence on the cochlear nucleus and beyond. *Hear. Res.* 216–217, 90–99. doi: 10.1016/j.heares.2006.01.006

Simon, M., Campbell, E., Genest, F., MacLean, M., Champoux, F., and Lepore, F. (2020). The impact of early deafness on brain plasticity: a systematic review of the white and gray matter changes. *Front. Neurosci.* 14:206. doi: 10.3389/fnins.2020.00206

Skotara, N., Salden, U., Kügow, M., Hänel-Faulhaber, B., and Röder, B. (2012). The influence of language deprivation in early childhood on L2 processing: an ERP comparison of deaf native signers and deaf signers with a delayed language acquisition. *BMC Neurosci.* 13:44. doi: 10.1186/1471-2202-13-44

Smiley, J. F., and Falchier, A. (2009). Multisensory connections of monkey auditory cerebral cortex. *Hear. Res.* 258, 37–46. doi: 10.1016/j.heares.2009.06.019

Smith, K. M., Mecoli, M. D., Altaye, M., Komlos, M., Maitra, R., Eaton, K. P., et al. (2011). Morphometric differences in the Heschl's gyrus of hearing impaired and normal hearing infants. *Cereb. Cortex* 21, 991–998. doi: 10.1093/cercor/bhq164

Smittenaar, C. R., MacSweeney, M., Sereno, M. I., and Schwarzkopf, D. S. (2016). Does congenital deafness affect the structural and functional architecture of primary visual cortex? *Open Neuroimag. J.* 10, 1–19. doi: 10.2174/1874440001610010001

Stakhovskaya, O., Hradek, G. T., Snyder, R. L., and Leake, P. A. (2008). Effects of age at onset of deafness and electrical stimulation on the developing cochlear nucleus in cats. *Hear. Res.* 243, 69–77. doi: 10.1016/j.heares.2008.05.007

Stanton, S. G., and Harrison, R. V. (2000). Projections from the medial geniculate body to primary auditory cortex in neonatally deafened cats. *J. Comp. Neurol.* 426, 117–129. doi: 10.1002/1096-9861(20001009)426:1<117::aid-cne8>3.0.co;2-s

Stoodley, C. J., and Schmahmann, J. D. (2009). Functional topography in the human cerebellum: a meta-analysis of neuroimaging studies. *Neuroimage* 44, 489–501. doi: 10.1016/j.neuroimage.2008.08.039

Sun, Z., Seo, J. W., Park, H. J., Lee, J. Y., Kwak, M. Y., Kim, Y., et al. (2021). Cortical reorganization following auditory deprivation predicts cochlear implant performance in postlingually deaf adults. *Hum. Brain Mapp.* 42, 233–244. doi: 10.1002/hbm.25219

Tan, L., Holland, S. K., Deshpande, A. K., Chen, Y., Choo, D. I., and Lu, L. J. (2015). A semi-supervised support vector machine model for predicting the language outcomes following cochlear implantation based on pre-implant brain fMRI imaging. *Brain Behav.* 5:e00391. doi: 10.1002/brb3.391

Tarabichi, O., Kozin, E. D., Kanumuri, V. V., Barber, S., Ghosh, S., Sitek, K., et al. (2018). Diffusion tensor imaging of central auditory pathways in patients with sensorineural hearing loss: a systematic review. *Syst. Rev.* 158, 432–442. doi: 10.1177/0194599817739838

Tierney, T., Russell, F., and Moore, D. (1997). Susceptibility of developing cochlear nucleus neurons to deafferentation-induced death abruptly ends just before the onset of hearing. *J. Comp. Neurol.* 378, 295–306. doi: 10.1002/(SICI)1096-9861(19970210)378:2<295::AID-CNE11>3.0.CO;2-R

Tomaiuolo, F., Campana, S., Collins, D. L., Fonov, V. S., Ricciardi, E., Sartori, G., et al. (2014). Morphometric changes of the corpus callosum in congenital blindness. *PLoS One* 9:e107871. doi: 10.1371/journal.pone.0107871

Touj, S., Gallino, D., Chakravarty, M. M., Bronchti, G., and Piché, M. (2021). Structural brain plasticity induced by early blindness. *Eur. J. Neurosci.* 53, 778–795. doi: 10.1111/ejn.15028

Turkeltaub, P. E., Eden, G. F., Jones, K. M., and Zeffiro, T. A. (2002). Meta-analysis of the functional neuroanatomy of single-word reading: method and validation. *Neuroimage* 16, 765–780. doi: 10.1006/nimg.2002.1131

Voss, P., Pike, B. G., and Zatorre, R. J. (2014). Evidence for both compensatory plastic and disuse atrophy-related neuroanatomical changes in the blind. *Brain* 137, 1224–1240. doi: 10.1093/brain/awu030

Voss, P., and Zatorre, R. J. (2012). Occipital cortical thickness predicts performance on pitch and musical tasks in blind individuals. *Cereb. Cortex* 22, 2455–2465. doi: 10.1093/cercor/bhr311

Wandell, B. A., Dumoulin, S. O., and Brewer, A. A. (2007). Visual field maps in human cortex. *Neuron* 56, 366–383. doi: 10.1016/j.neuron.2007.10.012

Wang, H., Liang, Y., Fan, W., Zhou, X., Huang, M., Shi, G., et al. (2019). DTI study on rehabilitation of the congenital deafness auditory pathway and speech center by cochlear implantation. *Eur. Arch. Oto Rhino Laryngol.* 276, 2411–2417. doi: 10.1007/s00405-019-05477-7

Wang, Y., Metoki, A., Smith, D. V., Medaglia, J. D., Zang, Y., Benear, S., et al. (2020). Multimodal mapping of the face connectome. *Nat. Hum. Behav.* 4, 397–411. doi: 10.1038/s41562-019-0811-3

Weiner, K. S., and Zilles, K. (2016). The anatomical and functional specialization of the fusiform gyrus. *Neuropsychologia* 83, 48–62. doi: 10.1016/j.physbeh.2017.03.040

Wells, G., Shea, B., O'Connell, D., and Peterson, J. (2000). *The Newcastle-Ottawa Scale (NOS) for Assessing the Quality of Nonrandomised Studies in Meta-Analyses*. Ottawa, ON: Ottawa Hospital Research Institute.

Wong, C., Chabot, N., Kok, M. A., and Lomber, S. G. (2014). Modified areal cartography in auditory cortex following early- and late-onset deafness. *Cereb. Cortex* 24, 1778–1792. doi: 10.1093/cercor/bht026

Wong, C., Chabot, N., Kok, M. A., and Lomber, S. G. (2015). Amplified somatosensory and visual cortical projections to a core auditory area, the anterior auditory field, following early- and late-onset deafness. *J. Comp. Neurol.* 523, 1925–1947. doi: 10.1002/cne.23771

World Health Organization (2021). *World Report on Hearing*. Geneva: World Health Organization.

Wu, C., Huang, L., Tan, H., Wang, Y., Zheng, H., Kong, L., et al. (2016). Diffusion tensor imaging and MR spectroscopy of microstructural alterations and metabolite concentration changes in the auditory neural pathway of pediatric congenital sensorineural hearing loss patients. *Brain Res.* 1639, 228–234. doi: 10.1016/j.brainres.2014.12.025

Wu, C., Stefanescu, R. A., Martel, D. T., and Shore, S. E. (2015). Listening to another sense: somatosensory integration in the auditory system. *Cell Tissue Res.* 361, 233–250. doi: 10.1007/s00441-014-2074-7

Wu, C. M., Ng, S. H., Wang, J. J., and Liu, T. C. (2009). Diffusion tensor imaging of the subcortical auditory tract in subjects with congenital cochlear nerve deficiency. *Am. J. Neuroradiol.* 30, 1773–1777. doi: 10.3174/ajnr.A1681

Yaka, R., Yinon, U., and Wollberg, Z. (1999). Auditory activation of cortical visual areas in cats after early visual deprivation. *Eur. J. Neurosci.* 11, 1301–1312. doi: 10.1046/j.1460-9568.1999.00536.x

Yusuf, P. A., Hubka, P., Tillein, J., Vinck, M., and Kral, A. (2021). Deafness weakens interareal couplings in the auditory cortex. *Front. Neurosci.* 14:625721. doi: 10.3389/fnins.2020.625721

Zheng, W., Wu, C., Huang, L., and Wu, R. (2017). Diffusion kurtosis imaging of microstructural alterations in the brains of paediatric patients with congenital sensorineural hearing loss. *Sci. Rep.* 7:1543. doi: 10.1038/s41598-017-01263-9

Znamenskiy, P., and Zador, A. M. (2013). Corticostriatal neurons in auditory cortex drive decisions during auditory discrimination. *Nature* 497, 482–485. doi: 10.1038/nature12077

Zwolan, T., Kileny, P. R., Smith, S., Mills, D., Koch, D., and Osberger, M. J. (2001). Adult cochlear implant patient performance with evolving electrode technology. *Otol. Neurotol.* 22, 844–849. doi: 10.1097/00129492-200111000-00022

Conflict of Interest: The authors declare that the research was conducted in the absence of any commercial or financial relationships that could be construed as a potential conflict of interest.

frontiers | Frontiers in Neuroscience

TYPE Original Research
PUBLISHED 23 September 2022
DOI 10.3389/fnins.2022.902866

OPEN ACCESS

EDITED BY
Maurice Ptito,
Université de Montréal, Canada

REVIEWED BY
Claudia Lunghi,
UMR 8248 Laboratoire des Systèmes Perceptifs, France
Mikhail Lipin,
University of Pennsylvania, United States

*CORRESPONDENCE
Negin Nadvar
nadvarn@gmail.com
James Weiland
weiland@umich.edu

SPECIALTY SECTION
This article was submitted to Perception Science, a section of the journal Frontiers in Neuroscience

RECEIVED 23 March 2022
ACCEPTED 29 August 2022
PUBLISHED 23 September 2022

CITATION
Nadvar N, Stiles N, Choupan J, Patel V, Ameri H, Shi Y, Liu Z, Jonides J and Weiland J (2022) Sight restoration reverses blindness-induced cross-modal functional connectivity changes between the visual and somatosensory cortex at rest. *Front. Neurosci.* 16:902866. doi: 10.3389/fnins.2022.902866

Sight restoration reverses blindness-induced cross-modal functional connectivity changes between the visual and somatosensory cortex at rest

Negin Nadvar[1]*, Noelle Stiles[2], Jeiran Choupan[2], Vivek Patel[3], Hossein Ameri[2], Yonggang Shi[2], Zhongming Liu[1,4], John Jonides[5] and James Weiland[1,6]*

[1]Department of Biomedical Engineering, University of Michigan, Ann Arbor, MI, United States, [2]Laboratory of Neuro Imaging, USC Mark and Mary Stevens Neuroimaging and Informatics Institute, Keck School of Medicine of USC, University of Southern California, Los Angeles, CA, United States, [3]Irvine School of Medicine, The University of California, Irvine, Irvine, CA, United States, [4]Department of Electrical Engineering and Computer Science, University of Michigan, Ann Arbor, MI, United States, [5]Department of Psychology, University of Michigan, Ann Arbor, MI, United States, [6]Department of Ophthalmology and Visual Sciences, University of Michigan, Ann Arbor, MI, United States

Resting-state functional connectivity (rsFC) has been used to assess the effect of vision loss on brain plasticity. With the emergence of vision restoration therapies, rsFC analysis provides a means to assess the functional changes following sight restoration. Our study demonstrates a partial reversal of blindness-induced rsFC changes in Argus II retinal prosthesis patients compared to those with severe retinitis pigmentosa (RP). For 10 healthy control (HC), 10 RP, and 7 Argus II subjects, four runs of resting-state functional magnetic resonance imaging (fMRI) per subject were included in our study. rsFC maps were created with the primary visual cortex (V1) as the seed. The rsFC group contrast maps for RP > HC, Argus II > RP, and Argus II > HC revealed regions in the post-central gyrus (PostCG) with significant reduction, significant enhancement, and no significant changes in rsFC to V1 for the three contrasts, respectively. These findings were also confirmed by the respective V1-PostCG ROI-ROI analyses between test groups. Finally, the extent of significant rsFC to V1 in the PostCG region was 5,961 in HC, 0 in RP, and 842 mm^3 in Argus II groups. Our results showed a reduction of visual-somatosensory rsFC following blindness, consistent with previous findings. This connectivity was enhanced following sight recovery with Argus II, representing a reversal of changes in cross-modal functional plasticity as manifested during rest, despite the rudimentary vision obtained by Argus II patients. Future investigation with a larger number of test subjects into this rare condition can further unveil the profound ability of our brain to reorganize in response to vision restoration.

KEYWORDS

resting-state functional connectivity, blindness, sight restoration, cross-modal plasticity, retinal prosthesis, fMRI

Introduction

Visual impairment has a negative effect on the quality of life of those afflicted by limiting their day-to-day activities, including environmental engagement and social opportunities. Vision rehabilitation teaches skills that help them play a more active and satisfying role in society (Bourne et al., 2012; Khorrami-Nejad et al., 2016; National Academies of Sciences Engineering and Medicine et al., 2016); however, rehabilitation does not improve vision itself. Sight restoration approaches have reached clinical trials and, in some cases, regulatory approval. Gene therapy (Bennett et al., 2016; Ashtari et al., 2017; Apte, 2018; Lee et al., 2019; Wang et al., 2020), optogenetic (McClements et al., 2020; Simon et al., 2020), and retinal prostheses (Zrenner et al., 2011; Fernandes et al., 2012; Stingl et al., 2013; Zrenner, 2013; Cheng et al., 2017; BLoch et al., 2019) have all been tested in patients with retinal disease. The degree of vision restoration provides patients with improved mobility and object detection. However, in most cases, recipients of these new therapies still have a significant visual impairment despite the regained function. While behavioral experiments that assess functional vision in real-world scenarios are the most important endpoints, measures of the cortical response to vision restoration can provide complementary information that explains clinical outcomes and guides future development of improvements in these therapies.

A need for biomarkers that help gauge patients' improvement during post-sight restoration rehabilitation becomes consequential. The functional magnetic resonance imaging (fMRI) blood-oxygen-level dependent (BOLD) activation response has been utilized for assessing brain plasticity following sight restoration. One study showed that prolonged use of the Argus II implant increased the fMRI BOLD response to visual stimuli in the primary visual cortex (Castaldi et al., 2016). Another neuroimaging experiment performed on retinal gene therapy patients demonstrated significantly enhanced fMRI activation in the visual cortex in response to visual checkerboard stimulation (Ashtari et al., 2017) compared to the same measurement made in the same individuals before therapy.

Resting-state functional connectivity (rsFC) has been used to gauge the plastic changes in the brain following sensory deprivation. This approach has been extensively studied with different analysis methods (Biswal et al., 1995; Bullmore and Sporns, 2009; Li et al., 2009; van den Heuvel and Hulshoff Pol, 2010; Van Dijk et al., 2010; Peltier and Shah, 2011; Barkhof et al., 2014; Iraji et al., 2016; Lv et al., 2018; Seitzman et al., 2019). The rsFC analysis reveals the relationship between spontaneous brain activity in different parts of the brain in the absence of any cognitive or sensory stimulation. Numerous rsFC studies have examined alterations in functional connectivity between the visual cortex and other brain sensory or cognitive areas following vision loss. This literature robustly shows that following visual sensory deprivation in congenital, early, and late blindness, rsFC decreases both within the visual cortical areas (Liu et al., 2008; Dai et al., 2013; Qin et al., 2014; Heine et al., 2015; Murphy et al., 2016; Hou et al., 2017; Huang et al., 2019; Hu et al., 2020) and between the visual cortex and other sensory (somatosensory or auditory) cortices (Wittenberg et al., 2004; Liu et al., 2008; Yu et al., 2008; Dai et al., 2013; Striem-Amit et al., 2015; Murphy et al., 2016; Bauer et al., 2017; Wen et al., 2018; Huang et al., 2019). In contrast, the rsFC between the visual cortex and cognitive regions of the brain has been shown to have enhanced the following vision loss (Heine et al., 2015; Striem-Amit et al., 2015; Murphy et al., 2016; Sabbah et al., 2016, 2017; Bauer et al., 2017; Wen et al., 2018; Hu et al., 2020); a phenomenon that has been attributed to increased top-down influence in the visual cortex due to visual deprivation.

In contrast to the abundant literature supporting the functional plastic changes in the brain following blindness, few studies have examined alterations in functional connectivity after sight restoration. A single analysis study on the effect of sight recovery 3 years after gene therapy application showed that rsFC between the visual and auditory areas was enhanced after sight restoration, partially reversing the effect of blindness (Mowad et al., 2020) and supporting the feasibility of using rsFC as a biomarker of vision restoration. To further investigate the relationship between rsFC and vision restoration, we studied functional connectivity in a cohort of patients with retinitis pigmentosa (RP) who were implanted with the Argus II retinal prosthesis to determine if this treatment, which partially restores vision, also reverses, in full or in part, the plastic changes induced by the vision loss.

Materials and methods

Human subjects

A total of 27 subjects were included in the analysis and divided into three groups: 10 healthy controls (HC-5 women, age 54.50 ± 13.84), 10 RP blind (RP-3 women, age 51.10 ± 12.92), and 7 Argus II subjects (3 women, age 64 ± 9.71)—the difference in age among the groups was insignificant (F2, 24) = 2.40, p = 0.11). Details of subjects' demographic and clinical information are included in **Supplementary Tables 1, 2**. The RP subjects were all blind with visual acuity of worse than 20/200 and a visual field of less than 20°, except for subject 13, which had a visual acuity of 20/80-2 and 20/50 + 2 and a visual field of 2° or less in both eyes. The Argus II subjects were legally blind from RP. Their baseline vision was bare light or no light perception, per the FDA-approved indication for Argus II. Out of the 27 subjects, 20 were recruited and consented to at 2 Human Connectome for Low Vision (HCLV) data collection centers per the approved Institutional Review Board at each center: the

University of Michigan (UM) and the University of Southern California (USC); this included 3 HC, 10 RP, and 5 Argus II subjects at USC and 2 Argus II subjects at UM. The remaining 7 HC subjects' data was sourced from the Human Connectome Project for Aging (HCP-A) public database (Bookheimer et al., 2019). One additional Argus II subject's neuroimaging data were collected at USC. However, the subject was determined to be a significant outlier and was removed from the analysis. For more details, please see the Subject Outlier Identification section in **Supplementary Material**. Resting-state functional runs showing the subject motion of more than 1 mm in any of the x, y, or z directions were excluded from the analysis. Moreover, the resting-state runs were included in the analysis only if they were acquired at the beginning of the sessions before any other task performance. These criteria excluded 22 out of 112 runs from the analysis among all the subjects in all the sessions.

Argus II retinal prosthesis

The Argus II retinal prosthesis is an epiretinal implant that was the first retinal prosthesis with FDA approval obtained in 2013 and CE approval in 2011. The system comprises an internal implant unit and an externally worn unit. The internal system contains an intraocular array with an area of 3.5 by 6 mm, covering an area of 11 × 19 degrees of the visual field. The array is a 6 × 10 grid of platinum surface electrodes that are 200 μm in diameter and spaced 575 μm apart. The electronic supporting case is sutured to the sclera and inductively receives power/data from the external system. The external unit contains a video camera mounted on a pair of glasses worn by the patient, a video processing unit (VPU), and a battery. The camera transmits the visual data to the VPU, where data are processed, sent to the external coil, and relayed to the internal circuitry. RP patients using Argus II could perceive motion (Dorn et al., 2013) and showed the best visual acuity of 20/1,260 (Humayun et al., 2012).

Experimental paradigm

The UM, USC, and HCP-A data neuroimaging experiments followed the same paradigm. Each scan visit was composed of two scanning sessions separated by a break. The MRI scans comprised structural and resting-state fMRI (rsfMRI) scans. During the rsfMRI runs, subjects were asked not to engage in any tasks while lying in the scanner. Upon completing the T1W scan, the technicians reviewed the quality of the structural images captured during the first scan session. A re-scan was performed during the second scanning session if the scan quality was deemed low from the first session. The participants completed a total of four runs of rsfMRI with their eyes open under a dark foam mask at UM and USC. This was performed due to the inability of blind subjects to fixate. For HCP-A rsfMRI runs, healthy controls were asked to fixate while lying in the scanner.

Data acquisition

Each subject acquired one anatomical and four resting-state functional runs (2 runs per scan session). Structural MRI scans at USC were acquired using a 3T Siemens Prisma scanner. The T1W structural scans used MPRAGE (Magnetization Prepared Rapid Gradient Echo) 3D acquisition, voxel dimension 0.8 × 0.8 × 0.8 mm^3, TI (inversion time)/TE (echo time)/FA (flip angle) = 1,000 ms/2.22 ms/8°. The resting-state functional runs were obtained with 2D gradient-echo (GRE) echo-planar imaging (EPI) acquisition with multiband (MB) acceleration factor = 8, voxel size of 2 × 2 × 2 mm^3 with TR (repetition time)/TE/FA = 800 ms/37 ms/52° with a total of 420 volumes for each run. At UM, T1W images were obtained with a 3T GE MR750 scanner with 3D spoiled gradient echo (SPGR) with inversion recovery magnetization preparation, voxel size of 0.5 × 0.5 × 0.8 mm^3, TI/TE/FA = 1,060 ms/Min Full/8° ("Min Full" refers to the minimum TE to obtain full echo acquisition). Functional runs were acquired with interleaved GRE-EPI, MB = 6, voxel size 2.4 × 2.4 × 2.4 mm^3 and TR/TE/FA = 800 ms/30 ms/52°. Field maps were acquired and used to correct the geometric distortion in EPI due to magnetic field inhomogeneities. Scan parameters for HCP-A structural and functional data were identical to USC parameters (Harms et al., 2018). Harmonization of the data between the HCLV collection centers at USC and UM was investigated using the data from a traveling subject and a Function Biomedical Informatics Research Network (fBIRN) phantom as a part of a previous study (Nadvar et al., 2019). Refer to **Supplementary Material** for a summary of the results of this analysis.

Data preprocessing

The field inhomogeneity inside the scanner (field map) was calculated with the FSL Topup function and an in-house Linux bash and MATLAB script. Using the Realign and Unwarp functions in combination with the field map toolbox in SPM, the susceptibility distortion, motion artifact, and susceptibility-by-movement interaction were corrected. The first 12 volumes were removed to ensure reaching a steady state (and additionally, the last 46 volumes were removed for HCP-A data due to a different length), yielding 420 volumes for each functional run. The reference volume for motion and field map correction was the 10th for UM data and the single-band reference volume (SBRef) for USC and HCP-A data. Motion correction parameters were created and used as regression covariates. The origin of the structural and functional

images was manually set at the anterior commissure to enhance the outcome of the co-registration and normalization to the standard template. Potential outlier volumes were flagged using the MATLAB CONN toolbox (Whitfield-Gabrieli and Nieto-Castanon, 2012) with the global BOLD signal above 5 standard deviations or frame-wise displacement of more than 0.9 mm, creating the scrubbing regression covariate. Using indirect segmentation and normalization in CONN, the functional and anatomical images were first co-registered using an affine transformation. The structural image was then normalized to standard MNI space and segmented into gray matter (GM), white matter (WM), and cerebrospinal fluid (CSF). This process continued iteratively until convergence, yielding non-linear spatial transformation parameters that were then applied to both anatomical and functional images; these images were resampled to isotropic 1 mm and 2 mm voxels, respectively. Functional images were spatially smoothed with a Gaussian kernel with a 4 mm full-width-at-half-maximum (FWHM). The anatomical component-based noise correction (aCompCor) was also implemented using CONN to minimize physiological noise further; the first five principal components of the BOLD in WM and CSF were extracted to be used as confounding effects. All the confounding factors, including the six translation/rotation motion parameters and their derivatives, scrubbing covariates, and WM/CSF covariates, were linearly regressed out of the BOLD signal. Finally, the time series were bandpass filtered between 0.008 and 0.0 Hz and linearly detrended.

Statistical analysis

Seed-based connectivity (SBC) maps were calculated using CONN; bivariate Pearson's correlation coefficients between the average BOLD signal in primary visual cortex (V1) Region of Interest (ROI) and the BOLD time series in the rest of the brain were first computed and Fisher z-transformed. Group-level SBC maps were created by applying a one-sample t-test to Fisher's z values associated with each voxel across subjects. A two-sample t-test was used for contrast analysis between the groups. The second-level analysis results were corrected for multiple comparisons using cluster-level inference to control for false positives. Parametric statistics were applied using Gaussian Random Field theory (Worsley, 1996) with an uncorrected voxel threshold of $p < 0.001$ and a cluster-level threshold of $p < 0.05$ for cluster size false discovery rate (FDR) correction. The ROI-ROI functional connectivity between V1 and post-central gyrus (PostCG) was also calculated as Fisher-transformed correlation coefficients between these 2 ROIs in BOLD time series, representing the effect size. Additionally, we looked at the spread of significant FC in a target ROI. This was defined as the cortical volume (in mm^3) with a statistically significant connection to the seed in group-level FC maps corrected at the cluster level. Considerations of data normality, effect size, and power are further investigated as a part of section 5 in **Supplementary Material**.

ROI selection

The 2020 Julich-Brain atlas (V2.9), an intricate volumetric atlas based on the cytoarchitecture of the brain (Amunts et al., 2020), was used to define ROIs. Given our *a priori* hypothesis regarding the primary visual and somatosensory cortex, we extracted these 2 ROIs from the atlas: the V1 was formed by combining the respective left and right ROIs from the atlas. PostCG, the location of the primary somatosensory cortex, was defined by merging the areas 1, 2, 3a, and 3b on the left and right sides as defined by the atlas.

Results

How does retinitis pigmentosa blindness affect functional connectivity to V1 at rest?

In order to evaluate the impact of blindness on functional connectivity with the primary visual cortex, we obtained the SBC maps for HC and RP groups as well as the between-group contrast as indicated in **Figures 1A–C**), each corrected for multiple comparisons using Gaussian Random Field Theory with an uncorrected voxel-level threshold of $p < 0.001$ and a cluster-level threshold of $p < 0.05$ FDR corrected for cluster size. In both the HC and RP groups, V1 showed strong functional connectivity to different parts of the occipital cortex, primary and secondary somatosensory cortex, and inferior temporal areas. Blue color-coded regions in **Figure 1C** highlight areas in the RP group with significantly lower functional connectivity to V1 than HC. In the indicated seed-to-voxel functional connectivity map in **Figure 1C**, these areas overlap with parts of higher-level visual areas such as the cuneus and lateral occipital cortex, as well as regions in primary and secondary somatosensory areas, motor cortex, and some parietal association areas. In the ROI-to-ROI analysis (**Figure 1D**) between V1 and PostCG, the effect size (Fisher z-transformed correlation coefficient value) was significantly lower in RP compared with HC [$t\,(18) = -5.39$, $p = 4 \times 10^{-5}$].

How does partial sight restoration with Argus II alter functional connectivity to V1 at rest?

We evaluated how partial sight restoration with Argus II can alter intrinsic brain connectivity in RP blindness. SBC

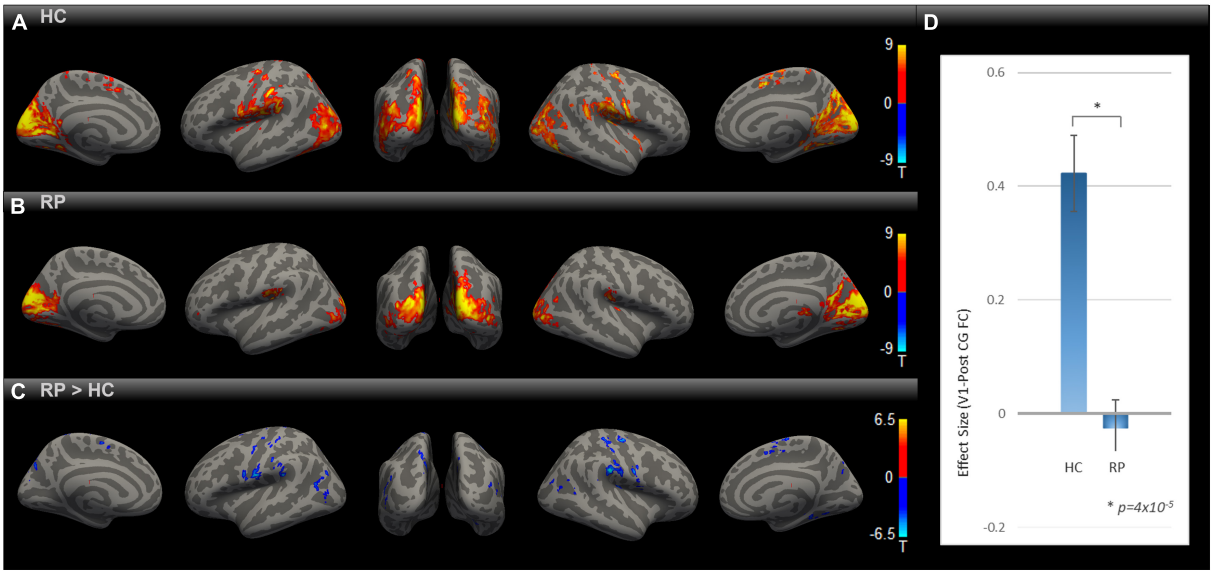

FIGURE 1
Comparing rsFC between RP and HC. Group-level rsFC maps using V1 as the seed for HC **(A)**, RP **(B),** and RP > HC contrast **(C)** were corrected for multiple comparisons using Gaussian Random Field Theory with an uncorrected voxel-level threshold of $p < 0.001$ and a cluster-level threshold of $p < 0.05$ FDR corrected for cluster size. Areas with lower rsFC to V1 covered regions of higher-level visual, primary/secondary somatosensory, motor, and parietal association cortex [blue blobs in **(C)**]. V1-to-PostCG ROI analysis **(D)** showed significantly lower rsFC effect size in RP vs. HC, using two-sample *t*-test [$t\ (18) = -5.39$, $*p = 4 \times 10^{-5}$].

maps for RP and Argus II (Figures 2A,B) groups were calculated and corrected for multiple comparisons with an uncorrected voxel-level threshold of $p < 0.001$ and a cluster-level threshold of $p < 0.05$ FDR corrected for cluster size. Both groups demonstrated functional connectivity between V1 and other visual and inferior temporal areas. The contrast map between the two groups, corrected for multiple comparisons, is shown in Figure 2C. Intriguingly, the seed-to-voxel functional connectivity map in Figure 2C revealed parts of primary motor and somatosensory (pre- and PostCG) with enhanced rsFC to V1 in the Argus II compared with the RP group. The ROI-to-ROI analysis between our two areas of interest (V1 and PostCG) in Figure 2D showed that the functional connectivity significantly increased after partial sight restoration with Argus II [$t\ (15) = 3.62$, $p = 0.002$].

How close are the results in the sight-restored to normally sighted?

Having observed enhanced rsFC after sight restoration, as demonstrated in Figure 2, an intriguing question is whether this was a partial or full reversal compared to normally sighted individuals. To that end, we compared the functional connectivity maps for HC and Argus II groups (Figures 3A–C) after correcting for multiple comparisons using Gaussian Random Field Theory with an uncorrected voxel-level threshold of $p < 0.001$ and a cluster-level threshold of $p < 0.05$ FDR corrected for cluster size. The seed-to-voxel functional connectivity map in Figure 3C shows that sight restoration with Argus II was not able to fully reverse the blindness-induced decrease in rsFC within the visual cortex, especially between V1 and higher visual areas, as indicated by small blue color-coded regions in the medial and lateral sides of the higher-level occipital cortex. Interestingly, partial sight restoration reversed alterations in V1 functional connections with the pre- and PostCG. As indicated in Figure 3D, ROI-to-ROI functional connectivity between V1 and PostCG showed no significant difference between the HC and Argus II groups in a two-sample *t*-test with $t\ (15) = -1.72$, $p = 0.10$.

Effect of blindness and sight restoration on the spread of significant functional connectivity to V1

In order to evaluate how blindness and sight restoration affect functional connectivity, one approach is to look at the strength of this connection, as described in Figures 1–3. Another way of evaluating such alterations is to consider how broadly the connectivity patterns spread over a target ROI. To examine this, we defined another metric that measures the extent of significant functional connectivity as the volumetric area in the target ROI with a significant functional connection to the source ROI. Using V1 as the source ROI and PostCG as the

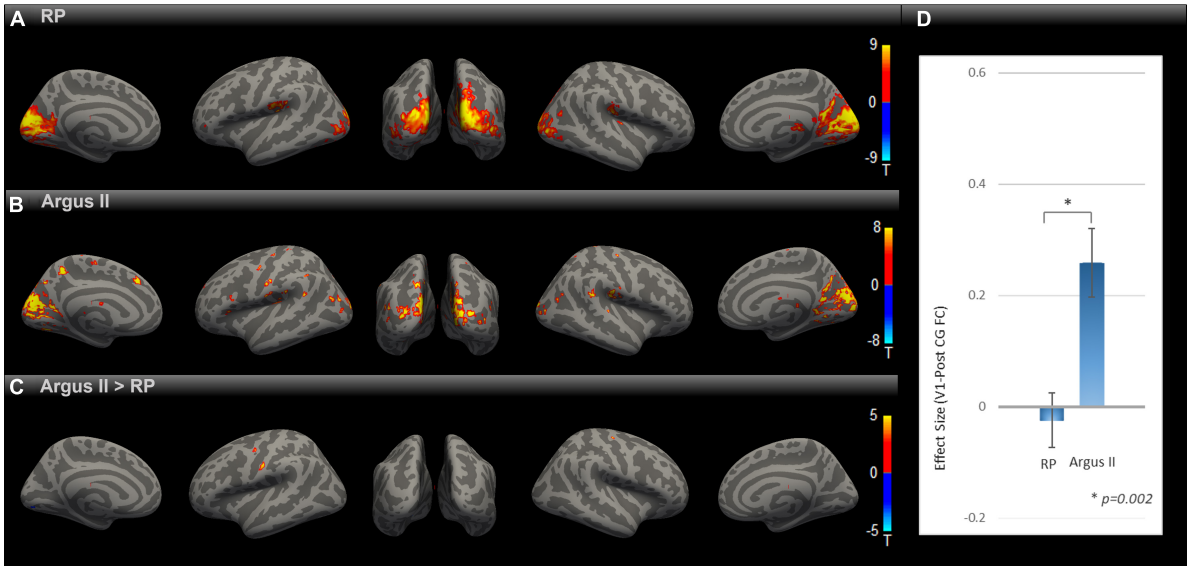

FIGURE 2
Comparing rsFC between Argus and RP. Whole-brain rsFC map using V1 as the seed is calculated at the group level for RP **(A)** Argus II **(B)** and contrast Argus II > RP **(C)**. rsFC maps were corrected for multiple comparisons using the Gaussian Random Field Theory with an uncorrected voxel-level threshold of $p < 0.001$ and a cluster-level threshold of $p < 0.05$ FDR corrected for cluster size. Areas with higher rsFC in Argus II than RP involved pre- and PostCG regions. The ROI-to-ROI rsFC analysis between V1 and PostCG **(D)** additionally showed significant [$t(15) = 3.62$, $^*p = 0.002$] enhancement of this connectivity in Argus II compared with RP.

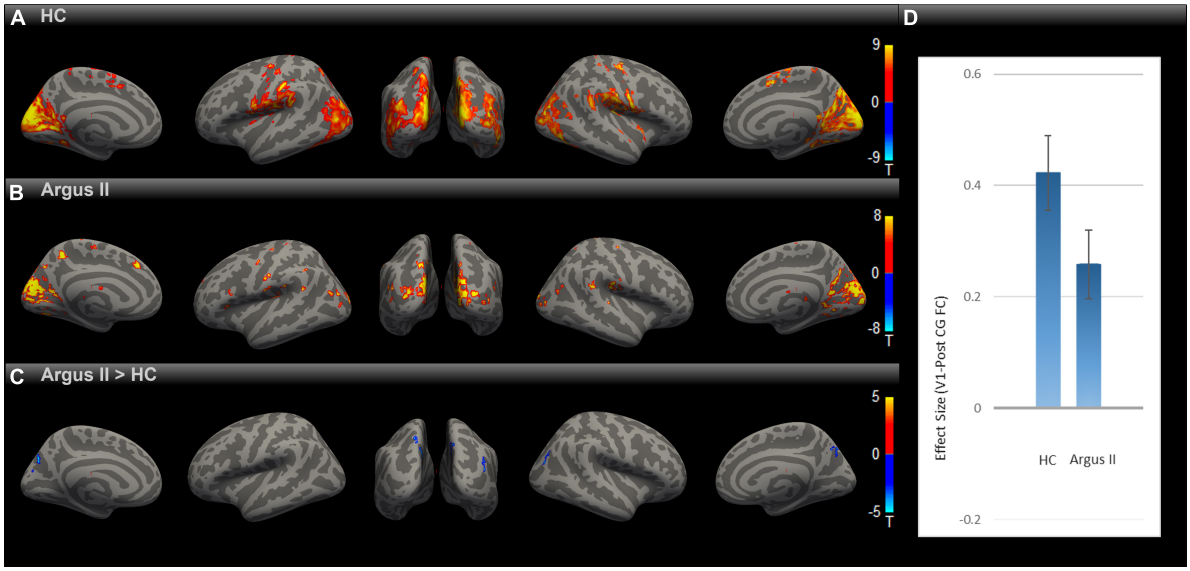

FIGURE 3
Comparing rsFC between Argus II and HC. Using the V1 seed, the group-level rsFC maps for Argus II **(A)**, HC **(B),** and Argus II > HC contrast **(C)** were corrected for multiple comparisons using the Gaussian Random Field Theory with an uncorrected voxel-level threshold of $p < 0.001$ and a cluster-level threshold of $p < 0.05$ FDR corrected for cluster size. The contrast map shows that the areas depicting lower rsFC to V1 were found in some higher-level visual areas (shown in blue). The ROI-to-ROI rsFC analysis **(D)** revealed no significant difference in the V1-PostCG rsFC effect size between Argus II and HC groups, $t(15) = -1.72$, $p = 0.1$.

target ROI, we computed the extent of significant connections for HC, RP, and Argus II groups, as indicated in Figure 4B. Figure 4A shows that the calculated volumetric spread of functional connectivity to V1 in PostCG was 5,961 mm^3 in the HC group. This metric decreased to 0 mm^3 for RP and then increased to 842 mm^3 for the Argus II group.

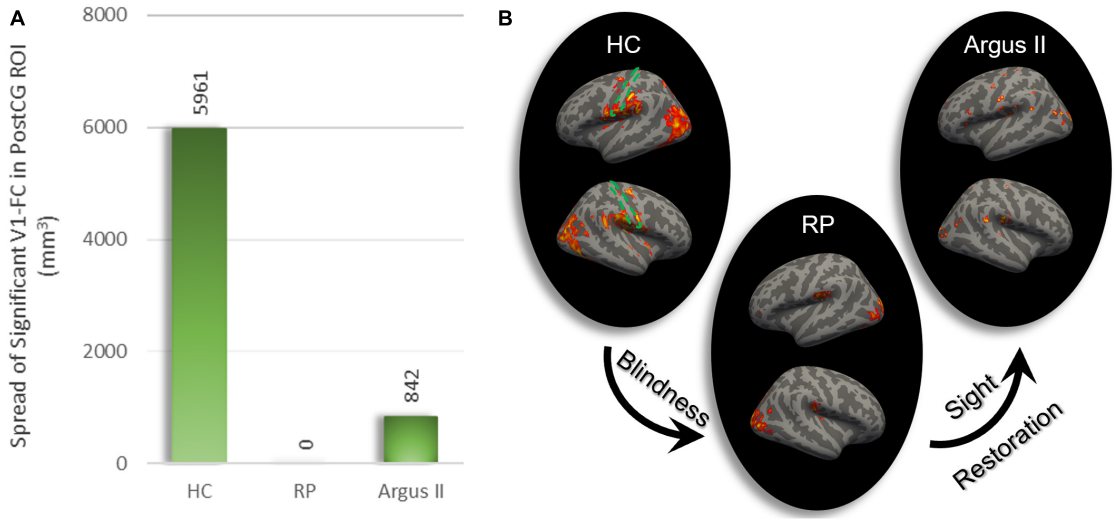

FIGURE 4
The extent of rsFC to V1. The volumetric extent in PostCG shows significant rsFC to V1 as the seed was calculated in mm^3 **(A)**. This spread of connectivity drastically reduced after blindness and partially increased following sight restoration in Argus II. Areas in the whole brain with significant rsFC to V1 for each of the three study groups are shown on the right **(B)**. The dotted green area represents PostCG/primary somatosensory cortex boundary.

Discussion

This study investigated how the loss and subsequent re-introducing of visual input can affect visual-somatosensory functional connectivity at rest. At the group level, the healthy controls demonstrated somatosensory cortex areas with significant rsFC to V1. In the blind RP group, these regions were significantly reduced in rsFC with V1. Additionally, we evaluated the effect of partial sight restoration with the Argus II retinal prosthesis at the group level. The results clearly indicated a change in the opposite direction as a significant increase in visual-PostCG rsFC in Argus II compared with the blind RP group. Importantly, this level of increase rendered the somatosensory-visual rsFC in the Argus II group at a level close to the healthy controls, as no significant rsFC was observed between the two regions in the contrast analyses, with either connectivity maps or ROI analyses. Additionally, the extent of regions in the somatosensory cortex with significant rsFC to V1 followed the same direction as the strength: reduction in the RP blind compared with HC and enhancement in Argus II vs. the fully blind RP group.

We focused on visual-somatosensory rsFC. This choice allowed us to take advantage of the many prior studies of the effects of blindness on visual-somatosensory cross-modal plasticity, against which we could compare our findings. We observed that RP blindness reduces visual-somatosensory rsFC; this finding is consistent with many prior experiments that evaluated rsFC in late-blind individuals (Wittenberg et al., 2004; Dai et al., 2013; Murphy et al., 2016; Wen et al., 2018; Huang et al., 2019). There is also similar evidence for this reduction in rsFC in the congenitally (Striem-Amit et al., 2015; Murphy et al., 2016) and early blind (Wittenberg et al., 2004; Liu et al., 2008; Bauer et al., 2017). Strikingly, some other studies on the blind observed the involvement of the visual cortex in the processing of language and mathematics as well—examples of higher-level cognitive tasks (Bedny et al., 2011; Kanjlia et al., 2016). rsFC has been shown to increase between visual and cognitive areas following blindness (Heine et al., 2015; Striem-Amit et al., 2015; Murphy et al., 2016; Sabbah et al., 2016, 2017; Bauer et al., 2017; Wen et al., 2018). Such an effect on functional connectivity following vision loss has been attributed to an increase in the top-down impact on the visual cortex. One model proposed to explain these unexpected alterations is the reverse hierarchy. In normally sighted individuals, as information is fed through the visual hierarchy, more and more complex and abstract visual features will be processed, which will then serve as an input to cognitive regions such as attention and decision. The feedback connection from higher to lower regions in the visual hierarchy serves to enforce selective attention and learning. It has been proposed that in early-blind individuals, this reverse connection serves to further elaborate information from higher-level visual areas and provide an input containing abstract information into the lower-level visual areas, giving rise to cognitive processing in these regions. Reverse hierarchy, however, has its own limitations in explaining the observed cognitive processing in the visual cortex (Bareket et al., 2017; Fine and Park, 2018).

Previous studies have attempted to evaluate brain alteration following visual restoration using fMRI BOLD activation as the metric. A study looked at the tactile-evoked cross-modal

BOLD responses in occipital regions in two Argus II prosthesis patients (Cunningham et al., 2015), one at 5 weeks and the other at 15 weeks following implantation. The qualitative assessment of their results indicated that the strength and extent of activation in these subjects seemed to be affected by the time since implantation in these two cases, with the subject with a longer time post-surgery demonstrating tactile-evoked visual activation levels closer to the group with normal vision. However, given that only two subjects were evaluated, no firm conclusions can be drawn from this study. Another study evaluated auditory-evoked cross-modal BOLD responses in patients whose sight was restored using RPE65 gene therapy technology (Mowad et al., 2020). Their qualitative comparison of the study groups discovered that the baseline blind RPE65 subjects had enhanced activations within the bilateral visual cortices due to auditory stimulation. However, 3 years later, these activation patterns were significantly elevated. Furthermore, in their study, the visual-auditory rsFC was qualitatively shown to be reduced in the baseline blind RPE65 subjects compared to healthy controls, whereas it slightly increased 3 years following gene therapy compared to baseline RPE65 subjects. Although the results were based on a qualitative comparison of activation maps between groups and not based on group-level contrast maps, their findings have important scientific implications.

Similar to gene therapy observations, our study revealed enhanced rsFC between V1 and PostCG following partial sight recovery with the Argus II retinal prosthesis. This represents a reversal of the cross-modal plasticity initially induced by blindness, as manifested at rest by using functional connectivity as the metric. The noted alteration in rsFC is remarkable in that it was observed even though retinal prosthesis patients regain only basic vision and only occasionally use their prosthetic implant. It is important to note that functional connectivity during rest was used as the metric in our study to investigate plastic changes in the brain following vision loss and restoration. How functional plastic changes manifest during task execution has been shown to be different from rest in blindness. In a study on early blind individuals, Pelland et al. (2017) looked at the apparent disagreement between task-dependent activation or connectivity and resting-state functional connectivity in the blind, i.e., an increase in cross-modal responses in the visual cortex during a non-visual sensory task and the decrease in rsFC between non-visual sensory and visual cortex. They hypothesized that such a decrease in rsFC in early blind individuals might be due to the involvement of the visual cortex in a larger number of processing modes during rest, when the brain is more available to explore various modes, resulting in an increase in functional connectivity variability at rest. On the other hand, increased functional connectivity during task execution might be due to brain involvement in limited modes, resulting in lower functional connectivity variability during the task. Therefore, it is essential to note that the rsFC for groups presented in our study does not smoothly generalize to the brain state during the execution of sensory tasks, such as tactile tasks. However, our finding shows that rsFC could be potentially used as a measure of functional plastic changes detectable during the resting state in response to visual sensory loss and restoration.

Our findings are limited by the relatively small number of participants. As such, we could not conduct a deeper analysis that might have revealed links between patient characteristics and rsFC. Recruitment is a challenge for any study, and Argus II patients are rare. Yet, a larger study that allows stratification and correlation analysis (using patient characteristics) has the potential to provide valuable information that can benefit the ongoing development of visual prostheses and other sight-restoration therapies. Factors such as device usage, duration of blindness, age, and time since implantation could all conceivably play a role in the brain's functional organization after the therapeutic intervention. Our findings can serve as a starting point for such a study or be included in a meta-analysis of other similar studies that can increase the robustness of the results through a pooling of data.

Conclusion

We showed that decreases in resting-state functional connectivity due to blindness were partially reversed by vision restoration. Despite advancements in vision restoration technologies, the vision provided remains well below healthy vision, and patient outcomes vary greatly. To better understand this variability, metrics associated with vision improvement are essential. The rsFC is a tool that has been broadly used to track functional changes in the brain following blindness. Studies of rsFC to investigate sight recovery are relatively rare. Our study aimed to evaluate the effect of blindness on visual-somatosensory rsFC and to further track changes in this quantity after partial sight restoration with the Argus II retinal prosthesis. Our investigation showed that visual-somatosensory rsFC has the potential to serve as a biomarker for functional plastic changes in the brain following vision recovery.

Data availability statement

The datasets presented in this study can be found in online repositories. The names of the repository/repositories and accession number(s) can be found below: The Retinitis Pigmentosa (RP) and Argus II Human Connectome for Low Vision (HCLV) data that support the findings of this study have been provided to the Connectome Coordination Facility (CCF) at Human Connectome Project organization. This data is not yet available at CCF on https://humanconnectome.org because CCF is still processing it. The Lifespan Human Connectome Project Aging (HCP-A) data is openly available

and can be accessed at the Lifespan dataset in NDA: https://nda.nih.gov/general-query.html?q=query=featured-datasets:HCP%20Aging%20and%20Development. Commercial application software used for the analysis includes FSL, SPM, CONN, FreeSurfer and MATLAB. Custom scripts for data management are available upon request.

Ethics statement

The studies involving human participants were reviewed and approved by the Institutional Review Board at University of Michigan and the Institutional Review Board at University of Southern California. The patients/participants provided their written informed consent to participate in this study.

Author contributions

NN, NS, JC, VP, YS, JJ, and JW contributed to the experimental design. NN, NS, JC, VP, HA, YS, and JW performed the data collection. NN, ZL, and JW carried out the data analysis. NS, HA, ZL, JJ, and JW contributed to manuscript editing. NN drafted the manuscript. All authors contributed to the article and approved the submitted version.

Funding

This work was supported in part by the National Institutes of Health, National Eye Institute (U01 EY025864), the National Institutes of Health, BRAIN Initiative (1 K99 EY031987-01), the University of Southern California, Roski Eye Institute, the Michigan Endowment of Biosciences, the Arnold O. Beckman Postdoctoral Scholars Fellowship Program, and the National Institute on Aging of the National Institutes of Health (Award Number: U01AG052564).

Acknowledgments

We gratefully acknowledge all the subjects involved in the study. We thank Drs. Luis Hernandez-Garcia and Yizhen Zhang for providing feedback for data acquisition and analysis, respectively. Additionally, we appreciate the statistical consultation provided by Dr. Ivo Dinov.

Conflict of interest

JW received research support from Second Sight Medical Products, Inc. outside of this study.

The remaining authors declare that the research was conducted in the absence of any commercial or financial relationships that could be construed as a potential conflict of interest.

Publisher's note

All claims expressed in this article are solely those of the authors and do not necessarily represent those of their affiliated organizations, or those of the publisher, the editors and the reviewers. Any product that may be evaluated in this article, or claim that may be made by its manufacturer, is not guaranteed or endorsed by the publisher.

Author disclaimer

The content was solely the responsibility of the authors and does not necessarily represent the official views of the National Institutes of Health.

Supplementary material

The Supplementary Material for this article can be found online at: https://www.frontiersin.org/articles/10.3389/fnins.2022.902866/full#supplementary-material

References

Amunts, K., Mohlberg, H., Bludau, S., and Zilles, K. (2020). Julich-Brain: A 3D probabilistic atlas of the human brain's cytoarchitecture. *Science* 4588, 988–992. doi: 10.1126/science.abb4588

Apte, R. S. (2018). Gene Therapy for Retinal Degeneration. *Cell* 173:5. doi: 10.1016/j.cell.2018.03.021

Ashtari, M., Nikonova, E. S., Marshall, K. A., Young, G. J., Aravand, P., Pan, W., et al. (2017). The Role of the Human Visual Cortex in Assessment of the Long-Term Durability of Retinal Gene Therapy in Follow-on RPE65 Clinical Trial Patients. *Ophthalmology* 124, 873–883. doi: 10.1016/j.ophtha.2017.01.029

Bareket, L., Barriga-Rivera, A., and Zapf, M. P. (2017). Learning to see again: Biological constraints on cortical plasticity and the implications for sight restoration technologies Related content Progress in artificial vision through suprachoroidal retinal implants. *J. Neural Eng.* 14:051003. doi: 10.1088/1741-2552/aa795e

Barkhof, F., Haller, S., and Rombouts, S. A. R. B. (2014). Resting-state Functional mR imaging: A New Window to the Brain. *Radiology* 272, 29–49. doi: 10.1148/radiol.14132388

Bauer, C. M., Hirsch, G. V., Zajac, L., Koo, B. B., Collignon, O., and Merabet, L. B. (2017). Multimodal MR-imaging reveals large-scale structural and functional connectivity changes in profound early blindness. *PLoS One* 12:e0173064. doi: 10.1371/journal.pone.0173064

Bedny, M., Pascual-Leone, A., Dodell-Feder, D., Fedorenko, E., and Saxe, R. (2011). Language processing in the occipital cortex of congenitally blind adults. *Proc. Natl. Acad. Sci. U. S. A.* 108, 4429–4434. doi: 10.1073/pnas.1014818108

Bennett, J., Wellman, J., Marshall, K. A., McCague, S., Ashtari, M., DiStefano-Pappas, J., et al. (2016). Safety and durability of effect of contralateral-eye administration of AAV2 gene therapy in patients with childhood-onset blindness caused by RPE65 mutations: A follow-on phase 1 trial. *Lancet* 388, 661–672. doi: 10.1016/S0140-6736(16)30371-3

Biswal, B., Zerrin Yetkin, F., Haughton, V. M., and Hyde, J. S. (1995). Functional connectivity in the motor cortex of resting human brain using echo-planar mri. *Magn. Reson. Med.* 34, 537–541. doi: 10.1002/mrm.1910340409

BLoch, E., Luo, Y., and Da Cruz, L. (2019). Advances in retinal prosthesis systems. *Ther. Adv. Ophthalmol.* 11:2515841418817501.

Bookheimer, S. Y., Salat, D. H., Terpstra, M., Ances, B. M., Barch, D. M., Buckner, R. L., et al. (2019). The Lifespan Human Connectome Project in Aging: An overview. *Neuroimage* 185, 335–348. doi: 10.1016/j.neuroimage.2018.10.009

Bourne, R., Price, H., and Stevens, G. (2012). Global Burden of Visual Impairment and Blindness. *Arch. Ophthalmol.* 130, 645–647. doi: 10.1001/archophthalmol.2012.1032

Bullmore, E., and Sporns, O. (2009). Complex brain networks: Graph theoretical analysis of structural and functional systems. *Nat. Rev. Neurosci.* 10, 186–198. doi: 10.1038/nrn2575

Castaldi, E., Cicchini, G. M., Cinelli, L., Biagi, L., Rizzo, S., and Morrone, M. C. (2016). Visual BOLD Response in Late Blind Subjects with Argus II Retinal Prosthesis. *PLoS Biol.* 14:e1002569. doi: 10.1371/journal.pbio.1002569

Cheng, D. L., Greenberg, P. B., and Borton, D. A. (2017). Advances in Retinal Prosthetic Research: A Systematic Review of Engineering and Clinical Characteristics of Current Prosthetic Initiatives. *Curr. Eye Res.* 42, 334–347. doi: 10.1080/02713683.2016.1270326

Cunningham, S. I., Shi, Y., Weiland, J. D., Falabella, P., Koo, C. O., De Zacks, D. N., et al. (2015). Feasibility of Structural and Functional MRI Acquisition with Unpowered Implants in Argus II Retinal Prosthesis Patients?: A Case Study. *Transl. Vis. Sci. Technol.* 4:6. doi: 10.1167/tvst.4.6.6

Dai, H., Morelli, J. N., Ai, F., Yin, D., Hu, C., Xu, D., et al. (2013). Resting-state functional MRI: Functional connectivity analysis of the visual cortex in primary open-angle glaucoma patients. *Hum. Brain Mapp.* 34, 2455–2463. doi: 10.1002/hbm.22079

Dorn, J. D., Ahuja, A. K., Caspi, A., Da Cruz, L., Dagnelie, G., Sahel, J. A., et al. (2013). The detection of motion by blind subjects with the epiretinal 60-electrode (Argus II) retinal prosthesis. *JAMA Ophthalmol.* 131, 183–189. doi: 10.1001/2013.jamaophthalmol.221

Fernandes, R. A. B., Diniz, B., Ribeiro, R., and Humayun, M. (2012). Artificial vision through neuronal stimulation. *Neurosci. Lett.* 519, 122–128. doi: 10.1016/J.NEULET.2012.01.063

Fine, I., and Park, J.-M. (2018). Blindness and Human Brain Plasticity. *Annu. Rev. Vis. Sci.* 4, 337–356. doi: 10.1146/annurev-vision-102016

Harms, M. P., Somerville, L. H., Ances, B. M., Andersson, J., Barch, D. M., Bastiani, M., et al. (2018). Extending the Human Connectome Project across ages: Imaging protocols for the Lifespan Development and Aging projects. *Neuroimage* 183, 972–984. doi: 10.1016/j.neuroimage.2018.09.060

Heine, L., Bahri, M. A., Cavaliere, C., Soddu, A., Laureys, S., Ptito, M., et al. (2015). Prevalence of increases in functional connectivity in visual, somatosensory, and language areas in congenital blindness. *Front. Neuroanat.* 9:86. doi: 10.3389/fnana.2015.00086

Hou, F., Liu, X., Zhou, Z., Zhou, J., and Li, H. (2017). Reduction of Interhemispheric Functional Brain Connectivity in Early Blindness: A Resting-State fMRI Study. *Biomed. Res. Int.* 2017:6756927. doi: 10.1155/2017/6756927

Hu, S. L., Tang, L. Y., Fang, J. W., Su, T., Ge, Q. M., Lin, Q., et al. (2020). Intrinsic functional connectivity alterations of the primary visual cortex in patients with proliferative diabetic retinopathy: A seed-based resting-state fMRI study. *Neuropsychiatr. Dis. Treat.* 16, 1571–1581. doi: 10.2147/NDT.S238463

Huang, X., Zhou, F.-Q., Dan, H. D., and Shen, Y. (2019). Impaired interhemispheric synchrony in late blindness. *Acta Radiol.* 61, 414–423. doi: 10.1177/0284185119864843

Humayun, M. S., Dorn, J. D., Da Cruz, L., Dagnelie, G., Sahel, J. A., Stanga, P. E., et al. (2012). Interim Results from the International Trial of Second Sight's Visual Prosthesis. *OPHTHA* 119, 779–788. doi: 10.1016/j.ophtha.2011.09.028

Iraji, A., Calhoun, V. D., Wiseman, N. M., Davoodi-Bojd, E., Avanaki, M. R. N., Haacke, E. M., et al. (2016). The connectivity domain: Analyzing resting state fMRI data using feature-based data-driven and model-based methods. *Neuroimage* 134, 494–507. doi: 10.1016/j.neuroimage.2016.04.006

Kanjlia, S., Lane, C., Feigenson, L., and Bedny, M. (2016). Absence of visual experience modifies the neural basis of numerical thinking. *Proc. Natl. Acad. Sci. U. S. A.* 113, 11172–11177. doi: 10.1073/pnas.1524982113

Khorrami-Nejad, M., Sarabandi, A., Akbari, M. R., and Askarizadeh, F. (2016). The Impact of Visual Impairment on Quality of Life. *Med. Hypothesis Discov. Innov. Ophthalmol.* 5, 96–103.

Lee, J. H., Wang, J. H., Chen, J., Li, F., Edwards, T. L., Hewitt, A. W., et al. (2019). Gene therapy for visual loss: Opportunities and concerns. *Prog. Retin. Eye Res.* 68, 31–53. doi: 10.1016/j.preteyeres.2018.08.003

Li, K., Guo, L., Nie, J., Li, G., and Liu, T. (2009). Review of methods for functional brain connectivity detection using fMRI. *Comput. Med. Imaging Graph.* 33, 131–139. doi: 10.1016/j.compmedimag.2008.10.011

Liu, Y., Yu, C., Liang, M., Li, J., Tian, L., Zhou, Y., et al. (2008). Whole brain functional connectivity in the early blind. *Brain* 130, 2085–2096. doi: 10.1093/brain/awm121

Lv, X. H., Wang, X. Z., Tong, X. E., Williams, X. L. M., Zaharchuk, X. G., Zeineh, X. M., et al. (2018). Resting-State Functional MRI: Everything That Nonexperts Have Always Wanted to Know. *Am. J. Neuroradiol.* 39, 1390–1399. doi: 10.3174/ajnr.A5527

McClements, M. E., Staurenghi, F., MacLaren, R. E., and Cehajic-Kapetanovic, J. (2020). Optogenetic Gene Therapy for the Degenerate Retina: Recent Advances. *Front. Neurosci.* 14:570909. doi: 10.3389/fnins.2020.570909

Mowad, T. G., Willett, A. E., Mahmoudian, M., Lipin, M., and Fritz, J. B. (2020). Compensatory Cross-Modal Plasticity Persists After Sight Restoration. *Front. Neurosci.* 14:291. doi: 10.3389/fnins.2020.00291

Murphy, M. C., Nau, A. C., Fisher, C., Kim, S. G., Schuman, J. S., and Chan, K. C. (2016). Top-down influence on the visual cortex of the blind during sensory substitution. *Neuroimage* 125, 932–940. doi: 10.1016/j.neuroimage.2015.11.021

Nadvar, N., Choupan, J., Litinas, K., Shi, Y., Hernandez-Garcia, L., and Weiland, J. (2019). "*Implementation of human connectome low vision (HCLV) imaging protocol* at University of Michigan," in Proceedings of the annual society for neuroscience conference abstract.

National Academies of Sciences Engineering and Medicine, Health and Medicine Division, Board on Population Health and Public Health Practice, Committee on Public Health Approaches to Reduce Vision Impairment and Promote Eye Health, Welp, A., Woodbury, R. B., et al. (2016). *The Impact of Vision Loss in Making Eye Health a Population Health Imperative: Vision for Tomorrow*. Available online at: https://www.ncbi.nlm.nih.gov/books/NBK402367/ (accessed January 10, 2022).

Pelland, M., Orban, P., Dansereau, C., Lepore, F., Bellec, P., and Collignon, O. (2017). State-dependent modulation of functional connectivity in early blind individuals. *Neuroimage* 147, 532–541. doi: 10.1016/j.neuroimage.2016.12.053

Peltier, S. J., and Shah, Y. (2011). Biophysical Modulations of Functional Connectivity. *Brain Connect.* 1, 267–277. doi: 10.1089/brain.2011.0039

Qin, W., Xuan, Y., Liu, Y., Jiang, T., and Yu, C. (2014). Functional Connectivity Density in Congenitally and Late Blind Subjects. *Cereb. Cortex* 25, 2507–2516. doi: 10.1093/cercor/bhu051

Sabbah, N., Authié, C. N., Sanda, N., Mohand-Saïd, S., Sahel, J. A., Safran, A. B., et al. (2016). Increased functional connectivity between language and visually deprived areas in late and partial blindness. *Neuroimage* 136, 162–173. doi: 10.1016/j.neuroimage.2016.04.056

Sabbah, N., Sanda, N., Authié, C. N., Mohand-Saïd, S., Sahel, J. A., Habas, C., et al. (2017). Reorganization of early visual cortex functional connectivity following selective peripheral and central visual loss. *Sci. Rep.* 7:43223. doi: 10.1038/srep43223

Seitzman, B. A., Snyder, A. Z., Leuthardt, E. C., and Shimony, J. S. (2019). The State of Resting State Networks. *Top. Magn. Reson. Imaging* 28, 189–196. doi: 10.1097/rmr.0000000000000214

Simon, C. J., Sahel, J. A., Duebel, J., Herlitze, S., and Dalkara, D. (2020). Opsins for vision restoration. *Biochem. Biophys. Res. Commun.* 527, 325–330. doi: 10.1016/j.bbrc.2019.12.117

Stingl, K., Ulrich Bartz-Schmidt, K., Besch, D., Braun, A., Bruckmann, A., Gekeler, F., et al. (2013). Artificial vision with wirelessly powered subretinal

electronic implant alpha-IMS. *Proc. Biol. Sci.* 280:20130077. doi: 10.1098/rspb.2013.0077

Striem-Amit, E., Ovadia-Caro, S., Caramazza, A., Margulies, D. S., Villringer, A., and Amedi, A. (2015). Functional connectivity of visual cortex in the blind follows retinotopic organization principles. *Brain* 138, 1679–1695.

van den Heuvel, M. P., and Hulshoff Pol, H. E. (2010). Exploring the brain network: A review on resting-state fMRI functional connectivity. *Eur. Neuropsychopharmacol.* 20, 519–534. doi: 10.1016/j.euroneuro.2010.03.008

Van Dijk, K. R. A., Hedden, T., Venkataraman, A., Evans, K. C., Lazar, S. W., and Buckner, R. L. (2010). Intrinsic functional connectivity as a tool for human connectomics: Theory, properties, and optimization. *J. Neurophysiol.* 103, 297–321. doi: 10.1152/jn.00783.2009

Wang, X., Yu, C., Tzekov, R. T., Zhu, Y., and Li, W. (2020). The effect of human gene therapy for RPE65-associated Leber's congenital amaurosis on visual function: A systematic review and meta-analysis. *Orphanet J. Rare Dis.* 15:49.

Wen, Z., Zhou, F. Q., Huang, X., Dan, D., Xie, B. J., and Shen, Y. (2018). Altered functional connectivity of primary visual cortex in late blindness. *Neuropsychiatr. Dis. Treat.* 14, 3317–3327. doi: 10.2147/NDT.S183751

Whitfield-Gabrieli, S., and Nieto-Castanon, A. (2012). Conn: A Functional Connectivity Toolbox for Correlated and Anticorrelated Brain Networks. *Brain Connect.* 2, 125–141. doi: 10.1089/brain.2012.0073

Wittenberg, G. F., Werhahn, K. J., Wassermann, E. M., Herscovitch, P., and Cohen, L. G. (2004). Functional connectivity between somatosensory and visual cortex in early blind humans. *Eur. J. Neurosci.* 20, 1923–1927. doi: 10.1111/j.1460-9568.2004.03630.x

Worsley, K. J. (1996). The Geometry of Random Images. *CHANCE* 9, 27–40. doi: 10.1080/09332480.1996.10542483

Yu, C., Liu, Y., Li, J., Zhou, Y., Wang, K., Tian, L., et al. (2008). Altered functional connectivity of primary visual cortex in early blindness. *Hum. Brain Mapp.* 29, 533–543. doi: 10.1002/hbm.20420

Zrenner, E. (2013). Fighting blindness with microelectronics. *Sci. Transl. Med.* 5:210s16. doi: 10.1126/scitranslmed.3007399

Zrenner, E., Ulrich Bartz-Schmidt, K., Benav, H., Besch, D., Bruckmann, A., Gabel, V. P., et al. (2011). Subretinal electronic chips allow blind patients to read letters and combine them to words. *Proc. R. Soc. B Biol. Sci.* 278, 1489–1497. doi: 10.1098/rspb.2010.1747

frontiers | Frontiers in Neuroscience

TYPE Original Research
PUBLISHED 03 October 2022
DOI 10.3389/fnins.2022.921321

OPEN ACCESS

EDITED BY
Maurice Ptito,
Université de Montréal, Canada

REVIEWED BY
N. Apurva Ratan Murty,
Massachusetts Institute of Technology, United States
Yousuke Kawachi,
Tohoku University, Japan

*CORRESPONDENCE
Roni Arbel
roni.arbel@mail.huji.ac.il

SPECIALTY SECTION
This article was submitted to Perception Science, a section of the journal Frontiers in Neuroscience

RECEIVED 15 April 2022
ACCEPTED 05 September 2022
PUBLISHED 03 October 2022

CITATION
Arbel R, Heimler B and Amedi A (2022) Face shape processing *via* visual-to-auditory sensory substitution activates regions within the face processing networks in the absence of visual experience. *Front. Neurosci.* 16:921321. doi: 10.3389/fnins.2022.921321

Face shape processing *via* visual-to-auditory sensory substitution activates regions within the face processing networks in the absence of visual experience

Roni Arbel[1,2,3]*, Benedetta Heimler[1,4,5] and Amir Amedi[1,4]

[1]Department of Medical Neurobiology, Hadassah Ein-Kerem, Hebrew University of Jerusalem, Jerusalem, Israel, [2]Faculty of Medicine, Hebrew University of Jerusalem, Jerusalem, Israel, [3]Department of Pediatrics, Hadassah University Hospital-Mount Scopus, Jerusalem, Israel, [4]Ivcher School of Psychology, The Institute for Brain, Mind, and Technology, Reichman University, Herzeliya, Israel, [5]Center of Advanced Technologies in Rehabilitation, Sheba Medical Center, Ramat Gan, Israel

Previous evidence suggests that visual experience is crucial for the emergence and tuning of the typical neural system for face recognition. To challenge this conclusion, we trained congenitally blind adults to recognize faces *via* visual-to-auditory sensory-substitution (SDD). Our results showed a preference for trained faces over other SSD-conveyed visual categories in the fusiform gyrus and in other known face-responsive-regions of the deprived ventral visual stream. We also observed a parametric modulation in the same cortical regions, for face orientation (upright vs. inverted) and face novelty (trained vs. untrained). Our results strengthen the conclusion that there is a predisposition for sensory-independent and computation-specific processing in specific cortical regions that can be retained in life-long sensory deprivation, independently of previous perceptual experience. They also highlight that if the right training is provided, such cortical preference maintains its tuning to what were considered visual-specific face features.

KEYWORDS

fMRI, fusiform gyrus, visual deprivation, face perception, sensory substitution device, blindness, training

Introduction

Visual face processing is a complex visual skill that enables the identification of others, as well as the interpretation of expressions and affect. This skill develops through the exposure to hundreds of thousands of face exemplars over the years in varying conditions of light, changes in expression, gaze, and age (Maurer et al., 2002;

McKone et al., 2007; Haist et al., 2013). A broad network of brain regions involved in visual face recognition has been identified using Functional Magnetic Resonance Imaging (fMRI). The Fusiform Face Area (FFA) is located in the visual extrastriate cortex and it is considered the hallmark of face cortical processing in the human brain. FFA has notable reproducibility for face identification and is part of the object-recognition system within the ventral visual stream (Kanwisher et al., 1997; Spiridon et al., 2006). This ventral-stream node has been shown to be strongly responsive to the invariant face components used for identity judgment when presented in the upright orientation (Haxby et al., 2000; Ishai, 2008) and to have a preference for familiar over unfamiliar face exemplars (Visconti di Oleggio Castello et al., 2017). Additional face-responsive regions include the occipital face area (OFA) and the temporal face area in the superior temporal sulcus (STS); these, along with the FFA, compose the core network for face identification (Haxby et al., 2000; Ishai, 2008). The extended network for face recognition includes the amygdala and insula, where emotional responses to faces are processed, the anterior temporal lobe, which mediates aspects of biological information, and the inferior frontal gyrus (IFG), where face-related semantic aspects are processed (Haxby et al., 2000, 2002; Ishai et al., 2005; Gobbini and Haxby, 2007; Ishai, 2008; Avidan et al., 2014).

Since experience with faces relies heavily on visual input, will face-responsive regions retain their preference and unique properties in cases of life-long visual deprivation? This question is particularly relevant when embedded within accumulating evidence documenting that in congenitally blind adults, nearly all the known regions in higher-order visual cortices which were heretofore considered "visual" can be activated by any sensory modality (e.g., by audition or touch rather than vision), while retaining their functional selectivity, for example, to objects in the lateral occipital complex (e.g., Amedi et al., 2007), to spatial localization in the middle-occipital gyrus (e.g., Collignon et al., 2011), to spatial layout in the parahippocampal area (Wolbers et al., 2011), to motion detection in MT+/V5 (e.g., Ricciardi et al., 2007), or to letters and number identification in visual word form area and in number form area, respectively (e.g., Reich et al., 2011; Striem-Amit et al., 2012; Abboud et al., 2015).

This evidence has given rise to a new theory of brain organization proposing that brain specializations are driven by specific sensory-independent computations rather than by sensory-specific processes as classically conceived (Heimler et al., 2015; Amedi et al., 2017).

However, cortical regions in the ventral visual stream normally responding to visual faces, with a special emphasis on FFA, are suggested to diverge from this theory, as evidence of FFA-preserved computational-selectivity in congenitally blind adults is inconsistent (Bi et al., 2016). Specifically, one line of research investigated whether FFA becomes responsive to human-emitted sounds when lacking visual experience across the lifespan and thus not developing typical face preference. Within this framework, one study reported FFA-like activations in congenitally blind adults in response to certain types of human-emitted sounds [e.g., chewing sounds; see van den Hurk et al., 2017, and a replication in Murty et al. (2020)]. However, other studies failed to show any FFA compatible activations for a more distinctive set of person-specific sounds, namely voices (Hölig et al., 2014; Dormal et al., 2018). Voices are a "special" human-related sound for people who are blind, as they represent the type of sensory information the blind rely on the most to identify people in their everyday lives. This lack of FFA-related activation for voices suggests that the computation of FFA may not specifically rely on identity judgments and may be more related to the components of human shapes (Konkle and Caramazza, 2013; Shultz and McCarthy, 2014; Bi et al., 2016).

In accordance with this latter consideration, another line of research investigated whether potential face preference in congenitally blind individuals may arise from haptic exploration of 3D face images. Despite social constraints limiting the extent of human identification *via* touch in people who are congenitally blind (Murty et al., 2020), they are still able to gain some experience of the general structure of faces from their own faces and those of their loved ones. This is evidenced by studies showing the ability of the congenitally blind to successfully classify 3D objects as belonging to the face category (Kilgour and Lederman, 2002; Murty et al., 2020). These behavioral results have been explained by suggesting that their extensive experience with touch for the purposes of object recognition, could result in connections between the somatosensory system and the object-identification regions within the ventral visual stream, therefore also including face regions (Bi et al., 2016). A recent study tested this hypothesis by asking congenitally blind adults to explore 3D faces *via* touch, while investigating face preferences within a pre-defined region in the deprived ventral visual stream (Murty et al., 2020). Results revealed preferential activation for 3D haptically explored faces over other categories in the blind in a location similar to that of the sighted FFA. This study suggested that in the absence of visual experience, some aspects of face preference in the ventral visual stream can arise through the haptic modality. This result, however, stands in contrast with a previous investigation which failed to report ventral stream activations in the congenitally blind for haptic face exploration (Pietrini et al., 2004).

All these results highlight some unexplored questions about the properties of face preference in congenitally blind adults. First, it is still unknown whether face preference in the deprived ventral visual stream is retained only for tactile processing or it extends to other spared sensory modalities, i.e., audition, namely a sensory-modality that people who are blind do not typically use for object recognition. Previous studies showed that congenitally blind adults can successfully perceive various object shapes (but not faces) *via* audition using visual-to-auditory Sensory Substitution Devices (Amedi et al., 2007; Striem-Amit and Amedi, 2014; Abboud et al., 2015).

These SSDs transform visual information into audition using a specific algorithm that maintains core visual features such as objects' shapes, locations, and even color (Meijer, 1992; Abboud et al., 2014). However, the little overall experience with face-shapes that blind acquire through touch may not be anchored enough in the deprived visual cortex to support a generalization to an entirely novel sensory-modality (i.e., SSD-conveyed auditory face-shapes). Second, and furthermore, other distinctive characteristics of face specificity within the ventral visual stream, such as the preference for upright over inverted faces (Yovel and Kanwisher, 2005; Rosenthal et al., 2016) or the difference between familiar and novel faces (Visconti di Oleggio Castello et al., 2017) remain unexplored in the visually deprived population. Finally, previous studies mainly focused on FFA activations alone, and therefore it is still unclear whether other regions of the face network become also activated by atypical sensory modalities.

To address these open issues, we trained a group of congenitally blind adults to perceive face shapes *via* audition using visual-to-auditory SSDs. Our blind participants were expert SSD users with dozens of hours of previous training with SSDs, albeit tailored to the perception of simpler objects. To teach participants the perception of the much more complicated colorful face soundscapes, we designed a ∼12 h training program specifically tailored to teach the perception of face shapes in their upright orientation, alongside additional similarly long training targeting other "visual" categories. Specifically, we trained our participants to perceive short words *via* SSD using a novel auditory SSD alphabet we developed (Arbel et al., 2020). This allowed us to explore the role of subordinate object identification associated with face exemplars, as well as experience with a novel category of stimuli (Gauthier and Tarr, 1997; Gauthier et al., 1999, 2000a).

We also trained our participants to use SSDs to recognize hand gestures to investigate the extent to which deprived cortical regions retain their preference for general animate objects in addition to face processing in the blind brain, as in the sighted brain (Peelen and Downing, 2005; Konkle and Caramazza, 2013; Kaiser et al., 2014; Shultz and McCarthy, 2014; Fisher and Freiwald, 2015; Thorat et al., 2019). Hand gestures, like faces, are stimuli for which congenitally blind adults have significantly lower perceptual experience through their remaining sensory-modalities during daily life compared to the sighted, with the exception of proprioceptive cues (Bi et al., 2016).

Finally, we tested the responses of congenitally blind adults to human voices, the stimulus congenitally blind individuals rely on the most across their lifespan to identify other people. With this additional control, we investigated whether general person-specific sound processing overlaps with putative face-shape related preferences in the congenitally blind brain or rather emerges in distinctive voice-specific regions (Gougoux et al., 2009; Dormal et al., 2018) (for results in the deaf brain, see Benetti et al., 2017).

After training, we presented our participants with stimuli belonging to all the above categories, while testing their neural responses using fMRI.

Taken together, our results show a maintained preference for face shapes in the ventral visual stream of the congenitally blind brain, with properties largely similar to those reported for the sighted brain. Specifically, we show preference for trained upright faces vs. words in a location near the sighted FFA, as well as a preference for faces over scramble faces in a similar location, accompanied by activations in a location near the sighted OFA, another core face region. In addition, we also observed a modulation by orientation and novelty of faces such that trained upright faces activated the face-responsive regions more than untrained inverted faces and of entirely novel faces. Crucially, both hand-gestures and faces activated the fusiform gyrus, albeit a Region of Interest (ROI) analysis suggests stronger activations for faces than hand-gestures. This latter result suggests that animacy processing is retained in the deprived fusiform gyrus. Finally, and in line with previous evidence, no activation for voices emerged in the deprived ventral visual stream. Taken together, these results further suggest that visual experience early in life is not the key factor shaping the emergence and properties of typical face preference in the ventral visual stream.

Materials and methods

Participants

Seven congenitally blind participants (five women, average age: 39 ± 5.3 years) with no reported neurological conditions or contra-indications for undergoing MRI scans, and with extensive (>50 h) experience with SSDs participated in the experiments. For detailed characteristics of participants see **Table 1**.

The Hadassah Medical Center Ethics Committee approved the experimental procedure; written informed consent was obtained from each participant. Participants were reimbursed for their participation in the study.

The EyeMusic algorithm

The EyeMusic visual-to-auditory SSD was used to teach participants to identify whole-face shapes, as well as words and hand gestures (see details in the following section). EyeMusic transforms each pixel of a given image into what we term auditory soundscapes, namely an auditory pattern preserving shape, color, and spatial layout of objects. In brief, the EyeMusic algorithm down-samples each image to 50*30 pixels. Then, using a sweep-line approach, it transforms each pixel in a given image into a corresponding sound using the following parameters. First, the *x*-axis is mapped to time; each image is

scanned column-by-column from left to right, such that pixels on the left side of the image are played before those on the right. Second, the *y*-axis is mapped to pitch variations using the pentatonic scale, such that the lower the pixel in the image, the lower the corresponding pitch sonifying it. Third, color is conveyed through timbre manipulations, such that each color is played using a different musical instrument, and brightness levels are conveyed *via* sound volume variations. EyeMusic has five colors (white, green, red, blue, and yellow), and black is mapped as silence (**Figure 1A**) (for full details, see Abboud et al., 2014).

EyeMusic training sessions

Face identification

Face identification *via* shape recognition is a visually dominant skill with which congenitally blind adults have little if any experience. Therefore, before training, our congenitally blind participants were largely unaware of face-related shapes. Thus, a crucial aspect of our structured training program was familiarization with this novel object category.

Furthermore, auditory face identification is an extremely challenging behavioral task because of the complexity of the soundscapes created by faces. Therefore, our training program also focused on teaching participants how to interpret such auditory complex soundscapes. This is why we selected participants who were already proficient EyeMusic users with extensive previous training with the device (>50 h) before face training began. Note, however, that unlike their previous training which consisted mostly of line drawing of simple shapes, participants were presented with images filled with color and with colorful features embedded within the images whose interpretation was crucial to succeed in the task.

We constructed a training program that included five sessions of 2 h each (participants received additional "refresher" sessions up to 12 h in total). For full details of the training program see Arbel et al., 2022. In brief, participants were introduced to 6 cartoon faces which were adapted from the children's game "guess who" and translated into soundscapes using EyeMusic (see **Supplementary Figure 2A**). In the first stages of the training, participants learned to interpret only horizontal strips of the images (bottom, top, and middle), to gradually advance their skill so they could focus on perceiving small details embedded within the complex sounds (**Supplementary Figure 1**). Even if during this phase we presented portions of faces, we never trained single facial features in isolation: each strip contained multiple facial features (e.g., each top strip contained hair, eyes, glasses, etc.). This is very different from tactile exploration where each facial feature is generally explored alone, separately from the others.

After familiarization with face-strips, participants were gradually introduced to the full face images, until they learned to identify all 6 cartoon faces. Identification consisted of learning the perception of each of these faces as a whole, as well as the features included in each face (e.g., eye or hair color, glasses, beard, etc.), and only then learning the name associated with the face. This latter training strategy was introduced because it was shown that assigning names to new faces improves face recognition skills (Schwartz and Yovel, 2016). In addition, it was introduced to make the training program more similar to our other training programs (see below) where each trained object had distinctive names.

Word training and other visual category training

The word training aimed at teaching our participants a novel orthography that we created by merging Braille and Morse features and transformed *via* EyeMusic to soundscapes (for full details see Arbel et al., 2020). During this structured training program, participants learned to read using this new orthography. The duration of training was the same as for face training. Training also included color, as each letter was consistently presented in one of three possible colors. Specifically, during training, participants first learned to identify half of the Hebrew alphabet (11 letters), and then learned to read short words and pseudo-words of up to five characters comprised of these letters. In the experiments described in this work, we included three 3-letter words using only trained letters.

Participants were trained to identify stimuli belonging to additional visual categories in similar computation-specific training programs. These included hand gestures (e.g., closed

TABLE 1 Participants' demographic information.

Participant	Age	Blindness cause	Light perception	Age at blindness onset	Braille reading	Handedness
FO	32	Microphthalmia	No	0	Yes (since age 5)	Right
FH	41	Leber's disease	Faint	0	Yes (since age 5)	Ambidextrous
NN	44	Retinopathy of prematurity	No	0	Yes (since age 6)	Right
PC	40	Retinopathy of prematurity	No	0	Yes (since age 6)	Right
PH	41	Retinopathy of prematurity	No	0	Yes (since age 5)	Right
FN	32	Leber's disease	Faint	0	Yes (since age 5)	Ambidextrous
DS	33	Retinopathy of prematurity	No	0	Yes (since age 6)	Right

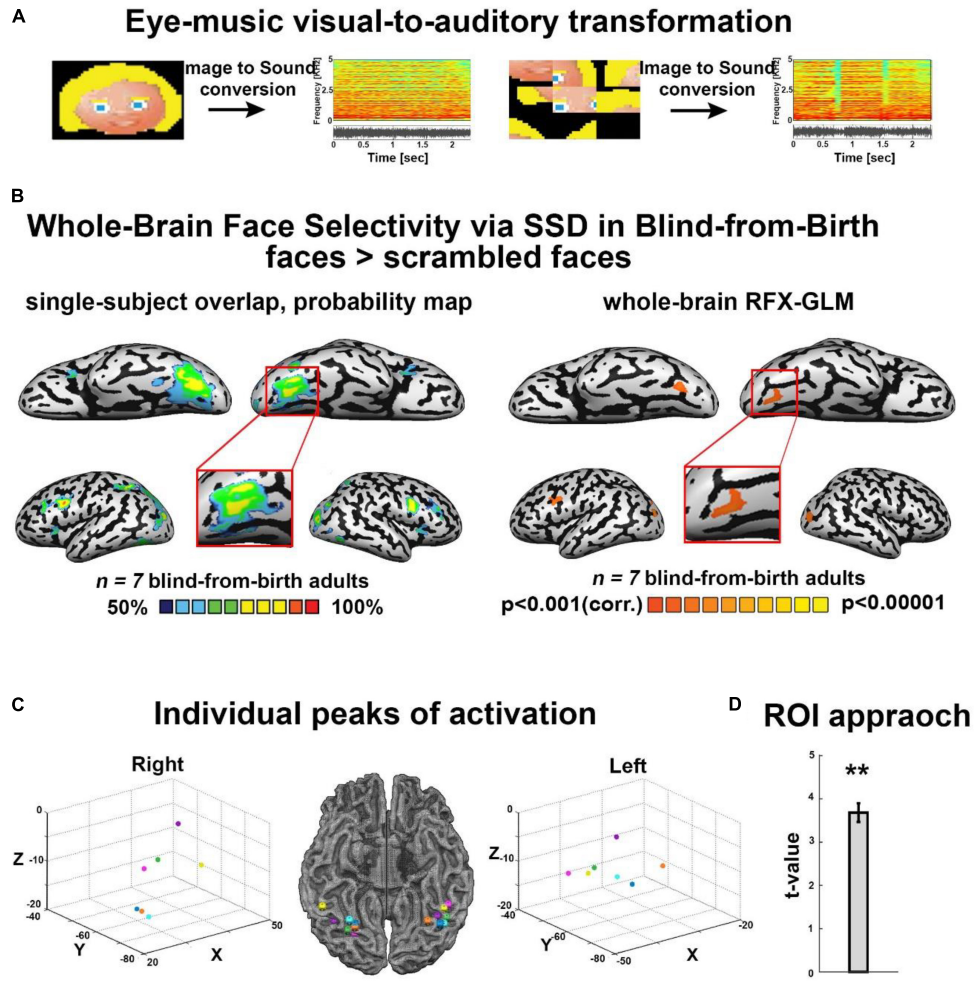

FIGURE 1
(A) Examples of some of the visual stimuli used, with their corresponding spectrograms after sonification *via* the Eye-Music visual-to-auditory SSD for trained and scrambled faces. **(B)** Trained faces > scrambled faces. Left: RFX-general linear model (GLM) analysis showed a bilateral cluster in fusiform gyrus (FG) (Talairach coordinates: right: 19, −68, −13 (zoom); left: −34, −65, −14). We also found bilateral clusters of activation in a region within the middle occipital gyrus, including the location of occipital face area (OFA) as described in the sighted (Talairach coordinates: right: 21, −94, −5; left: −33, −82, −8) and a cluster of activation in the left inferior frontal gyrus (IFG, Talairach coordinates: −45, 8, 31), two other cortical regions known to be involved in face processing. No preference for faces was observed in the auditory cortex (top panel). Right: The probability map obtained from the overlap of single participants' activations for the same contrast reveals a remarkably consistent face preference in FG. **(C)** Trained faces > Scrambled faces. Individual peaks of activation in bilateral FG for all participants are located around the canonical location of the fusiform face area (FFA) in the sighted, lateral to the mid-fusiform sulcus. **(D)** Region of interest (ROI) approach: significant preference for trained faces > scrambled faces within the canonical location of the sighted right FFA. $^{**}P < 0.005$.

hands in a fist, fully open hands, closed fist with index, and middle finger stretched out – the three hand-gestures used in the game "rock, paper, and scissors"). A detailed description and results of these additional training programs will be reported more thoroughly in future publications.

Behavioral experiments

Prior to the fMRI experiment, to ensure training effectiveness and the feasibility of the tasks inside the scanner, each participant completed three behavioral tasks [results are detailed in Arbel et al. (2022)]. Briefly, the first was a *naming task* in which participants named each of the six characters learned during training. Each character was played repeatedly until participant named it (roughly within two repetitions). Each character was presented in 16 separate trials, 96 trials overall presented in random order. Each face soundscape lasted 2.5 s, the same length as the soundscape presentations in the scanner. Participants provided their responses verbally, and the experimenter entered them into the computer. The rate of correct responses was analyzed using a *t*-test against chance level (17%) (see **Supplementary Figure 2B**).

The second task was an *orientation task*. A character was repeatedly played in either the standard upright (trained) or inverted (up-side down) orientation (untrained) until participants identified the orientation (roughly within two repetitions). Participants were instructed to verbalize their answer, and the experimenter entered the results into the computer. Each character in each orientation was presented five times (five separate trials) for a total of 60 trials presented in random order. Each face soundscape lasted 2.5 s, the same length as the soundscape presentations in the scanner. The rate of correct responses was analyzed, using a *t*-test against chance level (50%) (see **Supplementary Figure 2A**).

The third task was a *new-faces task*. Each of the six trained faces, as well as each of the six untrained faces, was presented repeatedly until participants identified whether the character was familiar or unfamiliar. Untrained faces were created using visual attributes similar to those of the trained faces (see **Supplementary Figure 2A**). Participants were instructed to verbalize their response, and the experimenter entered it into the computer. Each character was presented six times (six separate trials) for a total of 72 trials presented in random order. Each face soundscape lasted 2.5 s, the same length as the soundscape presented in the scanner. The rate of correct responses was analyzed (see **Supplementary Figure 2B**) using a *t*-test against chance level (50%).

The order of tasks was always the same: first, the naming task; then, the orientation task, and finally, the new-faces task following the fMRI session, to avoid presentation of the novel faces prior to investigation of neural processes mediating face perception. All behavioral tasks were programmed with the Presentation software.

Functional magnetic resonance imaging experiments

Functional and anatomical magnetic resonance imaging acquisition

BOLD functional magnetic resonance imaging measurements were obtained in a whole-body, 3–T Magnetom Skyra scanner (Siemens, Germany). Scanning sessions included anatomical and functional imaging. Functional protocols were based on multi-slice gradient echoplanar imaging (EPI) and a 20 channel head coil. The functional data were collected under the following timing parameters: TR = 2 s, TE = 30 ms, FA = 70°, imaging matrix = 80 × 80, field of view (FOV) = 24 × 24 cm^2 (i.e., in-plane resolution of 3 mm). Twenty-nine slices with slice thickness = 4 mm and 0.4 mm gap were oriented −22° from the axial position, for complete coverage of the whole cortex while minimizing artifacts from the frontal sinus. The first 10 images (during the first baseline rest condition) were excluded from the analysis because of non-steady state magnetization.

High resolution three-dimensional anatomical volumes were collected using a 3D-turbo field echo (TFE) T1-weighted sequence (equivalent to MP-RAGE). Typical parameters were: FOV 23 cm (RL) x 23 cm (VD) x 17 cm (AP); Foldover- axis: RL, data matrix: 160 × 160 × 144 zero-filled to 256 in all directions (approx. 1 mm isovoxel native data), TR/TE = 2,300 ms/2.98 ms, flip angle = 9°.

Pre-processing functional magnetic resonance imaging data

Data analysis was performed using Brain Voyager QX 2.0.8 software package (Brain Innovation, Maastricht, Netherlands). fMRI data pre-processing steps included head motion correction, slice scan time correction, and high-pass filtering (cut-off frequency: 2 cycles/scan). No head movement beyond 2 mm was detected in the collected data; thus, all participants were included in the subsequent analyses. Functional data underwent spatial smoothing (spatial Gaussian smoothing, full width at half maximum = 6 mm) to overcome inter-subject anatomical variability within and across experiments. Functional and anatomical datasets for each subject were first aligned (co-registered) and then transformed to fit the standardized Talairach space (Talairach and Tournoux, 1988).

Functional imaging experiments

Block-design experiment, modulated faces

First, to isolate the neural network recruited for auditory (Eye Music SSD) face recognition, we conducted a block-design experiment using four sets of face stimuli: condition a, *trained faces*; condition b, *trained faces in the untrained inverted orientation* (inverted faces); condition c, *entirely new, untrained faces* (new faces); condition d, *scrambled faces*. Condition a, trained faces, comprised six colorful faces participants learned to identify during training. In condition b, inverted faces, each of the six trained faces was sonified using EyeMusic in its untrained, inverted (upside down) orientation. In condition c, new faces, six visually similar faces that were not introduced during training were presented. In condition d, scrambled faces, the six familiar faces were divided into nine parts, and then scrambled randomly using MATLAB. The resulting images were sonified *via* EyeMusic (see **Supplementary Figure 2A** for visual representations of all stimuli, as well as spectrograms of the soundscapes in the experiment).

The conditions were presented in a block design paradigm. The experiment was programmed using Presentation software. Each condition was repeated 6 times, in a pseudorandom order, for a total of 24 blocks. To increase data robustness, we collected data over 4 runs using the following design. In each block, two different stimuli belonging to the same experimental condition were displayed, each lasting 5 s (two consecutive repetitions of 2.5 s per stimulus), followed by a response interval of 2 s. Each block started with an auditory cue indicating the tested

category which lasted for 2 s (trained faces, inverted, new, and scrambled). Participants were instructed to listen carefully to the soundscapes and to provide their responses using a response box at the end of both repetitions of a stimulus. Motor tasks were added to confirm participants remained engaged during the entire length of the experiment. For trained and inverted conditions, participants were instructed to identify the character. To limit the number of stimuli of each condition to three and thus allow only one response box in the scanner, two of the four runs consisted of female characters in all blocks presented, and two runs consisted of male characters in all blocks presented. Each block lasted 16 s and was followed by a 10 s rest interval. New faces could not be asked to be directly identified, as they were introduced to participants for the first time during training. Thus, participants were instructed to listen carefully to each soundscape; to control for motor response and to ensure that participants paid attention to the shape characteristics of the presented soundscapes, we used a vision-related task: if they could identify yellow features, they were instructed to press 1, if not, 2. For scrambled faces, participants were instructed to closely attend to the auditory stimuli. Additionally, to ensure engagement and attendance to these stimuli, as well as a motor control, they were also instructed to press any response key at the end of each stimulus presentation.

Before entering the scanner, participants were familiarized with the tasks inside the scanner, especially concerning the response box, to make sure the response mapping was fully understood by all. Digital auditory soundscapes were generated on a PC, played on a stereo system, and transferred binaurally to the subjects through a pneumatic device and silicone tubes into commercially available noise shielding headphones.

Visual categories experiments

Event-related experiment

Stimuli from three categories were included. Faces: soundscapes of the three male trained characters. Written words: soundscapes of three 3-letter words presented in a novel auditory orthography designed for EyeMusic compatibility. Hand gestures: soundscapes of three trained hand gestures were included in the experiment, taken from the paper-rock-scissors game: a hand featuring the gesture of a "rock" (fist), a gesture of "paper" (open hand), and "scissors" (two straight fingers, other fingers in a fist). The conditions were presented in an event-related paradigm. The experiment was programmed using Presentation software. Each trial consisted of two repetitions of a stimulus, lasting 2.5 s each, followed by a rest interval of 11 s.

Participants were instructed to covertly classify each of the stimuli as belonging to the face, words or hand-gesture category and to identify each exemplar (i.e., identify the specific face character, read the specific word or identify the specific hand-gesture presented). The experiment consisted of two identical runs. Over the two runs, each stimulus was repeated 10 times, for a total of 30 trials per category.

Block design experiment

The same nine stimuli from the above experiment were included, together with three soundscapes of scrambled images of houses as control stimuli, presented in a block design. The experiment was programmed using Presentation software.

In each block, two different stimuli of the same condition were presented, each lasting 5 s (two consecutive repetitions of 2.5 s per stimulus), followed by a response interval of 2 s. Each block started with an auditory cue indicating tested category (faces, words, hand gestures) lasting 2 s. All blocks lasted 16 s and were followed by a 10 s rest interval. Participants were instructed to identify each stimulus and provide their responses using a response box after listening carefully. Before entering the scanner, all participants were familiarized with the stimulus-finger mapping. For the "scrambled" condition participants were instructed to press randomly, for a motor response.

Data were pooled for analysis across block and event-related designs for the "visual categories" experiments to increase the data's robustness.

Human voice localizer

To localize the temporal-voice area (TVA) in our congenitally blind participants and explore possible ventral stream activations in response to human voices, we used the seminal fMRI voice localizer introduced by Belin (for details, see Belin et al., 2000; Pernet et al., 2015). In brief, the 10 min localizer contains blocks of vocal and non-vocal sounds in similar power spectra, allowing direct comparison of the two categories while avoiding auditory sampling bias. Vocal blocks contain human vocal sounds from different speakers, speech sounds and non-speech sounds (i.e., emotional and neutral sounds, such a cough). Non-vocal sounds contain natural sounds (e.g., wind), animals (e.g., sea waves), man-made sources (e.g., cars), and classical musical instruments (e.g., bells, harps). Each block lasted 20 s with 10 s of silence between consecutive blocks.

Quantification and statistical analysis

Probability mapping

To probe the anatomical consistency of face-specific regions among blind participants, we used overlap probability mapping. For each participant, we obtained individual activation maps for the specific contrast (Face > Scramble; Voice > Natural sounds; Faces > Baseline), with a threshold of $p < 0.001$ before correction, then corrected for multiple comparison using the spatial extent method based on the theory of Gaussian random fields (Friston et al., 1994; Forman et al., 1995). This was done based on the Monte Carlo stimulation approach, extended to 3D datasets using the threshold size plug-in for BrainVoyager QX with $p < 0.05$. Then, we computed the overlap probability. This was a way to investigate the consistency of activations across participants, as this analysis provided the percentage of

participants who showed a given active voxel in the specific contrast of interest.

Whole-brain general linear model analysis

To compute statistical maps, we applied a general linear model (GLM) using predictors convoluted with a typical hemodynamic response function (Friston et al., 1999). Across-subject statistical maps were calculated using hierarchical random-effects model analysis (Friston et al., 1999). All GLM contrasts between two or more conditions included an additional comparison of the first conditions of the subtraction to baseline (rest times between the epochs), to ensure only positive BOLD changes would be included in the analysis. The minimum significance level of all results obtained using GLM analysis was set to $p < 0.001$ before correction, and then corrected for multiple comparisons to $p < 0.05$ using a cluster-size threshold adjustment for Monte Carlo simulation approach extended to 3D datasets, using the threshold size plug-in Brain Voyager QX (Forman et al., 1995). The minimum cluster size for the contrast Face > Scramble was 30 voxels. The minimum cluster size for the contrast Face > Words was 23 voxels. The minimum cluster size for the contrast Human voices > Natural sounds was 20 voxels.

Whole-brain parametric general linear model analyses

To find regions showing modulated response to faces due to face novelty and change in orientation, we conducted a whole-brain parametric analysis. Parametric modulation analysis is used to identify modulations in brain activation in response to consistent variations in stimuli belonging to the same group of objects (Büchel et al., 1998; Wood et al., 2008; Eck et al., 2013).

Each of the four conditions (trained faces, inverted faces, new faces, and scrambled faces) was assigned a predictor value used as a regressor in GLM analysis. All predictors were convoluted with a typical hemodynamic response function (Friston et al., 1999). This analysis was carried out twice. First, we used ordinal weights based on objective experience with the specific stimulus type: trained faces, followed by inverted and untrained faces (both untrained), followed by scrambled faces as a control. Second, weights were assigned to match the ratio of activation as reported in the literature for sighted individuals who perceive faces visually. The ratio of BOLD signal change between familiar faces and scrambled faces was calculated from Kanwisher et al. (1997) to be 3.2. The ratio of BOLD signal change between faces and inverted faces was calculated from Yovel and Kanwisher (2005) to be 1.23. The predictor weight for new faces received the same value as inverted faces in both analyses, following the hypothesis that strength of activation for novel faces will follow experience-related predictions.

To obtain regions showing not only face-related modulations but also differential activations in relation to change in orientation and face familiarity, we applied a conjunction (AND) condition, comprising the parametrically modulated condition and the "main" unmodulated face activation.

All parametric analyses were reported using a threshold of $p < 0.005$ before correction (Eck et al., 2013) (see **Supplementary Figure 3A** for results with $p < 0.001$), and then corrected for multiple comparisons using a cluster-size threshold adjustment for the Monte Carlo simulation approach extended to 3D datasets, using the threshold size plug-in Brain Voyager QX at $p < 0.05$ (Forman et al., 1995). The minimum cluster size for the parametric modulation using ordinal weights based on objective experience was 59 voxels, and the minimum cluster size for the analysis using literature-based weights was 57 voxels.

Single-subject fusiform gyrus peaks

To assess the individual variability of fusiform gyrus recruitment for auditory SSD face processing, and to ensure the peak of the activation in the ventral visual stream was indeed in the fusiform gyrus, we extracted the peak activation of each participant in the ventral visual stream, bilaterally for the contrast Trained faces > Scrambled faces. For demonstration purposes, a 6 mm sphere was created around these peaks and then plotted on a 3D graph. Results were also projected on a 3D brain.

Region of interest analysis

First, to investigate the preference for auditory faces over scrambled faces within the location of the right FFA in sighted individuals, we created a 6 mm sphere ROI around its canonical coordinates (Talairach coordinates: 40, −55, −10 (Kanwisher et al., 1997). Activation parameter estimates and *t*-values were sampled from this ROI in a group-level random-effects analysis. Second, to further investigate the results we obtained from the category experiments, namely to clarify the properties of activation in our FFA-like face-responding cluster in face versus other visual categories, we created a 6 mm sphere ROI around the peak of maximal overlap in the right fusiform gyrus in the probabilistic map obtained from the contrast Faces > Baseline, computed from the block design experiment on face-related modulations. This peak represented 100% overlap for face soundscapes, meaning that all participants showed activation for faces in this location (see **Supplementary Figure 4B**). Within this cluster, we extracted the average beta value per condition (faces, words, hand gestures). We first calculated the individual average activation for each of the three categories and then averaged them across the group, over both block and event-related experiments containing the three visual categories.

ANCOVA model

To explore the relationship between neural response and behavioral performance, we performed a whole-brain ANCOVA model. An average beta-value map for each participant resulting from the contrast upright faces > baseline across all face

blocks was created. Beta values were then correlated with the corresponding individual behavioral identification performance for upright faces (average of percent correct across blocks). Due to technical issues resulting in loss of behavioral data from one participant, leading to a low number of participants in the analysis, results are reported uncorrected for multiple comparisons with $p < 0.05$.

Visualization of the results

For representational purposes, cortical reconstruction included the segmentation of the white matter using a grow-region function embedded in the Brain Voyager QX 2.0.8 software package. The cortical surface was then inflated. Group results were superimposed on a 3D cortical reconstruction of a Talairach normalized brain (Talairach and Tournoux, 1988).

Results

Face preferences in fusiform gyrus and its modulation by face properties

First, we analyzed the results of the block-design experiment containing blocks of trained cartoon faces, scrambled faces, untrained inverted faces, and entirely new faces (**Supplementary Figure 1**). fMRI results revealed face-shape preference in the fusiform gyrus (FG) largely resembling typical face processing as documented in the sighted. First, as shown in **Figure 1B**, we investigated the cross-subject overlap probability map created from the individual activation maps for the contrast Trained faces > Scrambled faces. This analysis aimed at assessing the anatomical consistency of activations across participants, and revealed bilateral FG activations across all individual subjects (**Figure 1B**), with activation peaks located lateral to the mid fusiform sulcus (**Figure 1C**). In addition, this analysis also revealed across-participants anatomically consistent bilateral clusters of activation in a region within the middle occipital gyrus, including the location of OFA as identified in the sighted, i.e., a core region of the face network, and a cluster of activation in the left IFG, another region implicated in face processing (**Figure 1B**). We also tested the same contrast again, this time using whole-brain RFX-GLM analysis. This result showed compatible results, namely, bilateral recruitment of FG and of the middle occipital sulcus, again including the location of OFA. Finally, to assess the dependency of our observed activations with the behavioral performance inside the scanner during the face identification task, we applied an ANCOVA model. Specifically, we conducted a whole-brain analysis correlating individual neural activation for upright-face blocks, with the individual success rate in upright-faces identification (see section "Materials and methods"). This analysis revealed a trend of stronger correlation between neural activation and behavioral performance in the fusiform gyrus only, in close proximity to the FG recruitment for the contrast of upright faces > scrambled faces (**Supplementary Figure 4C**).

Second, to explore the anatomical relationship between face-responsive activation in the blind and the face-responsive activation reported in the sighted, we conducted an ROI-GLM analysis using the canonical coordinates of the right FFA (see section "Materials and methods"; Talairach coordinates of ROI peak: 40, −55, −10). Results for the contrast Trained Faces > Scrambled Faces showed a significant recruitment for face soundscapes in our group of congenitally blind participants, within this defined ROI (**Figure 1D**).

Third, we investigated the extent to which FFA-like activations are modulated by untrained changes in orientation (upright/inverted faces) or by face novelty (trained/entirely new faces) as in the sighted. Whole-brain analyses for the direct contrasts between these conditions did not yield fusiform gyrus activations. However, when using a more permissive threshold, we observed recruitment of the right FG for trained faces versus novel faces (**Supplementary Figure 3E**), while the contrast of upright trained faces over inverted faces did not show any significant activation in the fusiform gyrus. Interestingly, this latter contrast yielded a bilateral activation of the sub-insular cortex, a region that has been suggested to be involved in the processing of configural aspects of face perception in the sighted brain (see **Supplementary Figures 3C,D,F**, for the results of inverted and novel faces vs scrambled faces). Importantly, however, when we performed a whole-brain rank-order parametric analysis on these data, we observed a bilateral cluster peaking in the FG which was maximally activated by trained faces, followed by inverted and untrained faces, and then by scrambled faces – in other words, a modulation resembling face-preference properties reported in the sighted brain (**Figure 2A**). These results were replicated when we performed the same analysis using weights derived from the literature (**Supplementary Figure 4A**).

Faces versus other categories

Next, we tested whether our reported FFA-like preference for face shapes was maintained when faces were contrasted with other object categories: words and hand gestures, also conveyed *via* SSD and trained in parallel to faces. As seen in **Figure 2B**, the whole-brain RFX-GLM analysis comparing activations for SSD-trained faces to activations for SSD-trained written words showed a cluster of significant preference for faces, with a whole-brain peak in the right FG. A second peak of activation was in an anatomical location near the location of the right OFA. Importantly, these results exclude the possibility that the FFA-like activations resulted mainly from acquired experience in perceiving shapes belonging to a novel set of stimuli.

In addition, the direct contrast of SSD-conveyed faces and hand gestures showed no face preference in FG. However, beta

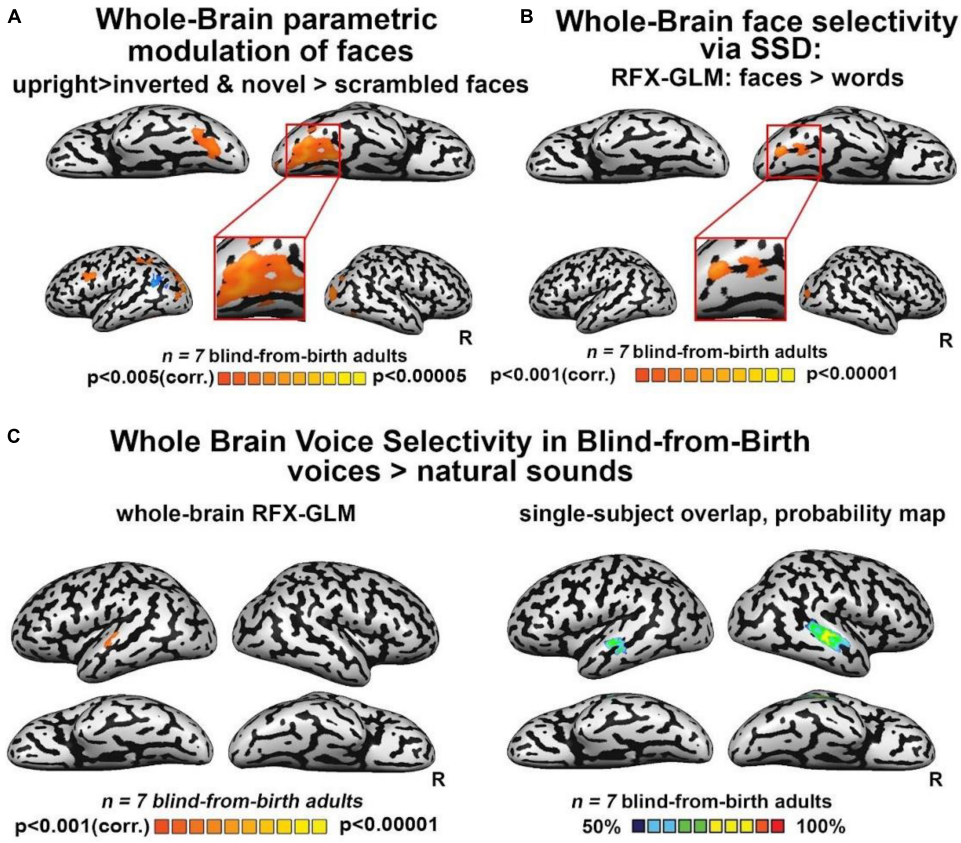

FIGURE 2
(A) Whole-brain parametric general linear model (GLM) shows that bilateral clusters in fusiform gyrus (FG) are maximally activated by trained faces, then by face orientation and face novelty, and last by scrambled faces. A similar modulation was observed also for occipital face area (OFA) and inferior frontal gyrus (IFG), two other cortical regions known to be involved in face processing. **(B)** Whole-brain RFX-GLM with the contrast Faces > Words shows recruitment of the right FG (Talairach coordinates of peak 31, −57, −16), together with a cluster in the right middle occipital gyrus, including OFA, another cortical region known to prefer face-related information. **(C)** Human voices > natural sounds. Left: RFX-GLM analysis shows the expected recruitment of the left superior temporal gyrus (Talairach coordinates: −60, −19, 10), compatible with the known location of the TVA but crucially, no recruitment of FG. Right: The probability map obtained from the overlap of single participants' activations for the same contrast, reveals consistent activations in the bilateral TVA but crucially, no activation in the ventral visual stream nor in FG.

values for the three conditions (faces, words, hand gestures) obtained from an independent FFA-like cluster (see section "Materials and methods"), revealed a trend of activation: the FFA-compatible region was maximally activated by faces, then by hand gestures, and last by words (**Supplementary Figure 4B**). These results suggest that similarly to what has been reported for the sighted, the lateral posterior fusiform gyrus of congenitally blind adults responds to animate objects.

Finally, to characterize the response of our blind participants to human voices, we employed the seminal human-voice localizer protocol used to unravel voice specializations in the healthy population (see section "Materials and methods"). As seen in **Figure 2C**, mirroring what is typically documented in the sighted, whole-brain RFX-GLM analysis showed activations in the TVA for the contrast Voices > Natural sounds (see also **Supplementary Figure 3B**). Crucially, no voice preference emerged in FG or in any other location compatible with a known face-responsive region in the sighted. The cross-subject overlap probability map created from all the individual participants' activations for the same contrast (**Figure 2C**) confirmed there were no anatomically consistent activations in the ventral stream of our congenitally blind participants for human voices. These results indicate that the activation in the visual cortex elicited by whole-face soundscapes is not due to high-level interpretation of person-specific information or human-generated sounds.

Discussion

This study explored the properties of face-shape preference in the ventral visual stream of the congenitally blind, following tailored face training *via* the atypical auditory modality. Specifically, a group of SSD-expert congenitally blind adults learned to perceive cartooned faces in a ∼12 h unique training

program aimed at conveying faces auditorily *via* soundscapes, in a shape, spatial layout, and color-preserving manner, using a visual-to-auditory SSD (Arbel et al., 2022). Following training, the ventral visual stream in the blind brain showed preference for faces versus scrambled sounds in the fusiform gyrus as well as a parametrically modulated preference for trained SSD-faces over inverted, novel, and scrambled faces, also peaking in the fusiform gyrus. The same preference also emerged when faces were contrasted with stimuli belonging to another category of newly learned SSD-stimuli (reading words composed of letters from an entirely new alphabet), even though both categories were trained for a comparable time (**Figure 2B**). In contrast to the visual cortex, no modulation of the auditory cortex was observed in any of the analyses suggesting that participants attended all stimuli similarly. Importantly, activations in all the aforementioned analyses, also included a cluster within the middle occipital gyrus, including the location of the sighted OFA, namely, another region of the core face network. This suggests that acquired experience in recognizing exemplars of stimuli belonging to a novel category of objects cannot entirely explain the pattern of reported FG activation.

In addition, in contrast to the preference of faces over words, the ventral visual stream in the blind brain showed no preference for faces over hand gestures. Hand gestures represent another animate category of objects for which, like faces, blind people have little perceptual experience through their remaining sensory modalities (although they can access them to some extent *via* proprioceptive cues). While the direct contrast between trained faces and hand gestures did not yield any preference within the ventral visual stream, ROI analyses showed a trend for a preference in the blind right ventral stream for faces, as faces activated it the most, followed by hand gestures and words (**Supplementary Figure 3G**), similarly to the haptic domain (Murty et al., 2020). These results fit well with accumulating evidence on the sighted brain suggesting that bodies and faces share brain representations in the fusiform gyrus, thus allowing the building of a unified whole-person representation, leading to the perception of naturalistic stimuli (Kaiser et al., 2014; Fisher and Freiwald, 2015). Our results indicate the same process might be preserved and at work in the blind brain, thereby suggesting that such integrated body-faces representations are sensory-independent. Moreover, our results highlight that their emergence is not constrained to the exposure to visual inputs early in life or across the lifespan. Future studies may further investigate this intriguing conclusion. For instance, they might investigate through MVPA whether body-responsive and face-responsive voxels within this region are dissociable in congenitally blind adults, as has been demonstrated in the sighted (Kim et al., 2014). Our results strengthen the initial conclusions already suggesting that animate and not only inanimate object representations are retained in the blind ventral "visual" stream (Bi et al., 2016; Murty et al., 2020), with properties largely resembling typical specializations observed in the sighted brain.

Finally, we found no recruitment in the fusiform gyrus or in any other location compatible with a known face-responsive region in the sighted brain, to human voices, the main person-identification method used by blind adults in everyday life (**Figure 2C**). These results excludes the possibility that the observed FG activations were driven by general person-specific associations rather than by the processing of whole-face SSD-conveyed shapes and are in line with previous results (Hölig et al., 2014; Dormal et al., 2018).

Taken together, these results strengthen the emerging notion that brain specializations are driven by predispositions to process sensory-independent computations rather than unisensory-specific inputs, as classically conceived (James et al., 2002; Amedi et al., 2007, 2017; Ricciardi et al., 2007; Kupers et al., 2010; Collignon et al., 2011; Reich et al., 2011; Wolbers et al., 2011; Ptito et al., 2012; Striem-Amit et al., 2012; Striem-Amit and Amedi, 2014). It has recently been proposed that this computation-selective and sensory-independent organization originates from two non-mutual exclusive principles: (1) local tuning to sensory-independent task/computation distinctive features (e.g., a predisposition of FFA to process sensory-independent face-distinctive shapes); (2) preserved network connectivity (e.g., preserved connection between FFA and the rest of the face-network) (Hannagan et al., 2015; Heimler et al., 2015; Amedi et al., 2017).

Furthermore, the results argue against some aspects of the classic assumptions that stem from the seminal studies by Hubel and Wiesel (Hubel and Wiesel, 1962; Wiesel and Hubel, 1963, 1965) positing that the key driver of the emergence of typical brain specializations is the exposure to unisensory-specific inputs during early infancy, i.e., during specific time windows termed "critical/sensitive-periods" when the brain is particularly plastic (Knudsen, 2004). Indeed, our findings suggest that the potential to process specific computations in specific cortical regions may not vanish with the closure of critical periods but might be re-awakened at any time across the lifespan, if computation-tailored training is provided (Heimler and Amedi, 2020). Specifically, the current results are compatible with the conclusion that our tailored SSD training may have guided/facilitated the recruitment of typical face regions in the deprived visual brain *via* auditory inputs by relying on the two non-mutually exclusive – and possibly hard-wired – principles proposed above as underlying the emergence of computation-selective and sensory-independent cortical organization. In the case of face processing, the existence of hard-wired face-selective regions is supported by studies of infants showing face preference and discrimination abilities at birth (Turati et al., 2006), together with hard-wired connectivity within the face-related network (Buiatti et al., 2019; Kamps et al., 2020), possibly even suggesting a genetic component of face-related processing, as highlighted by studies with homozygote

twins (Polk et al., 2007; Wilmer et al., 2010). The connectivity properties of the whole face network still need to be explored in congenitally blind adults, as do the connections after dedicated face training (for evidence of preserved network-connectivity for other SSD-trained visual categories, see Abboud et al., 2014; Striem-Amit and Amedi, 2014. Another open issue concerns the pathway through which auditory information reaches the deprived visual cortex. Future studies should disentangle whether this is mediated by top-down connections from higher-order regions or *via* direct audio-visual connections (Collignon et al., 2013; Sigalov et al., 2016), or by bottom-up projections from sub-cortical regions (Müller et al., 2019).

Importantly, these results also carry implications for sensory recovery. While some studies on visually restored patients have reported lack of face selectivity even years after sight recovery (Fine et al., 2003; Röder et al., 2013; Grady et al., 2014), none has provided patients with a tailored, computation-oriented training aimed at teaching face-shape recognition.

Evidence in favor of the beneficial role of (multisensory) computation-specific training in sensory recovery is starting to emerge (i.e., pairing the restored sense, e.g., vision, with a familiar one, and audition). This evidence, mostly coming from animals, documents more efficient computation-selective neural recruitment in sensory restored individuals who have undergone multisensory computation-oriented training (DeGutis et al. (2007) and Isaiah et al. (2014); for comparable results for partial deprivation, see Jiang et al., 2015). This approach might be a promising rehabilitative venue to further tune face classification abilities developed *via* natural experience in visually restored patients (Gandhi et al., 2017). We suggest that such multisensory training approach might maximize the restoration outcomes, as the familiar sense (e.g., audition) might guide the restored sense (e.g., vision) to recruit its typical sensory cortex by promoting a network adaptability process (Heimler et al., 2015; Heimler and Amedi, 2020; Maimon et al., 2022). Future studies may more systematically investigate this intriguing hypothesis and track the extent to which such types of training might indeed aid the (re) establishment of typical cortical recruitment by the restored visual input, in line with the predictions of the computational-selective cortical organization.

While some face preference activations observed in our congenitally blind participants were largely similar to typical results in the sighted population, there were also some differences. First, preference in the fusiform gyrus was bilateral rather than right-lateralized as classically reported (Kanwisher et al., 1997; **Figure 1**). A possible explanation of this difference is our congenitally blind participants' lack of experience in the processing of whole faces *via* audition (∼12 h SSD training), i.e., we cannot exclude that with additional experience the activation will become right lateralized. Another possibility is that these bilateral FG activations might relate to the reduced left-lateralization for language repeatedly documented in the blind population (Lane et al., 2015, 2017; Pant et al., 2020). Indeed, previous studies showed reduced face-related lateralization in other populations with reduced language-lateralization, such as ambidextrous or left-handed individuals (Badzakova-Trajkov et al., 2010; Willems et al., 2010; Bukowski et al., 2013; Dundas et al., 2015; Gerrits et al., 2019). Specifically, several accounts currently propose that face and language processing compete for the same representational space in the human brain, and faces become right lateralized as a consequence of left regions being recruited by reading due to proximity to the rest of the language areas (Dundas et al., 2015).

Finally, our results showed preserved face preference in the blind brain not only in the fusiform gyrus, but also in other regions known to belong to the face network. Specifically, we showed consistent activations in all our main contrasts in the middle occipital gyrus, including a region compatible with OFA (**Figures 1B, 2A,B**), which is a core region of the face network and it is described as involved in the perceptual processing of facial features (Kanwisher et al., 1997; Gauthier et al., 2000b; Rossion et al., 2003; Pitcher et al., 2011). Further investigations into the roles of the FFA and OFA in people who are congenitally blind are still required to assess more systematically the similarities as well as the potential differences between blind and sighted brains regarding specific properties of both nodes. For instance, the role of both regions in the identification of complete face-images (i.e., holistic processing) vs. facial features (i.e., parts-based processing), as evidenced by the increased sensitivity documented in the sighted brain for the scrambling of faces in the FFA compared with OFA (Lerner et al., 2001). Future studies should also explore aspects directly related to cognitive processes mediating auditory face identification *via* sweep-line algorithms such as the present SSD, namely whether these processes involve object-based mechanisms or rather approaches more specific to visual faces perception such as holistic face processing and the extent to which specific characteristics of SSD-mediated processing influence recruitment of face-related regions within the face-network.

In contrast to observed recruitment of the OFA, we did not observe any activation in the STS another core face region, which is known to process the changeable aspects of faces, such as expressions (Phillips et al., 1997), direction of eye-gaze, and lip movements (Puce et al., 1998; Allison et al., 2000; Haxby et al., 2000; Lahnakoski et al., 2012; Zhen et al., 2015). Notably, however, these computations were not part of our training program nor where taken into consideration in the behavioral tasks performed by our participants in the scanner. Future studies addressing these specific aspects of face perception may provide crucial insight into possible constraints of visual experience on the development of face-specific cortical regions and on the face network as a whole.

While the present work investigated auditory face perception in congenitally blind for the first time, the novelty of the chosen stimuli imposes some limitations on

the experimental design. First, due to the presentation of novel images during the experiment, participants could not perform the exact same identification task for all presented stimuli. Second, while we investigated neural responses following extensive face training, we are unable to attest to the role of the fusiform gyrus and the rest of the face-identification network in congenitally blind, prior to any face training. Future investigations could further explore the effect of training on the engagement of the face-processing network, the potential role of "face imagination" or the abstract representation congenitally blind have of faces prior to face training, as well as further balance task and task-free designs to further define the properties of the neural face network in the congenital absence of vision.

Taken together, our results show that the ventral visual stream of congenitally blind adults can be recruited by face processing *via* non-traditional, non-visual, sensory information acquired during adulthood, and retain some of its properties despite life-long visual deprivation. Our results provide evidence supporting the presence of a predisposition for sensory-independent and computation-specific processing in the human brain. We show that this predisposition is retained even in life-long sensory deprivation when a given category of stimuli, face-shapes in the current case, has been largely inaccessible across the lifespan through the available sensory inputs. Our results thus have implications for visual recovery by suggesting that such predispositions can be (re) awakened in adulthood if tailored computation-oriented training is provided.

Data availability statement

The raw data supporting the conclusions of this article will be made available upon request to the authors, without undue reservation.

Ethics statement

The studies involving human participants were reviewed and approved by the Hadassah Medical Center Ethics Committee and the Hadassah Helsinki Committee. The patients/participants provided their written informed consent to participate in this study.

Author contributions

RA and AA conceived and designed the experiments. RA performed the experiments. AA and BH contributed to the data analysis supervision and guidance and analyzed the data. RA, BH, and AA wrote the manuscript. All authors contributed to the article and approved the submitted version.

Conflict of interest

The authors declare that the research was conducted in the absence of any commercial or financial relationships that could be construed as a potential conflict of interest.

Publisher's note

All claims expressed in this article are solely those of the authors and do not necessarily represent those of their affiliated organizations, or those of the publisher, the editors and the reviewers. Any product that may be evaluated in this article, or claim that may be made by its manufacturer, is not guaranteed or endorsed by the publisher.

Supplementary material

The Supplementary Material for this article can be found online at: https://www.frontiersin.org/articles/10.3389/fnins.2022.921321/full#supplementary-material

References

Abboud, S., Hanassy, S., Levy-Tzedek, S., Maidenbaum, S., and Amedi, A. (2014). EyeMusic: Introducing a "visual" colorful experience for the blind using auditory sensory substitution. *Restor. Neurol. Neurosci.* 32, 247–257. doi: 10.3233/RNN-130338

Abboud, S., Maidenbaum, S., Dehaene, S., and Amedi, A. (2015). A number-form area in the blind. *Nat. Commun.* 6:6026. doi: 10.1038/ncomms7026

Allison, T., Puce, A., and McCarthy, G. (2000). Social perception from visual cues: Role of the STS region. *Trends Cogn. Sci.* 4, 267–278. doi: 10.1016/S1364-6613(00)01501-1

Amedi, A., Hofstetter, S., Maidenbaum, S., and Heimler, B. (2017). Task selectivity as a comprehensive principle for brain organization. *Trends Cogn. Sci.* 21, 307–310. doi: 10.1016/j.tics.2017.03.007

Amedi, A., Stern, W. M., Camprodon, J. A., Bermpohl, F., Merabet, L., Rotman, S., et al. (2007). Shape conveyed by visual-to-auditory sensory substitution activates the lateral occipital complex. *Nat. Neurosci.* 10, 687–689. doi: 10.1038/nn1912

Arbel, R., Heimler, B., and Amedi, A. (2020). The sound of reading: Color-to-timbre substitution boosts reading performance

via OVAL, a novel auditory orthography optimized for visual-to-auditory mapping. *PLoS One* 15:e0242619. doi: 10.1371/journal.pone.0242619

Arbel, R., Heimler, B., and Amedi, A. (2022). Congenitally blind adults can learn to identify face-shapes via auditory sensory substitution and successfully generalize some of the learned features. *Sci. Rep.* 12:4330. doi: 10.1038/s41598-022-08187-z

Avidan, G., Tanzer, M., Hadj-Bouziane, F., Liu, N., Ungerleider, L. G., and Behrmann, M. (2014). Selective dissociation between core and extended regions of the face processing network in congenital prosopagnosia. *Cereb. Cortex* 24, 1565–1578. doi: 10.1093/CERCOR/BHT007

Badzakova-Trajkov, G., Häberling, I. S., Roberts, R. P., and Corballis, M. C. (2010). Cerebral asymmetries: Complementary and independent processes. *PLoS One* 5:e9682. doi: 10.1371/journal.pone.0009682

Belin, P., Zatorre, R. J., Lafaille, P., Ahad, P., and Pike, B. (2000). Voice-selective areas in human auditory cortex. *Nature* 403, 309–312. doi: 10.1038/35002078

Benetti, S., Van Ackeren, M. J., Rabini, G., Zonca, J., Foa, V., Baruffaldi, F., et al. (2017). Functional selectivity for face processing in the temporal voice area of early deaf individuals. *Proc. Natl. Acad. Sci. U.S.A.* 114, E6437–E6446. doi: 10.1073/pnas.1618287114

Bi, Y., Wang, X., and Caramazza, A. (2016). Object domain and modality in the ventral visual pathway. *Trends Cogn. Sci.* 20, 282–290. doi: 10.1016/j.tics.2016.02.002

Büchel, C., Holmes, A. P., Rees, G., and Friston, K. J. (1998). Characterizing stimulus-response functions using nonlinear regressors in parametric fMRI experiments. *Neuroimage* 8, 140–148. doi: 10.1006/nimg.1998.0351

Buiatti, M., Di Giorgio, E., Piazza, M., Polloni, C., Menna, G., Taddei, F., et al. (2019). Cortical route for facelike pattern processing in human newborns. *Proc. Natl. Acad. Sci. U.S.A.* 116, 4625–4630. doi: 10.1073/pnas.1812419116

Bukowski, H., Dricot, L., Hanseeuw, B., and Rossion, B. (2013). Cerebral lateralization of face-sensitive areas in left-handers: Only the FFA does not get it right. *Cortex* 49, 2583–2589. doi: 10.1016/j.cortex.2013.05.002

Collignon, O., Dormal, G., Albouy, G., Vandewalle, G., Voss, P., Phillips, C., et al. (2013). Impact of blindness onset on the functional organization and the connectivity of the occipital cortex. *Brain* 136, 2769–2783. doi: 10.1093/brain/awt176

Collignon, O., Vandewalle, G., Voss, P., Albouy, G., Charbonneau, G., Lassonde, M., et al. (2011). Functional specialization for auditory-spatial processing in the occipital cortex of congenitally blind humans. *Proc. Natl. Acad. Sci. U.S.A.* 108, 4435–4440. doi: 10.1073/pnas.1013928108

DeGutis, J. M., Bentin, S., Robertson, L. C., and D'Esposito, M. (2007). Functional plasticity in ventral temporal cortex following cognitive rehabilitation of a congenital prosopagnosic. *J. Cogn. Neurosci.* 19, 1790–1802. doi: 10.1162/jocn.2007.19.11.1790

Dormal, G., Pelland, M., Rezk, M., Yakobov, E., Lepore, F., and Collignon, O. (2018). Functional preference for object sounds and voices in the brain of early blind and sighted individuals. *J. Cogn. Neurosci.* 30, 86–106. doi: 10.1162/jocn_a_01186

Dundas, E. M., Plaut, D. C., and Behrmann, M. (2015). Variable left-hemisphere language and orthographic lateralization reduces right-hemisphere face lateralization. *J. Cogn. Neurosci.* 27, 913–925. doi: 10.1162/jocn_a_00757

Eck, J., Kaas, A. L., and Goebel, R. (2013). Crossmodal interactions of haptic and visual texture information in early sensory cortex. *Neuroimage* 75, 123–135. doi: 10.1016/j.neuroimage.2013.02.075

Fine, I., Wade, A. R., Brewer, A. A., May, M. G., Goodman, D. F., Boynton, G. M., et al. (2003). Long-term deprivation affects visual perception and cortex. *Nat. Neurosci.* 6, 915–916. doi: 10.1038/nn1102

Fisher, C., and Freiwald, W. A. (2015). Whole-agent selectivity within the macaque face-processing system. *Proc. Natl. Acad. Sci. U.S.A.* 112, 14717–14722. doi: 10.1073/pnas.1512378112

Forman, S. D., Cohen, J. D., Fitzgerald, M., Eddy, W. F., Mintun, M. A., and Noll, D. C. (1995). Improved assessment of significant activation in functional magnetic resonance imaging (fMRI): Use of a cluster-size threshold. *Magn. Reson. Med.* 33, 636–647. doi: 10.1002/mrm.1910330508

Friston, K. J., Holmes, A. P., Price, C. J., Büchel, C., and Worsley, K. J. (1999). Multisubject fMRI studies and conjunction analyses. *Neuroimage* 10, 385–396. doi: 10.1006/NIMG.1999.0484

Friston, K. J., Worsley, K. J., Frackowiak, R. S. J., Mazziotta, J. C., and Evans, A. C. (1994). Assessing the significance of focal activations using their spatial extent. *Hum. Brain Mapp.* 1, 210–220. doi: 10.1002/hbm.460010306

Gandhi, T. K., Singh, A. K., Swami, P., Ganesh, S., and Sinha, P. (2017). Emergence of categorical face perception after extended early-onset blindness. *Proc. Natl. Acad. Sci. U.S.A.* 114, 6139–6143. doi: 10.1073/pnas.1616050114

Gauthier, I., and Tarr, M. J. (1997). Becoming a "Greeble" expert: Exploring mechanisms for face recognition. *Vis. Res.* 37, 1673–1682. doi: 10.1016/S0042-6989(96)00286-6

Gauthier, I., Tarr, M. J., Anderson, A. W., Skudlarski, P., and Gore, J. C. (1999). Activation of the middle fusiform "face area" increases with expertise in recognizing novel objects. *Nat. Neurosci.* 2, 568–573. doi: 10.1038/9224

Gauthier, I., Skudlarski, P., Gore, J. C., and Anderson, A. W. (2000a). Expertise for cars and birds recruits brain areas involved in face recognition. *Nat. Neurosci.* 3, 191–197. doi: 10.1038/72140

Gauthier, I., Tarr, M. J., Moylan, J., Skudlarski, P., Gore, J. C., and Anderson, A. W. (2000b). The fusiform "face area" is part of a network that processes faces at the individual level. *J. Cogn. Neurosci.* 12, 495–504. doi: 10.1162/089892900562165

Gerrits, R., Van der Haegen, L., Brysbaert, M., and Vingerhoets, G. (2019). Laterality for recognizing written words and faces in the fusiform gyrus covaries with language dominance. *Cortex* 117, 196–204. doi: 10.1016/j.cortex.2019.03.010

Gobbini, M. I., and Haxby, J. V. (2007). Neural systems for recognition of familiar faces. *Neuropsychologia* 45, 32–41. doi: 10.1016/J.NEUROPSYCHOLOGIA.2006.04.015

Gougoux, F., Belin, P., Voss, P., Lepore, F., Lassonde, M., and Zatorre, R. J. (2009). Voice perception in blind persons: A functional magnetic resonance imaging study. *Neuropsychologia* 47, 2967–2974. doi: 10.1016/j.neuropsychologia.2009.06.027

Grady, C. L., Mondloch, C. J., Lewis, T. L., and Maurer, D. (2014). Early visual deprivation from congenital cataracts disrupts activity and functional connectivity in the face network. *Neuropsychologia* 57, 122–139. doi: 10.1016/J.NEUROPSYCHOLOGIA.2014.03.005

Haist, F., Adamo, M., Han Wazny, J., Lee, K., and Stiles, J. (2013). The functional architecture for face-processing expertise: FMRI evidence of the developmental trajectory of the core and the extended face systems. *Neuropsychologia* 51, 2893–2908. doi: 10.1016/J.NEUROPSYCHOLOGIA.2013.08.005

Hannagan, T., Amedi, A., Cohen, L., Dehaene-Lambertz, G., and Dehaene, S. (2015). Origins of the specialization for letters and numbers in ventral occipitotemporal cortex. *Trends Cogn. Sci.* 19, 374–382. doi: 10.1016/j.tics.2015.05.006

Haxby, J. V., Hoffman, E. A., and Gobbini, M. I. (2000). The distributed human neural system for face perception. *Trends Cogn. Sci.* 4, 223–233. doi: 10.1016/S1364-6613(00)01482-0

Haxby, J. V., Hoffman, E. A., and Gobbini, M. I. (2002). Human neural systems for face recognition and social communication. *Biol. Psychiatry* 51, 59–67. doi: 10.1016/S0006-3223(01)01330-0

Heimler, B., and Amedi, A. (2020). Are critical periods reversible in the adult brain? Insights on cortical specializations based on sensory deprivation studies. *Neurosci. Biobehav. Rev.* 116, 494–507. doi: 10.1016/j.neubiorev.2020.06.034

Heimler, B., Striem-Amit, E., and Amedi, A. (2015). Origins of task-specific sensory-independent organization in the visual and auditory brain: Neuroscience evidence, open questions and clinical implications. *Curr. Opin. Neurobiol.* 35, 169–177. doi: 10.1016/J.CONB.2015.09.001

Hölig, C., Föcker, J., Best, A., Röder, B., and Büchel, C. (2014). Brain systems mediating voice identity processing in blind humans. *Hum. Brain Mapp.* 35, 4607–4619. doi: 10.1002/hbm.22498

Hubel, D. H., and Wiesel, T. N. (1962). Receptive fields, binocular interaction and functional architecture in the cat's visual cortex. *J. Physiol.* 160, 106–154.

Isaiah, A., Vongpaisal, T., King, A. J., and Hartley, D. E. H. (2014). Multisensory training improves auditory spatial processing following bilateral cochlear implantation. *J. Neurosci.* 34, 11119–11130. doi: 10.1523/JNEUROSCI.4767-13.2014

Ishai, A. (2008). Let's face it: It's a cortical network. *Neuroimage* 40, 415–419. doi: 10.1016/J.NEUROIMAGE.2007.10.040

Ishai, A., Schmidt, C. F., and Boesiger, P. (2005). Face perception is mediated by a distributed cortical network. *Brain Res. Bull.* 67, 87–93. doi: 10.1016/J.BRAINRESBULL.2005.05.027

James, T. W., Humphrey, G. K., Gati, J. S., Servos, P., Menon, R. S., and Goodale, M. A. (2002). Haptic study of three-dimensional objects activates extrastriate visual areas. *Neuropsychologia* 40, 1706–1714. doi: 10.1016/S0028-3932(02)00017-9

Jiang, H., Stein, B. E., and McHaffie, J. G. (2015). Multisensory training reverses midbrain lesion-induced changes and ameliorates haemianopia. *Nat. Commun.* 6:7263. doi: 10.1038/ncomms8263

Kaiser, D., Strnad, L., Seidl, K. N., Kastner, S., and Peelen, M. V. (2014). Whole person-evoked fMRI activity patterns in human fusiform gyrus are accurately modeled by a linear combination of face- and body-evoked activity patterns. *J. Neurophysiol.* 111, 82–90. doi: 10.1152/jn.00371.2013

Kamps, F. S., Hendrix, C. L., Brennan, P. A., and Dilks, D. D. (2020). Connectivity at the origins of domain specificity in the cortical face and place networks. *Proc. Natl. Acad. Sci. U.S.A.* 117, 6163–6169. doi: 10.1073/pnas.1911359117

Kanwisher, N., McDermott, J., and Chun, M. M. (1997). The fusiform face area: A module in human extrastriate cortex specialized for face perception. *J. Neurosci.* 17, 4302–4311. doi: 10.1523/JNEUROSCI.17-11-04302.1997

Kilgour, A. R., and Lederman, S. J. (2002). Face recognition by hand. *Percept. Psychophys.* 64, 339–352. doi: 10.3758/BF03194708

Kim, N. Y., Lee, S. M., Erlendsdottir, M. C., and McCarthy, G. (2014). Discriminable spatial patterns of activation for faces and bodies in the fusiform gyrus. *Front. Hum. Neurosci.* 8:632. doi: 10.3389/fnhum.2014.00632

Knudsen, E. I. (2004). Sensitive periods in the development of the brain and behavior. *J. Cogn. Neurosci.* 16, 1412–1425. doi: 10.1162/0898929042304796

Konkle, T., and Caramazza, A. (2013). Tripartite organization of the ventral stream by animacy and object size. *J. Neurosci.* 33, 10235–10242. doi: 10.1523/JNEUROSCI.0983-13.2013

Kupers, R., Chebat, D. R., Madsen, K. H., Paulson, O. B., and Ptito, M. (2010). Neural correlates of virtual route recognition in congenital blindness. *Proc. Natl. Acad. Sci. U.S.A.* 107, 12716–12721. doi: 10.1073/pnas.1006199107

Lahnakoski, J. M., Glerean, E., Salmi, J., Jääskeläinen, I. P., Sams, M., Hari, R., et al. (2012). Naturalistic fMRI mapping reveals superior temporal sulcus as the hub for the distributed brain network for social perception. *Front. Hum. Neurosci.* 6:233. doi: 10.3389/fnhum.2012.00233

Lane, C., Kanjlia, S., Omaki, A., and Bedny, M. (2015). "Visual" cortex of congenitally blind adults responds to syntactic movement. *J. Neurosci.* 35, 12859–12868. doi: 10.1523/JNEUROSCI.1256-15.2015

Lane, C., Kanjlia, S., Richardson, H., Fulton, A., Omaki, A., and Bedny, M. (2017). Reduced left lateralization of language in congenitally blind individuals. *J. Cogn. Neurosci.* 29, 65–78. doi: 10.1162/jocn_a_01045

Lerner, Y., Hendler, T., Ben-Bashat, D., Harel, M., and Malach, R. (2001). A hierarchical axis of object processing stages in the human visual cortex. *Cereb. Cortex* 11, 287–297. doi: 10.1093/CERCOR/11.4.287

Maimon, A., Yizhar, O., Buchs, G., Heimler, B., and Amedi, A. (2022). A case study in phenomenology of visual experience with retinal prosthesis versus visual-to-auditory sensory substitution. *Neuropsychologia* 173:108305. doi: 10.1016/J.NEUROPSYCHOLOGIA.2022.108305

Maurer, D., Le Grand, R., and Mondloch, C. J. (2002). The many faces of configural processing. *Trends Cogn. Sci.* 6, 255–260. doi: 10.1016/S1364-6613(02)01903-4

McKone, E., Kanwisher, N., and Duchaine, B. C. (2007). Can generic expertise explain special processing for faces? *Trends Cogn. Sci.* 11, 8–15. doi: 10.1016/j.tics.2006.11.002

Meijer, P. B. L. (1992). An experimental system for auditory image representations. *IEEE Trans. Biomed. Eng.* 39, 112–121.

Müller, F., Niso, G., Samiee, S., Ptito, M., Baillet, S., and Kupers, R. (2019). A thalamocortical pathway for fast rerouting of tactile information to occipital cortex in congenital blindness. *Nat. Commun.* 10:5154. doi: 10.1038/s41467-019-13173-7

Murty, N. A. R., Teng, S., Beeler, D., Mynick, A., Oliva, A., and Kanwisher, N. (2020). Visual experience is not necessary for the development of face-selectivity in the lateral fusiform gyrus. *Proc. Natl. Acad. Sci. U.S.A.* 117, 23011–23020. doi: 10.1073/PNAS.2004607117/-/DCSUPPLEMENTAL

Pant, R., Kanjlia, S., and Bedny, M. (2020). A sensitive period in the neural phenotype of language in blind individuals. *Dev. Cogn. Neurosci.* 41:100744. doi: 10.1016/j.dcn.2019.100744

Peelen, M. V., and Downing, P. E. (2005). Selectivity for the human body in the fusiform gyrus. *J. Neurophysiol.* 93, 603–608. doi: 10.1152/jn.00513.2004

Pernet, C. R., McAleer, P., Latinus, M., Gorgolewski, K. J., Charest, I., Bestelmeyer, P. E. G., et al. (2015). The human voice areas: Spatial organization and inter-individual variability in temporal and extra-temporal cortices. *Neuroimage* 119, 164–174. doi: 10.1016/J.NEUROIMAGE.2015.06.050

Phillips, M. L., Young, A. W., Senior, C., Brammer, M., Andrew, C., Calder, A. J., et al. (1997). A specific neural substrate for perceiving facial expressions of disgust. *Nature* 389, 495–498. doi: 10.1038/39051

Pietrini, P., Furey, M. L., Ricciardi, E., Gobbini, M. I., Wu, W.-H. C., Cohen, L., et al. (2004). Beyond sensory images: Object-based representation in the human ventral pathway. *Proc. Natl. Acad. Sci. U.S.A.* 101, 5658–5663. doi: 10.1073/pnas.0400707101

Pitcher, D., Walsh, V., and Duchaine, B. (2011). The role of the occipital face area in the cortical face perception network. *Exp. Brain Res.* 209, 481–493. doi: 10.1007/s00221-011-2579-1

Polk, T. A., Park, J., Smith, M. R., and Park, D. C. (2007). Nature versus nurture in ventral visual cortex: A functional magnetic resonance imaging study of twins. *J. Neurosci.* 27, 13921–13925. doi: 10.1523/JNEUROSCI.4001-07.2007

Ptito, M., Matteau, I., Zhi Wang, A., Paulson, O. B., Siebner, H. R., and Kupers, R. (2012). Crossmodal recruitment of the ventral visual stream in congenital blindness. *Neural Plast.* 2012:304045. doi: 10.1155/2012/304045

Puce, A., Allison, T., Bentin, S., Gore, J. C., and McCarthy, G. (1998). Temporal cortex activation in humans viewing eye and mouth movements. *J. Neurosci.* 18, 2188–2199. doi: 10.1523/jneurosci.18-06-02188.1998

Reich, L., Szwed, M., Cohen, L., and Amedi, A. (2011). A ventral visual stream reading center independent of visual experience. *Curr. Biol.* 21, 363–368. doi: 10.1016/j.cub.2011.01.040

Ricciardi, E., Vanello, N., Sani, L., Gentili, C., Scilingo, E. P., Landini, L., et al. (2007). The effect of visual experience on the development of functional architecture in hMT+. *Cereb. Cortex* 17, 2933–2939. doi: 10.1093/cercor/bhm018

Röder, B., Ley, P., Shenoy, B. H., Kekunnaya, R., and Bottari, D. (2013). Sensitive periods for the functional specialization of the neural system for human face processing. *Proc. Natl. Acad. Sci. U.S.A.* 110, 16760–16765. doi: 10.1073/pnas.1309963110

Rosenthal, G., Sporns, O., and Avidan, G. (2016). Stimulus dependent dynamic reorganization of the human face processing network. *Cereb. Cortex* 27, 4823–4834. doi: 10.1093/cercor/bhw279

Rossion, B., Caldara, R., Seghier, M., Schuller, A., Lazeyras, F., and Mayer, E. (2003). A network of occipito-temporal face-sensitive areas besides the right middle fusiform gyrus is necessary for normal face processing. *Brain* 126, 2381–2395. doi: 10.1093/brain/awg241

Schwartz, L., and Yovel, G. (2016). The roles of perceptual and conceptual information in face recognition. *J. Exp. Psychol. Gen.* 145, 1493–1511. doi: 10.1037/xge0000220

Shultz, S., and McCarthy, G. (2014). Perceived animacy influences the processing of human-like surface features in the fusiform gyrus. *Neuropsychologia* 60, 115–120. doi: 10.1016/j.neuropsychologia.2014.05.019

Sigalov, N., Maidenbaum, S., and Amedi, A. (2016). Reading in the dark: Neural correlates and cross-modal plasticity for learning to read entire words without visual experience. *Neuropsychologia* 83, 149–160. doi: 10.1016/J.NEUROPSYCHOLOGIA.2015.11.009

Spiridon, M., Fischl, B., and Kanwisher, N. (2006). Location and spatial profile of category-specific regions in human extrastriate cortex. *Hum. Brain Mapp.* 27, 77–89. doi: 10.1002/HBM.20169

Striem-Amit, E., and Amedi, A. (2014). Visual cortex extrastriate body-selective area activation in congenitally blind people "Seeing" by using sounds. *Curr. Biol.* 24, 687–692. doi: 10.1016/j.cub.2014.02.010

Striem-Amit, E., Cohen, L., Dehaene, S., and Amedi, A. (2012). Reading with sounds: Sensory substitution selectively activates the visual word form area in the blind. *Neuron* 76, 640–652. doi: 10.1016/j.neuron.2012.08.026

Talairach, J., and Tournoux, P. (1988). *Co-planar stereotaxic atlas of the human brain: 3-Dimensional proportional system: An approach to cerebral imaging*. Stuttgart: Thieme Medical Publishers.

Thorat, S., Proklova, D., and Peelen, M. V. (2019). The nature of the animacy organization in human ventral temporal cortex. *eLife* 8:e47142. doi: 10.7554/eLife.47142

Turati, C., Macchi Cassia, V., Simion, F., and Leo, I. (2006). Newborns' face recognition: Role of inner and outer facial features. *Child Dev.* 77, 297–311. doi: 10.1111/j.1467-8624.2006.00871.x

van den Hurk, J., Van Baelen, M., and Op de Beeck, H. P. (2017). Development of visual category selectivity in ventral visual cortex does not require visual experience. *Proc. Natl. Acad. Sci. U.S.A.* 114, E4501–E4510. doi: 10.1073/pnas.1612862114

Visconti di Oleggio Castello, M., Halchenko, Y. O., Guntupalli, J. S., Gors, J. D., and Gobbini, M. I. (2017). The neural representation of personally familiar and unfamiliar faces in the distributed system for face perception. *Sci. Rep.* 7:12237. doi: 10.1038/s41598-017-12559-1

Wiesel, T. N., and Hubel, D. H. (1963). Single-cell responses in striate cortex of kittens deprived of vision in one eye. *J. Neurophysiol.* 26, 1003–1017. doi: 10.1152/jn.1963.26.6.1003

Wiesel, T. N., and Hubel, D. H. (1965). Extent of recovery from the effects of visual deprivation in kittens. *J. Neurophysiol.* 28, 1060–1072. doi: 10.1152/jn.1965.28.6.1060

Willems, R. M., Peelen, M. V., and Hagoort, P. (2010). Cerebral lateralization of face-selective and body-selective visual areas depends on handedness. *Cereb. Cortex* 20, 1719–1725. doi: 10.1093/cercor/bhp234

Wilmer, J. B., Germine, L., Chabris, C. F., Chatterjee, G., Williams, M., Loken, E., et al. (2010). Human face recognition ability is specific and highly heritable. *Proc. Natl. Acad. Sci. U.S.A.* 107, 5238–5241. doi: 10.1073/pnas.0913053107

Wolbers, T., Klatzky, R. L., Loomis, J. M., Wutte, M. G., and Giudice, N. A. (2011). Modality-independent coding of spatial layout in the human brain. *Curr. Biol.* 21, 984–989. doi: 10.1016/j.cub.2011.04.038

Wood, G., Nuerk, H. C., Sturm, D., and Willmes, K. (2008). Using parametric regressors to disentangle properties of multi-feature processes. *Behav. Brain Funct.* 4:38. doi: 10.1186/1744-9081-4-38

Yovel, G., and Kanwisher, N. (2005). The neural basis of the behavioral face-inversion effect. *Curr. Biol.* 15, 2256–2262. doi: 10.1016/J.CUB.2005.10.072

Zhen, Z., Yang, Z., Huang, L., Kong, X., Wang, X., Dang, X., et al. (2015). Quantifying interindividual variability and asymmetry of face-selective regions: A probabilistic functional atlas. *Neuroimage* 113, 13–25. doi: 10.1016/J.NEUROIMAGE.2015.03.010

frontiers | Frontiers in Neuroscience

TYPE Original Research
PUBLISHED 05 October 2022
DOI 10.3389/fnins.2022.924938

OPEN ACCESS

EDITED BY
Maurice Ptito,
Université de Montréal, Canada

REVIEWED BY
Givago Silva Souza,
Federal University of Pará, Brazil
Adam Kirton,
University of Calgary, Canada
Chao-Ying Chen,
Chang Gung University, Taiwan

*CORRESPONDENCE
Yannick Bleyenheuft
yannick.bleyenheuft@uclouvain.be

†These authors have contributed equally to this work and share first authorship

SPECIALTY SECTION
This article was submitted to Perception Science, a section of the journal Frontiers in Neuroscience

RECEIVED 20 April 2022
ACCEPTED 22 August 2022
PUBLISHED 05 October 2022

CITATION
Araneda R, Ebner-Karestinos D, Dricot L, Herman E, Hatem SM, Friel KM, Gordon AM and Bleyenheuft Y (2022) Impact of early brain lesions on the optic radiations in children with cerebral palsy. *Front. Neurosci.* 16:924938. doi: 10.3389/fnins.2022.924938

Impact of early brain lesions on the optic radiations in children with cerebral palsy

Rodrigo Araneda[1,2†], Daniela Ebner-Karestinos[1,2†], Laurance Dricot[1], Enimie Herman[1], Samar M. Hatem[1,3,4,5], Kathleen M. Friel[6], Andrew M. Gordon[7] and Yannick Bleyenheuft[1*]

[1]Institute of Neuroscience, Université Catholique de Louvain, Ottignies-Louvain-la-Neuve, Belgium, [2]Exercise and Rehabilitation Science Institute, School of Physical Therapy, Faculty of Rehabilitation Science, Universidad Andrés Bello, Santiago, Chile, [3]Physical and Rehabilitation Medicine, Brugmann University Hospital, Brussels, Belgium, [4]Faculty of Medicine and Pharmacy, Vrije Universiteit Brussel, Brussels, Belgium, [5]Faculty of Physical Education and Physiotherapy, Vrije Universiteit Brussel, Brussels, Belgium, [6]Burke-Cornell Medical Research Institute, White Plains, NY, United States, [7]Department of Biobehavioral Sciences, Teachers College, Columbia University, New York, NY, United States

Due to their early brain lesion, children with unilateral spastic cerebral palsy (USCP) present important changes in brain gray and white matter, often manifested by perturbed sensorimotor functions. We predicted that type and side of the lesion could influence the microstructure of white matter tracts. Using diffusion tensor imaging in 40 children with USCP, we investigated optic radiation (OR) characteristics: fractional anisotropy (FA), mean diffusivity (MD), axial diffusivity (AD) and radial diffusivity (RD). First, we compared the OR of the lesional and non-lesional hemisphere. Then we evaluated the impact of the brain lesion type (periventricular or cortico-subcortical) and side in the differences observed in the lesional and non-lesional OR. Additionally, we examined the relationship between OR characteristics and performance of a visuospatial attention task. We observed alterations in the OR of children with USCP on the lesional hemisphere compared with the non-lesional hemisphere in the FA, MD and RD. These differences were influenced by the type of lesion and by the side of the lesion. A correlation was also observed between FA, MD and RD and the visuospatial assessment mainly in children with periventricular and right lesions. Our results indicate an important role of the timing and side of the lesion in the resulting features of these children's OR and probably in the compensation resulting from neuroplastic changes.

KEYWORDS

diffusion tensor imaging, early brain lesion type, hemiparesis, lesion side, white matter

Abbreviations: USCP, unilateral spastic cerebral palsy; OR, optic radiation; FA, fractional anisotropy; MD, mean diffusivity; CP, Cerebral palsy; ROI, regions of interest; OR-LH, optic radiation scores on the lesional hemisphere; OR-NLH, optic radiation scores on the non-lesional hemisphere.

Introduction

Cerebral palsy (CP) is a group of movement and posture disorders resulting from early brain injury. With an incidence of 4–10 per 1,000 children (Graham et al., 2016), CP is the most common cause of pediatric motor deficits, and is often accompanied by disabilities in cognitive and sensory functions (Krageloh-Mann and Cans, 2009; Weierink et al., 2013). These persistent deficits are attributable to brain structural abnormalities arising at different stages of brain development, with consequences for neuronal proliferation, migration, and differentiation, as well as neuronal growth and myelination (de Graaf-Peters and Hadders-Algra, 2006; Stiles and Jernigan, 2010). Therefore, the timing of the brain lesion influences the nature of subsequent perturbations in brain development (Chugani et al., 1996; Brizzolara et al., 2002). The two most common types of structural defect in children with unilateral spastic cerebral palsy (USCP) are periventricular lesions and cortical/subcortical lesions. Periventricular lesions arise early in the 3rd trimester of gestation and are associated mainly with white matter damage, whereas cortical/subcortical lesions, typically arise at the end of the 3rd trimester (Volpe, 1997; Cowan et al., 2003; Krageloh-Mann and Horber, 2007) and are associated mainly with gray matter damage (Bax et al., 2006; Krageloh-Mann and Horber, 2007; Reid et al., 2015). Periventricular lesions of the white matter mainly affect sensorimotor functions (Staudt et al., 2000, 2003; Pavlova and Krageloh-Mann, 2013). The cortical/subcortical lesions, on the other hand, also affect sensory and motor structures such as the basal ganglia and the primary motor cortex; the extent of a subcortical lesion is closely related to the severity of sensorimotor impairments (Martinez-Biarge et al., 2010). Less commonly, USCP may also arise from brain malformations occurring in the 2nd trimester of gestation (Volpe, 1997; Cowan et al., 2003; Krageloh-Mann and Horber, 2007).

Given that some functions such as language, visuospatial attention and (fine) hand motor control (Springer et al., 1999; Gotts et al., 2013) are lateralized, the side of the lesion may have some bearing on functional (re)organization of the developing brain. These lateralized functions accommodate differently depending on whether damage is congenital or acquired in the adult. For instance, a left brain lesion involving Broca's or Wernicke's areas will frequently induce permanent language impairments in adult stroke patients (Willmes and Poeck, 1993; Perani et al., 2003), whereas lesions in comparable regions of children with CP may result only in delayed language acquisition (Krageloh-Mann et al., 2017). Conversely, visuospatial abilities are usually lateralized to the non-dominant right hemisphere (Corballis, 2003). Adult stroke patients with right hemisphere lesions may show unilateral spatial neglect (Karnath et al., 2004), with absence of perception of the contralateral hemispace (Laplane and Degos, 1983). Interestingly, unilateral spatial neglect, notably in visual cancelation tasks (Laurent-Vannier et al., 2003; Trauner, 2003), is evident in children with early brain injury to either hemisphere (Thareja et al., 2012). This suggests spatial attention functions have greater plasticity in the damaged developing brain than in adults. Spatial neglect has been associated both with lesions in parietal cortex (Corbetta and Shulman, 2011) and in white mater tracts, including the optic radiations (OR) (Chechlacz et al., 2010). Although reorganization of motor pathways is well-documented in children with USCP (Cioni et al., 2011), less is known about corresponding reorganization of visuospatial functions. Guzzetta (2010) proposed a model wherein a primary visual cortex lesion would provoke reorganization of visual function in occipital areas extending beyond the primary visual cortex. On the other hand, subcortical lesions affecting the retro-geniculate pathway might entail remodeling of the OR to attain the preferred target in primary visual cortex. While intriguing, there has been little direct empirical evidence supporting this twofold model.

In the present study, we therefore aimed to (1) describe the reorganization of the OR in children with USCP, (2) investigate the effects of the type and side of the lesion on white matter changes in the OR of children with USCP due to an early brain lesion, and (3) assess the relationship between changes in the OR and performance of visuospatial attention tasks. We hypothesized that white matter characteristics of the OR would differ according to the side and type of lesion, and that OR findings would correlate with the extent of visuospatial neglect in children with USCP.

Materials and methods

Participants

Forty children with diagnosis of USCP participated in this study, of whom 26 were recruited at the Université Catholique de Louvain in Belgium, and 14 at Teachers College of Columbia University in New York City (19 girls; mean age: 9.1 ± 2.8 years; 22 right hemiparesis) from among children who participated or were interested in participating in intensive rehabilitation day camps (Bleyenheuft et al., 2020). Teachers College participants were recruited from local clinics, the laboratory website,[1] and online parents' forums. In Belgium, children were recruited from university hospital centers dedicated to treatment of children with CP. The parents/legal tutors of potential participants were contacted by e-mail or telephone. All parents/legal tutor and children provided their written, informed consent to participate in the study, which had been approved by the respective Institutional Review Boards.

1 www.tc.edu/centers/cit/

Participants (see **Table 1**) were classified following the Manual Ability Classification System (Eliasson et al., 2006) as levels I (n = 8), II (n = 30) or III (n = 2). Children were also evaluated by a pediatric neurologist and a neuroradiologist using the criteria of Krageloh-Mann and Horber (2007), to classify the origin of their brain lesion (cortical malformation, n = 6; periventricular lesion, n = 18; cortical/subcortical lesion, n = 16).

The inclusion criteria were (1) children diagnosed with unilateral CP, (2) aged 6–16 years, (3) ability to grasp light objects and lift the more affected arm 15 cm above a table surface, (4) school level equal to that of typically developing peers, (5) ability to follow instructions and complete testing. Exclusion criteria were (1) uncontrollable seizures, (2) botulinum toxin injections in the previous 6 months or planned for the following 6 months, (3) orthopedic surgery in the previous 12 months or planned within the study period, (4) uncorrectable visual problems likely to interfere with treatment/testing.

3D-magnetic resonance imaging and diffusion tensor imaging

In a single scanning session, children underwent an MRI scan at 3T with a 32-channel phased array head coil to record 3D heavily T1-weighted structural and diffusion tensor imaging (DTI) images. In Brussels, 26 children were scanned using a Philips Achieva magnet (Philips Healthcare, Eindhoven, The Netherlands). Nine children were scanned using a Philips Achieva at Columbia Medical School and five using a Siemens Prisma 3T scanner (Siemens, Erlangen, Germany) at Cornell-Weil Hospital in New York.

The anatomical 3D sequence obtained on the Philips magnet consisted of a gradient echo sequence with an inversion prepulse (Turbo Field Echo, TFE) acquired in the sagittal plane employing the following parameters: repetition time (TR) = 9.1 ms, echo time (TE) = 4.6 ms, flip angle = 8°, 150 slices, slice thickness = 1 mm, in-plane resolution = 0.81 × 0.95 mm^2 (acquisition) reconstructed in 0.75 × 0.75 mm^2, field of view (FOV) = 220 × 197 mm^2, acquisition matrix = 296 × 247 (reconstruction 3202), SENSE factor = 1.5 (parallel imaging), with a total scan time of 8 min and 26 s. The anatomical 3D sequence obtained on the Siemens magnet consisted of a magnetization-prepared rapid gradient-echo (MP-RAGE) sequence acquired in the axial plane employing the following parameters: TR = 2170 ms, TE = 4.33 ms, flip angle = 7°, 176 slices, slice thickness = 1 mm, in-plane resolution = 1 × 1 mm^2 (acquisition and reconstruction), FOV = 256 × 256 mm^2, acquisition matrix = 256 × 256, GRAPPA factor = 2 (parallel imaging), in a 4 min 27 s of total scan time.

DTI images on the Achieva scanner were obtained using the following sequence: spin-echo planar imaging, TE = 83 ms, TR = 6,422 ms, Bandwidth = 2,790 hz/pixel, 70 slices, slice thickness = 2 mm, in-plane resolution = 2 × 2 mm^2, matrix size = 112 × 112, FOV = 224 × 224 mm^2, 55 directions, b = 800 s/mm^2, in a total scan time of 8 min. DTI images on the Prisma scanner were acquired employing the following sequence: spin-echo planar imaging, TE = 83 ms, TR = 9,000 ms, Bandwidth = 1,860 hz/pixel, 75 slices, slice thickness = 2 mm, in-plane resolution = 2 × 2 mm^2, matrix size = 112 × 112, FOV = 224 × 224 mm^2, 64 directions, b = 1,000 s/mm^2, in a total scan time of 10 min and 14 s.

The DTI data were pre-processed using BrainVoyager (Version 20.6, Brain Innovation, Maastricht, The Netherlands). The diffusion data were first corrected for eddy current-induced distortions and motion-induced artifacts. To create the fractional anisotropy (FA) map and to calculate the radial (RD), axial (AD), and mean diffusivity (MD), the DTI data were co-registered with the 3D anatomy of the subject without normalization (native space).

To determine individual measures of the DTI metrics (FA, MD, AD, and RD) of the OR within the lesional and non-lesional hemispheres, axial planes were first imposed based on anatomical landmarks (see **Figure 1**). For each hemisphere, we used two regions of interest (ROIs) to trace the OR: an initial ROI was defined at the level of the lateral geniculate nucleus and a second in the visual primary cortex near the calcarine sulcus. These regions were identified on the echo planar images with no diffusion weighting and were verified later, in all planes, by an investigator uninvolved in the tracking. Fibers passing over the lateral geniculate nucleus were excluded from the analysis. A deterministic tracking was finally performed to reconstruct and track the OR. Only those fibers with FA > 0.20 and a deviation angle < 50° were included in the tracking. The MRI acquisition was performed by examiners unaware of the study purpose.

Visuospatial assessment

We used a star cancelation test to assess impairments in visuospatial attention specifically related to unilateral spatial neglect. In this test, the child is asked to cancel all small stars in a sheet of paper marked with stars of two different sizes. This test separately records the total number of omissions as well as the omissions on the more affected and the less affected hemispaces (Wilson et al., 1987).

Data analysis

Diffusion tensor imaging analyses

First, a t-test (or Mann-Whitney rank sum test when the normality was not respected) was performed to identify possible differences between the OR scores of the lesional hemisphere (OR-LH) and the non-lesional hemisphere (OR-NLH) for FA,

TABLE 1 Group's characteristics.

Lesion type	Gender	Age	MACS	Lesion side
Cortical/subcortical lesion (n = 16)	Girls = 9 Boys = 7	8 y 6 m	I = 5 II = 11	Right = 6 Left = 10
Periventricular lesion (n = 15)	Girls = 6 Boys = 9	9 y 6 m	I = 3 II = 12	Right = 8 Left = 7
Lesion side	**Gender**	**Age**	**MACS**	**Lesion type**
Right hemisphere (n = 16)	Girls = 9 Boys = 7	8 y 6 m	I = 5 II = 11	C/Sc = 6 PVL = 10
Left hemisphere (n = 19)	Girls = 9 Boys = 7	8 y 6 m	I = 5 II = 11	C/Sc = 6 PVL = 10

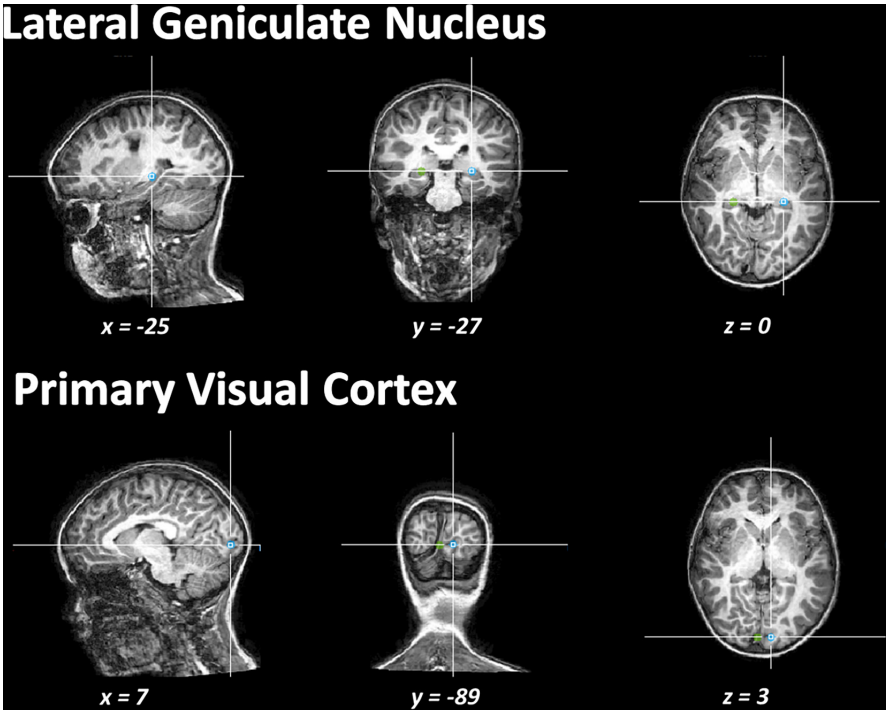

FIGURE 1
Illustration of the regions of interest drawn to execute the tracking of the fibers.

MD, AD, and RD. Next, we used a two-way ANOVA to identify the influence of type of lesion (periventricular/cortical-subcortical) on the differences between the OR-LH and the OR-NLH scores for FA, MD, AD, and RD. We performed Student-Newman-Keuls *post hoc* tests, after adjustment of the alpha level for multiple comparisons. Finally, we performed a two-way ANOVA with a Student-Newman-Keuls *post hoc* ($\alpha = 0.05$) to identify the influence of side of lesion (right/left) in the differences between the OR-LH and the OR-NLH scores for FA, MD, AD, and RD.

Visuospatial assessment analyses

We used a Mann-Whitney rank sum test to evaluate impairment in visuospatial attention in relation to unilateral spatial neglect. Here, we separately compared each result of the star cancelation test (total number of omissions, more affected hemispace omission and less affected hemispace omission) with lesion type (periventricular or cortical/subcortical lesion) and lesion side (right/left).

Correlation analyses

A Spearman's correlation was performed to investigate the relationships between the visuospatial test results and DTI measures (FA, MD AD, and RD) in the OR-LH and in the OR-NLH as functions of the lesion type and side.

Results

After the data acquisition, five children were excluded from the analyses because of inadequate quality of neuroimaging data

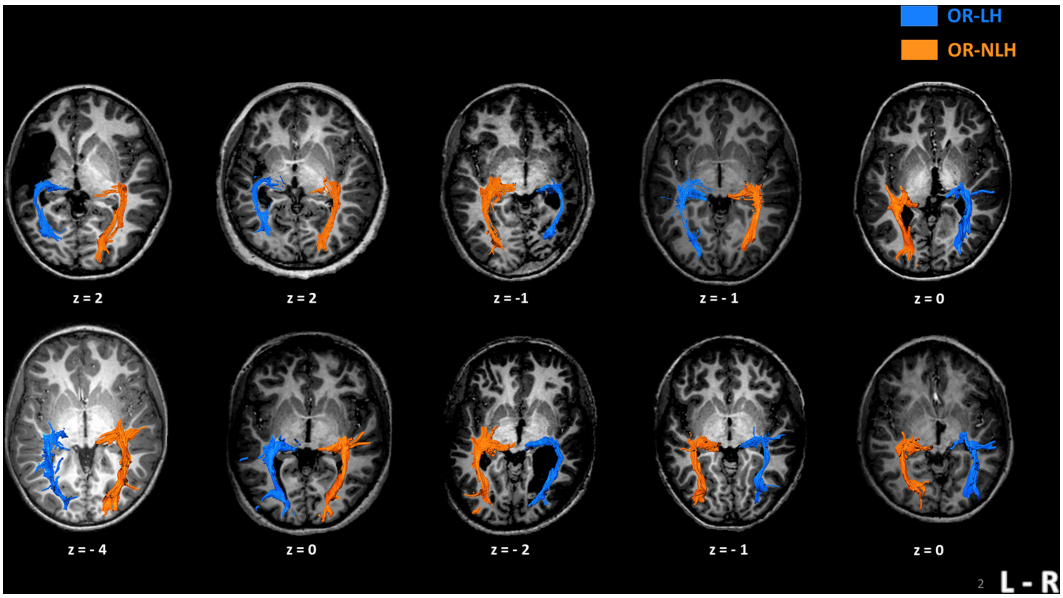

FIGURE 2
Imaging results in 10 children with unilateral spastic cerebral palsy, displaying their individual optic radiation bypasses. The upper row shows examples of children with cortico-subcortical lesions and the lower row depicts children with periventricular lesions. *Z*-values represent the coordinates in Talairach space. OR-LH, optic radiation of the lesional hemisphere; OR-NLH, optic radiations of the non-lesional hemisphere; L-R, left-right.

produced mainly by head movement. Therefore, the final sample for the analyses was of 35 children.

Description of optic radiations organization

For every participant, we could identify the OR between the lateral geniculate nucleus and the visual cortex, regardless of the type and side of lesion. We distinguished two types of lesion "bypasses" to the visual cortex; in children with a cortico-subcortical lesion, the OR-LH passed through the lesion, while in children with a periventricular lesion, the OR-LH systematically followed the outer contour of the lesion (Figure 2).

Interhemispheric differences in diffusion tensor imaging measures

We observed significant differences in DTI parameters of the OR-LH and OR-NLH. The FA values were lower in OR-LH compared to OR-NLH (Mann-Whitney U = 261.00, $p < 0.001$). Conversely, there were higher values in OR-LH compared to OR-NLH for MD (Mann-Whitney U = 433.00, $p < 0.05$) and RD (Mann-Whitney U = 424.00, $p < 0.05$). No significant difference were observed for the AD (Mann-Whitney U = 549.00, $p = 0.459$) (Figure 3).

Influence of lesion type

The final sample implicated in the analyses of the influence of the lesion was of 31 children; due to the small sample, children presenting a brain malformation were excluded from this analysis.

To identify the influence of the type of lesion on the differences in the FA, MD, AD, and RD between the OR-LH and the OR-NLH, we performed a 2 (optic radiations condition: OR-LH vs. OR-NLH) × 2 (type of lesion: periventricular vs. cortical/subcortical) ANOVA. These analyses revealed an optic radiations condition effect on FA values [$F(1, 58) = 18.30$; $p < 0.001$, $\eta^2 = 0.102$]. Lesion type had no such effect [$F(1, 58) = 0.01$; $p = 0.993$, $\eta^2 = 0.131$], but there was a significant optic radiations condition × lesion type interaction effect [$F(1, 58) = 4.63$; $p < 0.05$, $\eta^2 = 0.174$]. Figure 4 shows the results of the *post hoc* analysis. In cases of cortico-subcortical lesions ($p < 0.001$) mean FA values were lower in the OR-LH compared to OR-NLH.

The same analyses for the diffusivity showed an effect on the MD for the optic radiations condition [$F(1, 58) = 5.17$; $p < 0.05$, $\eta^2 = 0.152$] with lower values for the OR-NLH, but no significant difference for the lesion type [$F(1, 58) = 1.77$; $p = 0.19$, $\eta^2 = 0.130$] or interaction [$F(1, 58) = 0.18$; $p = 0.671$, $\eta^2 = 0.103$]. In addition, for the AD a trend was observed for the optic radiations condition [$F(1, 58) = 3.55$; $p = 0.65$, $\eta^2 = 0.155$], but a significant effect on the lesion type conditions [$F(1, 58) = 5.00$; $p < 0.05$, $\eta^2 = 0.229$] with higher values for the cortical/subcortical lesion and no interaction [$F(1, 58) = 0.15$;

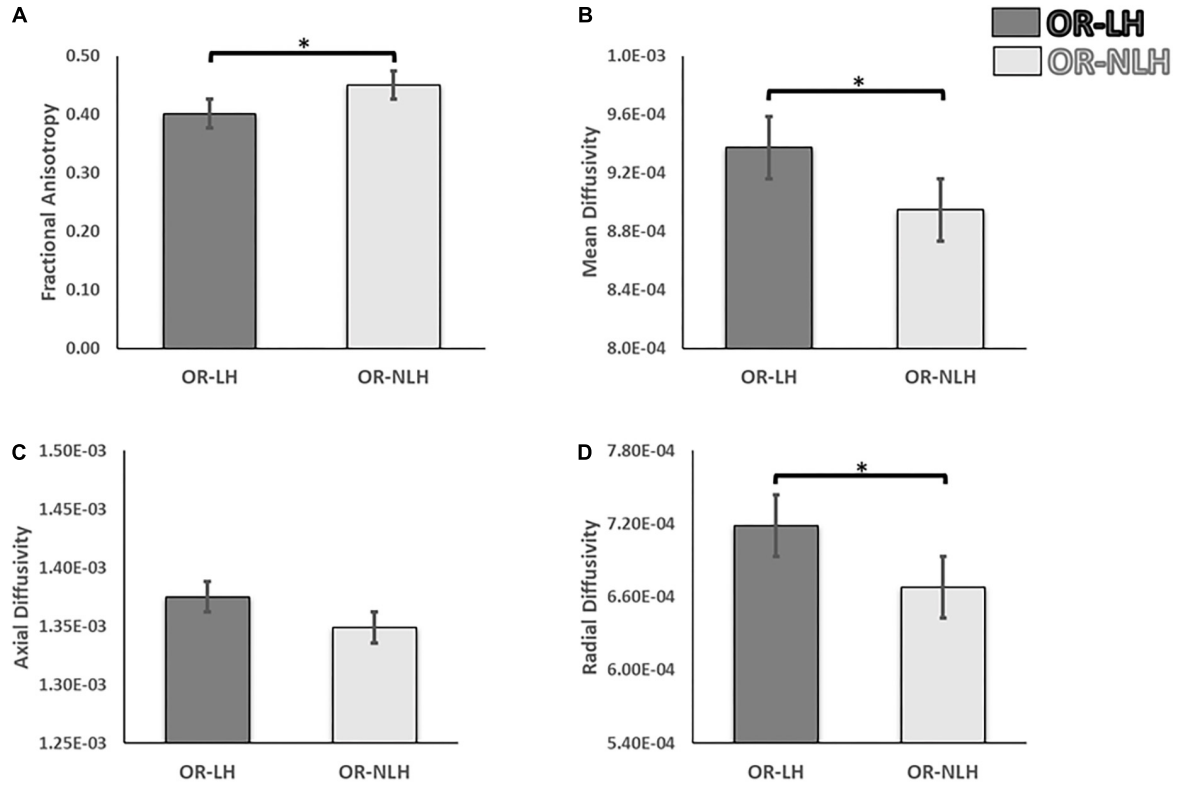

FIGURE 3
Differences in white matter integrity of the OR of the lesional and non-lesional hemispheres in children with USCP. **(A)** Mean fractional anisotropy, **(B)** mean diffusivity **(C)** mean axial diffusivity and **(D)** mean radial diffusivity. OR-LH, optic radiation of the lesional hemisphere; OR-NLH, optic radiations of the non-lesional hemisphere. Error bars represent standard errors of the mean. *$p < 0.05$.

$p = 0.701$, $\eta^2 = 0.121$]. Also, a significant effect was observed for the RD for the optic radiations conditions [$F(1, 58) = 4.92$; $p < 0.05$, $\eta^2 = 0.178$], but none for the lesion type conditions [$F(1, 58) = 0.74$; $p = 0.394$, $\eta^2 = 0.113$] and no interactions [$F(1, 58) = 0.16$; $p = 0.688$, $\eta^2 = 0.116$] (Figure 4).

Influence of lesion side

To test for effects of lesion side on group differences between the OR-LH and the OR-NLH group means of the FA, MD, AD, and RD, we performed a 2 (optic radiations condition: OR-LH vs. OR-NLH) × 2 (side of lesion: right vs. left) ANOVA. We found a significant effect on the FA of the OR condition [$F(1, 66) = 24.98$; $p < 0.001$, $\eta^2 = 0.275$], lesion side conditions [$F(1, 66) = 7.64$; $p < 0.05$, $\eta^2 = 0.204$] and a significant interaction effect between the OR condition and side of the lesion [$F(1, 66) = 4.37$; $p < 0.05$, $\eta^2 = 0.192$]. As depicted in Figure 5, children with a right lesion had lower values in OR-LH ($p < 0.001$) compared with children with a left lesion. Additionally, we observed lower mean FA values in OR-LH compared with the OR-NLH in children with a right ($p < 0.001$) and a left ($p < 0.05$) lesion.

The same analyses for the diffusivity showed an effect on the MD for the optic radiations condition [$F(1, 66) = 4.62$; $p < 0.05$, $\eta^2 = 0.265$] with lower values for the OR-NLH and significant difference for the lesion side [$F(1, 66) = 5.10$; $p < 0.05$, $\eta^2 = 0.272$] with lower values for the left lesion, but no interaction [$F(1, 66) = 1.20$; $p = 0.278$, $\eta^2 = 0.119$]. There were no significant effects of OR condition [$F(1, 66) = 2.07$; $p = 0.155$, $\eta^2 = 0.130$], lesion side [$F(1, 66) = 1.95$; $p = 0.167$, $\eta^2 = 0.127$] or their interaction [$F(1, 66) = 1.08$; $p = 0.302$, $\eta^2 = 0.116$] for AD results. In addition, for the RD a significant effect was observed for the optic radiations condition [$F(1, 66) = 5.04$; $p < 0.05$, $\eta^2 = 0.271$] with lower values for the OR-NLH and a significant effect on the lesion type conditions [$F(1, 66) = 5.79$; $p < 0.05$, $\eta^2 = 0.282$] with lower values for the left lesion and no interaction [$F(1, 58) = 0.15$; $p = 0.701$, $\eta^2 = 0.115$].

Visuospatial assessment

Children with USCP showed a mean of 2.91 ± 3.64 total omissions in the star cancelation test. These results are in line with those described in the literature in children with USCP (Ickx et al., 2018). Compared to aged-matched typically developing peers, only few children presented abnormal values (Ickx et al., 2017). Lesion side and type had no effect on the total number of omitted small stars, neither in the more affected

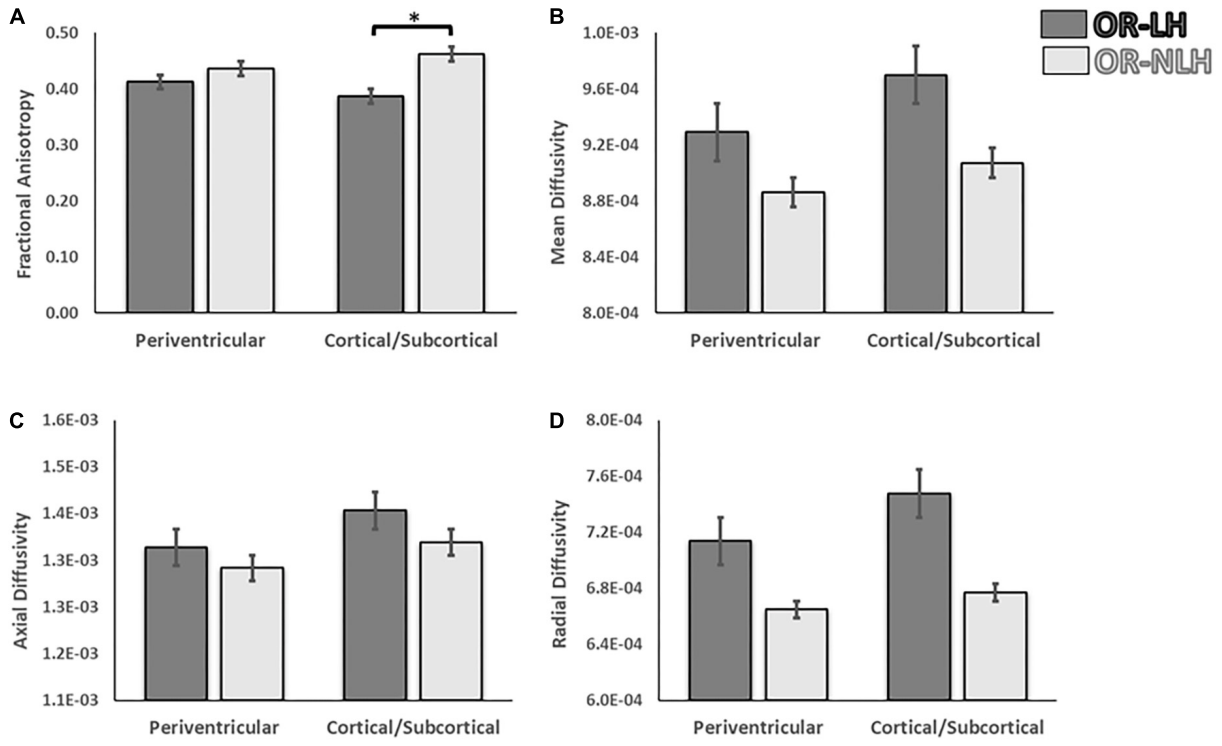

FIGURE 4
Differences in white matter integrity of the OR of the lesional and non-lesional hemispheres as functions of lesion type in children with USCP. **(A)** Fractional anisotropy, **(B)** mean diffusivity, **(C)** mean axial diffusivity and **(D)** mean radial diffusivity. OR-LH, optic radiation of the lesional hemisphere; OR-NLH, optic radiations of the non-lesional hemisphere. Error bars represent standard errors of the mean. *$p < 0.05$.

nor the less affected hemispace (all $p > 0.235$, Table 2; see also Table 3).

Correlation between diffusion tensor imaging measures and visuospatial assessment

In children with a periventricular lesion, the FA of the OR-LH correlated significantly with the total number of stars omitted ($r = -0.546$; $p = 0.034$) and the FA of the OR-NLH correlated significantly with the total number of stars omitted ($r = -0.638$; $p = 0.01$).

In children with a right-side brain lesion, the MD of the OR-NLH correlated significantly with the total number of stars omitted ($r = 0.536$; $p = 0.038$) and the RD of the OR-NLH with the total number of stars omitted ($r = 0.561$; $p = 0.029$). There were no other significant correlations with test scores.

Discussion

The aim of this study was to assess the organization and white matter characteristics of the OR in children with USCP, and test for an association with impairment in their performance of a visuospatial test. We also tested the hypothesis that type and side of the lesion would influence parameters of white matter microstructure, i.e., FA, MD, AD, and RD. Our results support this hypothesis, highlighting differences in the white matter properties of the OR between the lesional and the non-lesional hemisphere. These microstructural differences were influenced by the type of lesion and the side of the lesion, and may contribute to the visuospatial impairments often observed in children with USCP.

We observed two different patterns of white matter reorganization, apparently in response to the lesion. In one scenario, OR fibers in the lesion hemisphere passed through cortico-subcortical injuries, and in other cases, the OR followed the contour periventricular lesions (Figure 6). This last finding is in agreement with the proposal by Guzzetta (2010) that, when the lesion affects the retro-geniculate pathway, the OR circumvents the lesion contours to reach the primary visual cortex (Guzzetta, 2010). Moreover, in our study the two bypass routes also differed with respect to the microstructure of white matter fibers, as indicated by FA values. We suggest that the distinct modes of reorganization of the visual pathway may bear relation to the timing and the location of the lesion (Chugani et al., 1996; Feys et al., 2010). Indeed, an association

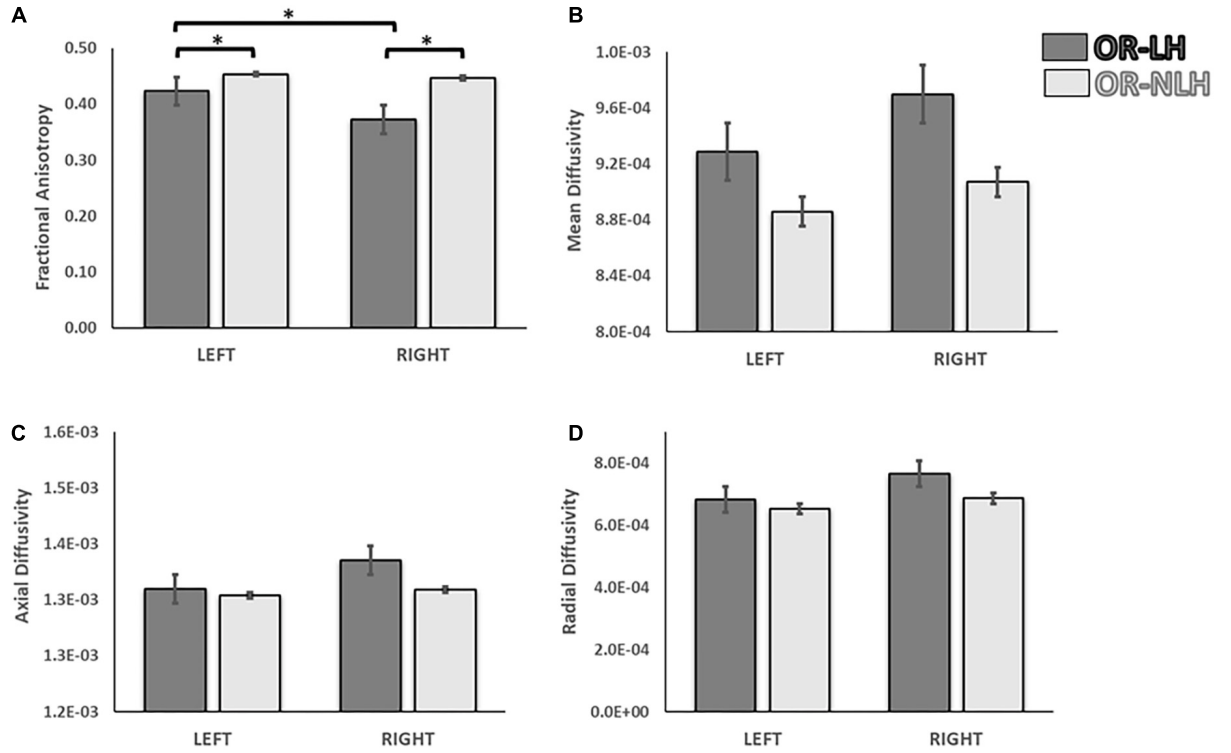

FIGURE 5
Differences in white matter integrity of the OR of the lesional and non-lesional hemispheres as functions of side of lesion in children with USCP. **(A)** Fractional anisotropy, **(B)** mean diffusivity, **(C)** mean axial diffusivity and **(D)** mean radial diffusivity. OR-LH: optic radiation of the lesional hemisphere; OR-NLH: optic radiations of the non-lesional hemisphere. Error bars represent standard errors of the mean. *$p < 0.05$.

between reorganization and lesional features is critical for the development of motor, sensory as well as cognitive deficits in children with USCP (Lidzba et al., 2006; Guzzetta et al., 2007; Staudt, 2010; Hadders-Algra, 2014). Thus, the importance of lesion features for reorganization of the visual pathway is a novel finding of this study, demonstrating the far-reaching consequences of early brain lesions in children with CP.

In this study we observed a significant difference between the OR-LH and OR-NLH, with the OR-LH showing lower values in the FA and higher values in MD and RD, but no difference in AD. These results indicate an impact of the brain lesion on the structure of the OR. The FA difference could indicate an impairment of the white matter microstructure, although this measure is affected by many factors including myelination, axon size, and density (Beaulieu, 2002; Mukherjee et al., 2002; Ciccarelli et al., 2008). However, the results observed in the FA were accompanied with higher values in the MD and RD of OR-LH without significant differences in AD. The RD has been associated with the myelin (Song et al., 2002, 2005) and AD with axonal microstructure (Sun et al., 2008; Budde et al., 2009). Therefore, our results suggest that the low FA associated with higher values in the AD and MD observed in OR-LH are potentially manifestations of impaired microstructure associated with altered myelin development process.

In this study, we observed lower FA values in OR-LH of children with a cortico-subcortical lesions compared to those with a periventricular lesion. The differences in FA between the lesional and non-lesional hemispheres is in line with previous studies showing an association between early brain lesions and damage to OR, specifically in children with lesions in the periventricular area (Leviton and Paneth, 1990; Rodriguez et al., 1990; Cioni et al., 2000). Our results are also consistent with findings of Chokron and Dutton (2016), indicating a correlation between white matter lesions in OR and impaired visual function in children with CP.

The difference in FA could relate to the specific cortical phase of development at the time of brain damage, i.e., start of 3rd trimester for periventricular lesions and end of 3rd trimester for cortical/subcortical lesions. Myelinization of the OR begins around the middle of the 3rd trimester (de Graaf-Peters and Hadders-Algra, 2006), such that a lesion occurring at around the 35th week of gestation is apt to have a higher impact on white matter in childhood. Similar differences between these two broad types of lesion have been shown in relation to motor function, since impairments of upper extremity function (Feys et al., 2010) and language skills (Coleman et al., 2013) are more common in CP children with cortical/subcortical compared to periventricular lesions. It is noteworthy that the

TABLE 2 Star cancelation scores.

All children (n = 35)	Total omissions mean (SD)		
	2.91 (3.64)		
Lesion side	**Total omissions**	**More affected hemispace omissions**	**Less affected hemispace omissions**
	Median [25–75%]	Median [25–75%]	Median [25–75%]
Right hemisphere (n = 16)	2.00 [0.00–4.00]	1.00 [0.00–4.00]	0.00 [0.00–1.00]
Left hemisphere (n = 19)	1.50 [0.00–5.00]	0.50 [0.00–2.00]	0.50 [0.00–2.00]
p-value	0.904	0.412	0.235
Lesion type	**Total omissions**	**More affected hemispace omissions**	**Less affected hemispace omissions**
	Median [25–75%]	Median [25–75%]	Median [25–75%]
Cortical/subcortical lesion (n = 16)	2.50 [0.00–5.00]	1.00 [0.00–4.00]	0.00 [0.00–2.50]
Periventricular lesion (n = 15)	1.00 [0.00–5.00]	1.00 [0.00–2.00]	0.00 [0.00–3.00]
p-value	0.822	0.563	0.912

myelination of projections from the precentral and postcentral gyrus, which are key substrates of sensorimotor functions, also begins during the 35th gestational week (de Graaf-Peters and Hadders-Algra, 2006). Damage occurring after the onset of myelination thus likely results in larger deficits than do earlier injuries. This phenomenon may represent a general pattern whereby lesions occurring prior to onset of the myelination process may have less impact on white matter and on functional abilities, while lesions occurring after the start of myelination are more deleterious. The difference observed between both lesion types could be related with the injury consequences such as microglial activation, excitotoxicity and free radical that produced, among other effects, damage of the oligodendrocyte and/or its precursors that play a crucial role in the myelination (Volpe et al., 2011). However, the consequences of the different lesion types for oligodendrocyte development are not completely understood (Silbereis et al., 2010).

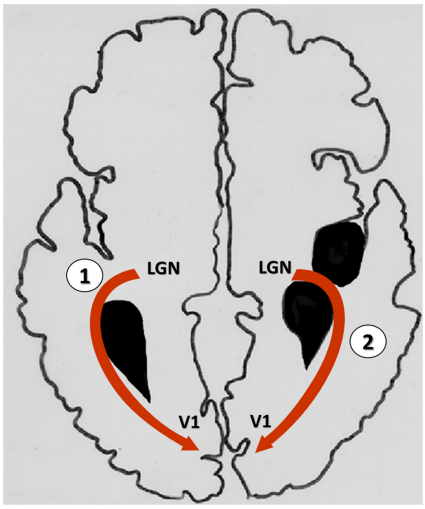

FIGURE 6
Graphical representation of the two bypass routes of the optic radiations in the lesional hemisphere. **(1)** Optic radiations contouring the edge of lesion to reach the primary visual cortex; **(2)** Optic radiations passing through the lesion attain the visual cortex. LGN, Lateral geniculate nucleus; V1, primary visual cortex.

Although we saw systematically larger deficits in the OR of the lesional vs. the non-lesional hemisphere, deficits in the OR of the lesional hemisphere were larger in children with right hemispheric lesions. These results indicate an impact of the lesion side on the characteristics of the OR fibers. A larger impact of right hemispheric lesions on visuospatial skills has been described in children with USCP (Kolk and Talvik, 2000), suggesting that a lesion of the right hemisphere could drive changes in the OR or other white matter structures involved in visuospatial abilities (Tuch et al., 2005). However, children with USCP with a left hemispheric lesion also show deficits in visuospatial abilities (Thareja et al., 2012). This could be explained by the "crowding hypothesis," according to which a lesion in the left hemisphere likely produces a functional shift of the areas normally subserving language from the left to the right hemisphere, which may compromise visuospatial function of the right hemisphere (Lidzba et al., 2006). Therefore, a lesion of either hemisphere could impact the OR and thus affect visuospatial abilities, but by different mechanisms. This sensitivity of visuospatial function to lesion in either hemisphere is predictable from the requirement of intra-hemispheric integration for a bilateral representation of visual space (Corbetta and Shulman, 2011). In this scenario, the lesional side could influence the FA or other aspects of OR microstructure in children with USCP. We suggest that, although lesions on either hemisphere may have an impact on OR microstructure, the effects of right hemispheric

TABLE 3 Amount of children presenting impaired visuospatial assessment.

Lesion type	Total omissions	More affected hemispace omissions	Less affected hemispace omissions
Cortical/subcortical lesion (n = 16)	3	3	2
Periventricular lesion (n = 15)	4	4	1
Lesion side	**Total omissions**	**More affected hemispace omissions**	**Less affected hemispace omissions**
Right hemisphere (n = 16)	3	2	0
Left hemisphere (n = 19)	4	4	3

lesions are greater due to the specialization of the right hemisphere for visuospatial function. However, despite the different characteristics of the lesion are influenced by the stage of brain maturation, the effects of the lesion may be influenced by other characteristics of the lesion such as the location, size and mechanisms involved (Graham et al., 2016).

At a behavioral level, different studies have shown a deficit in children with cerebral palsy on visuospatial assessments compared with reference values or control peers (Lidzba et al., 2006; Ickx et al., 2017, 2018). In addition, in this study we observed some correlation between FA, MD and RD with the number of omissions in the star cancelation test, suggesting a possible association between visuospatial attention deficits, specifically related to visuospatial impairments, and the damage of the white matter projections of the visual pathway. Tuch et al. (2005) showed a correlation between reaction times in a visual task and FA of the OR in healthy adult subjects, demonstrating that the OR mediates aspects of visual attention (Tuch et al., 2005). This is congruent with other studies of children with CP showing cortical visual impairments due to damage to the retrochiasmatic part of the visual pathway (Mercuri et al., 1996; Guzzetta et al., 2001), particularly in the OR (Ramenghi et al., 2010). However, the development of visual functions, including visuospatial attention, requires the integrity of a wide cortical and subcortical network, including the OR and the primary visual cortex, but also involving frontal and temporal regions, as well as the basal ganglia (Ramenghi et al., 2010). Therefore, while the present finding of disturbances in the OR of children with USCP are likely relevant to their visuospatial impairments, the OR is but one element among many.

Finally, this study presents some limitations regarding the information about the cerebral palsy cause and the extension of the lesion that could contribute to better understand the development of visuospatial functions. In addition, the assessment used in this study could have been complemented with a visual fields assessment, as well as, we could have used more than one test to evaluate the deficit in visuospatial attention. However, the knowledge about the visuospatial function should contribute to open a new perspective to understand the relevance of this function in rehabilitation programs.

Conclusion

We found differences in white matter characteristics of the OR between the lesional and the non-lesional hemispheres of children with USCP. These differences were apparently influenced by the timing of the lesion and by the side of the lesion, perhaps due to competition between language and visuospatial function. The observed differences may contribute to the different degrees of visuospatial impairments observed in children with USCP. We suggest that the timing of the lesion relative to myelination landmarks contributes importantly to the outcome for these children, probably in relation to compensation for injury to visual pathways through neuroplastic changes.

Data availability statement

The data will be made available upon publication to researchers who provide a methodologically sound proposal for use in achieving the goals of the approved proposal. Proposals should be submitted to YB, yannick.bleyenheuft@uclouvain.be.

Ethics statement

The studies involving human participants were reviewed and approved by the Comité d'Ethique Hospitalo-Facultaire, Université Catholique de Louvain, Brussels, Belgium and Teachers College, Columbia University Institutional Review Board, New York, United States. Written informed consent to participate in this study was provided by the participants' legal guardian/next of kin.

Author contributions

RA and DE-K participated to data collection, data analysis, and writing. LD participated to project design, data collection,

data analysis, and writing. EH participated to data collection and writing. SMH, KMF, and AMG participated to project design and writing. YB participated to project design, recruitment, data collection, data analysis, and writing. All authors contributed to the article and approved the submitted version.

Funding

RA had a grant from La Fondation Motrice/Fondation Paralysie Cérébrale. Data collection was supported by the Fondation JED-Belgique. AMG and KMF had a grant from the National Institutes of Health R01HD076436-01. SMH was a postdoctoral fellow of FRS-FNRS Belgium (FNRS—SPD).

Conflict of interest

The authors declare that the research was conducted in the absence of any commercial or financial relationships that could be construed as a potential conflict of interest.

Publisher's note

All claims expressed in this article are solely those of the authors and do not necessarily represent those of their affiliated organizations, or those of the publisher, the editors and the reviewers. Any product that may be evaluated in this article, or claim that may be made by its manufacturer, is not guaranteed or endorsed by the publisher.

References

Bax, M., Tydeman, C., and Flodmark, O. (2006). Clinical and MRI correlates of cerebral palsy: The European Cerebral Palsy Study. *JAMA* 296, 1602–1608. doi: 10.1001/jama.296.13.1602

Beaulieu, C. (2002). The basis of anisotropic water diffusion in the nervous system - a technical review. *NMR Biomed.* 15, 435–455. doi: 10.1002/nbm.782

Bleyenheuft, Y., Dricot, L., Ebner-Karestinos, D., Paradis, J., Saussez, G., Renders, A., et al. (2020). Motor skill training may restore impaired corticospinal tract fibers in children with cerebral palsy. *Neurorehabil. Neural Repair* 34, 533–546. doi: 10.1177/1545968320918841

Brizzolara, D., Pecini, C., Brovedani, P., Ferretti, G., Cipriani, P., and Cioni, G. (2002). Timing and type of congenital brain lesion determine different patterns of language lateralization in hemiplegic children. *Neuropsychologia* 40, 620–632. doi: 10.1016/S0028-3932(01)00158-0

Budde, M. D., Xie, M., Cross, A. H., and Song, S. K. (2009). Axial diffusivity is the primary correlate of axonal injury in the experimental autoimmune encephalomyelitis spinal cord: A quantitative pixelwise analysis. *J. Neurosci.* 29, 2805–2813. doi: 10.1523/JNEUROSCI.4605-08.2009

Chechlacz, M., Rotshtein, P., Bickerton, W. L., Hansen, P. C., Deb, S., and Humphreys, G. W. (2010). Separating neural correlates of allocentric and egocentric neglect: Distinct cortical sites and common white matter disconnections. *Cogn. Neuropsychol.* 27, 277–303. doi: 10.1080/02643294.2010.519699

Chokron, S., and Dutton, G. N. (2016). Impact of cerebral visual impairments on motor skills: implications for developmental coordination disorders. *Front. Psychol.* 7:1471. doi: 10.3389/fpsyg.2016.01471

Chugani, H. T., Müller, R.-A., and Chugani, D. C. (1996). Functional brain reorganization in children. *Brain Dev.* 18, 347–356. doi: 10.1016/0387-7604(96)00032-0

Ciccarelli, O., Catani, M., Johansen-Berg, H., Clark, C., and Thompson, A. (2008). Diffusion-based tractography in neurological disorders: Concepts, applications, and future developments. *Lancet Neurol.* 7, 715–727. doi: 10.1016/S1474-4422(08)70163-7

Cioni, G., Bertuccelli, B., Boldrini, A., Canapicchi, R., Fazzi, B., Guzzetta, A., et al. (2000). Correlation between visual function, neurodevelopmental outcome, and magnetic resonance imaging findings in infants with periventricular leucomalacia. *Arch. Dis. Child. Fetal Neonatal Ed.* 82, F134–F140.

Cioni, G., D'Acunto, G., and Guzzetta, A. (2011). Perinatal brain damage in children: Neuroplasticity, early intervention, and molecular mechanisms of recovery. *Prog. Brain Res.* 189, 139–154. doi: 10.1016/B978-0-444-53884-0.00022-1

Coleman, A., Weir, K. A., Ware, R. S., and Boyd, R. N. (2013). Relationship between communication skills and gross motor function in preschool-aged children with cerebral palsy. *Arch. Phys. Med. Rehabil.* 94, 2210–2217. doi: 10.1016/j.apmr.2013.03.025

Corballis, P. M. (2003). Visuospatial processing and the right-hemisphere interpreter. *Brain Cogn.* 53, 171–176.

Corbetta, M., and Shulman, G. L. (2011). Spatial neglect and attention networks. *Annu. Rev. Neurosci.* 34, 569–599. doi: 10.1146/annurev-neuro-061010-113731

Cowan, F., Rutherford, M., Groenendaal, F., Eken, P., Mercuri, E., Bydder, G. M., et al. (2003). Origin and timing of brain lesions in term infants with neonatal encephalopathy. *Lancet* 361, 736–742. doi: 10.1016/S0140-6736(03)12658-X

de Graaf-Peters, V. B., and Hadders-Algra, M. (2006). Ontogeny of the human central nervous system: What is happening when? *Early Hum. Dev.* 82, 257–266. doi: 10.1016/j.earlhumdev.2005.10.013

Eliasson, A. C., Krumlinde-Sundholm, L., Rosblad, B., Beckung, E., Arner, M., Ohrvall, A. M., et al. (2006). The Manual Ability Classification System (MACS) for children with cerebral palsy: Scale development and evidence of validity and reliability. *Dev. Med. Child Neurol.* 48, 549–554. doi: 10.1017/S0012162206001162

Feys, H., Eyssen, M., Jaspers, E., Klingels, K., Desloovere, K., Molenaers, G., et al. (2010). Relation between neuroradiological findings and upper limb function in hemiplegic cerebral palsy. *Eur. J. Paediatr. Neurol.* 14, 169–177. doi: 10.1016/j.ejpn.2009.01.004

Gotts, S. J., Jo, H. J., Wallace, G. L., Saad, Z. S., Cox, R. W., and Martin, A. (2013). Two distinct forms of functional lateralization in the human brain. *Proc. Natl. Acad. Sci. U.S.A.* 110, E3435–E3444. doi: 10.1073/pnas.1302581110

Graham, H. K., Rosenbaum, P., Paneth, N., Dan, B., Lin, J. P., Damiano, D. L., et al. (2016). Cerebral palsy. *Nat. Rev. Dis. Primers* 2:15082. doi: 10.1038/nrdp.2015.82

Guzzetta, A. (2010). Plasticity of the visual system after congenital brain damage: A few weeks can matter. *Dev. Med. Child Neurol.* 52:699. doi: 10.1111/j.1469-8749.2010.03678.x

Guzzetta, A., Bonanni, P., Biagi, L., Tosetti, M., Montanaro, D., Guerrini, R., et al. (2007). Reorganisation of the somatosensory system after early brain damage. *Clin. Neurophysiol.* 118, 1110–1121. doi: 10.1016/j.clinph.2007.02.014

Guzzetta, A., Mercuri, E., and Cioni, G. (2001). Visual disorders in children with brain lesions: 2. Visual impairment associated with cerebral palsy. *Eur. J. Paediatr. Neurol.* 5, 115–119. doi: 10.1053/ejpn.2001.0481

Hadders-Algra, M. (2014). Early diagnosis and early intervention in cerebral palsy. *Front. Neurol.* 5:185. doi: 10.3389/fneur.2014.00185

Ickx, G., Bleyenheuft, Y., and Hatem, S. M. (2017). Development of visuospatial attention in typically developing children. *Front. Psychol.* 8:2064. doi: 10.3389/fpsyg.2017.02064

Ickx, G., Hatem, S. M., Riquelme, I., Friel, K. M., Henne, C., Araneda, R., et al. (2018). Impairments of visuospatial attention in children with unilateral spastic cerebral palsy. *Neural Plast.* 2018:1435808. doi: 10.1155/2018/1435808

Karnath, H. O., Fruhmann Berger, M., Kuker, W., and Rorden, C. (2004). The anatomy of spatial neglect based on voxelwise statistical analysis: A study of 140 patients. *Cereb. Cortex* 14, 1164–1172. doi: 10.1093/cercor/bhh076

Kolk, A., and Talvik, T. (2000). Cognitive outcome of children with early-onset hemiparesis. *J. Child Neurol.* 15, 581–587. doi: 10.1177/088307380001500903

Krageloh-Mann, I., and Cans, C. (2009). Cerebral palsy update. *Brain Dev.* 31, 537–544. doi: 10.1016/j.braindev.2009.03.009

Krageloh-Mann, I., and Horber, V. (2007). The role of magnetic resonance imaging in elucidating the pathogenesis of cerebral palsy: A systematic review. *Dev. Med. Child Neurol.* 49, 144–151. doi: 10.1111/j.1469-8749.2007.00144.x

Krageloh-Mann, I., Lidzba, K., Pavlova, M. A., Wilke, M., and Staudt, M. (2017). Plasticity during early brain development is determined by ontogenetic potential. *Neuropediatrics* 48, 66–71. doi: 10.1055/s-0037-1599234

Laplane, D., and Degos, J. D. (1983). Motor neglect. *J. Neurol. Neurosurg. Psychiatry* 46, 152–158.

Laurent-Vannier, A., Pradat-Diehl, P., Chevignard, M., Abada, G., and De Agostini, M. (2003). Spatial and motor neglect in children. *Neurology* 60, 202–207.

Leviton, A., and Paneth, N. (1990). White matter damage in preterm newborns–an epidemiologic perspective. *Early Hum. Dev.* 24, 1–22. doi: 10.1016/0378-3782(90)90002-z

Lidzba, K., Staudt, M., Wilke, M., and Krageloh-Mann, I. (2006). Visuospatial deficits in patients with early left-hemispheric lesions and functional reorganization of language: Consequence of lesion or reorganization? *Neuropsychologia* 44, 1088–1094. doi: 10.1016/j.neuropsychologia.2005.10.022

Martinez-Biarge, M., Diez-Sebastian, J., Rutherford, M. A., and Cowan, F. M. (2010). Outcomes after central grey matter injury in term perinatal hypoxic-ischaemic encephalopathy. *Early Hum. Dev.* 86, 675–682. doi: 10.1016/j.earlhumdev.2010.08.013

Mercuri, E., Spano, M., Bruccini, G., Frisone, M. F., Trombetta, J. C., Blandino, A., et al. (1996). Visual outcome in children with congenital hemiplegia: Correlation with MRI findings. *Neuropediatrics* 27, 184–188. doi: 10.1055/s-2007-973784

Mukherjee, P., Miller, J. H., Shimony, J. S., Philip, J. V., Nehra, D., Snyder, A. Z., et al. (2002). Diffusion-tensor MR imaging of gray and white matter development during normal human brain maturation. *AJNR Am. J. Neuroradiol.* 23, 1445–1456.

Pavlova, M. A., and Krageloh-Mann, I. (2013). Limitations on the developing preterm brain: Impact of periventricular white matter lesions on brain connectivity and cognition. *Brain* 136(Pt 4), 998–1011. doi: 10.1093/brain/aws334

Perani, D., Cappa, S. F., Tettamanti, M., Rosa, M., Scifo, P., Miozzo, A., et al. (2003). A fMRI study of word retrieval in aphasia. *Brain Lang.* 85, 357–368.

Ramenghi, L. A., Ricci, D., Mercuri, E., Groppo, M., De Carli, A., Ometto, A., et al. (2010). Visual performance and brain structures in the developing brain of pre-term infants. *Early Hum. Dev.* 86(Suppl. 1), 73–75. doi: 10.1016/j.earlhumdev.2010.01.010

Reid, L. B., Rose, S. E., and Boyd, R. N. (2015). Rehabilitation and neuroplasticity in children with unilateral cerebral palsy. *Nat. Rev. Neurol.* 11, 390–400. doi: 10.1038/nrneurol.2015.97

Rodriguez, J., Claus, D., Verellen, G., and Lyon, G. (1990). Periventricular leukomalacia: Ultrasonic and neuropathological correlations. *Dev. Med. Child Neurol.* 32, 347–352. doi: 10.1111/j.1469-8749.1990.tb16947.x

Silbereis, J. C., Huang, E. J., Back, S. A., and Rowitch, D. H. (2010). Towards improved animal models of neonatal white matter injury associated with cerebral palsy. *Dis. Model. Mech.* 3, 678–688. doi: 10.1242/dmm.002915

Song, S. K., Sun, S. W., Ramsbottom, M. J., Chang, C., Russell, J., and Cross, A. H. (2002). Dysmyelination revealed through MRI as increased radial (but unchanged axial) diffusion of water. *Neuroimage* 17, 1429–1436. doi: 10.1006/nimg.2002.1267

Song, S. K., Yoshino, J., Le, T. Q., Lin, S. J., Sun, S. W., Cross, A. H., et al. (2005). Demyelination increases radial diffusivity in corpus callosum of mouse brain. *Neuroimage* 26, 132–140. doi: 10.1016/j.neuroimage.2005.01.028

Springer, J. A., Binder, J. R., Hammeke, T. A., Swanson, S. J., Frost, J. A., Bellgowan, P. S., et al. (1999). Language dominance in neurologically normal and epilepsy subjects: A functional MRI study. *Brain* 122(Pt 11), 2033–2046.

Staudt, M. (2010). Reorganization after pre- and perinatal brain lesions. *J. Anat.* 217, 469–474. doi: 10.1111/j.1469-7580.2010.01262.x

Staudt, M., Niemann, G., Grodd, W., and Krageloh-Mann, I. (2000). The pyramidal tract in congenital hemiparesis: Relationship between morphology and function in periventricular lesions. *Neuropediatrics* 31, 257–264. doi: 10.1055/s-2000-9239

Staudt, M., Pavlova, M., Bohm, S., Grodd, W., and Krageloh-Mann, I. (2003). Pyramidal tract damage correlates with motor dysfunction in bilateral periventricular leukomalacia (PVL). *Neuropediatrics* 34, 182–188. doi: 10.1055/s-2003-42206

Stiles, J., and Jernigan, T. L. (2010). The basics of brain development. *Neuropsychol. Rev.* 20, 327–348. doi: 10.1007/s11065-010-9148-4

Sun, S. W., Liang, H. F., Cross, A. H., and Song, S. K. (2008). Evolving Wallerian degeneration after transient retinal ischemia in mice characterized by diffusion tensor imaging. *Neuroimage* 40, 1–10. doi: 10.1016/j.neuroimage.2007.11.049

Thareja, T., Ballantyne, A. O., and Trauner, D. A. (2012). Spatial analysis after perinatal stroke: Patterns of neglect and exploration in extra-personal space. *Brain Cogn.* 79, 107–116. doi: 10.1016/j.bandc.2012.02.009

Trauner, D. A. (2003). Hemispatial neglect in young children with early unilateral brain damage. *Dev. Med. Child Neurol.* 45, 160–166.

Tuch, D. S., Salat, D. H., Wisco, J. J., Zaleta, A. K., Hevelone, N. D., and Rosas, H. D. (2005). Choice reaction time performance correlates with diffusion anisotropy in white matter pathways supporting visuospatial attention. *Proc. Natl. Acad. Sci. U.S.A.* 102, 12212–12217. doi: 10.1073/pnas.0407259102

Volpe, J. J. (1997). Brain injury in the premature infant–from pathogenesis to prevention. *Brain Dev.* 19, 519–534. doi: 10.1016/s0387-7604(97)00078-8

Volpe, J. J., Kinney, H. C., Jensen, F. E., and Rosenberg, P. A. (2011). The developing oligodendrocyte: Key cellular target in brain injury in the premature infant. *Int. J. Dev. Neurosci.* 29, 423–440. doi: 10.1016/j.ijdevneu.2011.02.012

Weierink, L., Vermeulen, R. J., and Boyd, R. N. (2013). Brain structure and executive functions in children with cerebral palsy: A systematic review. *Res. Dev. Disabil.* 34, 1678–1688. doi: 10.1016/j.ridd.2013.01.035

Willmes, K., and Poeck, K. (1993). To what extent can aphasic syndromes be localized? *Brain* 116(Pt 6), 1527–1540.

Wilson, B., Cockburn, J., and Halligan, P. (1987). Development of a behavioral test of visuospatial neglect. *Arch. Phys. Med. Rehabil.* 68, 98–102.

frontiers | Frontiers in Neuroscience

TYPE Original Research
PUBLISHED 05 October 2022
DOI 10.3389/fnins.2022.947390

OPEN ACCESS

EDITED BY
Maurice Ptito,
Université de Montréal, Canada

REVIEWED BY
Ted Mau,
University of Texas Southwestern Medical Center, United States
Berit Schneider-Stickler,
Medical University of Vienna, Austria

*CORRESPONDENCE
Marie Dedry
marie.dedry@uclouvain.be

SPECIALTY SECTION
This article was submitted to Perception Science, a section of the journal Frontiers in Neuroscience

RECEIVED 18 May 2022
ACCEPTED 17 August 2022
PUBLISHED 05 October 2022

CITATION
Dedry M, Dricot L, Van Parys V, Boucquey D, Delinte N, van Lith-Bijl J, Szmalec A, Maryn Y and Desuter G (2022) Brain adaptation following various unilateral vocal fold paralysis treatments: A magnetic resonance imaging based longitudinal case series.
Front. Neurosci. 16:947390.
doi: 10.3389/fnins.2022.947390

Brain adaptation following various unilateral vocal fold paralysis treatments: A magnetic resonance imaging based longitudinal case series

Marie Dedry[1,2]*, Laurence Dricot[2], Vinciane Van Parys[3], Donatienne Boucquey[4], Nicolas Delinte[2,5], Julie van Lith-Bijl[6], Arnaud Szmalec[1,2,7], Youri Maryn[8,9,10,11] and Gauthier Desuter[2,4]

[1]Psychological Sciences Research Institute, Université catholique de Louvain, Louvain-la-Neuve, Belgium, [2]Institute of Neuroscience, Université catholique de Louvain, Brussels, Belgium, [3]Neuromuscular Reference Center, Cliniques Universitaires Saint-Luc, Université catholique de Louvain, Brussels, Belgium, [4]Otolaryngology, Head and Neck Surgery Department, Voice and Swallowing Clinic, Cliniques Universitaires Saint-Luc, Université catholique de Louvain, Brussels, Belgium, [5]Institute of Information and Communication Technologies, Electronics and Applied Mathematics (ICTM), Université catholique de Louvain, Louvain-la-Neuve, Belgium, [6]ENT Department, Flevoziekenhuis, Almere, Netherlands, [7]Department of Experimental Psychology, Faculty of Psychology and Educational Science, Ghent University, Ghent, Belgium, [8]Department of Otorhinolaryngology and Head and Neck Surgery, European Institute for ORL-HNS, Sint-Augustinus (GZA), Antwerp, Belgium, [9]Department of Rehabilitation Sciences and Physiotherapy, Faculty of Medicine and Health Sciences, Ghent University, Ghent, Belgium, [10]Faculty of Education, Health and Social Work, University College Ghent, Ghent, Belgium, [11]Phonanium, Lokeren, Belgium

Aim: Examination of central compensatory mechanisms following peripheral vocal nerve injury and recovery is essential to build knowledge about plasticity of the neural network underlying phonation. The objective of this prospective multiple-cases longitudinal study is to describe brain activity in response to unilateral vocal fold paralysis (UVFP) management and to follow central nervous system adaptation over time in three patients with different nervous and vocal recovery profiles.

Materials and methods: Participants were enrolled within 3 months of the onset of UVFP. Within 1 year of the injury, the first patient did not recover voice or vocal fold mobility despite voice therapy, the second patient recovered voice and mobility in absence of treatment and the third patient recovered voice and vocal fold mobility following an injection augmentation with hyaluronic acid in the paralyzed vocal fold. These different evolutions allowed comparison of individual outcomes according to nervous and vocal recovery. All three patients underwent functional magnetic resonance imaging (fMRI task and resting-state) scans at three (patient 1) or four (patients 2 and 3) time points. The fMRI task included three conditions: a condition of phonation and audition of the sustained [a:] vowel for 3 s, an audition condition of this vowel and a resting condition. Acoustic and aerodynamic measures

as well as laryngostroboscopic images and laryngeal electromyographic data were collected.

Results and conclusion: This study highlighted for the first time two key findings. First, hyperactivation during the fMRI phonation task was observed at the first time point following the onset of UVFP and this hyperactivation was related to an increase in resting-state connectivity between previoulsy described phonatory regions of interest. Second, for the patient who received an augmentation injection in the paralyzed vocal fold, we subsequently observed a bilateral activation of the voice-related nuclei in the brainstem. This new observation, along with the fact that for this patient the resting-state connectivity between the voice motor/sensory brainstem nuclei and other brain regions of interest correlated with an aerodynamic measure of voice, support the idea that there is a need to investigate whether the neural recovery process can be enhanced by promoting the restoration of proprioceptive feedback.

KEYWORDS

unilateral vocal fold paralysis, UVFP, early intervention, fMRI, sustained phonation, brain plasticity, nerve recovery, voice recovery

Abbreviations

LEMG	Laryngeal electromyography
MeAF	Mean air flow
P (1, 2, 3)	Patient (1, 2, 3)
T (1, 2, 3, 4)	Time/Session (1, 2, 3, 4)
PHONATION contrast	[PHONATION_AUDITION condition minus AUDITION condition]
MOBILE map	P2T3 + P2T4 + P3T3 + P3T4 + C1T1 + C1T2 + C1T3 + C1T4
PARALYZED map	P1T1 + P1T2 + P1T3 + P2T1 + P2T2 + P3T1 + P3T2
PARALYZED times (for P2 or P3)	T1 + T2
MOBILE times (for P2 or P3)	T3 + T4

Introduction

Unilateral vocal fold paralysis (UVFP) results in the majority of cases from peripheral nerve damage in the path of the vagus nerve (CN X). The motor neurons of this nerve relay to the ventrolateral portion of the medulla oblongata of the brainstem at the level of the nucleus ambiguus. The intrinsic muscles of the larynx receive motor innervation *via* the recurrent laryngeal nerve except for the crico-thyroid muscle that is innervated by the superior laryngeal nerve. An injury to the vagus nerve or its recurrent branch can therefore lead to the immobility of the vocal fold on the same side of the injury (Rosen et al., 2016). Sensory afferents from the larynx are transmitted by the superior laryngeal nerve and probably also by sensory anastomoses with the recurrent laryngeal nerve to the nucleus of the solitary tract that is also located in the medulla oblongata (Foote and Thibeault, 2021). According to a recent study (Wang H. W. et al., 2020), paralysis is mainly caused, in decreasing order of prevalence, by surgery (mainly following thyroidectomy), tumors (mainly in the lung), or idiopathic causes. Rarer causes include, in the same order, central nerve damage, cardiovascular disorder, trauma and radiation-related disorder. Vocal impairment following paralysis can be very disabling as the voice is often described as hoarse, breathy and of low intensity or aphonic. Patients may also have respiratory or swallowing complaints (Misono and Merati, 2012). This condition can substantially impair the quality of life with repercussions in familial, social and professional spheres. Patients with UVFP report frustration, isolation, fear and an altered self-identity (Francis et al., 2018).

Regarding the management of the UVFP, a first critical question concerns the timing to intervene. Indeed, following nerve damage, there is systematically an attempt of spontaneous reinnervation. This process can either lead to a recovery of mobility of the vocal fold and thus of the voice, or to an improvement of the voice, without recovery of mobility (through synkinetic reinnervation that prevents atrophy of the paralyzed vocal fold and/or favors in a more medial position of the vocal fold), or it can be unsuccessful. Mau et al. (2017) and Mau (2019) reported that, in 96% of cases, if voice recovery was to occur, it would be before 9 months after nerve damage. After 12 months, this percentage increased to 99%. It was therefore recommended not to perform definitive surgical modification (such as medialization laryngoplasty or laryngeal reinnervation) before this time, unless the prognosis for recovery, as assessed

with laryngeal electromyography (LEMG), is very poor or that life expectancy is very short (so the patient cannot wait for spontaneous voice recovery). Mau et al. (2017) and Mau (2019) also suggested that the probability and speed of spontaneous recovery are dependent on the severity of the nerve damage as well as the distance of the site of the nerve injury to the vocal muscle. Patients with idiopathic paralysis, mostly due to neurapraxia, would therefore be to expected to recover more frequently and more quickly than those with neurotmesis or axonotmesis following surgery.

A second key question is what to propose as an effective intervention for UVFP. The time course of the injury, the severity of the nerve damage and its location can therefore guide the choice of a treatment option. In addition, the position of the paralyzed vocal fold is a determining factor as it influences the severity of vocal, respiratory and/or swallowing symptoms. Lastly, although some recommendations are reported in this introduction, these do not prevail over the patient's needs and expectations in determining the most appropriate treatment option. Permanent interventions recommended after a waiting period of 9–12 months will not be discussed here. In the waiting period, two types of interventions could be offered to patients, behavioral voice therapy and injection augmentation. Reviews of the literature supported that behavioral voice therapy is effective in improving the voice of patients with UVFP as well as avoiding the development of maladaptive compensatory vocal behaviors (Walton et al., 2017; Maryn et al., 2020). A majority of studies on the behavioral voice therapy for these patients reported improvement in voice quality or glottic closure (the paralyzed vocal fold moving into a more favorable position for the voice). Only the study of Mattioli et al. (2015), discussed results in terms of improvement of mobility of the paralyzed vocal fold. Since there was no control group and since the improvements of the paralyzed vocal fold were mainly observed in the early behavioral voice therapy groups (before 2 months), authors agreed that it was difficult to distinguish the part of the progress related to the therapy and the part related to possible spontaneous reinnervation. In a more complex way, it is also possible to hypothesize that early intervention might support this process, but this cannot be confirmed. The second intervention option, augmentation injection of a temporary and fully resorbable material, allows to improve the patient's voice immediately by filling the paralyzed vocal fold (Courey and Naunheim, 2020; Wang C. C. et al., 2020), placing it in a more medial position and thus more favorable position for glottic closure during phonation. This is an effective and temporary procedure. The time of complete resorption, ranging from 1 month to 1 year depends on the injected material (Kwon and Buckmire, 2004). Furthermore, this intervention does not prevent the reinnervation process (Marques et al., 2021). Several retrospective studies, have suggested that early injection would reduce the need for permanent intervention at the end of the waiting period (Mau, 2019). However, most of these studies did not specify whether this decrease was related to a recovery of a satisfactory voice in the absence of vocal fold mobility or to a recovery of vocal fold mobility. Furthermore, except for the prospective study of Pei et al. (2015), no experimental design has attempted to evaluate the possible reinnervation process (Mau, 2019). Pei et al. (2015) showed that 6 months after the injection, there was no difference in quantitative LEMG (peak turn frequency measure) between an injection group and a control group. They also emphasized that the decision to perform a permanent intervention is usually influenced by other considerations besides the voice function, such as the patient's general and mental health, their confidence in the medical procedure, and the interactions with their physician. Therefore, the permanent intervention rate would not be a reliable indicator of recovery. This study did not detail how many patients had recovered voice and/or mobility in the two groups at the end of 6 months. Besides, in the injection group assessments were also performed at 1 and 3 months, but not in the control group. It would have been interesting if these results had been detailed and compared with similar assessments in the control group. Indeed, it may be considered that an injection of a temporary material could generate modifications or influence the recovery process differently than natural recovery, even if the final state is similar.

Different hypotheses have been suggested as to how early intervention might promote spontaneous recovery of voice and/or mobility. Accordingly, it would be interesting to analyze what happens at the level of the peripheral nervous system, but also at the level of the brainstem and the brain; neuroplasticity required for such hypotheses, occurring more central than the recurrent laryngeal nerve.

Only four studies have used Magnetic Resonance Imaging (MRI) to investigate changes that occur in patients with vocal fold paralysis. The study of Kiyuna et al. (2020) compared a group of 12 patients with left UVFP for more than 6 months (M = 21.17 months, SD = 22.6) to a group of 12 matched control subjects sustaining 3 s. [i:] vowel in an MRI scanner. The comparison of these two groups between rest and phonation revealed that the UVFP patients showed increased brain activation in the following regions: in the right secondary motor areas (BA 6), primary somatosensory areas (BA 1 and 2), angular gyrus (BA 39), bilateral SMA (BA 6), left inferior parietal lobule (BA 40), superior parietal lobule (BA 7), and middle frontal gyrus (BA 8). The right superior temporal gyrus (BA 22) showed reduced brain activity in UVFP patients. This shows that, in case of chronic vocal fold paralysis, sustained vowel phonation involves an hyperactivation of the phonatory motor network and that a peripheral nerve damage leads to neuroplasticity. Furthermore, two case studies investigated brain changes following voice improvement. Galgano et al. (2009) investigated central neural activation changes after a permanent intervention (type I medialization thyroplasty) in a patient with an UVFP for 3 months. fMRI scans were

completed prior to surgical rehabilitation, 1 month following surgery and 6 months following surgery during following four tasks: a sustained "uh" phonation task at high pitch, sustained "uh" at comfortable pitch, sustained "uh" at low pitch, and a repetition task of the "uh" sound over 4 s. Increased activation was reported in premotor planning (middle frontal gyri) and motor execution areas (precentral gyri) in the frontal lobe, in the inferior and superior parietal lobes, in the superior temporal gyrus, in the thalamus and in the cerebellum 1 month post-surgery. The results at 6 months, however, were difficult to interpret because the patient's health had deteriorated significantly and she was undergoing chemotherapy. Joshi et al. (2011) selectively blocked (i.e., temporarily paralyzed) the right recurrent laryngeal nerve by injecting a solution of lidocaine and epinephrine in this nerve. Brain activations were compared in a sentence reading task before induced paralysis, during paralysis and 1 h after recovery. Greater activation was reported during recovery phase compared to baseline or paralysis period. Although this was different from pathological nerve damage leading to more chronic UVFP and the recovery process was quick, this study showed evidence that neuroplastic changes were observed directly after paralysis and recovery. Perez et al. (2020) compared a group of 10 patients who presented UVFP for more than 12 months and who had been treated with a permanent intervention (type I medialization thyroplasty) for at least 3 months, to a group of 12 control subjects. They investigated resting-state connectivity and reported significant differences in connectivity between the two groups: increased resting-state connectivity between both caudate nuclei and the precuneus and decreased connectivity between these nuclei and the left cerebellar hemisphere, for UVFP patients. Their study testifies that some long-term changes underlying learning processes can be observed in resting state. These studies indicate that (a) UVFP triggers different phonatory activation patterns than that observed in healthy subjects and that (b) improvement of voice following intervention may lead to adapted phonatory brain function.

Considering this information, and in an attempt to improve understanding of the spontaneous reinnervation process, as well as the possible impact of early interventions on voice recovery and/or vocal fold mobility, it appears interesting to evaluate peripheral and central neuroplasticity at several time points, such as shortly after nerve injury and subsequently for a period up to 9/12 months. Therefore, the present study followed three UVFP patients for 1 year with several multiparametric voice assessments and MRI. First, we will comment on the task proposed in this study with regard to our previous review of the literature on activated regions in sustained vowel phonation tasks (Dedry et al., 2022). Second, we will describe the evolution of brain and brainstem activations for this phonation task in three UVFP patients according to time, proposed interventions and vocal and/or nervous recovery. Third, we will focus on the neural recovery of the two patients who recovered vocal fold mobility. Finally, we will look at how the resting-state connectivity was related to the other results. Due to this small number of patients (as a consequence of hindered recruitment during the COVID-19 pandemic), we were restricted to an exploratory and qualitative multiple-cases study.

Materials and methods

Participants

The protocol of this prospective multiple-cases longitudinal study was approved by the Ethics Committee of the University Hospital of Saint-Luc (number: B403201837695) and was conducted in accordance with the principles of the Declaration of Helsinki. All participants signed a written informed consent. The inclusion criterium for the study was to have had a UVFP for less than 3 months.

Three women with UVFP and one healthy control participant with no history of neurologic, hearing or voice disorder were enrolled. The first patient (P1) was a 61-year-old left-handed female with left UVFP with vocal fold in abductory position for 87 days at the time of study inclusion. The identified cause of her paralysis was the excision of a mediastinal paraganglioma. The second patient (P2) was a 30-year-old right-handed female and had a right UVFP in paramedian position resulting from a thermoablation of a thyroid nodule 78 days before inclusion in the study. The third patient (P3) was a 54-year-old and right-handed female with a right UVFP in abductory position. She identified the onset of symptoms as following an upper respiratory tract infection that had occurred 41 days prior to study inclusion. The female control participant (C) was right-handed and 55 years old. All participants were French speaking.

Intervention and assessment procedures

The three patients received different treatments and had several multiparametric voice assessments during the 9 months of their participation. The healthy control participant received no intervention.

In terms of treatment, P1 had fifteen 30-min sessions of voice therapy as well as video-guided homework to be performed between sessions. The sessions were scheduled over 10 weeks (two sessions per week for 5 weeks and then one session per week for the next 5 weeks). The objective of the therapy was to progressively improve the opening and closing movements of the vocal folds by exerting the intrinsic abductor and adductor muscles of

the larynx. This therapy included resonant voice exercises, pitch and loudness variation training, glottal fry exercises, humming exercises, soft glottal closure exercises, phonation on inhalation, Valsalva training, sustaining vowel phonation and sniffing/smelling exercises. At the beginning of vocal therapy, P1 also received a sham injection, which consisted of a subdermic injection of saline solution in the neck (supra-hyoid puncture site), under conditions similar to an acid hyaluronic augmentation injection (described below). Sham interventions (sham injection or sham voice therapy) were set up so that each patient would receive two similar interventions without knowing which one and whether they were effective and specific to UVFP.

P2 received a sham voice therapy consisting of exercises that were designed to not actively mobilize the vocal folds. These exercises aimed at avoiding maladaptive compensatory behaviors, promoting neck and shoulder muscles relaxation and optimizing breathing and posture. The planning of the sessions, their duration and the homework requirements were identical to the protocol of P1. P2 was intended to receive a hyaluronic acid injection but due to anatomical reason (thyroid gland enlargement), the injection could not be performed during the laryngology consultation, hence she also received a sham injection. Therefore, P2 did not receive any effective or specific treatment for UVFP.

P3 underwent vocal fold augmentation with a supra-thyroid injection of 1 ml of hyaluronic acid under local anesthesia and controlled by laryngoscopy in the right/paralyzed vocal fold. She also had the same sham voice therapy as P2.

In terms of timing, the COVID-19 pandemic has disrupted the originally planned timelines for assessments; P1 had three assessments while P2 and P3 had four. Considering that day + 0 is the presumed day of the nerve damage, P1 had three assessments at D + 87, D + 270, and D + 370. Voice therapy was started at D + 92. P2 had four assessments at D + 78, D + 99, D + 161, and D + 358. Finally, P3 had four assessments at D + 41, D + 83, D + 218, and D + 315. The hyaluronic injection occurred at D + 60. The delays in days from the paralysis to the different follow-up points are represented in Figure 1.

Unilateral vocal fold paralysis assessment

Multiparametric assessment as recommended by Dejonckere et al. (2001) and Mattei et al. (2018) was carried out at three or four moments.

Videostroboscopic examination confirmed UVFP and allowed to qualitatively track the evolution of the following parameters with visual analogue scale: glottic closure, position of vocal folds, mucosal wave and vibratory amplitude, regularity and symmetry. Participants were asked to breathe, to sustain [a:], to produce [i:] at high pitch, to repeat three times the sentence "Le petit chat fait sa toilette" and to sniff. These examinations were then scored by three experienced otolaryngologists in order to classify the mobility of the vocal fold on the Ricci-Maccarini et al. (2018) 6-point scale (1: immobile in median position, 2: immobile in paramedian position, 3: immobile in intermediate position, 4: immobile in abducted position, 5: hypomobile, 6: normally mobile). In case of disagreement, the score proposed by 2 of 3 raters was retained.

The following acoustic measures were collected: intensity range, mean fundamental frequency, fundamental frequency range, jitter, shimmer, noise-to-harmonic ratio, smoothed cepstral peak prominence. The following aerodynamic measures were collected: maximum phonation time, phonatory quotient,

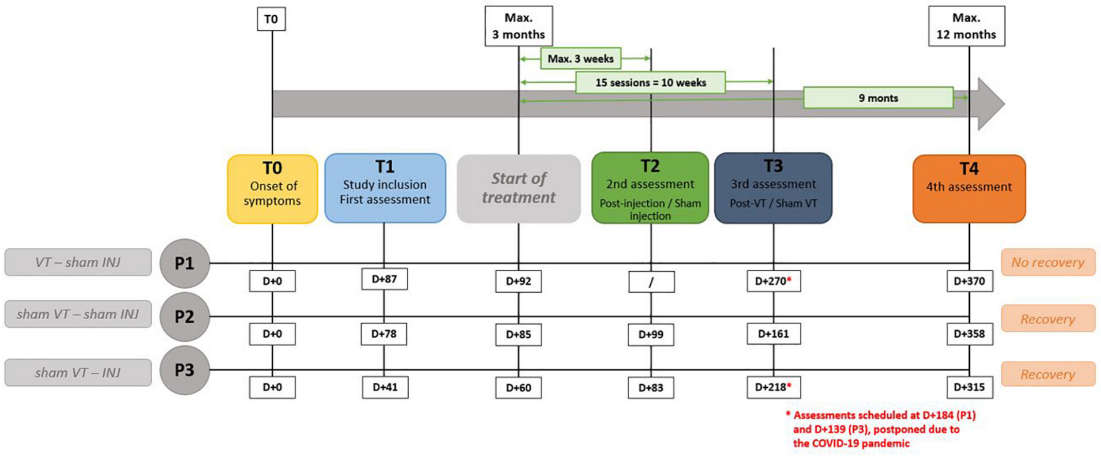

FIGURE 1
Description of experimental procedure. "VT" means voice speech therapy and "INJ" means injection. D + 0 is the presumed day of the nerve damage. "T" represents the different time points of the study.

estimated subglottic pressure, mean air flow (MeAF). The collection procedure of these measures is described in the **Supplementary Table 1**. Multiparametric indices such as the Acoustic Voice Quality Index (v.02.02) (Maryn et al., 2010) and Dysphonia Severity Index (original version) (Wuyts et al., 2000) were calculated. The Hirano's GRBASI scale (Hirano, 1989) and the Voice Handicap Index-30 (Jacobson et al., 1997) were completed.

Finally, laryngeal electromyography (LEMG) of the right and left thyroarytenoid and cricothyroid muscles was performed using concentric needle electrodes with a recording area of 0.07 mm^2 (length = 37 mm, diameter = 0.46 mm), connected to the Nicolet Viking AT2 + 6 amplifier electromyography acquisition system (Natus Medical Incorporated, Pleasanton, CA, United States). For thyroarytenoid muscles, recordings were made at rest, during sustained phonation of the [a:] at habitual pitch and comfortable loudness for at least 3 s and during a series of three sniff inspirations. Potentials in the cricothyroid muscles were measured during phonation of a high-pitched [i:]. Qualitative LEMG interpretation was completed by three professionals (one neurologist, one otorhinolaryngologist and one speech-therapist), based on the characteristics of the EMG waveforms described in Kneisz et al. (2020) (high-pass filter set to 20 Hz, low-pass filter setting 10 kHz, sampling frequency set to 20 kHz). Only the recording of the thyroarytenoid muscle on the paralyzed side during the sustained phonation task was qualitatively scale-coded. The volitional electromyographic activity during phonation in the thyroarytenoid muscle of the paralyzed side was scored on a 4-point scale (1: dense volitional activity, 2: midly decreased volitional activity, 3: strongly decreased volitional activity, 4: single fiber activity) (Kneisz et al., 2020). Again, in case of disagreement, the score proposed by 2/3 was retained.

During the first assessment, a hearing test was also performed (tonal and vocal audiometry). At this time, if patients had a hearing impairment, were unable to produce the sustained [a:] for 3 s or did not have an electromyographic signal in the thyroarytenoid muscle during the LEMG, they would have been excluded from the study. For evident reasons, patients with contraindications for MRI examinations could not be recruited. This was never the case in this study.

Neuroimaging assessment

Functional magnetic resonance imaging tasks

Before each fMRI scanning session, participants had a 15-min appointment with the experimenter to record the sustained [a:], to review the task and to practice it outside the MRI scanner. Participants were asked to sustained [a:] on habitual pitch and intensity levels for 4 s. This sustained phonation was recorded and was then edited to retain 3 s of continuous sound (the onset of the production was removed from the recording). The sustained [a:] vowel was chosen because it is generally used in the laryngology/voice clinics for acoustic and aerodynamic measurements as well as during videostroboscopy and LEMG. The short 3-s duration was chosen to ensure that all patients would be able to produce the sustained [a:] at all times during the time course of their vocal fold paralysis.

The experimental protocol consisted of three conditions. For the PHONATION_AUDITION condition, participants were asked to produce the [a:] on habitual pitch and intensity for 3 s. To ensure sufficient auditory feedback of the sound (in addition to bone conduction) in the noisy MRI scanner, the prerecorded sustained [a:] was also played through MRI compatible audio headphones simultaneous with the voice production. Participants were told that, in this condition, they were hearing herself live. In the AUDITION condition the participants were asked only to listen to their pre-recorded sustained [a:]. In this condition, they had no phonatory task. In the REST condition, the participants had nor phonatory nor listening task.

Functional magnetic resonance imaging paradigm and procedure

The fMRI experiment was presented with a randomized event-related design. Each condition was repeated 15 times for PHONATION_AUDITION and AUDITION conditions and 10 times for REST condition. The run total duration was 11 min 3 s.

Each event began with the presentation of an instruction slide for 2 s. On this slide, the same two visual symbols were presented to participants in all three conditions: a talking mouth and a hearing ear. When these symbols were presented in black color (on a gray background), no "phonation" and "audition" should be performed (REST). When they both were in yellow color, participants had to listen to the sustained [a:] while producing it (PHONATION_AUDITION). When only the hearing symbol was in yellow color, participants only need to listen to their prerecorded sustained [a:] (AUDITION). After the instruction slide, there was a visual countdown from 3-to-1 before presentation of a green loading bar that progressed during the 3 s of the task. Finally, there was a rest period ranging between 7 s and 9.8 s with a black fixation cross. An example of such sequence is demonstrate in **Figure 2**. These visual instructions were generated using Eprime 2.0.8.90 (Psychology Software Tools, Pittsburgh, PA, United States[1]) and presented on a screen (NordicNeuroLab, Norway[2]). A MRI-compatible headset was needed to attenuate the background noise and play the pre-recorded sustained [a:] (NordicNeuroLab, Norway, see text footnote 2). A coil angle-mirror was used to allow participants to see the screen located over the head of the subject.

Two specific instructions were given to reduce non-experimental variability between all three conditions due to

1 http://www.pstnet.com

2 https://www.nordicneurolab.com

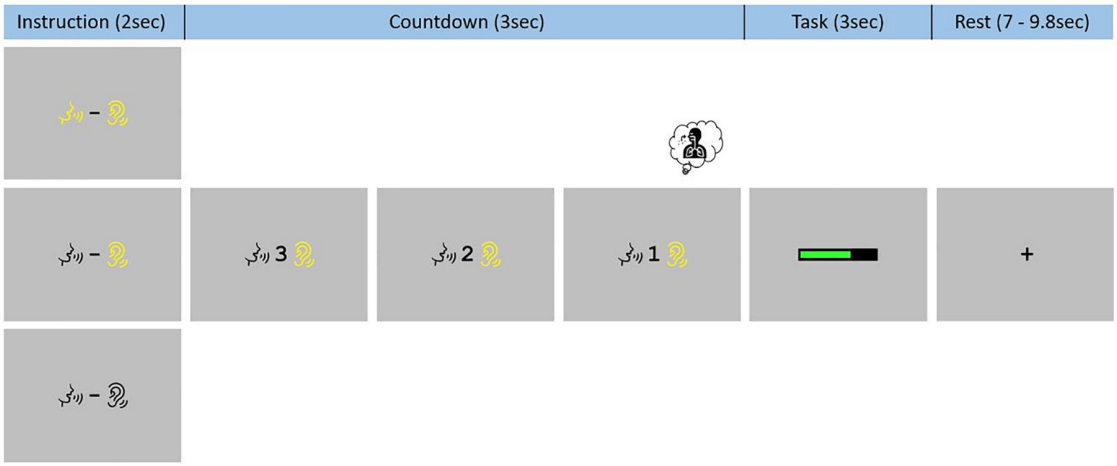

FIGURE 2
Functional magnetic resonance imaging task paradigm. Participants were trained to systematically inhale on the "1" of the 3-to-1 countdown and had to keep the mouth slightly open, in the articulatory position for the [a:] phonation, during the whole experiment.

articulatory and respiratory movements. Participants were instructed to place themselves in the articulatory position for the [a:] phonation at the beginning of the task and to remain with their mouths slightly open during the entire functional acquisition. They were also asked to systematically inhale on the "1" of the 3-to-1 countdown regardless of the condition.

In the absence of an MRI-compatible microphone, it was not possible to monitor the correct execution of the task during or after the examination. Different specific questions about the procedure were therefore asked to the participant directly after the examination to confirm the correct completion of the tasks in the three conditions.

Imaging acquisition parameters

Anatomical, functional (resting-state and task) and multishell diffusion sequences were acquired at the Cliniques Universitaires Saint-Luc (UCLouvain, Belgium) using a 3T head scanner (Signa Premier, General Electric Company, United States) equipped with a 48-channel coil. Diffusion images were not used for the current study. A three-dimensional (3D) T1-weighted data set encompassing the whole brain was selected to provide detailed anatomy (1 mm^3) thanks to a MPRAGE sequence (inversion time = 900 ms, repetition time (TR) = 2188.16 ms, echo time (TE) = 2.96 ms, flip angle (FA) = 8°, field of view (FOV) = 256*256 mm^2, matrix size = 256*256, 156 slices, slice thickness = 1 mm, no gap, total scan time = 5 min 36 s). Task and resting-state MRI T2-weighted sequences of brain activity were collected with echo-planar imaging: FOV = 220*220 mm^2, matrix size = 110*110, TE = 30 ms, TR = 1700 ms, FA = 90°, 75 slices (order ascending and interleaved), slice thickness = 2 mm, parallel imaging (ARC2) and hyperband factor = 3. For the task sequence, the whole brain slices were scanned 390 times per run (= 11 min 3 s) and for the resting-state, the whole brain slices were scanned 210 times per run (= 5 min 57 s).

Neuroimaging data processing

The MRI data were analyzed using BrainVoyager (Version 22.2.2, Brain Innovation, Maastricht, Netherlands). Preprocessing of the resting-state and functional data consisted of linear trend removal to exclude scanner-related signal drift, a temporal high-pass filter to remove frequencies lower than 0.07 Hz (task) and 0.005 Hz (resting-state) and correction for head movements using a rigid body algorithm for rotating and translating each functional volume in 3D space. The data were also corrected for time differences in the acquisition of the different slices. For the resting-state, because spontaneous low-frequency fluctuations are not exclusively BOLD-related fluctuations, but also contaminated by non-neural signals (i.e., artifacts), several additional pre-processing steps were added to remove these undesirable sources of variance. Regression analyses were performed to remove artifacts due to residual motion (the six movement regressors were obtained during the previous motion correction) and changes in ventricles (the signal from the ventricular mask defined in each participant). The data were smoothed in the spatial domain (Gaussian filter, FWHM – 5 mm). To compare the locations of activated brain areas across participants, all anatomical and functional volumes were spatially normalized in Montreal Neurological Institute – MNI space and flipped for P1, and the statistical maps computed were overlaid on the 3D T1-weighted scans. In this way, the acquisitions of the three patients are consistent with paralysis of the right vocal fold. All co-registrations were

verified and movement corrections were optimized, using a sinc interpolation.

Data analyses

Since all MRI scans acquired for P1 were flipped (inverted), all analyses assumed right UVFP. Furthermore, the analyses were performed for a particular contrast, the PHONATION contrast, which includes the activations of the PHONATION_AUDITION condition fMRI scans minus the activations of the AUDITION condition scans (PHONATION = [PHONATION_AUDITION – AUDITION]). The MOBILE map was also investigated independently of the PARALYZED map. The MOBILE map was computed by grouping the "mobile" time points; these were sessions 3 and 4 of P2 and P3, as well as the four sessions of C1 (8 runs). The PARALYZED map included the three sessions of P1, as well as session 1 and 2 of P2 and P3 (7 runs). Besides, four behavioral measures were also selected for analysis of correlations with MRI observations. These were selected because they represented different aspects of the voice and vocal fold mobility. The Acoustic Voice Quality Index – AVQI (Maryn et al., 2010) is an acoustic measure, the mean air flow (MeAF) is an aerodynamic measure, the scale-coding of qualitative LEMG is a peripheral nerve measure and the qualitative laryngoscopy scale is a visual measure of vocal fold mobility. These are provided in **Table 1** for the different time points of the study.

Functional magnetic resonance imaging analysis

Functional data were analyzed using a multiple regression model (general linear model; GLM) consisting of predictors, which corresponded to the particular experimental conditions: PHONATION_AUDITION, AUDITION and REST. The predictor time courses used were obtained by convolution of a condition box-car time course with a standard hemodynamic response function (two-gamma HRF). We conducted two types of analyses, based on regions of interest (ROI) and in the whole brain.

To define the regions of interest (ROI) (Dedry et al., 2022), the present experiment used a previous literature review. This study highlighted 20 left-sided coordinates or clusters of activation and 23 right-sided coordinates or clusters of activation in fifteen different regions in the brain and cerebellum (named according to the atlas of Mai et al., 2006). In this previous literature review, it was decided to exclude regions that were cited only once in the articles included in the literature review from the qualitative analysis. These 28 regions were added to our analyses to ensure a complete overview. Finally, we chose to include two coordinates in the brainstem since no study had investigated it so far. All ROI were created by generating a spherical volume of interest around these coordinates with a radius of 5 mm (515 mm^3). The region of the brainstem identified was the nucleus ambiguus since it is the first motor relay of the recurrent laryngeal nerve. MNI coordinates of this nucleus have been determined from the obex thanks to the atlas of Paxinos et al. (2012) and were validated by a neurosurgeon. The solitary tract nucleus, as first sensory relay of the superior laryngeal nerve and the recurrent laryngeal nerve, was also examined. However, since MNI coordinates of the nucleus ambiguus (from ±5, −40, −49 to ±5, −40, −67) were so close to those of the solitary tract nucleus (±2, −46, −58) (Frangos and Komisaruk, 2017) and as the radius of the volume of interest was 5 mm, it was decided to consider this location as a single region: the motor/sensory nuclei of voice, located in the medulla oblongata of the brainstem. A total of 73

TABLE 1 Behavioral measures at different assessment times.

	AVQI	MeAF	LEMG	Laryngoscopy
P1_T1	6.75	0.23	4	4
P1_T3	7.03	0.26	3	3
P1_T4	5.83	0.32	3	3
P2_T1	4.63	0.21	3	2
P2_T2	4.62	0.16	3	2
P2_T3	4.70	0.22	4	5
P2_T4	5.51	0.19	1	5
P3_T1	6.73	0.61	4	2
P3_T2	4.54	0.23	4	2
P3_T3	4.39	0.16	1	6
P3_T4	6.28	0.10	1	6

The Acoustic Voice Quality Index – AVQI (Maryn et al., 2010) is a multiparametric acoustic indicator rated between 1 and 10. The higher it is, the lower the voice quality. The Men Air Flow (MeAF) is an indicator of the airflow used for the production of a voiced sentence (in L/sec). For laryngeal electromyography, the volitional activity in the thyroarytenoid muscle of the paralyzed side was scored on a 4-point scale (1: dense volitional activity, 2: midly decreased volitional activity, 3: strongly decreased volitional activity, 4: single fiber activity) (Kneisz et al., 2020). For laryngoscopy, the mobility of the paralyzed vocal fold was assessed based on Ricci-Maccarini et al. (2018) 6-point scale (1: immobile in median position, 2: immobile in paramedian position, 3: immobile in intermediate position, 4: immobile in abducted position, 5: hypomobile, 6: normally mobile).

ROI were used for the analyses (cfr. **Supplementary Table 2**). First, to validate the sustained vowel phonation task performed in the MRI scanner with regard to the selected ROI, analyses were conducted to highlight significant brain activation for the PHONATION contrast in the 73 ROIs for the MOBILE map (one-sample Student's *t*-Test). Second, for P2 and P3 separate analyses were run to identify the ROI in which the MOBILE times (3rd and 4th sessions) and the PARALYZED times (1st and 2nd sessions) ([MOBILE – PARALYZED]) showed significant differences in activation (independent sample Student's *t*-Test). To further investigate the MOBILE versus PARALYZED differences, correlational analyses (Pearson correlation) between behavioral measures and beta-weights in the ROIs were also run for P2 and P3.

In order to complement, a whole brain analysis was conducted for each participant and for each assessment time point, to determine, without *a priori* functional localization, the involved regions for the PHONATION contrast. The fifteen maps (3 × P1, 4 × P2, 4 × P3, 4 × C1) were corrected for multiple comparisons using Bonferroni correction ($p < 0.05$).

Resting-state functional connectivity analyses

We used BrainVoyager and a customized Matlab code (The Mathworks) to calculate cross-correlations between the average time-course signals, extracted from 55 ROI (cfr. **Supplementary Table2**). Fifty-four regions were derived from the 73 ROI (described in the previous paragraph) intersected with the MOBILE map. The region of voice motor/sensory nuclei in the brainstem was included in these 54 ROI on the right but not on the left; we therefore chose to add the left nuclei region. This resulted in 1,485 pairs of resting-state functional connectivity per subject. We entered these pairs in an ANOVA to investigate differences between the MOBILE and PARALYZED maps. Independent sample Student's *t*-Test was also conducted between the MOBILE and PARALYZED times particularly for P2 and P3. For P3, correlational analyses using Pearson's *r* coefficient were conducted between behavioral measures and ROI.

Results

Validation of the sustained phonation task

Regions activated for the PHONATION contrast when the MOBILE runs were pooled, compared to forty-three coordinates or clusters of activation highlighted in our literature review of fMRI sustained vowel phonation tasks (Dedry et al., 2022), are illustrated in **Figure 3**. When examined, 35/43 ROI were significantly activated or contained an activation peak ($p < 0.05$). Non-activated clusters were the following: OP47_InfFrontF_orbit_L1, OP47_InfFrontF_orbit_R3, BA42_PlanTemp_Cl_R1, Insula_L1, Putamen_L1, Thalamus_L1, Thalamus_R2, and Cerebellum_CrusII_R4. With the exception of the cerebellar Crus II, other ROI in the inferior frontal gyrus, planum temporale, insula, putamen and thalamus showed activation. Furthermore, when considering the PARALYZED map, the cluster in the left putamen was activated. This does not imply that these regions could not be activated individually for a participant.

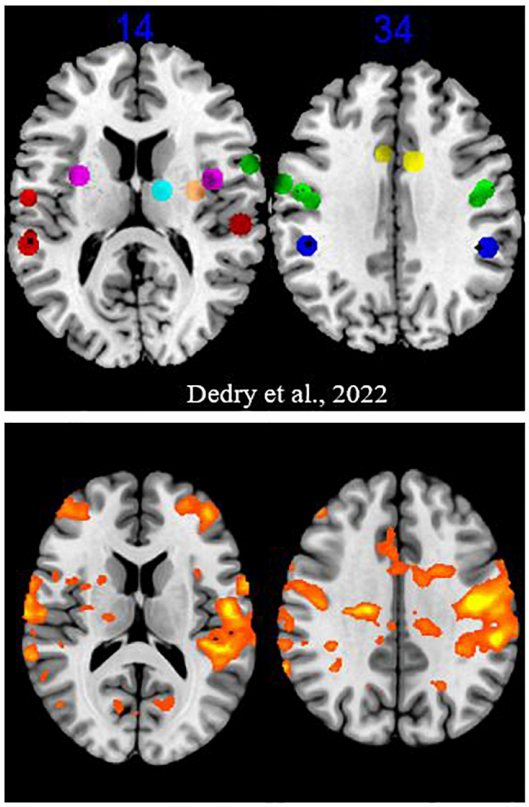

FIGURE 3
Activation map for the "Mobile" runs. The upper part is excerpted from a figure in the Dedry et al. (2022) review of literature. The clusters and coordinates of interest were represented on a brain map at two Z coordinates in MNI. The colors were assigned as follows: green = frontal lobe, red = temporal lobe, dark blue = parietal lobe, yellow = cingulate gyrus, purple = insula, orange = putamen, light blue = thalamus. The bottom part reports activation at a liberal significance threshold ($p = 0.05$) for the "MOBILE" runs of the present experiment.

To further validate the ROI of the present study, the thirty newly added ROI were also examined. Six did not present any significant activation ($p < 0.05$) (BA8_SupFrontG_Cl_L1, BA8_SupFrontG_R1, BA37_MidTempG_L1, BA37_MidTempG_R2, PiriformCortex_R1, AmygdaloidIsland_L1). Two other ROI in the middle temporal gyrus (BA37, BA21) showed

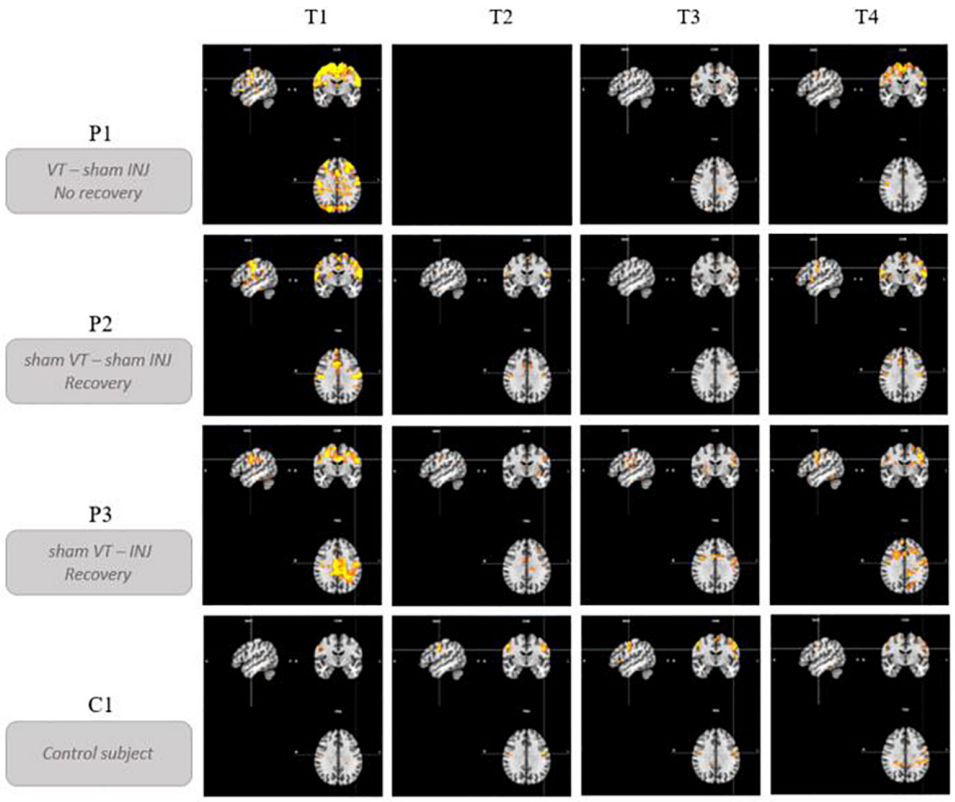

FIGURE 4
Brain activation profiles over time. Evolution of brain activations for the PHONATION contrast using a Bonferroni correction for each patient and the control subject over time. "VT" means voice speech therapy and "INJ" means injection. "T" represents the different time points of the study. These images are centered on the left laryngeal motor cortex cluster located at [−50, −8, 32] (in MNI coordinates).

activation. Brodmann area 8 in the superior frontal gyrus and the amygdalian areas did not appear to play a role in phonation.

Brain activation profiles over time

Figure 4 illustrates the evolution of brain activations for the PHONATION contrast using a Bonferroni correction for each patient and the control participant over time. Only the second MRI scan was missing for P1. These images are centered on the only cluster output from the ALE meta-analysis performed in the previous literature review (Dedry et al., 2022), located at [−50, −8, 32] (in MNI coordinates). This coordinate corresponds to the dorsal laryngeal motor control area and more precisely, the ventromedial peak (Brown et al., 2008, 2009; Belyk et al., 2021).

Qualitatively, hyperactivation was observed for the three patients at the first fMRI session (between 41 and 87 days post-paralysis) in comparison with the control participant. This hyperactivation was mainly localized bilaterally in the premotor, motor and somatosensory integration regions of the frontal lobe (pre- and post-central gyri – BA1, BA2, BA4, BA6, BA43), in the cingulate gyrus (BA24, BA32) and also but less consistently, in the parietal lobe (supramarginal gyrus and parietal operculum – BA40). In general, there was a decrease in activation at times 2 and 3. Time 4, which corresponded to stable state (reinnervation process no longer occurring because the delay was about 1 year after the nerve injury), resulted in more activation than at times 2 and 3 but not in the hyperactivation observed at time 1.

P1, who did not recover vocal fold mobility, is the patient showing the most activation on the last session, mainly in the same frontal regions as at time 1. Unlike P2 and P3, she already had activations in the superior frontal gyrus at time 1 that were still present at the final time. P2 and P3 recovered vocal fold mobility between the second and the third session. Different recovery profiles can be considered. P2, who recovered mobility without injection between time 2 and time 3, showed a progressive bilateral reactivation (on the third and the fourth fMRI scans). Her last scan was more similar to that of the control participant. P3 recovered mobility (between time 2 and time 3) following an injection of hyaluronic acid just before time 2 in the right vocal fold. Her recovery profile seems to be lateralized with a more important activation in the left hemisphere.

It is also interesting to look at what happens in the region of the nucleus ambiguus (that is the first central motor nervous relay) and of the solitary tract nucleus (that is the first central sensory nervous relay) of the vagus nerve (cfr. Figure 5). No activation was detected in this region, for any participant and at any time, except for the second fMRI scan for P3, that was acquired 23 days after the injection of hyaluronic acid in the right vocal fold. Although the injection was unilateral, the activation observed in these nuclei was bilateral and predominantly on the left side. This activation did not last in time, since it was no longer present at times 3 and 4.

Brain activation mobility recovery profiles for P2 and P3

Given these differences, the recovery profiles of P2 and P3 were investigated in more detail by highlighting the activation differences in the 73 ROI between the MOBILE runs (first and second MRI sessions) and the PARALYZED runs (third and fourth MRI sessions) for the PHONATION contrast. Independent samples Student's *t*-Test was run and only significant differences ($p < 0.05$) are reported below. The reason for grouping the times two by two was to increase the statistical power. For a detail of the individual times, please refer to Figure 4. To support the activation variations observed in some of these ROI, correlations with behavioral measures were investigated. Only Pearson's r coefficients greater than $r = 0.6$ were reported, none of them were significant since with four assessment times, the correlation should have been $r = 0.95$ to reach significance ($p < 0.05$).

For P2, three ROI deactivated significantly when reinnervation had occurred and the vocal fold was mobile. These were the following ROI: BA6_PreG_Cl_R2, BA37_MidTempG_R2, PostCingulateG_R3. No correlation was observed with MeAF, AVQI or the scale-coding of qualitative LEMG. Deactivation of these three regions correlated negatively with the qualitative laryngoscopy scale.

P3 had a more complex profile. She presented deactivations but also significant activations when the vocal fold was mobile. First, deactivations were observed in the following ROI: BA4_PreG_R2, BA4_PreG_L3, BA4_PreG_Cl_R3, BA6_ParacentralLobule_R2, BA7_SupramarginalG_R1, Thalamus_R1, Brainstem_MotSens_L. However, this deactivation observed in the voice motor/sensory nuclei in the brainstem was probably only due to the isolated post-injection hyperactivation at time 2. These deactivations correlated positively with (a) the MeAF (r from 0.73 to 0.88) in the precentral gyrus and paracentral lobule (4/7 ROI), (b) AVQI (r from 0.69 to 0.87) in 3 of these 4 deactivated regions (except BA4_PreG_Cl_R3), and (c) negatively ($r = -0.61$) with the deactivation of the voice motor/sensory nuclei in the brainstem. As explained above, since these nuclei were never activated except after injection, this correlation must be considered with caution. (d) A positive correlation (r from 0.61 to 0.66) was also observed with the scale-coding of qualitative LEMG (and reversely with qualitative laryngoscopy scale) in the right precentral and paracentral gyrus, supramarginal gyrus and thalamus (5/7 ROI). Second, when the vocal fold was mobile the following ROI were more activated: BA44_InfFrontG_oper_Cl_R1, OP47_InfFrontF_orbit_L2, BA22_SupTempG_Cl_L1, Insula_L2, Insula_R3, Putamen_R3, Thalamus_R2. A negative correlation (r from −0.72 to −0.80) with the MeAF (a) was found for all the regions except the left inferior frontal gyrus. (b) AVQI generally did not correlate with increased activation except for left superior temporal gyrus ($r = -0.85$). (c) The scale-coding of qualitative LEMG correlated negatively and the qualitative laryngoscopy scale positively (r from ±0.67 to ±0.79) with 4/7 ROIs (all except those in the inferior frontal gyrus and the one in the right thalamus).

These ROIs did not contain significant deactivations or activations in the control participant when comparing runs 1 and 2 to runs 3 and 4 except for the BA7_SupramarginalG_R1 that showed a significant difference but in the opposite direction to the one observed in P3 and with a less significant activation peak in the investigated region.

Resting-state connectivity analyses

Differences in connectivity between the MOBILE and PARALYZED maps

Qualitatively, Figure 6 shows that functional connectivity between the 55 ROI selected for resting-state analyses was higher in the PARALYZED map than in the MOBILE map, there were thus more regions whose functional activations vary simultaneously. Quantitatively, only significant ($p < 0.05$) differences will be reported in the text below.

Resting-state connectivity decreased mainly between motor (BA4) and premotor (BA6, BA43) regions and between those regions and the cingulate gyrus and the lobule VI of the cerebellum. Resting-state connectivity also decreased between the parietal regions (BA40, BA7), and between those regions and the motor and premotor regions, insula, putamen and cerebellum. A reduction was also observed between the ROI of cerebellar lobule VI. At the level of the right voice motor/sensory nuclei in the brainstem, resting-state connectivity decreased with the right premotor regions (BA6 and BA43), the right cingulate cortex (BA32), and right lobule VI of the cerebellum. For the left voice motor/sensory nuclei, decreased resting-state connectivity was observed with the left premotor regions (BA43), the right globus pallidus and thalamus, as well as the VI cerebellum lobule. Finally, resting-state connectivity decreased between the insula, putamen, thalamus and cerebellum.

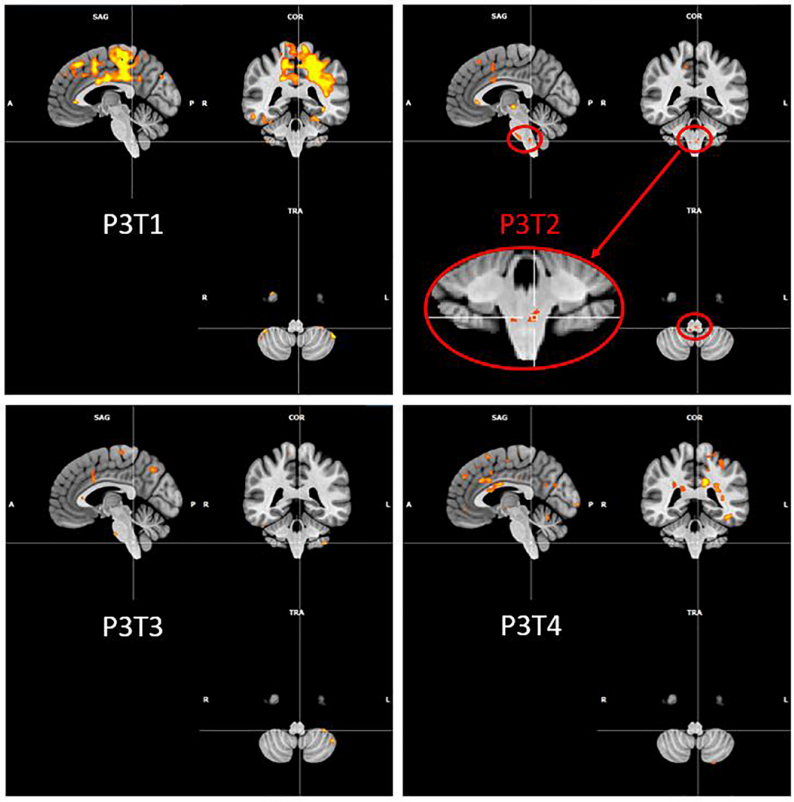

FIGURE 5
P3 over time activation of the region of ambiguus and solitary tract nuclei. Evolution of Patient 3 activation in the region of ambiguus and solitary tract nuclei for the PHONATION contrast using a Bonferroni correction. These images are centered at [−5, −40, −52] (in MNI coordinates).

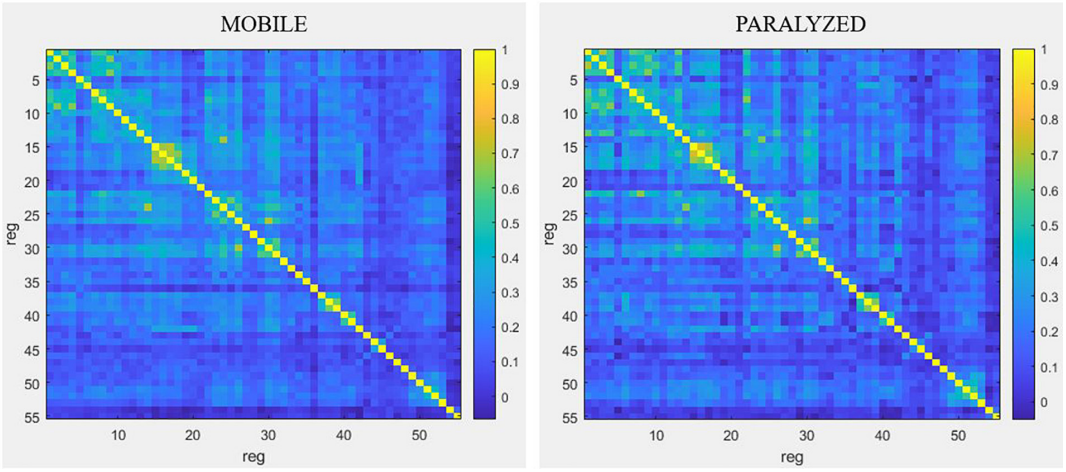

FIGURE 6
Resting-state connectivity matrices for the MOBILE map and the PARALYZED map. This figure is a symmetric matrix representing the connectivity between the 55 ROI. "reg" means regions. The color scale represents the correlation coefficients from −1 to 1.

Although decreased connectivity was most often present, some regions showed significant increased functional resting-state connectivity when the paralyzed vocal fold was mobile. The temporal ROI showed mainly increased bilateral resting-state connectivity with each other but also with some right motor (BA4) and premotor (BA6)

regions, with the putamen as well as with the post cingulate gyrus.

The highest degree of resting-state connectivity changes (either increase or decrease) between MOBILE and PARALYZED maps was found in the following six ROI: Cerebellum_VI_R1, BA43_PreG_Cl_L1, BA7_SupramarginalG_R1, Cerebellum_Cl_VI_L1, BA42_PlanTemp_R2, and Brainstem_ MotSens_L.

Differences in connectivity at the brainstem level for P3

Following the observation of activation for P3 just after injection in the area of the voice motor and sensory nuclei in the brainstem, it appeared interesting to investigate the modification of functional resting-state connectivity between these nuclei (left and right) and other ROI. MeAF showed the highest rate of correlation with changes in resting-state connectivity between the brainstem nuclei of interest and other regions. Moreover, the variations of the MeAF were important for P3 and reflected the immediate effect of the received injection. Having an UVFP in abduction, the MeAF of P3 was very high at time 1 (0.61 L/s) due to glottal air leakage. Immediately after the injection, at time 2, an important decrease of the MeAF was observed (0.23 L/s) due to mechanically restored glottic closure (by filling the paralyzed vocal fold with hyaluronic acid). At times 3 and 4, the MeAF continued to decrease slightly (0.16 and 0.10 L/s) and even normalize (Joshi, 2020) due to recovery of vocal fold mobility as confirmed by videostroboscopy. Therefore, we chose to report these correlations. The significant correlations had to reach a Pearson's r coefficient ≥ 0.95. Ten correlations reached this score for the right nuclei and five for the left nuclei. Considering the high number of correlations between $r = 0.9$ and $r = 0.95$ (six on the right and five on the left), we chose to consider them as well.

The resting-state connectivity changes correlated with the MeAF between voice motor/sensory brainstem nuclei and other regions are illustrated in **Figure 7**. Qualitatively, right nuclei showed more MeAF correlations with connectivity changes than left nuclei. Also, the left nuclei showed only positive correlations while those on the right had both positive and negative correlations depending on the regions.

For the left nuclei, changes in resting-state connectivity with several regions in the precentral gyrus were positively correlated with MeAF. These ROI were the first cluster in the left laryngeal motor cortex, which corresponded to the ventromedial peak of the dorsal laryngeal motor control area (Brown et al., 2008, 2009; Belyk et al., 2021), and some premotor regions (BA6 and BA43). Connectivity between the left nuclei and the right superior frontal gyrus (BA6) was also positively correlated with MeAF. Similar correlations were also observed with the thalamus and cerebellum. Hence, the correlations were always positive, indicating that the higher the MeAF was (thus, the larger the glottic air leakage), the higher the resting-state connectivity was between these regions and the left nuclei.

For the right side, the resting-state connectivity of the voice motor/sensory nuclei and the two clusters of the laryngeal motor cortex (BA4) correlated with changes in the MeAF. For cluster 1 on the left and bilaterally for cluster 2, which corresponded to the dorsolateral peak of this same region (Brown et al., 2008, 2009; Belyk et al., 2021), connectivity was positively correlated. For the third cluster in BA4 bilaterally, the correlation was reversed. Thus, connectivity was higher when MeAF was low (and glottic air leakage was reduced). This difference in the direction of correlations was also found elsewhere. Resting-state connectivity with the premotor area of the paracentral lobule, the inferior frontal gyrus (BA44), the auditory regions (planum temporale and middle temporal gyrus) and the cingulate gyrus correlated negatively with the MeAF. Consequently, resting-state connectivity was higher when MeAF was low. Conversely, resting-state connectivity with the premotor regions of the precentral gyrus (BA6), supramarginal gyrus, putamen and globus pallidus was increased when MeAF was high. For regions outside the laryngeal motor cortex, laterality was not always assessed because the ROIs did not systematically include identical clusters on both sides.

Finally, changes in resting-state connectivity between right and left voice motor/sensory brainstem nuclei were positively correlated with MeAF. The higher the MeAF was, the higher the connectivity was between the two regions of nuclei.

P2 had an UVFP in paramedian position and her MeAF was within the normal range (Joshi, 2020) from time 1 and relatively stable at all other times (0.21, 0.16, 0.22, and 0.19 L/s). It was therefore clinically irrelevant to analyze the correlations with this measure.

Discussion

In order to describe the central nervous changes observed in our three patients, part of the analyses of this study were performed using the regions of interest of our previous literature review on sustained phonation tasks in healthy subjects (Dedry et al., 2022). As detailed in the "Results" section, most of the expected regions were also active in the "MOBILE" map of this study. These regions were therefore considered relevant and were used in the analyses.

The qualitative analysis of the different evolutions changes in the three patients revealed a brain hyperactivation for the PHONATION contrast compared to the control participant. This enhanced brain activation was already described in the study by Kiyuna et al. (2020). The authors reported that activity was greater in the regions involved in voice control in patients with chronic UVFP ($n = 12$) compared to the control group. In

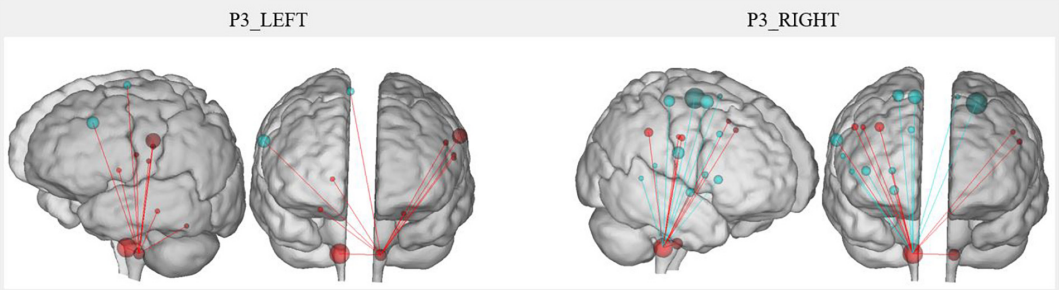

FIGURE 7
P3 resting-state connectivity changes correlated with the MeAF from the voice motor/sensitive brainstem nuclei. The correlation between the MeAF (L/s) and Patient 3 connectivity changes from the left and right voice motor/sensitive brainstem nuclei is presented. Positive correlations are shown in red and negative correlations in blue. The size of the spheres represents the degree of change in connectivity of each region (either in the direction of more or less connectivity).

contrast, Galgano et al. (2009) did not report such significantly increased activation in their patient scanned preoperatively 3 months after onset of UVFP. Our case series study provides an additional precision; hyperactivation seems to take place rapidly after the nerve damage (within 3 months) and seems to be even more increased in this acute phase. Indeed, the activation was very strong at time 1 compared to the other study times. P1, who did not recover vocal fold mobility, was also the one who showed greater activity at time 4. This greater activation compared to the control participant was also observed to a lesser extent for P2 and P3. It would have been interesting to scan these two patients a fifth time to see if, once recovery was stabilized, they returned to a level of activation completely similar to that of the control participant. After 1 year, we cannot state that the recovery of mobility after paralysis activates the brain regions similarly to the activations observed in someone who has never had an UVFP. The resting-state connectivity analyses also provided supplementary and novel information. Indeed, in our patients, the UVFP-related hyperactivation during paralysis observed for the PHONATION contrast in fMRI was associated with an increase in resting-state connectivity (without doing any task) between most regions of interest. Paralysis would therefore lead to an increase in activation in the phonation task but also to an increase in resting-state connectivity between the hyperactivated regions. These resting-state results cannot be compared with those of the only previous study that conducted connectivity analyses (Perez et al., 2020). Indeed, these authors recruited patients who had experienced UVFP for more than 1 year and who had received a permanent intervention. They were outside the time course of nerve recovery. The central plasticity processes at work in their study were therefore quite different from those investigated in the current study.

These qualitative observations also enabled to observe a different brain plasticity in the process of nervous recovery for P2 than for P3. We therefore investigated the changes in ROI activation for the MOBILE time compared to the PARALYZED time. In order to support the assumption that the observed changes were indeed related to the recovery process, we looked at whether these correlated with certain behavioral measures. Few significant changes were observed for P2. These differences were observed on the right side, the "healthy" cerebral side, contralateral to the lesion [since cortico-motoneuronal projections are bilateral but with a contralateral dominance (Jürgens, 2002)]. These were in the direction of deactivation and correlated negatively with qualitative laryngoscopy scale (no correlation with MeAF, AVQI or qualitative LEMG scale-coding). P2, who recovered spontaneously from paralysis in the paramedian position, seemed to show milder and progressive changes. The correlations with behavioral measures were also fewer, but in view of the position in which the paralyzed vocal fold was positioned, the MeAF and the AVQI were already less impacted at baseline. The changes observed in P3 were more frequent, more bilateral, were in the direction of deactivation or activation and were correlated with behavioral measures. Finally, at the final MRI session, activations observed qualitatively for the PHONATION contrast in P2 were more similar to those of the control subject. The profile of P3 showed more activation and a more lateralized activation on the left brain side. A precise analysis or any conclusion with these two patients is not possible, but we hypothesize that the abrupt change induced by the injection may have resulted in greater plasticity and that the post-injection nerve recovery process may differ from the spontaneous nerve recovery process.

It is still a matter of debate whether and how the injection augmentation could promote voice recovery and/or recovery of vocal fold mobility (Mau, 2019). This study is the first to investigate the changes in brain activation following an injection with several MRI scans. We found that, following the injection, the region of the voice motor and sensory nuclei in the medulla oblongata (brainstem) was activated bilaterally. This was the only scan in the study where activation at this location was observed. Furthermore, it is important to note that, at this time,

P3 had not yet recovered mobility of the vocal fold (UVFP confirmed at time 2 by videostroboscopy) and that the scale-coding of her thyroarytenoid muscle electromyography was equivalent to time 1. Therefore, there was no indication yet that reinnervation was going to be successful. As this was a multiple-cases study, we applied a Bonferroni correction in order to obtain robuster results. There could also be activation of these nuclei in all mobile vocal fold phonation tasks at a threshold that cannot be reliably assessed with the methodology of this study. It is therefore still uncertain whether this is a one-time activation or a hyperactivation compared to all other assessment times and subjects.

Different hypotheses were summarized by Mau (2019) on the possible impact of injection on voice recovery or vocal fold mobility recovery. Only one of them can be applied to mobility recovery; the injection would restore proprioceptive feedback that would favor spontaneous reinnervation process. The sensory receptors of the muscles of the glottic level would recover sensations similar to those of a healthy voice due to the restoration of the subglottic pressure during phonation and/or due to the vibro-tactile stimulation due to the contact between the paralyzed vocal fold with the healthy vocal fold. Furthermore, auditory perception of clearer and/or louder sounding voice is restored as a result of this early injection (Smith et al., 2020). Restoring feedbacks could therefore play a role in the peripheral reinnervation process, but it remains unclear how these processes occur. Two aspects of our study are in line with the first hypothesis.

First, the activation observed in the nuclei of interest was bilateral but more prominent on the left side, contralateral to the paralyzed vocal fold. The motor and sensory innervation between the vocal folds and the voice-related nuclei in the brainstem being unilateral, it may be surprising to see a bilateral medulla response after an injection into a unilaterally paralyzed vocal fold. One possible explanation is that by injecting the paralyzed vocal fold and restoring the tightness of the glottic closure, the sensation of subglottic pressure and of vocal fold contact would be restored for both vocal folds. Furthermore, the greatest response on the healthy side would be expected since more sensory nerve fibers would be preserved on this side. LEMG at times 1 and 2 confirmed that the nerve damage was low in the vagus nerve pathway and that the superior laryngeal nerve was preserved. Indeed, the signal observed in the crico-thyroid muscle was normal. The middle division of this nerve internal branch is responsible for sensory innervation of the vocal folds (Foote and Thibeault, 2021). Moreover, according to the synthesis written by Foote and Thibeault (2021) on the sensory innervation of the larynx, Galen's anastomosis and/or the arytenoid plexus are highly prevalent in humans and consequently, the posterior branch of the recurrent laryngeal nerve (classically described as only motor) would play an important role in the sensory innervation of the subglottic region. That this nerve was injured on the paralyzed side and preserved on the mobile side could contribute to a greater sensory response in the left nuclei of the solitary tract.

Second, for Patient 3, MeAF was the measure that showed the highest rate of correlations with changes in resting-state connectivity between the voice-related nuclei in the brainstem and other regions. MeAF is an indicator of the glottic air leakage present during phonation; it is therefore indirectly related to glottic closure and thus to the restoration of proprioceptive perception of subglottic pressure. Furthermore, the observation of the correlation of the MeAF with the connectivity at rest in this patient has allowed to highlight different points. The resting-state connectivity between voice motor/sensory nuclei bilaterally was more important when the MeAF was high; therefore, when the glottic air leak was important, when the vocal cord was paralyzed. The resting-state connectivity between the left brainstem nuclei and the motor, premotor, thalamic and cerebellar regions was also more important when the MeAF was high. This increased connectivity could reflect an attempt to compensate from the healthy side. On the paralyzed vocal fold side (right), direction of the correlations varied.

Although both of these elements support the hypothesis that restoring proprioceptive feedback could be beneficial, the effect of restoring auditory feedback cannot be isolated in the present study. Indeed, the injection generates both a restoration of the subglottic pressure and an improvement of the vocal quality. The patient could therefore hear herself again with a more stable and powerful voice after the intervention. Auditory feedback may also play a role. The study of Smith et al. (2020), which investigated the effect of disrupting auditory feedback and proprioceptive feedback on the laryngeal compensatory response, concluded that when both sources of feedback were available and the information received by these two perceptual systems was congruent, the compensatory response was greater. Although this study was not conducted in patients with voice disorders, the presence of auditory feedback may potentiate the effect of proprioceptive feedback detected in the voice-related nuclei in the brainstem.

Qualitatively, an important observation was that the patient reported being able to clearly identify the moment her "normal" voice started to return. This occurred 3 months after the injection (between time 2 and time 3). She then commented that her voice was clearer already in the morning, that there was no longer a hitch, and that the voice always came out as she expected. This patient was therefore particularly attentive to her senses, whether they were sensory or audible.

All the observations above invited questions about the conditions that might foster the reinnervation process. Some of these have been described previously. First, the severity of the nerve injury as well as the distance between the damage and the vocal muscle impact the possibilities of nervous recovery (Mau et al., 2017). Neurotmesis or axonotmesis are less likely

to result in reinnervation to restore mobility than neurapraxia. Indeed, the more the nerve fibers are damaged, the more the risk of having a synkinetic reinnervation is important (Mau et al., 2017). Although it is not easy to have a clear indication of these parameters, different aspects can provide an indication. LEMG shows a good positive predictive value for screening patients with poor recovery prognosis (Wang et al., 2015) but can also inform on the topology of the injury. When the nerve signal is intact in the crico-thyroid muscle, the damage is located further along the vagus nerve, at the level of the recurrent laryngeal nerve. In addition, the etiology is also informative. Indeed, recoveries are more frequent in idiopathic or infectious UVFP (Sulica, 2008). A hypothesis on the severity can also be formulated according to the type of surgery performed. Second, the activation observed of the brainstem voice-related nuclei leads us to consider the need for sensory innervation to remain available for proprioceptive feedback to be transmitted. Regarding the vocal folds contact, this transmission is ensured by the superior laryngeal nerve. Regarding the subglottic pressure, it could be ensured by some sensory anastomosis with the recurrent laryngeal nerve. The impairment or not of these nerves could therefore be a determining factor. Third, in order for proprioceptive feedback to be effective, glottic closure must be complete during phonation. This condition depends on the position and the possible amyotrophy of the paralyzed vocal fold. The vocal fold could be paralyzed in the paramedian position but, when this is not the case, the injection could carry out this function. If this procedure is required, it is preferably performed as early as possible after the nerve injury. Indeed, it has been described that the chances of nerve recovery are higher just after the injury and decrease significantly with time to be minimal from 9 months (Mau, 2019). This would be a fourth condition.

This study presents several points of improvement for future studies. First, regarding the experimental design, it would be beneficial to record the patients with a microphone during the task and have them hear themselves live with auditory feedback from the microphone. This would permit the use of the prerecorded [a:] only in the AUDITION task and ensure that the task was performed as instructed. In addition, a choice was made regarding the analyzed behavioral measures. This choice was justified based on the principle of having a representative measure of the different parameters of the voice: acoustic, aerodynamic, vocal fold mobility and peripheral innervation. These last two parameters were analyzed with qualitative scales previously reported. Other teams may consider it more relevant to measure quantitative parameters for these two aspects. Concerning the fMRI analyses performed, some of them were based on regions of interest defined in a previous literature review. They were representative of the regions reported to be activated by a sustained vowel phonation task but were not always bilateral. It was therefore not always possible to distinguish between compensation of the healthy vocal fold and reinnervation attempts in the paralyzed vocal fold. Bilaterality could only be commented on at the level of the brainstem voice-related nuclei and of the laryngeal motor cortex for which the clusters were systematically bilateral as also for the qualitative analyses in the whole brain. In the future, the contralateral coordinates should always be included for each ROI in the investigated regions. Finally, given the intrinsic heterogeneity of this voice disorder, we recommend privileging case series analyses.

More hypotheses than answers were addressed in this study. Given the small number of profiles analyzed, it was only possible to describe and share the methodology and our observations. Only one patient received injection, we formulated several conditions for the replicability of our observations with this patient and we hope that other patients with similar profiles will support our assumptions. Furthermore, we have to be aware of the possibility that P3 could have recovered spontaneously without the injection. Our assumptions are therefore not intended to encourage a more systematic early injection but to encourage understanding of whether and how early injection augmentation might influence the nerve recovery process. We hope that both the experimental design and the results discussed will encourage further research on this exciting and crucial issue in order to develop and provide the best possible intervention for each UVFP patient.

Conclusion

This multiple-cases longitudinal study highlighted several points. In our three patients, an hyperactivation was observed at time 1 for the sustained vowel phonation task. This hyperactivation was related to an increase in resting-state connectivity between phonatory regions of interest. Moreover, two patients recovered vocal fold mobility but the brain plasticity related to this nerve recovery did not follow a similar trend. We did not identify a single pattern of brain plasticity related to recovery; this could depend on whether the recovery is spontaneous or supported by an early intervention. Finally, for the patient who received an augmentation injection in the paralyzed vocal fold, we subsequently observed a bilateral activation of the voice-related nuclei in the brainstem. This last observation, as well as the fact that, for this same patient, the resting-state connectivity between the voice motor/sensory brainstem nuclei and other brain ROI correlated with the MeAF, support the hypothesis that promoting the restoration of proprioceptive feedback enhances the neural recovery process. These observations should be investigated in future research. We have therefore provided a list of conditions in which we believe that a similar observation at the level of the voice-related nuclei in the brainstem could be expected. The qualitative results obtained with our multiple-cases report provides further insight

about the process at play in vocal recovery and pave the way for more efficient treatments for patients dealing with UVFP.

Data availability statement

The datasets presented in this article are not readily available because this is a multiple-case study and the patients included did not give their consent for the data to be used by other research teams. Requests to access the datasets should be directed to MD, marie.dedry@uclouvain.be.

Ethics statement

The studies involving human participants were reviewed and approved by the Ethics Committee of the University Hospital of Saint-Luc (number: B403201837695). The patients/participants provided their written informed consent to participate in this study.

Author contributions

MD, LD, VV, AS, YM, and GD contributed to the conception and design of the study. MD, LD, VV, DB, and GD participated in the data collection. MD and LD performed the analysis. MD, LD, AS, YM, and GD contributed to the interpretation of the results. MD wrote the first draft of the manuscript. LD wrote sections of the manuscript. All authors contributed to the manuscript revision, read, and approved the submitted version.

Acknowledgments

We thank Dr. Gilles Delahaut, otorhinolaryngologist, for his expertise in the analysis of videostroboscopic recordings as well as Prof. Aleksandar Jankovski, neurosurgeon, for his help in locating the nucleus ambiguus.

Conflict of interest

YM was employed by company Phonanium.

The remaining authors declare that the research was conducted in the absence of any commercial or financial relationships that could be construed as a potential conflict of interest.

Publisher's note

All claims expressed in this article are solely those of the authors and do not necessarily represent those of their affiliated organizations, or those of the publisher, the editors and the reviewers. Any product that may be evaluated in this article, or claim that may be made by its manufacturer, is not guaranteed or endorsed by the publisher.

Supplementary material

The Supplementary Material for this article can be found online at: https://www.frontiersin.org/articles/10.3389/fnins.2022.947390/full#supplementary-material

References

Belyk, M., Brown, R., Beal, D. S., Roebroeck, A., McGettigan, C., Guldner, S., et al. (2021). Human larynx motor cortices coordinate respiration for vocal-motor control. *Neuroimage* 239:118326. doi: 10.1016/j.neuroimage.2021.118326

Brown, S., Laird, A. R., Pfordresher, P. Q., Thelen, S. M., Turkeltaub, P., and Liotti, M. (2009). The somatotopy of speech: Phonation and articulation in the human motor cortex. *Brain Cogn.* 70, 31–41. doi: 10.1016/j.bandc.2008.12.006

Brown, S., Ngan, E., and Liotti, M. (2008). A larynx area in the human motor cortex. *Cereb. Cortex* 18, 837–845. doi: 10.1093/cercor/bhm

Courey, M. S., and Naunheim, M. R. (2020). Injection laryngoplasty for management of neurological vocal fold immobility. *Adv. Neurolaryngol.* 85, 68–84. doi: 10.1159/000456684

Dedry, M., Maryn, Y., Szmalec, A., van Lith-Bijl, J., Dricot, L., and Desuter, G. (2022). Neural correlates of healthy sustained vowel phonation tasks: A systematic review and meta-analysis of neuroimaging studies. *J. Voice* doi: 10.1016/j.jvoice.2022.02.008

Dejonckere, P. H., Bradley, P., Clemente, P., Cornut, G., Crevier-Buchman, L., Friedrich, G., et al. (2001). A basic protocol for functional assessment of voice pathology, especially for investigating the efficacy of (phonosurgical) treatments and evaluating new assessment techniques. *Eur. Arch. Otorhinolaryngol.* 258, 77–82. doi: 10.1007/s004050000299

Foote, A. G., and Thibeault, S. L. (2021). Sensory Innervation of the larynx and the search for mucosal mechanoreceptors. *J. Speech Lang. Hear. Res.* 64, 371–391. doi: 10.1044/2020_JSLHR-20-00350

Francis, D. O., Sherman, A. E., Hovis, K. L., Bonnet, K., Schlundt, D., Garrett, C. G., et al. (2018). Life experience of patients with unilateral vocal fold paralysis. *JAMA Otolaryngol. Head Neck Surg.* 144, 433–439. doi: 10.1001/jamaoto.2018.0067

Frangos, E., and Komisaruk, B. R. (2017). Access to vagal projections via cutaneous electrical stimulation of the neck: fMRI evidence in healthy humans. *Brain Stimul.* 10, 19–27. doi: 10.1016/j.brs.2016.10.008

Galgano, J. F., Peck, K. K., Branski, R. C., Bogomolny, D., Mener, D., Ho, M., et al. (2009). Correlation between functional MRI and voice improvement following type I thyroplasty in unilateral vocal fold paralysis—a case study. *J. Voice* 23, 639–645. doi: 10.1016/j.jvoice.2008.01.016

Hirano, M. (1989). Objective evaluation of the human voice: Clinical aspects. *Folia Phoniatr (Basel)* 41, 89–144. doi: 10.1159/000265950

Jacobson, B. H., Johnson, A., Grywalski, C., Silbergleit, A., Jacobson, G., Benninger, M. S., et al. (1997). The voice handicap index (VHI) development and validation. *Am. J. Speech Lang. Pathol.* 6, 66–70. doi: 10.1044/1058-0360.0603.66

Joshi, A. (2020). A comparison of the s/z ratio to instrumental aerodynamic measures of phonation. *J. Voice* 34, 533–538. doi: 10.1016/j.jvoice.2019.02.014

Joshi, A., Jiang, Y., Stemple, J. C., Archer, S. M., and Andreatta, R. D. (2011). Induced unilateral vocal fold paralysis and recovery rapidly modulate brain areas related to phonatory behavior: A case study. *J. Voice* 25, e53–e59. doi: 10.1016/j.jvoice.2010.07.002

Jürgens, U. (2002). Neural pathways underlying vocal control. *Neurosci. Biobehav. Rev.* 26, 235–258. doi: 10.1016/S0149-7634(01)00068-9

Kiyuna, A., Kise, N., Hiratsuka, M., Maeda, H., Hirakawa, H., Ganaha, A., et al. (2020). Brain activity in patients with unilateral vocal fold paralysis detected by functional magnetic resonance imaging. *J. Voice.* doi: 10.1016/j.jvoice.2020.08.008

Kneisz, L., Volk, G. F., Mayr, W., Leonhard, M., Pototschnig, C., and Schneider-Stickler, B. (2020). Objectivation of laryngeal electromyography (LEMG) data: Turn number vs. qualitative analysis. *Eur. Arch. Otorhinolaryngol.* 277, 1409–1415. doi: 10.1007/s00405-020-05846-7

Kwon, T. K., and Buckmire, R. (2004). Injection laryngoplasty for management of unilateral vocal fold paralysis. *Curr. Opin. Otolaryngol. Head Neck Surg.* 12, 538–542. doi: 10.1097/01.moo.0000144393.40874.98

Mai, J. K., Majtanik, M., and Paxinos, P. (2006). *Atlas of the human brain*, 4th Edn. Cambridge, MA: Academic Press.

Marques, J. A., Marronnier, A., Crampon, F., Lagier, A., and Marie, J. P. (2021). Early management of acute unilateral vocal fold paralysis: Update of the literature. *J. Voice* 35, 924–926. doi: 10.1016/j.jvoice.2020.02.021

Maryn, Y., De Bodt, M., and Roy, N. (2010). The acoustic voice quality index: Toward improved treatment outcomes assessment in voice disorders. *J. Commun. Disorder* 43, 161–174. doi: 10.1016/j.jcomdis.2009.12.004

Maryn, Y., Dedry, M., Szmalec, A., and Desuter, G. (2020). Behavioural treatment of unilateral vocal fold paralysis of the recurrent laryngeal nerve: Literature overview [Logopädische Behandlung unilateraler Stimmlippenparalysen]. *Spr. Stimme Gehor* 44, 34–43. doi: 10.1055/a-0949-7863

Mattei, A., Desuter, G., Roux, M., Lee, B. J., Louges, M. A., Osipenko, E., et al. (2018). International consensus (ICON) on basic voice assessment for unilateral vocal fold paralysis. *Eur. Anna. Otorhinolaryngol. Head. Neck Dis.* 135, S11–S15. doi: 10.1016/j.anorl.2017.12.007

Mattioli, F., Menichetti, M., Bergamini, G., Molteni, G., Alberici, M. P., Luppi, M. P., et al. (2015). Results of early versus intermediate or delayed voice therapy in patients with unilateral vocal fold paralysis: Our experience in 171 patients. *J. Voice* 29, 455–458. doi: 10.1016/j.jvoice.2014.09.027

Mau, T. (2019). "Timing of intervention for unilateral vocal fold paralysis," in *Decision making in vocal fold paralysis*, (Cham: Springer), 13–28.

Mau, T., Pan, H. M., and Childs, L. F. (2017). The natural history of recoverable vocal fold paralysis: Implications for kinetics of reinnervation. *Laryngoscope* 127, 2585–2590. doi: 10.1002/lary.26734

Misono, S., and Merati, A. L. (2012). Evidence-based practice: Evaluation and management of unilateral vocal fold paralysis. *Otolaryngol. Clin. North America* 45, 1083–1108. doi: 10.1016/j.otc.2012.06.011

Paxinos, G., Huang, X., Sengul, G., and Watson, C. (2012). *Organization of brainstem nuclei*. Amsterdam: Elsevier Academic Press.

Pei, Y. C., Fang, T. J., Hsin, L. J., Li, H. Y., and Wong, A. M. (2015). Early hyaluronate injection improves quality of life but not neural recovery in unilateral vocal fold paralysis: An open-label randomized controlled study. *Restor. Neurol. Neurosci.* 33, 121–130. doi: 10.3233/rnn-140439

Perez, P. L., Cueva, K. L., Rosen, C. A., Young, V. N., Naunheim, M. L., Yung, K. C., et al. (2020). Cortical-basal ganglia-cerebellar networks in unilateral vocal fold paralysis: A pilot study. *Laryngoscope* 130, 460–464. doi: 10.1002/lary.28004

Ricci-Maccarini, A., Bergamini, G., and Fustos, R. (2018). Proposal of a form for the collection of videolaryngostroboscopy basic findings. *Eur. Arch. Otorhinolaryngol.* 275, 1927–1933. doi: 10.1007/s00405-018-4991-7

Rosen, C. A., Mau, T., Remacle, M., Hess, M., Eckel, H. E., Young, V. N., et al. (2016). Nomenclature proposal to describe vocal fold motion impairment. *Eur. Arch. Otorhinolaryngol.* 273, 1995–1999. doi: 10.1007/s00405-015-3663-0

Smith, D. J., Stepp, C., Guenther, F. H., and Kearney, E. (2020). Contributions of auditory and somatosensory feedback to vocal motor control. *J. Speech Lang. Hear. Res.* 63, 2039–2053. doi: 10.1044/2020_JSLHR-19-00296

Sulica, L. (2008). The natural history of idiopathic unilateral vocal fold paralysis: Evidence and problems. *Laryngoscope* 118, 1303–1307. doi: 10.1097/MLG.0b013e31816f27ee

Walton, C., Conway, E., Blackshaw, H., and Carding, P. (2017). Unilateral vocal fold paralysis: A systematic review of speech-language pathology management. *J. Voice* 31, 509–e7. doi: 10.1016/j.jvoice.2016.11.002

Wang, C. C., Chang, M. H., De Virgilio, A., Jiang, R. S., Lai, H. C., Wang, C. P., et al. (2015). Laryngeal electromyography and prognosis of unilateral vocal fold paralysis—a long-term prospective study. *Laryngoscope* 125, 898–903. doi: 10.1002/lary.24980

Wang, C. C., Wu, S. H., Tu, Y. K., Lin, W. J., and Liu, S. A. (2020). Hyaluronic acid injection laryngoplasty for unilateral vocal fold paralysis—A systematic review and meta-analysis. *Cells* 9:2417. doi: 10.3390/cells9112417

Wang, H. W., Lu, C. C., Chao, P. Z., and Lee, F. P. (2020). Causes of vocal fold paralysis. *Ear Nose Throat J.* 101, N294–N298. doi: 10.1177/0145561320965212

Wuyts, F. L., Bodt, M. S. D., Molenberghs, G., Remacle, M., Heylen, L., Millet, B., et al. (2000). The dysphonia severity index: An objective measure of vocal quality based on a multiparameter approach. *J. Speech Lang. Hear. Res.* 43, 796–809. doi: 10.1044/jslhr.4303.796

frontiers | Frontiers in Neuroscience

TYPE Systematic Review
PUBLISHED 20 October 2022
DOI 10.3389/fnins.2022.1010354

OPEN ACCESS

EDITED BY
Hamidreza Namazi,
Monash University, Malaysia

REVIEWED BY
Maria Arioli,
University of Milano-Bicocca, Italy
Amber Maimon,
Reichman University, Israel

*CORRESPONDENCE
Maurice Ptito
maurice.ptito@umontreal.ca

SPECIALTY SECTION
This article was submitted to Perception Science, a section of the journal Frontiers in Neuroscience

RECEIVED 03 August 2022
ACCEPTED 30 September 2022
PUBLISHED 20 October 2022

CITATION
Bleau M, Paré S, Chebat D-R, Kupers R, Nemargut JP and Ptito M (2022) Neural substrates of spatial processing and navigation in blindness: An activation likelihood estimation meta-analysis. *Front. Neurosci.* 16:1010354. doi: 10.3389/fnins.2022.1010354

Neural substrates of spatial processing and navigation in blindness: An activation likelihood estimation meta-analysis

Maxime Bleau[1], Samuel Paré[1], Daniel-Robert Chebat[2,3], Ron Kupers[1,4,5], Joseph Paul Nemargut[1] and Maurice Ptito[1,5,6]*

[1]École d'Optométrie, Université de Montréal, Montreal, QC, Canada, [2]Visual and Cognitive Neuroscience Laboratory (VCN Lab), Department of Psychology, Faculty of Social Sciences and Humanities, Ariel University, Ariel, Israel, [3]Navigation and Accessibility Research Center of Ariel University (NARCA), Ariel University, Ariel, Israel, [4]Institute of Neuroscience, Faculty of Medicine, Université de Louvain, Brussels, Belgium, [5]Department of Neuroscience, University of Copenhagen, Copenhagen, Denmark, [6]Department of Neurology and Neurosurgery, Montreal Neurological Institute, McGill University, Montreal, QC, Canada

Even though vision is considered the best suited sensory modality to acquire spatial information, blind individuals can form spatial representations to navigate and orient themselves efficiently in space. Consequently, many studies support the *amodality hypothesis* of spatial representations since sensory modalities other than vision contribute to the formation of spatial representations, independently of visual experience and imagery. However, given the high variability in abilities and deficits observed in blind populations, a clear consensus about the neural representations of space has yet to be established. To this end, we performed a meta-analysis of the literature on the neural correlates of spatial processing and navigation via sensory modalities other than vision, like touch and audition, in individuals with early and late onset blindness. An activation likelihood estimation (ALE) analysis of the neuroimaging literature revealed that early blind individuals and sighted controls activate the same neural networks in the processing of non-visual spatial information and navigation, including the posterior parietal cortex, frontal eye fields, insula, and the hippocampal complex. Furthermore, blind individuals also recruit primary and associative occipital areas involved in visuo-spatial processing via cross-modal plasticity mechanisms. The scarcity of studies involving late blind individuals did not allow us to establish a

clear consensus about the neural substrates of spatial representations in this specific population. In conclusion, the results of our analysis on neuroimaging studies involving early blind individuals support the *amodality hypothesis* of spatial representations.

KEYWORDS

visual impairments and blindness, spatial navigation, spatial processing, neuroplasticity, amodality, neuroimaging, MRI, meta-analysis

Introduction

Vision is the most adapted sense in humans for moving around and wayfinding (Ekstrom, 2015) and the most prominent spatio-cognitive sensory modality (Foulke, 1982). It has been hypothesized that all spatial inputs are recoded into *visual* representations in the brain (Pick, 1974; Lehnert and Zimmer, 2008). Consequently, blindness is often associated with an inability to move and orient oneself properly in space (Ptito et al., 2021a). However, through orientation and mobility (O&M) training, blind individuals learn to rely on other sensory modalities such as audition (i.e., echolocation), olfaction, touch and proprioception (Juurmaa and Suonio, 1975; Kupers et al., 2010; Long and Giudice, 2010; Teng et al., 2012; Kolarik et al., 2017) for resolving spatial tasks. Blind individuals also learn adaptive orientation strategies and the use of navigation and orientation aids, such as the long cane and tactile maps, which extend their perception of the environment and allow them to learn its layout (Long and Giudice, 2010; Chebat et al., 2018a, 2020a; Giudice, 2018; Ptito et al., 2021a). This training thus allows safe and independent navigation for both early blind (EB) and late blind (LB) individuals (Long and Giudice, 2010; Schinazi et al., 2016). In fact, EB, even without visual experience, are able to form cognitive spatial representations (or cognitive maps) of various environments (Passini and Proulx, 1988; Passini et al., 1990; Thinus-Blanc and Gaunet, 1997; Fortin et al., 2006a; Connors et al., 2014; Chebat et al., 2018b; Nelson et al., 2018) through a process known as spatial learning, cognitive mapping or spatial knowledge acquisition (Schinazi et al., 2016; Chebat et al., 2020a). Hence, EB can integrate paths (Loomis et al., 1993, 2012), as well as encode and recognize routes and locations (Passini and Proulx, 1988; Passini et al., 1990; Thinus-Blanc and Gaunet, 1997; Fortin et al., 2006a).

Empirical data thus indicate that EB can represent space, and that their deficit is purely *perceptual,* and not *cognitive.* This conjecture is demonstrated by studies investigating the use of sensory substitution devices (SSDs) which translate visual information into other sensory modalities (i.e., vibrotactile or auditory feedback). These studies showed that when given the same amount of spatial information through SSDs, EB are able to locate and avoid obstacles as efficiently as LB and blindfolded sighted controls (SC), sometimes outperforming them (Segond et al., 2005; Auvray and Myin, 2009; Chebat et al., 2011; Maidenbaum et al., 2014; Stoll et al., 2015; Bleau et al., 2021; Paré et al., 2021) or performing as well as SC using vision (Chebat et al., 2015, 2017). Furthermore, EB, and even LB, outperformed blindfolded SC in various spatial tasks, such as non-visual path integration (Loomis et al., 1993) and locating sound sources on the horizontal plane (Voss et al., 2004; Doucet et al., 2005; Gougoux et al., 2005; Collignon et al., 2011). However, other studies suggests that EB exhibit impairments in auditory and proprioceptive spatial perception (Cappagli et al., 2017) and have deficits in many spatial tasks such as sound localization in the vertical plane (Zwiers et al., 2001; Lewald, 2002), auditory spatial bisection (Gori et al., 2014, 2020) and motion encoding (Finocchietti et al., 2015). Furthermore, other studies showed that even though EB can form and use spatial representations, they fail to achieve the same level of proficiency than LB and SC (Fortin et al., 2006b; Pasqualotto and Newell, 2007; Ruggiero et al., 2018, 2021). Hence, there is no consensus on the abilities and deficits of blind individuals, as they seem to vary depending on the chosen paradigms and testing conditions (Schinazi et al., 2016; Giudice, 2018).

It is however clear that blindness is associated with complex behavioral changes that vary with types of tasks, context, and different personal and social factors such as age, blindness onset, physical exercise and O&M training (Cappagli and Gori, 2016; Giudice, 2018; Rogge et al., 2021). The large variability in behavioral performances may thus be attributable to the wide range of adaptive strategies and abilities (e.g., Braille reading, echolocation) used by blind individuals to compensate for their lack of visual input. These life-long changes are also accompanied by underlying changes at the neural level (Merabet and Pascual-Leone, 2010; Kupers and Ptito, 2014). Indeed, it is now well known that the brain of blind individuals (EB and LB) undergoes important modifications both at the anatomical and functional levels. Occipital visual areas are cross-modally recruited by other sensory modalities through various neuroplastic mechanisms (Harrar et al., 2018; Chebat et al., 2020b; Ptito et al., 2021a). This cross-modal recruitment enables the visual cortex to stay functional and leads to better performances in non-visual tasks (Kupers and Ptito, 2014;

Silva et al., 2018; Ptito et al., 2021a). However, this finding is at odds with reports of significant atrophy in visual pathways and occipital cortex (Shimony et al., 2006; Ptito et al., 2008b, 2021b; Wang et al., 2013; Jiang et al., 2015). Furthermore, brain structures involved in navigation such as the posterior hippocampus, the parahippocampal gyrus and the entorhinal gyrus (Fyhn et al., 2007; Epstein et al., 2017), are reduced in EB, and to a certain extent in LB (Chebat et al., 2007; Ptito et al., 2008b; Modi et al., 2012; Ankeeta et al., 2021).

Studies conducted in blind individuals have led to the concept of an *amodal* foundation of the neural representation of space which has been conceptualized in the *amodality hypothesis* (Loomis et al., 2013). This hypothesis suggests that spatial representations can be formed through many different sensory inputs, are encoded in a format that transcends specific sensory modalities and are *spatial* in nature. According to this theory, all subsequent spatial mental operations are independent from their input modalities and from visual experience (Loomis et al., 2012; Chebat et al., 2018a; Giudice, 2018; Harrar et al., 2018). Thus, spatial deficits in the blind may not arise from the loss of vision *per se*, but from the insufficient access to spatial information due to the lack of non-visual alternatives and the poor accessibility of the environment built by and for the sighted. Consequently, cumulating and integrating spatial information for spatial knowledge acquisition is a longer and more cognitively demanding process that heavily depends on the individual's attentional resources and memory (Long and Giudice, 2010; Giudice, 2018). This may lead to delays in the development of spatial abilities in the blind who rely more frequently on egocentric frames of reference (based on the subject's viewpoint) instead of allocentric ones (independent from the individual's perspective). Blind individuals therefore often prefer route-based strategies rather than cognitive map-based, or "survey knowledge," strategies that are more prone to error in this population (Passini and Proulx, 1988; Millar, 1994; Thinus-Blanc and Gaunet, 1997; Ungar et al., 1997; Espinosa et al., 1998; Pasqualotto and Proulx, 2012; Iachini et al., 2014; Giudice, 2018; Ruggiero et al., 2021).

As highlighted in the previous paragraphs, there is still no clear consensus regarding the nature of spatial processing and its independence from visual experience and imagery (Giudice, 2018). To the best of our knowledge, only two meta-analyses investigated neural correlates of non-visual functions in individuals with blindness (Ricciardi et al., 2014; Zhang et al., 2019). These studies however mainly focused on the cross-modal recruitment of the occipital cortex and not on the functioning of the larger neural network underlying spatial navigation in the absence of vision (Chebat et al., 2018a, 2020b). Furthermore, results from LB were excluded. Therefore, it is relevant and timely to conduct a meta-analysis specifically on the neural correlates of non-visual spatial navigation and orientation in both EB and LB. This type of analysis may help to shed light on potential knowledge gaps and lead to new research directions in the field of O&M, visual rehabilitation and restoration. The present study hence examines brain activations patterns in a large data set of spatio-cognitive paradigms in EB, LB, and SC. The systematic literature search focuses on paradigms investigating cognitive processes involved in (1) the processing of spatial information through tactile and auditory modalities; and (2) spatial navigation and orientation in the absence of vision. Activation likelihood estimation (ALE) analyses were performed to investigate general agreements across the selected neuroimaging studies. Results identified shared activations in frontoparietal networks involved in visuospatial attention, and recruitment of navigation networks (e.g., hippocampus, parahippocampus, and other areas of the visual dorsal stream) in EB, as compared to LB and SC. Current data thus support the view that spatial representations in these networks are indeed independent from the input modality.

Methods

The literature search conducted in the present study as well as the screening and selection process followed the *Preferred reporting items for systematic reviews and meta-analyses* (PRISMA) guidelines (Moher et al., 2009). We systematically searched seven databases: PubMed (NCBI), PsycINFO (EBSCO), MEDLINE (NLM), Global Health (PSI), Embase (Elsevier), ERIC (IES), and Web of Science (Clarivate Analytics), to identify neuroimaging studies that investigated spatial navigation or spatial processing in individuals with total blindness, and that were published between January 1990 and January 2022. Since spatial navigation tasks generally integrate different spatial and decision-making tasks, data in the selected articles were extracted and divided into two categories: (1) Non-visual *Spatial Processing* (tasks generally involving one specific type of spatial computing) and (2) Non-visual *Spatial Navigation* (tasks involving higher order processes, i.e., navigating, recognizing routes or important features used during wayfinding). Following this classification, ALE meta-analyses were performed to identify the neural correlates in EB, LB and SC for these two categories. Contrast and conjunction meta-analyses were also conducted to identify the neural correlates that are common, or different, across the three groups. In the context of this paper, we defined EB as individuals who either were born blind or acquired blindness early in life ($<$1 year of age), whereas individuals who acquired blindness later in life were considered as LB.

Literature search

The *population* of interest was defined as adult ($\geq$18 years of age) individuals with total blindness resulting from peripheral (eye or optic nerve) pathologies, or damages, without

neurological disorders or psychiatric illness. The topic of interest was related to the neural substrates of spatial processing, spatial navigation, and orientation, using sensory information other than vision (i.e., tactile and auditory). In the meta-analysis, we considered neuroimaging studies published before January 2022, and written in English. Thereupon, a broad list of keywords relating to "spatial navigation" or "spatial processing" and "neural correlates" and "blindness" was then developed to collect relevant articles (**Supplementary Table 1**). In addition, through snowballing (Jalali and Wohlin, 2012), reference lists of the most relevant empirical articles and reviews were also screened to identify any other eligible articles. All identified sources were imported into End-Note v.9.3.3 (Clarivate Analytics, PA, USA) and exported into Covidence (Veritas Health Innovation, Melbourne, Australia), a screening software for the conduction of systematic reviews. All duplicates were then automatically removed, and a two-stage screening process was conducted: (1) title and abstract screening; and (2) full-text screening. This procedure allowed for the identification of eligible articles based on the inclusion criteria and *post hoc* exclusion criteria (**Table 1**). During title and abstract screening, only articles including blind participants, investigating spatial navigation or spatial sensory processing, and employing task-based fMRI or PET techniques were withheld. During the full-text screening process, we followed guidelines for conducting meta-analysis (Müller et al., 2018) and only accepted papers that (1) reported activation coordinates in standardized Talairach space (Talairach and Tournoux, 1988) or Montreal Neurological Institute (MNI) space (Collins et al., 1994); (2) conducted within-group based contrasts; (3) performed whole-brain analyses; (4) used an univariate approach to reveal localized increased activations; and (5) included a minimum of three participants per group in the final analyses. The final criterion was modified due to recruitment challenges often encountered when working with blind populations (see "Study limitations and considerations for future research" section).

Ultimately, 31 studies were included in the meta-analysis that were grouped into two categories: (1) *spatial processing* (21 studies), including articles with spatial tasks (i.e., localization, spatial attention, spatial working memory), that required the processing of non-visual sensory stimuli (of these, 13 studies investigated the auditory modality and seven, the tactile modality, while only one investigated both); and (2) *spatial navigation* (9 studies), including articles with spatial navigation tasks in a given environment or spatial tasks that required the processing of important information used by individuals with blindness during navigation and spatial learning (i.e., spatial language, landmarks or spatially significant textures).

Figure 1 illustrates the literature search process and the classification of the included papers.

Data from every included article was extracted and organized based on authors' names, year of publication, characteristics of participants, neuroimaging methodology (fMRI or PET), contrasts of interest (only those reflecting spatial processes), coordinates space (MNI or Talairach), number of activation foci identified for the performed contrasts, and significant finding related to the aim of the present study. **Table 2** presents a detailed overlook of the 31 studies included in the meta-analysis, including to which category dataset articles belonged and the functional domain of the task (in other words, the nature of the task or of the investigated spatial process). Since four out of 31 studies (Gougoux et al., 2005; Voss et al., 2006, 2008, 2011) performed the same experiments in three independent samples (EB, LB, and SC), included articles may feature potential overlaps of subject samples. Information about sources that were not included in the meta-analysis is provided in **Supplementary Table 2**.

Datasets associated with non-visual spatial processing and navigation

The meta-analysis included a total of 263 EB, 50 LB and 232 SC, from 30, 9 and 26 studies, respectively. Reported coordinates of foci from all 31 included studies were extracted into seven datasets. For experiments in the *spatial processing* category, two datasets were constructed: "*EB Spatial Processing*" (20 contrasts, 461 foci; 183 subjects) and "*SC Spatial Processing*"

TABLE 1 Inclusion and exclusion criteria.

Inclusion criteria	Exclusion criteria
• Studies on non-visual spatial navigation or spatial sensory processing. • Studies involving individuals with total blindness (bilateral & peripheral). • Neuroimaging methods of interest: only fMRI and PET.	***According to Participants, Concept and Context*** • Presence of concomitant neurological disorders or psychiatric illnesses. • Spatial tasks not relevant to spatial navigation or with no sufficient control (i.e., imagery with no sensory stimuli/task, etc.). ***According to Meta-analysis guidelines*** • *MNI* or *Talairach* coordinates not reported. • No univariate analysis (i.e., multivoxel analysis, machine learning, functional connectivity). • No "within group"- based contrasts. • Region of Interest (ROI) instead of whole brain analysis. • Less than three participants per group.

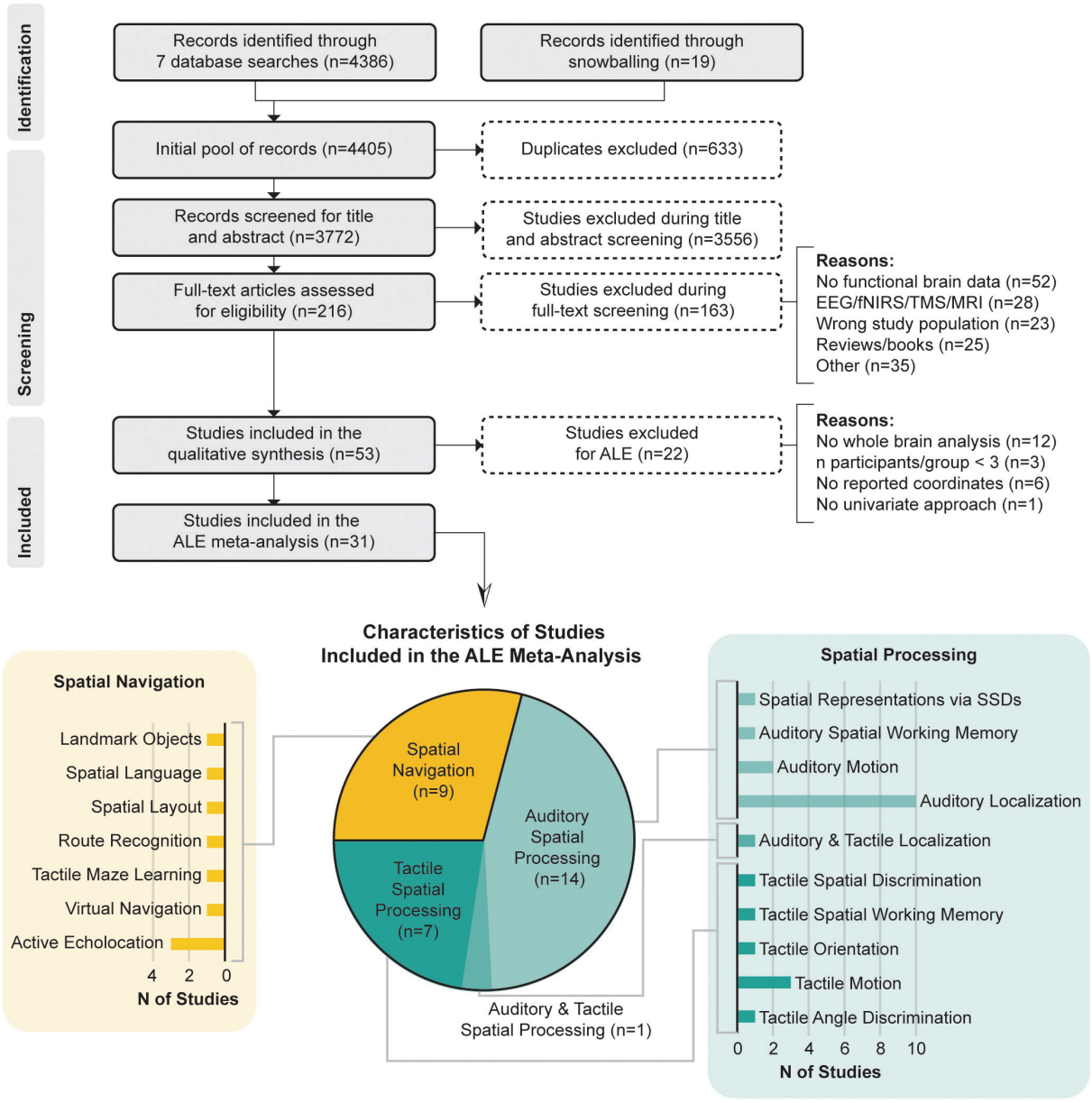

FIGURE 1
PRISMA flow chart and characteristics of studies included in the meta-analysis according to datasets and the specific functional domains they investigated.

(15 contrasts, 237 foci; 157 subjects). For the *spatial navigation* category, two datasets were constructed: "*EB Spatial Navigation*" (11 contrasts, 157 foci; 80 subjects) and "*SC Spatial Navigation*" (8 contrasts, 93 foci; 75 subjects). Furthermore, three datasets combining both spatial processing and navigation were formed: "*EB Spatial Processing + Spatial Navigation*" (31 contrasts, 618 foci; 263 subjects); "*SC Spatial Processing + Spatial Navigation*" (23 contrasts, 330 foci; 232 subjects); and "*LB Spatial Processing + Spatial Navigation.*" Since only a limited number of studies involved LB, the "*LB Spatial Processing + Spatial Navigation*" dataset only included 6 contrasts (78 foci; 50 subjects) which is well below guidelines criteria (Müller et al., 2018). Therefore, a meta-analysis specific to LB is still unachievable as of the current literature. In constructing these datasets, clusters with positive activations were included, while deactivation clusters were excluded. Different contrasts obtained from the same sample within the same article and/or across multiple articles (Gougoux et al., 2005; Voss et al., 2006, 2008, 2011) were pooled into one experiment to avoid counting a single experiment multiple time (Müller et al., 2018).

TABLE 2 Overview of included studies.

REFERENCES	FUNCTIONAL DOMAIN	METHOD	*N* SUBJECTS	TASK CONTRASTS	FOCI EB	FOCI LB	FOCI SC	MAIN FINDINGS
SPATIAL NAVIGATION								
Dodsworth, 2019*	Active echolocation	fMRI	5 Blind (4 EB, 1 LB), 8 SC	Active echolocation for navigation, with echoes > No echoes; Route > Scrambled route	30	–	19	During echolocation-based navigation, expert echolocators recruited parts of the occipital cortex (MOG, cuneus, precuneus) and small area in the parahippocampus.
Fiehler et al., 2015	Active echolocation	fMRI	6 EB, 3 SC	[expert or novice] Active echolocation for path direction, with echoes > No echoes	6	–	9	Path direction discrimination via echoes recruited premotor cortex, SPL, IPL and IFC in all groups. EB additionally recruited parts of the occipital cortex.
Gagnon et al., 2012	Tactile maze learning	fMRI	11 EB, 14 SC	Maze learning > Rest	16	–	5	EB activated the right hippocampus and parahippocampus, occipital cortex and fusiform gyrus. Those activations increased across three runs.
Halko et al., 2014	Virtual navigation	fMRI	9 EB	Virtual navigation > Motor control; Planning period > Motor control	14	–	–	Right TPJ activation during planning and execution of the task, which correlated with performance and subjective independence level in daily travels.
He et al., 2013	Landmark objects	fMRI	16 EB, 17 SC	Large non-manipulable objects > tools & animals	5	–	5	EB and SC activate PPA, RSC and left TOS in both visual (pictures of objects and scenes) and auditory (language) modalities.
Kupers et al., 2010	SSD & route recognition	fMRI	10 EB, 10 SC	Route recognition > Scrambled route	30	–	20	Like SC (full Vision), EB activated areas in the visual cortex (IOG, SOG, MOG, cuneus and fusiform gyrus), right parahippocampus, superior and inferior PPC, precuneus, anterior cingulate cortex, anterior insula, dorsolateral PFC, and cerebellum.
Milne et al., 2015	Active echolocation	fMRI	6 EB, 3 SC	[expert or novice] Active echolocation, with material echoes > No echoes	20	–	6	EB expert echolocators activated calcarine sulcus during echolocation and parahippocampal cortex (parahippocampal gyrus, fusiform gyrus, and anterior CoS) to identify surface material through echoes. No parahippocampal, nor occipital responses were found in EB novice echolocators and SC.
Struiksma et al., 2011	Spatial language	fMRI	13 EB, 13 SC	Spatial > Non-spatial sentences	24	–	24	EB activated left SMG, left MOG and right cuneus when spatial sentences were presented
Wolbers et al., 2011*	Spatial layout	fMRI	4 EB, 3 LB, 7 SC	Spatial Layout > Non-spatial object	12	12	5	For spatial layouts, EB activated PPA, RSC, parieto-occipital sulcus, SPL area 7p and middle frontal gyrus. Compared to SC, EB had stronger activation of occipital and middle temporal areas.
SPATIAL PROCESSING								
Anurova et al., 2015	Auditory localization	fMRI	12 EB, 12 SC	Auditory identification and localization > Detection	25	–	13	In the auditory localization task, EB displayed higher (compared to SC) activations in regions of the occipital cortex, in the bilateral SPL, and in the left middle frontal gyrus and sulcus.
Bedny et al., 2010	Auditory motion processing	fMRI	10 EB, 5 LB, 21 SC	High motion + low motion > Rest	3	0	9	hMT/hMST response only found in EB.

(Continued)

10.3389/fnins.2022.1010354

TABLE 2 (Continued)

REFERENCES	FUNCTIONAL DOMAIN	METHOD	*N* SUBJECTS	TASK CONTRASTS	FOCI EB	FOCI LB	FOCI SC	MAIN FINDINGS
Bonino et al., 2008	Tactile spatial working memory	fMRI	4 EB	Tactile recognition and spatial memory maintenance > Rest	76	–	–	EB activate (pre)frontal (premotor, SMA, PFC) and parietal cortical (SPL, precuneus, IPS) areas, as well as lateral occipital cortex and cerebellum.
Bonino et al., 2015	Tactile angle discrimination	fMRI	9 EB, 10 SC	Angle discrimination > Control	3	–	9	EB and SC recruited PPC, intraparietal regions, middle frontal and premotor areas. EB also recruited ventro-temporal, temporo-occipital and dorsal occipital regions. These activations were correlated to behavioral performance.
Chan et al., 2012	Auditory localization	fMRI	11 EB, 14 SC	Distance estimation > Detection	18	–	16	After training, EB increasingly activated R-inferior parietal cortex, L-hippocampus, R-cuneus, whereas no difference was found for SC in pre *vs* post-training.
Collignon et al., 2011	Auditory localization	fMRI	11 EB, 11 SC	Spatial judgment > Pitch judgment	36	–	14	Spatial judgments involved the dorsal network (IPL, SPL, middle occipito-temporal gyrus, etc.). EB showed higher activations in occipital regions known for visuospatial processing (cuneus, MOG, lingual gyrus).
Dormal et al., 2016	Auditory motion processing	fMRI	16 EB, 15 SC	Motion perception > Static	9	–	10	Auditory motion activated fronto-temporo-parietal network in both groups; only EB activated occipital areas (bilateral MOG and SOG), including areas hMT + /V5 and V3A.
Gougoux et al., 2005	Auditory localization	PET	12 EB, 7 SC	[Superior or Normal] Binaural and Monaural Sound Localization > Control	36	–	24	Both groups activated inferior parietal cortex. Occipital activations (striate and ventral extrastriate cortex) only in EB with superior sound localization. More extensive frontal activations for monaural localization.
Matteau et al., 2010	Tactile motion processing	fMRI	8 EB, 9 SC	Motion perception > Rest	24	–	17	hMT + , parietal (IPL, SPL) and frontal activations in EB and SC. EB also recruited right occipital cortex (BA 19).
Park et al., 2011	Auditory spatial working memory	fMRI	10 EB, 10 SC	2-back Working Memory of Location > 0-back Detection	11	–	7	Both groups activated prefrontal and parietal regions, and cerebellum. Fusiform gyrus and visual occipital areas (MOG, lingual gyrus, cuneus) showed increased functional connectivity with frontoparietal regions and default mode network in both groups.
Ptito and Kupers, 2005	SSD & tactile orientation processing	PET	6 EB, 5 SC	Pattern Orientation Detection > Random dots (no pattern)	19	–	18	After training with TDU, only EB activated occipital (cuneus, inferior, medial and lateral occipital cortex), occipito-parietal (dorsal IPS) and occipito-temporal (fusiform gyrus) areas. EB and SC activated frontal (IFG, SFG, MedFG, Insula) and parietal (anterior IPS) areas.
Ptito et al., 2009	Tactile motion processing	PET	7 EB, 6 SC	Motion Discrimination > Rest	10	–	10	EB recruited hMT, V1 (cuneus), V3 (MOG), IPS. EB and SC activated frontal areas (MFG, MedFG), SMG and cerebellum. SC activated PCG and insula.
Renier et al., 2010	Auditory and tactile localization	fMRI	12 EB, 12 SC	Localization > Identification or Detection	26	–	17	R-MOG activity during auditory and tactile spatial processing in EB; this activity was correlated with localization performance. R-MOG deactivation in blindfolded SC.

(Continued)

10.3389/fnins.2022.1010354

TABLE 2 (Continued)

REFERENCES	FUNCTIONAL DOMAIN	METHOD	*N* SUBJECTS	TASK CONTRASTS	FOCI EB	FOCI LB	FOCI SC	MAIN FINDINGS
Ricciardi et al., 2007	Tactile motion processing	fMRI	4 EB, 7 SC	Motion Stimuli > Static Stimuli	38	–	25	EB and SC activated hMT + , parietal (IPS), and ventral and inferior temporal regions. Only EB activated motion-responsive areas V3A and V7.
Stilla et al., 2008	Tactile spatial processing	fMRI	5 EB, 5 LB	Tactile microspatial discrimination > Tactile temporal discrimination	41	20	–	Somatosensory, posterior and ventral IPS, frontal (FEF, PMv) and occipital (IOS, LOC, fusiform gyrus) areas were spatially responsive in both EB and LB.
Striem-Amit et al., 2012	SSD & spatial representations	fMRI	11 EB, 9 SC	Location > Shape	14	–	15	In both EB and SC, the location task activated parts of the dorsal stream, including the precuneus. Only EB activated occipital visual areas, including V1.
Tao et al., 2015	Auditory localization	fMRI	15 EB, 17 LB	Localization > differentiation	11	4	–	EB more strongly activate occipital areas (R-MOG), while LB more strongly activated prefrontal areas involved in visuospatial working memory.
Tao et al., 2017	Auditory localization	fMRI	11 EB, 13 LB	Localization > discrimination	7	7	–	After sound localization training, precuneus activation decreased in EB and increased in LB. In LB, visuospatial working memory capacities were linked to a precuneus-lingual gyrus network and enhanced learning of sound localization. The precuneus seems important to learn sound localization, independently from visual experience.
Voss et al., 2006	Auditory localization	PET	6 LB, 7 SC	Binaural and monaural sound localization > Control	–	7	0	LB did not demonstrate enhanced performances compared to SC, but showed occipital activations (in MOG, SOG, and lingual gyrus) during sound localization tasks. These activations were mostly in the right hemisphere during binaural localization but extended bilaterally in monaural localization. SC showed occipital deactivations. Parietal and frontal activations were also present.
Voss et al., 2008	Auditory localization	PET	12 EB, 6 LB, 7 SC	Binaural and monaural sound localization > Control	19	16	7	EB, but not LB, activated occipital visual areas. LB activated right medial and lateral occipitotemporal cortex.
Voss et al., 2011	Auditory localization	PET	12 EB, 6 LB, 7 SC	[Supperior or normal] Monaural sound localization with spectral cues > Control	15	19	14	Occipital activations (cuneus, lingual gyrus, IOG) in all groups but stronger in EB and LB. Activations in left lingual gyrus, left precentral sulcus and inferior frontal cortex boundary correlated with performance.
Weeks et al., 2000	Auditory localization	PET	9 EB, 9 SC	Localization > Rest	17	–	12	EB activated occipital cortex (parieto-occipital, dorsal, ventral). Both EB and SC activated IPL. Correlations between right IPL, temporal and occipital cortex (parieto-occipital, ventral, dorsal and peristriate) activations in EB.

*Studies that included a blind group with mixed EB and LB participants. CoS, collateral sulcus; FEF, frontal eye fields; IFC, Inferior frontal cortex; IOG, inferior occipital gyrus; IOS, intra-occipital sulcus; IPL, inferior parietal lobule; IPS, intraparietal sulcus; LOC, lateral occipital cortex; MedFG, medial frontal gyrus; MFG, middle frontal gyrus; MOG, middle occipital gyrus; hMST, human medial superior temporal area; hMT, human middle temporal area; MTG, middle temporal Gyrus; PFC, prefrontal cortex; PMv, ventral premotor cortex; PPA, parahipocampal place area; ROI, region of interest; RSC, retrosplenial complex; SMA, supplementary motor area; SMG, supramarginal gyrus; SOG, superior occipital gyrus; SSD, sensory substitution device; TDU, tongue display unit; TOS, transverse occipital sulcus; TPJ, temporal parietal junction.

10.3389/fnins.2022.1010354

Meta-analysis

We used the *Ginger*ALE software (version 3.0)[1] to perform the meta-analysis. First, we converted foci from Talairach coordinates into MNI space. Then, three types of meta-analysis were conducted to determine the neural correlates of non-visual spatial navigation and spatial processing. Single meta-analyses (Eickhoff et al., 2012) were conducted on each dataset independently, to discover convergent clusters across tasks and participants. Contrast meta-analyses (Eickhoff et al., 2011) were conducted to detect clusters with significantly stronger activations (BOLD signal) in one group compared to the other. Contrast meta-analyses were performed to determine group differences in brain activations. The contrasts of interest were EB > SC, SC > EB. Conjunction meta-analyses (Eickhoff et al., 2011) were conducted to detect overlapping activated brain regions between groups. The specific investigated conjunctions were EB∩SC.

Statistical analysis

For the single meta-analyses, an ALE value was calculated for each voxel, using cluster-level family-wise error (FWE) correction (Eickhoff et al., 2016) to correct for multiple comparisons. The meta-analyses were performed with a cluster-level FWE correction set at $p < 0.05$ (Müller et al., 2018), a threshold for forming clusters at $p < 0.001$ and 5,000 permutations. Additional exploratory meta-analyses were conducted for datasets that did not respect criteria of number of experiments (Müller et al., 2018): "*EB Spatial Navigation*" and *"SC Spatial Navigation."* For these analyses, the threshold for forming clusters was set at $p < 0.01$. Thus, it is important to state that results from these exploratory analyses with less conservatory thresholds constitute preliminary data that should be more thoroughly investigated in future studies. As for the contrasts meta-analyses, they were performed with a significance level set at $p < 0.01$ and 1,000 permutations (Eickhoff et al., 2011). Finally, the conjunction meta-analyses, detecting the overlap between two ALE maps, were performed with a significance level set at $p < 0.01$ and 1,000 permutations (Eickhoff et al., 2011). The obtained results were overlaid on the Colin_27_T1_seg_MNI template (see text footnote 2) using Mango.[2] Reported coordinates are in MNI space.

Results

Results obtained from the performed meta-analyses report the neural correlates of spatial navigation and spatial processing in 31 neuroimaging studies, spanning more than 20 years of research. As mentioned above, as spatial navigation tasks usually integrate spatial and decision-making tasks, we separated *spatial processing* and *spatial navigation* analyses and presented them individually. However, due to the limited number of studies investigating spatial navigation, we performed an additional "*Spatial Processing + Spatial Navigation*" analysis, combining spatial processing and spatial navigation studies, which revealed extra clusters when compared to the "*Spatial Processing*" meta-analysis.

Spatial processing analysis

The spatial processing analysis included many spatial tasks such as sound localization, motion processing, auditory distance judgments, and auditory spatial working memory. Detailed information of all clusters is shown in **Table 3** and **Figure 2**.

Single meta-analyses

The ALE analysis revealed eight significant clusters in EB that were located in parietal, (pre)frontal, temporal, and occipital gyri. Parietal clusters included the precuneus, superior parietal lobule (SPL), inferior parietal lobule (IPL), supramarginal gyrus (SMG). Clusters in the (pre)frontal lobe included the precentral gyrus (PCG), middle frontal gyrus (MFG), right medial frontal gyrus (MedFG), superior frontal gyrus (SFG) and anterior cingulate cortex (ACC). Temporal clusters included the middle and inferior temporal gyri (MTG and ITG). Occipital clusters included the cuneus, and right middle and inferior occipital gyri (MOG and IOG). The ALE analysis revealed seven clusters in SC, located in parietal and (pre)frontal lobes, as well as in sub-lobar structures. Parietal clusters included the IPL, SMG, and left SPL. Clusters in the (pre)frontal lobe included the PCG, MFG, right inferior frontal gyrus (IFG), and right SFG. Sub-lobar clusters included the insula and claustrum. As stated previously, given the paucity of studies strictly dealing with LB populations, no datasets were possible in this category.

Contrast and conjunction meta-analyses

Contrast meta-analyses revealed that EB recruited a larger network than SC. These included the precuneus, cuneus, MOG, IOG, MTG, and ITG. The conjunction analysis revealed shared activations in EB and SC in precuneus, IPL, SMG, MFG and PCG.

Exploratory spatial navigation analysis

The spatial navigation exploratory analysis included tasks such as route recognition, maze learning, and discrimination of spatial layouts and landmark objects/features through various

1 http://brainmap.org/ale/
2 http://rii.uthscsa.edu/mango

TABLE 3 Brain clusters obtained from the activation likelihood estimation (ALE) meta-analysis for spatial processing and contributing studies.

# Cluster	Brain regions (% of cluster volume)	Brodmann areas (% of cluster volume)	Cluster center (MNI x,y,z)	Cluster size (mm^3)	Max ALE or Z value	Contributing studies
EB						
1	Precuneus (69%), Cuneus (28%), SPL (3%)	7 (62%), 19 (36%), 18 (2%)	(20,-73,47)	3,608	0.0203	Weeks et al., 2000; Gougoux et al., 2005; Ptito and Kupers, 2005; Stilla et al., 2008; Voss et al., 2008; Renier et al., 2010; Collignon et al., 2011; Voss et al., 2011; Anurova et al., 2015; Tao et al., 2015
2	SPL (52%), Precuneus (42%), IPL (4%)	7 (93%), 40 (7%)	(33, –47,48)	2,960	0.0197	Weeks et al., 2000; Gougoux et al., 2005; Stilla et al., 2008; Voss et al., 2008; Matteau et al., 2010; Renier et al., 2010; Collignon et al., 2011; Voss et al., 2011; Bonino et al., 2015; Dormal et al., 2016
3	IPL (54%), SPL (24%), SMG (11%), Precuneus (11%)	40 (65%), 7 (35%)	(–35, –44,49)	2,096	0.0213	Weeks et al., 2000; Matteau et al., 2010; Renier et al., 2010; Collignon et al., 2011; Park et al., 2011; Anurova et al., 2015; Tao et al., 2015; Dormal et al., 2016
4	PCG (58%), MFG (42%)	6 (100%)	(34, –4,53)	1,920	0.0185	Gougoux et al., 2005; Ricciardi et al., 2007; Stilla et al., 2008; Voss et al., 2008; Renier et al., 2010; Collignon et al., 2011; Voss et al., 2011; Striem-Amit et al., 2012; Anurova et al., 2015; Tao et al., 2015
5	MFG (71%), PCG (22%), Sub-gyral (7%)	6 (98%), 4 (1%)	(–25, –6,56)	1,808	0.0226	Stilla et al., 2008; Matteau et al., 2010; Renier et al., 2010; Collignon et al., 2011; Anurova et al., 2015; Tao et al., 2015
6	Precuneus (78%), Cuneus (22%)	7 (86%), 19 (14%)	(–15, –74,46)	1,576	0.0163	Weeks et al., 2000; Ptito and Kupers, 2005; Ricciardi et al., 2007; Stilla et al., 2008; Renier et al., 2010; Chan et al., 2012; Tao et al., 2015
7	ITG (30%), IOG (25%), MTG (25%), MOG (21%),	19 (45%), 37 (40%)	(49, –68, –2)	1,424	0.0146	Gougoux et al., 2005; Bonino et al., 2008; Voss et al., 2008; Ptito et al., 2009; Renier et al., 2010; Voss et al., 2011; Anurova et al., 2015; Dormal et al., 2016
8	MedFG (51%), Cingulate Gyrus (25%), SFG (24%),	6 (54%), 32 (21%), 24 (19%), 8 (5%)	(7,12,48)	4,136	0.0184	Ricciardi et al., 2007; Stilla et al., 2008; Matteau et al., 2010; Renier et al., 2010; Anurova et al., 2015; Tao et al., 2015
SC						
1	IPL (88%), SMG (9%), Sub-Gyral (3%)	40 (100%)	(44, –42,38)	2,208	0.0156	Weeks et al., 2000; Ptito et al., 2009; Matteau et al., 2010; Renier et al., 2010; Collignon et al., 2011; Chan et al., 2012; Anurova et al., 2015; Dormal et al., 2016
2	Insula (67%), Claustrum (24%), IFG (9%)	13 (74%), 47 (1%), 45 (1%)	(36,22,4)	2,080	0.0248	Ptito et al., 2005; Gougoux et al., 2005; Voss et al., 2008; Ptito et al., 2009; Bedny et al., 2010; Matteau et al., 2010; Renier et al., 2010; Voss et al., 2011; Anurova et al., 2015
2	MFG (53%), PCG (25%), Sub-Gyral (18%), SFG (5%)	6 (100%)	(32,1,58)	2,064	0.0221	Gougoux et al., 2005; Ricciardi et al., 2007; Voss et al., 2008; Ptito et al., 2009; Renier et al., 2010; Collignon et al., 2011; Park et al., 2011; Voss et al., 2011; Dormal et al., 2016

(Continued)

TABLE 3 (Continued)

# Cluster	Brain regions (% of cluster volume)	Brodmann areas (% of cluster volume)	Cluster center (MNI x,y,z)	Cluster size (mm^3)	Max ALE or Z value	Contributing studies
4	Insula (64%), Claustrum (36%)	13 (64%)	(−32,21,5)	1,600	0.0238	Gougoux et al., 2005; Ptito et al., 2005; Voss et al., 2008; Bedny et al., 2010; Matteau et al., 2010; Renier et al., 2010; Voss et al., 2011; Anurova et al., 2015
5	IFG (57%), MFG (34%), PCG (9%)	9 (90%), 6 (9%), 8 (1%)	(57,15,30)	1,520	0.0148	Gougoux et al., 2005; Ricciardi et al., 2007; Voss et al., 2008; Bedny et al., 2010; Voss et al., 2011; Chan et al., 2012; Bonino et al., 2015; Dormal et al., 2016
6	IPL (83%), SMG (15%), SPL (2%)	40 (98%), 7 (2%)	(−37, −47,46)	1,368	0.0159	Gougoux et al., 2005; Voss et al., 2008; Renier et al., 2010; Park et al., 2011; Voss et al., 2011; Dormal et al., 2016
7	PCG (62%), MFG (38%)	6 (88%), 4 (12%)	(−30, −8,53)	1,072	0.0168	Matteau et al., 2010; Collignon et al., 2011; Anurova et al., 2015; Dormal et al., 2016
EB > SC						
1	ITG (30%), IOG (25%), MTG (25%), MOG (20%)	19 (45%), 37 (40%)	(50, −69, −3)	1,256	3.29 Z	Gougoux et al., 2005; Bonino et al., 2008; Voss et al., 2008; Ptito et al., 2009; Renier et al., 2010; Voss et al., 2011; Anurova et al., 2015
2	Precuneus (58%), Cuneus (42%)	19 (61%), 7 (32%), 18 (7%)	(21, −80,44)	1,024	3.29 Z	Ptito et al., 2005); Renier et al., 2010
3	Precuneus (97%), Cuneus (3%)	7 (89%), 19 (11%)	(−14, −76,46)	648	3.29 Z	Ptito et al., 2005; Tao et al., 2015
SC > EB						
NA						
EB ∩ SC						
1	MFG (53%), PCG (47%)	6 (97%), 4 (3%)	(−29, −8,53)	736	0.0159	Matteau et al., 2010; Renier et al., 2010; Collignon et al., 2011; Dormal et al., 2016
2	IPL (83%), SMG (15%), SPL (2%)	40 (98%), 7 (2%)	(−37, −45,47)	688	0.0142	Weeks et al., 2000; Renier et al., 2010; Collignon et al., 2011; Dormal et al., 2016
3	PCG (58%), MFG (42%)	6 (100%)	(33, −3,54)	488	0.014	Ptito et al., 2009; Renier et al., 2010; Collignon et al., 2011
4	Precuneus	7	(35, −41,44)	456	0.013	Matteau et al., 2010; Collignon et al., 2011; Dormal et al., 2016

MFG, middle frontal gyrus; MedFG, medial frontal gyrus; MOG, middle occipital gyrus; MTG, middle temporal gyrus; IFG, inferior frontal gyrus; IOG, inferior occipital gyrus; IPL, inferior parietal lobule; ITG, inferior temporal gyrus; SFG, superior frontal gyrus; SMG, supramarginal gyrus; SPL, superior parietal lobule.

means such as SSDs, echolocation, and tactile exploration. Detailed information about all clusters can be found in Table 4 and Figure 3.

Single meta-analyses

The ALE analysis revealed six clusters in EB located in the parietal, occipital, and temporal cortices in the right hemisphere. Parietal clusters included the precuneus and SPL. Occipital clusters included the cuneus, MOG, IOG and lingual gyrus. The temporal cluster included the fusiform gyrus and parahippocampal gyrus (PHIP) and extended to a portion of the hippocampus (HIP). The ALE analysis revealed three significant clusters of activation in the right hemisphere in SC. The first cluster included the SPL and IPL; the second, the precuneus and cuneus; and the third, the insula, claustrum and IFG. No LB datasets were possible in this category.

Contrast and conjunction meta-analyses

Given the small number of studies in the *spatial navigation* datasets, the contrast analysis revealed no significant clusters that were more activated in either EB or SC. The conjunction meta-analysis identified one small (144 mm^3) cluster in the precuneus that was commonly activated by EB and SC.

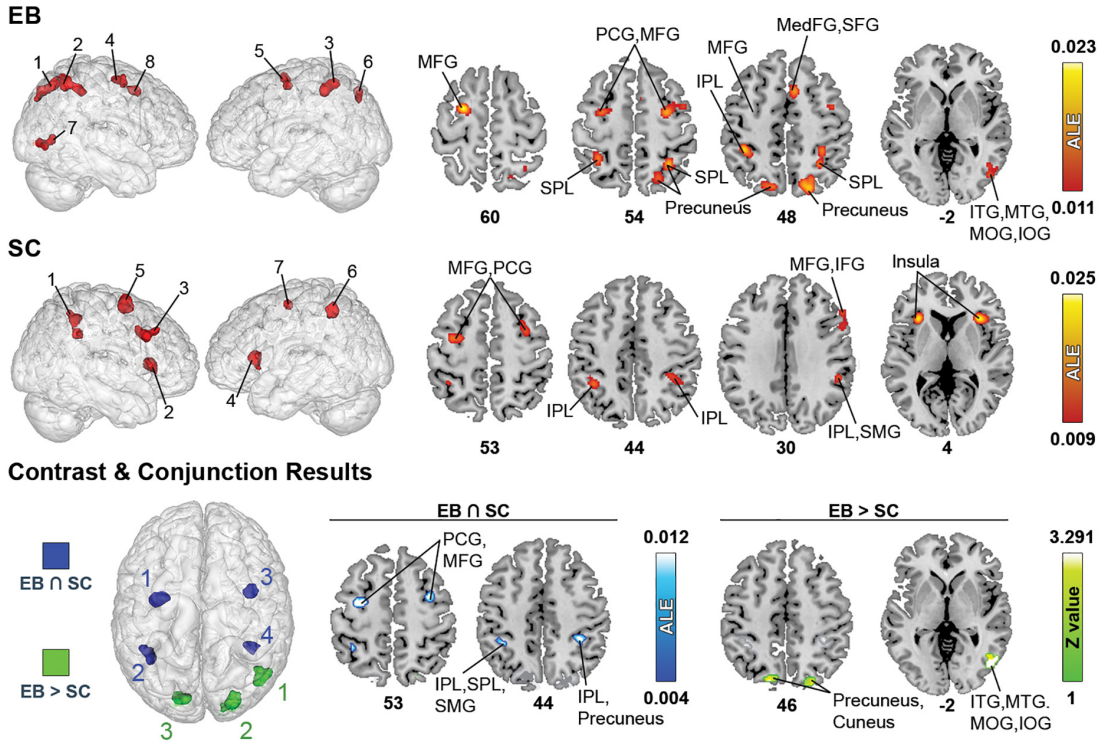

FIGURE 2
Brain areas activated by spatial processing in EB and SC and results of contrast and conjunction analyses. **(Left)** 3D renders of the brain and activation clusters (see **Table 4** for reference). **(Right)** Axial cuts of the brain with identified clusters of activation. The number below the slices refer to the z coordinate in MNI space. ALE (for single and conjunction meta-analyses) and Z values (for contrast meta-analyses) are displayed to the right. The ALE values, calculated for each voxel, represent the probability of activation across included studies (Turkeltaub et al., 2012). For the contrast analysis, Z-values show the significance of ALE subtractions between two groups. More details regarding the ALE and Z values are presented in **Table 3**. IOG, inferior occipital gyrus; IPL, inferior parietal lobule; ITG, inferior temporal gyrus; MedFG, medial frontal gyrus; MFG, middle frontal gyrus; MTG, medial temporal gyrus; PCG, precentral gyrus; SFG, superior frontal gyrus; SMG, supramarginal gyrus; SPL, superior parietal lobule.

Spatial processing + spatial navigation analyses

Here, we performed ALE analyses on *spatial processing* and *spatial navigation* tasks combined. Detailed information about all significant clusters can be found in **Table 5** and **Figure 4**.

Single meta-analyses

The ALE analysis revealed nine significant clusters in EB, located in parietal, (pre)frontral, and occipital lobes, as well as sub-lobar structures. In the parietal lobe, clusters included the precuneus, SPL, and IPL. Clusters in the (pre)frontal lobe covered the MFG, PCG, right MedFG, right SFG, and right ACC. Clusters in the occipital lobe included the cuneus, lingual gyrus, and right MOG. Clusters in sub-lobar structures included the insula and claustrum. For SC, six clusters were found in the parietal and (pre)frontal lobes, and in sub-lobar structures. In the parietal lobe, these included the IPL, SPL and SMG. Clusters in the (pre)frontal lobe included the IFG and right MFG, PCG, and SFG. Sub-lobar clusters included the insula and claustrum.

Contrast and conjunction meta-analyses

Only one contrast meta-analysis (EB > SC) produced significant results and revealed that EB recruited a larger network of brain structures than their SC counterparts. This network included the precuneus, cuneus, MOG and lingual gyrus. Conjunction meta-analyses revealed shared clusters between EB and SC in SPL, IPL, insula, claustrum, MFG and PCG. Clusters common to EB and LB were located in the left MFG and PCG. There were no shared clusters common for LB and SC.

Qualitative review of neural activity in late blind

There was an insufficient number of studies to conduct a meta-analysis in LB. We therefore performed a qualitative analysis of the literature. The results show that LB had similar activity in parietal and (pre)frontal cortices (Stilla et al., 2008; Tao et al., 2015, 2017); however, there was a lack of consensus

TABLE 4 Brain clusters obtained from the activation likelihood estimation (ALE) meta-analysis for spatial navigation and contributing studies.

# Cluster	Brain regions (% of cluster volume)	Brodmann areas (% of cluster volume)	Cluster center (MNI x,y,z)	Cluster size (mm^3)	Max ALE value	Contributing studies
EB						
1*	Cuneus (42%), Lingual Gyrus (36%), MOG (19%), IOG (2%)	18 (52%), 17 (30%), 23 (7%), 30 (4%)	(19, −82,8)	5,992	0.0152	Kupers et al., 2010; Struiksma et al., 2011; Gagnon et al., 2012; Halko et al., 2014; Milne et al., 2015; Dodsworth, 2019
2*	Precuneus (79%), SPL (12%), Cuneus (9%)	7 (79%), 19 (21%)	(18, −70,49)	4,728	0.0158	Kupers et al., 2010; Wolbers et al., 2011; Gagnon et al., 2012; Halko et al., 2014; Fiehler et al., 2015
3*	Parahippocampal Gyrus (55%), Fusiform Gyrus (45%)	37 (56%), 36 (33%), 20 (6%), 19 (5%)	(38, −43, −11)	2,600	0.0125	Kupers et al., 2010; Gagnon et al., 2012; He et al., 2013
4	Precuneus (84%), SPL (15%), Cuneus (2%)	7 (97%), 19 (3%)	(18, −68,50)	1,880	0.0158	Kupers et al., 2010; Wolbers et al., 2011; Gagnon et al., 2012; Halko et al., 2014; Fiehler et al., 2015
5	Cuneus (52%), MOG (45%), Lingual Gyrus (3%)	17 (55%), 18 (45%)	(29, −85,9)	1,600	0.0151	Kupers et al., 2010; Gagnon et al., 2012; Dodsworth, 2019
6	Lingual Gyrus (93%), Cuneus (7%)	18 (96%)	(1, −78,5)	928	0.0152	Kupers et al., 2010; Struiksma et al., 2011; Gagnon et al., 2012
SC						
1	IPL (58%), SPL (42%)	7 (55%), 40 (45%)	(38, −55,50)	808	0.0108	Kupers et al., 2010; Struiksma et al., 2011; Fiehler et al., 2015
2	Precuneus (87%), Cuneus (13%)	7 (100%)	(8, −71,43)	752	0.012	Kupers et al., 2010; Gagnon et al., 2012
3	Insula (58%), IFG (21%), Claustrum (21%)	13 (52%), 47 (12%), 45 (9%)	(35,25, −1)	744	0.0094	Kupers et al., 2010; Struiksma et al., 2011; Fiehler et al., 2015; Dodsworth, 2019
EB > SC						
NA						
SC > EB						
NA						
EB ∩ SC						
1	Precuneus (100%)	7 (100%)	(11, −71,42)	144	0.0091	Gagnon et al., 2012

*Thresholded at $P < 0.01$. IFG, inferior frontal gyrus; IOG, inferior occipital gyrus; IPL, inferior parietal lobule; MOG, middle occipital gyrus; SPL, superior parietal lobule.

on the presence and magnitude of occipital activation during spatial tasks. On the one hand, occipital activation in EB and LB were found during tactile drawing (Likova, 2012), tactile microspatial discrimination (Stilla et al., 2008), and auditory localization (Voss et al., 2006, 2011; Collignon et al., 2013). Moreover, this activation often correlated with performance (Collignon et al., 2013) or level of expertise in the task (Thaler et al., 2011; Norman and Thaler, 2019). On the other hand, such visual occipital activity was superior in EB (Collignon et al., 2013; Tao et al., 2015, 2017; Jiang et al., 2016) or was only present in EB (Voss et al., 2008). In terms of spatial patterns of observed activations, LB often showed activations of the lateral occipital cortex, MOG, lingual gyrus, and cuneus (Voss et al., 2006, 2011; Stilla et al., 2008; Tao et al., 2017). LB also showed greater reliance on the precuneus and other parietal and (pre)frontal areas (Tao et al., 2015, 2017), in line with results obtained in SC. In conclusion, consistent with the idea of cross-modal plasticity being experience-driven (Ptito et al., 2021a), LB often show activations that are intermediary between EB and SC patterns.

Discussion

In the present study, we used ALE meta-analyses to identify brain regions commonly activated in neuroimaging

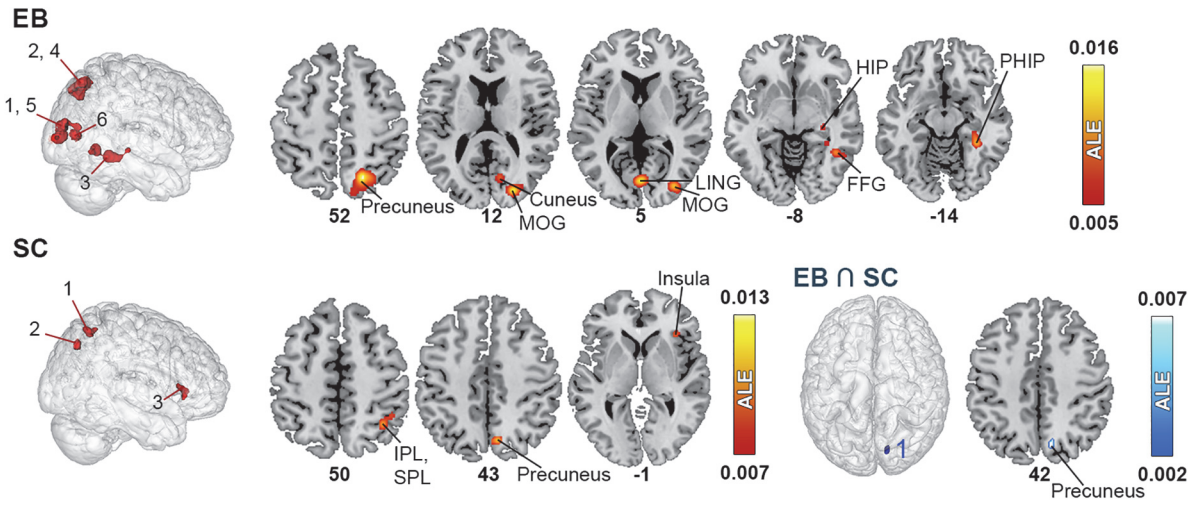

FIGURE 3
Brain areas activated by spatial navigation in EB and SC and results of conjunction analysis. **(Left)** 3D renders of the brain and activation clusters (see **Table 4** for reference). **(Right)** Axial cuts of the brain with identified clusters of activation. The number below the slices refer to the z coordinate in MNI space. The ALE values, calculated for each voxel, represent the probability of activation across included studies (Turkeltaub et al., 2012) and are disclosed to the right. More details regarding the ALE values are presented in **Table 4**. FFG, fusiform gyrus; HIP, hippocampus; IPL, inferior parietal lobule; LING, lingual gyrus; MOG, middle occipital gyrus; PHIP, parahippocampus.

studies of non-visual spatial processing and navigation in blind and sighted individuals. Our analyses identified supramodal brain areas that are activated by spatial tasks in both EB and SC. In addition, we identified occipital brain areas that are cross-modally recruited by blind individuals. Due to the limited literature on LB (nine studies, six contrasts), we could not identify the neural correlates of spatial processing and spatial navigation in this population. The next sections will thus strongly focus on findings in EB and SC populations.

Neural correlates of non-visual spatial processing

The ALE analysis revealed that non-visual spatial information processing via tactile and auditory modalities activates a neural network that comprises dorsal frontal and parietal regions in both hemispheres. This core network was shown to be recruited in both SC and EB participants and includes the SPL, IPL, MFG, MedFG, and pre-central gyrus. A shared activation of the right insula in EB and SC was also identified when navigation tasks were included in the meta-analysis. Furthermore, the ALE analysis revealed that EB individuals also activated the pre-SMA and cross-modally recruited occipital areas during spatial tasks. These activations are similar to those reported in previous meta-analyses in blind (Zhang et al., 2019) and sighted individuals (Parlatini et al., 2017; Cona and Scarpazza, 2019). Indeed, Zhang et al. (2019) also reported that blind participants consistently activated precuneus, SPL, IPL, MFG, pre-central gyrus, insula, cuneus and other occipital areas along with extra parahippocampal gyrus activations. Taken together, these meta-analyses indicate that both blind and sighted participants recruit two interlinked frontoparietal networks for performing spatial tasks, a dorsal frontoparietal network, also known as the dorsal attention network (DAN), and a ventral frontoparietal network.

The DAN includes the SPL, intraparietal sulcus (IPS), dorsal premotor areas and frontal eye fields (FEF), an area located around the intersection of the precentral gyrus and MFG (Corbetta et al., 2008; Power et al., 2011; Vernet et al., 2014). The DAN mediates both spatial attention and spatial working memory and allows for the selection of sensory stimuli that are not only salient, but also relevant to the individual's goals (top-down attention) in order to plan contextually appropriate responses (Serences and Yantis, 2007; Corbetta et al., 2008; Cona and Scarpazza, 2019). DAN regions are organized in topographic maps corresponding to areas of the visual field (Hagler and Sereno, 2006; Jerde and Curtis, 2013), most specifically to a range of polar angles and eccentricities (Mackey et al., 2017). It is therefore theorized that the DAN serves to implement internal spatial representations (i.e., priority maps of space) and to allocate top-down attention toward them (Cona and Scarpazza, 2019). Our meta-analysis suggests that these internal spatial representations in DAN regions are not necessarily organized according to the visual field but are in fact *amodal*, and independent from visual experience. The most commonly activated DAN regions in the ALE analysis were the SPL and dorsal premotor areas including the FEF (Paus, 1996; Luna et al., 1998; Ioannides et al., 2004; Garg et al., 2007;

TABLE 5 Brain clusters obtained from the activation likelihood estimation (ALE) meta-analysis for spatial processing + spatial navigation and contributing studies.

# Cluster	Brain regions (% of cluster volume)	Brodmann areas (% of cluster volume)	Cluster center (MNI x,y,z)	Cluster size (mm^3)	Max ALE or Z value	Contributing studies
EB						
1	Precuneus (58%), Cuneus (20%), SPL (19%), IPL (3%)	7 (72%), 19 (22%), 40 (3%), 18 (2%), 31 (1%)	(25, −62,48)	11,248	0.0319	Weeks et al., 2000; Gougoux et al., 2005; Ptito et al., 2005; Stilla et al., 2008; Voss et al., 2008; Kupers et al., 2010; Matteau et al., 2010; Renier et al., 2010; Collignon et al., 2011; Park et al., 2011; Struiksma et al., 2011; Voss et al., 2011; Wolbers et al., 2011; Gagnon et al., 2012; Halko et al., 2014; Anurova et al., 2015; Bonino et al., 2015; Fiehler et al., 2015; Tao et al., 2015; Dormal et al., 2016
2	MOG (73%), Cuneus (27%)	18 (55%), 17 (27%), 19 (19%)	(32, −84,9)	3,168	0.0255	Weeks et al., 2000; Stilla et al., 2008; Ptito et al., 2009; Kupers et al., 2010; Matteau et al., 2010; Gagnon et al., 2012; Anurova et al., 2015; Dodsworth, 2019
3	Precuneus (70%), Cuneus (31%)	7 (82%), 19 (15%), 18 (4%)	(−14, −74,47)	2,448	0.0213	Chan et al., 2012; Tao et al., 2015; Weeks et al., 2000; Stilla et al., 2008; Ptito et al., 2005; Ricciardi et al., 2007; Kupers et al., 2010; Gagnon et al., 2012; Wolbers et al., 2011
4	IPL (61%), SPL (25%), Precuneus (8%), SMG (6%)	40 (64%), 7 (36%)	(−35, −46,49)	2,400	0.0254	Weeks et al., 2000; Kupers et al., 2010; Matteau et al., 2010; Renier et al., 2010; Collignon et al., 2011; Park et al., 2011; Struiksma et al., 2011; Anurova et al., 2015; Tao et al., 2015; Dormal et al., 2016
5	PCG (59%), MFG (40%)	6 (100%)	(35, −3,52)	2,304	0.024	Gougoux et al., 2005; Bonino et al., 2008; Stilla et al., 2008; Voss et al., 2008; Renier et al., 2010; Collignon et al., 2011; Striem-Amit et al., 2012; Struiksma et al., 2011; Voss et al., 2011; Anurova et al., 2015; Fiehler et al., 2015; Tao et al., 2015; Dormal et al., 2016
6	MedFG (63%), Cingulate Gyrus (19%), SFG (19%)	6 (63%), 32 (24%), 24 (13%)	(7,12,49)	1,536	0.019	Ricciardi et al., 2007; Stilla et al., 2008; Kupers et al., 2010; Renier et al., 2010; Collignon et al., 2011; Park et al., 2011; Struiksma et al., 2011; Anurova et al., 2015; Tao et al., 2015
7	MFG (67%), PCG (26%), Sub-Gyral (7%)	6 (97%), 4 (3%)	(−26, −6,56)	1,528	0.0227	Stilla et al., 2008; Matteau et al., 2010; Renier et al., 2010; Collignon et al., 2011; Anurova et al., 2015; Tao et al., 2015
8	Lingual gyrus (72%), Cuneus (28%)	18 (46%), 17 (44%)	(−3, −86,7)	1,480	0.0166	Gougoux et al., 2005; Voss et al., 2008; Ptito et al., 2009; Kupers et al., 2010; Collignon et al., 2011; Struiksma et al., 2011; Voss et al., 2011; Gagnon et al., 2012; Anurova et al., 2015

(Continued)

TABLE 5 (Continued)

# Cluster	Brain regions (% of cluster volume)	Brodmann areas (% of cluster volume)	Cluster center (MNI x,y,z)	Cluster size (mm^3)	Max ALE or Z value	Contributing studies
9	Claustrum (59%), Insula (41%)	13 (41%)	(34,20,5)	1,304	0.0242	Gougoux et al., 2005; Voss et al., 2008; Kupers et al., 2010; Matteau et al., 2010; Renier et al., 2010; Park et al., 2011; Struiksma et al., 2011; Voss et al., 2011; Anurova et al., 2015
SC						
1	Insula (62%), Claustrum (22%), IFG (15%), Extra-Nuclear (2%)	13 (60%), 47 (7%), 45 (4%)	(36,23,2)	3,000	0.033	Gougoux et al., 2005; Ptito et al., 2005; Voss et al., 2008; Ptito et al., 2009; Bedny et al., 2010; Kupers et al., 2010; Matteau et al., 2010; Renier et al., 2010; Struiksma et al., 2011; Voss et al., 2011; Anurova et al., 2015; Fiehler et al., 2015; Dodsworth, 2019
2	IPL (79%), SPL (18%), SMG (2%)	40 (78%), 7 (22%)	(40, −47,47)	2,984	0.0174	Gougoux et al., 2005; Ptito et al., 2005; Voss et al., 2008; Kupers et al., 2010; Matteau et al., 2010; Struiksma et al., 2011; Voss et al., 2011; Chan et al., 2012; Anurova et al., 2015; Fiehler et al., 2015; Dormal et al., 2016
3	Insula (65%), Claustrum (29%), extra-nuclear (3%), IFG (2%)	13 (60%), 47 (5%)	(−32,21,3)	2,400	0.0279	Ptito and Kupers, 2005; Gougoux et al., 2005; Voss et al., 2008; Matteau et al., 2010; Bedny et al., 2010; Kupers et al., 2010; Renier et al., 2010; Voss et al., 2011; Struiksma et al., 2011; Anurova et al., 2015; Dodsworth, 2019
4	MFG (55%), PCG (25%), Sub-Gyral (16%), SFG (4%)	6 (100%)	(32,0,57)	2,392	0.0233	Gougoux et al., 2005; Ricciardi et al., 2007; Voss et al., 2008; Ptito et al., 2009; Renier et al., 2010; Collignon et al., 2011; Park et al., 2011; Struiksma et al., 2011; Voss et al., 2011; Dormal et al., 2016
5	IPL (78%), SMG (18%), SPL (3%), Sub-Gyral (1%)	40 (98%), 7 (2%)	(−37, −47,46)	2,288	0.0232	Weeks et al., 2000; Gougoux et al., 2005; Voss et al., 2008; Renier et al., 2010; Kupers et al., 2010; Park et al., 2011; Struiksma et al., 2011; Voss et al., 2011; Fiehler et al., 2015; Dormal et al., 2016
6	IFG (64%), MFG (31%), PCG (6%),	9 (94%), 6 (6%)	(57,17,29)	1,000	0.0148	Ricciardi et al., 2007; Bedny et al., 2010; Chan et al., 2012; Bonino et al., 2015; Dormal et al., 2016
EB > SC						
1	MOG (83%), Cuneus (18%)	18 (62%), 19 (21%), 17 (18%)	(33, −84,9)	3,008	3.29 Z	Weeks et al., 2000; Stilla et al., 2008; Ptito et al., 2009; Kupers et al., 2010; Gagnon et al., 2012; Anurova et al., 2015; Dodsworth, 2019
2	Cuneus (67%), Precuneus (33%)	19 (53%), 7 (29%), 18 (12%), 31 (5%)	(21, −82,39)	1,416	3.29 Z	Renier et al., 2010; Collignon et al., 2011; Wolbers et al., 2011; Dormal et al., 2016
3	Precuneus	7	(20, −66,52)	224	2.65 Z	Stilla et al., 2008; Renier et al., 2010; Gagnon et al., 2012; Halko et al., 2014

(Continued)

TABLE 5 (Continued)

# Cluster	Brain regions (% of cluster volume)	Brodmann areas (% of cluster volume)	Cluster center (MNI x,y,z)	Cluster size (mm^3)	Max ALE or Z value	Contributing studies
SC > EB						
NA						
EB ∩ SC						
1	SPL (75%), IPL (25%)	7 (83%), 40 (17%)	(36, −45,46)	1,504	0.0171	Kupers et al., 2010; Matteau et al., 2010; Collignon et al., 2011; Struiksma et al., 2011; Fiehler et al., 2015; Dormal et al., 2016
2	IPL (85%), SMG (9%), SPL (6%)	40 (96%), 7 (4%)	(−36, −46,48)	1,208	0.021	Weeks et al., 2000; Gougoux et al., 2005; Voss et al., 2008; Kupers et al., 2010; Renier et al., 2010; Collignon et al., 2011; Park et al., 2011; Struiksma et al., 2011; Voss et al., 2011; Anurova et al., 2015; Fiehler et al., 2015; Dormal et al., 2016
3	Claustrum (56%), Insula (44%)	13 (44%)	(34,20,4)	1,072	0.0242	Ptito et al., 2009; Bedny et al., 2010; Kupers et al., 2010; Matteau et al., 2010; Park et al., 2011; Renier et al., 2010; Struiksma et al., 2011; Anurova et al., 2015
4	PCG (52%), MFG (48%)	6 (100%)	(31, −3,54)	728	0.0181	Stilla et al., 2008; Ptito et al., 2009; Renier et al., 2010; Collignon et al., 2011; Struiksma et al., 2011; Bonino et al., 2015

MFG, middle frontal gyrus; MedFG, medial frontal gyrus; MOG, middle occipital gyrus; IFG, inferior frontal gyrus; IPL, inferior parietal lobule; PCG, precentral gyrus; SFG, superior frontal gyrus; SMG, supramarginal gyrus; SPL, superior parietal lobule.

Vernet et al., 2014). The SPL is classically associated with visual guidance of actions (Karnath and Perenin, 2005; Prado et al., 2005) and visuospatial attention (Silver et al., 2005; Saygin and Sereno, 2008; Vandenberghe et al., 2012; Wu et al., 2016), and codes space in an egocentric reference frame, including the known space outside the visual field such as the rear space (Schindler and Bartels, 2013). The FEF is strongly involved in the control of different types of eye movements (mostly saccadic eye movements, but also fixation, pursuit, and vergence), the orientation of attention, visual awareness and perceptual modulation (Moore and Fallah, 2001; Squire et al., 2013; Vernet et al., 2014). However, the SPL and FEF are also recruited in non-visual spatial tasks such as auditory distance judgments (Collignon et al., 2011), localization of sounds on the horizontal axis (Weeks et al., 2000; Gougoux et al., 2005; Renier et al., 2010; Anurova et al., 2015), covert allocation of auditory spatial attention (Garg et al., 2007), auditory motion processing (Dormal et al., 2016), auditory spatial working memory (Park et al., 2011) and tactile microspatial discrimination Stilla et al. (2008) in both blind and sighted individuals. It is therefore proposed that these regions most likely code peripersonal space based on the available or contextually relevant sensory information. Whereas in sighted persons this is mostly based on visual information, blind individuals primarily rely on haptic and auditory cues.

The ventral frontoparietal network includes the temporo-parietal junction (encompassing IPL and superior temporal sulcus), parts of the middle and inferior frontal gyri, the frontal operculum, and the insula. This network is associated with bottom-up attention; it mediates the detection of unattended salient and behaviorally relevant stimuli, and consequently guides actions (Seeley et al., 2007; Corbetta et al., 2008; Cona and Scarpazza, 2019). The ALE revealed activations of the IPL and insula. The IPL is a multimodal brain region that is mostly involved in the detection of salient novel stimuli, in sustaining attention (Singh-Curry and Husain, 2009), and in motor imagery (Kraeutner et al., 2019). Studies in the macaque monkey demonstrated that the IPL is involved in the transformation of information from all sensory modalities into motor behaviors (Borra and Luppino, 2017; Niu et al., 2021). This is corroborated by studies in humans that have identified numerous connections between IPL and frontal, occipital and temporal regions (Caspers et al., 2011; Sun et al., 2022). The insula was the other node of the ventral frontoparietal network that was identified by the ALE analysis. The insula is involved in prioritizing stimuli and spatial maps in the DAN. This is based on both bottom-up inputs and top-down internal information from higher association cortices including, but not limited to, the individual's goals and previous sensory input (Serences and Yantis, 2007; Myers et al., 2017).

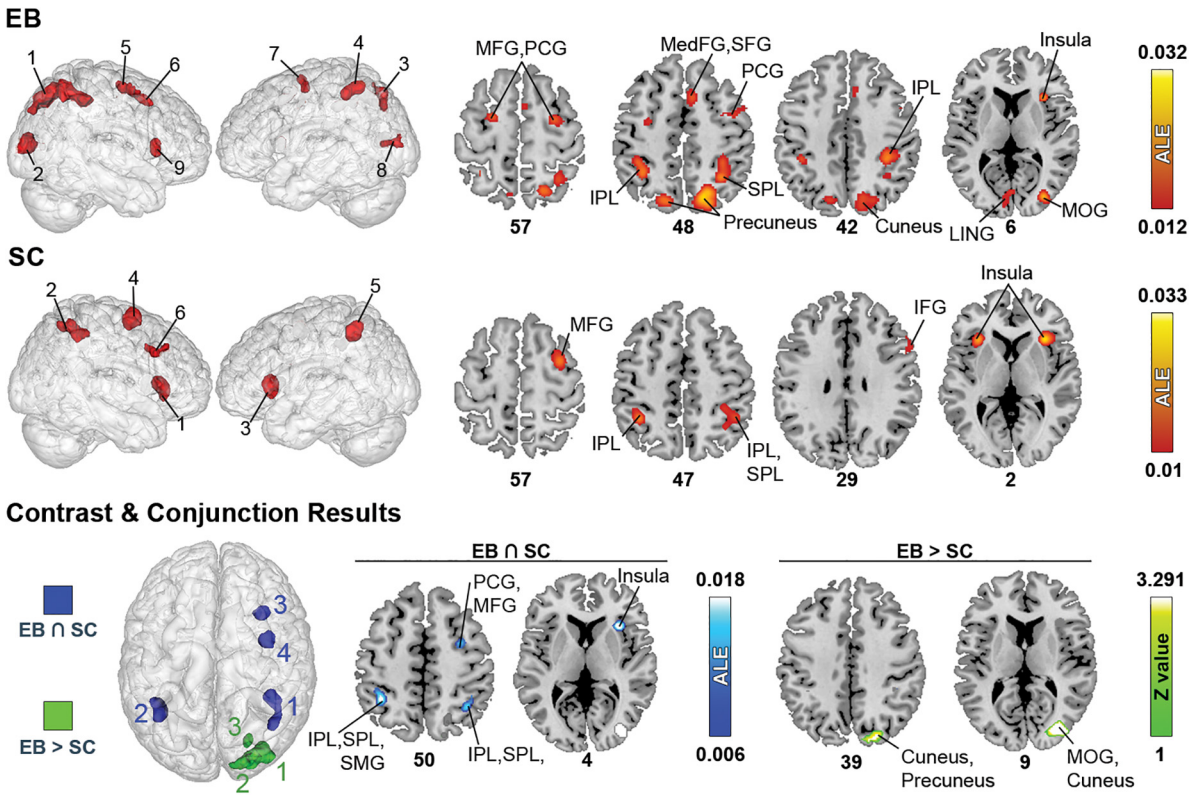

FIGURE 4
Brain areas activated in spatial processing + spatial navigation in EB, LB, and SC and results of contrast and conjunction analyses. **(Left)** 3D renders of the brain and activation clusters (see **Table 4** for reference). **(Right)** Axial cuts of the brain with identified clusters of activation. The number below the slices refer to the z coordinate in MNI space. ALE (for single and conjunction meta-analyses) and Z values (for contrast meta-analyses) are displayed to the right. The ALE values, calculated for each voxel, represent the probability of activation across included studies (Turkeltaub et al., 2012). For the contrast analysis, Z-values are used to show the significance of ALE subtractions between two groups. More details regarding the ALE and Z values are presented in **Table 5**. IOG, inferior occipital gyrus; IPL, inferior parietal lobule; ITG, inferior temporal gyrus; LING, lingual gyrus; MedFG, medial frontal gyrus; MFG, middle frontal gyrus; MOG, middle occipital gyrus; MTG, medial temporal gyrus; PCG, precentral gyrus; SFG, superior frontal gyrus; SPL, superior parietal lobule.

Similarly to findings from Zhang et al. (2019), we also found that EB recruited a larger network than SC including the precuneus, cuneus, lingual gyrus, and MTG. Moreover, we found additional activations in the pre-SMA, MOG, IOG, and ITG. The pre-SMA activation might be explained by its extensive role in the sequential integration of spatial information to form higher order representations (Cona and Semenza, 2017; Cona and Scarpazza, 2019). Furthermore, there is now ample evidence that the cuneus, lingual gyrus, MOG, IOG, MTG and ITG are cross-modally recruited by other senses, and thus maintain their spatial function in EB individuals (Ricciardi et al., 2007; Ptito et al., 2009; Matteau et al., 2010; Renier et al., 2010; Collignon et al., 2011; Dormal et al., 2016; Huber et al., 2019); they might even serve a multisensory role in normal sighted subjects (Palejwala et al., 2021). This could explain why in the absence of vision, the dorsal visual stream appears to be preserved both structurally (Reislev et al., 2016) and functionally (Fiehler et al., 2009; Zhang et al., 2019).

There is some evidence that the cross-modal recruitment of occipital areas in EB is topographically organized, forming new "retinotopic-like" cortical maps. These include new cortical representations of the fingers in the occipital cortex of Braille reading experts (Ptito et al., 2008a), and of the tongue in blind individuals trained with the tongue display unit (Kupers et al., 2006). Spatiotopic representations of auditory information in individuals trained in echolocation (Thaler et al., 2011; Arnott et al., 2013; Norman and Thaler, 2019; Van der Heijden et al., 2020) or trained with auditory SSDs (Hofstetter et al., 2021) have also been reported. It therefore seems that in the blind, visual areas in the occipital cortex maintain their function and form lower-level cortical maps of the perceived sensory information, similarly to frontoparietal networks. These new cortical maps are mostly egocentric and comparable to the retinotopic maps found in sighted subjects (Linton, 2021). It is theorized that this cross-modal recruitment in EB might arise from: (1) strengthened cortico-cortical connections between the occipital cortex with other sensory cortices and parietal associative areas

(Wittenberg et al., 2004; Ptito et al., 2005; Kupers et al., 2006); or (2) new connections between the sensory nuclei of the thalamus enabling non-visual sensory information to arrive directly to the occipital cortex via the optic radiations (Kupers and Ptito, 2014; Müller et al., 2019).

Neural correlates of non-visual spatial navigation

While previous meta-analyses (Ricciardi et al., 2014; Zhang et al., 2019) investigated spatial (navigation) tasks, they did not allow to distinguish between spatial processing and more complex spatial navigation tasks. As navigation integrates many tasks such as locomotion, echolocation, attention to stimuli, mental rotation, decision making, as well as working memory and long-term memory, this distinction is important for the present research question. Therefore, we also assessed the neural correlates of non-visual spatial navigation in EB individuals in one exploratory ALE analysis using a dataset of 11 contrasts. Clusters for spatial navigation included the precuneus, SPL, hippocampus, parahippocampal gyrus, fusiform gyrus, lingual gyrus and cuneus, all in the right hemisphere. Comparing with results from "*spatial processing + spatial navigation*" and "*spatial processing*," an additional significant cluster was found in the right insula and claustrum. These results are in line with those of previous meta-analyses investigating the neural correlates of navigation in SC (Epstein et al., 2017; Cona and Scarpazza, 2019; Qiu et al., 2019; Li et al., 2021), giving further credit to the idea that SC and EB share the same neural networks, despite differences in sensory modalities and navigational strategies. Spatial navigation in SC has been related to large cortical and subcortical networks, including the medial temporal lobe (comprised of HIP and entorhinal, perirhinal and parahippocampal cortices), posterior parietal cortex, insula/claustrum, prefrontal cortex, and a "scene perception" network comprised of the parahippocampal place area (PPA), the retrosplenial complex (RSC), and occipital place area (OPA) (Epstein et al., 2017; Epstein and Baker, 2019; Qiu et al., 2019; Li et al., 2021).

The activations in EB of the precuneus and SPL during virtual navigation (Halko et al., 2014), route and path recognition (Kupers et al., 2010; Fiehler et al., 2015), and tactile maze learning (Gagnon et al., 2012) are consistent with results in SC in spatial tasks (Cona and Scarpazza, 2019). These areas are mostly involved in egocentric navigation, more specifically in coding the environment, objects, and landmarks around the individual, or along routes, to plan and execute movements in relation to them (Farrell, 1996; Farrell and Robertson, 2000; Milner and Goodale, 2006). Other studies reported that these areas are involved in mental navigation (Ghaem et al., 1997), imagining places or scenes (Bisiach et al., 1993; Burgess et al., 2001) and help sustaining navigation in virtual mazes (Ohnishi et al., 2006). Furthermore, route recognition (Kupers et al., 2010) and maze learning (Gagnon et al., 2012) was associated with activations of primary and secondary visual areas: the cuneus, MOG, and lingual gyrus, a region involved in the discrimination of direction and motion (Cornette et al., 1998) and spatial learning of an environment (Nemmi et al., 2013). The lingual gyrus is also linked to allocentric, as opposed to egocentric, navigational strategies (Li et al., 2021).

The next cluster included the hippocampus, parahippocampal gyrus and fusiform gyrus. This cluster was activated by route recognition (Kupers et al., 2010), maze learning (Gagnon et al., 2012), and the processing of tactile spatial layouts (Wolbers et al., 2011) and large non-manipulable objects (He et al., 2013). The hippocampus is extensively linked to spatial navigation as it is involved in the formation and use of cognitive maps (Hartley et al., 2003; Iaria et al., 2003, 2007; Marchette et al., 2011; Epstein et al., 2017). It contains spatial codes representing distance and time relationships in small and large environments (Hassabis et al., 2009; Morgan et al., 2011; Deuker et al., 2016) and its activity can predict navigational performance (Suthana et al., 2009). Volume of the right posterior hippocampus correlates with navigational performance, experience, and spatial learning (Woollett and Maguire, 2011; Hartley and Harlow, 2012; Schinazi et al., 2013). The portion of the cluster in the parahippocampal gyrus closely overlapped with the PPA (Park and Chun, 2009). The PPA is a region that shows stronger responses to (1) visual scenes containing spatial information relevant for navigation (Harel et al., 2013; Epstein et al., 2017; Epstein and Baker, 2019); and (2) location-related – or large non-manipulable – objects that may serve as environmental landmarks or be linked to decision points (Epstein et al., 1999; Janzen and Van Turennout, 2004; Schinazi and Epstein, 2010; Julian et al., 2017; Epstein and Baker, 2019). Consequently, the PPA is thought to have a role in encoding a representation of specific scenes and landmarks, enabling their recognition (Epstein, 2008).

The "scene perception" network, comprised of the PPA, RSC and OPA, subserves different roles in long-term spatial memory and navigation; damage to these areas causes wayfinding deficits (Aguirre and D'esposito, 1999). While the PPA is involved in the representation of spatial layouts of scenes, the RSC and OPA are involved in the representation of spatial relationships between the observer and the parts of a scene (Epstein and Baker, 2019). Activity in the RSC increases with the acquisition of spatial knowledge of an environment (Wolbers and Büchel, 2005) and codes for the allocentric heading direction (Spiers and Maguire, 2007; Epstein, 2008). It is believed that the RSC is more involved in providing allocentric representations, thus situating scenes within more extensive environments (Epstein and Higgins, 2007; Epstein et al., 2007; Epstein, 2008). However, there is less consensus about its role in spatial navigation. Whereas some authors suggest that the RSC may serve as a relay structure that converts allocentric spatial representations

from the hippocampal complex to the egocentric representation in the posterior parietal cortex, others claim that it encodes and stores its own allocentric spatial representations (Epstein, 2008; Epstein and Baker, 2019). While specific clusters were not identified in the RSC, this region was activated by both visual and tactile spatial layouts in EB and SC (Wolbers et al., 2011). Taken together with PPA responses to scenes and spatially relevant information conveyed through visual, tactile and auditory stimuli (Kupers et al., 2010; Wolbers et al., 2011; Gagnon et al., 2012; Milne et al., 2015; Dodsworth, 2019) as well as through language (He et al., 2013), this result suggests that the spatial representations in this "scene perception" network may also be independent from visual experience and hence, amodal in nature.

Finally, activations of the anterior insula and claustrum, identified in the *spatial processing* + *spatial navigation* meta-analysis, are consistent with their known role in the processing goal-related sensory stimuli, in guiding behaviors, and in spatial learning (Hartley and Harlow, 2012). However, no other activations in (pre)frontal cortices were found even though they are associated with multiple wayfinding tasks such as switching navigational strategy, route planning, detours, and shortcuts (Cona and Scarpazza, 2019; Li et al., 2021). As it is the case for RSC, this null result may arise from the limited number of studies involving blind participants in such complex navigational tasks as only one study required participants to plan routes in a virtual environment (Halko et al., 2014).

Amodal nature of spatial cognition and navigation

The present study adds to a growing body of research suggesting that the brain of EB and SC are similarly organized at the functional level (Proulx et al., 2014; Cecchetti et al., 2016; Arioli et al., 2021). Particularly, our ALE analysis supports the *amodal* spatial processing hypothesis (Loomis et al., 2012; Chebat et al., 2018a; Giudice, 2018) as it indicates that EB and SC share common neural networks mediating spatial processing of sensory information, spatial navigation, and the formation of spatial representations. Our data suggest that fronto-parietal networks, typically involved in visuospatial attention and visually guided movements, maintain their function even though spatial information is obtained from sensory modalities other than vision. It is quite unlikely that this can be explained by visual imagery since EB, as defined in this paper, have limited or no visual experience. Furthermore, it is reasonable to assume that scene representations in the PPA is also amodal (Wolbers et al., 2011), as this region is recruited by tactile and auditory information relevant for navigation. However, further evidence is needed to establish the amodal character of the "scene perception" network.

In **Figure 5**, we present a new model of amodal spatial navigation that builds upon the work of various authors (Cisek and Kalaska, 2010; Epstein et al., 2017; Giudice, 2018; Epstein and Baker, 2019). According to this model, amodal spatial representations (2 in **Figure 5A**), stored in working memory, reflect the external space surrounding the individual (Loomis et al., 2002). These mental representations of space can be formed by sensory experiences and language (1 in **Figure 5A**), mental imagery or long-term memory, and can persist even after sensory inputs are removed (Giudice, 2018). Through a spatial computation system (3 in **Figure 5A**), likely the frontoparietal networks identified in the current meta-analysis, amodal spatial representations can serve to plan and execute many types of responses (i.e., locomotion, reaching or eye movements, attentional shifts, etc.; 4 in **Figure 5A**). According to this model, locomotion (also referred to as egocentric or response-based navigation; **Figure 5B**), is a sensorimotor loop in which actions lead to new sensory experiences (i.e., a new viewpoint, optic flow, etc.) and, in turn, to new (or updated) spatial representations used to plan subsequent actions. It is also well known that during locomotion, predictive feedback is utilized by the cerebellum to anticipate the consequences of actions and to refine further motor commands (Cisek and Kalaska, 2010; Hull, 2020). According to this model, spatial learning (also referred to as path integration and/or cognitive mapping; **Figure 5C**) is the process in which amodal spatial representations can be integrated to form a more allocentric (viewpoint-independent) or *global* spatial representation of an environment to be encoded in long-term memory (mediated by the hippocampal complex). These higher-level spatial representations (also known as cognitive maps; 6 in **Figure 5A**) generally preserve properties and relationships between environmental features such as landmarks, paths and directions (Golledge, 1999; Long and Giudice, 2010). These spatial representations can serve in wayfinding (**Figure 5D**), as the individual must constantly relate these to perceived features in the environment (5 in **Figure 5A**) while continuously keeping track of his/her position in relation to those features during locomotion (Long and Giudice, 2010; Epstein et al., 2017; Epstein and Baker, 2019). This constant comparison (5 in **Figure 5A**) of transient amodal spatial representations (2 in **Figure 5A**) and long-term global spatial representations (6 in **Figure 5A**) is likely mediated by the "scene perception" network (Epstein et al., 2017; Epstein and Baker, 2019) and its interaction with frontoparietal networks. This process likely serves different roles during wayfinding: 1) if the individual is in a new environment, a new global spatial representation can be encoded through path integration; 2) if the individual is in a known environment, the global spatial representation can be anchored to the perceived space and, thus, be utilized to orient the individual in this environment. Finally, this model also integrates the individual's motivations in the processes of wayfinding and locomotion.

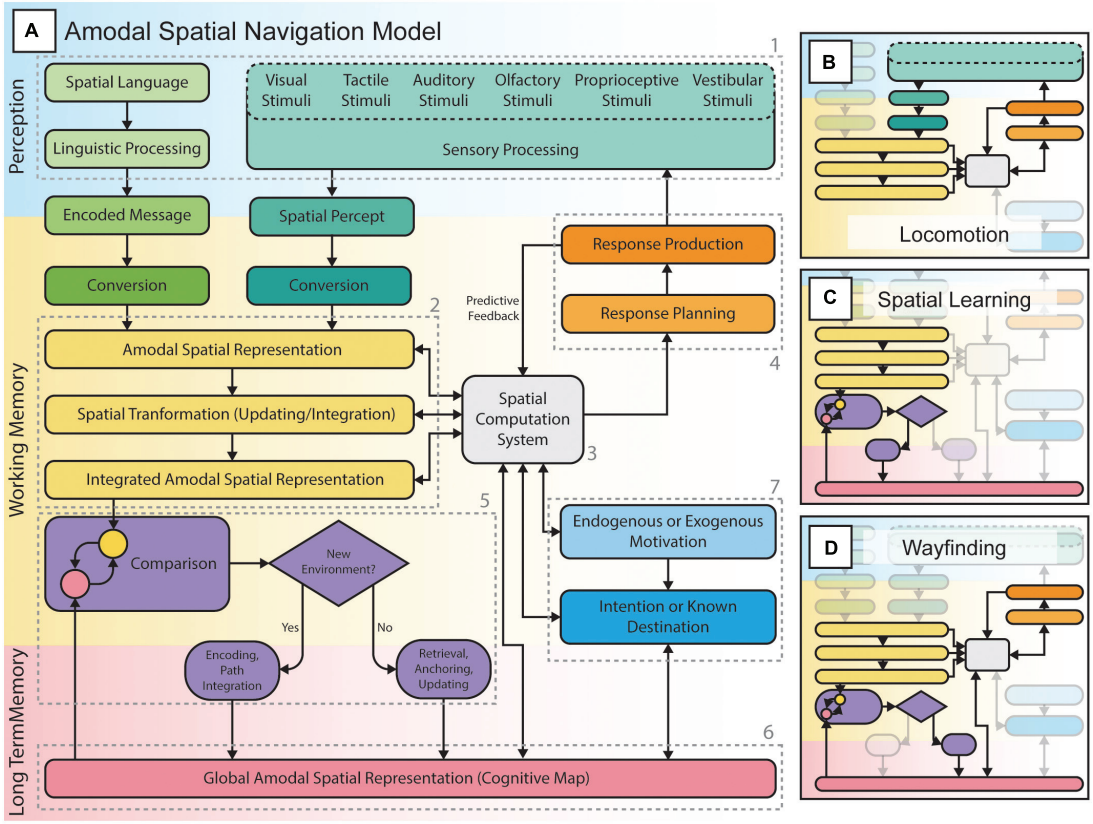

FIGURE 5
The amodal spatial navigation model including locomotion, spatial learning, and wayfinding. **(A)** Spatial navigation from perception to action, through various spatial computations, planning and execution of responses (actions such as movements and/or attentional allocation to sensory stimuli) according to endogenous or exogenous goals, and the formation and/or use of internal spatial representations (e.g., cognitive maps) to orient oneself in the environment. **(B)** Locomotion or "response-based" navigation consists of a sensorimotor loop that allows the individual to negotiate his path in the environment while considering the presence of obstacles or changes in the ground surface and level. The individual perceives the environment through sensory channels, extracts spatial information and uses it to plan and execute actions. These will then lead to a change (i.e., a new position or viewpoint) in the perceived environment followed by the planning of subsequent actions. This loop is involved in all forms of spatial navigation, including spatial learning and wayfinding tasks. **(C)** Spatial learning is the process of encoding an environment during locomotion (e.g., exploration): the individual integrates various spatial representations and forms a more global cognitive map to be stored in long-term memory. Such spatial representations can either be survey or route knowledge. **(D)** Wayfinding or "cognitive map-based" navigation is the process of retrieving a specific cognitive map and constantly relating it to the perceived environment during locomotion in order to reach known locations while staying oriented in the environment.

These motivations can be endogenous (e.g., hunger) or exogenous (e.g., seeing an obstacle or smelling food). These motivations can lead to an intention (e.g., fetch food) or to a known destination (e.g., a restaurant) to make decisions and/or actions (e.g., going to the restaurant). Accordingly, motivations can serve to retrieve global spatial representations and to find a certain destination.

Navigational abilities in the absence of vision

Spatial navigation involves numerous higher level cognitive processes such as spatial attention, working memory, long-term memory and decision making; consequently, it recruits a large network of brain areas (Epstein et al., 2017; Cona and Scarpazza, 2019; Li et al., 2021). These cognitive processes gain in importance for blind individuals who rely on less precise sensory inputs. Consequently, the formation of spatial representations in blind individuals will require more time and physical exploration of the environment. The difference between blind and sighted individuals is therefore not so much in the ability to form and use spatial representations, but in the temporal aspect of encoding these representations during spatial learning.

Referring to the model of amodal navigation (**Figure 5**), during locomotion, EB and SC will not only rely on incoming sensory information to guide their movements, but also on the proprioceptive feedback from their own body to judge traveled distances and turns taken. During spatial learning and

wayfinding, blind individuals constantly need to memorize this information and keep track of their movements in space as they cannot access all environmental information. Furthermore, wayfinding requires that the individual pays close attention to the limited environmental information they have access to in order to estimate their location in space, to recognize memorized landmarks and other relevant information such as textures on the floor. Consequently, spatial navigation in the absence of vision poses heavier demands on memory and attentional resources which can easily lead to exhaustion (Giudice, 2018). Consequently, many blind individuals tend to limit themselves to familiar environments and routes, which may lead to spatial deficits or delays in the development of spatial and mobility skills during childhood (Millar, 1994; Ungar et al., 1997; Cappagli and Gori, 2016).

There is substantial disagreement as to whether blind individuals possess the same spatial abilities as their sighted counterparts. **Figure 6** shows three models of spatial knowledge acquisition in the absence of vision: the *convergent* model, the *deficiency/cumulative* model, and the *inefficiency/persistent* model (reviewed in Schinazi et al., 2016; Giudice, 2018). The *convergent* model suggests that blind subjects are first disadvantaged but that through experience (exposure to an environment, repetition of a task, development of spatial abilities with age) they can reach similar performance as SC. The *cumulative* model proposes that vision plays a critical role in the development of spatial representations and abilities, and that blindness therefore leads to a slower progression in those abilities that will create a disparity between blind and non-blind populations over time. Finally, the *persistent* model suggests that individuals with blindness show a disadvantage from the start that, with age and experience, remains constant as vision is the most effective spatial modality. While firm evidence in support of one of these models is still lacking, novel technologies which aim to substitute or restore vision should bring us as close as possible to performance levels as proposed in the *convergent* model.

While it may be relevant to study and test such models and how tactile and auditory modalities compare to vision for spatial knowledge acquisition, spatial abilities of blind individuals are influenced by numerous internal and external factors. For instance, spatial knowledge and independence vary with age, experience, age at onset of blindness, amount of physical exercise, proficiency with navigational aids (long cane, guide dogs, GPS), the amount of O&M training (use of orientation strategies, practice, echolocation), environmental adaptations and, even, to the specific rehabilitation policies of the country of living. Indeed, O&M specialists often do not have the time to see clients as often as needed to help them develop all spatial skills and concepts that support the formation of allocentric spatial representations of the environment (Giudice, 2018). It is therefore not surprising that there are substantial inter-individual differences in reported spatial performance of blind individuals (Halko et al., 2014; Schinazi et al., 2016). It is hence important to study the numerous factors and neural mechanisms influencing the rate at which spatial abilities can develop and improve in visually impaired subjects of all ages in respect to the degree and onset of their visual condition.

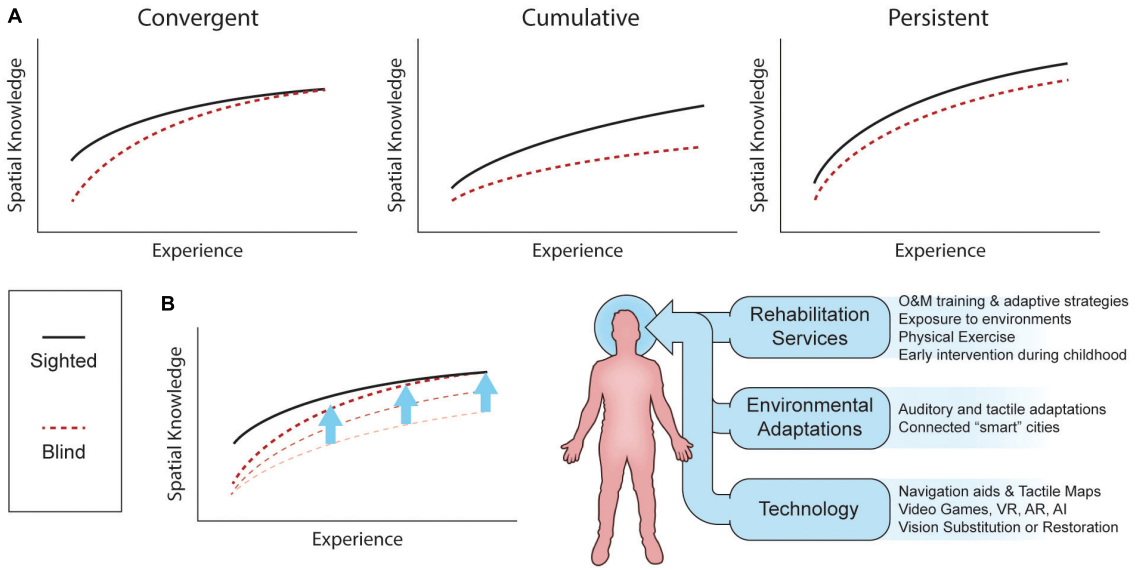

FIGURE 6
Spatial knowledge acquisition by sighted and blind individuals. **(A)** Three different models of spatial knowledge acquisition: the convergent, cumulative, and persistent models. **(B)** Spatial knowledge acquisition can be improved by the combination of rehabilitation services, environment adaptations and technologies. Adapted, with permission, from Schinazi et al. (2016). AI, artificial intelligence; AR, augmented reality; VR, virtual reality.

For this purpose, virtual environments and videogames show great potential (Connors et al., 2014; Li et al., 2021), but remain largely underused in the field of blindness. Indeed, identifying the neural networks underlying spatial learning and wayfinding in complex, but controlled and low-stress, virtual environments may lead to more adapted rehabilitative strategies and exercises to (1) support better navigational skills and improve autonomy; and (2) develop spatial concepts in children with visual impairments in a way that may decrease developmental delays and cortical atrophy caused by limited experiences and interactions with the environment.

Study limitations and considerations for future research

The present study is subject to various limitations inherent to the ALE meta-analysis and to working with small study populations. First, the ALE coordinate-based approach is prone to publication bias, false positives, and does not take effect size into account (Müller et al., 2018). Second, studies on blind subjects often deal with recruitment challenges and/or limited sample sizes. Moreover, included blind participants can be very heterogeneous in terms of blindness onset, duration, and cause, factors that may all affect functional outcomes. Many studies did not include LB subjects, implying that this group is underrepresented in the literature. Consequently, the ALE meta-analysis on spatial tasks could only be conducted for EB and SC. Furthermore, very few studies have dealt with the neural mechanisms of navigation, wayfinding and formation of allocentric cognitive maps (Ottink et al., 2022). Future research should therefore focus on better studying these processes; an endeavor that can be facilitated by the recent advances in audio-based virtual reality (Halko et al., 2014; Afonso-Jaco and Katz, 2022; Andrade et al., 2022).

Conclusion

The present meta-analysis study identified shared neural networks for non-visual spatial processing and navigation in blind and sighted individuals, thus lending further support to the hypothesis stating that neural representations of space are *amodal* or encoded independently of sensory modalities. However, given the limited data on spatial learning and wayfinding in blind populations, future research is still needed to understand their neural correlates. In addition, the paucity of data in late blind subjects also makes it difficult to arrive at firm conclusions regarding the neural correlates of spatial navigation and processing in this group. Since the incidence of late onset blindness is on the rise due to increased longevity and the associated prevalence of age-related diseases and diabetes, it is important to conduct further research in this group of patients.

Data availability statement

The raw data supporting the conclusions of this article will be made available by the authors, without undue reservation.

Author contributions

MB, JN, and MP conceptualized the study and planned the experiment. MB planned the methodology. MB, SP, and JN performed the literature search, curated the data, and performed the final formal statistical analysis. MB, SP, D-RC, RK, JN, and MP wrote the original draft, reviewed and edited the manuscript. All authors contributed to the article and approved the submitted version.

Funding

This study was supported by grants from the Canadian Institutes of Health Research (163014-2019: MP) and the Harland-Sanders Chair in Vision Science, the Vision Health Research Network (MB), Fonds de Recherche en Santé du Québec (MB), and the Centre Interdisciplinaire de Recherche sur le Cerveau et l'Apprentissage (MB).

Conflict of interest

The authors declare that the research was conducted in the absence of any commercial or financial relationships that could be construed as a potential conflict of interest.

Publisher's note

Supplementary material

The Supplementary Material for this article can be found online at: https://www.frontiersin.org/articles/10.3389/fnins.2022.1010354/full#supplementary-material

References

Afonso-Jaco, A., and Katz, B. F. (2022). Spatial Knowledge via Auditory Information for Blind Individuals Spatial Cognition Studies and the Use of Audio V R. *Sensors* 22:4794. doi: 10.3390/s22134794

Aguirre, G. K., and D'esposito, M. (1999). Topographical disorientation: A synthesis and taxonomy. *Brain* 122, 1613–1628. doi: 10.1093/brain/122.9.1613

Andrade, R., Baker, S., Waycott, J., and Vetere, F. (2022). *A Participatory Design Approach to Creating Echolocation-Enabled Virtual Environments*. New York, NY: Association for Computing Machinery. doi: 10.1145/3516448

Ankeeta, A., Senthil Kumaran, S., Saxena, R., Dwivedi, S. N., and Jagannathan, N. R. (2021). Visual Cortex Alterations in Early and Late Blind Subjects During Tactile Perception. *Perception* 50, 249–265. doi: 10.1177/0301006621991953

Anurova, I., Renier, L. A., De Volder, A. G., Carlson, S., and Rauschecker, J. P. (2015). Relationship Between Cortical Thickness and Functional Activation in the Early Blind. *Cereb. Cortex* 25, 2035–2048. doi: 10.1093/cercor/bhu009

Arioli, M., Ricciardi, E., and Cattaneo, Z. (2021). Social cognition in the blind brain: A coordinate-based meta-analysis. *Hum. Brain Mapp.* 42, 1243–1256. doi: 10.1002/hbm.25289

Arnott, S. R., Thaler, L., Milne, J. L., Kish, D., and Goodale, M. A. (2013). Shape-specific activation of occipital cortex in an early blind echolocation expert. *Neuropsychologia* 51, 938–949. doi: 10.1016/j.neuropsychologia.2013.01.024

Auvray, M., and Myin, E. (2009). Perception with compensatory devices: From sensory substitution to sensorimotor extension. *Cogn. Sci.* 33, 1036–1058. doi: 10.1111/j.1551-6709.2009.01040.x

Bedny, M., Konkle, T., Pelphrey, K., Saxe, R., and Pascual-Leone, A. (2010). Sensitive Period for a Multimodal Response in Human Visual Motion Area MT/MST. *Curr. Biol.* 20, 1900–1906. doi: 10.1016/j.cub.2010.09.044

Bisiach, E., Brouchon, M., Poncet, M., and Rusconi, M. L. (1993). Unilateral neglect in route description. *Neuropsychologia* 31, 1255–1262. doi: 10.1016/0028-3932(93)90072-8

Bleau, M., Paré, S., Djerourou, I., Chebat, D. R., Kupers, R., and Ptito, M. (2021). Blindness and the Reliability of Downwards Sensors to Avoid Obstacles: A Study with the EyeCane. *Sensors* 21:2700. doi: 10.3390/s21082700

Bonino, D., Ricciardi, E., Bernardi, G., Sani, L., Gentili, C., Vecchi, T., et al. (2015). Spatial imagery relies on a sensory independent, though sensory sensitive, functional organization within the parietal cortex: A fmri study of angle discrimination in sighted and congenitally blind individuals. *Neuropsychologia* 68, 59–70. doi: 10.1016/j.neuropsychologia.2015.01.004

Bonino, D., Ricciardi, E., Sani, L., Gentili, C., Vanello, N., Guazzelli, M., et al. (2008). Tactile spatial working memory activates the dorsal extrastriate cortical pathway in congenitally blind individuals. *Arch. Ital. Biol.* 146, 133–146.

Borra, E., and Luppino, G. (2017). Functional anatomy of the macaque temporo-parieto-frontal connectivity. *Cortex* 97, 306–326. doi: 10.1016/j.cortex.2016.12.007

Burgess, N., Becker, S., King, J. A., and O'keefe, J. (2001). Memory for events and their spatial context: Models and experiments. *Philos. Trans. R. Soc. Lond. B Biol. Sci.* 356, 1493–1503. doi: 10.1098/rstb.2001.0948

Cappagli, G., and Gori, M. (2016). Auditory spatial localization: Developmental delay in children with visual impairments. *Res. Dev. Disabil.* 5, 391–398. doi: 10.1016/j.ridd.2016.02.019

Cappagli, G., Cocchi, E., and Gori, M. (2017). Auditory and proprioceptive spatial impairments in blind children and adults. *Dev. Sci.* 20:e12374. doi: 10.1111/desc.12374

Caspers, S., Eickhoff, S. B., Rick, T., Von Kapri, A., Kuhlen, T., Huang, R., et al. (2011). Probabilistic fibre tract analysis of cytoarchitectonically defined human inferior parietal lobule areas reveals similarities to macaques. *NeuroImage* 58, 362–380. doi: 10.1016/j.neuroimage.2011.06.027

Cecchetti, L., Kupers, R., Ptito, M., Pietrini, P., and Ricciardi, E. (2016). Are Supramodality and Cross-Modal Plasticity the Yin and Yang of Brain Development? From Blindness to Rehabilitation. *Front. Syst. Neurosci.* 10:89. doi: 10.3389/fnsys.2016.00089

Chan, C. C. H., Wong, A. W. K., Ting, K. H., Whitfield-Gabrieli, S., He, J. F., and Lee, T. M. C. (2012). Cross auditory-spatial learning in early-blind individuals. *Hum. Brain Mapp.* 33, 2714–2727. doi: 10.1002/hbm.21395

Chebat, D. R., Chen, J. K., Schneider, F., Ptito, A., Kupers, R., and Ptito, M. (2007). Alterations in right posterior hippocampus in early blind individuals. *Neuroreport* 18, 329–333. doi: 10.1097/WNR.0b013e32802b70f8

Chebat, D. R., Maidenbaum, S., and Amedi, A. (2015). Navigation Using Sensory Substitution in Real and Virtual Mazes. *PLoS One* 10:e0126307. doi: 10.1371/journal.pone.0126307

Chebat, D. R., Maidenbaum, S., and Amedi, A. (2017). "The Transfer of Non-Visual Spatial Knowledge Between Real and Virtual Mazes via Sensory Substitution," in *2017 International Conference On Virtual Rehabilitation*, (Canada: IEEE). doi: 10.1109/ICVR.2017.8007542

Chebat, D.-R., Schneider, F. C., and Ptito, M. (2020a). Spatial Competence and Brain Plasticity in Congenital Blindness via Sensory Substitution Devices. *Front. Neurosci.* 14:815. doi: 10.3389/fnins.2020.00815

Chebat, D. R., Schneider, F. C., and Ptito, M. (2020b). Neural Networks Mediating Perceptual Learning in Congenital Blindness. *Sci. Rep.* 10:495. doi: 10.1038/s41598-019-57217-w

Chebat, D.-R., Harrar, V., Kupers, R., Maidenbaum, S., Amedi, A., and Ptito, M. (2018a). ". Sensory Substitution and the Neural Correlates of Navigation in Blindness," in *Mobility of Visually Impaired People: Fundamentals and ICT Assistive Technologies*, eds E. Pissaloux and R. Velazquez (Cham: Springer International Publishing). doi: 10.1007/978-3-319-54446-5_6

Chebat, D.-R., Heimler, B., Hofsetter, S., and Amedi, A. (2018b). "The Implications of Brain Plasticity and Task Selectivity for Visual Rehabilitation of Blind and Visually Impaired Individuals," in *The Neuroimaging of Brain Diseases: Structural and Functional Advances*, ed. C. Habas (Cham: Springer International Publishing). doi: 10.1007/978-3-319-78926-2_13

Chebat, D.-R., Schneider, F. C., Kupers, R., and Ptito, M. (2011). Navigation with a sensory substitution device in congenitally blind individuals. *Neuroreport* 22, 342–347. doi: 10.1097/WNR.0b013e3283462def

Cisek, P., and Kalaska, J. F. (2010). Neural Mechanisms for Interacting with a World Full of Action Choices. *Annu. Rev. Neurosci.* 33, 269–298. doi: 10.1146/annurev.neuro.051508.135409

Collignon, O., Dormal, G., Albouy, G., Vandewalle, G., Voss, P., Phillips, C., et al. (2013). Impact of blindness onset on the functional organization and the connectivity of the occipital cortex. *Brain* 136, 2769–2783. doi: 10.1093/brain/awt176

Collignon, O., Vandewalle, G., Voss, P., Albouy, G., Charbonneau, G., Lassonde, M., et al. (2011). Functional specialization for auditory-spatial processing in the occipital cortex of congenitally blind humans. *Proc. Natl. Acad. Sci. U S A.* 108, 4435–4440. doi: 10.1073/pnas.1013928108

Collins, D. L., Neelin, P., Peters, T. M., and Evans, A. C. (1994). Automatic 3D intersubject registration of Mr volumetric data in standardized Talairach space. *J. Comput. Assist. Tomogr.* 18, 192–205. doi: 10.1097/00004728-199403000-00005

Cona, G., and Scarpazza, C. (2019). Where is the "where" in the brain? A meta-analysis of neuroimaging studies on spatial cognition. *Hum. Brain Mapp.* 40, 1867–1886. doi: 10.1002/hbm.24496

Cona, G., and Semenza, C. (2017). Supplementary motor area as key structure for domain-general sequence processing: A unified account. *Neurosci. Biobehav. Rev.* 72, 28–42. doi: 10.1016/j.neubiorev.2016.10.033

Connors, E. C., Chrastil, E. R., Sánchez, J., and Merabet, L. B. (2014). Virtual environments for the transfer of navigation skills in the blind: A comparison of directed instruction vs. video game based learning approaches. *Front. Hum. Neurosci.* 8:223. doi: 10.3389/fnhum.2014.00223

Corbetta, M., Patel, G., and Shulman, G. L. (2008). The Reorienting System of the Human Brain: From Environment to Theory of Mind. *Neuron* 58, 306–324. doi: 10.1016/j.neuron.2008.04.017

Cornette, L., Dupont, P., Rosier, A., Sunaert, S., Hecke, P. V., Michiels, J., et al. (1998). Human brain regions involved in direction discrimination. *J. Neurophysiol.* 79, 2749–2765. doi: 10.1152/jn.1998.79.5.2749

Deuker, L., Bellmund, J. L. S., Schröder, T. N., and Doeller, C. F. (2016). An event map of memory space in the hippocampus. *eLife* 5:e16534. doi: 10.7554/eLife.16534

Dodsworth, C. (2019). *Changes in the Human Brain Cortex in Response to Learning Click-Based Echolocation: A Virtual Navigation Paradigm*, Ph.D thesis, Durham: Durham University.

Dormal, G., Rezk, M., Yakobov, E., Lepore, F., and Collignon, O. (2016). Auditory motion in the sighted and blind: Early visual deprivation triggers a large-scale imbalance between auditory and "visual" brain regions. *NeuroImage* 134, 630–644. doi: 10.1016/j.neuroimage.2016.04.027

Doucet, M. E., Guillemot, J. P., Lassonde, M., Gagné, J. P., Leclerc, C., and Lepore, F. (2005). Blind subjects process auditory spectral cues more efficiently

than sighted individuals. *Exp. Brain Res.* 160, 194–202. doi: 10.1007/s00221-004-2000-4

Eickhoff, S. B., Bzdok, D., Laird, A. R., Kurth, F., and Fox, P. T. (2012). Activation likelihood estimation meta-analysis revisited. *NeuroImage* 59, 2349–2361. doi: 10.1016/j.neuroimage.2011.09.017

Eickhoff, S. B., Bzdok, D., Laird, A. R., Roski, C., Caspers, S., Zilles, K., et al. (2011). Co-activation patterns distinguish cortical modules, their connectivity and functional differentiation. *NeuroImage* 57, 938–949. doi: 10.1016/j.neuroimage.2011.05.021

Eickhoff, S. B., Nichols, T. E., Laird, A. R., Hoffstaedter, F., Amunts, K., Fox, P. T., et al. (2016). Behavior, sensitivity, and power of activation likelihood estimation characterized by massive empirical simulation. *NeuroImage* 137, 70–85. doi: 10.1016/j.neuroimage.2016.04.072

Ekstrom, A. D. (2015). Why vision is important to how we navigate. *Hippocampus* 25, 731–735. doi: 10.1002/hipo.22449

Epstein, R. A. (2008). Parahippocampal and retrosplenial contributions to human spatial navigation. *Trends Cogn. Sci.* 12, 388–396. doi: 10.1016/j.tics.2008.07.004

Epstein, R. A., and Baker, C. I. (2019). Scene Perception in the Human Brain. *Annu. Rev. Vis. Sci.* 5, 373–397. doi: 10.1146/annurev-vision-091718-014809

Epstein, R. A., and Higgins, J. S. (2007). Differential parahippocampal and retrosplenial involvement in three types of visual scene recognition. *Cereb. Cortex* 17, 1680–1693.

Epstein, R. A., Higgins, J. S., Jablonski, K., and Feiler, A. M. (2007). Visual scene processing in familiar and unfamiliar environments. *J. Neurophysiol.* 97, 3670–3683.

Epstein, R. A., Patai, E. Z., Julian, J. B., and Spiers, H. J. (2017). The cognitive map in humans: Spatial navigation and beyond. *Nat. Neurosci.* 20, 1504–1513. doi: 10.1038/nn.4656

Epstein, R., Harris, A., Stanley, D., and Kanwisher, N. (1999). The parahippocampal place area: Recognition, navigation, or encoding? *Neuron* 23, 115–125. doi: 10.1016/S0896-6273(00)80758-8

Espinosa, M. A., Ungar, S., Ochaıta, E., Blades, M., and Spencer, C. (1998). Comparing Methods for Introducing Blind and Visually Impaired People to Unfamiliar Urban Environments. *J. Environ. Psychol.* 18, 277–287. doi: 10.1006/jevp.1998.0097

Farrell, M. J. (1996). Topographical disorientation. *Neurocase* 2, 509–520. doi: 10.1080/13554799608402427

Farrell, M. J., and Robertson, I. H. (2000). The automatic updating of egocentric spatial relationships and its impairment due to right posterior cortical lesions. *Neuropsychologia* 38, 585–595. doi: 10.1016/S0028-3932(99)00123-2

Fiehler, K., Burke, M., Bien, S., Röder, B., and Rösler, F. (2009). The Human Dorsal Action Control System Develops in the Absence of Vision. *Cereb. Cortex* 19, 1–12. doi: 10.1093/cercor/bhn067

Fiehler, K., Schütz, I., Meller, T., and Thaler, L. (2015). Neural Correlates of Human Echolocation of Path Direction During Walking. *Multisens. Res.* 28, 195–226. doi: 10.1163/22134808-00002491

Finocchietti, S., Cappagli, G., and Gori, M. (2015). Encoding audio motion: Spatial impairment in early blind individuals. *Front. Psychol.* 6:1357. doi: 10.3389/fpsyg.2015.01357

Fortin, M., Voss, P., Rainville, C., Lassonde, M., and Lepore, F. (2006a). Blind subjects are as good as sighted ones on a topographical orientation task. *Brain Cogn.* 60, 309–309.

Fortin, M., Voss, P., Rainville, C., Lassonde, M., and Lepore, F. (2006b). Impact of vision on the development of topographical orientation abilities. *Neuroreport* 17, 443–446. doi: 10.1097/01.wnr.0000203626.47824.86

Foulke, E. (1982). "Perception, cognition and the mobility of blind pedestrians," in *Spatial Abilities: Development and Physiological Foundations*, ed. M. Potegal (New York, NY: Academic Press), 55–76.

Fyhn, M., Hafting, T., Treves, A., Moser, M.-B., and Moser, E. I. (2007). Hippocampal remapping and grid realignment in entorhinal cortex. *Nature* 446, 190–194. doi: 10.1038/nature05601

Gagnon, L., Schneider, F. C., Siebner, H. R., Paulson, O. B., Kupers, R., and Ptito, M. (2012). Activation of the hippocampal complex during tactile maze solving in congenitally blind subjects. *Neuropsychologia* 50, 1663–1671. doi: 10.1016/j.neuropsychologia.2012.03.022

Garg, A., Schwartz, D., and Stevens, A. A. (2007). Orienting auditory spatial attention engages frontal eye fields and medial occipital cortex in congenitally blind humans. *Neuropsychologia* 45, 2307–2321. doi: 10.1016/j.neuropsychologia.2007.02.015

Ghaem, O., Mellet, E., Crivello, F., Tzourio, N., Mazoyer, B., Berthoz, A., et al. (1997). Mental navigation along memorized routes activates the hippocampus, precuneus, and insula. *NeuroReport* 8, 739–744. doi: 10.1097/00001756-199702100-00032

Giudice, N. A. (2018). "Navigating without vision: Principles of blind spatial cognition," in *Handbook of Behavioral and Cognitive Geography*, ed. D. R. Montello (Cheltenham: Edward Elgar Publishing), 432

Golledge, R. G. (1999). *Wayfinding Behavior: Cognitive Mapping and Other Spatial Processes*. Baltimore: John hopkins university press.

Gori, M., Amadeo, M. B., and Campus, C. (2020). Spatial metric in blindness: Behavioural and cortical processing. *Neurosci. Biobehav. Rev.* 109, 54–62. doi: 10.1016/j.neubiorev.2019.12.031

Gori, M., Sandini, G., Martinoli, C., and Burr, D. C. (2014). Impairment of auditory spatial localization in congenitally blind human subjects. *Brain* 137, 288–293. doi: 10.1093/brain/awt311

Gougoux, F., Zatorre, R. J., Lassonde, M., Voss, P., and Lepore, F. (2005). A Functional Neuroimaging Study of Sound Localization: Visual Cortex Activity Predicts Performance in Early-Blind Individuals. *PLoS Biol.* 3:e27. doi: 10.1371/journal.pbio.0030027

Hagler, D. J., and Sereno, M. I. (2006). Spatial maps in frontal and prefrontal cortex. *NeuroImage* 29, 567–577. doi: 10.1016/j.neuroimage.2005.08.058

Halko, M. A., Connors, E. C., Sanchez, J., and Merabet, L. B. (2014). Real world navigation independence in the early blind correlates with differential brain activity associated with virtual navigation. *Hum. Brain Mapp.* 35, 2768–2778. doi: 10.1002/hbm.22365

Harel, A., Kravitz, D. J., and Baker, C. I. (2013). Deconstructing visual scenes in cortex: Gradients of object and spatial layout information. *Cereb. Cortex* 23, 947–957. doi: 10.1093/cercor/bhs091

Harrar, V., Aubin, S., Chebat, D.-R., Kupers, R., and Ptito, M. (2018). "The Multisensory Blind Brain," in *Mobility of Visually Impaired People: Fundamentals and Ict Assistive Technologies*, eds E. Pissaloux and R. Velazquez (Cham: Springer International Publishing). doi: 10.1007/978-3-319-54446-5_4

Hartley, T., and Harlow, R. (2012). An association between human hippocampal volume and topographical memory in healthy young adults. *Front. Hum. Neurosci.* 6:338. doi: 10.3389/fnhum.2012.00338

Hartley, T., Maguire, E. A., Spiers, H. J., and Burgess, N. (2003). The well-worn route and the path less traveled: Distinct neural bases of route following and wayfinding in humans. *Neuron* 37, 877–888. doi: 10.1016/S0896-6273(03)00095-3

Hassabis, D., Chu, C., Rees, G., Weiskopf, N., Molyneux, P. D., and Maguire, E. A. (2009). Decoding neuronal ensembles in the human hippocampus. *Curr. Biol.* 19, 546–554. doi: 10.1016/j.cub.2009.02.033

He, C. X., Peelen, M. V., Han, Z. Z., Lin, N., Caramazza, A., and Bi, Y. C. (2013). Selectivity for large nonmanipulable objects in scene-selective visual cortex does not require visual experience. *Neuroimage* 79, 1–9. doi: 10.1016/j.neuroimage.2013.04.051

Hofstetter, S., Zuiderbaan, W., Heimler, B., Dumoulin, S. O., and Amedi, A. (2021). Topographic maps and neural tuning for sensory substitution dimensions learned in adulthood in a congenital blind subject. *Neuroimage* 235:118029. doi: 10.1016/j.neuroimage.2021.118029

Huber, E., Jiang, F., and Fine, I. (2019). Responses in area hMT+ reflect tuning for both auditory frequency and motion after blindness early in life. *Proc. Natl. Acad. Sci. U S A.* 116, 10081–10086. doi: 10.1073/pnas.1815376116

Hull, C. (2020). Prediction signals in the cerebellum: Beyond supervised motor learning. *eLife* 9:e54073. doi: 10.7554/eLife.54073

Iachini, T., Ruggiero, G., and Ruotolo, F. (2014). Does blindness affect egocentric and allocentric frames of reference in small and large scale spaces? *Behav. Brain Res.* 273, 73–81. doi: 10.1016/j.bbr.2014.07.032

Iaria, G., Chen, J.-K., Guariglia, C., Ptito, A., and Petrides, M. (2007). Retrosplenial and hippocampal brain regions in human navigation: Complementary functional contributions to the formation and use of cognitive maps. *Eur. J. Neurosci.* 25, 890–899. doi: 10.1111/j.1460-9568.2007.05371.x

Iaria, G., Petrides, M., Dagher, A., Pike, B., and Bohbot, V. D. (2003). Cognitive strategies dependent on the hippocampus and caudate nucleus in human navigation: Variability and change with practice. *J. Neurosci. Res.* 23, 5945–5952. doi: 10.1523/JNEUROSCI.23-13-05945.2003

Ioannides, A. A., Corsi-Cabrera, M., Fenwick, P. B. C., Del Rio, Portilla, Y., Laskaris, N. A., et al. (2004). Meg Tomography of Human Cortex and Brainstem Activity in Waking and Rem Sleep Saccades. *Cereb. Cortex* 14, 56–72. doi: 10.1093/cercor/bhg091

Jalali, S., and Wohlin, C. (2012). *Systematic Literature Studies: Database Searches vs. Backward Snowballing*. Sweden: IEEE. doi: 10.1145/2372251.2372257

Janzen, G., and Van Turennout, M. (2004). Selective neural representation of objects relevant for navigation. *Nat. Neurosci.* 7, 673–677. doi: 10.1038/nn1257

Jerde, T. A., and Curtis, C. E. (2013). Maps of space in human frontoparietal cortex. *J. Physiol. Paris* 107, 510–516. doi: 10.1016/j.jphysparis.2013.04.002

Jiang, A., Tian, J., Li, R., Liu, Y., Jiang, T., Qin, W., et al. (2015). Alterations of Regional Spontaneous Brain Activity and Gray Matter Volume in the Blind. *Neural Plast.* 2015:141950. doi: 10.1155/2015/141950

Jiang, F., Stecker, G. C., Boynton, G. M., and Fine, I. (2016). Early Blindness Results in Developmental Plasticity for Auditory Motion Processing within Auditory and Occipital Cortex. *Front. Hum. Neurosci.* 10:324. doi: 10.3389/fnhum.2016.00324

Julian, J. B., Ryan, J., and Epstein, R. A. (2017). Coding of object size and object category in human visual cortex. *Cereb. Cortex* 27, 3095–3109. doi: 10.1093/cercor/bhw150

Juurmaa, J., and Suonio, K. (1975). The role of audition and motion in the spatial orientation of the blind and the sighted. *Scand. J. Psychol.* 16, 209–216. doi: 10.1111/j.1467-9450.1975.tb00185.x

Karnath, H.-O., and Perenin, M.-T. (2005). Cortical Control of Visually Guided Reaching: Evidence from Patients with Optic Ataxia. *Cereb. Cortex* 15, 1561–1569. doi: 10.1093/cercor/bhi034

Kolarik, A. J., Pardhan, S., Cirstea, S., and Moore, B. C. J. (2017). Auditory spatial representations of the world are compressed in blind humans. *Exp. Brain Res.* 235, 597–606. doi: 10.1007/s00221-016-4823-1

Kraeutner, S. N., El-Serafi, M., Lee, J., and Boe, S. G. (2019). Disruption of motor imagery performance following inhibition of the left inferior parietal lobe. *Neuropsychologia* 127, 106–112. doi: 10.1016/j.neuropsychologia.2019.02.016

Kupers, R., and Ptito, M. (2014). Compensatory plasticity and cross-modal reorganization following early visual deprivation. *Neurosci. Biobehav. Rev.* 41, 36–52. doi: 10.1016/j.neubiorev.2013.08.001

Kupers, R., Chebat, D. R., Madsen, K. H., Paulson, O. B., and Ptito, M. (2010). Neural correlates of virtual route recognition in congenital blindness. *Proc. Natl. Acad. Sci. U S A.* 107, 12716–12721. doi: 10.1073/pnas.1006199107

Kupers, R., Fumal, A., De Noordhout, A. M., Gjedde, A., Schoenen, J., and Ptito, M. (2006). Transcranial magnetic stimulation of the visual cortex induces somatotopically organized qualia in blind subjects. *Proc. Natl. Acad. Sci. U S A.* 103, 13256–13260. doi: 10.1073/pnas.0602925103

Lehnert, G., and Zimmer, H. D. (2008). Common coding of auditory and visual spatial information in working memory. *Brain Res.* 1230, 158–167.

Lewald, J. (2002). Opposing effects of head position on sound localization in blind and sighted human subjects. *Eur. J. Neurosci.* 15, 1219–1224. doi: 10.1046/j.1460-9568.2002.01949.x

Li, J., Zhang, R., Liu, S., Liang, Q., Zheng, S., He, X., et al. (2021). Human spatial navigation: Neural representations of spatial scales and reference frames obtained from an Ale meta-analysis. *NeuroImage* 238:118264. doi: 10.1016/j.neuroimage.2021.118264

Likova, L. (2012). The Spatiotopic 'Visual' Cortex of the Blind. *Proc. SPIE* 8291:82910L. doi: 10.1117/12.912257

Linton, P. (2021). V1 as an egocentric cognitive map. *Neurosci. Conscious.* 2021:niab017. doi: 10.1093/nc/niab017

Long, R. G., and Giudice, N. A. (2010). "Establishing and Maintaining Orientation for Mobility," in *Foundations of Orientation and Mobility*, 3 Edn, eds W. R. Wiener, R. L. Welsh, and B. B. Blasch (New York, NY: American Foundation for the Blind.). doi: 10.21307/ijom-2010-008

Loomis, J. M., Klatzky, R. L., and Giudice, N. A. (2013). "Representing 3D Space in Working Memory: Spatial Images from Vision, Hearing, Touch, and Language," in *Multisensory Imagery*, eds S. Lacey and R. Lawson (New York, NY: Springer). doi: 10.1007/978-1-4614-5879-1_8

Loomis, J. M., Klatzky, R. L., Golledge, R. G., Cicinelli, J. G., Pellegrino, J. W., and Fry, P. A. (1993). Nonvisual navigation by blind and sighted: Assessment of path integration ability. *J. Exp. Psychol.* 122:73. doi: 10.1037/0096-3445.122.1.73

Loomis, J. M., Klatzky, R. L., Mchugh, B., and Giudice, N. A. (2012). Spatial working memory for locations specified by vision and audition: Testing the amodality hypothesis. *Atten. Percept. Psychophys.* 74, 1260–1267. doi: 10.3758/s13414-012-0311-2

Loomis, J. M., Lippa, Y., Klatzky, R. L., and Golledge, R. G. (2002). Spatial updating of locations specified by 3-d sound and spatial language. *J. Exp. Psychol. Learn. Mem. Cogn.* 28:335. doi: 10.1037/0278-7393.28.2.335

Luna, B., Thulborn, K. R., Strojwas, M. H., Mccurtain, B. J., Berman, R. A., Genovese, C. R., et al. (1998). Dorsal cortical regions subserving visually guided saccades in humans: An fmri study. *Cereb. Cortex* 8, 40–47. doi: 10.1093/cercor/8.1.40

Mackey, W. E., Winawer, J., and Curtis, C. E. (2017). Visual field map clusters in human frontoparietal cortex. *eLife* 6:e22974. doi: 10.7554/eLife.22974

Maidenbaum, S., Hanassy, S., Abboud, S., Buchs, G., Chebat, D. R., Levy-Tzedek, S., et al. (2014). The "EyeCane", a new electronic travel aid for the blind: Technology, behavior & swift learning. *Restor. Neurol. Neurosci.* 32, 813–824. doi: 10.3233/RNN-130351

Marchette, S. A., Bakker, A., and Shelton, A. L. (2011). Cognitive mappers to creatures of habit: Differential engagement of place and response learning mechanisms predicts human navigational behavior. *J. Neurosci. Res.* 31, 15264–15268. doi: 10.1523/JNEUROSCI.3634-11.2011

Matteau, I., Kupers, R., Ricciardi, E., Pietrini, P., and Ptito, M. (2010). Beyond visual, aural and haptic movement perception: HMT+ is activated by electrotactile motion stimulation of the tongue in sighted and in congenitally blind individuals. *Brain Res. Bull.* 82, 264–270. doi: 10.1016/j.brainresbull.2010.05.001

Merabet, L. B., and Pascual-Leone, A. (2010). Neural reorganization following sensory loss: The opportunity of change. *Nat. Rev. Neurosci.* 11, 44–52. doi: 10.1038/nrn2758

Millar, S. (1994). *Understanding and Representing Space: Theory and Evidence from Studies with Blind and Sighted Children*. Oxford: Oxford University Press. doi: 10.1093/acprof:oso/9780198521426.001.0001

Milne, J. L., Arnott, S. R., Kish, D., Goodale, M. A., and Thaler, L. (2015). Parahippocampal cortex is involved in material processing via echoes in blind echolocation experts. *Vis. Res.* 109, 139–148. doi: 10.1016/j.visres.2014.07.004

Milner, D., and Goodale, M. (2006). *The Visual Brain in Action*. Oxford: Oup Oxford. doi: 10.1093/acprof:oso/9780198524724.001.0001

Modi, S., Bhattacharya, M., Singh, N., Tripathi, R. P., and Khushu, S. (2012). Effect of visual experience on structural organization of the human brain: A voxel based morphometric study using Dartel. *Eur. J. Radiol.* 81, 2811–2819. doi: 10.1016/j.ejrad.2011.10.022

Moher, D., Liberati, A., Tetzlaff, J., and Altman, D. G. (2009). Preferred Reporting Items for Systematic Reviews and Meta-Analyses: The Prisma Statement. *Ann. Intern. Med.* 151, 264–269. doi: 10.7326/0003-4819-151-4-200908180-00135

Moore, T., and Fallah, M. (2001). Control of eye movements and spatial attention. *Proc. Natl. Acad. Sci. U S A.* 98, 1273–1276. doi: 10.1073/pnas.98.3.1273

Morgan, L. K., Macevoy, S. P., Aguirre, G. K., and Epstein, R. A. (2011). Distances between real-world locations are represented in the human hippocampus. *J. Neurosci. Res.* 31, 1238–1245. doi: 10.1523/JNEUROSCI.4667-10.2011

Müller, F., Niso, G., Samiee, S., Ptito, M., Baillet, S., and Kupers, R. (2019). A thalamocortical pathway for fast rerouting of tactile information to occipital cortex in congenital blindness. *Nat. Commun.* 10:5154. doi: 10.1038/s41467-019-13173-7

Müller, V. I., Cieslik, E. C., Laird, A. R., Fox, P. T., Radua, J., Mataix-Cols, D., et al. (2018). Ten simple rules for neuroimaging meta-analysis. *Neurosci. Biobehav. Rev.* 84, 151–161. doi: 10.1016/j.neubiorev.2017.11.012

Myers, N. E., Stokes, M. G., and Nobre, A. C. (2017). Prioritizing Information during Working Memory: Beyond Sustained Internal Attention. *Trends Cogn. Sci.* 21, 449–461. doi: 10.1016/j.tics.2017.03.010

Nelson, J. S., Kuling, I. A., Gori, M., Postma, A., Brenner, E., and Smeets, J. B. J. (2018). Spatial representation of the workspace in blind, low vision, and sighted human participants. *i-Perception* 9:2041669518781877. doi: 10.1177/2041669518781877

Nemmi, F., Boccia, M., Piccardi, L., Galati, G., and Guariglia, C. (2013). Segregation of neural circuits involved in spatial learning in reaching and navigational space. *Neuropsychologia* 51, 1561–1570. doi: 10.1016/j.neuropsychologia.2013.03.031

Niu, M., Rapan, L., Funck, T., Froudist-Walsh, S., Zhao, L., Zilles, K., et al. (2021). Organization of the macaque monkey inferior parietal lobule based on multimodal receptor architectonics. *NeuroImage* 231:117843. doi: 10.1016/j.neuroimage.2021.117843

Norman, L. J., and Thaler, L. (2019). Retinotopic-like maps of spatial sound in primary 'visual' cortex of blind human echolocators. *Proc. Biol. Sci.* 286:20191910. doi: 10.1098/rspb.2019.1910

Ohnishi, T., Matsuda, H., Hirakata, M., and Ugawa, Y. (2006). Navigation ability dependent neural activation in the human brain: An fMRI study. *Neurosci. Res.* 55, 361–369. doi: 10.1016/j.neures.2006.04.009

Ottink, L., Buimer, H., Van Raalte, B., Doeller, C. F., Van Der Geest, T. M., and Van Wezel, R. J. A. (2022). Cognitive map formation supported by auditory, haptic, and multimodal information in persons with blindness. *Neurosci. Biobehav. Rev.* 140:104797. doi: 10.1016/j.neubiorev.2022.104797

Palejwala, A. H., Dadario, N. B., Young, I. M., O'connor, K., Briggs, R. G., Conner, A. K., et al. (2021). Anatomy and white matter connections of the lingual

gyrus and cuneus. *World Neurosurg.* 151, e426–e437. doi: 10.1016/j.wneu.2021.04.050

Paré, S., Bleau, M., Djerourou, I., Malotaux, V., Kupers, R., and Ptito, M. (2021). Spatial navigation with horizontally spatialized sounds in early and late blind individuals. *PLoS One* 16:e0247448. doi: 10.1371/journal.pone.0247448

Park, H.-J., Chun, J.-W., Park, B., Park, H., Kim, J. I., Lee, J. D., et al. (2011). Activation of the Occipital Cortex and Deactivation of the Default Mode Network During Working Memory in the Early Blind. *J. Int. Neuropsychol. Soc.* 17, 407–422. doi: 10.1017/S1355617711000051

Park, S., and Chun, M. M. (2009). Different roles of the parahippocampal place area (Ppa) and retrosplenial cortex (Rsc) in panoramic scene perception. *NeuroImage* 47, 1747–1756. doi: 10.1016/j.neuroimage.2009.04.058

Parlatini, V., Radua, J., Dell'acqua, F., Leslie, A., Simmons, A., Murphy, D. G., et al. (2017). Functional segregation and integration within fronto-parietal networks. *NeuroImage* 146, 367–375. doi: 10.1016/j.neuroimage.2016.08.031

Pasqualotto, A., and Newell, F. N. (2007). The role of visual experience on the representation and updating of novel haptic scenes. *Brain Cogn.* 65, 184–194. doi: 10.1016/j.bandc.2007.07.009

Pasqualotto, A., and Proulx, M. J. (2012). The role of visual experience for the neural basis of spatial cognition. *Neurosci. Biobehav. Rev.* 36, 1179–1187. doi: 10.1016/j.neubiorev.2012.01.008

Passini, R., and Proulx, G. (1988). Wayfinding without Vision: An Experiment with Congenitally Totally Blind People. *Environ. Behav.* 20, 227–252. doi: 10.1177/0013916588202006

Passini, R., Proulx, G., and Rainville, C. (1990). The spatio-cognitive abilities of the visually impaired population. *Environ. Behav.* 22, 91–118. doi: 10.1177/0013916590221005

Paus, T. (1996). Location and function of the human frontal eye-field: A selective review. *Neuropsychologia* 34, 475–483. doi: 10.1016/0028-3932(95)00134-4

Pick, H. L. (1974). "Visual coding of nonvisual spatial information," in *Perception: Essays in honor of James J. Gibson*, eds R. B. MacLeod, and H. L. Pickeds (Ithaca, NY: Cornell University Press).

Power, Jonathan, D., Cohen, Alexander, L., Nelson, Steven, M., et al. (2011). Functional Network Organization of the Human Brain. *Neuron* 72, 665–678. doi: 10.1016/j.neuron.2011.09.006

Prado, J., Clavagnier, S., Otzenberger, H., Scheiber, C., Kennedy, H., and Perenin, M.-T. (2005). Two Cortical Systems for Reaching in Central and Peripheral Vision. *Neuron* 48, 849–858. doi: 10.1016/j.neuron.2005.10.010

Proulx, M. J., Brown, D. J., Pasqualotto, A., and Meijer, P. (2014). Multisensory perceptual learning and sensory substitution. *Neurosci. Biobehav. Rev.* 41, 16–25. doi: 10.1016/j.neubiorev.2012.11.017

Ptito, M., and Kupers, R. (2005). Cross-modal plasticity in early blindness. *J. Integr. Neurosci.* 4, 479–488. doi: 10.1142/S0219635205000951

Ptito, M., Bleau, M., Djerourou, I., Paré, S., Schneider, F. C., and Chebat, D.-R. (2021a). Brain-Machine Interfaces to Assist the Blind. *Front. Hum. Neurosci.* 15:46388876. doi: 10.3389/fnhum.2021.638887

Ptito, M., Fumal, A., De Noordhout, A. M., Schoenen, J., Gjedde, A., and Kupers, R. (2008a). Tms of the occipital cortex induces tactile sensations in the fingers of blind Braille readers. *Exp. Brain Res.* 184, 193–200. doi: 10.1007/s00221-007-1091-0

Ptito, M., Matteau, I., Gjedde, A., and Kupers, R. (2009). Recruitment of the middle temporal area by tactile motion in congenital blindness. *NeuroReport* 20, 543–547. doi: 10.1097/WNR.0b013e3283279909

Ptito, M., Moesgaard, S. M., Gjedde, A., and Kupers, R. (2005). Cross-modal plasticity revealed by electrotactile stimulation of the tongue in the congenitally blind. *Brain* 128, 606–614. doi: 10.1093/brain/awh380

Ptito, M., Paré, S., Dricot, L., Cavaliere, C., Tomaiuolo, F., and Kupers, R. (2021b). A quantitative analysis of the retinofugal projections in congenital and late-onset blindness. *NeuroImage* 32:102809. doi: 10.1016/j.nicl.2021.102809

Ptito, M., Schneider, F. C. G., Paulson, O. B., and Kupers, R. (2008b). Alterations of the visual pathways in congenital blindness. *Exp. Brain Res.* 187, 41–49. doi: 10.1007/s00221-008-1273-4

Qiu, Y., Wu, Y., Liu, R., Wang, J., Huang, H., and Huang, R. (2019). Representation of human spatial navigation responding to input spatial information and output navigational strategies: An ALE meta-analysis. *Neurosci. Biobehav. Rev.* 103, 60–72. doi: 10.1016/j.neubiorev.2019.06.012

Reislev, N. L., Kupers, R., Siebner, H. R., Ptito, M., and Dyrby, T. B. (2016). Blindness alters the microstructure of the ventral but not the dorsal visual stream. *Brain Struct. Funct.* 221, 2891–2903. doi: 10.1007/s00429-015-1078-8

Renier, L. A., Anurova, I., De Volder, A. G., Carlson, S., Vanmeter, J., and Rauschecker, J. P. (2010). Preserved functional specialization for spatial processing in the middle occipital gyrus of the early blind. *Neuron* 68, 138–148. doi: 10.1016/j.neuron.2010.09.021

Ricciardi, E., Tozzi, L., Leo, A., and Pietrini, P. (2014). Modality Dependent Cross-Modal Functional Reorganization Following Congenital Visual Deprivation within Occipital Areas: A Meta-Analysis of Tactile and Auditory Studies. *Multisensory Res.* 27, 247–262. doi: 10.1163/22134808-00002454

Ricciardi, E., Vanello, N., Sani, L., Gentili, C., Scilingo, E. P., Landini, L., et al. (2007). The effect of visual experience on the development of functional architecture in hMT. *Cereb. Cortex* 17, 2933–2939. doi: 10.1093/cercor/bhm018

Rogge, A. K., Hamacher, D., Cappagli, G., Kuhne, L., Hötting, K., Zech, A., et al. (2021). Balance, gait, and navigation performance are related to physical exercise in blind and visually impaired children and adolescents. *Exp. Brain Res.* 239, 1111–1123. doi: 10.1007/s00221-021-06038-3

Ruggiero, G., Ruotolo, F., and Iachini, T. (2018). Congenital blindness limits allocentric to egocentric switching ability. *Exp. Brain Res.* 236, 813–820. doi: 10.1007/s00221-018-5176-8

Ruggiero, G., Ruotolo, F., and Iachini, T. (2021). How ageing and blindness affect egocentric and allocentric spatial memory. *Q. J. Exp. Psychol.* 75, 1628–1642. doi: 10.1177/17470218211056772

Saygin, A. P., and Sereno, M. I. (2008). Retinotopy and Attention in Human Occipital Temporal, Parietal, and Frontal Cortex. *Cereb. Cortex* 18, 2158–2168. doi: 10.1093/cercor/bhm242

Schinazi, V. R., and Epstein, R. A. (2010). Neural correlates of real-world route learning. *Neuroimage* 53, 725–735. doi: 10.1016/j.neuroimage.2010.06.065

Schinazi, V. R., Nardi, D., Newcombe, N. S., Shipley, T. F., and Epstein, R. A. (2013). Hippocampal size predicts rapid learning of a cognitive map in humans. *Hippocampus* 23, 515–528. doi: 10.1002/hipo.22111

Schinazi, V. R., Thrash, T., and Chebat, D.-R. (2016). Spatial navigation by congenitally blind individuals. *Wires Cogn. Sci.* 7, 37–58. doi: 10.1002/wcs.1375

Schindler, A., and Bartels, A. (2013). Parietal Cortex Codes for Egocentric Space beyond the Field of View. *Curr. Biol.* 23, 177–182. doi: 10.1016/j.cub.2012.11.060

Seeley, W. W., Menon, V., Schatzberg, A. F., Keller, J., Glover, G. H., Kenna, H., et al. (2007). Dissociable Intrinsic Connectivity Networks for Salience Processing and Executive Control. *J. Neurosci.* 27:2349. doi: 10.1523/JNEUROSCI.5587-06.2007

Segond, H., Weiss, D., and Sampaio, E. (2005). Human spatial navigation via a visuo-tactile sensory substitution system. *Perception* 34, 1231–1249. doi: 10.1068/p3409

Serences, J. T., and Yantis, S. (2007). Spatially Selective Representations of Voluntary and Stimulus-Driven Attentional Priority in Human Occipital Parietal, and Frontal Cortex. *Cereb. Cortex* 17, 284–293. doi: 10.1093/cercor/bhj146

Shimony, J. S., Burton, H., Epstein, A. A., Mclaren, D. G., Sun, S. W., and Snyder, A. Z. (2006). Diffusion Tensor Imaging Reveals White Matter Reorganization in Early Blind Humans. *Cereb. Cortex* 16, 1653–1661. doi: 10.1093/cercor/bhj102

Silva, P. R., Farias, T., Cascio, F., Dos Santos, L., Peixoto, V., Crespo, E., et al. (2018). Neuroplasticity in Visual Impairments. *Neurol. Int.* 10:7326. doi: 10.4081/ni.2018.7326

Silver, M. A., Ress, D., and Heeger, D. J. (2005). Topographic Maps of Visual Spatial Attention in Human Parietal Cortex. *J. Neurophysiol.* 94, 1358–1371. doi: 10.1152/jn.01316.2004

Singh-Curry, V., and Husain, M. (2009). The functional role of the inferior parietal lobe in the dorsal and ventral stream dichotomy. *Neuropsychologia* 47, 1434–1448. doi: 10.1016/j.neuropsychologia.2008.11.033

Spiers, H. J., and Maguire, E. A. (2007). Decoding human brain activity during real-world experiences. *Trends Cogn. Sci.* 11, 356–365. doi: 10.1016/j.tics.2007.06.002

Squire, R. F., Noudoost, B., Schafer, R. J., and Moore, T. (2013). Prefrontal Contributions to Visual Selective Attention. *Annu. Rev. Neurosci.* 36, 451–466. doi: 10.1146/annurev-neuro-062111-150439

Stilla, R., Hanna, R., Hu, X. P., Mariola, E., Deshpande, G., and Sathian, K. (2008). Neural processing underlying tactile microspatial discrimination in the blind: A functional magnetic resonance imaging study. *J. Vis.* 8:13. doi: 10.1167/8.10.13

Stoll, C., Palluel-Germain, R., Fristot, V., Pellerin, D., Alleysson, D., and Graff, C. (2015). Navigating from a depth image converted into sound. *Appl. Bionics. Biomech.* 2015:543492. doi: 10.1155/2015/543492

Striem-Amit, E., Dakwar, O., Reich, L., and Amedi, A. (2012). The large-Scale Organization of Visual Streams Emerges Without Visual Experience. *Cereb. Cortex* 22, 1698–1709. doi: 10.1093/cercor/bhr253

Struiksma, M. E., Noordzij, M. L., Neggers, S. F., Bosker, W. M., and Postma, A. (2011). Spatial language processing in the blind: Evidence for a supramodal representation and cortical reorganization. *PLoS One* 6:e24253. doi: 10.1371/journal.pone.0024253

Sun, J., Huang, J., Wang, A., Zhang, M., and Tang, X. (2022). The role of the interaction between the inferior parietal lobule and superior temporal gyrus in the multisensory Go/No-go task. *NeuroImage* 254:119140. doi: 10.1016/j.neuroimage.2022.119140

Suthana, N. A., Ekstrom, A. D., Moshirvaziri, S., Knowlton, B., and Bookheimer, S. Y. (2009). Human hippocampal CA1 involvement during allocentric encoding of spatial information. *J. Neurosci.* 29, 10512–10519. doi: 10.1523/JNEUROSCI.0621-09.2009

Talairach, J., and Tournoux, P. (1988). *Co-Planar Stereotaxic Atlas of the Human Brain*. New York, NY: Thieme.

Tao, Q., Chan, C. C. H., Luo, Y. J., Li, J. J., Ting, K. H., Lu, Z. L., et al. (2017). Prior Visual Experience Modulates Learning of Sound Localization Among Blind Individuals. *Brain Topography* 30, 364–379. doi: 10.1007/s10548-017-0549-z

Tao, Q., Chan, C. C. H., Luo, Y.-J., Li, J.-J., Ting, K.-H., Wang, J., et al. (2015). How Does Experience Modulate Auditory Spatial Processing in Individuals with Blindness? *Brain Topography* 28, 506–519. doi: 10.1007/s10548-013-0339-1

Teng, S., Puri, A., and Whitney, D. (2012). Ultrafine spatial acuity of blind expert human echolocators. *Exp. Brain Res.* 216, 483–488. doi: 10.1007/s00221-011-2951-1

Thaler, L., Arnott, S. R., and Goodale, M. A. (2011). Neural correlates of natural human echolocation in early and late blind echolocation experts. *PLoS One* 6:e20162. doi: 10.1371/journal.pone.0020162

Thinus-Blanc, C., and Gaunet, F. (1997). Representation of space in blind persons: Vision as a spatial sense? *Psychol. Bull.* 121, 20–42. doi: 10.1037/0033-2909.121.1.20

Turkeltaub, P. E., Eickhoff, S. B., Laird, A. R., Fox, M., Wiener, M., and Fox, P. (2012). Minimizing within-experiment and within-group effects in activation likelihood estimation meta-analyses. *Hum. Brain Mapp.* 33, 1–13. doi: 10.1002/hbm.21186

Ungar, S., Blades, M., and Spencer, C. (1997). Teaching visually impaired children to make distance judgments from a tactile map. *J. Vis. Impair. Blind.* 91, 163–174. doi: 10.1177/0145482X9709100209

Van der Heijden, K., Formisano, E., Valente, G., Zhan, M., Kupers, R., and De Gelder, B. (2020). Reorganization of Sound Location Processing in the Auditory Cortex of Blind Humans. *Cereb. Cortex* 30, 1103–1116. doi: 10.1093/cercor/bhz151

Vandenberghe, R., Molenberghs, P., and Gillebert, C. R. (2012). Spatial attention deficits in humans: The critical role of superior compared to inferior parietal lesions. *Neuropsychologia* 50, 1092–1103. doi: 10.1016/j.neuropsychologia.2011.12.016

Vernet, M., Quentin, R., Chanes, L., Mitsumasu, A., and Valero-Cabré, A. (2014). Frontal eye field, where art thou? Anatomy, function, and non-invasive manipulation of frontal regions involved in eye movements and associated cognitive operations. *Front. Integr. Neurosci.* 8:66. doi: 10.3389/fnint.2014.00066

Voss, P., Gougoux, F., Lassonde, M., Zatorre, R. J., and Lepore, F. (2006). A positron emission tomography study during auditory localization by late-onset blind individuals. *NeuroReport* 17, 383–388. doi: 10.1097/01.wnr.0000204983.21748.2d

Voss, P., Gougoux, F., Zatorre, R. J., Lassonde, M., and Lepore, F. (2008). Differential occipital responses in early- and late-blind individuals during a sound-source discrimination task. *NeuroImage* 40, 746–758. doi: 10.1016/j.neuroimage.2007.12.020

Voss, P., Lassonde, M., Gougoux, F., Fortin, M., Guillemot, J. P., and Lepore, F. (2004). Early- and late-onset blind individuals show supra-normal auditory abilities in far-space. *Curr. Biol.* 14, 1734–1738. doi: 10.1016/j.cub.2004.09.051

Voss, P., Lepore, F., Gougoux, F., and Zatorre, R. J. (2011). Relevance of spectral cues for auditory spatial processing in the occipital cortex of the blind. *Front. Psychol.* 2:48. doi: 10.3389/fpsyg.2011.00048

Wang, D., Qin, W., Liu, Y., Zhang, Y., Jiang, T., and Yu, C. (2013). Altered White Matter Integrity in the Congenital and Late Blind People. *Neural Plast.* 2013:128236. doi: 10.1155/2013/128236

Weeks, R., Horwitz, B., Aziz-Sultan, A., Tian, B., Wessinger, C. M., Cohen, L. G., et al. (2000). A positron emission tomographic study of auditory localization in the congenitally blind. *J. Neurosci.* 20, 2664–2672. doi: 10.1523/JNEUROSCI.20-07-02664.2000

Wittenberg, G. F., Werhahn, K. J., Wassermann, E. M., Herscovitch, P., and Cohen, L. G. (2004). Functional connectivity between somatosensory and visual cortex in early blind humans. *Eur. J. Neurosci.* 20, 1923–1927. doi: 10.1111/j.1460-9568.2004.03630.x

Wolbers, T., and Büchel, C. (2005). Dissociable retrosplenial and hippocampal contributions to successful formation of survey representations. *J. Neurosci.* 25, 3333–3340. doi: 10.1523/JNEUROSCI.4705-04.2005

Wolbers, T., Klatzky, R. L., Loomis, J. M., Wutte, M. G., and Giudice, N. A. (2011). Modality-independent coding of spatial layout in the human brain. *Curr. Biol.* 21, 984–989. doi: 10.1016/j.cub.2011.04.038

Woollett, K., and Maguire, E. A. (2011). Acquiring "the Knowledge" of London's layout drives structural brain changes. *Curr. Biol.* 21, 2109–2114. doi: 10.1016/j.cub.2011.11.018

Wu, Y., Wang, J., Zhang, Y., Zheng, D., Zhang, J., Rong, M., et al. (2016). The Neuroanatomical Basis for Posterior Superior Parietal Lobule Control Lateralization of Visuospatial Attention. *Front. Neuroanat.* 10:32. doi: 10.3389/fnana.2016.00032

Zhang, C., Lee, T. M. C., Fu, Y., Ren, C., Chan, C. C. H., and Tao, Q. (2019). Properties of cross-modal occipital responses in early blindness: An Ale meta-analysis. *NeuroImage* 24:102041. doi: 10.1016/j.nicl.2019.102041

Zwiers, M. P., Van Opstal, A. J., and Cruysberg, J. R. (2001). A spatial hearing deficit in early-blind humans. *J. Neurosci.* 21:RC142. doi: 10.1523/JNEUROSCI.21-09-j0002.2001

frontiers | Frontiers in Neuroscience

TYPE Original Research
PUBLISHED 09 November 2022
DOI 10.3389/fnins.2022.970878

OPEN ACCESS

EDITED BY
Maurice Ptito,
Université de Montréal, Canada

REVIEWED BY
Alberto Inuggi,
University of Genoa, Italy
S. Senthil Kumaran,
All India Institute of Medical Sciences, India

*CORRESPONDENCE
Isabel Arend
arend.psy@gmail.com

SPECIALTY SECTION
This article was submitted to Perception Science, a section of the journal Frontiers in Neuroscience

RECEIVED 16 June 2022
ACCEPTED 14 October 2022
PUBLISHED 09 November 2022

CITATION
Arend I, Yuen K, Yizhar O, Chebat D-R and Amedi A (2022) Gyrification in relation to cortical thickness in the congenitally blind. *Front. Neurosci.* 16:970878. doi: 10.3389/fnins.2022.970878

Gyrification in relation to cortical thickness in the congenitally blind

Isabel Arend[1]*, Kenneth Yuen[2,3], Or Yizhar[4,5,6], Daniel-Robert Chebat[7,8] and Amir Amedi[4]

[1]The Joseph Sagol Neuroscience Center, The Chaim Sheba Medical Center, Ramat Gan, Israel, [2]Neuroimaging Center (NIC), Focus Program Translational Neuroscience, Johannes Gutenberg University Medical Center, Mainz, Germany, [3]Leibniz Institute for Resilience Research, Mainz, Germany, [4]The Institute for Brain, Mind and Technology, The Baruch Ivcher School of Psychology, Reichman University, Herzliya, Israel, [5]Max Planck Institute for Human Development, Research Group Adaptive Memory and Decision Making, Berlin, Germany, [6]Max Planck Institute for Human Development, Berlin, Germany, [7]Department of Psychology, Navigation and Accessibility Research Center of Ariel University (NARCA), Ariel, Israel, [8]Visual and Cognitive Neuroscience Laboratory (VCN Lab), Department of Psychology, Faculty of Social Sciences and Humanities, Ariel University, Ariel, Israel

Greater cortical gyrification (GY) is linked with enhanced cognitive abilities and is also negatively related to cortical thickness (CT). Individuals who are congenitally blind (CB) exhibits remarkable functional brain plasticity which enables them to perform certain non-visual and cognitive tasks with supranormal abilities. For instance, extensive training using touch and audition enables CB people to develop impressive skills and there is evidence linking these skills to cross-modal activations of primary visual areas. There is a cascade of anatomical, morphometric and functional-connectivity changes in non-visual structures, volumetric reductions in several components of the visual system, and CT is also increased in CB. No study to date has explored GY changes in this population, and no study has explored how variations in CT are related to GY changes in CB. T1-weighted 3D structural magnetic resonance imaging scans were acquired to examine the effects of congenital visual deprivation in cortical structures in a healthy sample of 11 CB individuals (6 male) and 16 age-matched sighted controls (SC) (10 male). In this report, we show for the first time an increase in GY in several brain areas of CB individuals compared to SC, and a negative relationship between GY and CT in the CB brain in several different cortical areas. We discuss the implications of our findings and the contributions of developmental factors and synaptogenesis to the relationship between CT and GY in CB individuals compared to SC. F.

KEYWORDS

vision, voxel-based morphometry, MRI, cortical thickness, gyrification, congenital blindness, late onset blindness, cross-modal plasticity

Introduction

The congenitally blind (CB) brain exhibits remarkable functional plasticity (Bavelier and Neville, 2002; Merabet and Pascual-Leone, 2010; Voss, 2013), influencing both white and gray matter (Noppeney et al., 2005; Shimony et al., 2006; Ptito et al., 2008; Jiang et al., 2009; Modi et al., 2012; Reislev et al., 2016, 2017). Indeed, there is a cascade of anatomical (Noppeney et al., 2005; Yang et al., 2014; Cecchetti et al., 2016), structural (Shimony et al., 2006; Bridge et al., 2009; Bridge and Watkins, 2019), morphological (Park et al., 2009), morphometric (Rombaux et al., 2010; Tomaiuolo et al., 2014; Aguirre et al., 2016; Maller et al., 2016), functional-connectivity (Heine et al., 2015), and metabolic changes (de Volder et al., 1997) in visual areas. Complete absence of vision from birth alters the cortical thickness (CT) of the brain and specifically in the primary visual cortex, which has been shown to be increased compared to sighted individuals (Jiang et al., 2009; Park et al., 2009; Kupers and Ptito, 2014; Anurova et al., 2015). CT is defined as the distance between the white/gray matter surface and pial surface. There is increased thickness in cortical visual areas of the CB relative to SC including the left visual association cortex (Jiang et al., 2009), the pericalcarine sulcus, lingual gyrus, right rostral middle frontal gyrus, left caudate and anterior cingulate cortices (Park et al., 2009). Both CB and LB showed thinner entorhinal cortex relative to SC (Jiang et al., 2009). These brain modifications are believed to be triggered at first by sensory deprivation (i.e., disuse related mechanisms), and later by the training of the other senses (i.e., training induced brain plasticity) (Chebat et al., 2020). The changes in CT of the CB brain have been explained in terms of disuse related mechanisms, but also in terms of cross-modal functional recruitment of brain areas (Jiang et al., 2009; Park et al., 2009; Voss and Zatorre, 2012; Anurova et al., 2015).

During the early stages of brain development there is notable increase in the formation of synaptic contacts, immediately followed by sensory dependent pruning of inactive synapses (Inuggi et al., 2020). In the visual cortex, synaptogenesis reaches a maximum of synaptic density around 8 months to 1 year of age. A long period of pruning, which lasts up to 11 years of age, eliminates about 40% of synapses. Prolonged visual deprivation during development alters pruning mechanisms which are dependent on sensory input (Pascual-Leone et al., 2005). Increased CT in the visual cortex in CB has been attributed to disuse related mechanisms during development (Jiang et al., 2009). In line with this time frame, changes in the thickness of the cortex are not observed in late blind (LB) individuals (Jiang et al., 2009; Park et al., 2009; Voss and Zatorre, 2012; Anurova et al., 2015), and CT gradually is linked with the age of blindness onset (Li et al., 2017). These differences between CB and LB individuals suggest that CT in occipital cortex is dependent on sensory experience during early development. The lack of visual experience must start influencing CT early on in development since, like adults, CB children have a thicker cortex than their sighted counterparts, while blind children with low vision do not (Inuggi et al., 2020; Ankeeta et al., 2021). Furthermore, these brain changes are long lasting, and not fully reversible, since people who had their sight restored by cataract surgery had decreased visual cortical area and higher CT than sighted individuals (Hölig et al., 2022). Indeed, a short and transient lack of visual experience early in life can have long lasting effects on brain development. Patients born with congenital cataracts exhibit long lasting changes in CT to the visual cortex and other visual areas, as well as resting state connectivity changes (Feng et al., 2021). Even slight changes to the quality of vision, such as in congenital achromatopsia, can also cause increases in CT in the visual cortex (Molz et al., 2022).

These first stages of development are characterized by delay (Begeer et al., 2014) or impairment (Gori et al., 2014) of certain abilities and altered brain development (Levtzion-Korach, 2001). During later stages of brain development, however, extensive training using touch and sound enables CB people to develop impressive skills that are linked to cross-modal activations of primary visual areas (Ptito et al., 2005; Merabet and Pascual-Leone, 2010; Voss et al., 2010; Kupers and Ptito, 2014). For example, CB possess enhanced verbal memory (Amedi et al., 2003), working memory (Heled et al., 2022), perceptual (Voss et al., 2004; Chebat et al., 2007; Arnaud et al., 2018), attention (Collignon et al., 2006), and cognitive (Fortin et al., 2008; Kupers et al., 2010; Chebat et al., 2015, 2017) skills compared to their sighted counterparts. This cross-modal recruitment keeps the primary visual cortex functional despite visual disuse for non-visual tasks (Amedi et al., 2003; Gougoux et al., 2005; Stevens et al., 2007; Jiang et al., 2009; Kupers and Ptito, 2014; Silva et al., 2018; Ptito et al., 2021). Variations in the thickness of the cortex in CB are linked to better performances on pitch and musical discrimination tasks. These changes are attributed to mechanisms of cross-modal training induced brain plasticity (Voss and Zatorre, 2012). Anurova et al. (2015) examined the relationship between CT and the magnitude of cortical activations in CB individuals during an attentionally demanding auditory task. They find that functional activations were negatively correlated with CT in all cortical areas involved in the auditory task (i.e., middle occipital gyrus, aSTG, pSTG). Meanwhile, cortical thinning in the CB brain is found in auditory and somatosensory areas, which is interpreted to reflect the interplay between developmental and adult training-induced plasticity (Park et al., 2009).

Reports of impaired performances and delayed brain development seem at odds with studies showing enhanced behavioral performances associated with cortical plastic changes in CB. In order to better understand the link between morphological changes and functional changes, it is imperative to look at several different measures of morphological changes. Gyrification (GY) is a complimentary measure to CT and is defined as the amount of cortical folding

(Hogstrom et al., 2013). CT and GY have been shown to be complementary measures, the former being sensitive to environmental changes whereas the latter is assumed to reflect rather stable inherent morphological characteristics. Indeed, although GY also shows levels of increment and/or decrement during aging, these changes seem to be driven by loss of volume and surface area (White et al., 2010; Striedter et al., 2015). Furthermore, in terms of the link between structure and function, there are differential contributions of CT and GY to different forms of intelligence (Tadayon et al., 2020). It is possible that CT and GY may also be affected differently by complete absence of visual experience from birth. No study to date has investigated GY in CB adults, and this is also the first study to explore the link between CT and GY in CB. In sighted humans, CT is negatively related to GY (Gautam et al., 2015), and greater cortical GY is usually linked with enhanced cognitive abilities (Hogstrom et al., 2013; Gautam et al., 2015; Green et al., 2018). The mechanisms underlying changes in GY are still unknown (White et al., 2010), and the forces driving the relationship between GY and CT is still largely misunderstood (Striedter et al., 2015). There are many non-mutually exclusive hypotheses describing why the cortex folds during development (White et al., 2010; Striedter et al., 2015). The observation of increase or decrease in GY might lead to different hypotheses concerning the mechanisms underlying plastic changes of the cortex of the blind during development. For example, GY changes might underlie some of the functional-anatomical modulations observed in the visual areas of the blind following cross-modal associations (Amedi et al., 2004, 2010; Ptito et al., 2005). The functional-anatomical modulations observed in the visual areas of CB following cross-modal associations (Desikan et al., 2006; Luders et al., 2006; Dahnke et al., 2013) including CT might reflect GY changes, and possibly also changes in the nature of the relationship between CT and GY.

We report here for the first time GY changes in CB adults compared to sighted people, and the link between CT and GY. We examine the effects of congenital visual deprivation in cortical structures GY and CT by comparing a group of healthy CB individuals with age-matched sighted controls (SC). We hypothesize that the relationship between CT and GY in targeted areas should be consistent with the effects of early visual deprivation and also to cross-modal experience dependent plasticity.

Materials and methods

Participant

We studied 11 CB (6 males) and 16 SC (10 males). Blindness was of peripheral causes in all cases and without any cognitive or neurological comorbidities. CB participants were born blind and had no history of light perception, except GA who lost his sight at the age of 1. Average ages of CB and SC were 34 (range 20–48) and 30 (range 20–40) years. Demographic data and the causes of blindness are summarized in **Table 1**. All subjects gave informed consent and the study protocol was approved by the local research ethics committee.

Magnetic resonance imaging data acquisition

High resolution three-dimensional anatomical volumes were collected using MP-RAGE T1-weighted sequence with a magnetic field 3T GE Signa scanner (GE Medical Systems, USA). Typical parameters were: Field of View (FOV) 23 cm (RL) × 23 cm (VD) × 17 cm (AP); Fold over- axis: RL, data matrix: 160 × 160 × 144 zero-filled to 256 in all directions (approx. 1 mm isovoxel native data), TR/TE = 3 ms/2300 ms, flip angle = 8°, resulting in 160 scans per subject.

Surface based morphometry analysis

Surface based morphometry analyses were computed using the CAT 12 toolbox (Structural Brain Mapping group, Jena University Hospital, Jena, Germany) implemented in SPM12 (Statistical Parametric Mapping, Institute of Neurology, London, UK). All T1-weighted images were corrected for bias e field inhomogeneities, then segmented into gray matter (GM), white matter (WM), and cerebrospinal fluid (CSF) (Gautam et al., 2015) and spatially normalized. The segmentation process was further extended by accounting for partial volume effects (Ptito et al., 2005), applying adaptive maximum *a posteriori* estimates. After pre-processing and in addition to visual checks for artifacts all scans passed an automated quality check protocol. CT and GY indices are determined by the

TABLE 1 Demographic information of the congenitally blind group.

	Sex	Age	Causes of blindness
AK	M	30	Congenital–cause unknown.
DK	M	33	Congenital–cause unknown.
EM	F	33	Congenital–cause unknown.
EN	F	30	Congenital–cause unknown.
GA	F	32	Early (1 year)–Left eye didn't develop during pregnancy, lost right eye when fell at the age of 1.
IG	M	42	Congenital–cause: Leiber disease.
MM	M	48	Congenital–cause: excess of oxygen.
OB	F	38	Congenital–cause: excess of oxygen.
OG	F	38	Congenital–cause: Rubella.
SH	M	30	Congenital–cause unknown.
SS	M	20	Congenital–cause unknown.

projection based thickness (PBT) method (Desikan et al., 2006). GY index refers to the estimated surface complexity in 3D, indirectly reflecting the amount of cortical folding and an increase in surface areas housing more gray matter. For both indices, scans were smoothed with a Gaussian kernel of 20 mm (FWHM). Automated ROI based analysis was performed for both GY and CT. ROIs were based on cortical parcelation using Desikan-Killiany Atlas (Pietrini et al., 2004).

Statistical analysis

Statistical analyses were carried out using the approach implemented in the CAT toolbox for SPM12. All values entered in the analysis were Z-transformed based on the mean and STD of the groups. We first examined group differences in CT by conducting a whole-brain analysis using a two-sample *t*-test adjusting for age and sex ($p < 0.05$, FDR correction). Comparisons between CB and SC groups was performed using independent *t*-tests separately for CT and GY indices. In all analyses, sex and age were entered as covariates in order to remove variance related to these potentially confounding variables. CAT 12 allows the estimation of surface parameters by surface-based atlas maps (Amedi et al., 2010). The atlas-based ROI analysis applies the information contained in the design matrix in order to extract parcellation based ROI values. False Discovery Rate correction was used to determine significant areas (FDR at $p < 0.05$).

We used paired *t*-tests to examine differences within each group concerning GY and CT. Data for all the areas except otherwise specified (see **Table 2**), were normally distributed according to Shapiro–Wilk test for normality (significant $p < 0.05$ suggesting deviation from normality).

TABLE 2 Desikan-Killiany (DK) Atlas brain areas ($p < 0.05$, FDR corrected) showing group differences (CB > SC) in Gyrification (GY).

	T-value	*Z*-value	*P*-value
Left hemisphere			
1. Left pars opercularis	3.77593	3.29	0.03
2. Left middle temporal	2.75599	2.53	0.048
3. Left temporal pole	2.66305	2.46	0.048
4. Left rostral middle frontal	2.64442	2.44	0.048
Right hemisphere			
5. Superior frontal	3.39	3.39	0.045
6. Pericalcarine	2.98	2.71	0.048
7. Frontal pole	2.68	2.47	0.048
8. Rostral middle frontal	2.85	2.61	0.048
9. Inferior temporal	2.68	2.47	0.048
10. Lateral occipital	2.64	2.438	0.048

General linear model testing the interaction between group, gyrification and cortical thickness

We first examined the relationship between GY and CT in cortical areas showing significant increase in GY ($p < 0.05$, FDR correction). A two-step regression approach was used to examine the relationship between GY and CT in the targeted cortical areas. The first model aimed at examining whether there was an association between GY and CT as a function of group and ROI. Therefore, GY was taken as dependent variable, CT, group and ROIs were chosen as the independent variables while adjusting for age and sex. The second model served as a *post-hoc* analysis examining the association between GY and CT within each ROI as a function of group (see: 31, for a similar approach). Checks for normality assumption were performed by using adequacy of Q-Q plots and residuals (see **Supplementary material**: Q-Q plots standardized residuals).

Results

Analysis of cortical thickness

In order to examine group differences in CT, we first conducted a whole-brain using a two-sample *t*-test adjusting for age and sex (FDR corrected $p = 0.05$). This analysis did not reveal any significant difference for the contrast SC > CB or for the reversed contrast CB > SC. Considering the small sample size used in the present study, and the fact that previous studies reported thickening of the cortex in CB individuals, we further explored group differences by using a less stringent exploratory threshold ($p = 0.001$ and $p = 0.005$, uncorrected) for the CB > SC contrast. Our analyses revealed a blob in the right fusiform area, and two additional blobs at the left middle occipital cortex and in the right superior motor area. Results for the whole-brain analysis are reported in (see **Supplementary material**: Analysis of CT, **Supplementary Figure 1**).

We also examined group differences by means of an atlas-based ROI analysis using FDR at $p < 0.05$. There was no significant group difference under FDR corrected threshold. The uncorrected threshold ($p < 0.05$) revealed differences for SC > CB and CB > SC contrasts. The results of this analyses are presented in full in **Supplementary material**. Although not reaching multiple comparisons threshold, CB > SC contrast revealed differences in the left and right occipital cortex. Despite not reaching statistical significance under FDR correction, the pattern from both whole-brain and ROI-based analysis are consistent with previous findings showing thickening of the occipital cortex in CB relative to controls (Pan et al., 2007; Jiang et al., 2009; Park et al., 2009; Voss and Zatorre, 2012).

Analysis of gyrification

In terms of group differences for GY (CB > SC) several brain areas are increased for the CB group (Figure 1). Namely, we find increases in the left hemisphere, the pars opercularis (BA44), temporal pole and middle temporal cortex, lateral orbitofrontal cortex and rostral middle frontal cortex. In the right hemisphere, we find a significant increase in GY in the following areas: superior frontal cortex, pericalcarine, frontal pole and inferior temporal, rostral frontal and lateral occipital cortex (Table 3 for the list of areas). The reverse contrast (SC > CB) did not reveal any differences.

Relationship between gyrification and cortical thickness in targeted cortical areas

We used Pearson's correlation coefficient to determine which brain areas had significant correlations between GY and CT for the CB group. Most areas show a negative link between CT and GY except for the right superior frontal and pericalcarine areas for CB and the left pars opercularis for SC (Table 3). For SC, although the correlations follow a similar negative trend, it only reached significance in the left temporal pole and in the right inferior temporal cortex.

We applied a linear regression analysis taking GY as dependent variable, Group, ROI and CT as regressors, while controlling for sex and age). We find a significant 3-way interaction $F_{(9,228)} = 2.34$, $p = 0.015$, as well as a significant main effect of CT, $F_{(1,228)} = 23.52$, $p < 0.001$. We further examined the association between GY and CT in a *post-hoc* analysis, for each ROI by means of separate linear regression models, taking GY as dependent variable, CT and group as independent variables adjusting for age and sex (Table 4). We observe a correlation between CT and GY changes for most areas except for the left rostral middle frontal, right pericalcarine, right inferior frontal, right inferior temporal and right calcarine areas. Of main relevance for the present report is the interaction involving Group and CT. We find that the level of CT in the left pars opercularis (BA 44) and in the right rostral middle frontal cortex had a significant impact on the amount of GY. We find a significant difference between the relationship between GY and CT between CB and SC groups. The impact of Group and CT as regressors of GY is illustrated in Figure 2.

TABLE 3 Pearson correlation coefficients between GY and CT for each DK atlas area showing increase in GY.

D.K Atlas label	Correlation between GY and CT	
	CB	SC
1. Left Pars opercularis (BA 44, 45, 47)	−0.53 ($p = 0.09$)	0.24 ($p = 0.37$)
2. Left middle temporal	**−0.64 ($p = 0.03$)**	−0.43 ($p = 0.10$)
3. Left temporal pole	**−0.81 ($p = 0.002$)**	−0.64 (**$p < 0.007$**)
4. Left rostral middle frontal	−0.15 ($p = 0.70$)	−0.32 ($p = 0.23$)
5. R superior frontal	**0.62 ($p = 0.04$)**	−0.11 ($p = 0.70$)
6. R pericalcarine	0.26 ($p = 0.45$)	−0.05 ($p = 0.85$)
7. R frontal pole	**−0.67 ($p = 0.02$)***	−0.41 ($p = 0.11$)
8. R rostral middle frontal	**−0.85 ($p = 0.009$)**	−0.18 ($p = 0.52$)
9. R inferior temporal	−0.06 ($p = 0.87$)	**−0.64 ($p = 0.007$)***
10. R lateral occipital	−0.27 ($p = 0.42$)	−0.16 ($p = 0.57$)

*Spearman correlation coefficient. Significant values are shown in bold font.

Discussion

Although our results are limited by our small sample size and by the absence of any cognitive assessment data for our subjects (see "Limitations"), several distinct trends emerged from our data. We focus on three specific themes: comparisons of CT, cortical GY, and the relationship between CT and GY between our groups. We did not find statistically significant differences in CT between CB and SC in whole-brain analysis. However, using less stringent threshold, thickening of the occipital cortex was observed, consistent with previous findings (Pan et al., 2007; Jiang et al., 2009; Park et al., 2009; Voss and Zatorre, 2012). In terms of GY, several brain areas are increased for the CB group (Figure 1). We find that most of the areas that have increased GY are also correlated negatively with CT for the CB group (see Table 3). Of those areas where GY was increased, we find interactions involving Group and CT in the left pars opercularis (BA 44) and in the right rostral middle frontal cortex (Figure 2). We discuss our findings in the following sections in terms of the existing literature on the subject.

Cortical thickness and gyrification following blindness in humans

Several brain areas are increased in terms of GY for the CB group (Figure 1). Namely, we find increases in the left the pars opercularis (BA44), temporal pole, middle temporal cortex, lateral orbitofrontal cortex, rostral middle frontal cortex, in the right superior frontal cortex, pericalcarine, frontal pole and inferior temporal, rostral frontal and lateral occipital cortex (Table 2). Interestingly, the temporal pole which we find increased in terms of GY, has been shown in previous reports to be reduced in terms of CT in CB (Park et al., 2009). Given that GY and CT are inversely related (Gautam et al., 2015), our results are congruent with these previous reports. Our report is congruent with CT increases in visual, sensory-motor, and auditory areas, and GI in bilateral visual cortex in CB children (Ankeeta et al., 2021).

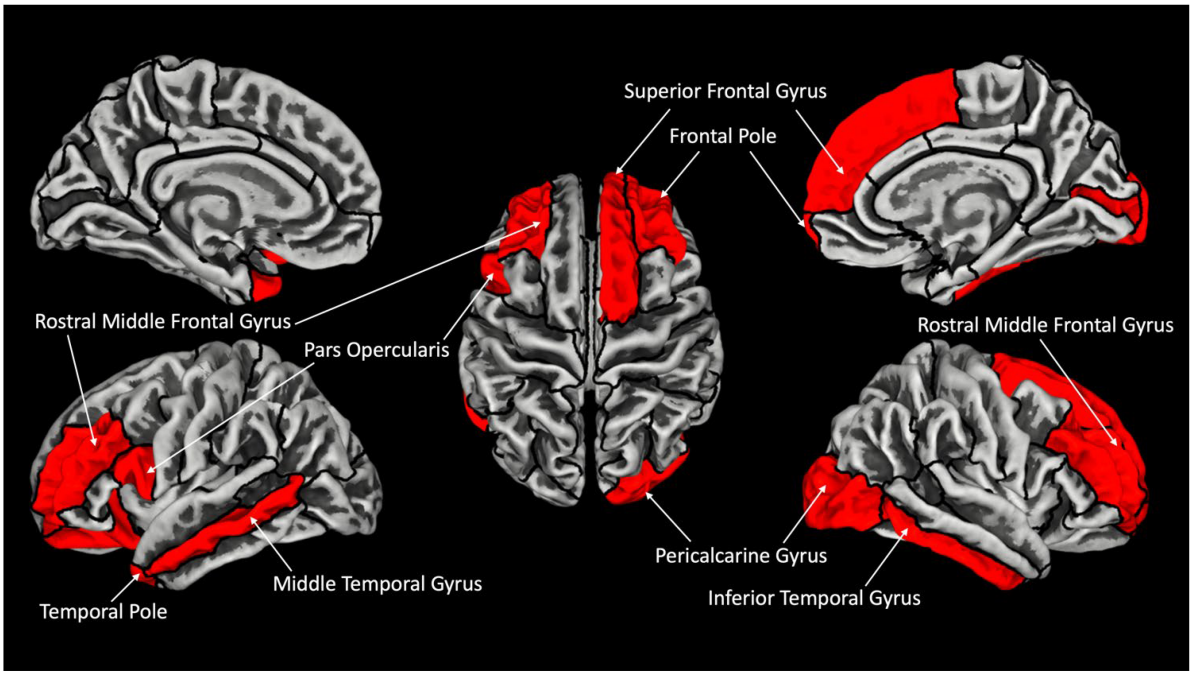

FIGURE 1
Increased gyrification in CB with respect to SC. Areas showing significant increase in gyrification are labeled in red (FDR corrected $p < 0.05$). Outline represent ROIs composing the Desikan–Killiani Atlas (Desikan et al., 2006) (DK40) (**Table 2** for full presentation of results).

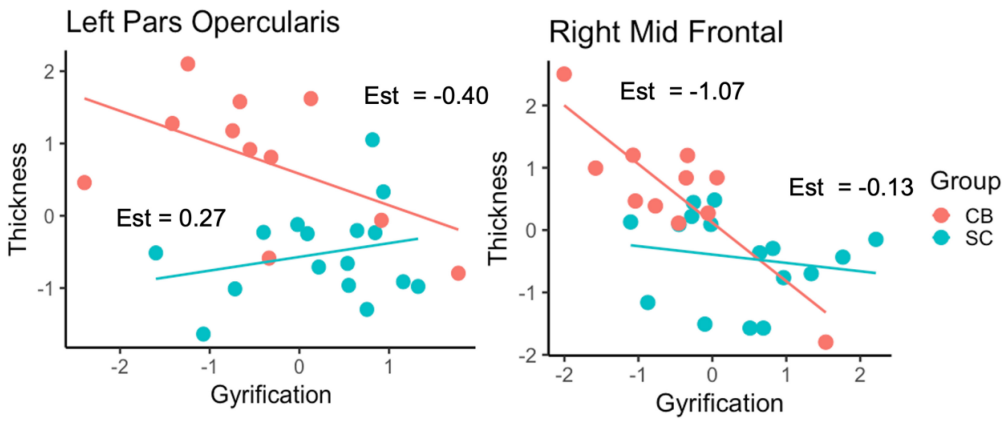

FIGURE 2
Relationship between GY and CT as a function of Group for the left pars opercularis and right rostral middle frontal cortex. Est = estimates of individual slopes.

The morphological changes we find in terms of GY and CT in the visual cortex of the CB are probably linked to mechanisms of general loss and compensatory plasticity. It has been shown that the lack of visual experience has an effect early on during development since CB children have increased CT compared to their sighted peers (Inuggi et al., 2020). Changes in CT have been described as "multi-systemic" since they affect several distinct brain areas. The areas that we find show increase GY in CB individuals are areas that have been consistently linked with cross modal activations in this population. For example, brain imaging studies in CB individuals show an increase in activation in these brain areas to non-visual stimuli (Amedi et al., 2003; Ptito et al., 2005; Kupers et al., 2010) recruiting the ventral stream for response to object recognition (Ptito et al., 2005, 2012; Striem-Amit et al., 2012), and the dorsal stream in responses to perceived motion of non-visual stimuli (Ricciardi et al., 2007; Ptito et al., 2009; Sani et al., 2010), and superior occipital cortex responses to spatial localization of

TABLE 4 Results of linear regression models taking mean CT and GROUP as regressors, and the interaction term CT × Group adjusting for sex and age.

		Beta values	CI	*p*	Adjusted R^2
L pars opercularis		−1.20	−1.83 to 0.56	0.001	0.48
	CT	−0.40	−0.96 to 0.16	0.001	
	Group × CT	**0.67**	**0.03 to 1.32**	**0.041**	
L middle temporal	Group	−0.68	−1.32 to 0.30	0.040	0.51
	CT	−0.93	−1.66 to −0.20	0.015	
	Group × CT	0.56	−0.23 to 1.35	0.157	
L temporal pole	Group	−0.44	−1.07 to 0.19	0.165	0.59
	CT	−0.93	−1.60 to 0.25	0.010	
	Group × CT	0.42	−0.31 to 1.16	0.244	
Left rostral middle frontal	Group	−0.84	−1.72 to 0.03	0.057	0.14
	CT	−0.13	−0.73 to 0.46	0.65	
	Group × CT	−0.26	−1.15 to −0.62	0.54	
R pericalcarine	Group	−1.21	−2.02 to −0.39	0.006	0.17
	CT	0.35	-0.32 to 1.03	0.29	
	Group × CT	−0.29	−1.10 to 0.52	0.46	
R frontal pole	Group	−0.52	−1.29 to 0.24	0.167	0.39
	CT	−0.75	−1.33 to −0.17	0.014	
	Group × CT	0.33	−0.38 to 1.05	0.345	
R rostral middle frontal	Group	−0.59	−1.23 to 0.06	0.074	
	CT	−1.07	−1.62 to −0.51	0.001	
	Group × CT	**0.94**	**0.26 to 1.61**	**0.009**	
R inferior temporal	Group	−0.76	−1.41 to 0.10	0.026	0.37
	CT	0.003	−0.51 to 0.51	0.991	
	Group × CT	−0.52	−1.15 to 0.12	0.104	
R lateral occipital	Group	−1.00	−1.73 to −0.28	0.009	0.45
	CT	−0.22	−0.69 to 0.24	0.33	
	Group × CT	−0.005	−0.64 to −0.63	0.988	

CI, confidence intervals. Beta values = unstandardized coefficients.

sounds (Gougoux et al., 2005; Collignon et al., 2011). Our results show an increase in GY in the left pars opercularis, and rostral middle frontal cortex that carry language and memory for verbal stimuli. These areas are co-activated with the left triangular cortex and occipital cortex during a verbal-memory task in CB (Amedi et al., 2003), and connectivity between these areas and striate cortex is altered in congenital blindness (Butt et al., 2013), suggesting that mechanisms of cross-modal plasticity also influence measurements of GY in the CB brain.

Relationship between gyrification and cortical thickness in targeted cortical areas

We find associations between GY and CT in various areas (Table 3). CT in the left pars opercularis (BA 44) and in the right rostral middle frontal cortex is correlated to the amount of GY in CB. Furthermore, the relationship between GY and CT is significantly different between CB and SC (Figure 2). These findings could suggest that GY and CT are not related in the same way for our two groups. We further explored the relationship between GY and CT by means of linear regression models, taking GY as dependent variable and CT and group as regressors (Table 4). We observe that CT is reliably correlated to GY changes in pars opercularis and in the right rostral middle frontal cortex. We further examined the association between GY and CT in a *post-hoc* analysis, for each ROI by means of separate linear regression models, taking GY as dependent variable, CT and group as independent variables (Table 4). Of main relevance for the present report is the interaction involving Group and CT. We find that the level of CT in the left pars opercularis (BA 44) and in the right rostral middle frontal cortex had a significant impact on the amount of GY (Figure 2).

We report a novel finding connecting two anatomical markers, GY and CT in CB individuals. Our findings are in line with previous work showing that there is increased thickness in cortical visual areas of the CB relative to SC including the pericalcarine sulcus, lingual gyrus, right rostral middle frontal gyrus, left caudate and anterior cingulate cortices

(Park et al., 2009), and that both CB and LB have a thinner entorhinal cortex relative to SC (Jiang et al., 2009). The thickness of the cortex in CB is linked with better performance in a melody discrimination task (Voss and Zatorre, 2012). Changes in CT and GY are linked with duration of Braille education in CB and LB children (Ankeeta et al., 2021). These results were interpreted to reflect the interaction of cross-modal plasticity and mechanisms of synaptic pruning, possibly driving the relationship between CT and GY. We find that in these specific areas, GY changes are correlated to changes in CT.

The biological significance for the expansion of cortical surface, and the consequential increase in GY, is that it enables the increase in computational capacity of the brain (Toro and Burnod, 2005). Indeed, phylogenic increases in GY is associated with increased cognitive abilities and more complex behaviors (e.g., rodents versus primate cortex) (Gregory et al., 2016). Furthermore, cortical GY is associated with better cognitive function (Burgaleta et al., 2014; Gautam et al., 2015; Youn et al., 2021), and GY is inversely correlated with CT (McIntosh et al., 2009; Hogstrom et al., 2013; Gautam et al., 2015; Schmitt et al., 2022), meaning that in most brain areas increases in GY are usually, but not always accompanied by decreases in CT. CT and GY are both influenced by early experiences of maltreatment (Kelly et al., 2013), the acquisition of a new language (Vaughn et al., 2021) or being born preterm (Papini et al., 2020), showing its vast malleability. Different cognitive measures in older adults, revealed positive correlations between GY and cognitive abilities in the superior temporal gyrus, the insular cortex and in the post-central gyrus (Lamballais et al., 2020), and GY decreases with age (Frangou et al., 2022). The CB brain is greatly modified for processing tactile and auditory stimuli as well as braille reading, speech processing and verbal memory (Kujala et al., 1995; Röder et al., 2002; Amedi et al., 2003; Ptito et al., 2005). We show that the areas responsible for these processes also show differences in terms of GY and the relationship between CT and GY may also be an important measure of synaptic plasticity.

Limiting factors

The present study is subject to various limitations inherent to working with small study populations. Different from previous studies, we did not find significant difference in CT in visual areas between CB and SC. We believe this null result could be possibly due to sample size issues since we did find differences in CT under less stringent threshold. Studies on blind subjects often deal with recruitment challenges and/or limited sample sizes. Moreover, included blind participants can be very heterogeneous in terms of blindness onset, duration, and cause, factors that may all affect functional outcomes. CB individuals represent an exceptionally rare population, even more so when strict selection requirements are enforced. Our sample of 12 participants can be considered as large and within the range of other classical brain morphometry studies in this population (for review see: Kupers and Ptito, 2014). Regardless, this is a major limiting factor of our study, and the relatively small sample size of CB participants forces us to be very cautious in our conclusions. Another major limiting factor is the absence of subject's cognitive information. Indeed, it would be interesting to correlate changes in GY and CT with measures of performance in different cognitive tasks. Future studies should explore behavioral correlates of perceptual training and CT/GY changes, training induced brain plasticity and training of abilities in CB people and its impact on the relationship between GY and CT in a larger sample of participants including late blind and low vision participants.

Conclusion

In this report, we show for the first time an increase in GY in several brain areas of CB adults compared to SC, and a negative relationship between GY and CT in the CB brain in several different cortical areas. We find that GY and CT covary differently in targeted areas, suggesting CB and SC may use these measures may be affected differently by the lack of visual experience, possibly reflecting disuse related mechanisms for CT changes, and training induced brain plasticity changes for GY changes in the CB. Furthermore, this differential relationship is highlighted by the fact that the relationship between GY and CT is not the same way in these two groups. Our results show that areas that are consistently implicated in cross-modal associations in CB are correlated in terms of CT/GY changes. Further exploration of ratio changes between GY and CT linked with perceptual learning skills in CB would enable us to disentangle the relation between cortical thickness, GY and behavioral abilities and the contributions of training induced plasticity vs. disuse related mechanisms.

Data availability statement

The data supporting the conclusions of this article will be made available upon request by the corresponding author.

Ethics statement

The studies involving human participants were reviewed and approved by The Hebrew University's Ethics Committee. The patients/participants provided their written informed consent to participate in this study.

Author contributions

IA, AA, and D-RC conceived and designed the experiments. IA, OY, KY, D-RC, and AA performed the experiments. IA, KY, D-RC, and AA analyzed the data. IA, KY, and D-RC wrote the manuscript. All authors contributed to the article and approved the submitted version.

Funding

This work was supported by the Ariel University Research Authority Absorption Grant # RA1700000192 (D-RC).

Conflict of interest

The authors declare that the research was conducted in the absence of any commercial or financial relationships that could be construed as a potential conflict of interest.

Publisher's note

All claims expressed in this article are solely those of the authors and do not necessarily represent those of their affiliated organizations, or those of the publisher, the editors and the reviewers. Any product that may be evaluated in this article, or claim that may be made by its manufacturer, is not guaranteed or endorsed by the publisher.

Supplementary material

The Supplementary Material for this article can be found online at: https://www.frontiersin.org/articles/10.3389/fnins.2022.970878/full#supplementary-material

References

Aguirre, G. K., Datta, R., Benson, N. C., Prasad, S., Jacobson, S. G., Cideciyan, A. V., et al. (2016). Patterns of individual variation in visual pathway structure and function in the sighted and blind. *PLoS One* 11:e0164677. doi: 10.1371/journal.pone.0164677

Amedi, A., Floel, A., Knecht, S., Zohary, E., and Cohen, L. G. (2004). Transcranial magnetic stimulation of the occipital pole interferes with verbal processing in blind subjects. *Nat. Neurosci.* 7, 1266–1270. doi: 10.1038/nn1328

Amedi, A., Raz, N., Azulay, H., Malach, R., and Zohary, E. (2010). Cortical activity during tactile exploration of objects in blind and sighted humans. *Restor. Neurol. Neurosci.* 28, 143–156. doi: 10.3233/RNN-2010-0503

Amedi, A., Raz, N., Pianka, P., Malach, R., and Zohary, E. (2003). Early "visual" cortex activation correlates with superior verbal memory performance in the blind. *Nat. Neurosci.* 6, 758–766. doi: 10.1038/nn1072

Ankeeta, A., Kumaran, S. S., Saxena, R., and Jagannathan, N. R. (2021). Structural and white matter changes associated with duration of Braille education in early and late blind children. *Vis. Neurosci.* 38:E011. doi: 10.1017/S0952523821000080

Anurova, I., Renier, L. A., de Volder, A. G., Carlson, S., and Rauschecker, J. P. (2015). Relationship between cortical thickness and functional activation in the early blind. *Cereb. Cortex* 25, 2035–2048. doi: 10.1093/cercor/bhu009

Arnaud, L., Gracco, V., and Ménard, L. (2018). Enhanced perception of pitch changes in speech and music in early blind adults. *Neuropsychologia* 117, 261–270. doi: 10.1016/j.neuropsychologia.2018.06.009

Bavelier, D., and Neville, H. J. (2002). Cross-modal plasticity: Where and how? *Nat. Rev. Neurosci.* 3, 443–452. doi: 10.1038/nrn848

Begeer, S., Dik, M., Voor De Wind, M. J., Asbrock, D., Brambring, M., and Kef, S. (2014). A new look at theory of mind in children with ocular and ocular-plus congenital blindness. *J. Vis. Impair. Blind.* 108, 17–27. doi: 10.1177/0145482X1410800103

Bridge, H., and Watkins, K. E. (2019). Structural and functional brain reorganisation due to blindness: The special case of bilateral congenital anophthalmia. *Neurosci. Biobehav. Rev.* 107, 765–774. doi: 10.1016/j.neubiorev.2019.10.006

Bridge, H., Cowey, A., Ragge, N., and Watkins, K. (2009). Imaging studies in congenital anophthalmia reveal preservation of brain architecture in "visual" cortex. *Brain* 132, 3467–3480. doi: 10.1093/brain/awp279

Burgaleta, M., Johnson, W., Waber, D. P., Colom, R., and Karama, S. (2014). Cognitive ability changes and dynamics of cortical thickness development in healthy children and adolescents. *Neuroimage* 84, 810–819. doi: 10.1016/j.neuroimage.2013.09.038

Butt, O. H., Benson, N. C., Datta, R., and Aguirre, G. K. (2013). The fine-scale functional correlation of striate cortex in sighted and blind people. *J. Neurosci.* 33, 16209–16219. doi: 10.1523/JNEUROSCI.0363-13.2013

Cecchetti, L., Ricciardi, E., Handjaras, G., Kupers, R., Ptito, M., and Pietrini, P. (2016). Congenital blindness affects diencephalic but not mesencephalic structures in the human brain. *Brain Struct. Funct.* 221, 1465–1480. doi: 10.1007/s00429-014-0984-5

Chebat, D. R., Maidenbaum, S., and Amedi, A. (2015). Navigation using sensory substitution in real and virtual mazes. *PLoS One* 10:e0126307. doi: 10.1371/journal.pone.0126307

Chebat, D. R., Maidenbaum, S., and Amedi, A. (2017). "The transfer of non-visual spatial knowledge between real and virtual mazes via sensory substitution," in *Proceedings of the international conference on virtual rehabilitation, ICVR* (Montreal: IEEE).

Chebat, D. R., Rainville, C., Kupers, R., and Ptito, M. (2007). Tactile-'visual' acuity of the tongue in early blind individuals. *Neuroreport* 18, 1901–1904. doi: 10.1097/WNR.0b013e3282f2a63

Chebat, D. R., Schneider, F. C., and Ptito, M. (2020). Spatial competence and brain plasticity in congenital blindness via sensory substitution devices. *Front. Neurosci.* 14:815. doi: 10.3389/fnins.2020.00815

Collignon, O., Renier, L., Bruyer, R., Tranduy, D., and Veraart, C. (2006). Improved selective and divided spatial attention in early blind subjects. *Brain Res.* 1075, 175–182. doi: 10.1016/j.brainres.2005.12.079

Collignon, O., Vandewalle, G., Voss, P., Albouy, G., Charbonneau, G., Lassonde, M., et al. (2011). Functional specialization for auditory-spatial processing in the occipital cortex of congenitally blind humans. *Proc. Natl. Acad. Sci. U.S.A.* 108, 4435–4440. doi: 10.1073/pnas.1013928108

Dahnke, R., Yotter, R. A., and Gaser, C. (2013). Cortical thickness and central surface estimation. *Neuroimage* 65, 336–348. doi: 10.1016/j.neuroimage.2012.09.050

de Volder, A. G., Bol, A., Blin, J., Robert, A., Arno, P., Grandin, C., et al. (1997). Brain energy metabolism in early blind subjects: Neural activity in the visual cortex. *Brain Res.* 750, 235–244. doi: 10.1016/S0006-8993(96)01352-2

Desikan, R. S., Ségonne, F., Fischl, B., Quinn, B. T., Dickerson, B. C., Blacker, D., et al. (2006). An automated labeling system for subdividing the human cerebral

cortex on MRI scans into gyral based regions of interest. *Neuroimage* 31, 968–980. doi: 10.1016/j.neuroimage.2006.01.021

Feng, Y., Collignon, O., Maurer, D., Yao, K., and Gao, X. (2021). Brief postnatal visual deprivation triggers long-lasting interactive structural and functional reorganization of the human cortex. *Front. Med. (Lausanne)* 8:752021. doi: 10.3389/fmed.2021.752021

Fortin, M., Voss, P., Lord, C., Lassonde, M., Pruessner, J., Saint-Amour, D., et al. (2008). Wayfinding in the blind: Larger hippocampal volume and supranormal spatial navigation. *Brain* 131, 2995–3005. doi: 10.1093/brain/awn250

Frangou, S., Modabbernia, A., Williams, S. C. R., Papachristou, E., Doucet, G. E., Agartz, I., et al. (2022). Cortical thickness across the lifespan: Data from 17,075 healthy individuals aged 3–90 years. *Hum. Brain Mapp.* 43, 431–451. doi: 10.1002/hbm.25364

Gautam, P., Anstey, K. J., Wen, W., Sachdev, P. S., and Cherbuin, N. (2015). Cortical gyrification and its relationships with cortical volume, cortical thickness, and cognitive performance in healthy mid-life adults. *Behav. Brain Res.* 287, 331–339. doi: 10.1016/j.bbr.2015.03.018

Gori, M., Sandini, G., Martinoli, C., and Burr, D. C. (2014). Impairment of auditory spatial localization in congenitally blind human subjects. *Brain* 137, 288–293. doi: 10.1093/brain/awt311

Gougoux, F., Zatorre, R. J., Lassonde, M., Voss, P., and Lepore, F. (2005). A functional neuroimaging study of sound localization: Visual cortex activity predicts performance in early-blind individuals. *PLoS Biol.* 3:e27. doi: 10.1371/journal.pbio.0030027

Green, S., Blackmon, K., Thesen, T., DuBois, J., Wang, X., Halgren, E., et al. (2018). Parieto-frontal gyrification and working memory in healthy adults. *Brain Imaging Behav.* 12, 303–308. doi: 10.1007/s11682-017-9696-9

Gregory, M. D., Kippenhan, J. S., Dickinson, D., Carrasco, J., Mattay, V. S., Weinberger, D. R., et al. (2016). Regional variations in brain gyrification are associated with general cognitive ability in humans. *Curr. Biol.* 26, 1301–1305. doi: 10.1016/j.cub.2016.03.021

Heine, L., Bahri, M. A., Cavaliere, C., Soddu, A., Laureys, S., Ptito, M., et al. (2015). Prevalence of increases in functional connectivity in visual, somatosensory and language areas in congenital blindness. *Front. Neuroanat.* 9:86. doi: 10.3389/fnana.2015.00086

Heled, E., Elul, N., Ptito, M., and Chebat, D. R. (2022). Deductive reasoning and working memory skills in individuals with blindness. *Sensors* 22:2062. doi: 10.3390/s22052062

Hogstrom, L. J., Westlye, L. T., Walhovd, K. B., and Fjell, A. M. (2013). The structure of the cerebral cortex across adult life: Age-related patterns of surface area, thickness, and gyrification. *Cereb. Cortex* 23, 2521–2530. doi: 10.1093/cercor/bhs231

Hölig, C., Guerreiro, M. J. S., Lingareddy, S., Kekunnaya, R., and Röder, B. (2022). Sight restoration in congenitally blind humans does not restore visual brain structure. *Cereb. Cortex* bhac197. doi: 10.1093/cercor/bhac197

Inuggi, A., Pichiecchio, A., Ciacchini, B., Signorini, S., Morelli, F., and Gori, M. (2020). Multisystemic increment of cortical thickness in congenital blind children. *Cereb. Cortex Commun.* 1:tgaa071. doi: 10.1093/texcom/tgaa071

Jiang, J., Zhu, W., Shi, F., Liu, Y., Li, J., Qin, W., et al. (2009). Thick visual cortex in the early blind. *J. Neurosci.* 29, 2205–2211.

Kelly, P. A., Viding, E., Wallace, G. L., Schaer, M., de Brito, S. A., Robustelli, B., et al. (2013). Cortical thickness, surface area, and gyrification abnormalities in children exposed to maltreatment: Neural markers of vulnerability? *Biol. Psychiatry* 74, 845–852. doi: 10.1016/j.biopsych.2013.06.020

Kujala, T., Alho, K., Kekoni, J., Hämäläinen, H., Reinikainen, K., Salonen, O., et al. (1995). Auditory and somatosensory event-related brain potentials in early blind humans. *Exp. Brain Res.* 104, 519–526. doi: 10.1007/BF00231986

Kupers, R., and Ptito, M. (2014). Compensatory plasticity and cross-modal reorganization following early visual deprivation. *Neurosci. Biobehav. Rev.* 41, 36–52. doi: 10.1016/j.neubiorev.2013.08.001

Kupers, R., Chebat, D. R., Madsen, K. H., Paulson, O. B., and Ptito, M. (2010). Neural correlates of virtual route recognition in congenital blindness. *Proc. Natl. Acad. Sci. U.S.A.* 107, 12716–12721. doi: 10.1073/pnas.1006199107

Lamballais, S., Vinke, E. J., Vernooij, M. W., Ikram, M. A., and Muetzel, R. L. (2020). Cortical gyrification in relation to age and cognition in older adults. *Neuroimage* 212:116637.

Levtzion-Korach, O. (2001). Early motor development of blind children. *J. Paediatr. Child Health* 36, 226–229.

Li, Q., Song, M., Xu, J., Qin, W., Yu, C., and Jiang, T. (2017). Cortical thickness development of human primary visual cortex related to the age of blindness onset. *Brain Imaging Behav.* 11, 1029–1036. doi: 10.1007/s11682-016-9576-8

Luders, E., Thompson, P. M., Narr, K. L., Toga, A. W., Jancke, L., and Gaser, C. (2006). A curvature-based approach to estimate local gyrification on the cortical surface. *Neuroimage* 29, 1224–1230. doi: 10.1016/j.neuroimage.2005.08.049

Maller, J. J., Thomson, R. H., Ng, A., Mann, C., Eager, M., Ackland, H., et al. (2016). Brain morphometry in blind and sighted subjects. *J. Clin. Neurosci.* 33, 89–95.

McIntosh, A. M., Moorhead, T. W. J., McKirdy, J., Hall, J., Sussmann, J. E. D., Stanfield, A. C., et al. (2009). Prefrontal gyral folding and its cognitive correlates in bipolar disorder and schizophrenia. *Acta Psychiatr. Scand.* 119, 192–198. doi: 10.1111/j.1600-0447.2008.01286.x

Merabet, L. B., and Pascual-Leone, A. (2010). Neural reorganization following sensory loss: The opportunity of change. *Nat. Rev. Neurosci.* 11, 44–52. doi: 10.1038/nrn2758

Modi, S., Bhattacharya, M., Singh, N., Tripathi, R. P., and Khushu, S. (2012). Effect of visual experience on structural organization of the human brain: A voxel based morphometric study using DARTEL. *Eur. J. Radiol.* 81, 2811–2819. doi: 10.1016/j.ejrad.2011.10.022

Molz, B., Herbik, A., Baseler, H. A., de Best, P. B., Vernon, R. W., Raz, N., et al. (2022). Structural changes to primary visual cortex in the congenital absence of cone input in achromatopsia. *Neuroimage Clin.* 33:102925. doi: 10.1016/j.nicl.2021.102925

Noppeney, U., Friston, K. J., Ashburner, J., Frackowiak, R., and Price, C. J. (2005). Early visual deprivation induces structural plasticity in gray and white matter. *Curr. Biol.* 15, R488–R490.

Pan, W. J., Wu, G., Li, C. X., Lin, F., Sun, J., and Lei, H. (2007). Progressive atrophy in the optic pathway and visual cortex of early blind Chinese adults: A voxel-based morphometry magnetic resonance imaging study. *Neuroimage* 37, 212–220. doi: 10.1016/j.neuroimage.2007.05.014

Papini, C., Palaniyappan, L., Kroll, J., Froudist-Walsh, S., Murray, R. M., and Nosarti, C. (2020). Altered cortical gyrification in adults who were born very preterm and its associations with cognition and mental health. *Biol. Psychiatry Cogn. Neurosci. Neuroimaging* 5, 640–650.

Park, H. J., Lee, J. D., Kim, E. Y., Park, B., Oh, M. K., Lee, S. C., et al. (2009). Morphological alterations in the congenital blind based on the analysis of cortical thickness and surface area. *Neuroimage* 47, 98–106. doi: 10.1016/j.neuroimage.2009.03.076

Pascual-Leone, A., Amedi, A., Fregni, F., and Merabet, L. B. (2005). The plastic human brain cortex. *Annu. Rev. Neurosci.* 28, 377–401.

Pietrini, P., Furey, M. L., Ricciardi, E., Gobbini, M. I., Wu, W. H. C., Cohen, L., et al. (2004). Beyond sensory images: Object-based representation in the human ventral pathway. *Proc. Natl. Acad. Sci. U.S.A.* 101, 5658–5663. doi: 10.1073/pnas.0400707101

Ptito, M., Bleau, M., Djerourou, I., Paré, S., Schneider, F. C., and Chebat, D. R. (2021). Brain-machine interfaces to assist the blind. *Front. Hum. Neurosci.* 15:638887. doi: 10.3389/fnhum.2021.638887

Ptito, M., Matteau, I., Gjedde, A., and Kupers, R. (2009). Recruitment of the middle temporal area by tactile motion in congenital blindness. *Neuroreport* 20, 543–547. doi: 10.1097/WNR.0b013e3283279909

Ptito, M., Matteau, I., Zhi Wang, A., Paulson, O. B., Siebner, H. R., and Kupers, R. (2012). Crossmodal recruitment of the ventral visual stream in congenital blindness. *Neural Plast.* 2012:304045.

Ptito, M., Moesgaard, S. M., Gjedde, A., and Kupers, R. (2005). Cross-modal plasticity revealed by electrotactile stimulation of the tongue in the congenitally blind. *Brain* 128, 606–614. doi: 10.1093/brain/awh380

Ptito, M., Schneider, F. C. G., Paulson, O. B., and Kupers, R. (2008). Alterations of the visual pathways in congenital blindness. *Exp. Brain Res.* 187, 41–49.

Reislev, N. H., Dyrby, T. B., Siebner, H. R., Lundell, H., Ptito, M., and Kupers, R. (2017). Thalamocortical connectivity and microstructural changes in congenital and late blindness. *Neural Plast.* 2017:9807512. doi: 10.1155/2017/9807512

Reislev, N. L., Dyrby, T. B., Siebner, H. R., Kupers, R., and Ptito, M. (2016). Simultaneous assessment of white matter changes in microstructure and connectedness in the blind brain. *Neural Plast.* 2016:6029241. doi: 10.1155/2016/6029241

Ricciardi, E., Vanello, N., Sani, L., Gentili, C., Scilingo, E. P., Landini, L., et al. (2007). The effect of visual experience on the development of functional architecture in hMT+. *Cereb. Cortex* 17, 2933–2939. doi: 10.1093/cercor/bhm018

Röder, B., Stock, O., Bien, S., Neville, H., and Rösler, F. (2002). Speech processing activates visual cortex in congenitally blind humans. *Eur. J. Neurosci.* 16, 930–936.

Rombaux, P., Huart, C., de Volder, A. G., Cuevas, I., Renier, L., Duprez, T., et al. (2010). Increased olfactory bulb volume and olfactory function in early blind subjects. *Neuroreport* 21, 1069–1073. doi: 10.1097/WNR.0b013e32833fcb8a

Sani, L., Ricciardi, E., Gentili, C., Vanello, N., Haxby, J. V., and Pietrini, P. (2010). Effects of visual experience on the human MT+ functional connectivity networks: An fMRI study of motion perception in sighted and congenitally blind individuals. *Front. Syst. Neurosci.* 4:159. doi: 10.3389/fnsys.2010.00159

Schmitt, S., Ringwald, K. G., Meller, T., Stein, F., Brosch, K., Pfarr, J. K., et al. (2022). Associations of gestational age with gyrification and neurocognition in healthy adults. *Eur. Arch. Psychiatry Clin. Neurosci.* 1–13.

Shimony, J. S., Burton, H., Epstein, A. A., McLaren, D. G., Sun, S. W., and Snyder, A. Z. (2006). Diffusion tensor imaging reveals white matter reorganization in early blind humans. *Cereb. Cortex* 16, 1653–1661.

Silva, P. R., Farias, T., Cascio, F., dos Santos, L., Peixoto, V., Crespo, E., et al. (2018). Neuroplasticity in visual impairments. *Neurol. Int.* 10:7326.

Stevens, A. A., Snodgrass, M., Schwartz, D., and Weaver, K. (2007). Preparatory activity in occipital cortex in early blind humans predicts auditory perceptual performance. *J. Neurosci.* 27, 10734–10741. doi: 10.1523/JNEUROSCI.1669-07.2007

Striedter, G. F., Srinivasan, S., and Monuki, E. S. (2015). Cortical folding: When, where, how, and why? *Annu. Rev. Neurosci.* 38, 291–307.

Striem-Amit, E., Dakwar, O., Reich, L., and Amedi, A. (2012). The large-scale organization of "visual" streams emerges without visual experience. *Cereb. Cortex* 22, 1698–1709.

Tadayon, E., Pascual-Leone, A., and Santarnecchi, E. (2020). Differential contribution of cortical thickness, surface area, and gyrification to fluid and crystallized intelligence. *Cereb. Cortex* 30, 215–225. doi: 10.1093/cercor/bhz082

Tomaiuolo, F., Campana, S., Collins, D. L., Fonov, V. S., Ricciardi, E., Sartori, G., et al. (2014). Morphometric changes of the corpus callosum in congenital blindness. *PLoS One* 9:e107871. doi: 10.1371/journal.pone.0107871

Toro, R., and Burnod, Y. (2005). A morphogenetic model for the development of cortical convolutions. *Cereb. Cortex* 15, 1900–1913. doi: 10.1093/cercor/bhi068

Vaughn, K. A., Nguyen, M. V. H., Ronderos, J., and Hernandez, A. E. (2021). Cortical thickness in bilingual and monolingual children: Relationships to language use and language skill. *Neuroimage* 1:243. doi: 10.1016/j.neuroimage.2021.118560

Voss, P. (2013). Sensitive and critical periods in visual sensory deprivation. *Front. Psychol.* 4:664. doi: 10.3389/fpsyg.2013.00664

Voss, P., and Zatorre, R. J. (2012). Occipital cortical thickness predicts performance on pitch and musical tasks in blind individuals. *Cereb. Cortex* 22, 2455–2465.

Voss, P., Collignon, O., Lassonde, M., and Lepore, F. (2010). Adaptation to sensory loss. *Wiley Interdiscip. Rev. Cogn. Sci.* 1, 308–328.

Voss, P., Lassonde, M., Gougoux, F., Fortin, M., Guillemot, J. P., and Lepore, F. (2004). Early-and late-onset blind individuals show supra-normal auditory abilities in far-space. *Curr. Biol.* 14, 1734–1738. doi: 10.1016/j.cub.2004.09.051

White, T., Su, S., Schmidt, M., Kao, C. Y., and Sapiro, G. (2010). The development of gyrification in childhood and adolescence. *Brain Cogn.* 72, 36–45.

Yang, C., Wu, S., Lu, W., Bai, Y., and Gao, H. (2014). Anatomic differences in early blindness: A deformation-based morphometry MRI study. *J. Neuroimaging* 24, 68–73. doi: 10.1111/j.1552-6569.2011.00686.x

Youn, H. C., Choi, M., Lee, S., Kim, D., Suh, S., Han, C. E., et al. (2021). Decreased cortical thickness and local gyrification in individuals with subjective cognitive impairment. *Clin. Psychopharmacol. Neurosci.* 19, 640–652. doi: 10.9758/cpn.2021.19.4.640

frontiers | Frontiers in Neuroscience

TYPE Original Research
PUBLISHED 11 January 2023
DOI 10.3389/fnins.2022.962817

OPEN ACCESS

EDITED BY
Maurice Ptito,
University of Montreal, Canada

REVIEWED BY
Laurence Dricot,
Université Catholique de Louvain, Belgium
Stuart Trenholm,
McGill University, Canada

*CORRESPONDENCE
Amber Maimon
✉ amber.maimon@runi.ac.il

SPECIALTY SECTION
This article was submitted to Perception Science, a section of the journal Frontiers in Neuroscience

RECEIVED 06 June 2022
ACCEPTED 19 December 2022
PUBLISHED 11 January 2023

CITATION
Maimon A, Netzer O, Heimler B and Amedi A (2023) Testing geometry and 3D perception in children following vision restoring cataract-removal surgery. *Front. Neurosci.* 16:962817. doi: 10.3389/fnins.2022.962817

Testing geometry and 3D perception in children following vision restoring cataract-removal surgery

Amber Maimon[1,2]*, Ophir Netzer[3], Benedetta Heimler[4] and Amir Amedi[1,2]

[1]The Baruch Ivcher Institute for Brain, Cognition, and Technology, Baruch Ivcher School of Psychology, Reichman University, Herzliya, Israel, [2]The Ruth & Meir Rosenthal Brain Imaging Center, Reichman University, Herzliya, Israel, [3]Gonda Brain Research Center, Bar-Ilan University, Ramat Gan, Israel, [4]Center of Advanced Technologies in Rehabilitation (CATR), Sheba Medical Center, Ramat Gan, Israel

As neuroscience and rehabilitative techniques advance, age-old questions concerning the visual experience of those who gain sight after blindness, once thought to be philosophical alone, take center stage and become the target for scientific inquiries. In this study, we employ a battery of visual perception tasks to study the unique experience of a small group of children who have undergone vision-restoring cataract removal surgery as part of the Himalayan Cataract Project. We tested their abilities to perceive in three dimensions (3D) using a binocular rivalry task and the Brock string task, perceive visual illusions, use cross-modal mappings between touch and vision, and spatially group based on geometric cues. Some of the children in this study gained a sense of sight for the first time in their lives, having been born with bilateral congenital cataracts, while others suffered late-onset blindness in one eye alone. This study simultaneously supports yet raises further questions concerning Hubel and Wiesel's critical periods theory and provides additional insight into Molyneux's problem, the ability to correlate vision with touch quickly. We suggest that our findings present a relatively unexplored intermediate stage of 3D vision development. Importantly, we spotlight some essential geometrical perception visual abilities that strengthen the idea that spontaneous geometry intuitions arise independently from visual experience (and education), thus replicating and extending previous studies. We incorporate a new model, not previously explored, of testing children with congenital cataract removal surgeries who perform the task *via* vision. In contrast, previous work has explored these abilities in the congenitally blind *via* touch. Taken together, our findings provide insight into the development of what is commonly known as the visual system in the visually deprived and highlight the need to further empirically explore an amodal, task-based interpretation of specializations in the development and structure of the brain.

Moreover, we propose a novel objective method, based on a simple binocular rivalry task and the Brock string task, for determining congenital (early) vs. late blindness where medical history and records are partial or lacking (e.g., as is often the case in cataract removal cases).

KEYWORDS

vision restoration, sensory perception, sensory development, visual perception, cataract removal, visual development, geometry, 3D perception

1. Introduction

"You'll learn," the blind man answered. "There is much to learn in the world." And indeed, as discovered by the protagonist in Wells, 1921 short story "The Country of the Blind," we have much to learn from the blind and the visually impaired. Particularly with regard to the neuroscience of vision and the development of the brain and the senses. Today, actual attempts at restoring vision allow for true exploration concerning these themes. In particular, by way of cataract removal. Though cataract removal methods and techniques have been documented for hundreds of years–with one of the first reported cases taking place as early as 1615 (Leffler et al., 2021), case studies and reports on the visual abilities and experiences of people who undergo cataract removal surgeries are still relatively few and far between (Fine et al., 2003; Ostrovsky et al., 2006).

Cataracts are the leading cause of vision impairment in children, particularly those residing in low-income countries worldwide (World Health Organization [WHO], 2021). Several humanitarian efforts are currently underway to change this unfortunate circumstance and rectify the situation. Among these projects is project Prakash (Thomas, 2011; Sinha, 2013; Sinha et al., 2013), a project with humanitarian and scientific goals led by Prof. Pawan Sinha, and the Himalayan Cataract Project (Welling et al., 2013; Brant et al., 2021), founded by Drs. Geoffrey Tabin and Sanduk Ruit that aims to eradicate curable blindness.

David Hubel and Torsten Wiesel, who later won the 1981 Nobel Prize for this work, found that deprivation of visual input in the first few months of the lives of animals (such as cats and monkeys) led to irreversibly abnormal visual processing (Wiesel and Hubel, 1965; Hubel et al., 1977; LeVay et al., 1980). They found that when monocularly deprived of vision, the percentage of cells driven by the sensory-deprived eye is reduced (Wiesel and Hubel, 1963). When binocularly deprived of vision, they found a decrease in the number of binocularly influenced cells. They suggested that this indicates "a deterioration of innate connections subserving binocular convergence" (Wiesel and Hubel, 1974, p. 1060).

Following from these findings, Hubel and Wiesel (1963) concluded that while there is a basic organization in place at birth, for proper development and visual processing, visual input is necessary. They thus formulated the critical periods hypothesis, which postulates that there is a critical period for developing the sense of vision (and other senses). If sensory information is deprived during the critical period, the neuronal morphology and connectivity are altered in such a way that the sense cannot be gained or recovered at a later stage (Wiesel and Hubel, 1965; Hubel and Wiesel, 1970). In humans, while the greatest chance of visual recovery in the case of detected and treated visual abnormality is under the age of 5 (Siu and Murphy, 2018), the critical period for binocularity was thought to decrease by age 6–8 (Aslin and Banks, 1978), with some studies pointing to the end of the critical period for stereopsis as falling between the age of 4–5 (Fawcett et al., 2005). Despite this, research conducted specifically on congenital cataract removal by Prof. Pawan Sinha and others indicates that the human brain "retains the capacity" for the acquisition of vision even after extended sensory deprivation during critical periods (Held et al., 2011). A wealth of research indicates that neuroplasticity can bring about enhanced development in the intact skills and abilities of the sensory deprived (Amedi et al., 2005; Heimler et al., 2014; Heimler and Amedi, 2020). Further support for this comes from studies showing compensatory neuroplasticity, for example, switching of tasks performed by a specific brain area leading to enhancement in high-level cognitive functions, such as memory or language (Amedi et al., 2003; Bedny et al., 2011 or memory in a causal relationship Amedi et al., 2004), or neuroplasticity that underlies the ability to perform substitution of one sense by another. Contemporary research on blind users trained with sensory substitution devices that translate vision to audition show activation in category-specific visual areas when using the devices for various tasks, such as identification of objects (Striem-Amit et al., 2012a), letters (Reich et al., 2011), and numbers (Abboud et al., 2015).

A cataract is a lens opacity that causes visual impairment, sometimes to complete blindness (Grałek et al., 2007). Cases of visual restoration following cataract removal represent the true core of both the philosophical and scientific debate on sight, the

senses, and neuroplasticity. Would one who underwent surgery that allowed them to gain a previously inexperienced sense of vision be able to "know" what they were seeing? If so, how rapidly and to what level would the ability to use this knowledge, for example, for perceiving three dimensions (3D) vision and geometry, come about? These findings are also interesting for the nature vs. nurture debate concerning visual properties. This debate dates back to the time of John Locke and his acquaintance William Molineux, who pondered in correspondence whether a blind person who could recognize objects by touch would be able to recognize those same objects by vision, were their vision miraculously restored (Locke, 1847; Ferretti and Glenney(eds), 2021). We aim to weigh in on several core questions in this case study. Would children blind from birth in one or both eyes gain true visual properties? If so, to what extent and how similar or different is their visual experience from those of the normally sighted? Would they achieve the level of visual knowledge experienced by the normally sighted children?

In addition, we specifically explore some still-open questions at the forefront of research conducted with vision restoration patients. Would these children have 3D vision? Fine et al. (2003) conducted a case study that showed that long-term visual deprivation leads to deficits in processing complex forms, specifically 3D. Would the children be able to correspond what they now see with what they feel through touch? Prior research indicates, for example, that the cross-modal transfer of information between the tactile sense and the newly acquired visual one does not develop immediately. However, it develops within a few days (Held et al., 2011). Later research indicates that this correspondence occurs quicker than previously thought (Chen et al., 2016). Would these children be susceptible to visual illusions? It was commonly believed that susceptibility to visual illusions is visual experience-dependent (Gillam, 1980). Yet, a study showed that children who underwent cataract removal surgery (as part of project Prakash) are susceptible to certain illusions immediately after surgery (Gandhi et al., 2015). Moreover, how would they perform on tasks requiring the spatial grouping of visual geometric cues? Research conducted with haptic geometric cues has led to conflicting conclusion. On the one hand, Marlair et al. (2021) showed lower performance in the blind than the sighted, but on the other, Heimler et al. (2021) showed similar performance in the blind as in the sighted.

This paper aims to provide insight into these key questions, to some extent, through the individual experiences of eight children who underwent cataract-removal surgery in Quiha hospital in Ethiopia as part of the Himalayan Cataract Project. We were able to explore the children's visual state a few days after surgery (but due to the circumstances–not before) to shed some light on the relationship between the behavioral and the neurological. A case study is particularly warranted in these circumstances due to the exceptional nature of these cases. The extensive battery of tests we employ allows for ascertaining the fine details of the children's visual experience. We believe this paper serves as a springboard for more research in this challenging field and paves the way for a deeper understanding of the development of vision and the senses in general.

In addition, we wish to propose a novel and more objective method for determining congenital (early) vs. late blindness in children undergoing cataract-removal surgery. In these cases, particularly in, but not limited to, low and middle-income countries, it is often difficult to determine the precise medical background of the children, and their clinical state is often not adequately documented, leaving the medical and rehabilitative staff often dependent on reports of the parents alone. We suggest utilizing the findings of this study, particularly concerning the binocular rivalry and the Brock String task, as a method for distinguishing cases of congenital (early) and late blindness in children following cataract surgery.

2. Materials and methods

2.1. Participants and ethics

Eight children participated in the study, all of whom underwent vision restoring or rehabilitating ophthalmological surgery in the days before the study as part of the Himalayan Cataract Project (see **Table 1** for more details). For the purpose of this study, childhood is defined as below the universally accepted age of 18 (McGoldrick, 1991). The children presented with various visual impairments but had no other known diseases or medical conditions. RS (male, 11 years old) and HB (male, 13 years old) had congenital cataracts in both eyes. IG (male, 14 years old) had a congenital cataract in one eye. OB (male, 7 years old), GA (male, 7 years old), AC (female, 10 years old), AB (male, 12 years old), and GH (female, 10 years old) had trauma-induced cataracts in one eye. While RS and HB had been blind from birth in both eyes, and IG blind from birth in one eye, the others had much shorter periods of vision loss, between 2 weeks to a month, before surgery (see **Table 1** for demographic and medical information about the children). All the children underwent the operation 4–6 days before the study. The children's legal guardians gave informed consent to their participation in this study. In addition, the study was conducted within the hospital setting while the children were under the care of the hospital staff and adhered to the ethical guidelines of the declaration of Helsinki.

2.2. Binocular rivalry

All subjects performed a binocular rivalry task and a depth perception task. The subjects wore classic (generic) paper 3D viewing glasses in the binocular rivalry task. They were presented with stimuli consisting of two superimposed cartoon figures (cartoon figures were used as stimuli as the subjects

TABLE 1 Demographic and medical information about the children.

Subject	Gender	Age	Days from surgery	Schooling	Type of cataract	Reported visual acuity
RS	Male	11	5	None	Congenital	*Pre-op*: Right: Hand motion (HM) Left: HM *Post-op*: Right: 6/36 Left: 6/6
HB	Male	13	4	2 years	Congenital	*Pre-op*: Right: 1/2 M Left: HM *Post-op*: Right: 6/18 Left: 6/12
IG	Male	14	6	2 years	Congenital/ one eye	*Post-op*: Right: Counting fingers (CF) 1M Left: 6/6
OB	Male	7	6	None	Acquired/ one eye	*Pre-op*: Right: Light perception (LP) *Post-op*: Right: 6/6
GA	Male	7	5	None	Acquired/ one eye	*Pre-op*: Left: LP *Post-op*: Left: 6/12
AC	Female	10	5	2 years	Acquired/ one eye	*Post-op*: Left: CF 2M Lacking color perception
AB	Male	12	5	1 year	Acquired/ one eye	*Post-op*: Right: CF 2M
GH	Female	10	5	2 years	Acquired/ one eye	*Post-op*: Right: 6/6 Left: 6/6

were children) in red and blue (see examples in Figure 1D). We asked participants to close one eye at a time to see each figure separately and then to look at the image on the screen with both eyes and report whether they see the two figures alternating. In those with normally developed vision, the simultaneous presentation of two different images in two colors superimposed through the red/blue filter leads to a well-documented perceptual phenomenon of image dominance switching (Wade, 1998). The perceptual dominance of the images changes such that only one image is perceived at a time, with the images switching between them (coming in and out of active perception) every few seconds (Miller et al., 2000; Pettigrew, 2001; Blake and Logothetis, 2002).

On the other hand, when one eye or the other is covered, only one image is perceived at a time without changing. This phenomenon is closely correlated with the two-dimensional information presented to our eyes from the outside world, which is combined into a single three-dimensional representation in the brain (Levelt, 1965). In this study, the children were instructed to look at the images first with one eye, then with the other, then with both eyes while fixating their gaze on the fixation cross at the top center of the image (Figure 1A).

2.3. Depth perception with the Brock string task

In addition to the binocular rivalry task, all children performed a Brock string task to test their ability to converge the information acquired by their two eyes to create binocular 3D vision (Brock, 1955). The instrument employed in the task is a white string with three beads, one green, one yellow, and one red, placed along the string's length at different intervals. The string and beads used for the task were homemade and not commercial instruments. One end of the string is held precisely at the tip of the subject's nose, while the other is placed at a fixed location with the string pulled tautly. In this task, the experimenter points sequentially at the three balls, and the participant must gaze at them, reporting what they (see Figure 1B). Participants prepared for ∼1 min using the

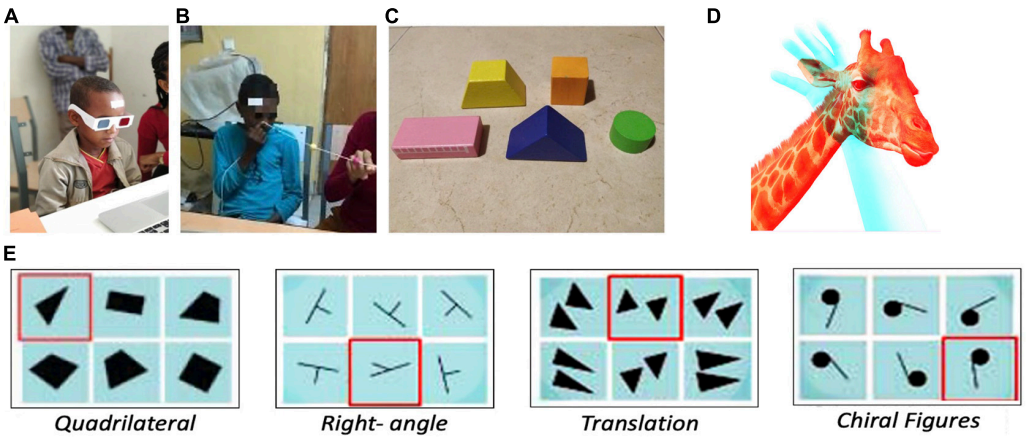

FIGURE 1
(A) A child in the study that had cataract removal surgery 4–6 days prior to undergoing the binocular rivalry task. **(B)** A child in the study undergoing the Brock string task and binocular rivalry task. **(C)** Geometrical three dimensional (3D) shapes used for the three-dimensional cross-modal object recognition task. **(D)** Superimposed images were used to test binocular rivalry. **(E)** Spatial grouping task based on geometric cues from Dehaene et al. (2006) (detection of the outlier in each group of geometric cues, for example, the triangle among the quadrilaterals).

string: the experimenter pointed sequentially to the different balls on the thread, and the participants needed to direct their gaze to the ball pointed to by the experimenter. If the beads appear double to the subject, then it indicates an inadequacy in the convergence of visual input. If one has binocular depth perception, s/he will start to see two lines rather than only one line.

2.4. Spatial grouping based on geometric cues

Four children, RS, HB (the two who had bilateral congenital cataracts removed), AC and GH (who had trauma-induced cataracts removed and were close in age to RS and HB), performed a spatial grouping task based on geometric cues (Dehaene et al., 2006) in which they are shown six images–five images depicting a specific geometric concept, and one outlier which does not abide by the given regularity (for example, right angles, or parallel lines). The children were asked to identify the outlier among the given geometric groups (see, for instance, **Figure 1E**).

2.5. Cross-modal object recognition

RS, HB, and IG were also tested for cross-modal object recognition. During this task, they were asked to feel a 3D geometrically shaped wooden shape (store-bought generic wooden blocks) they had never been exposed to before (using touch alone–without seeing the shape as it was placed in a black, opaque bag) corresponding to some of the shapes in a geometrical cues task (see below). They were asked to look at one shape and report whether it was the same or different from the shape they were touching; then, to match among alternatives: look at two shapes and point to the one that matched the tactile shape they were touching (**Figure 1C**–the same wooden shapes they touched were placed on a table in front of them). This task was repeated twice: once using 3D real shapes for visual matching; once using 2D figures of the same shapes presented on the computer.

2.6. Visual illusions

These three children were also tested on their perception of visual illusions. The children were presented with classic visual illusions: Length illusions: the Muller-Lyer (1889) illusion, the vertical-horizontal illusion (Künnapas, 1955), and the Ponzo (1911), Size illusions: Delboeuf (1865) and Ebbinghaus (1902) illusions. In the length and depth illusions, the children were asked whether one of the two lines appeared to be longer, while in size illusions, they were asked whether one of the two circles looked bigger (see **Figure 2**).

3. Results

3.1. Binocular rivalry

The two children with bilateral congenital cataracts removed (RS and HB) did not show binocular rivalry despite reporting that they accurately saw each image with the two eyes separately, meaning that they did not see the two images alternating at any

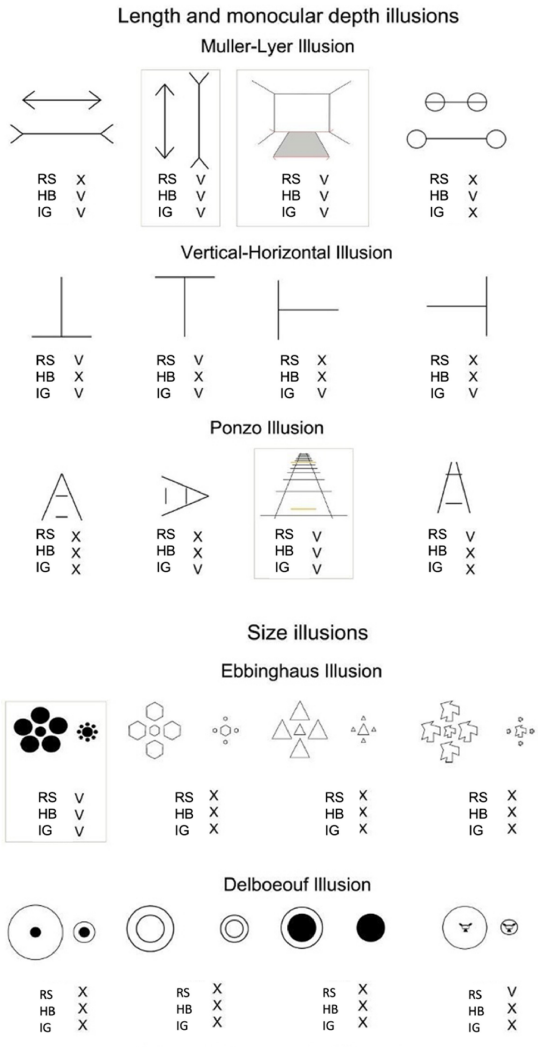

FIGURE 2
The single subject susceptibility to visual illusions. V represents the subject's susceptibility to the illusion, and X means that the subject was not susceptible to the illusion.

point of the task. IG, who had a congenital cataract in one eye removed, did not report binocular rivalry. AC had a unilateral trauma-induced cataract removed, lacked color perception in the eye, and did not show binocular rivalry. The other children showed binocular rivalry when tested 4–6 days after surgery.

3.2. Depth perception with the Brock string task

If one has binocular depth perception, they will see two lines crossing instead of only one line after some time. The two children with bilateral congenital cataracts removed (RS and HB) had no binocular depth perception. Four of the five children with unilateral trauma-induced cataract removals did have depth perception. IG, who had a congenital cataract in one eye removed, did not have depth perception during the task.

3.3. Spatial grouping based on geometric cues

RS and HB (who had bilateral congenital cataracts removed), compared to AC and GH, who had unilateral trauma-induced cataracts removed, performed this task. Correct identification of the outlier was considered to be a "success." All the children tested had no or minimal prior schooling. The results showed that RS and HB (congenital cataracts) outperformed AC and GH on this task with an average success of 53% vs. 38%, much higher than the chance level of 16.6%. Of course, it is difficult to reach generalized conclusion with such a low number of subjects and trials, given the nature of this field research (Figures 3, 4).

3.4. Cross-modal object recognition

RS and HB (who had bilateral congenital cataracts removed), and IG (who had a unilateral congenital cataract removed), underwent testing for cross-modal object recognition. If the child correctly pointed to the visual shape that matched the tactile shape they were touching, it was considered a "success." When tested 4–6 days after surgery, the children after bilateral cataract removals showed very high accuracy in both the 2D and the 3D conditions. RS and HB each succeeded in 9/10 trials with an accuracy of 90% (much higher than the 50% chance level), and IG succeeded in 6/10 with an accuracy of 60%.

3.5. Visual illusions

A total of 4–6 days after surgery, RS, HB, and IG were tested on visual illusions. RS and HB (who had bilateral congenital cataracts removed) showed higher susceptibility to length illusions (Muller-Lyer, Vertical-Horizontal, and Ponzo) than to size illusions (Ebbinghaus, Delboeouf). This test was binary. Either the child perceived the illusion or not. Higher susceptibility, in this case, refers to the fact that the children were influenced more by the length illusions than the size illusions (as seen in Figure 2).

4. Discussion

In this case study, eight children underwent a battery of numerous visual tests and tasks in a challenging field setting,

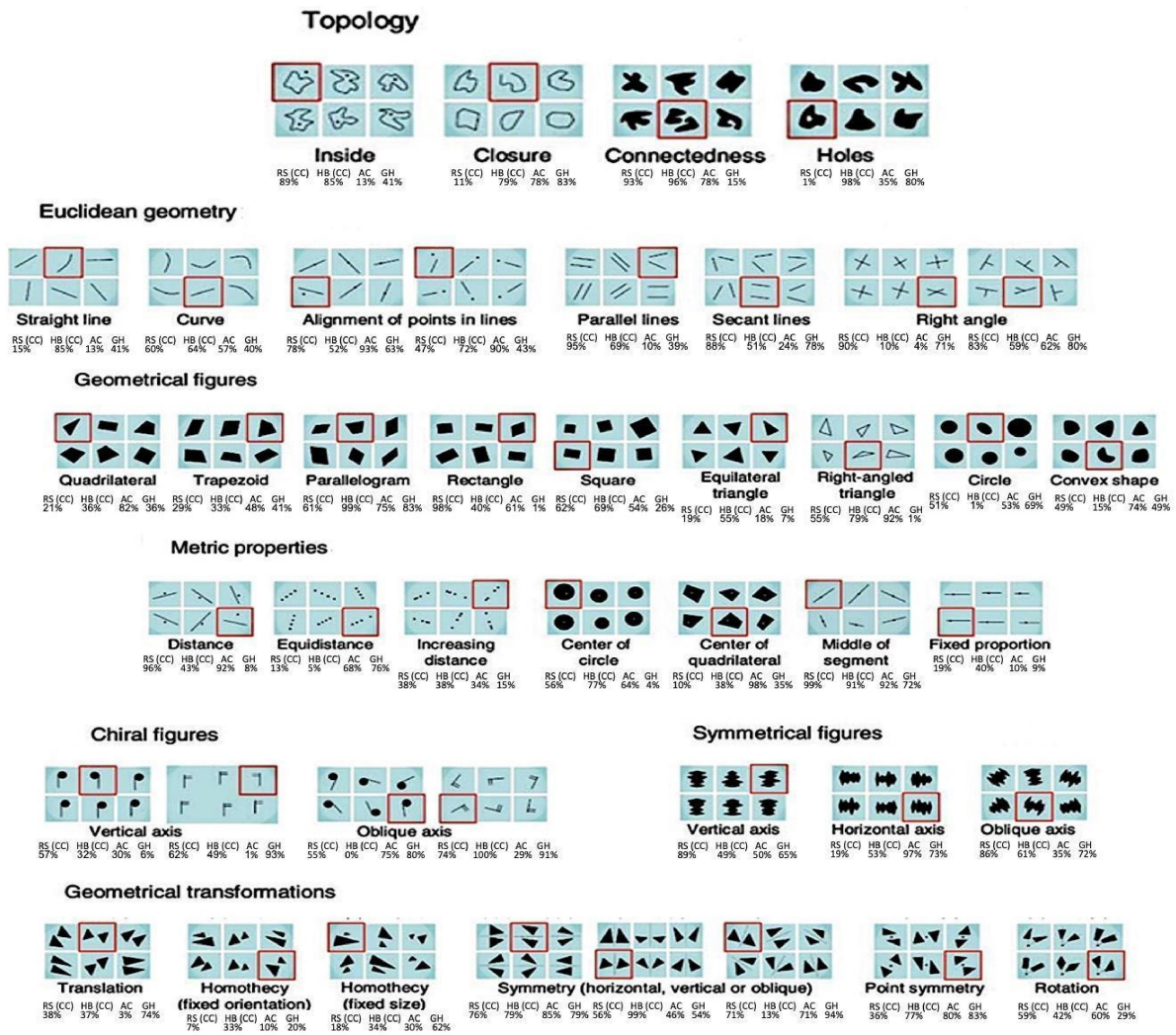

FIGURE 3
The single subject average results on the spatial grouping task based on geometric cues from Dehaene et al. (2006) (chance level is 16.6% in these tasks).

including the classic binocular rivalry red/blue filtered glasses task and the Brock string task of depth perception. Of the eight children who participated in the study, Two of them were born with bilateral congenital cataracts, thereby experiencing true unobscured sight for the first time in their lives only in the few days preceding the study. One child was unilaterally congenitally blind, thereby experiencing binocular vision for the first time in his life. The remaining five were normally sighted children who lost vision in one eye due to trauma-induced cataracts. As such, these children served as important control cases, representing age-matched children with normal visual development during the standard critical periods. The children with congenital cataracts were the only ones in the group not to display either binocular rivalry or depth perception on the Brock string task. In contrast, the other cases of trauma-induced and later onset/short-term cataracts did show these abilities. Out of the group, the two children with congenital cataract removals (bilateral and unilateral) were also tested on visual illusions and cross-modal correspondence. The children were susceptible to some depth illusions relying on monocular cues, such as the Ponzo illusion. They showed high accuracy in both the 2D and the 3D conditions of the cross-modal correspondences task (the two with bilateral congenital cataracts showed nearly ceiling-level accuracy). In addition, the two children with bilateral cataract removals were compared to two children with trauma-induced cataract removals in a task of spontaneous use of geometric cues. In this task, the children with bilateral congenital cataract removals displayed an even higher success rate than their peers.

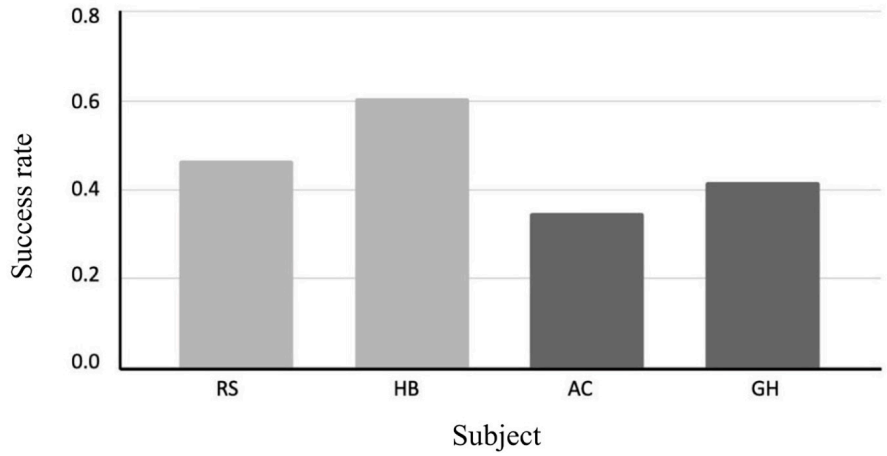

FIGURE 4
The single subject grand average success on the spatial grouping task.

4.1. The results in the context of the theory of critical periods

Hubel and Wiesel's Nobel prize-winning studies claim that sensory deprivation, specifically of visual input in the early stages of life, would prevent the rehabilitation of vision later in life (Wiesel and Hubel, 1965; Hubel et al., 1977; LeVay et al., 1980). On the one hand, the visual properties we observed in the children who were deprived of vision during the critical period (those who underwent bilateral or unilateral congenital cataract removals) support the theory of critical periods (with regard to binocular vision and depth perception in particular). But on the other hand, some findings we observed in other tasks hint at a different interpretation overall. It has been suggested that the unnatural, immediate increase in visual acuity following congenital cataract removal does not follow the course of events of vision acquisition in newborns, which in itself may delay the proper encoding of visual information in the period directly following the surgery (Vogelsang et al., 2018).

In this study, when tested a few days after the surgery, the children who underwent congenital cataract removal showed neither binocular rivalry nor depth perception on the Brock string test. The obvious and clear implication of this is that, as expressed by Bach-y-Rita (1972), we see with our brains, not with our eyes. Though the children's eyes were no longer occluded, and they achieved moderate-mild visual acuity (the WHO defines mild visual acuity as worse than 6/12 to 6/18 and moderate visual acuity as worse than 6/18 to 6/60), their higher-level visual processing of the information was not fully established.

Interestingly, on the visual illusion tasks in our study, the children who had congenital cataracts removed were susceptible to some of the depth illusions that rely on monocular depth cues, such as the Ponzo illusion. This might indicate that at the time of testing, a few days after surgery, the children were at an intermediate stage of visual recovery. This is further strengthened by our findings concerning cross-modal object recognition and grouping based on geometric cues, and by animal research that indicates sensory-motor stimulation can promote recovery from visual deprivation (Baroncelli et al., 2010; Levelt and Hübener, 2012). The children's success on these tasks could represent the initial stages of development of a sense of 3D in the visual domain. It is possible that recovery of bilateral depth is not as quick as other aspects of visual recovery, compared to the results of the other tasks, which the children were able to perform at a level similar to the children who underwent trauma-induced cataract removal. This point is raised with caution, as we lack information concerning the continued development of the children's vision at a later time. Yet we believe this indicates that further research into the long-term visual recovery of children who have undergone bilateral congenital cataract removal is particularly warranted.

4.2. A novel, objective method for determining congenital (early) vs. late blindness

As described above, the children's results on the binocular rivalry task and the Brock string task are particularly interesting. Taken together, these two tasks seem to be the primary distinguishing factor between congenitally blind children and those who developed cataracts later in life. We propose utilizing these two simple, straightforward tests as a method of making this differentiation precisely in the field. This is particularly important for, but not

limited to, projects operating in low or middle-income countries where access to medical records and documentation is less readily available or even scarce (Röder et al., 2021).

To promote and reliably conduct research involving people who have undergone cataract removal or other surgeries and procedures for sight restoration in childhood or even adulthood. Conducting research with these individuals necessitates a very high degree of certainty that the study participants were indeed devoid of vision from birth/very early life, specifically during the critical periods (Röder et al., 2021).

Following our study's findings, we propose a novel method for retroactively identifying individuals born congenitally blind. Potential subjects can be screened on the binocular rivalry task and the Brock string task in combination a few days after surgery. Our findings would allow the researcher to confirm or disaffirm a congenital cataract diagnosis retroactively since children with trauma-induced cataracts later in childhood could perform these two specific tasks while children with congenital cataracts were not.

4.3. Replication and extension of previous studies on cross-modal correspondence following congenital cataracts

The children's results on the cross-modal object recognition tasks and the spatial grouping based on geometric cues have significant scientific and philosophical implications. Cross-modal object recognition tasks are historically based on a philosophical thought experiment known as Molyneux's problem (Ferretti and Glenney(eds), 2021). Molyneux, whose wife was blind, pondered upon whether a blind person who could recognize objects by touch would be able to recognize those same objects by vision, were his/her vision miraculously restored. Molyneux pondered whether sighted and touch can or cannot be linked immediately upon first sight Molyneux's answer to his proposed question was that they cannot, a stance backed by his friend Locke (1847) and further agreed upon and expanded by George Berkley. Berkley (1709) further stated that visual experience gained by the blind upon visual restoration represents a "new set of ideas, perfectly distinct and different from the former, and which can in no sort make themselves perceived by touch." This philosophical stance represents that of the empiricists, who opposed the idea that there are innate amodal mechanisms in common between the senses and that true sensory knowledge can only be gained through modality-specific sensory experience.

Previous research conducted on children following congenital cataract removal surgeries through Project Prakash found evidence that was consistent with Molyneux's idea in that the children could not immediately correspond between what they saw and what they had felt (Held et al., 2011). Yet they showed that the children's abilities to perform this matching improved rapidly, developing within a few days. Another study by Chen et al. (2016) also showed very rapid development of these abilities in a child who had undergone cataract-removal surgery in under 2 days, concluding that the merging between the senses is "prearranged." Our results are consistent with these findings, as the children in our study reached nearly top performance on this task when tested a few days following their surgeries after having never encountered these items in the visual domain. In addition, unlike Held et al. (2011), the stimuli used in our study were naturally occurring geometric shapes, further correlated to the task of spatial grouping by geometric cues (as expanded upon below). Held et al. (2011) suggested that the performance improvement may be due to their ability to create a three-dimensional visual representation. Yet, the children in our study (who had congenital cataracts removed) could not create three-dimensional representations at the stage at which they could perform with very high accuracy on the cross-modal object recognition task.

So while our findings are consistent with those of Held et al. (2011) who show the development of this ability in such a consistently rapid way. We interpret these findings differently with respect to the conclusion drawn with respect to Molyneux's problem. We claim that the extremely rapid development of this ability, within days following surgery, could serve as evidence for precisely the opposite interpretation, an uncovering of innate preexisting connections between these senses (Chen et al., 2016; Bola et al., 2017; Maimon and Hemmo, 2022) or a re-calibration (Gallagher, 2020). This interpretation, which we believe is warranted by the findings, supports an amodal understanding of brain development and structure. This is further supported by the results of this study concerning spatial grouping based on geometric cues. This interpretation is supported by prior research conducted in our lab that has shown that the lateral-occipital tactile-visual area (LOtv) is an area activated by visual and tactile exploration of objects (Amedi et al., 2002) that can also be activated in the blind for processing object shapes after training with a visual to auditory sensory substitution device, indicating that this area is involved in the task of processing the geometry and shape of objects, irrespective of the sensory modality through which the information was conveyed (Amedi et al., 2007).

4.4. Replication and expansion of previous studies on the spontaneous emergence of geometry concepts in congenital cataracts

Spatial grouping tasks based on geometric cues have been used in prior research to show that spontaneous geometry intuitions arise independently from education in

normally sighted Amazonian adults (Dehaene et al., 2006). This research was later expanded in our lab, showing that geometric knowledge and reasoning develop irrespective of vision (Heimler et al., 2021). This study showed that both normally sighted blindfolded people and the congenitally blind showed geometrical sense driven by touch alone. The results of this current study further strengthen and elaborate on these findings, now repeating the task for the first time *via* vision. The four children tested on this task in our study had very little formal education, with RS having never attended school at all and the other three children reaching up to second-grade education. The findings showed that all four children (RS and HB, who underwent surgery for bilateral congenital cataracts, and AC and GH, who underwent surgery for unilateral trauma-induced cataracts) performed above chance level, with RS and HB performing better than their peers who were born with intact vision. These findings further support the amodal nature of the brain, at least for geometry, and the innate preexisting links between the senses. More generally, these findings support the revised "neuronal recycling theory (Dehaene, 2005; Dehaene and Cohen, 2007)" that posits a task-selective, sensory independent interpretation of specialization in the brain (Striem-Amit et al. 2011, 2012a; Reich et al., 2012; Heimler et al., 2015; Amedi et al., 2017). Under this interpretation, areas such as the visual cortex are not "visual" *per se* as they do not undergo specialization for vision but rather undergo specialization for performing a specific task (where usually vision is the most accurate and easy way to perform the task) and thereby can be activated by corresponding information delivered through other senses. For example, the Lateral Occipital Cortex (LOC), commonly correlated with visual object and shape recognition, could be recruited for processing 3D geometric shapes, irrespective of the sensory modality through which the information was provided, as was indeed shown in Amedi et al. (2001).

Another example would be the Visual Word Form Area (VWFA) commonly associated with visual letter recognition. According to the task selective, sensory independent interpretation, this area would be designated for the task of symbol-to-phoneme conversion (independent of the visual modality), as supported by Striem-Amit et al. (2012b). There are many more such examples of task selectivity as opposed to sensory-dependent organization. For a full review, see Amedi et al. (2017). Similar views of the brain as a-modal or supramodal (see Pascual-Leone and Hamilton, 2001; Kupers and Ptito, 2011; Ricciardi et al., 2014; Cecchetti et al., 2016) fit well with this notion and theory.

4.5. Limitations and future directions

A practical limitation of the study pertains to the partial nature of the children's medical histories, which were reported by the parents, and the lack of digitized medical data related to the children and their medical reports (the post-operative surgical report was handwritten). Due to this partial or illegible information, we did not, for example, have data concerning some of the children's pre-op visual acuity. Furthermore, as these results represent the individual cases of the experiences of a number of children, the results cannot be generalized. Yet, we feel that this research indicates several future study directions. With respect to future directions, we suggest implementing this battery of tests on children undergoing congenital cataract removal, with data acquired pre-surgery, immediately following surgery, and months after surgery. This way, the progressive development can be tracked, further shedding light on the questions and issues we have discussed. In addition, future research on the neural underpinnings of children's visual recovery in similar circumstances is warranted to further elucidate the link between the behavioral and the neurological. As such, fMRI studies can be conducted pre and post-surgery to investigate the mechanisms in the brain corresponding to the visual experiences of the children following surgery. This study presents a select few of the many lessons to be learned from these cases regarding the deepest aspects of visual development specifically and the profound interaction between the sensory experience and the brain more generally.

5. Conclusion

This study focused on the visual and geometry abilities of children who had undergone cataract removal surgery at Quiha hospital in Ethiopia as part of the Himalayan Cataract Project. The findings of the study reveal, first and foremost, that out of the cohort of children, those with congenital cataracts did not exhibit binocular rivalry, nor did they show depth perception when tested with the Brock string test. These two tests clearly delineated the congenitally blind children from the normally sighted at birth (who developed cataracts later in life). As such, we novelly propose the utilization of these two tests in retroactively confirming the blindness status of a child, particularly in cases where medical history and records are lacking. In addition, the current study replicates and expands upon previous studies conducted on cross-modal correspondence following congenital cataract removal in children. The children in this study reached nearly ceiling-level performance on the cross-modal correspondence task when tested a mere few days following their surgeries. Finally, this study strengthens the findings of previous studies indicating that geometry concepts arise independently from experience and education, thus supporting a task-selective, sensory-independent interpretation of specialization and development in the brain.

Data availability statement

The original contributions presented in this study are included in the article/supplementary material, further inquiries can be directed to the corresponding author.

Ethics statement

Ethical approval was not provided for this study on human participants because the study was conducted while the children were under the care and supervision of the local Quiha Hospital medical staff, with the parents present. The parents of all of the children signed written consent forms approving the participation of the children in the study. Written informed consent to participate in this study was provided by the participants' legal guardian/next of kin. Written informed consent was obtained from the participant's next of kind for the publication of any identifiable images or data included in this article.

Author contributions

AM: writing—original draft, review, and editing, conceptualization, visualization, and project administration. ON and BH: conceptualization, investigation, and visualization. AA: writing—original draft, review, and editing, project administration, supervision, resources, conceptualization, investigation, methodology, and funding acquisition. All authors contributed to the article and approved the submitted version.

Funding

This research was supported by an ERC Consolidator Grant (773121 NovelExperiSense) and a Horizon GuestXR (101017884) grant (both to AA).

Acknowledgments

We wish to acknowledge and thank Dr. Geoffrey Tabin, co-founder and chairman of the Himalayan Cataract Project, and Dr. Yonas Mitku, head of the ophthalmology unit at Quiha General Hospital, who led the clinical operation to restore vision and test the patients postsurgery. We would also like to thank Prof. Stanislas Dehaene for providing us with material to test spatial grouping based on geometric cues.

Conflict of interest

The authors declare that the research was conducted in the absence of any commercial or financial relationships that could be construed as a potential conflict of interest.

Publisher's note

References

Abboud, S., Maidenbaum, S., Dehaene, S., and Amedi, A. (2015). A number-form area in the blind. *Nat. Commun.* 6, 1–9. doi: 10.1038/ncomms7026

Amedi, A., Floel, A., Knecht, S., Zohary, E., and Cohen, L. G. (2004). Transcranial magnetic stimulation of the occipital pole interferes with verbal processing in blind subjects. *Nat. Neurosci.* 7, 1266–1270. doi: 10.1038/nn1328

Amedi, A., Hofstetter, S., Maidenbaum, S., and Heimler, B. (2017). Task selectivity as a comprehensive principle for brain organization. *Trends Cogn. Sci.* 21, 307–310. doi: 10.1016/j.tics.2017.03.007

Amedi, A., Jacobson, G., Hendler, T., Malach, R., and Zohary, E. (2002). Convergence of visual and tactile shape processing in the human lateral occipital complex. *Cerebr. Cortex* 12, 1202–1212. doi: 10.1093/cercor/12.11.1202

Amedi, A., Malach, R., Hendler, T., Peled, S., and Zohary, E. (2001). Visuo-haptic object-related activation in the ventral visual pathway. *Nat. Neurosci.* 4, 324–330. doi: 10.1038/85201

Amedi, A., Merabet, L. B., Bermpohl, F., and Pascual-Leone, A. (2005). The occipital cortex in the blind: lessons about plasticity and vision. *Curr. Direct. Psychol. Sci.* 14, 306–311. doi: 10.1111/j.0963-7214.2005.00387.x

Amedi, A., Raz, N., Pianka, P., Malach, R., and Zohary, E. (2003). Early 'visual' cortex activation correlates with superior verbal memory performance in the blind. *Nat. Neurosci.* 6, 758–766. doi: 10.1038/nn1072

Amedi, A., Stern, W. M., Camprodon, J. A., Bermpohl, F., Merabet, L., Rotman, S., et al. (2007). Shape conveyed by visual-to-auditory sensory substitution activates the lateral occipital complex. *Nat. Neurosci.* 10, 687–689. doi: 10.1038/nn1912

Aslin, R. N., and Banks, M. S. (1978). "Early visual experience in humans: evidence for a critical period in the development of binocular vision," in *Psychology: From Research to Practice*, eds H. L. Pick, H. W. Leibowitz, J. E. Singer, A. Steinschneider, and H. W. Stevenson (Boston, MA: Springer). doi: 10.1007/978-1-4684-2487-4_14

Bola, Ł., Zimmermann, M., Mostowski, P., Jednoróg, K., Marchewka, A., Rutkowski, P., et al. (2017). Task-specific reorganization of the auditory cortex in deaf humans. *Proc. Natl. Acad. Sci. U.S.A.* 114, E600–E609.

Bach-y-Rita, P. (1972). *Brain Mechanisms in Sensory Substitution*. Cambridge, MA: Academic Press.

Baroncelli, L., Sale, A., Viegi, A., Vetencourt, J. F. M., De Pasquale, R., Baldini, S., et al. (2010). Experience-dependent reactivation of ocular dominance plasticity in the adult visual cortex. *Exp. Neurol.* 226, 100–109. doi: 10.1016/j.expneurol.2010.08.009

Bedny, M., Pascual-Leone, A., Dodell-Feder, D., Fedorenko, E., and Saxe, R. (2011). Language processing in the occipital cortex of congenitally blind

adults. *Proc. Natl. Acad. Sci. U.S.A.* 108, 4429–4434. doi: 10.1073/pnas.1014818108

Blake, R., and Logothetis, N. K. (2002). Visual competition. *Nat. Rev. Neurosci.* 3, 13–21. doi: 10.1038/nrn701

Brant, A. R., Hinkle, J., Shi, S., Hess, O., Zubair, T., Pershing, S., et al. (2021). Artificial intelligence in global ophthalmology: using machine learning to improve cataract surgery outcomes at Ethiopian outreaches. *J. Cataract Refract. Surg.* 47, 6–10. doi: 10.1097/j.jcrs.0000000000000407

Brock, F. W. (1955). The string as an aid to visual training. *Vis. Train. Work* 4, 29–33.

Cecchetti, L., Kupers, R., Ptito, M., Pietrini, P., and Ricciardi, E. (2016). Are supramodality and cross-modal plasticity the yin and yang of brain development? From blindness to rehabilitation. *Front. Syst. Neurosci.* 10:89. doi: 10.3389/fnsys.2016.00089

Chen, J., Wu, E., Chen, X., Zhu, L., Li, X., Thorn, F., et al. (2016). Rapid integration of tactile and visual information by a newly sighted child. *Curr. Biol.* 26, 1069–1074. doi: 10.1016/j.cub.2016.02.065

Dehaene, S. (2005). *8 Evolution of Human Cortical Circuits for Reading and Arithmetic: The From monkey brain to human brain: A Fyssen Foundation symposium*. Cambridge, MA: MIT press. doi: 10.7551/mitpress/3136.001.0001

Dehaene, S., and Cohen, L. (2007). Cultural recycling of cortical maps. *Neuron* 56, 384–398. doi: 10.1016/j.neuron.2007.10.004

Dehaene, S., Izard, V., Pica, P., and Spelke, E. (2006). Core knowledge of geometry in an Amazonian indigene group. *Science* 311, 381–384. doi: 10.1126/science.1121739

Delboeuf, F. J. (1865). Note sur certaines illusions d'optique: essai d'une théorie psychophysique de la maniere dont l'oeil apprécie les distances et les angles. *Bull. l'Académie R. Sci. Lett. Beaux Arts Belgique* 19, 195–216.

Ebbinghaus, H. (1902). *The Principles of Psychology*. Leipzig: VEIT GmbH.

Fawcett, S. L., Wang, Y. Z., and Birch, E. E. (2005). The critical period for susceptibility of human stereopsis. *Investig. Ophthalmol. Vis. Sci.* 46, 521–525. doi: 10.1167/iovs.04-0175

Ferretti, G., and Glenney, B. (eds) (2021). *Molyneux's Question and the History of Philosophy*. Milton Park: Routledge. doi: 10.4324/9780429020377

Fine, I., Wade, A. R., Brewer, A. A., May, M. G., Goodman, D. F., Boynton, G. M., et al. (2003). Long-term deprivation affects visual perception and cortex. *Nat. Neurosci.* 6, 915–916. doi: 10.1038/nn1102

Gallagher, S. (2020). "No yes answers to Molyneux," in *Molyneux's Question and the History of Philosophy*, eds G. Ferretti and B. Glenney (Milton Park: Routledge), 235–249. doi: 10.4324/9780429020377-21

Gandhi, T., Kalia, A., Ganesh, S., and Sinha, P. (2015). Immediate susceptibility to visual illusions after sight onset. *Curr. Biol.* 25, R358–R359.

Gillam, B. (1980). Geometrical illusions. *Sci. Am.* 242, 102–111. doi: 10.1038/scientificamerican0180-102

Grałek, M., Kanigowska, K., and Seroczyńska, M. (2007). Cataract in children–not only an ophthalmological problem. *Medycyna Wieku Rozwojowego* 11(2 Pt 2), 227–230.

Heimler, B., and Amedi, A. (2020). Are critical periods reversible in the adult brain? Insights on cortical specializations based on sensory deprivation studies. *Neurosci. Biobehav. Rev.* 116, 494–507.

Heimler, B., Behor, T., Dehaene, S., Izard, V., and Amedi, A. (2021). Core knowledge of geometry can develop independently of visual experience. *Cognition* 212:104716. doi: 10.1016/j.cognition.2021.104716

Heimler, B., Striem-Amit, E., and Amedi, A. (2015). Origins of task-specific sensory-independent organization in the visual and auditory brain: neuroscience evidence, open questions and clinical implications. *Curr. Opin. Neurobiol.* 35, 169–177. doi: 10.1016/j.conb.2015.09.001

Heimler, B., Weisz, N., and Collignon, O. (2014). Revisiting the adaptive and maladaptive effects of crossmodal plasticity. *Neuroscience* 283, 44–63. doi: 10.1016/j.neuroscience.2014.08.003

Held, R., Ostrovsky, Y., de Gelder, B., Gandhi, T., Ganesh, S., Mathur, U., et al. (2011). The newly sighted fail to match seen with felt. *Nat. Neurosci.* 14, 551–553. doi: 10.1038/nn.2795

Hubel, D. H., and Wiesel, T. N. (1963). Shape and arrangement of columns in cat's striate cortex. *J. Physiol.* 165:559. doi: 10.1113/jphysiol.1963.sp007079

Hubel, D. H., and Wiesel, T. N. (1970). The period of susceptibility to the physiological effects of unilateral eye closure in kittens. *J. Physiol.* 206, 419–436. doi: 10.1113/jphysiol.1970.sp009022

Hubel, D. H., Wiesel, T. N., LeVay, S., Barlow, H. B., and Gaze, R. M. (1977). Plasticity of ocular dominance columns in monkey striate cortex. *Philos. Trans. R. Soc. Lond. B Biol. Sci.* 278, 377–409. doi: 10.1098/rstb.1977.0050

Künnapas, T. M. (1955). "An analysis of the" vertical-horizontal illusion. *J. Exp. Psychol.* 49:134. doi: 10.1037/h0045229

Kupers, R., and Ptito, M. (2011). Insights from darkness: what the study of blindness has taught us about brain structure and function. *Prog. Brain Res.* 192, 17–31. doi: 10.1016/B978-0-444-53355-5.00002-6

Leffler, C. T., Schwartz, S. G., Peterson, E., Couser, N. L., and Salman, A.-R. (2021). The First Cataract Surgeons in the British Isles. *Am. J. Ophthalmol.* 230, 75–122. doi: 10.1016/j.ajo.2021.03.009

LeVay, S., Wiesel, T. N., and Hubel, D. H. (1980). The development of ocular dominance columns in normal and visually deprived monkeys. *J. Comp. Neurol.* 191, 1–51. doi: 10.1002/cne.901910102

Levelt, C. N., and Hübener, M. (2012). Critical-period plasticity in the visual cortex. *Annu. Rev. Neurosci.* 35, 309–330. doi: 10.1146/annurev-neuro-061010-113813

Levelt, W. J. (1965). *On Binocular Rivalry*. Doctoral dissertation. Assen: Van Gorcum Assen.

Locke, J. (1847). *An Essay Concerning Human Understanding*. Philadelphia, PA: Kay & Troutman.

Maimon, A., and Hemmo, M. (2022). Does Neuroplasticity Support the Hypothesis of Multiple Realizability? *Philos. Sci.* 89, 107–127. doi: 10.1017/psa.2021.16

Marlair, C., Pierret, E., and Crollen, V. (2021). Geometry intuitions without vision? A study in blind children and adults. *Cognition* 216:104861. doi: 10.1016/j.cognition.2021.104861

McGoldrick, D. (1991). The United Nations convention on the rights of the child. *Int. J. Law Policy Fam.* 5, 132–169. doi: 10.1093/lawfam/5.2.132

Miller, S. M., Liu, G. B., Ngo, T. T., Hooper, G., Riek, S., Carson, R. G., et al. (2000). Interhemispheric switching mediates perceptual rivalry. *Curr. Biol.* 10, 383–392.

Muller-Lyer, F. C. (1889). Optische urteilstauschungen. *Arch. Anatomie Physiol. Physiol. Abteilung* 2, 263–270.

Ostrovsky, Y., Andalman, A., and Sinha, P. (2006). Vision following extended congenital blindness. *Psychol. Sci.* 17, 1009–1014. doi: 10.1111/j.1467-9280.2006.01827.x

Pascual-Leone, A., and Hamilton, R. (2001). The metamodal organization of the brain. *Prog. Brain Res.* 134, 427–445. doi: 10.1016/S0079-6123(01)34028-1

Pettigrew, J. D. (2001). Searching for the switch: neural bases for perceptual rivalry alternations. *Brain Mind* 2, 85–118. doi: 10.1023/A:1017929617197

Ponzo, M. (1911). *Intorno Ad Alcune Illusioni Nel Campo Delle Sensazioni Tattili Sull'illusione Di Aristotele e Fenomeni Analoghi*. Berlin: Wilhelm Engelmann.

Reich, L., Maidenbaum, S., and Amedi, A. (2012). The brain as a flexible task machine: implications for visual rehabilitation using noninvasive vs. invasive approaches. *Curr. Opin. Neurol.* 25, 86–95. doi: 10.1097/WCO.0b013e32834ed723

Reich, L., Szwed, M., Cohen, L., and Amedi, A. (2011). A ventral visual stream reading center independent of visual experience. *Curr. Biol.* 21, 363–368. doi: 10.1016/j.cub.2011.01.040

Ricciardi, E., Bonino, D., Pellegrini, S., and Pietrini, P. (2014). Mind the blind brain to understand the sighted one! Is there a supramodal cortical functional architecture? *Neurosci. Biobehav. Rev.* 41, 64–77. doi: 10.1016/j.neubiorev.2013.10.006

Röder, B., Kekunnaya, R., and Guerreiro, M. J. (2021). Neural mechanisms of visual sensitive periods in humans. *Neurosci. Biobehav. Rev.* 120, 86–99. doi: 10.1016/j.neubiorev.2020.10.030

Sinha, P. (2013). Once blind and now they see. *Sci. Am.* 309, 48–55. doi: 10.1038/scientificamerican0713-48

Sinha, P., Chatterjee, G., Gandhi, T., and Kalia, A. (2013). Restoring vision through "Project Prakash": the opportunities for merging science and service. *PLoS Biol.* 11:e1001741. doi: 10.1371/journal.pbio.1001741

Siu, C. R., and Murphy, K. M. (2018). The development of human visual cortex and clinical implications. *Eye Brain* 10, 25–36. doi: 10.2147/EB.S130893

Striem-Amit, E., Bubic, A., and Amedi, A. (2012a). "Neurophysiological mechanisms underlying plastic changes and rehabilitation following sensory loss in blindness and deafness," in *The Neural Bases of Multisensory Processes*, eds M. M. Murray and M. T. Wallace (Boca Raton, FL: CRC Press/Taylor & Francis). doi: 10.1201/b11092-27

Striem-Amit, E., Cohen, L., Dehaene, S., and Amedi, A. (2012b). Reading with sounds: sensory substitution selectively activates the visual word form area in the blind. *Neuron* 76, 640–652. doi: 10.1016/j.neuron.2012.08.026

Striem-Amit, E., Dakwar, O., Reich, L., and Amedi, A. (2011). The large-scale organization of "visual" streams emerges without visual experience. *Cerebr. Cortex* 22, 1698–1709. doi: 10.1093/cercor/bhr253

Thomas, S. (2011). Project prakash: challenging the critical period: association of research in vision and ophthalmology national meeting. *Yale J. Biol. Med.* 84, 483–485.

Vogelsang, L., Gilad-Gutnick, S., Ehrenberg, E., Yonas, A., Diamond, S., Held, R., et al. (2018). Potential downside of high initial visual acuity. *Proc. Natl. Acad. Sci. U.S.A.* 115, 11333–11338. doi: 10.1073/pnas.1800901115

Wade, N. J. (1998). Early studies of eye dominances. *Lateral. Asymmetr. Body Brain Cogn.* 3, 97–108. doi: 10.1080/713754296

Welling, J., Newick, E., and Tabin, G. (2013). The economic impact of cataract surgery in a remote Ghanaian village three years after surgical intervention. *Investig. Ophthalmol. Vis. Sci.* 54, 4396–4396.

Wells, H. G. (1921). *The Country of the Blind*. New York, NY: Appeal Publishing Company.

Wiesel, T. N., and Hubel, D. H. (1963). Effects of visual deprivation on morphology and physiology of cells in the cat's lateral geniculate body. *J. Neurophysiol.* 26, 978–993.

Wiesel, T. N., and Hubel, D. H. (1965). Extent of recovery from the effects of visual deprivation in kittens. *J. Neurophysiol.* 28, 1060–1072. doi: 10.1152/jn.1965.28.6.1060

Wiesel, T. N., and Hubel, D. H. (1974). Ordered arrangement of orientation columns in monkeys lacking visual experience. *J. Comp. Neurol.* 158, 307–318.

World Health Organization [WHO] (2021). *Blindness and Vision Impairment*. Geneva: World Health Organization.

frontiers | Frontiers in Neuroscience

TYPE Original Research
PUBLISHED 03 March 2023
DOI 10.3389/fnins.2023.997357

OPEN ACCESS

EDITED BY
Maurice Ptito,
University of Montreal, Canada

REVIEWED BY
Matthew William Geoffrey Dye,
Rochester Institute of Technology, United States
Amir Amedi,
Interdisciplinary Center Herzliya, Israel

*CORRESPONDENCE
Stephen G. Lomber
✉ steve.lomber@mcgill.ca

†These authors have contributed equally to this work and share first authorship

SPECIALTY SECTION
This article was submitted to Perception Science, a section of the journal Frontiers in Neuroscience

RECEIVED 18 July 2022
ACCEPTED 24 January 2023
PUBLISHED 03 March 2023

CITATION
Mitzelfelt T, Bao X, Barnes P and Lomber SG (2023) Visually evoked potentials (VEPs) across the visual field in hearing and deaf cats. *Front. Neurosci.* 17:997357. doi: 10.3389/fnins.2023.997357

Visually evoked potentials (VEPs) across the visual field in hearing and deaf cats

Thomas Mitzelfelt[1†], Xiaohan Bao[2†], Paisley Barnes[1] and Stephen G. Lomber[1,2*]

[1]Department of Physiology, McGill University, Montreal, QC, Canada, [2]Integrated Program in Neuroscience, McGill University, Montreal, QC, Canada

Introduction: Congenitally deaf cats perform better on visual localization tasks than hearing cats, and this advantage has been attributed to the posterior auditory field. Successful visual localization requires both visual processing of the target and timely generation of an action to approach the target. Activation of auditory cortex in deaf subjects during visual localization in the peripheral visual field can occur either *via* bottom-up stimulus-driven and/or top-down goal-directed pathways.

Methods: In this study, we recorded visually evoked potentials (VEPs) in response to a reversing checkerboard stimulus presented in the hemifield contralateral to the recorded hemisphere in both hearing and deaf cats under light anesthesia.

Results: Although VEP amplitudes and latencies were systematically modulated by stimulus eccentricity, we found little evidence of changes in VEP in deaf cats that can explain their behavioral advantage. A statistical trend was observed, showing larger peak amplitudes and shorter peak latencies in deaf subjects for stimuli in the near- and mid-peripheral field. Additionally, latency of the P1 wave component had a larger inter-sweep variation in deaf subjects.

Discussion: Our results suggested that cross-modal plasticity following deafness does not play a major part in cortical processing of the peripheral visual field when the "vision for action" system is not recruited.

KEYWORDS

deafness, hearing loss, cross-modal plasticity, cortical magnification, EEG

Introduction

Visual enhancement in the far-peripheral visual field of congenitally deaf humans and animals is one of the most impressive examples of compensatory cross-modal plasticity (Neville and Lawson, 1987; Bavelier et al., 2000; Lomber et al., 2010). In cats, the neural mechanism of this observed enhancement has been demonstrated to involve deaf auditory cortex. Deactivation of the region posterior to primary auditory cortex (i.e., the posterior auditory field, PAF) decreases enhanced visual localization performance in deaf cats to a level no different from hearing cats, indicating its involvement (Lomber et al., 2010). It is particularly interesting that the greatest enhancement of visual localization in deaf cats is observed at the largest eccentricities (furthest into the periphery), suggesting they rely more on visual cues for orientation behavior. Conversely, in hearing cats, auditory cues contribute more significantly to orientation behavior whereas visual cues in the far periphery are less significant.

Visual orientation, in its most general definition, includes any visually guided behavior where gaze is redirected toward a target, e.g., predator or prey (primates: Lisberger and Fuchs, 1978a,b;

grasshopper: Szentesi et al., 1996; cat: Lomber and Payne, 2004), through movement in the body, head, and/or eyes (gaze). Orientation behavior is a vital neurological function for survival that involves both cortical and subcortical circuits. The superior colliculus (SC) is deemed as the most prominent modality-unspecific sensorimotor hub in mammals (King, 2004), which acquires the retinotopic map of its direct visual inputs from retinal ganglion neurons and receives modulation of its indirect inputs from cerebral cortex (Schiller et al., 1974; Mize and Murphy, 1976). In primate cortex, it has been identified that neurons in the frontal eye field respond specifically to locations in the visual field, that correspond to either the location of the visual stimulus or the destination of the intended saccade (Thompson et al., 2005). It is proposed that visual orientation (or saccadic eye movement, to be more specific) is triggered by a combination of neuronal activity related to both stimulus-driven bottom-up visual processing and goal-directed top-down motor generation. Human behavioral experiments have shown that subjects can make faster saccade responses when the visual stimulus is more salient, or when the target location is easier to predict (Marino and Munoz, 2009).

Considering permanent lesion or reversible deactivation studies, cat area 5 and part of area 6 have been found to be essential for the action of orientation behavior, as their deactivation eliminates both acoustic and visual localization (Malhotra et al., 2004). Some other areas are essential for acoustic-specific orientation, such as the primary auditory cortex, PAF, and anterior ectosylvian sulcus (AES) (Malhotra et al., 2004). Areas such as the posterior middle suprasylvian sulcus (pMS), dorsal posterior ectosylvian gyrus (dPE), and posterior suprasylvian sulcus (PS) are critical for visual orientation (Lomber and Payne, 2004). In cat auditory cortex, many areas including PAF contain neurons that respond to sound for selective source locations (Stecker et al., 2003; Lee and Middlebrooks, 2013). It has also been shown that AES in deaf cats is implicated in visual rather than auditory localization following cross-modal plastic changes (Meredith et al., 2011). It is unclear whether activity in AES contributes to the bottom-up, stimulus-driven, or top-down, goal-directed pathway.

Previous human studies have found that visually evoked potentials (VEPs) in congenital deaf subjects demonstrated shorter peak latency in early VEP component N85 (Hauthal et al., 2014), and larger magnitudes in P100 (Hauthal et al., 2014), N150, and P230 (Neville et al., 1983) when compared to normal hearing subjects. In cochlear-implanted children, shorter latency of the visual N1 component (Corina et al., 2017) and the higher occurrence and amplitude of oscillations in the N1-P2 complex (Campbell and Sharma, 2016) were found in comparison to normal hearing subjects. Brain imaging studies have also shown that areas in auditory cortex were activated by visual stimulus in deaf sign language users (Fine et al., 2005), in congenital deaf (Finney et al., 2001, 2003; Scott et al., 2014), when compared to hearing volunteers.

To investigate the stimulus-driven neural activity associated with visual localization, we recorded VEPs in response to a checkerboard stimulus present at one of seven eccentricity markers, between 0 and 90 degrees away from the midline in hearing and deaf cats under light anesthesia. Although VEPs are widely used in research and clinical applications (e.g., Laron et al., 2009), we were surprised to find that no existing documentation of VEP studies included far-peripheral stimuli as done previously in a cat visual localization task (Lomber et al., 2010). As expected, VEPs decayed exponentially with increasing eccentricity in both the hearing and deaf groups. However, we did not see a dramatic difference in VEPs between the two groups, suggesting a lack of cortical cross-modal plasticity involvement in sensory processing of the peripheral visual field.

Materials and methods

All procedures were conducted in compliance with the National Research Council's Guide for the Care and Use of Laboratory Animals (8th edition; 2011) and the Canadian Council on Animal Care's Guide to the Care and Use of Experimental Animals (1993). Furthermore, the following procedures were approved by the Animal Care Committee for Faculty of Medicine and Health Sciences at McGill University.

Deafening

Early deafness was produced in five cats using systemic ototoxic procedures. Before 21 days postnatal, three kittens received co-administration of subcutaneous kanamycin (300 mg/kg) and intravenous furosemide (2 mg/mL to effect; Valent Pharmaceuticals, Laval, QC, Canada). This drug combination has been identified to damage cochlear hair cells and induce profound, bilateral deafness (Schwaber et al., 1993). Throughout the procedure, auditory brainstem responses (ABRs) were measured to monitor the degree of hearing loss. Two other newborn cats received neomycin daily from the day of birth to between postnatal days 26 and 28 (Leake et al., 1991, 1997) before ABRs showed profound hearing loss. All five cats were confirmed deaf (click ABR threshold higher than 80 dB HL) in a follow-up ABR procedure at least 3 months later.

Animal preparation and anesthesia

In total, 12 cats (7 hearing and 5 early deaf) were examined. One hearing subject was excluded for poor signal quality leaving both groups with comparable sex and age distribution (hearing: 71.4% female and mean age 4.2 years; deaf: 60% female and mean age 3.1 years). After the subject was sedated using 0.04 mg/kg dexmedetomidine (Dexdomitor, Zoetis) injected intramuscularly, the left eye was occluded using a hard black contact lens so that visual stimuli were presented unilaterally. Phenylephrine (Mydfrin, Alcon) was applied to the right eye to dilate the pupil, and saline drops were used as lubrication. Hearing subjects were also ear-plugged to minimize auditory input. During stimulus presentation and EEG recording, the anesthesia level was closely monitored and remained stable so that there were rarely any cases of artifact from subject movement in the raw signal. Data collection was terminated either by 45 min after the injection or at the end of the session during which any sign of subject movement was noticed. After removing the electrodes, contact lens, and ear plugs, the subject received an intramuscularly injection with 0.4 mg/kg atipamezole (Antisedan, Zoetis) to facilitate recovery from sedation. Given the large range of stimulus eccentricities selected (0–90 degree), the minor horizontal eye movements previously reported in anesthetized but non-paralyzed cats (O'Keefe and Berkley, 1991) should not confound the effect of stimulus eccentricity. As such, our subjects were maintained in centrally-gazed position without the use of neuromuscular blockers.

Visual stimulation

The visual stimuli were presented to subjects from a 30-inch 2,560-by-1,600 LED screen with 178-degree horizontal and vertical viewing angles (Dell, U3014). To cover a wide azimuth range of visual field, the screen was placed 6.5 inch away from the right eye to the 45-deg front-right of subject (Figure 1A). The stimulus used to evoke VEPs was 12-deg-wide circular checkerboards with dartboard pattern (3 concentric rings, 8 divisions per ring). To occupy roughly the same size of visual field from the cat's perspective, stimuli presented on the screen were the warped projection of the checkerboard, depending on how much stimulus eccentricity (0-, 15-, 30-, or 45-deg) deviated from 45 degrees (Figure 1C). For the same reason, the luminance of the bright cells in the checkerboard was calibrated to 100 cd/m^2 individually for each eccentricity from different angles (Konica Minolta, LS160).

All stimuli were programmed and controlled with PsychToolbox (Brainard, 1997; Pelli, 1997; Kleiner et al., 2007) run on MATLAB, rendered by a graphic card (AMD, Radeon HD 6800 Series), and transited at a video processing unit (Cambridge Research System, Bits#) for generating stimulus timestamps. Once a subject was under stable sedation, EEG data was collected while visual stimuli were presented for 10 to 20 sessions (Figure 1B). Each session lasted for ∼1.5 min, consisting of 7 blocks for different eccentricities in randomized order. In each block, the stimulus inverted 20 times (i.e., 20 sweeps), with inter-sweep interval randomly set between 500 and 550 milliseconds. Between two blocks, there was a 2-second-long black screen. At the end of each session, the level of sedation was re-evaluated, with measurement of heart rate, SpO2, respiration, and electrode impedances taken if needed, before starting the next session.

EEG recording and signal processing

Three 25G stainless steel needles were placed subcutaneously as recording electrodes. The active electrode was placed near the midpoint of subject's interaural line, while the reference electrode was placed inferior to the right ear (ipsilateral to the side of visual stimulation). The ground electrode was placed on subject's dorsum. The impedance of both active and reference electrodes was maintained below 3 kOhm during recording. The signal was amplified and digitized with a pre-amplifier (TDT, RA4LI/RA4PA), streamed onto a digital signal processor (TDT, RZ2), and stored on a computer hard drive.

All data analysis was performed offline. The signal was digitally filtered between 1 and 30 Hz (about 10 dB/octave roll-off) and notch-filtered at 30, 60, 120, 180, and 240 Hz, before epochs were extracted from 80-ms pre-stimulus to 400-ms post-stimulus. All epochs were demeaned with their pre-stimulus baselines individually, before being grouped by stimulus eccentricity and further processed separately (e.g., averaging or resampling).

Data analysis

Root-mean-square values were obtained using MATLAB built-in function *rms()*. Each averaged waveform was separated into an 80-ms pre-stimulus zero-mean baseline window and 400-ms post-stimulus response window, producing two RMS values, respectively. The corrected RMS value was calculated as in the following equation:

$$RMS_{\text{corrected}} = \sqrt{RMS_{response}{}^2 - RMS_{baseline}{}^2}$$

Curve fitting of the corrected RMS as a function of stimulus eccentricity was performed in MATLAB and its Curve Fitting Toolbox^{TM}. We first obtained the initial values for the model coefficients using function *polyfit()*, where the corrected RMS values were first converted into logarithmic space for exponential modeling. Then, function *fit()* was used to fine tune the model coefficients with customized anonymous functions $RMS_{corrected} = a \cdot e^{b \cdot Eccentricity}$ for exponential modeling, and $RMS_{corrected} = k \cdot Eccentricty + b$ for linear modeling, and to evaluate the goodness of fit.

To analyze peak components (N1, P1, and N2 components), we first manually determined a window surrounding the candidate of interest by interactively overlaying a pair of cursors with the averaged VEP waveform. This process was visually guided with graphical information including polarity, amplitude, latency, as well as the entire waveform and other peak components. Bounded by this window, either a minimum or maximum was identified with MATLAB built-in function *min()* or *max()* for the calculation of amplitude and latency.

To quantify the inter-sweep variability, we chose 18 out of total 20 sweeps (90%) before averaging to generate 190 resampled waveforms for each stimulus eccentricity in each subject. Here we only included the first 10 sessions, even when there were more sessions recorded in some subjects. The reference latency was determined from the waveform averaged from all 200 sweeps in the same way as described above. In each resampled waveform, the peak with a latency closest to the reference latency was taken as a resampled latency. Probability density functions, which were re-centered to the reference latency, were given by MATLAB built-in function *ksdensity()*. Mean absolute deviations (MADs) were calculated using MATLAB built-in function *mad()*.

Statistical analysis

For corrected RMS values, peak amplitudes and latencies of the three components, we adopted two-way mixed-design ANOVA with deafness as the between-group variable and stimulus eccentricity as the within-group variable. As the motivation of the current study is to compare VEP traces between hearing and deaf cats, we enforced the "simple effect" test at each of seven stimulus eccentricity levels, regardless of whether the main effect of deafness is significant. Due to a small sample size in this study, both parametric (two-sample Student's *t*-test, *t-test2()* in MATLAB) and non-parametric (Mann–Whitney U test, *ranksum()* in MATLAB) methods were used, and the largest *p*-values of the two tests were used to report statistical significance, without correction for multiple comparison. For latency jitter MADs, data of different stimulus eccentricity from different subjects were pooled together for comparison between hearing and deaf cats. The effect of deafness on MADs was examined by ANCOVA with peak amplitude as a covariate. All statistics were performed in MATLAB and its Statistics and Machine Learning Toolbox^{TM}.

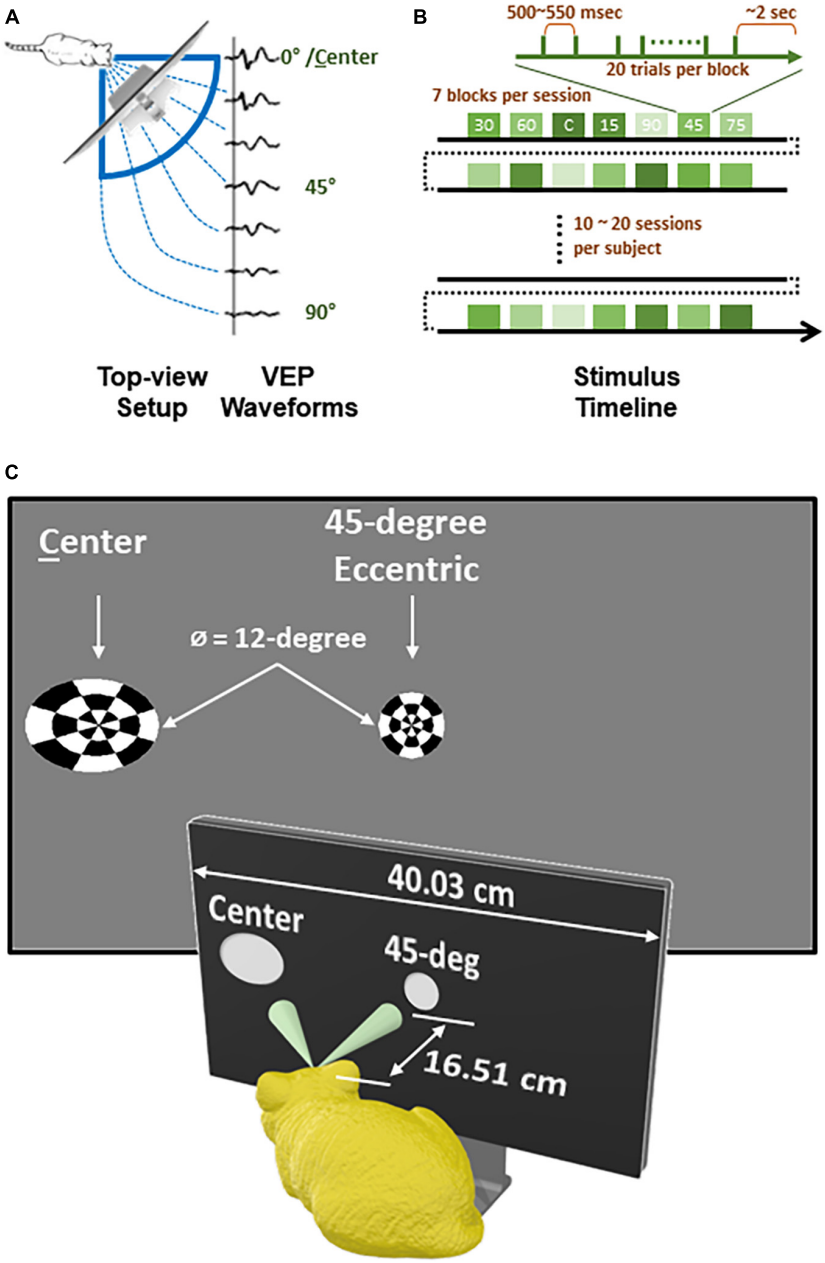

FIGURE 1
Experiment design and recording timeline of each subject. **(A)** A top-view diagram showing how checkerboard stimuli of varying eccentricity were present to animal subject and corresponding VEP waveforms for each eccentricity. **(B)** A timeline of recording for each subject. **(C)** Stimuli viewed from subject's perspective.

Results

In this study, we recorded VEPs in response to checkerboards presented at seven different eccentricities, from 0 to 90 degrees, in seven hearing and five early deaf cats. The recorded data in all except for one hearing subject were of good quality, in respect to the signal-to-noise ratio, and were further analyzed and reported below.

Waveforms

First, we vertically stacked the averaged VEP waveforms for each hearing and deaf subject in the order of stimulus eccentricity (Figure 2). For the smaller eccentricities (upper rows), the VEP waveforms were not distinctively different between the two groups. However, the VEP responses seemed to scale down more drastically in deaf subjects than in hearing subjects as stimulus eccentricity increased.

Root-mean-square (RMS) level

To quantify VEP responses with the least *in prior* bias, we calculated the noise-corrected root-mean-square (RMS) of the waveform in the entire post-stimulus window (i.e., 400-ms) for each subject and compared between hearing and deaf groups

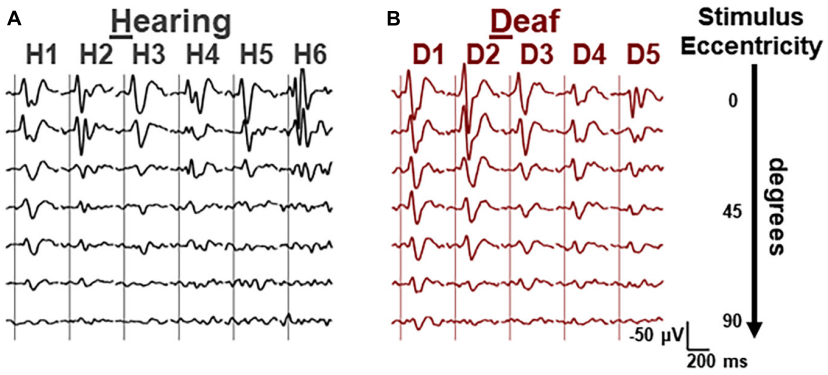

FIGURE 2
Averaged VEP waveforms for different eccentricities of each subject. **(A)** Waveforms from the data collected from 6 hearing cats, grouped by subject and stacked in each column. Stimulus eccentricity increases for the waveforms from the top (central) to the bottom (90 deg). **(B)** Waveforms of 6 deaf cats. Same scalars are applied to both hearing and deaf waveforms. Horizontal, 200 ms. Vertical, 50 μV, negative-up.

(Figure 3). In both groups, the median of the corrected RMSs decayed monotonously with increasing eccentricity (Figure 3A). A two-way mixed-design ANOVA showed that the effect of stimulus eccentricity was significant [$F(6,54) = 52.02$, $p < 0.001$], but not the effect of deafness or the interaction between eccentricity and deafness. For stimuli at the 45-degree and 60-degree eccentricities, the median of RMSs in the deaf group was higher than the hearing group with a large effect size quantified as Cohen's d (see Table 1). We also investigated the effect of stimulus eccentricity and the trend of decay in RMS at the individual subject level (Figure 3B). Both non-linear and linear models were adopted to fit the RMSs as a function of eccentricity. All 11 subjects fit well with the two-coefficient (gain and decay) exponential model with an adjusted r^2 above 0.75 (Figure 3C). Three deaf and five hearing subjects fit better with a non-linear exponential model than the linear model. A paired-test comparison of the Fisher's Z-transformed adjusted r^2 values showed that the advantage of the non-linear model was statistically significant ($t_{10} = 2.26$, $p = 0.047 < 0.05$). However, the gain yielded from the model fitting was not different between the two groups (Figure 4A). The decay rate was slightly higher in the deaf group ($U = 42$, $p = 0.030 < 0.05$) (Figure 4B).

From the analysis of RMSs, we found that there was no main effect of early deafness on the overall amount of cortical activation by the checkerboard stimuli. The visual activation, however, was modulated by stimulus eccentricity exponentially, in an analogous way for both hearing and early deaf cats.

TABLE 1 Effect size for the comparisons between the two groups.

	RMS	Peak amplitude			Peak latency		
		N1	P1	N2	N1	P1	N2
0	**−0.07**	**−0.28**	**−0.25**	**−0.12**	**−0.81**	**−0.38**	**−0.07**
15	**−0.57**	**−0.45**	**−0.53**	**−0.73**	**−0.2**	**−0.68**	0.05
30	**−0.93**	−1.77	−1.25	**−0.75**	**−0.13**	**−0.3**	**1.09**
45	−1.21	**−0.53**	−1.51	−1.14	0.77	0.74	**2.43**
60	−1.1	**−0.9**	−1.24	**−0.62**	0.06	0.02	0.52
75	**−0.86**	**−0.55**	**−0.94**	**−0.66**	0.34	0.25	0.88
90	**−0.54**	**−0.36**	**−0.59**	0.02	0.62	**−0.12**	0.01

Bold values represent the effect size larger than 1.

N1-P1-N2 complex

Next, we investigated the VEPs by different peak components. The VEP waveforms of all subjects showed at least 3 components, which are referred as N1-P1-N2 complex and characterized by the pattern of their peak polarities, relative amplitudes, and peak latencies. According to the VEPs from the total 12 subjects in the current study, it started with a negative component N1 peaking at 54∼144 ms, followed by a positive component P1 peaking at 86 ∼ 189 ms, and ends with a second negative component N2 peaking at 178∼367 ms. In four subjects (3 hearing and 1 deaf), there were extra peaks between N1 and P1, which were not further analyzed.

We started with the exploration on how the peak amplitude of each component was affected by the stimulus eccentricity and early deafness (Figure 5). All three components showed a clear trend of decrease in amplitude with increasing eccentricity [N1: $F(6,54) = 27.07$, $p < 0.001$; P1: $F(6,54) = 21.73$, $p < 0.001$; N2: $F(6,54) = 20.98$, $p < 0.001$]. However, the difference between the hearing and deaf groups was not significant. For individual stimulus eccentricity, the deaf group showed larger peak amplitude with a large effect size (a) in the N1 component for stimuli present at 30-degree eccentricity, (b) in the P1 component for stimuli present at 30-, 45-, and 60-degree eccentricity, and (c) in the N2 component for stimuli present at 45-degree eccentricity, when compared to the hearing group (see Table 1).

We also examined how the peak latency of each component was affected by the stimulus eccentricity and deafness (Figure 6). Both N1 and P1, but not N2, showed prolonged latency with increasing eccentricity [N1: $F(6,54) = 5.38$, $p < 0.001$; P1: $F(6,54) = 12.36$, $p < 0.001$]. For individual stimulus eccentricity, only N2 component revealed a shorter peak latency in the deaf group than the hearing group [$F(1,9) = 7.49$, $p = 0.023 < 0.05$], especially for stimuli present at 30- and 45-degree eccentricity (see Table 1).

Although the increase of peak amplitude and shorter peak latency in early deaf cats reported above showed minimal statistical significance, they seemed to preferably occur for middle-peripheral visual field (e.g., 30-, and 45-degree eccentricities). In contrast to the lack of group differences found with RMS level, the trend of an increase in peak amplitude and a shorter peak latency suggests that the signal morphology was more sensitive to the effect of early deafness than the RMS values of VEPs. The trend we found is also

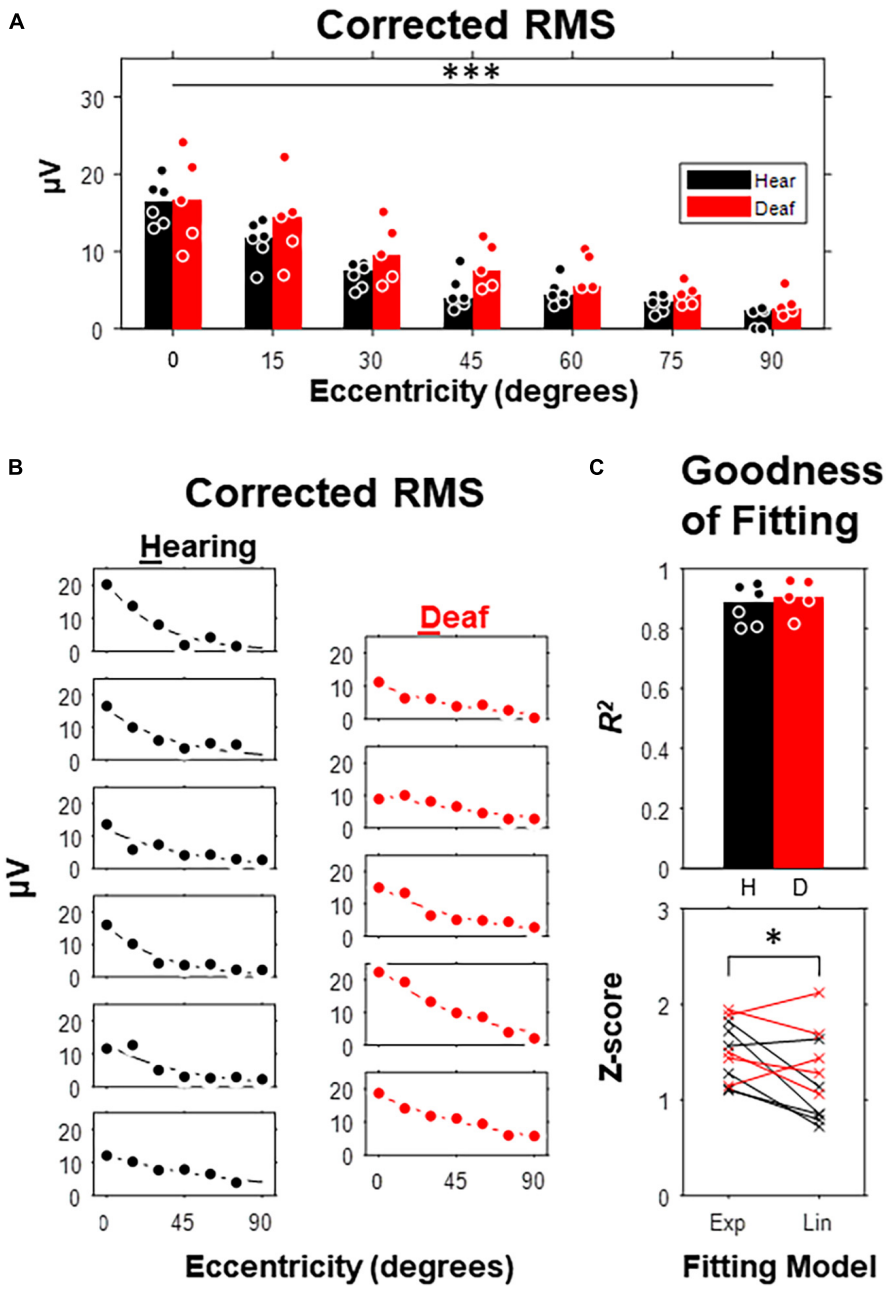

FIGURE 3
Corrected Root-Mean-Square (RMS) as a function of stimulus eccentricity. **(A)** RMS over a 420-ms post-stimulus window corrected with an 80-ms pre-stimulus baseline. Dot, data for individual subject. Bar, median. **(B)** Curve fitting with an exponentially decay model carried out for each of 6 hearing and 5 deaf subjects. **(C)** Goodness of fit. Top, adjusted R^2 compared between hearing and deaf group. Bottom, Fisher's Z scores of the adjusted R^2 derived from exponential and linear fitting for each subject. *$p < 0.05$; ***$p < 0.001$ for the main effect of eccentricity.

consistent with previous studies of VEPs in deaf human subjects (Neville et al., 1983).

Inter-sweep variability

Finally, we explored the inter-sweep variability of the peak latencies of N1 and P1 components. For each subject, 190 re-samples were taken by averaging 90% of the sweeps (i.e., with 2 sweeps per session excluded for each resampling average). The jitters of the resampled peak latencies followed a bell-shape distribution, with its width becoming larger as stimulus eccentricity increases (Figure 7A), because of larger inter-sweep variability. Hearing cats showed a smaller inter-sweep variability, especially at near-peripheral visual field (15- and 30-degree eccentricities) than deaf cats. This trend was even more apparent when the mean absolute deviations (MADs) of the jitters were quantified and plot as a function of the peak amplitude (Figure 7B). We performed an ANCOVA analysis regarding the effect of early deafness on MADs of latency jitter with peak amplitude as a covariate. We found a significant increase of MADs in early deaf cats compared to hearing cats for only P1 component [$F(1,72) = 8.52$, $p = 0.005 < 0.01$]. N1 component did not reveal such difference of statistical significance, neither was P1

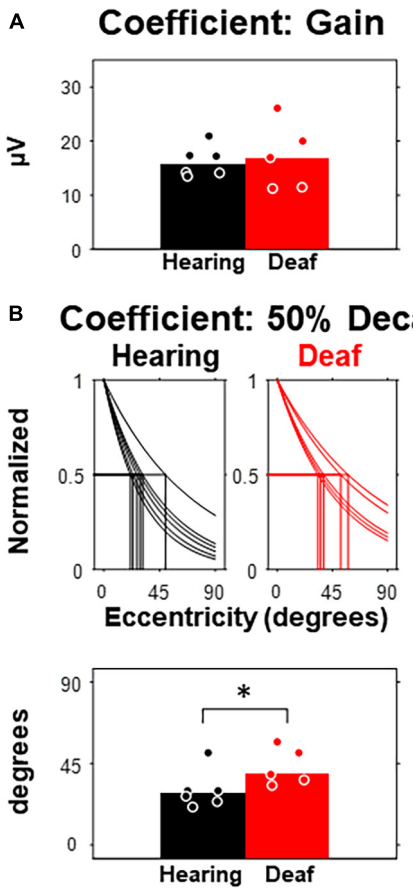

FIGURE 4
Comparison of model parameters between hearing and deaf subjects. **(A)** The fitting coefficient representing the gain of the model, which is equivalent to the model-estimated RMS at central eccentricity. **(B)** The fitting coefficient representing the rate of decay, which is equivalent to the amount of eccentricity increase that predicts 50% of RMS at central eccentricity. Top, model and 50% thresholds for each subject separated by group. Bottom, 50% threshold compared between hearing and deaf. *$p < 0.05$.

component without holding peak amplitude as a covariate. Our findings revealed an increase in VEP variability for early deafness that is specific to the P1 component. The larger variation identified within each deaf cat subject was similar to the larger individual differences in the VEP topographical distribution found in cochlear implanted subjects (Buckley and Tobey, 2011).

Discussion

In this study, we presented a checkerboard stimulus at seven different eccentricities, ranging from 0 to 90 degrees away from the midline, and compared the pattern-reversal visually evoked potentials (VEPs) between hearing and deaf cats. Overall, we observed no significant difference in response RMS values between the two groups, although some waveform components had larger amplitudes and shorter latencies in the deaf group, particularly for near- or mid-peripheral eccentricities. However, the inter-sweep variation analysis showed more variable latency in the deaf group for the peak component occurring about 100-ms post-stimulus.

The effect of deafness on VEPs

Considering previous findings in both behavioral studies (Lomber et al., 2010) as well as human VEP studies (Neville et al., 1983; Hauthal et al., 2014), it might be expected that VEPs would be larger in the deaf compared to hearing cats, especially at far-peripheral (60-, 75-, 90-degree) eccentricities. However, as we proposed in the introduction and evidenced by our data, that may not be the case.

In the visual localization task of an earlier study (Lomber et al., 2010), animal subjects were alert and motivated by reward in orienting/approaching the locations of visual stimuli, where the visual stimuli had small size (less than 1-degree) and locations randomized trial to trial. In the VEP recording of the current study, animal subjects were sedated, not previously trained on a visual localization task, and the stimuli were larger in size (6 degree) and repeated for 20 trials at the same location.

When subjects are neither alert nor responsive, visual neurons with motor functions involved in eye movement tasks may make no or little contribution to the visual responses evoked by stimulus. While there is little information on how head movements modulate cortical visual neurons in cats (Straschill and Schick, 1977), many studies have shown the effect of eye movements on visual neuron in both cats (Guitton and Mandl, 1978a,b; Toyama et al., 1984; Yin and Greenwood, 1992; Weyand and Gafka, 1998) and non-human primates (Colby and Goldberg, 1999; Glimcher, 2001; Munoz, 2002).

In macaque monkeys, a large proportion of neurons in the frontal eye field (FEF) show no response to visual stimuli but reliable pre-saccadic activities for certain areas of the visual field, which are therefore deemed "movement" neurons (Glimcher, 2001). In contrast, most neurons in the lateral intraparietal area (LIP) demonstrate visual receptive field and their responses are modulated by stimulus saliency and task-relevance (Colby and Goldberg, 1999).

Compared to hearing cats, visual orienting behavior is improved in deaf cats, where accuracies of orienting to peripheral targets is increased (Lomber et al., 2010). This implies that neuronal function must be enhanced in visual representations and/or motor planning. The deactivation of deaf PAF eliminated the improved performance in the peripheral visual field (Lomber et al., 2010), which suggests that neurons in PAF acquire some functions in visual representations and/or motor planning. While there is still no evidence of visual responsiveness of PAF neurons in either hearing or deaf cats, cortical deactivation experiments show that PAF in hearing animals is involved in auditory localization (Malhotra et al., 2004; Malhotra and Lomber, 2007) and that PAF neurons are better tuned for sound location than A1 or AAF (Harrington et al., 2008). Therefore, neurons in PAF in hearing cats may already carry information of space required for the motor planning in visually guided orienting behavior, and may acquire functions in processing visual inputs following deafness.

Cat area 6 has been suggested as a homologue to primate FEF. Microstimulation in the banks and fundus of the perisylvian sulcus or the ventral bank of the cruciate sulcus in anesthetized cats produces saccadic eye movements, neck EMG activity (Guitton and Mandl, 1978a,b), and neuronal activity in superior colliculus (Meredith, 1999). However, only a small fraction of neurons in these areas demonstrated pre-saccadic activity in alert cats, but with a larger population being visually responsive (Weyand and Gafka, 1998). Although some neurons showed preference for certain eye movement direction, there is a lack of evidence for the behavioral relevance of

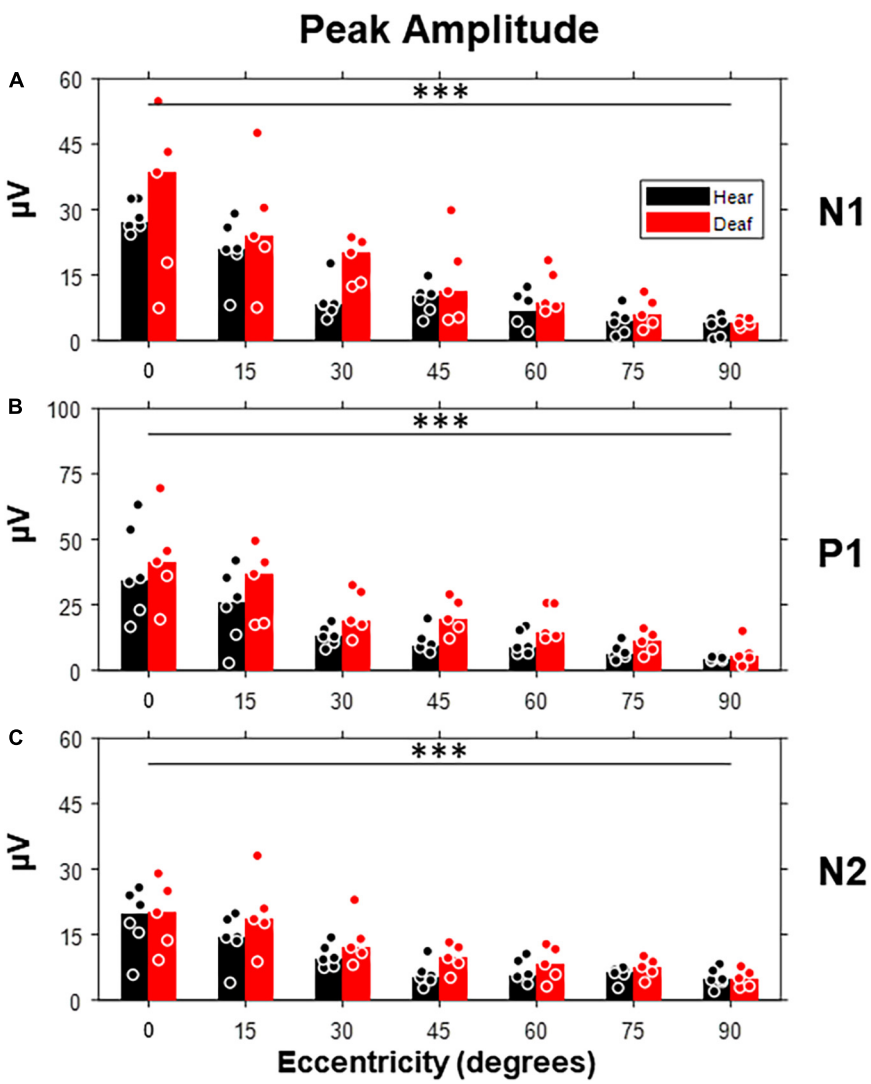

FIGURE 5
Peak amplitudes of three VEP components (N1, P1, and N2) as a function of stimulus eccentricity. **(A)** Peak amplitudes quantified from the N1 component, which is defined as the first negative deflection after stimulus onset. **(B)** Peak amplitudes quantified from the P1 component, which is defined as the first positive deflection after N1. **(C)** Peak amplitudes quantified from the N2 component, which is defined as the last negative deflection. Dot, individual subject; bar, median; ***$p < 0.001$ for the main effect of eccentricity.

these neurons as in primate FEF. However, area 6 may still serve as another potential target of cross-modal plasticity following deafness, by actively participating in the motor planning of eye and head movement.

While further investigation is still needed to support this hypothesis, we propose that a large proportion of functional cross-modal plasticity in cortex following deafness may reside in neural circuits associated with motor planning rather than those associated with visual processing.

It is also worth noting that neuromodulation systems, such as the dopaminergic (Anderson et al., 1994; Weil et al., 2010) and noradrenergic (McLean and Waterhouse, 1994; Treviño et al., 2019) systems, associated with reward and alertness, respectively, are actively involved in visually guided behaviors, as well as general task performance. Therefore, another possible explanation for the increased accuracy of peripheral visual localization in deaf cats may be found during the task training process, where reward are used to maintain subjects' alertness and motivation to perform the task.

The influence of dexmedetomidine

We did not attribute our negative results to the use of anesthetic agent, i.e., dexmedetomidine, because the anesthesia or sedation induced by dexmedetomidine is uniquely different from the other anesthetics, such as propofol and isoflurane, which directly interact with the GABAergic system (Hemmings et al., 2005) and may profoundly attenuate VEPs depending on their dosage (Sebel et al., 1986; Tanaka et al., 2020). One study has shown that the administration of dexmedetomidine does not affect VEPs in spine surgery patients undergoing general anesthesia with propofol (Rozet et al., 2015).

Although the VEPs recorded under dexmedetomidine cannot explain the enhanced performance in visual localization, our data is still the first report in cats on how early deafness changes VEPs that reflects stimulus-driven, bottom-up neural processing of visual inputs. Except when stimuli were positioned at central location or with 90-deg eccentricity, the medians of RMS and peak amplitude

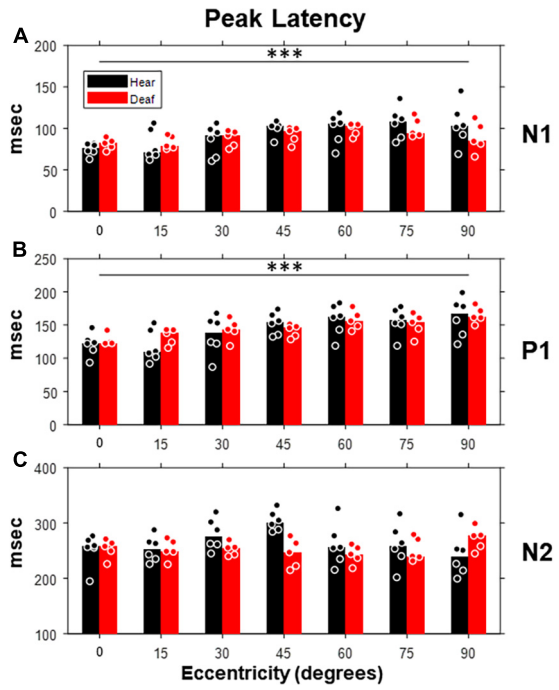

FIGURE 6
Peak latencies of three VEP components (N1, P1, and N2) as a function of stimulus eccentricity. Same layout of panels **(A–C)** as in Figure 5 but for peak latency. Dot, individual subject; bar, median; ***$p < 0.001$ for main effect of eccentricity.

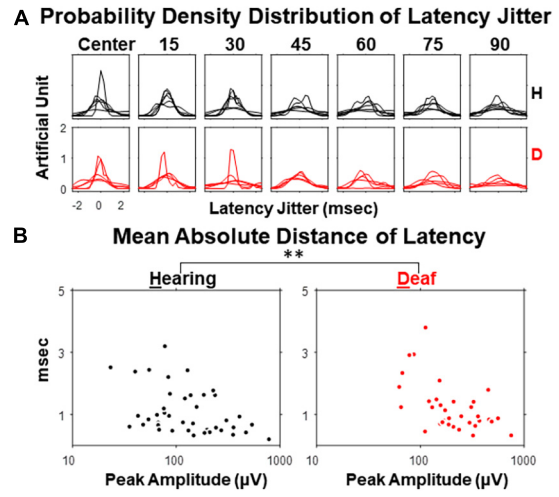

FIGURE 7
Jitter of peak latency for VEP P1 component in hearing and early deaf cats. **(A)** The estimated probability density for each of 7 stimulus eccentricities. Each line represents one of the subjects in both groups. **(B)** Mean absolute deviation (MAD) of resampled latency plot against the peak amplitude of the averaged waveform. Left, hearing. Right, deaf. Each dot represents one stimulus eccentricity in one subject. **$p < 0.01$ for the main effect of deafness in ANCOVA.

from the deaf group were almost unanimously larger than those from the hearing group. Although no main effect of deafness was revealed by ANOVA tests, a trend to increase in RMS and peak amplitude as well as decrease in peak latency seemed to appear at certain stimulus eccentricities with medium to large effect size worth being reported. Considering the low statistical power caused by small sample size used in the current study, a large effect size should have been expected to reveal statistical significance and avoid false negative. Similar cases were reported with a comparable sample size in previous histological investigations (Kok et al., 2014; Chabot et al., 2015; Wong et al., 2015; Meredith et al., 2016; Butler et al., 2018). Whereas a number of cat visual areas demonstrated increased or decreased number of afferents in several auditory areas in deaf cats when compared to hearing cats, only a few of such changes were statistically significant, such as the projections from posterolateral lateral suprasylvian area (PLLS) to the dorsal zone (DZ) of auditory cortex (Kok et al., 2014) and the projections from anterolateral lateral suprasylvian area (ALLS) to the anterior auditory fields (Wong et al., 2015).

Over all seven quantifications of VEPs and all seven stimulus eccentricities, the effect size values derived from the comparisons between the hearing and the deaf groups are mostly smaller than 1.5, and correspondingly led to a statistic power less than 59.8%. According to our calculation, at least 60% more than the current sample size in the deaf group is needed to achieve a statistic power higher than 80%, with the estimate of the current effect size assumed.

Regardless of the discussion above, we cannot completely exclude the possibility that the cross-modal plasticity shown in congenitally deaf cats is absent in early deaf cats or not sensitive to EEG recording technique. However, we consider these are the least likely, since several previous human ERP studies revealed different VEPs between hearing and deaf subjects (Neville et al., 1983; Hauthal et al., 2014; Campbell and Sharma, 2016; Corina et al., 2017).

We did find a statistically significant increase of latency variation in deaf subjects. The variability in neural activity in response to visual stimuli can be contributed by both neural and non-neural factors. Synaptic transmission is proposed to be a main source of neural variability due to its cascade nature of cellular and molecular process (Ribrault et al., 2011). Although we did not reveal a distinctive response amplitude in VEP from the deaf group, the reorganized auditory cortex may still participate in the early visual processing subtly, which involves synaptic transmission with less time precision. The increase we found in inter-sweep variability in deaf subjects, differentiating with respect to different VEP components, suggests a potential temporal specificity along the timeline of cortical sensory processing. Several neurological disorders (e.g., autism) have been associated with the increase in neural variability, which may share a similar underlying mechanism with this finding (Dinstein et al., 2015).

The effect of stimulus eccentricity

In this study, we also examined the effect of stimulus eccentricity on VEPs. This has been explored in previous studies (Albus, 1975; Van Essen et al., 1984; Harvey and Dumoulin, 2011; Ziccardi et al., 2015), but not at a range of eccentricity covering the entire quarter-sphere. To investigate the peripheral-specificity of cross-modal plasticity after deafness using VEPs, it is critical to understand how VEPs are affected by stimulus eccentricity in normal hearing subjects.

The contralateral visual field in the cat is represented by multiple cortical visual areas. Extracellular recording shows that whereas all of the visual areas studied are responsive to stimuli presented near central vision, only areas 17, 19, PMLS, and 21b are responsive to stimuli present beyond 70-degree eccentricity along the horizontal

meridian (Tusa et al., 1981). Except for area 17, the visual field represented in other cortical areas is more limited to the horizontal meridian at more peripheral positions (Tusa et al., 1981).

In this study, we quantified the effect of stimulus eccentricity on VEPs with an exponential model and found good fitness. This was in good consistent with a recent study in human subjects, where P1-N1 peak-to-peak amplitudes per squared-degree visual field as a function of stimulus eccentricities up to 20 degrees were exponentially modeled (Ziccardi et al., 2015). Our results suggest that the exponential model for the effect of stimulus eccentricity on VEPs can be generalized to the full range of quarter-sphere on the horizontal in non-primate species.

The attenuated VEP to stimulus present at peripheral field compared to central field that we observed is most likely due to cortical magnification, first observed with extracellular recording, where a larger proportion of visual cortical area were found representing a rather small central (foveal) visual field (Daniel and Whitteridge, 1961). Alternatively, it can also be argued that, because neurons in the peripheral visual field also have larger receptive field size in comparison to the central field (Albus, 1975; Van Essen et al., 1984), peripheral visual input can activate additional neurons as non-optimal stimulus as an advantage over central visual inputs. In virtue of such a trade-off, the product of cortical magnification factor (distance in cortex per degree in visual field) and receptive field size, also known as point-image size, was approximately constant for varying eccentricity (Harvey and Dumoulin, 2011). Our data showed that cortical activity measured using VEPs was not constant for varying eccentricity as point-image size.

One of the factors that interplays with cortical magnification in the effect of stimulus eccentricity is the respective participation of parvocellular and magnocellular pathways. Compared to the magnocellular pathway, the parvocellular pathway has a larger dynamic range for luminance contrast. It has been shown that VEPs to foveal stimuli (<2.5-degree eccentricity) demonstrate a broader range in response amplitude to various checkerboard contrasts when compared with peripheral stimuli (Laron et al., 2009), suggesting a maximized participation of the parvocellular pathway for the central visual field. Although its dominance decreases with eccentricity, the parvocellular pathway remains the major contributor in terms of the signal energy of VEPs as peripheral as 6.4 degrees (Baseler and Sutter, 1997). Given this majority position and high contrast stimuli being used, the results presented here reflect the unequal participation of both pathways, with the parvocellular pathway playing a greater part. However, it would be of interest for future studies to quantify the contribution of the parvocellular pathway for central versus peripheral visual field visual localization in deaf subjects.

It is also expected that there may be mutual benefits between future cat VEPs studies of this type and the development of source estimation algorithms for cat EEG signals. In humans, source estimation has been applied to VEPs with prior knowledge of generator locations derived from other brain imaging techniques such as PET (Woldorff et al., 1997) and fMRI (Hagler et al., 2009). Both human and cat cerebral cortex are gyrencephalic, which is a significant factor that compromises the performance of the source estimation algorithms using the concentric multi-sphere head models (Whittingstall et al., 2003). Although the smaller size of the cat head would raise the required spatial resolution of the scanners, such disadvantage is in the trade-off with an easier accessibility to invasive techniques such as extracellular recordings. In the current study, the error in VEP measurements regarding the lack of spatial resolution and unknown locations and orientation of VEP generators inevitably complicated the interpretation of our results. However, we speculate that the use of VEPs in assessing visual functions across visual fields in human and animal subjects is a promising approach.

In conclusion, our investigation of pattern reversal VEPs in response to peripherally present checkerboards in hearing and deaf cats demonstrated little functional plasticity in cortical activity driven by visual stimuli, suggesting that the enhanced visual localization previously reported in congenitally deaf cats is primarily due to plasticity in the neural circuit controlling orientation behavior instead of the lower-level visual system. In the future, we hope to use VEP techniques (1) to dissociate perception from orientation action, and (2) to adopt multi-channel recording and source localization.

Data availability statement

The raw data supporting the conclusions of this article will be made available by the authors, without undue reservation.

Ethics statement

The animal study was reviewed and approved by McGill University Animal Care Committee–DOWB.

Author contributions

TM, XB, and SL contributed to the conception of research question and design of the experiment. TM and PB carried out data collection and participated in editing the manuscript. XB and TM performed the data analysis. XB and SL drafted the manuscript. All authors contributed to the article and approved the submitted version.

Funding

This work was supported by grants from the Canadian Institutes of Health Research, the Natural Sciences and Engineering Research Council of Canada, and the Canada Foundation for Innovation.

Conflict of interest

The authors declare that the research was conducted in the absence of any commercial or financial relationships that could be construed as a potential conflict of interest.

Publisher's note

References

Albus, K. (1975). A quantitative study of the projection area of the central and the paracentral visual field in area 17 of the cat. *Exp. Brain Res.* 24, 159–179. doi: 10.1007/BF00234062

Anderson, T. J., Jenkins, I. H., Brooks, D. J., Hawken, M. B., Frackowiak, R. S., and Kennard, C. (1994). Cortical control of saccades and fixation in man. A PET study. *Brain* 117, 1073–1084. doi: 10.1093/brain/117.5.1073

Baseler, H. A., and Sutter, E. E. (1997). M and P components of the VEP and their visual field distribution. *Vision Res.* 37, 675–690. doi: 10.1016/S0042-6989(96)00209-X

Bavelier, D., Tomann, A., Hutton, C., Mitchell, T., Corina, D., Liu, G., et al. (2000). Visual attention to the periphery is enhanced in congenitally deaf individuals. *J. Neurosci.* 20:RC93–RC93. doi: 10.1523/JNEUROSCI.20-17-j0001.2000

Brainard, D. H. (1997). The psychophysics toolbox. *Spat. Vis.* 10, 433–436.

Buckley, K. A., and Tobey, E. A. (2011). Cross-modal plasticity and speech perception in pre- and postlingually deaf cochlear implant users. *Ear. Hear.* 32, 2–15. doi: 10.1097/AUD.0b013e3181e8534c

Butler, B. E., de la Rua, A., Ward-Able, T., and Lomber, S. G. (2018). Cortical and thalamic connectivity to the second auditory cortex of the cat is resilient to the onset of deafness. *Brain Struct. Funct.* 223, 819–835. doi: 10.1007/s00429-017-1523-y

Campbell, J., and Sharma, A. (2016). Visual cross-modal re-organization in children with cochlear implants. *PLoS One* 11:e0147793. doi: 10.1371/journal.pone.0147793

Chabot, N., Butler, B. E., and Lomber, S. G. (2015). Differential modification of cortical and thalamic projections to cat primary auditory cortex following early- and late-onset deafness. *J. Comp. Neurol.* 523, 2297–2320. doi: 10.1002/cne.23790

Colby, C. L., and Goldberg, M. E. (1999). Space and attention in parietal cortex. *Annu. Rev. Neurosci.* 22, 319–349. doi: 10.1146/annurev.neuro.22.1.319

Corina, D. P., Blau, S., LaMarr, T., Lawyer, L. A., and Coffey-Corina, S. (2017). Auditory and visual electrophysiology of deaf children with cochlear implants: Implications for cross-modal plasticity. *Front. Psychol.* 8:59. doi: 10.3389/fpsyg.2017.00059

Daniel, P. M., and Whitteridge, D. (1961). The representation of the visual field on the cerebral cortex in monkeys. *J. Physiol.* 159, 203–221. doi: 10.1113/jphysiol.1961.sp006803

Dinstein, I., Heeger, D. J., and Behrmann, M. (2015). Neural variability: Friend or foe? *Trends Cogn. Sci.* 19, 322–328. doi: 10.1016/j.tics.2015.04.005

Fine, I., Finney, E. M., Boynton, G. M., and Dobkins, K. R. (2005). Comparing the effects of auditory deprivation and sign language within the auditory and visual cortex. *J. Cogn. Neurosci.* 17, 1621–1637. doi: 10.1162/089892905774597173

Finney, E. M., Clementz, B. A., Hickok, G., and Dobkins, K. R. (2003). Visual stimuli activate auditory cortex in deaf subjects: Evidence from MEG. *Neuroreport* 14, 1425–1427. doi: 10.1097/00001756-200308060-00004

Finney, E. M., Fine, I., and Dobkins, K. R. (2001). Visual stimuli activate auditory cortex in the deaf. *Nat. Neurosci.* 4, 1171–1173. doi: 10.1038/nn763

Glimcher, P. W. (2001). Making choices: The neurophysiology of visual-saccadic decision making. *Trends Neurosci.* 24, 654–659. doi: 10.1016/s0166-2236(00)01932-9

Guitton, D., and Mandl, G. (1978a). Frontal 'oculomotor'area in alert cat. I. Eye movements and neck activity evoked by stimulation. *Brain Res.* 149, 295–312. doi: 10.1016/0006-8993(78)90477-8

Guitton, D., and Mandl, G. (1978b). Frontal 'oculomotor'area in alert cat. II. Unit discharges associated with eye movements and neck muscle activity. *Brain Res.* 149, 313–327. doi: 10.1016/0006-8993(78)90478-x

Hagler, D. J. Jr., Halgren, E., Martinez, A., Huang, M., Hillyard, S. A., and Dale, A. M. (2009). Source estimates for MEG/EEG visual evoked responses constrained by multiple, retinotopically-mapped stimulus locations. *Hum. Brain Mapp.* 30, 1290–1309. doi: 10.1002/hbm.20597

Harrington, I. A., Stecker, G. C., Macpherson, E. A., and Middlebrooks, J. C. (2008). Spatial sensitivity of neurons in the anterior, posterior, and primary fields of cat auditory cortex. *Hear. Res.* 240, 22–41. doi: 10.1016/j.heares.2008.02.004

Harvey, B. M., and Dumoulin, S. O. (2011). The relationship between cortical magnification factor and population receptive field size in human visual cortex: Constancies in cortical architecture. *J. Neurosci.* 31, 13604–13612. doi: 10.1523/JNEUROSCI.2572-11.2011

Hauthal, N., Thorne, J. D., Debener, S., and Sandmann, P. (2014). Source localisation of visual evoked potentials in congenitally deaf individuals. *Brain Topogr.* 27, 412–424.

Hemmings, H. C. Jr., Akabas, M. H., Goldstein, P. A., Trudell, J. R., Orser, B. A., and Harrison, N. L. (2005). Emerging molecular mechanisms of general anesthetic action. *Trends Pharmacol. Sci.* 26, 503–510.

King, A. J. (2004). The superior colliculus. *Curr. Biol.* 14:R335–R338. doi: 10.1016/j.cub.2004.04.018

Kleiner, M., Brainard, D. H., and Pelli, D. (2007). What's new in psychtoolbox-3? *Perception* 36, 1–16. doi: 10.1177/03010066070360S101

Kok, M. A., Chabot, N., and Lomber, S. G. (2014). Cross-modal reorganization of cortical afferents to dorsal auditory cortex following early- and late-onset deafness. *J. Comp. Neurol.* 522, 654–675. doi: 10.1002/cne.23439

Laron, M., Cheng, H., Zhang, B., and Frishman, L. J. (2009). The effect of eccentricity on the contrast response function of multifocal visual evoked potentials (mfVEPs). *Vision Res.* 49, 1711–1716. doi: 10.1016/j.visres.2009.03.021

Leake, P. A., Hradek, G. T., Rebscher, S. J., and Snyder, R. L. (1991). Chronic intracochlear electrical stimulation induces selective survival of spiral ganglion neurons in neonatally deafened cats. *Hear. Res.* 54, 251–271. doi: 10.1016/0378-5955(91)90120-x

Leake, P. A., Kuntz, A. L., Moore, C. M., and Chambers, P. L. (1997). Cochlear pathology induced by aminoglycoside ototoxicity during postnatal maturation in cats. *Hear. Res.* 113, 117–132. doi: 10.1016/s0378-5955(97)00133-0

Lee, C. C., and Middlebrooks, J. C. (2013). Specialization for sound localization in fields A1, DZ, and PAF of cat auditory cortex. *J. Assoc. Res. Otolaryngol.* 14, 61–82. doi: 10.1007/s10162-012-0357-9

Lisberger, S. G., and Fuchs, A. F. (1978a). Role of primate flocculus during rapid behavioral modification of vestibuloocular reflex. I. Purkinje cell activity during visually guided horizontal smooth-pursuit eye movements and passive head rotation. *J. Neurophysiol.* 41, 733–763. doi: 10.1152/jn.1978.41.3.733

Lisberger, S. G., and Fuchs, A. F. (1978b). Role of primate flocculus during rapid behavioral modification of vestibuloocular reflex. II. Mossy fiber firing patterns during horizontal head rotation and eye movement. *J. Neurophysiol.* 41, 764–777. doi: 10.1152/jn.1978.41.3.764

Lomber, S. G., Meredith, M. A., and Kral, A. (2010). Cross-modal plasticity in specific auditory cortices underlies visual compensations in the deaf. *Nat. Neurosci.* 13, 1421–1427. doi: 10.1038/nn.2653

Lomber, S. G., and Payne, B. R. (2004). Cerebral areas mediating visual redirection of gaze: Cooling deactivation of 15 loci in the cat. *J. Comp. Neurol.* 474, 190–208. doi: 10.1002/cne.20123

Malhotra, S., Hall, A. J., and Lomber, S. G. (2004). Cortical control of sound localization in the cat: Unilateral cooling deactivation of 19 cerebral areas. *J. Neurophysiol.* 92, 1625–1643. doi: 10.1152/jn.01205.2003

Malhotra, S., and Lomber, S. G. (2007). Sound localization during homotopic and heterotopic bilateral cooling deactivation of primary and nonprimary auditory cortical areas in the cat. *J. Neurophysiol.* 97, 26–43. doi: 10.1152/jn.00720.2006

Marino, R. A., and Munoz, D. P. (2009). The effects of bottom-up target luminance and top-down spatial target predictability on saccadic reaction times. *Exp. Brain Res.* 197, 321–335. doi: 10.1007/s00221-009-1919-x

McLean, J., and Waterhouse, B. D. (1994). Noradrenergic modulation of cat area 17 neuronal responses to moving visual stimuli. *Brain Res.* 667, 83–97. doi: 10.1016/0006-8993(94)91716-7

Meredith, M. A. (1999). The frontal eye fields target multisensory neurons in cat superior colliculus. *Exp. Brain Res.* 128, 460–470. doi: 10.1007/s002210050869

Meredith, M. A., Clemo, H. R., Corley, S. B., Chabot, N., and Lomber, S. G. (2016). Cortical and thalamic connectivity of the auditory anterior ectosylvian cortex of early-deaf cats: Implications for neural mechanisms of crossmodal plasticity. *Hear. Res.* 333, 25–36. doi: 10.1016/j.heares.2015.12.007

Meredith, M. A., Kryklywy, J., McMillan, A. J., Malhotra, S., Lum-Tai, R., and Lomber, S. G. (2011). Crossmodal reorganization in the early deaf switches sensory, but not behavioral roles of auditory cortex. *Proc. Natl. Acad. Sci. U.S.A.* 108, 8856–8861. doi: 10.1073/pnas.1018519108

Mize, R. R., and Murphy, E. H. (1976). Alterations in receptive field properties of superior colliculus cells produced by visual cortex ablation in infant and adult cats. *J. Comp. Neurol.* 168, 393–424. doi: 10.1002/cne.901680306

Munoz, D. P. (2002). Commentary: Saccadic eye movements: Overview of neural circuitry. *Prog. Brain Res.* 140, 89–96. doi: 10.1016/S0079-6123(02)40044-1

Neville, H. J., and Lawson, D. (1987). Attention to central and peripheral visual space in a movement detection task: An event-related potential and behavioral study. II. Congenitally deaf adults. *Brain Res.* 405, 268–283. doi: 10.1016/0006-8993(87)90296-4

Neville, H. J., Schmidt, A., and Kutas, M. (1983). Altered visual-evoked potentials in congenitally deaf adults. *Brain Res.* 266, 127–132. doi: 10.1016/0006-8993(83)91314-8

O'Keefe, L. P., and Berkley, M. A. (1991). Binocular immobilization induced by paralysis of the extraocular muscles of one eye: Evidence for an interocular proprioceptive mechanism. *J. Neurophysiol.* 66, 2022–2033. doi: 10.1152/jn.1991.66.6.2022

Pelli, D. G. (1997). The videotoolbox software for visual psychophysics: Transforming numbers into movies. *Spat. Vis.* 10, 437–442. doi: 10.1163/156856897x00366

Ribrault, C., Sekimoto, K., and Triller, A. (2011). From the stochasticity of molecular processes to the variability of synaptic transmission. *Nat. Rev. Neurosci.* 12, 375–387. doi: 10.1038/nrn3025

Rozet, I., Metzner, J., Brown, M., Treggiari, M. M., Slimp, J. C., Kinney, G., et al. (2015). Dexmedetomidine does not affect evoked potentials during spine surgery. *Anesth. Analg.* 121, 492–501. doi: 10.1213/ANE.0000000000000840

Schiller, P. H., Stryker, M., Cynader, M., and Berman, N. (1974). Response characteristics of single cells in the monkey superior colliculus following ablation or cooling of visual cortex. *J. Neurophysiol.* 37, 181–194. doi: 10.1152/jn.1974.37.1.181

Schwaber, M. K., Garraghty, P. E., and Kaas, J. H. (1993). Neuroplasticity of the adult primate auditory cortex following cochlear hearing loss. *Am. J. Otol.* 14, 252–258.

Scott, G. D., Karns, C. M., Dow, M. W., Stevens, C., and Neville, H. J. (2014). Enhanced peripheral visual processing in congenitally deaf humans is supported by multiple brain regions, including primary auditory cortex. *Front. Hum. Neurosci.* 8:177. doi: 10.3389/fnhum.2014.00177

Sebel, P. S., Ingram, D. A., Flynn, P. J., Rutherfoord, C. F., and Rogers, H. (1986). Evoked potentials during isoflurane anaesthesia. *Br. J. Anaesth.* 58, 580–585. doi: 10.1093/bja/58.6.580

Stecker, G. C., Mickey, B. J., Macpherson, E. A., and Middlebrooks, J. C. (2003). Spatial sensitivity in field PAF of cat auditory cortex. *J. Neurophysiol.* 89, 2889–2903. doi: 10.1152/jn.00980.2002

Straschill, M., and Schick, F. (1977). Discharges of superior colliculus neurons during head and eye movements of the alert cat. *Exp. Brain Res.* 27, 131–141. doi: 10.1007/BF00237694

Szentesi, A., Hopkins, T. L., and Collins, R. D. (1996). Orientation responses of the grasshopper, Melanoplus sanguinipes, to visual, olfactory and wind stimuli and their combinations. *Entomol. Exp. Appl.* 80, 539–549. doi: 10.1111/j.1570-7458.1996.tb00970.x

Tanaka, R., Tanaka, S., Ichino, T., Ishida, T., Fuseya, S., and Kawamata, M. (2020). Differential effects of sevoflurane and propofol on an electroretinogram and visual evoked potentials. *J. Anesth.* 34, 298–302. doi: 10.1007/s00540-020-02733-7

Thompson, K. G., Bichot, N. P., and Sato, T. R. (2005). Frontal eye field activity before visual search errors reveals the integration of bottom-up and top-down salience. *J. Neurophysiol.* 93, 337–351. doi: 10.1152/jn.00330.2004

Toyama, K., Komatsu, Y., and Shibuki, K. (1984). Integration of retinal and motor signals of eye movements in striate cortex cells of the alert cat. *J. Neurophysiol.* 51, 649–665. doi: 10.1152/jn.1984.51.4.649

Treviño, M., Medina-Coss y León, R., and Lezama, E. (2019). Adrenergic modulation of visually-guided behavior. *Front. Synaptic Neurosci.* 11:9. doi: 10.3389/fnsyn.2019.00009

Tusa, R. J., Palmer, L. A., and Rosenquist, A. C. (1981). "Multiple cortical visual areas," in *Multiple visual areas*, ed. C. Woolsey (Berlin: Springer), 1–31.

Van Essen, D. C., Newsome, W. T., and Maunsell, J. H. (1984). The visual field representation in striate cortex of the macaque monkey: Asymmetries, anisotropies, and individual variability. *Vision Res.* 24, 429–448. doi: 10.1016/0042-6989(84)90041-5

Weil, R. S., Furl, N., Ruff, C. C., Symmonds, M., Flandin, G., Dolan, R. J., et al. (2010). Rewarding feedback after correct visual discriminations has both general and specific influences on visual cortex. *J. Neurophysiol.* 104, 1746–1757. doi: 10.1152/jn.00870.2009

Weyand, T. G., and Gafka, A. C. (1998). Activity of neurons in area 6 of the cat during fixation and eye movements. *Vis. Neurosci.* 15, 123–140. doi: 10.1017/s0952523898151088

Whittingstall, K., Stroink, G., Gates, L., Connolly, J. F., and Finley, A. (2003). Effects of dipole position, orientation and noise on the accuracy of EEG source localization. *Biomed. Eng. Online* 2:14. doi: 10.1186/1475-925X-2-14

Woldorff, M. G., Fox, P. T., Matzke, M., Lancaster, J. L., Veeraswamy, S., Zamarripa, F., et al. (1997). Retinotopic organization of early visual spatial attention effects as revealed by PET and ERPs. *Hum. Brain Mapp.* 5, 280–286. doi: 10.1002/(SICI)1097-0193(1997)5:4<280::AID-HBM13>3.0.CO;2-I

Wong, C., Chabot, N., Kok, M. A., and Lomber, S. G. (2015). Amplified somatosensory and visual cortical projections to a core auditory area, the anterior auditory field, following early- and late-onset deafness. *J. Comp. Neurol.* 523, 1925–1947. doi: 10.1002/cne.23771

Yin, T. C., and Greenwood, M. (1992). Visuomotor interactions in responses of neurons in the middle and lateral suprasylvian cortices of the behaving cat. *Exp. Brain Res.* 88, 15–32. doi: 10.1007/BF02259125

Ziccardi, L., Parisi, V., Giannini, D., Sadun, F., de Negri, A. M., Barboni, P., et al. (2015). Multifocal VEP provide electrophysiological evidence of predominant dysfunction of the optic nerve fibers derived from the central retina in Leber's hereditary optic neuropathy. *Graefes Arch. Clin. Exp. Ophthalmol.* 253, 1591–1600. doi: 10.1007/s00417-015-2979-1

frontiers | Frontiers in Neuroscience

TYPE Original Research
PUBLISHED 09 March 2023
DOI 10.3389/fnins.2023.973525

OPEN ACCESS

EDITED BY
Ron Kupers,
University of Copenhagen, Denmark

REVIEWED BY
Ji Won Bang,
Grossman School of Medicine, New York University, United States
Jakub Limanowski,
Technical University Dresden, Germany

*CORRESPONDENCE
Or Yizhar
✉ or.yizhar@gmail.com

SPECIALTY SECTION
This article was submitted to Perception Science, a section of the journal Frontiers in Neuroscience

RECEIVED 20 June 2022
ACCEPTED 23 February 2023
PUBLISHED 09 March 2023

CITATION
Yizhar O, Tal Z and Amedi A (2023) Loss of action-related function and connectivity in the blind extrastriate body area. *Front. Neurosci.* 17:973525. doi: 10.3389/fnins.2023.973525

Loss of action-related function and connectivity in the blind extrastriate body area

Or Yizhar[1,2,3]*, Zohar Tal[4] and Amir Amedi[2,5]

[1]Department of Cognitive and Brain Sciences, The Hebrew University of Jerusalem, Jerusalem, Israel, [2]Ivcher School of Psychology, The Institute for Brain, Mind and Technology, Reichman University, Herzliya, Israel, [3]Research Group Adaptive Memory and Decision Making, Max Planck Institute for Human Development, Berlin, Germany, [4]Faculty of Psychology and Educational Sciences, University of Coimbra, Coimbra, Portugal, [5]The Ruth & Meir Rosenthal Brain Imaging Center, Reichman University, Herzliya, Israel

The Extrastriate Body Area (EBA) participates in the visual perception and motor actions of body parts. We recently showed that EBA's perceptual function develops independently of visual experience, responding to stimuli with body-part information in a supramodal fashion. However, it is still unclear if the EBA similarly maintains its action-related function. Here, we used fMRI to study motor-evoked responses and connectivity patterns in the congenitally blind brain. We found that, unlike the case of perception, EBA does not develop an action-related response without visual experience. In addition, we show that congenital blindness alters EBA's connectivity profile in a counterintuitive way—functional connectivity with sensorimotor cortices dramatically decreases, whereas connectivity with perception-related visual occipital cortices remains high. To the best of our knowledge, we show for the first time that action-related functions and connectivity in the visual cortex could be contingent on visuomotor experience. We further discuss the role of the EBA within the context of visuomotor control and predictive coding theory.

KEYWORDS

congenital blindness, neuroimaging, body representation, resting-state fMRI, visuomotor interactions, extrastriate body area, plasticity

Introduction

Visual processing in the brain features two pathways, the ventral-occipitotemporal "what" stream and the dorsal-occipitoparietal "where and how" stream (Goodale and Milner, 1992). For many years, researchers assumed that visual streams develop only during specific time windows of critical periods (Hensch, 2004; Knudsen, 2004). However, there is accumulating evidence that the two streams maintain some level of functional selectivity and connectivity independent of visual experience (Striem-Amit et al., 2012b; Fine and Park, 2018; Heimler and Amedi, 2020). Studies of congenitally blind individuals show that category-selective loci operate in a sensory-independent manner (Reich et al., 2012; Heimler et al., 2015) and respond to task-specific information derived from other sensory modalities (Amedi et al., 2002, 2007; Pietrini et al., 2004; Ptito et al., 2005; Poirier et al., 2006; Renier et al., 2010; Sani et al., 2010; Collignon et al., 2011; Reich et al., 2011; Striem-Amit et al., 2012a; Strnad et al., 2013; Striem-Amit and Amedi, 2014; Abboud et al., 2015; Sigalov et al., 2016; Mattioni et al., 2020). Category-specific brain areas can thus form without visual

experience in critical periods–the ideal time frames for development in infancy (Kupers and Ptito, 2014; Heimler and Amedi, 2020; Mattioni et al., 2020). For differences in the organization of higher cognitive functions between blind and sighted individuals, see (Amedi et al., 2003, 2004; Bedny, 2017).

These studies explored the stability of perceptual processing in the Occipital lobe. Yet, recent works on sighted individuals show that motor planning and execution can recruit visual cortical areas (Dinstein et al., 2007; Orlov et al., 2010; Lingnau and Downing, 2015; Gallivan et al., 2016). In particular, multiple studies reported that motor actions evoke a neural response in the visual Extrastriate Body Area (EBA) (Astafiev et al., 2004; Peelen and Downing, 2005; Kühn et al., 2011; Gallivan et al., 2013, 2016; Limanowski and Blankenburg, 2016; Zimmermann et al., 2016; Limanowski et al., 2017). Situated in the Lateral Occipital Temporal Cortex (LOTC) and connected to both visual streams, the EBA specializes in the perceptual processing of body parts (Downing, 2001). Even so, evidence from an array of studies finds that both seen and unseen movements recruit the EBA (Astafiev et al., 2004; Peelen and Downing, 2005; Limanowski et al., 2017) and that EBA's neural activity patterns can decode future motor actions (Kühn et al., 2011; Gallivan et al., 2013, 2016; Orgs et al., 2016). In amputees, the strength of functional connectivity between EBA and sensorimotor areas correlates with higher prosthesis usage (Van Den Heiligenberg et al., 2018). EBA is also active during the rubber-hand illusion and even passive arm movements (Gentile et al., 2015; Limanowski and Blankenburg, 2016; Limanowski et al., 2017), which suggests it is a target for proprioceptive as well as visual information. Although its location is remote from primary Sensorimotor cortices, it appears to play an integral functional part in motor actions, perhaps even independent of vision. Given the now-known task-selective sensory-independent nature of the visual streams, does the EBA develop its action-related functions regardless of visual and motor experience? And do perception and action follow the same developmental constraints?

In a previous study, we used a visual-to-auditory Sensory Substitution Device (SSD) to show that the EBA of blind individuals responds preferentially to stimuli with body-related information (Striem-Amit and Amedi, 2014). The response had a high degree of anatomical consistency across blind individuals, which overlapped with responses elicited by visual body-part images in sighted individuals (Striem-Amit and Amedi, 2014). Furthermore, the blind EBA preserves its functional connections to visual cortices, like the Ventral and Dorsal streams (Striem-Amit and Amedi, 2014). Other studies on the blind brain report maintenance of large-scale functional and structural organization within visual cortices (Striem-Amit et al., 2012b, 2015; Butt et al., 2013; Burton et al., 2014; Heine et al., 2015; Fine and Park, 2018). Moreover, as the principal role of the EBA is perceptual, one could predict that the lack of visual experience would cause even lower damage to EBA's action-related functions. Findings from sighted individuals support this prediction. The EBA is also active when visual information is absent, and researchers can decode future body postures from its activity (van Nuenen et al., 2012; Zimmermann et al., 2016, 2018). These results led some researchers to infer that EBA takes part in motor planning by receiving information on the current postural schema and determining a future postural configuration. Thus, we hypothesized that the lack of visual experience does not affect EBA's motor-related neural responses.

An opposing view is that EBA integrates visuomotor information, and its development is contingent on visual experience. Although much of the blind Visual cortex maintains its intrinsic large-scale organization (Striem-Amit et al., 2012b, 2015), its functional connections to frontal or sensorimotor cortices decrease (Burton et al., 2014; Heine et al., 2015; Wang et al., 2015; Bauer et al., 2017). In particular, the blind EBA seems to lack significant functional connections to somatosensory and motor cortices (Striem-Amit and Amedi, 2014), in stark contrast to the widespread and pronounced connectivity patterns common for EBA in the sighted (Zimmermann et al., 2018). While EBA retains its perceptual function, the lack of functional connections to sensorimotor cortices hints at a loss of action-related function. Thus, an alternative hypothesis could posit that EBA relies on visual information for actions, and its development is contingent on visual experience. One option is that rather than engaging in motor planning, EBA's motor-evoked response is part of a perceptual process that anticipates the sensory consequences of motor actions (Astafiev et al., 2004; Orlov et al., 2010; Gallivan et al., 2013). EBA integrates information from upcoming motor actions with incoming visual and proprioceptive sensations to encode limb position (Gallivan et al., 2013, 2016; Gallivan and Culham, 2015; Limanowski and Blankenburg, 2016). Such a dynamic visuomotor representation is redundant for blind individuals and thus would not evolve without visual experience.

Here, we study the effects of congenital blindness on the action-related function of the EBA with task-related and resting-state fMRI (functional Magnetic Resonance Imaging). We expand on our previous study by adapting a cortical parcellation and examining the seed-to-seed functional connections of the EBA to visual and motor regions of interest. Further, we compared the congenitally blind results to a group of sighted participants, where we expect EBA activity during motor tasks. We interpret and discuss our results in the context of the plasticity of action-related functions in visual cortices and their dependency on visual experience.

Materials and methods

Participant details

The study included 13 congenitally blind participants. Nine participants participated in the resting-state experiment [eight right-hand dominants, six females, age: 34.5 ± 6.2 (mean ± standard deviation)], and eight participated in the motor experiment (seven right-hand dominants, five females, age: 33.3 ± 9.1). Four blind participants took part in both experiments (see **Supplementary Table 1** for further details). We also recruited 29 sighted participants, 20 participated in the resting state experiment (18 right-hand dominants, 12 females, age: 29.5 ± 4.1), and nine participated in the motor experiment (eight right-hand dominants, five females, age: 26.3 ± 2.2). We excluded two additional sighted participants from the resting state analysis due to excessive head movement. Participants had no known neurological conditions, and hand dominance was self-reported. The study received full Helsinki Approval from the Hadassah Medical Center at the Hebrew University of Jerusalem. All participants signed a consent form, and blind participants signed with the companion of an impartial witness.

Experimental paradigm

fMRI motor experiment

The motor experiment included three scanning runs of body movements. Participants moved 12 body parts in succession while lying blindfolded in the MRI (Magnetic Resonance Imaging) scanner. To further decrease the effects of light and visual perception, we instructed participants to keep their eyes closed at all times, and we completely darkened the scanner room. The sequence is in line with the homunculus' spatial representation in primary Sensorimotor cortices (Penfield and Boldrey, 1937; Zeharia et al., 2012). This continuous paradigm is optimal for topographical mapping (Zeharia et al., 2012) and is also suitable for more conventional analyses (Tal et al., 2016, 2017; Hofstetter and Dumoulin, 2021). Each run consisted of six cycles in which participants moved the 12 body parts: right toes, right foot, right arm, right wrist, right fingers, lips, jaw, left fingers, left wrist, left arm, left foot, left toes (for more details, see **Supplementary Table 2**). Before the start of a cycle, participants heard a 3 s auditory cue with information about the cycle's direction (i.e., "start right/left"). Each cycle concludes with a rest period of 6–9 s. Three cycles in each run followed this sequence, while the other three cycles had the opposite direction, starting from the left toes and finishing with the right toes (**Supplementary Figure 1**). In sum, there were 18 trials for each body part. The sound sequences were produced using Adobe Premiere Pro (Adobe Inc.) and presented using Presentation (Neurobehavioral Systems). We instructed participants to execute movements for 3 s with an interstimulus interval of 1.5 s that included an auditory cue for the next body part. Each trial consisted of three body part movements synchronized with auditory metronome beeps. A body-part movement (e.g., flexion and extension of the arm) lasted 1 s, split evenly between the two actions. Before entering the scanner, we trained participants for 30 min to minimize excess movement.

Neuroimaging data collection

All brain imaging experiments included anatomical and functional scans from a 3T Siemens Skyra scanner using a 32-channel Head Matrix Coil at The Edmond and Lily Safra Center for Brain Sciences (ELSC) Neuroimaging Unit at the Hebrew University of Jerusalem.

fMRI motor experiment

The functional scans that included motor tasks used a multi-band (MB) imaging protocol with a factor of four. We collected the data under the following parameters: TR (Time Repetition) = 1,500 ms, TE (Time Echo) = 32.4 ms, FA (Flip Angle) = 78°, imaging matrix = 96*96, FOV (Field of View) = 192 mm*192 mm with an in-plane resolution of 2 mm*2 mm. We acquired 72 axial slices with 2 mm thickness and 0 mm gap for full cortex coverage. We omitted the first ten volumes of each functional run to ensure signal stabilization. High-resolution 3D T1-weighted anatomical images were collected using an MP-RAGE sequence with the following parameters: FOV = 256 mm*256 mm, 160 axial slices, TR = 2,300 ms, TE = 2.98 ms, flip angle = 9°, with an in-plane resolution of 1 mm*1 mm. In sum, we acquired between 254 and 272 functional volumes in each run.

fMRI resting-state experiment

We collected resting-state data under the following parameters: TR = 3,000 ms, TE = 30 ms, FA = 70°, imaging matrix = 64*64, FOV = 240 mm*240 mm with an in-plane resolution of 3.75*3.75 mm. We acquired 50 axial slices with 3 mm thickness and 0 mm gap for full cortex coverage. We acquired scans of 200 volumes for each participant in the blind group without a delayed acquisition and omitted the first 20 volumes to ensure magnetization stability. In the sighted group, we acquired 180 volumes per participant with an automatic system for stabilization. We collected High 3D T1–resolution weighted anatomical images using an MP-RAGE sequence with the following parameters: FOV = 256 mm*256 mm, 160 axial slices, with an in-plane resolution of 1 mm*1 mm.

Preprocessing

We analyzed data from both experiments using the BrainVoyager 20.6 software package (Brain Innovation, Maastricht). We corrected functional MRI data for slice timing (temporal interpolation to the middle slice of each functional volume), corrected for head motion (trilinear interpolation for detection), and applied a high-pass filter (cut-off frequency of two cycles per run). None of the scans included during the two experiments showed translational motion exceeding a maximum of 2 mm displacement or a maximum rotational motion exceeding 2° in any direction. We normalized anatomical T1 scans of each subject to a standardized MNI (Montreal Neurological Institute) space (ICBM-152). We then applied the calculated normalization parameters to all the subject's functional scans. Cortical reconstruction included the segmentation of white matter using a grow-region function. The remaining cortical surface was then inflated and aligned to a 3D cortical reconstruction of an MNI-normalized brain (FreeSurfer's fsAverage brain).

fMRI motor experiment

We spatially smoothed the data from the motor task runs (spatial Gaussian smoothing, Full Width at Half Maximum = 6 mm) to overcome inter-subject anatomical variability.

fMRI resting-state experiment

Functional resting-state data did not undergo spatial smoothing to avoid false correlations.

Cortex-based alignment

To acquire precise anatomical markers as Regions of Interest (ROI), we used a cortex-based alignment (CBA) algorithm implemented in BrainVoyager (Frost and Goebel, 2012) and aligned the hemispheres of all participants to a fsAverage brain surface. In short, the process morphs reconstructed and folded hemispheres into a sphere that produces a curvature map with

differing degrees of smoothness. The alignment itself is an iterative procedure that follows a coarse-to-fine matching strategy to a target brain that gradually decreases the smoothness of the sphere's surface. Importantly, we merged the aligned hemispheres to create a bilateral cortical alignment, rather than the more common procedure of aligning and analyzing each hemisphere in isolation. Using the alignment, we transformed all the functional datasets from a standard MR volume space to the target surface. This procedure enabled us to execute whole-brain analyses that produce statistical maps on both cortical hemispheres.

Parcellation and ROI selection

As some of our participants are blind, precise functional identification of the EBA was impossible on a subject level-basis. To identify the EBA and other relevant ROIs, we used anatomical landmarks delineated from the cortical parcellation suggested by Glasser et al. (2016). The parcellation considers structural and functional data collected in the Human Connectome Project (HCP). In localizing EBA, we used data provided by the HCP (van Essen et al., 2017) to identify cortical areas that preferentially respond to images of body parts compared to images of tools, faces, and lpaces (Glasser et al., 2016). We focused our analysis on the MT complex, a known location of the EBA (Ferri et al., 2013).

fMRI resting-state experiment

For the functional connectivity analysis, we selected eight ROIs (three for visual areas and five for sensory-motor areas) in addition to EBA. We chose visual regions associated with EBA's functions, the visual Ventral and Dorsal streams, and the primary Visual cortex (V1). For sensorimotor ROIs, we chose areas that produce consistent activity during motor planning and action, or process incoming proprioceptive inputs. These include the Premotor cortex (PMc), the primary Motor cortex (M1), the primary Somatosensory cortex (S1), the Operculum and Insular cortex (Operculum), and the Supplementary motor Area along with adjacent cingulate motor areas (SMA). For each ROI, we chose the corresponding parcellations from HCP-MMP1.0 (Glasser et al., 2016). A description of the ROIs and the cytoarchitecture regions that comprise them are in **Supplementary Table 3**. Following the fMRI motor experiment, we wanted to use a bilateral EBA seed and bilateral visual and motor ROIs. To establish that left and right EBAs have similar connectivity patterns, we analyzed the functional connections between left-lateralized EBA and right-lateralized ROIs, as well as between right-lateralized EBA and left-lateralized ROIs in the sighted group (**Supplementary Figure 2**).

GLM analyses

We performed our analyses on the reconstructed and inflated fsAverage brain surface to which we aligned all participants' cortices with cortex-based alignment.

fMRI motor experiment

We first computed statistical parametric maps from a single-subject General Linear Model (GLM). We chunked the body part movements into five predictors of major anatomical segments: right foot (toes and foot), right hand (digits, arm, and wrist), face (jaw and lips), left hand (digits, arm, and wrist), left foot (toes and foot). In our model, all body parts within each group are explained by the same predictor (e.g., "face" for jaw and lips). The model predictors were convoluted with a canonical Hemodynamic Response Function. Before fitting the GLM model, time courses of the preprocessed data underwent z-normalization. For the group-level analyses, we used a multi-level random-effects model. The statistical threshold criterion for individual vertices was $p < 0.05$. We corrected all the results for multiple comparisons using a cluster-size threshold estimator based on a Monte Carlo simulation approach with 500 iterations, as implemented in BrainVoyager 20.6. We conducted ROI analyses of the EBA by contrasting each of the five body part groups against a baseline parameter of zero (i.e., no response). We executed all these analyses using MATLAB software (MathWorks). ROI statistical tests were double-sided and corrected for multiple comparisons using False Discovery Rate (FDR, $\alpha = 0.05$). We also examined if between-group differences in EBA's motor-evoked response are bilateral and are anatomically consistent for left-and right-hand movements. We plotted the peak activity for the sighted group's right-hand movements within bilateral EBA. We defined a seed that includes all vertices within a 4 mm distance from the peak group activity (**Supplementary Figure 3**). To establish bilaterality, we analyzed the activity within that seed for left-hand movements (see **Supplementary Figure 4**) for a magnified view of motor-evoked response around EBA).

fMRI resting-state experiment

To describe the EBA connectivity patterns, we extracted the EBA signal time course by averaging the data across all EBA vertices at each time point. Next, we extracted the MR signal from the ventricles and subarachnoid spaces (i.e., Cerebrospinal Fluid). We wanted to use the signal as a confound in our model, as these voxels include noise factors such as global signal drift. We used an embedded function found in BrainVoygaer to remove skull tissue, head tissue and subcortical structures. From the resulting image, we created a mask of voxels with intensity levels below the threshold for white and gray matter segmentation. We repeated this procedure in each participant's brain following MNI normalization. Similar to the EBA, we averaged the time course across all voxels at each time point. Time-course samples were then z-normalized and modeled as predictors in a first-level GLM connectivity analysis - the EBA time course as an explanatory predictor and the Cerebrospinal Fluid (CSF) time courses as confounding predictors. In the group random effect analyses, we used beta images from first-level GLM analyses and treated the participants as a random factor. First, we performed a whole-brain analysis by contrasting connectivity estimates from both EBAs against the baseline. The vertex-wise statistical threshold for the whole-brain analysis was $p < 0.05$, corrected for multiple comparisons using a Monte Carlo permutation test. Next, we performed seed-to-seed ROI analyses from the EBA to five sensorimotor and three visual cortical areas (see ROI selection). As motor movements recruit both EBAs, we inspected the connectivity between bilateral ROIs and EBA predictors. The statistical threshold was $p < 0.05$, corrected for multiple comparisons with a False Detection Rate ($\alpha = 0.05$).

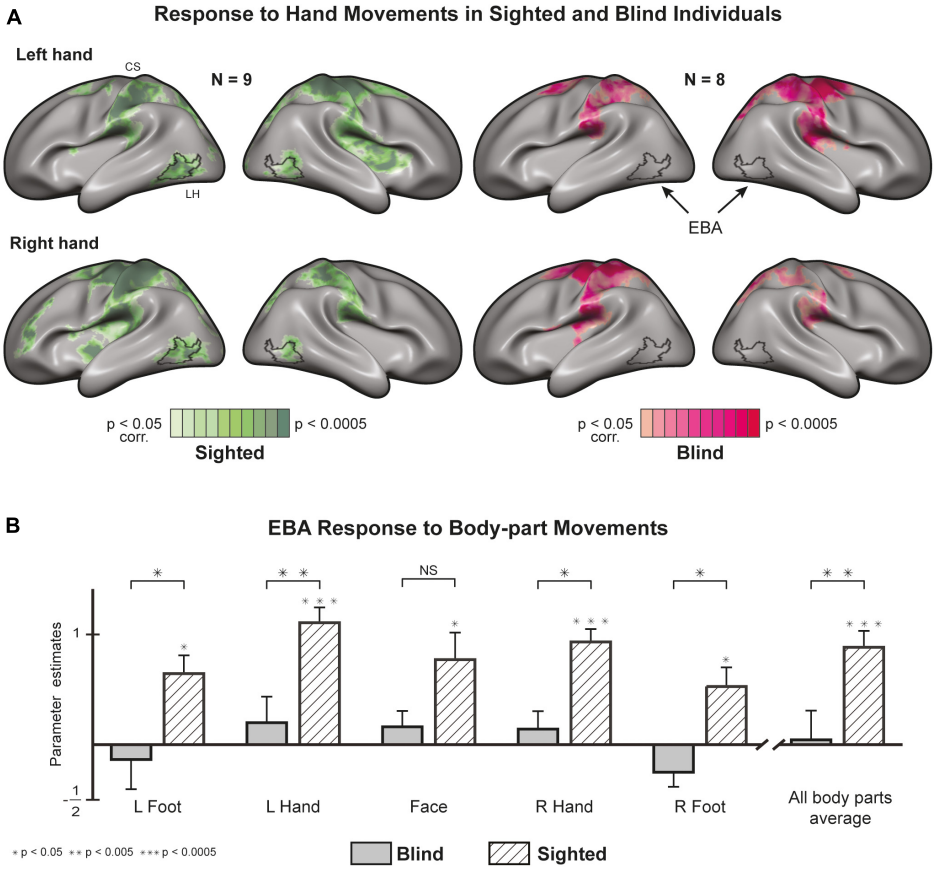

FIGURE 1
Motor-evoked responses to body part movements (whole-brain and EBA localizer). **(A)** Whole-brain statistical parametric maps of hand movements, most commonly associated with EBA activity, plotted on both cortical hemispheres after cortex-based alignment [random effects General Linear Model (GLM)]. Hand movements recruit EBA in sighted individuals but not in blind individuals (see **Supplementary Figure 5** for other body parts). EBA, Extrastriate Body Area; CS, central sulcus. **(B)** Regions of Interest (ROI) analysis of EBA response to various body parts. The region is significantly active in the sighted and not in the blind. A between-group analysis (random effects GLM, $n = 17$) reveals significant differences in the response to movements of the right foot, right hand, left foot, and left hand (for results in separate hemispheres, see **Supplementary Figure 6**).

Results

To explore the effects of visual experience on EBA's action-related function, we trained sighted and congenitally blind participants to move 12 unilateral body parts in search of motor-evoked responses. In a separate experiment, we investigated EBA connectivity patterns to sensorimotor and visual loci during rest. To characterize the whole-brain activity and functional connectivity, we used a Cortex Based Alignment technique (Frost and Goebel, 2012) that merges both hemispheres (see methods). We performed all group-level random-effects analyses on this aligned brain.

The blind EBA does not respond to active movements

A whole-brain GLM analysis in sighted individuals shows robust activations in and around bilateral EBA (**Figure 1A**) for hand movements (see **Supplementary Figure 5** for similar results of feet and face). In the blind group, we did not find activity in or around EBA for all unilateral movements. Hand movements in both groups result in localized activity in somatosensory and motor areas, suggesting a limited whole-brain noise effect. An ROI analysis of motor-evoked responses (**Figure 1B**) in EBA confirmed the previous observations, with statistically significant responses in the sighted and insignificant responses in the blind (**Supplementary Table 4**). An analysis of group differences showed that the sighted group had significantly stronger EBA responses for the left hand [$t(15) = 3.39$, $p = 0.004$, $d = 1.52$] and right hand [$t(15) = 2.44$, $p = 0.027$, $d = 1.08$], as well as the left foot [$t(15) = 2.81$, $p = 0.013$, $d = 1.26$] and right foot [$t(15) = 2.54$, $p = 0.022$, $d = 1.14$]. We did not find a significant difference between the groups in the face condition [$t(15) = 1.66$, $p = 0.118$].

M1 responses are comparable between blind and sighted individuals

An ROI analysis (**Figure 2**) of the Left primary Motor cortex (M1) shows no differences between the blind and sighted for movements of the right hand [$t(15) = 1.519$, $p = 0.15$] or right foot [$t(15) = 1.709$, $p = 0.108$]. The statistical difference between the groups for face movement did not survive a multiple comparison

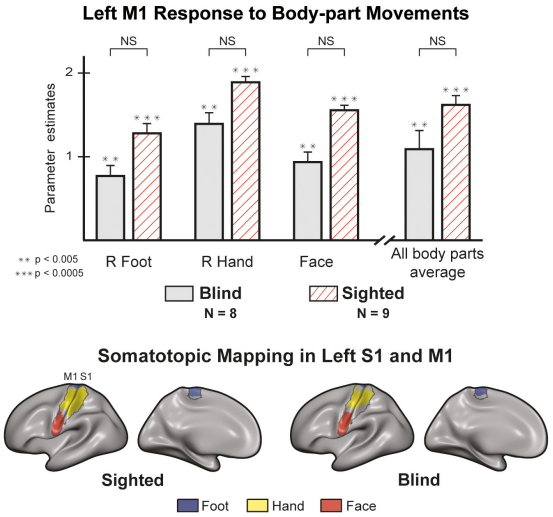

FIGURE 2
M1 responses are comparable between blind and sighted individuals [random effects General Linear Model (GLM)]. There were no significant group differences in M1 activity (left hemisphere) for all unilateral and face movements (**Supplementary Table 5**). Regions of Interest (ROI) analysis of right M1 produced similar results (**Supplementary Figure 7**). The sighted and blind groups show similar somatotopic organization in S1 and M1. We created the maps by contrasting each condition with all others. We then plotted and colored all statistically significant vertices ($p < 0.05$, corrected). The results on the left hemisphere represent the response to right hand, right foot, and face movements. We found similar results in the right hemisphere for contralateral effectors (**Supplementary Figure 5**). Error bars are for the standard error. Large asterisks indicate between-group significance, small asterisks indicate within-group significance against the baseline. NS, non-significant.

correction [t (15) = 1.28, p = 0.04]. Analysis of motor-evoked responses in Right M1 shows congruent results, with no significant differences between the groups (**Supplementary Table 5**). A mixed design ANOVA with a within-factor of body-part and a between-factor of the group found no differences in the group responses [F (1,135) = 3.619, p = 0.077, η^2 = 0.07] and no interaction between group and body-part [F (7,135) = 0.802, p = 0.587, η^2 = 0.016]. We also looked at the selectivity of neural responses in S1 and M1 (**Figure 2**). In both groups, we observed activity that follows a topographic organization (see **Supplementary Figure 7** for the right hemisphere), in line with the canonical Penfield homunculus (Penfield and Boldrey, 1937; Zeharia et al., 2012).

Congenital blindness drastically alters EBA's connectivity

We used resting-state fMRI data to examine the effects of visual development on EBA's connectivity to somatosensory and motor cortices. Under the assumption that neurons that fire together wire together, neural activity at rest should be reflective of activity during tasks. As such, neurons that are functionally co-activated should also have correlated activity during rest. To examine these connections, we extracted the resting-state time course of the EBA from each subject and used these as predictors in our second-level analysis. Given the bilateral nature of motor-related activity in the EBA, we defined the left and right EBA as a combined seed and analyzed their connectivity to the whole brain. To verify this assumption, we mapped the functional connectivity between the sighted EBA (left and right) and contralateral visual and motor ROIs. We found support for our assumption in comparable patterns of contralateral connectivity for left-lateralized and right-lateralized EBAs (**Supplementary Figure 2**). Both groups exhibited known connectivity patterns (Striem-Amit and Amedi, 2014; Zimmermann et al., 2018) to visual brain areas around the Occipital lobe (**Figure 3A**). EBA connectivity in the sighted group was more widespread. We found prominent connections to M1, S1, Inferior Parietal Lobule, and associative areas such as the Operculum. Next, we used probabilistic mapping to observe the consistency of connectivity patterns within the blind and sighted groups. We computed single-subject connectivity maps (corrected for multiple comparisons) and calculated the ratio of cross-subject overlap for each vertex on the cortex (**Figure 3B**). Both groups had a high degree of connectivity overlap in cortical visual areas, while sighted individuals also exhibited some cross-subject overlap around primary Somatosensory and Motor cortices. There was significantly higher connectivity (**Figure 3C**) in the sighted group around the Pre-and-post Central gyri, Operculum, Insula, Cingulate, and Superior Parietal Lobule (Glasser et al., 2016). EBA of the blind group had stronger connections with the Inferior-lateral Parietal cortex, Lateral Prefrontal cortex, and Precuneus. These areas are canonical to the brain's Default Mode Network (DMN), active during non-task states (Raichle, 2015).

There is a functional disconnection between the blind EBA and sensorimotor cortices

In addition to our whole-brain analysis, we wanted to classify the connectivity strength of the EBA with three visual and five sensorimotor cortical regions (**supplementary Table 6**). We based the categorization of ROIs on the parcellation offered by Glasser et al. (2016) (**Figure 4A**, See methods and **Supplementary Table 3** for detailed description). both groups showed a significant interaction between the EBA and cortical visual areas (**Figure 4B**). no statistical differences were found between the groups in the connectivity strength to the primary visual cortex [t (27) = 0.073, p = 0.942], or to the visual ventral stream [t (27) = 1.514, p = 0.141] and dorsal stream [t (27) = 0.41, p = 0.685]. In stunning contrast, the strength of connectivity to sensorimotor areas was significant in the sighted group and insignificant in the blind group. These findings show that blind participants preserve the intrinsic connectivity of the EBA to visual cortical perceptual areas, while on the other hand, there is a significant decrease in the extrinsic connectivity to sensorimotor cortices. In a direct group comparison, the sighted group showed stronger connectivity between the EBA and the primary motor cortex [t (27) = 3.376, p = 0.002, d = 1.07], primary somatosensory cortex [t (27) = 3.79, $p < 0.001$, d = 1.28], Supplementary motor area [t (27) = 3.796, $p < 0.001$, d = 1.27], premotor cortex [t (27) = 2.91, p = 0.007, d = 0.58], and operculum [t (27) = 3.881, $p < 0.001$, d = 1.42].

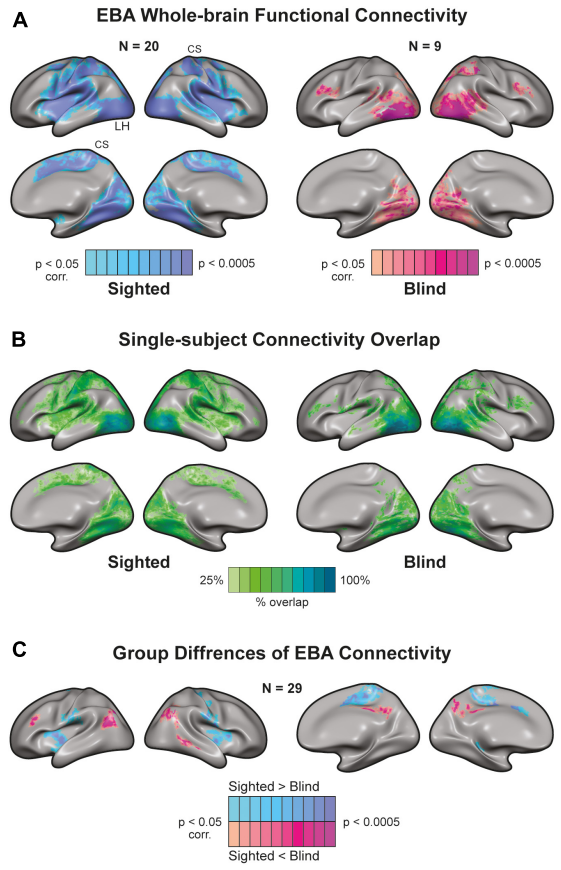

FIGURE 3
Whole-brain connectivity of Extrastriate Body Area (EBA) seed in blind and sighted individuals [random effects General Linear Model (GLM)]. **(A)** There is a high functional connection between the EBA [independent localizer from Human Connectome Project (HCP) atlas] and visual regions in sighted and blind individuals. However, EBA connectivity to sensorimotor areas exhibits a strikingly different picture. EBA has widespread connectivity to sensorimotor cortices in the sighted. Yet, there is a disconnection between EBA and sensorimotor regions in the congenitally blind. CS, central sulcus. **(B)** Single-subject connectivity overlap in sighted and blind groups. We created the probabilistic maps from single-subject EBA connectivity results. Connectivity to visual areas was consistent across blind and sighted participants. In addition, there was a connectivity overlap in the sighted around S1, M1, and associative sensorimotor cortices. **(C)** Group differences of EBA connectivity. The sighted had higher connectivity around sensorimotor regions and weaker connectivity around the Precuneus and lateral Parietal cortex.

Discussion

We studied the action-related function and connectivity of the EBA in both congenitally blind and healthy-sighted adults. We replicated previous results in the sighted and found that the EBA is indeed active during unseen motor actions of the hands and feet. However, the picture was completely different for the blind group, where the EBA did not show a significant response to any body part movements, a sharp contrast to its sensory-independent behavior in perceptual tasks (Heimler and Amedi, 2020). Our analysis of resting-state functional data revealed significant connectivity between EBA and visual cortices in both groups, but a decrease in connectivity between the blind EBA and sensorimotor regions compared to the sighted.

In a previous study, we showed that blind individuals' perception of body-related stimuli results in consistent activity in the EBA (Striem-Amit and Amedi, 2014). Other studies report a similar pattern for other category-selective areas in the visual Ventral and Dorsal streams (Pietrini et al., 2004; Ptito et al., 2005; Poirier et al., 2006; Amedi et al., 2007; Sani et al., 2010; Reich et al., 2011; Abboud et al., 2015). These areas display supramodal behavior, where a specific task defines their function (e.g., perceiving a stimulus with body-related information) and not the input modality (Pascual-Leone and Hamilton, 2001; Heimler et al., 2015; Cecchetti et al., 2016; Hurka et al., 2017; Fine and Park, 2018; Heimler and Amedi, 2020). Here, we found that this supramodal principle does not apply to action-related activity in the EBA. Body-part movements did not activate the EBA in the blind group, even for hand movements that elicit robust activity in the sighted. Additionally, the functional connectivity analysis showed that blind individuals have weaker connections between the EBA and sensorimotor areas, but the blind EBA maintain its internal connectivity profile to other visual cortices. Other supporting findings indicate that the deprived visual cortex of blind individuals maintains its large-scale intrinsic organization (Striem-Amit et al., 2012b, 2015; Butt et al., 2013; Burton et al., 2014; Heine et al., 2015; Bauer et al., 2017), coupled with a decrease in connectivity between visual and sensorimotor cortices (Burton et al., 2014; Striem-Amit and Amedi, 2014; Heine et al., 2015; Bauer et al., 2017).

The discrepancy in the EBA connectivity profile is, at first impression, a little counterintuitive. One might expect that visual deprivation results in weaker functional connections with visual cortices and stable functional connections with non-visual cortices. This assumption would also be consistent with previous findings of neural responses in the blind visual cortex to high-order tasks (Amedi et al., 2003, 2004; Bedny et al., 2011; Bedny, 2017). Instead, we found an absence of connectivity between the EBA and non-visual cortices. In turn, the maintenance of perception-related functions explains the stability within the visual system. A possible interpretation is that EBA engages in visuomotor computations (Orlov et al., 2010) that we need during typical sensory and motor development but are of no use for blind individuals. Differently, Ventral stream areas could have a computational bias for perception-related tasks and even respond to non-visual stimuli in healthy-sighted individuals (Amedi et al., 2001; Sathian, 2005; Lacey et al., 2009; Debowska et al., 2016; Siuda-Krzywicka et al., 2016; Tal et al., 2016; Bola et al., 2017). The differences observed here also point to the source of incoming signals to the EBA during action-related processing. While it is well established that EBA receives visual inputs from the primary Visual cortex via feedforward connections (Lamme and Roelfsema, 2000), the source of neural inputs during motor actions is less clear. One suggestion is that motor-related information travels through direct connections from the Frontoparietal to the Occipital cortices (Gallivan et al., 2013). Our results point to another option that inputs to the EBA are from Parietal and Premotor structures involved in somatosensory and motor processing (Gallivan et al., 2013, 2016; Lingnau and Downing, 2015; Limanowski and Blankenburg, 2016; Orgs et al., 2016; Simos et al., 2017). These types of lateral, rather than feedforward, connections are less hardwired (Fine and Park, 2018). In the blind brain, the lack of co-occurring inputs from

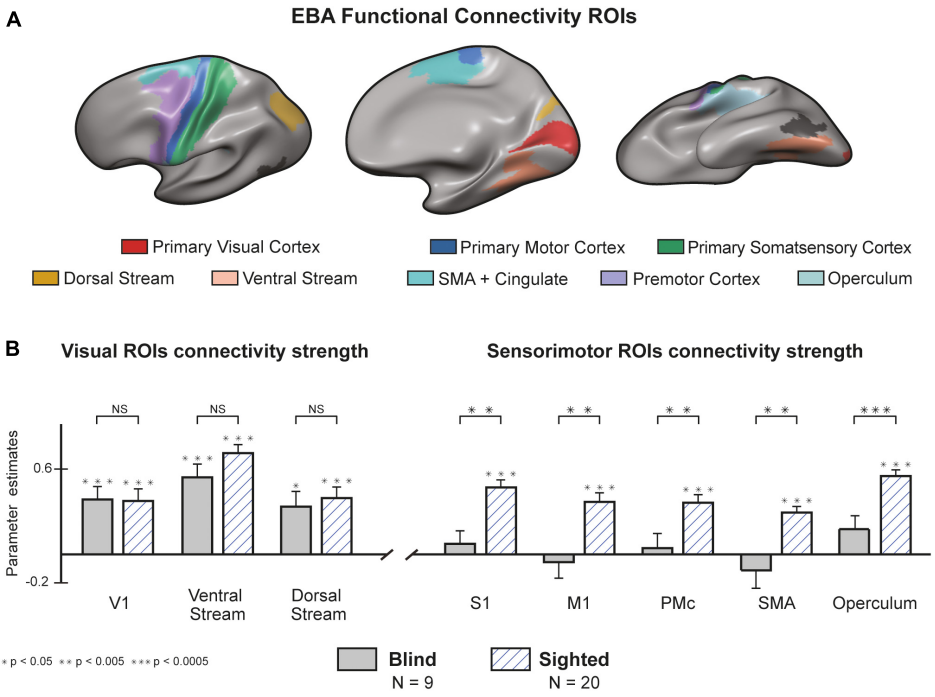

FIGURE 4
There is a functional disconnection between the blind Extrastriate Body Area (EBA) and sensorimotor cortices. **(A)** Regions of Interest (ROIs) from the Human Connectome Project (HCP) atlas (Glasser et al., 2016). A full cytoarchitectural breakdown of each area is in **Supplementary Table 3**. **(B)** Congenital blindness alters EBA's connectivity profile. Seed-to-seed analysis of connectivity strength from the EBA to sensorimotor and visual seeds. In both groups, resting-state connectivity to visual cortices was significantly higher than the baseline. Connectivity to sensorimotor regions was significantly higher in the sighted compared to the blind group (random effects GLM, n = 29). We found similar results when analyzing the connectivity from EBA to the right and left hemispheres separately (**Supplementary Figure 8**). Error bars are for the standard error. Large asterisks indicate between-group significance, small asterisks indicate within-group significance against the baseline. NS, non-significant.

visual and proprioceptive sensations into EBA would erode these weaker connections. Oppositely, EBA maintains its perceptual-related function through feedforward hardwired connections that are the pipeline for perceptual processing (Fine and Park, 2018). These contrasting behaviors also hint at the sensibility of the visual cortex during critical periods. The Occipital lobe might have low sensitivity to visual perceptual experience, which is hardwired, and high sensitivity to visuomotor action-related experience. At the very least, our results show that EBA's motor recruitment is contingent on visual experience and that its function does not depend only on sensorimotor experience.

How does the lack of EBA response in the blind inform us about EBA's role in motor-related processing in the sighted? Our findings suggest that EBA holds a whole-body motor representation. In sighted individuals, unilateral movements result in bilateral activations of EBA, especially for hand and foot movements. Unlike the typical contralateral or ipsilateral motor responses, each unilateral EBA computes information about both sides of the body, with an emphasis on the limbs. Moreover, action-related activity in bilateral EBA has been shown to correlate with the usage rate of hand prostheses in unilateral amputates (Van Den Heiligenberg et al., 2018), suggesting a possible connection between EBA function and the perception of limb position. Notably, bilateral EBA is active when participants perceive visual images of body parts (Orlov et al., 2010; Kühn et al., 2011; Gallivan et al., 2013; Zimmermann et al., 2018). These characteristics are beneficial for an EBA that takes part in motor control (Kühn et al., 2011; van Nuenen et al., 2012; Gallivan and Culham, 2015; Zimmermann et al., 2016) and predictive processing of sensory information (Astafiev et al., 2004; Orlov et al., 2010; Gallivan et al., 2013). Under the predictive processing theory, the brain generates representations to predict future sensory inputs (Keller and Mrsic-Flogel, 2018) and continuously compares these predictions to actual sensory inputs. The resulting error updates an internal representation that culminates in perception. EBA's activity patterns fit this framework, being active during active (Astafiev et al., 2004; Gallivan et al., 2013, 2016; Zimmermann et al., 2016; Limanowski et al., 2017) and passive (Limanowski and Blankenburg, 2016) movements and allowing for the decoding of future postures from its activity during motor planning (Kühn et al., 2011; Gallivan et al., 2013, 2016; Orgs et al., 2016; Zimmermann et al., 2016). Furthermore, visuo-proprioceptive incongruences decrease EBA's effective connectivity to Parietal cortices (Limanowski and Blankenburg, 2017), which may reflect a breakdown in the prediction process. The internal representation is thus available before and while incoming sensory information reaches the brain (Keller and Mrsic-Flogel, 2018), covering the duration of stimulus expectation and perception. Finally, EBA has strong connections with primary Sensorimotor and associative cortices, which are the source and target of information for the internal model (Keller and Mrsic-Flogel, 2018). Concerning our results, the EBA could provide a multimodal representation that predicts incoming visual information. EBA activity during unseen movement in the sighted reflects the recruitment of large networks that expects incoming

sensory information, even if it is not there. In congenital blindness, this internal model becomes redundant as visual information is unavailable.

In conclusion, our findings demonstrate that EBA's motor-related responses are contingent on visual experience and are absent in congenitally blind individuals. We provide initial steps toward studying plastic changes to action-related functions in the deprived visual cortex. Additionally, this work furthers our understanding of the EBA's dependence on visual information and experience in sighted individuals.

Data availability statement

The raw data supporting the conclusions of this article will be made available by the authors, without undue reservation.

Ethics statement

The studies involving human participants were reviewed and approved by Hadassah Medical Center, the Hebrew University of Jerusalem. The patients/participants provided their written informed consent to participate in this study.

Author contributions

OY and AA: conceptualization and validation. OY: data curation, formal analysis, methodology, visualization, and writing—original draft. AA: funding acquisition and supervision. OY and ZT: investigation and project administration. OY, ZT, and AA: reviewing, editing, and approving the submitted version.

Funding

This study was received funding from the European Research Council (ERC) under the EU Horizon 2020 Research and Innovation Programme (grant no. 773121), the EU Horizon 2020 FET Proactive (GuestXR, grant no. 101017884), and the Joy Ventures "Sphere-sound-body" grant.

Conflict of interest

The authors declare that the research was conducted in the absence of any commercial or financial relationships that could be construed as a potential conflict of interest.

Publisher's note

All claims expressed in this article are solely those of the authors and do not necessarily represent those of their affiliated organizations, or those of the publisher, the editors and the reviewers. Any product that may be evaluated in this article, or claim that may be made by its manufacturer, is not guaranteed or endorsed by the publisher.

Supplementary material

The Supplementary Material for this article can be found online at: https://www.frontiersin.org/articles/10.3389/fnins.2023.973525/full#supplementary-material

References

Abboud, S., Maidenbaum, S., Dehaene, S., and Amedi, A. (2015). A number-form area in the blind. *Nat. Commun.* 6:6026. doi: 10.1038/ncomms7026

Amedi, A., Floel, A., Knecht, S., Zohary, E., and Cohen, L. G. (2004). Transcranial magnetic stimulation of the occipital pole interferes with verbal processing in blind subjects. *Nat. Neurosci.* 7, 1266–1270. doi: 10.1038/nn1328

Amedi, A., Jacobson, G., Hendler, T., Malach, R., and Zohary, E. (2002). Convergence of visual and tactile shape processing in the human lateral occipital complex. *Cereb. Cortex* 12, 1202–1212. doi: 10.1093/cercor/12.11.1202

Amedi, A., Malach, R., Hendler, T., Peled, S., and Zohary, E. (2001). Visuo-haptic object-related activation in the ventral visual pathway. *Nat. Neurosci.* 4, 324–330. doi: 10.1038/85201

Amedi, A., Raz, N., Pianka, P., Malach, R., and Zohary, E. (2003). Early "visual" cortex activation correlates with superior verbal memory performance in the blind. *Nat. Neurosci.* 6, 758–766. doi: 10.1038/nn1072

Amedi, A., Stern, W. M., Camprodon, J. A., Bermpohl, F., Merabet, L., Rotman, S., et al. (2007). Shape conveyed by visual-to-auditory sensory substitution activates the lateral occipital complex. *Nat. Neurosci.* 10, 687–689. doi: 10.1038/nn1912

Astafiev, S. V., Stanley, C. M., Shulman, G. L., and Corbetta, M. (2004). Extrastriate body area in human occipital cortex responds to the performance of motor actions. *Nat. Neurosci.* 7, 542–548. doi: 10.1038/nn1241

Bauer, C. M., Hirsch, G. V., Zajac, L., Koo, B. B., Collignon, O., and Merabet, L. B. (2017). Multimodal MR-imaging reveals large-scale structural and functional connectivity changes in profound early blindness. *PLoS One* 12:e0173064. doi: 10.1371/journal.pone.0173064

Bedny, M. (2017). Evidence from blindness for a cognitively pluripotent cortex. *Trends Cogn. Sci.* 21, 637–648. doi: 10.1016/j.tics.2017.06.003

Bedny, M., Pascual-Leone, A., Dodell-Feder, D., Fedorenko, E., and Saxe, R. (2011). Language processing in the occipital cortex of congenitally blind adults. *Proc. Natl. Acad. Sci. U.S.A.* 108, 4429–4434. doi: 10.1073/pnas.1014818108

Bola, Ł, Siuda-Krzywicka, K., Paplińska, M., Sumera, E., Zimmermann, M., Jednoróg, K., et al. (2017). Structural reorganization of the early visual cortex following Braille training in sighted adults. *Sci. Rep.* 7, 1–12. doi: 10.1038/s41598-017-17738-8

Burton, H., Snyder, A. Z., and Raichle, M. E. (2014). Resting state functional connectivity in early blind humans. *Front. Syst. Neurosci.* 8:51. doi: 10.3389/fnsys.2014.00051

Butt, O. H., Benson, N. C., Datta, R., and Aguirre, G. K. (2013). The fine-scale functional correlation of striate cortex in sighted and blind people. *J. Neurosci.* 33, 16209–16219. doi: 10.1523/JNEUROSCI.0363-13.2013

Cecchetti, L., Kupers, R., Ptito, M., Pietrini, P., and Ricciardi, E. (2016). Are supramodality and cross-modal plasticity the yin and yang of brain development? From blindness to rehabilitation. *Front. Syst. Neurosci.* 10:89. doi: 10.3389/fnsys.2016.00089

Collignon, O., Vandewalle, G., Voss, P., Albouy, G., Charbonneau, G., Lassonde, M., et al. (2011). Functional specialization for auditory-spatial processing in the occipital cortex of congenitally blind humans. *Proc. Natl. Acad. Sci. U.S.A.* 108, 4435–4440. doi: 10.1073/pnas.1013928108

Debowska, W., Wolak, T., Nowicka, A., Kozak, A., Szwed, M., and Kossut, M. (2016). Functional and structural neuroplasticity induced by short-term tactile

training based on braille reading. *Front. Neurosci.* 10:460. doi: 10.3389/fnins.2016.00460

Dinstein, I., Hasson, U., Rubin, N., and Heeger, D. J. (2007). Brain areas selective for both observed and executed movements. *J. Neurophysiol.* 98, 1415–1427. doi: 10.1152/jn.00238.2007

Downing, P. E. (2001). A cortical area selective for visual processing of the human body. *Science* 293, 2470–2473. doi: 10.1126/science.1063414

Ferri, S., Kolster, H., Jastorff, J., and Orban, G. A. (2013). The overlap of the EBA and the MT/V5 cluster. *Neuroimage* 66, 412–425. doi: 10.1016/j.neuroimage.2012.10.060

Fine, I., and Park, J.-M. (2018). Blindness and Human Brain Plasticity. *Annu. Rev. Vis. Sci.* 4, 337–356. doi: 10.1146/annurev-vision-102016-061241

Frost, M. A., and Goebel, R. (2012). Measuring structural–functional correspondence: Spatial variability of specialised brain regions after macro-anatomical alignment. *Neuroimage* 59, 1369–1381. doi: 10.1016/j.neuroimage.2011.08.035

Gallivan, J. P., and Culham, J. C. (2015). Neural coding within human brain areas involved in actions. *Curr. Opin. Neurobiol.* 33, 141–149. doi: 10.1016/j.conb.2015.03.012

Gallivan, J. P., Chapman, C. S., Mclean, D. A., Flanagan, J. R., and Culham, J. C. (2013). Activity patterns in the category-selective occipitotemporal cortex predict upcoming motor actions. *Eur. J. Neurosci.* 38, 2408–2424. doi: 10.1111/ejn.12215

Gallivan, J. P., Johnsrude, I. S., and Randall Flanagan, J. (2016). Planning ahead: Object-directed sequential actions decoded from human frontoparietal and occipitotemporal networks. *Cereb. Cortex* 26, 708–730. doi: 10.1093/cercor/bhu302

Gentile, G., Björnsdotter, M., Petkova, V. I., Abdulkarim, Z., and Ehrsson, H. H. (2015). Patterns of neural activity in the human ventral premotor cortex reflect a whole-body multisensory percept. *Neuroimage* 109, 328–340. doi: 10.1016/j.neuroimage.2015.01.008

Glasser, M. F., Coalson, T. S., Robinson, E. C., Hacker, C. D., Harwell, J., Yacoub, E., et al. (2016). A multi-modal parcellation of human cerebral cortex. *Nature* 536, 171–178. doi: 10.1038/nature18933

Goodale, M. A., and Milner, A. D. (1992). Separate visual pathways for perception and action. *Trends Neurosci.* 15, 20–25. doi: 10.1016/0166-2236(92)90344-8

Heimler, B., and Amedi, A. (2020). Are critical periods reversible in the adult brain? Insights on cortical specializations based on sensory deprivation studies. *Neurosci. Biobehav. Rev.* 116, 494–507. doi: 10.1016/j.neubiorev.2020.06.034

Heimler, B., Striem-amit, E., and Amedi, A. (2015). Origins of task-specific sensory-independent organization in the visual and auditory brain?: Neuroscience evidence, open questions and clinical implications ScienceDirect implications. *Curr. Opin. Neurobiol.* 35, 169–177. doi: 10.1016/j.conb.2015.09.001

Heine, L., Bahri, M. A., Cavaliere, C., Soddu, A., Laureys, S., Ptito, M., et al. (2015). Prevalence of increases in functional connectivity in visual, somatosensory and language areas in congenital blindness. *Front. Neuroanat.* 9:86. doi: 10.3389/fnana.2015.00086

Hensch, T. K. (2004). Critical period regulation. *Annu. Rev. Neurosci.* 27, 549–579. doi: 10.1146/annurev.neuro.27.070203.144327

Hofstetter, S., and Dumoulin, S. O. (2021). Tuned neural responses to haptic numerosity in the putamen. *Neuroimage* 238:118178. doi: 10.1016/j.neuroimage.2021.118178

Hurka, J., Vanden, Van Baelena, M., and Beecka, H. P. O. (2017). Development of visual category selectivity in ventral visual cortex does not require visual experience. *Proc. Natl. Acad. Sci. U.S.A.* 114, E4501–E4510. doi: 10.1073/pnas.1612862114

Keller, G. B., and Mrsic-Flogel, T. D. (2018). Predictive processing: A canonical cortical computation. *Neuron* 100, 424–435. doi: 10.1016/j.neuron.2018.10.003

Knudsen, E. I. (2004). Sensitive periods in the development of the brain and behavior. *J. Cogn. Neurosci.* 16, 1412–1425. doi: 10.1162/0898929042304796

Kühn, S., Keizer, A. W., Rombouts, S. A. R. B., and Hommel, B. (2011). The functional and neural mechanism of action preparation: Roles of EBA and FFA in voluntary action control. *J. Cogn. Neurosci.* 23, 214–220. doi: 10.1162/jocn.2010.21418

Kupers, R., and Ptito, M. (2014). Compensatory plasticity and cross-modal reorganization following early visual deprivation. *Neurosci. Biobehav. Rev.* 41, 36–52. doi: 10.1016/j.neubiorev.2013.08.001

Lacey, S., Tal, N., Amedi, A., and Sathian, K. (2009). A putative model of multisensory object representation. *Brain Topogr.* 21, 269–274. doi: 10.1007/s10548-009-0087-4

Lamme, V. A. F., and Roelfsema, P. R. (2000). The distinct modes of vision offered by feedforward and recurrent processing. *Trends Neurosci.* 23, 571–579. doi: 10.1016/S0166-2236(00)01657-X

Limanowski, J., and Blankenburg, F. (2016). Integration of visual and proprioceptive limb position information in human posterior parietal, premotor, and extrastriate cortex. *J. Neurosci.* 36, 2582–2589. doi: 10.1523/JNEUROSCI.3987-15.2016

Limanowski, J., and Blankenburg, F. (2017). Posterior parietal cortex evaluates visuoproprioceptive congruence based on brief visual information. *Sci. Rep.* 7:16659. doi: 10.1038/s41598-017-16848-7

Limanowski, J., Kirilina, E., and Blankenburg, F. (2017). Neuronal correlates of continuous manual tracking under varying visual movement feedback in a virtual reality environment. *Neuroimage* 146, 81–89. doi: 10.1016/j.neuroimage.2016.11.009

Lingnau, A., and Downing, P. E. (2015). The lateral occipitotemporal cortex in action. *Trends Cogn. Sci.* 19, 268–277. doi: 10.1016/j.tics.2015.03.006

Mattioni, S., Rezk, M., Battal, C., Bottini, R., Mendoza, K. E. C., Oosterhof, N. N., et al. (2020). Categorical representation from sound and sight in the ventral occipito-temporal cortex of sighted and blind. *eLife* 9, 1–33. doi: 10.7554/eLife.50732

Orgs, G., Dovern, A., Hagura, N., Haggard, P., Fink, G. R., and Weiss, P. H. (2016). Constructing visual perception of body movement with the motor cortex. *Cereb. Cortex* 26, 440–449. doi: 10.1093/cercor/bhv262

Orlov, T., Makin, T. R., and Zohary, E. (2010). Topographic representation of the human body in the occipitotemporal cortex. *Neuron* 68, 586–600. doi: 10.1016/j.neuron.2010.09.032

Pascual-Leone, A., and Hamilton, R. (2001). "The metamodal organization of the brain," in *Progress in brain research*, eds C. Casanova and M. Ptito (Amsterdam: Elsevier), 427–445. doi: 10.1016/S0079-6123(01)34028-1

Peelen, M. V., and Downing, P. E. (2005). Is the extrastriate body area involved in motor actions? *Nat. Neurosci.* 8, 125–126. doi: 10.1038/nn0205-125b

Penfield, W., and Boldrey, E. (1937). Somatic motor and sensory representation in the cerbral cortex of mam as studied by electrical stimulation. *Brain* 60, 389–443.

Pietrini, P., Furey, M. L., Ricciardi, E., Gobbini, M. I., Wu, W.-H. C., Cohen, L., et al. (2004). Beyond sensory images: Object-based representation in the human ventral pathway. *Proc. Natl. Acad. Sci. U.S.A.* 101, 5658–5663. doi: 10.1073/pnas.0400707101

Poirier, C., Collignon, O., Scheiber, C., Renier, L., Vanlierde, A., Tranduy, D., et al. (2006). Auditory motion perception activates visual motion areas in early blind subjects. *Neuroimage* 31, 279–285. doi: 10.1016/j.neuroimage.2005.11.036

Ptito, M., Moesgaard, S. M., Gjedde, A., and Kupers, R. (2005). Cross-modal plasticity revealed by electrotactile stimulation of the tongue in the congenitally blind. *Brain* 128, 606–614. doi: 10.1093/brain/awh380

Raichle, M. E. (2015). The Brain's default mode network. *Annu. Rev. Neurosci.* 38, 433–447. doi: 10.1146/annurev-neuro-071013-014030

Reich, L., Maidenbaum, S., and Amedi, A. (2012). The brain as a flexible task machine. *Curr. Opin. Neurol.* 25, 86–95. doi: 10.1097/WCO.0b013e32834ed723

Reich, L., Szwed, M., Cohen, L., and Amedi, A. (2011). A ventral visual stream reading center independent of visual experience. *Curr. Biol.* 21, 363–368. doi: 10.1016/j.cub.2011.01.040

Renier, L. A., Anurova, I., De Volder, A. G., Carlson, S., VanMeter, J., and Rauschecker, J. P. (2010). Preserved functional specialization for spatial processing in the middle occipital gyrus of the early blind. *Neuron* 68, 138–148. doi: 10.1016/j.neuron.2010.09.021

Sani, L., Ricciardi, E., Gentili, C., Vanello, N., Haxby, J. V., and Pietrini, P. (2010). Effects of visual experience on the human MT+ Functional Connectivity Networks: An fMRI study of motion perception in sighted and congenitally blind individuals. *Front. Syst. Neurosci.* 4:159. doi: 10.3389/fnsys.2010.00159

Sathian, K. (2005). Visual cortical activity during tactile perception in the sighted and the visually deprived. *Dev. Psychobiol.* 46, 279–286. doi: 10.1002/dev.20056

Sigalov, N., Maidenbaum, S., and Amedi, A. (2016). Reading in the dark: Neural correlates and cross-modal plasticity for learning to read entire words without visual experience. *Neuropsychologia* 83, 149–160.

Simos, P. G., Kavroulakis, E., Maris, T., Papadaki, E., Boursianis, T., Kalaitzakis, G., et al. (2017). Neural foundations of overt and covert actions. *Neuroimage* 152, 482–496. doi: 10.1016/j.neuroimage.2017.03.036

Siuda-Krzywicka, K., Bola, Ł, Paplinska, M., Sumera, E., Jednorog, K., Marchewka, A., et al. (2016). Massive cortical reorganization in sighted braille readers. *eLife* 5, 1–26. doi: 10.7554/eLife.10762

Striem-Amit, E., and Amedi, A. (2014). Visual cortex extrastriate body-selective area activation in congenitally blind people "Seeing" by using sounds. *Curr. Biol.* 24, 687–692. doi: 10.1016/j.cub.2014.02.010

Striem-Amit, E., Dakwar, O., Reich, L., and Amedi, A. (2012b). The large-scale organization of "visual" streams emerges without visual experience. *Cereb. Cortex* 22, 1698–1709. doi: 10.1093/cercor/bhr253

Striem-Amit, E., Cohen, L., Dehaene, S., and Amedi, A. (2012a). Reading with sounds: Sensory substitution selectively activates the visual word form area in the blind. *Neuron* 76, 640–652. doi: 10.1016/j.neuron.2012.08.026

Striem-Amit, E., Ovadia-Caro, S., Caramazza, A., Margulies, D. S., Villringer, A., and Amedi, A. (2015). Functional connectivity of visual cortex in the blind follows retinotopic organization principles. *Brain* 138, 1679–1695. doi: 10.1093/brain/awv083

Strnad, L., Peelen, M. V., Bedny, M., and Caramazza, A. (2013). Multivoxel pattern analysis reveals auditory motion information in MT+ of both congenitally blind and sighted individuals. *PLoS One* 8:e63198. doi: 10.1371/journal.pone.0063198

Tal, Z., Geva, R., and Amedi, A. (2016). The origins of metamodality in visual object area LO: Bodily topographical biases and increased functional connectivity to S1. *Neuroimage* 127, 363–375. doi: 10.1016/j.neuroimage.2015.11.058

Tal, Z., Geva, R., and Amedi, A. (2017). Positive and negative somatotopic BOLD responses in contralateral versus ipsilateral penfield homunculus. *Cereb. Cortex* 27, 962–980. doi: 10.1093/cercor/bhx024

Van Den Heiligenberg, F. M. Z., Orlov, T., MacDonald, S. N., Duff, E. P., Henderson Slater, D., Beckmann, C. F., et al. (2018). Artificial limb representation in amputees. *Brain* 141, 1422–1433. doi: 10.1093/brain/awy054

van Essen, D. C., Smith, J., Glasser, M. F., Elam, J., Donahue, C. J., Dierker, D. L., et al. (2017). The brain analysis library of spatial maps and atlases (BALSA) database. *Neuroimage* 144, 270–274. doi: 10.1016/j.neuroimage.2016.04.002

van Nuenen, B. F. L., Helmich, R. C., Buenen, N., van de Warrenburg, B. P. C., Bloem, B. R., and Toni, I. (2012). Compensatory activity in the extrastriate body area of Parkinson's disease patients. *J. Neurosci.* 32, 9546–9553. doi: 10.1523/JNEUROSCI.0335-12.2012

Wang, X., Peelen, M. V., Han, Z., He, C., Caramazza, A., Bi, Y., et al. (2015). How visual is the visual cortex? comparing connectional and functional fingerprints between congenitally blind and sighted individuals. *J. Neurosci.* 35, 12545–12559. doi: 10.1523/jneurosci.3914-14.2015

Zeharia, N., Hertz, U., Flash, T., and Amedi, A. (2012). Negative blood oxygenation level dependent homunculus and somatotopic information in primary motor cortex and supplementary motor area. *Proc. Natl. Acad. Sci. U.S.A.* 109, 18565–18570. doi: 10.1073/pnas.1119125109

Zimmermann, M., Mars, R. B., de Lange, F. P., Toni, I., and Verhagen, L. (2018). Is the extrastriate body area part of the dorsal visuomotor stream? *Brain Struct. Funct.* 223, 31–46. doi: 10.1007/s00429-017-1469-0

Zimmermann, M., Verhagen, L., de Lange, F. P., and Toni, I. (2016). The extrastriate body area computes desired goal states during action planning. *eNeuro* 3, 1918–1921. doi: 10.1523/ENEURO.0020-16.2016

frontiers | Frontiers in Neuroscience

TYPE Original Research
PUBLISHED 06 October 2023
DOI 10.3389/fnins.2023.1132088

OPEN ACCESS

EDITED BY
Maurice Ptito,
Montreal University, Canada

REVIEWED BY
Daniel-Robert Chebat,
Ariel University, Israel
Matteo Diano,
University of Turin, Italy

*CORRESPONDENCE
Beatrice de Gelder
✉ b.degelder@maastrichtuniversity.nl

RECEIVED 26 December 2022
ACCEPTED 05 September 2023
PUBLISHED 06 October 2023

CITATION
Vaessen M, Van der Heijden K and de Gelder B (2023) Modality-specific brain representations during automatic processing of face, voice and body expressions.
Front. Neurosci. 17:1132088.
doi: 10.3389/fnins.2023.1132088

Modality-specific brain representations during automatic processing of face, voice and body expressions

Maarten Vaessen[1], Kiki Van der Heijden[2] and Beatrice de Gelder[3]*

[1]Zuyd University of Applied Science, Maastricht, Netherlands, [2]Radboud University, Nijmegen, Netherlands, [3]Maastricht University, Maastricht, Netherlands

A central question in affective science and one that is relevant for its clinical applications is how emotions provided by different stimuli are experienced and represented in the brain. Following the traditional view emotional signals are recognized with the help of emotion concepts that are typically used in descriptions of mental states and emotional experiences, irrespective of the sensory modality. This perspective motivated the search for abstract representations of emotions in the brain, shared across variations in stimulus type (face, body, voice) and sensory origin (visual, auditory). On the other hand, emotion signals like for example an aggressive gesture, trigger rapid automatic behavioral responses and this may take place before or independently of full abstract representation of the emotion. This pleads in favor specific emotion signals that may trigger rapid adaptative behavior only by mobilizing modality and stimulus specific brain representations without relying on higher order abstract emotion categories. To test this hypothesis, we presented participants with naturalistic dynamic emotion expressions of the face, the whole body, or the voice in a functional magnetic resonance (fMRI) study. To focus on automatic emotion processing and sidestep explicit concept-based emotion recognition, participants performed an unrelated target detection task presented in a different sensory modality than the stimulus. By using multivariate analyses to assess neural activity patterns in response to the different stimulus types, we reveal a stimulus category and modality specific brain organization of affective signals. Our findings are consistent with the notion that under ecological conditions emotion expressions of the face, body and voice may have different functional roles in triggering rapid adaptive behavior, even if when viewed from an abstract conceptual vantage point, they may all exemplify the same emotion. This has implications for a neuroethologically grounded emotion research program that should start from detailed behavioral observations of how face, body, and voice expressions function in naturalistic contexts.

KEYWORDS

multisensory affect, faces, voices, bodies, emotion perception, facial expressions, voice

Introduction

In reasoning about emotion expressions and their functional and brain basis, we tend to use abstract categories and to lump together different signals presumably referring to their shared meaning. Yet the specific conditions of subjective experience of an emotional stimulus in the natural environment often determine which affective signal triggers the adaptive behavior. For

example, an angry body posture alerts us already from a distance while an angry facial expression can only be seen from closer by and personal familiarity may play a role in how we react to it. Thus, the angry body expression viewed from a distance and the angry face expression seen from close by may each trigger a different reaction as adaptive behavior needs to fit the concrete context. Thus, another dimension of emotion signals besides the familiar abstract concept representation is related to their role in adaptive action. Given this essential role in triggering rapid automatic behavioral responses, sensory modality specific, local and context sensitive brain representations may play a role, suggesting that face, body, and voice expression perception may each have sensory modality specific emotion representations. Such a functional brain representation of affective signals that is sensitive to the naturalistic spatiotemporal contexts may exist besides the abstract higher order concept representations traditionally envisaged by emotion theorists (Ekman and Cordaro, 2011; but see Lindquist et al., 2012). Emotion perception in naturalistic conditions is often driven by a specific context that is relative to a behavioral goal. This specific context includes aspects that are currently not yet envisaged in human emotion research like for example the spatial parameters that matter for threat perception (de Borst et al., 2020) and convey a different behavioral status to signals from face, the body and the voice that, from an abstract vantage point, all have the same meaning. For example, since facial expressions can only be seen from sufficiently close by, decoding of facial expression may rely on processes related to personal memory more than this is the case for perception of voice or body expressions.

Previous studies comparing how the face, or the face and the voice and only in a few cases also the whole body convey emotions were motivated to find the common representations, variously referred amodal, supramodal or abstract, underlying these different expressions. They concentrated on where in the brain abstract representations of emotion categories are to be found (Peelen et al., 2010; Klasen et al., 2011). Such representations were found in high-level brain areas known for their role in categorization of mental states (Peelen et al., 2010). Specifically, medial prefrontal cortex (MPFC) and superior temporal cortex (STS) have been highlighted as representing emotions perceived in the face, voice, or body at a modality-independent level. Furthermore, these supramodal or abstract emotion representations presumably play an important role in multisensory integration by driving and sustaining convergence of the sensory inputs toward an amodal emotion representation (Gerdes et al., 2014). However, the existence of supramodal emotion representations was based on measurements of brain activity during explicit emotion recognition (Peelen et al., 2010; Klasen et al., 2011). As emotion perception in daily life is often automatic and rapid, it remains unclear whether supramodal emotion representations also emerge in the absence of explicit emotion processing.

To clarify the goal of our study it is important to distinguish the investigation of perpetual representations of emotion signals from studies on the neural basis of emotional experience, on how reward related processes are involved in processes shaping behavioral reactions and many related questions (Rolls, 2014, 2019). Clearly, perceptual representations of emotion signals do not be themselves define the emotional experience, its neural or its phenomenal basis. Other non-sensory brain areas like importantly orbitofrontal cortex are involved in defining how perception of an emotional signal ultimately gives rise to experience and behavior but these higher order issues are out of the scope of the present study.

To increase the ecological validity of our study of emotion processing in the human brain, we used naturalistic dynamic stimuli showing various emotion expressions of the body, the face or the voice. Importantly, to avoid explicit emotion recognition and verbal labeling, neither of which are normally part of daily emotion perception, participants performed a task related to another modality than that of the stimulus of interest. We used multivariate pattern analysis to identify cortical regions containing representations of emotion and to assess whether emotion representations were of supramodal nature or specific to the modality or stimulus. Following the literature we defined abstract or supramodal representation areas as regions that code what is common to a given emotion category regardless of the sensory modalities and thus have neither stimulus nor modality specific components. Our results show that during such automatic, implicit emotion processing, neuronal response patterns for varying emotions are differentiable within each stimulus type (i.e., face, body, or voice) but not across the stimulus types. This indicates that the brain represents emotions in a stimulus type and modality specific manner during implicit, ecologically valid emotion processing, as seemingly befits the requirements of rapid adaptive behavior.

Methods

Participants

Thirteen healthy participants (mean age = 25.3y; age range = 21–30y; two males) took part in the study. Participants reported no neurological or hearing disorders. Ethical approval was provided by the Ethical Committee of the Faculty of Psychology and Neuroscience at Maastricht University. Written consent was obtained from all participants. The experiment was carried out in accordance with the Declaration of Helsinki. Participants either received credit points or were reimbursed with a monetary reward after their participation in the scan session.

Stimuli

Stimuli consisted of color video and audio clips of four male actors expressing three different emotional reactions to specific events (e.g., fear in a car accident or happiness at a party). Images of such events were shown to the actors during their video recordings with the goal of triggering spontaneous and natural reactions of anger, fear, happiness, and an additional neutral reaction. Importantly, the vocal recordings were acquired simultaneously with the bodily or facial expression to obtain the most natural match between visual and auditory material. A full description of the recording procedure, the validation and the video selection is given in Kret et al. (2011a), see Figure 1 top panel for several examples of the stimulus set. In total there were 16 video clips of facial expressions, 16 video clips of body expressions, and 32 audio clips of vocal expressions, half of which were recorded in combination with the facial expressions and half of which were recorded in combination with the body expressions (i.e., two audio clips per emotional expression per actor). All actors were dressed in black and filmed against a green background under controlled lighting conditions.

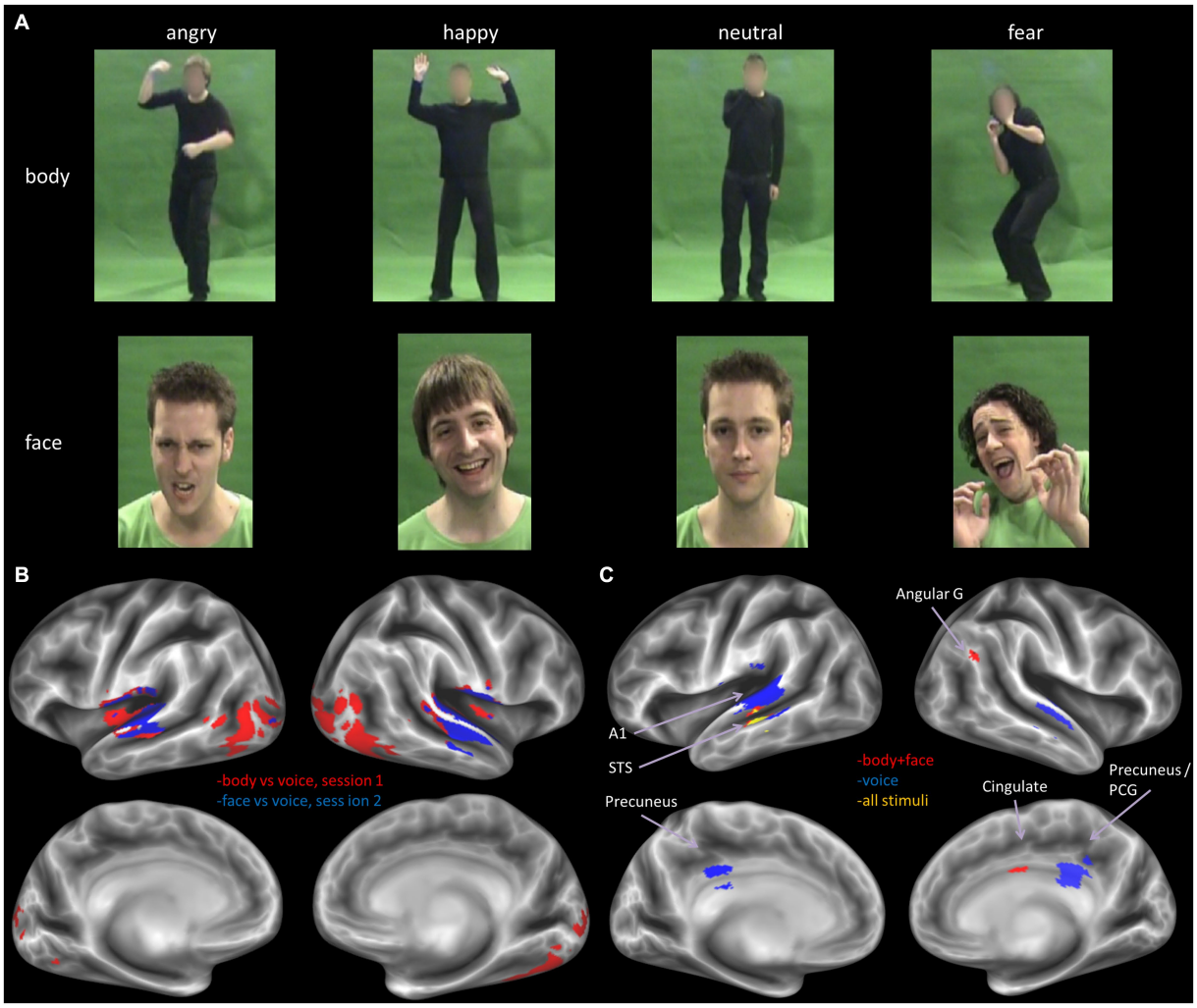

FIGURE 1
(A) Example stimuli from the body (top row) and face (middle row) set. The full set of stimuli can be accessed at: https://osf.io/7d83r/?view_only=a772df287d5a42d1ae7269d1eec4a14e. **(B)** Decoder trained to classify stimulus type, for the two sessions separately, results derived from thresholding the volume map at $p < 0.05$, FWE corrected. **(C)** Decoder trained to classify emotion from all stimuli (yellow), all visual stimuli (face and body, red) and all voice stimuli (blue), The displayed results are label maps derived from the volume map thresholded at $p < 0.001$ uncorrected, with a minimum cluster size threshold of $k = 25$ voxels. Angular G, angular gyrus; A1, primary auditory cortex; STS, superior temporal cortex; PCG, posterior cingulate gyrus.

Video clips were computer-edited using Ulead, After Effects, and Lightworks (EditShare). For the body stimuli, faces of actors were blurred with a Gaussian mask such that only the information of the body was available. The validity of the emotional expressions in the video clips was measured with a separate emotion recognition experiment (emotion recognition accuracy >80%). For more information regarding the recording and validation of these stimuli, see Kret et al. (2011a,b).

Experimental design and behavioral task

In a slow-event related design, participants viewed series of 1 s video clips on a projector screen or listened to series of 1 s audio clips through MR-compatible ear buds (Sensimetrics S14) equipped with sound attenuating circumaural muffs (attenuation >29 dB). The experiment consisted of 12 runs divided over 2 scan sessions. Six runs consisted of face and voice stimuli, followed by six runs consisting of body and voice stimuli. Each run was split in two halves where either *auditory* (consisting of 18 audio clips) or *visual* (consisting of 18 video clips) stimuli were presented. The 18 trials within each run half comprised 16 regular trials (consisting of 4 times 3 different emotion expressions and 4 times one neutral expression,) with an inter-stimulus interval of 10.7–11.3 s and two catch trials requiring a response. This design of using an orthogonal task was selected to divert attention from the modality of interest by blocking explicit recognition of the emotional expression and tap into automatic perception of the affective content (Vroomen et al., 2001; Rolls et al., 2006). The task instructions stipulated whether attention was to be allocated to the visual or to the auditory modality. During visual stimulus presentations, participants were instructed to detect an auditory change, and during auditory stimulus presentations,

participants were instructed to detect visual change catch trials. For the auditory catch trial task, a frequency modulated tone was presented and participants had to respond whether the direction of frequency modulation was up or down. For the visual distractor task, participants indicated whether the fixation cross turned lighter or darker during the trial. A separate localizer session was also performed where participants passively viewed stimuli of faces, bodies, houses, tools and words in blocks; see Zhan et al. (2018) for details.

Data acquisition

We measured blood-oxygen level-dependent (BOLD) signals with a 3 Tesla Siemens Trio whole body MRI scanner at the Scannexus MRI scanning facilities at Maastricht University (Scannexus, Maastricht). Functional images of the whole brain were obtained using T2*-weighted 2D echo-planar imaging (EPI) sequences [number of slices per volume = 50, 2 mm in-plane isotropic resolution, repetition time (TR) = 3,000 ms, echo time (TE) = 30 ms, flip angle (FA) = 90°, field of view (FoV) = 800 × 800 mm^2, matrix size = 100 × 100, multi-band acceleration factor = 2, number of volumes per run = 160, total scan time per run = 8 min]. A three-dimensional (3D) T1-weighted (MPRAGE) imaging sequence was used to acquire high-resolution structural images for each of the participants [1-mm isotropic resolution, TR = 2,250 ms, TE = 2.21 ms, FA = 9°, matrix size = 256 × 256, total scan time = 7 min approx.]. The functional localizer scan also used a T2*-weighted 2D EPI sequence [number of slices per volume = 64, 2 mm in-plane isotropic resolution, TR = 2,000 ms, TE = 30 ms, FA = 77, FoV = 800 × 800 mm^2, matrix size = 100 × 100, multi-band acceleration factor = 2, number of volumes per run = 432, total scan time per run = 14 min approx.].

Analysis

Pre-processing

Data were preprocessed and analyzed with BrainVoyager QX (Brain Innovation, Maastricht, Netherlands) and custom Matlab code (Mathworks, United States) (Hausfeld et al., 2012, 2014). Preprocessing of functional data consisted of 3D motion correction (trilinear/sync interpolation using the first volume of the first run as reference), temporal high pass filtering (thresholded at five cycles per run), and slice time correction. We co-registered functional images to the anatomical T1-weighted image obtained during the first scan session and transformed anatomical and functional data to the default Talairach template.

Univariate analysis

We estimated a random-effects General Linear Model (RFX GLM) in BrainVoyager 21.2[1] with a predictor for each stimulus condition of interest (12 conditions in total): four emotion conditions times three stimulus categories (face, body, voice). Additionally, we included predictors for the trials indicating the start of a new block and the catch trials. Predictors were created by convolving stimulus predictors with the canonical hemodynamic function. Finally, we included six motion parameters resulting from the motion correction as predictors of no interest. For this analysis, data was spatially smoothed with a 6 mm full-width half-maximum (FWMH) Gaussian kernel. To assess where in the brain the two different experimental factors had an influence, an ANOVA was run with either modality or emotion as a factor.

Multivariate analysis

We first estimated beta parameters for each stimulus trial and participant with custom MATLAB code by fitting an HRF function with a GLM to each trial in the time series. These beta values were then used as input for a searchlight multivariate pattern analysis (MVPA) with a Gaussian Naïve Bayes classifier (Ontivero-Ortega et al., 2017) which was also performed at the individual level. The searchlight was a sphere with a radius of five voxels. The Gaussian Naïve Bayes classifier is an inherently multi-class probabilistic classifier that performs similar to the much-used Support Vector Machine classifier in most scenarios, but it is computationally more efficient. The classifier was trained to decode (1) stimulus modality (visual or auditory); (2) stimulus emotion (e.g., fear in all stimulus types vs. angry in all stimulus types); (3) within-modality emotion (e.g., body angry vs. body fear); (4) cross-modal emotion (e.g., classify emotion by training on body stimuli and testing on the voice stimuli from the body session). As the GNB classifier is multi-class by design, the accuracies are calculated as the ratio of correct predictions to the total number of predictions regardless of class.

Classification accuracy was computed by averaging the decoding accuracy of all folds of a leave one-run out cross-validation procedure. We tested the significance of the observed decoding accuracies at the group level with a one-sample *t*-test against chance-level and corrected accuracy maps from each participant for multiple comparisons with the SPM Family Wise Error (FWE) procedure at $p < 0.05$ (Penny et al., 2011) (modality chance level = 50%, corresponding to two classes; emotion chance level = 25%, corresponding to four classes) with SPM12.[2] For visualization purposes, the group volume maps were mapped to the cortical surface. As this operation involves resampling the data (during which the original statistical values get lost), surface maps are displayed with discrete label values instead of continuous statistical values. Therefore, we do not include a color bar in the surface map figures.

An additional permutation analysis was performed to further investigate the robustness of the decoding results. In this method, decoding accuracies can be compared to results from permuted emotion labels (i.e., random decoding accuracies) at the *group level*. To accomplish this, we generated a set of randomized results ($n = 100$), by randomly permuting the emotion labels (these randomizations were the same for all participants). For each of the randomizations, the decoding accuracies were calculated for each participant by repeating the full leave one-run out cross-validation procedure of the main method at the single subject level with the randomized labels. These accuracy maps were then tested against the true label accuracies by performing a paired sample *t*-test over participants. By using a

1 https://www.brainvoyager.com/

2 https://www.fil.ion.ucl.ac.uk/spm/software/spm12/

paired *t*-test at the group level, we are able to assess how the true distribution of the decoding accuracies compare to random (supposedly chance level) accuracies at each voxel. Note that this method differs from the standard permutation method where the number of occurrences of the true accuracy being higher than the randomly sampled ones is counted (resulting in a *p*-value for each participant and voxel), but that we use it here because it enables assessing true vs. random accuracies directly at the group level. At the final stage, the t-maps were averaged for all participants resulting in a single averaged *t*-value group map, and thresholded at $t > 3.9$. This map was then qualitatively compared to the t-map of the main analysis described above.

ROI analysis

Lastly, to gain more insight into details of the responses regions known to be relevant for (emotional) sensory processing (V1, fusiform gyrus, EBA, A1 and amygdala), as well as regions known to be important for emotion or multi-modal integration: the STS and mPFC (Peelen et al., 2010), we extracted beta values from these ROIs.

Specifically, we used data of an independent localizer to identify, early visual cortex, rEBA, and rFFA. Multi-sensory regions pSTS and mPFC were located based on an anatomical definition of these areas. That is, we utilized a spherical ROI with a radius of 5 voxels centered on the reported cluster peak locations in Peelen et al. (2010). Finally, the amygdala was identified using an anatomic definition from the SPM Anatomy toolbox atlas where left and right Amygdala were combined in one ROI (Eickhoff et al., 2007). Early auditory cortex was defined bilaterally anatomically by a 5 mm sphere at the peak location for A1 reported in Warrier et al. (2009).

See Table 1 for details on location and size of the ROIs. From the ROI's we made several plots that (1) display the mean beta values for each of the 12 conditions; (2) display the multivoxel representational dissimilarity matrix (Kriegeskorte et al., 2008) constructed by calculating the 1-r (=Pearson's correlation coefficient) distance metric for all pairs of category averaged stimuli. The decoding accuracy of all the ROI voxels for stimulus modality, taken as the average of the accuracies for decoding of body vs. voice (of the body session) and face vs. voice (of face session) conditions is presented in Table 2. This table also includes the decoding accuracies for emotion from all stimuli, voice, face and body separately, and the crossmodal decoding accuracies for training the classifier on one modality (e.g., body emotion) and testing on the voice modality. Statistical results in this table are FDR corrected (Benjamini and Hochberg, 1995).

TABLE 1 Size and location of the ROIs.

ROI	Size	*x*	*y*	*Z*
FFA	1,784	39	−52	−26
EV	4,248	−12	−94	−8
EBA	5,488	45	−67	7
A1 L/R	6,152	−57/56	−17/−17	5/8
MPFC	2,976	11	48	17
pSTS	3,256	−47	−62	8
Amygdala L/R	784	−21/20	−6/−6	−10/−9

Size is in mm^3, location is in MNI coordinates.

Results

Modality-specific processing of face, body, and voice stimuli

First, we performed a univariate analysis of sensory-specific (i.e., visual vs. auditory) and emotion-specific neural processing. Using beta values estimated with an RFX GLM on the entire data set (see Methods), we ran an ANOVA with factors "stimulus type" and "emotion." Our results did not show an interaction between emotion and stimulus type ($p > 0.01$, FDR corrected for multiple comparisons). However, as expected, the F-map for stimulus type (Supplementary Figure S1) revealed significant activation clusters ($p < 0.01$, FDR corrected for multiple comparisons) with differential mean activation across stimulus types in primary and higher-order auditory and visual regions, as well as in motor, pre-motor and dorsal/superior parietal cortex. We did not observe significant activation clusters for emotion ($p > 0.01$, FDR corrected). We then tested whether emotions were processed differentially within stimulus type, i.e., for faces, bodies and voices separately. These ANOVAs did not reveal an effect of emotion for any stimulus type ($p < 0.01$, FDR corrected).

Multivariate pattern analysis of modality related emotion processing

Next, we performed a more sensitive multivariate pattern analysis (MVPA) using a searchlight approach (Ontivero-Ortega et al., 2017; see Methods). We sought to confirm the results of the univariate analysis and to assess whether more fine-grained emotion representations could be revealed either within a specific stimulus type or in a supramodal manner. To this end, we began by training the MVP classifier to decode stimulus type, i.e., visual vs. auditory stimuli. The classifier was trained separately for the two sessions: body vs. voice (session 1) and face vs. voice (session 2). In line with expectations, the classifier could accurately identify stimulus type in auditory and visual sensory cortices (chance level is 50%, $p < 0.05$, FWE corrected for multiple comparisons). In addition, we found clusters of above chance level decoding accuracy in fusiform cortex and large parts of the lateral occipital and temporo-occipital cortex, presumably including the extrastriatal body area (EBA; see Figure 1 bottom panel).

We then tested whether the MVP classifier trained to discriminate emotions on all stimulus types (i.e., face, body and voice combined) could accurately identify emotion from neural response patterns. Yet, like the results of the univariate analysis, we did not find classification accuracies above chance at the group level (that is, at $p < 0.05$, FWE corrected). Thus, while neural response patterns for stimulus type could be differentiated well by a MVP classifier, we did not observe a similarly robust, differentiable representation of emotions across stimulus types.

We then proceeded to evaluate our main hypothesis using the MVP classifier, that is, whether emotion specific representations emerge within modality specific neural response patterns. Specifically, we trained and tested the classifier to decode emotions within a specific stimulus modality. The visual stimulus modality consisted of the combined face and body stimuli and the auditory modality of the voice stimuli. Within the visual modality (i.e., faces and bodies), the

TABLE 2 Decoding accuracies group level *p*-values (FDR corrected) against chance level for the tested ROIs.

	Modality	Emotion	Emotion Body	Emotion Face	Emotion voice session 1	Emotion voice session 2	Emotion body ≥ voice	Emotion voice ≥ body	Emotion face ≥ voice	Emotion voice ≥ face
V1	0.0035	0.5235	0.5854	0.7936	0.5235	0.7002	0.7936	0.8732	0.0968	0.7002
FFA	0.0035	0.7936	0.713	0.893	0.1088	0.6185	0.6203	0.8732	0.7002	0.8147
EBA	0.0018	0.0661	0.3916	0.0968	0.7002	0.7002	0.8818	0.8818	0.7936	0.7936
A1	0	0.0445	0.9008	0.7936	0.2069	0.0168	0.1773	0.8732	0.7002	0.6203
MPFC	0.4624	0.7002	0.5477	0.713	0.5124	0.8392	0.7002	0.7936	0.5235	0.7002
pSTS	0.0445	0.8247	0.7466	0.7936	0.7009	0.7466	0.7002	0.7936	0.5124	0.7002
LR amy	0.689	0.6203	0.7936	0.8871	0.5854	0.0661	0.7002	0.168	0.5656	0.0968

Beta values of responses to the stimuli were extracted from an ROI and used to train and test a decoder on stimulus type and emotion from all stimuli or from a specific type and for crossmodal decoding. For these the header reading x ≥ y (e.g., body ≥ voice) indicated that the decoder was trained on body emotion and was tested on voice stimuli. The table shows uncorrected *p*-values as well an indication (*) where the *p*-value is significant at $p < 0.05$ after FDR correction.

TABLE 3 Results for the decoding of emotion.

	Cluster size	Cluster p(unc)	Peak T	Peak p(unc)	*x*	*y*	*z*
All stimuli							
STS L	38	0.0536	5.8422	0.0000	−62	−34	2
Voice stimuli only							
Planum temporale L	749	0.001	6.462	0.000	−58	−34	6
Posterior cingulate gyrus/precuneus	187	0.058	5.654	0.000	8	−34	30
Planum temporale R	210	0.046	5.206	0.000	62	−18	2
Face and body stimuli							
STS L	59	0.0200	6.8069	0.0000	−54	−26	−4
Cingulate gyrus R	92	0.0052	6.5513	0.0000	16	−12	20
Angular gyrus R	27	0.0979	6.4339	0.0000	60	−50	34

classifier could accurately (although not significantly, based on $p < 0.05$ FWE corrected) discriminate emotions in STS, cingulate gyrus and angular gyrus ($p < 0.001$ uncorrected, cluster size threshold = 25), but not in visual cortex. Within the auditory modality (i.e., voices), the classifier discriminated emotions accurately in primary and secondary auditory cortical regions (including the superior temporal gyrus [STS], and in the precuneus (Figure 1, bottom panel and Table 3) at $p < 0.001$ uncorrected, cluster size threshold = 25). When the classifier was trained and tested to decode emotion within a specific visual stimulus type, that is, either the face stimuli or body stimuli, classification performance was at chance level.

Additionally, we performed a permutation analysis on the obtained classification results to assess the robustness of the decoding results (see Methods). The permutation test confirmed that the classifier can accurately discriminate emotions (compared to randomized stimulus labels) based on neural activity patterns in response to stimuli in the auditory modality (voices). For the visual stimulus modality, the permutation analysis yielded slightly different results. More specifically, the classifier could discriminate emotions accurately (compared to randomized stimulus labels) only within either face stimuli (in STS and PCC) or body stimuli (in ACC), but not when trained or tested on all visual stimuli combined (Supplementary Figure S4). Classification results for the classifier trained and tested on all sensory modalities (i.e., voice, face and body) were not above the accuracy levels of the randomized stimulus labels in any region. The results show that in this study no evidence was found for visual–auditory modality independent representations.

Finally, we performed an additional MVP classification analysis to evaluate whether supramodal emotion processing regions can be identified in the brain by training a classifier to decode emotion across stimulus modalities. Being able to predict emotion by training on one modality and testing on another modality would be a strong indication of supramodal emotion encoding in the brain. Therefore, the cross-modal classifier was trained (or tested) on either the body or face stimuli and tested (or trained) on the voice stimuli from the body or face session, respectively. Thus, four whole-brain searchlight classifiers were trained in total (training on body and testing on voice, training on voice, and testing body, training on face and testing on voice, training on voice and testing on face). In contrast to the successful and significant decoding of modality and the successful decoding of emotion within stimulus type, none of these cross-modal classifiers resulted in accurate decoding of emotion ($p < 0.05$ FWE corrected, as well as at $p < 0.001$ uncorrected with cluster size threshold = 25).

Assessing emotion representations in neural response patterns in regions of interest

As a last step, we evaluated whether primary sensory regions (A1 and V1) and regions that have been previously implicated in emotion processing (fusiform gyrus, EBA, amygdala) or in multimodal regions implicated in supramodal emotion processing (pSTS and mPFC; Peelen et al., 2010) contained emotion processing using a more sensitive region-of-interest (ROI) analysis. In line with our approach in the previous analyses, we began by testing whether the classifier can discriminate sensory modality (visual vs. auditory) in the ROIs. The classifier could accurately identify the sensory modality of a stimulus in sensory cortices—as expected—but also in pSTS ($p < 0.05$, FDR corrected). We then assessed whether the classifier was able to discriminate emotion when trained and tested on all modalities together (face, body, voice). The classifier was successful only in primary auditory cortex (A1). Like our previous results, when the classifier operated on the data of each sensory modality in isolation, decoding accuracies were above chance level for voice session 2 emotion in A1. Emotion could not be decoded above chance level in the supramodal regions (mPFC and pSTS). Thus, while visual and auditory stimuli elicit distinct neural response patterns in the ROIs that can robustly be discriminated by a MVP classifier, the emotions used here do not elicit specific neural response patterns. A representational dissimilarity matrix (RDM) analysis confirms that most ROIs considered here exhibit a strong modulation by sensory modality, except for mPFC and amygdala. However, no robust emotion representations were observed in these ROIs (Figure 2, Supplementary Figure S2).

Discussion

This study addressed a central question in the emotion literature that arises once investigations of human emotion expressions move beyond the traditional focus on facial expression. Our goal was to investigate whether implicit, ecologically valid processing of emotion expressions in either the face, the voice or the whole body is specific for the stimulus category. We used MVPA to find evidence of abstract representations that would be common to the different stimulus modality categories. Our results show that the brain contains several regions with emotion-specific representations. Importantly, in the absence of explicit emotion recognition instructions these emotion-specific representations were restricted to the respective stimulus modality or category (i.e., face, body, voice) and we did not find evidence for abstract emotion representation. Our design was entirely motivated by the focus on the sensory processes useful for emotion decoding and not on the more traditional question of how emotions are represented in the brain or how emotions are subjectively experienced. In line with this, we opted for a task that turned attention away from the stimulus presented. One may argue that the fact that we did not find modality general results for the emotion categories *per se* might have been due to this distracting task. But this was exactly the purpose as we wanted to focus on attention independent processes.

Our study presents a novel approach to the neural mechanisms underlying implicit emotion processing because we used naturalistic stimuli from three different categories and a specific task paradigm that focused on implicit emotion processing. Our results, converging across analysis techniques, highlight the specific contributions and the neural basis of emotional signals provided by each sensory modality and stimulus category. In a departure from the few previous studies using a partially comparable approach, we found evidence for sensory specific rather than abstract supramodal representations during implicit emotion processing (different from recognition or experience) that sustain perception of various affective signals as a function of the modality (visual or auditory) and the stimulus category (face, voice, or body).

To understand our findings against the background of the literature, some specific aspects of our study must be highlighted. We used dynamic realistic face and body stimuli instead of point light displays or static images. The latter are also known to complicate comparisons with dynamic auditory stimuli (Campanella and Belin, 2007). Next, our stimuli do not present prototypical emotion representations obtained by asking actors to portray emotions but present spontaneous face, voice and whole body reactions to images of familiar events. The expressions we used may therefore be more spontaneous and trigger more sensorimotor processes in the viewer than posed expressions. Third, many previous studies used explicit emotion recognition (Lee and Siegle, 2012), passive viewing (Winston et al., 2003), implicit tasks like gender categorization (Dricu and Fruhholz, 2016) or oddball tasks presented in the same modality as the stimulus. In contrast, our modality specific oddball task is presented in the alternate modality of the stimulus presentation thereby diverting attention not only from the emotion content but also from the perceptual modality in which the target stimuli of that block are shown. We discuss separately the findings on the major research questions. However, before turning to detailed results we clarify whether a different definition of amodal representation than adopted here and in the literature influences the conclusions.

Amodal or supramodal representations

A supramodal representation of emotions in the brain is presumably a brain regions that exhibits activity patterns specific to the abstract meaning of the stimulus but that are independent from the sensory modality (visual, auditory) and the stimulus category (face, body, voice) as in Peelen et al. (2010). These authors speculated these areas possibly host abstract emotion coding neurons (Peelen et al., 2010). More recently, Schirmer and Adolphs (2017) also relate processing of face and voice expressions in pSTS and PFC to abstract emotion representations and emotional meaning.

However, it is important to underscore that those previous findings about amodal representations were obtained with an explicit recognition task that is very different from the orthogonal task we used here. Results obtained in emotion experiments are closely linked to the task used and this is certainly the case for measures of amygdalae activity (De Gelder et al., 2012). For example, in a recent study addressing the issue of explicit vs. implicit emotion tasks we found major differences in the brain representation of body emotion expressions as a function of explicit vs. implicit recognition

10.3389/fnins.2023.1132088

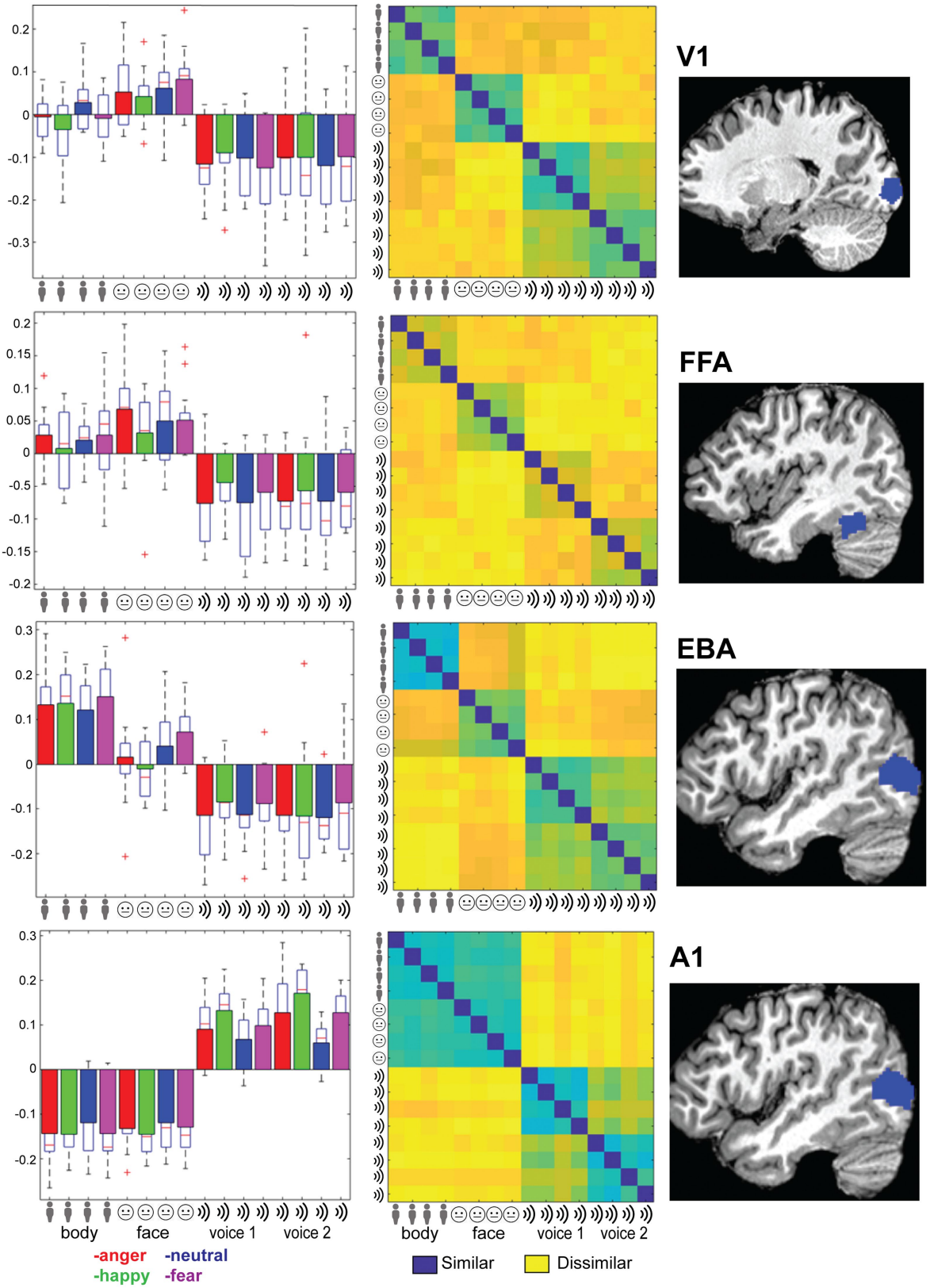

FIGURE 2
Right column: Location of the ROI (see main text for abbreviations). Left column: Trial-wise beta values for all 16 conditions: 4xtype (body, face, voice session 1 and voice session 2) and 4x emotion (indicated by color: anger-happy-neutral-fear) averaged over the ROI and group. Error bars indicate SE. Middle column: Representational dissimilarity matrix for the ROI. Blue colors indicate that responses to a pair of categories were similar (1-Pearson's r), yellow colors indicate dissimilarity. The matrices are ordered from top-left to bottom-right in blocks of 4 by 4 for the emotional expressions in order of angerhappy-neutral-fear. Blocks are ordered by stimulus type as indicated by the icons and text: body, face, voice session1 and voice session 2.

(Marrazzo et al., 2020). Furthermore, in older studies of our group that do not use MVPA we already systematically found that the similarities and differences between brain representation of face and body expressions is a function of the specific expression just as well as the stimulus category (Van de Riet et al., 2009; Kret et al., 2011a).

To put this issue in a boarder context, the notion of supramodal emotion representation has close conceptual links with the traditional theories of human emotions and mental states. Future experiments may start from other emotion theories focusing less on mental states and more on behavior and emotions as adaptive actions (de Gelder and Poyo Solanas, 2021). For example, it has long been argued that an action theory as opposed to a mental state theory of emotions (Frijda, 1987; De Gelder et al., 2004) implies a different picture of how the brain sustains emotional processes that the traditional notion of the six predefined basic emotions going back to Ekmans' emotion theory.

In the domain of emotion studies support for modality independent or abstract representations goes back to Ekmans' views but another area where this issue is debated is in studies on sensory deprivation. Studies of face, voice and whole body expressions in populations with sensory deprivation are very important to clarify and substantiate our findings underscoring the importance of category and modality specificity. Currently very few studies are available that address this issue. Interestingly, there is evidence for residual perception of face, body and voice perception in patients with cortical blindness following partial or complete striate cortex lesion (reviewed in Tamietto and De Gelder, 2010). These findings underscore the role of subcortical structures and draw attention to the fact that the issue is broader than that of cortical plasticity. Important as it is, this discussion is outside the scope of the present report.

An issue that is directly relevant is the following. Based on the literature it is not yet clear what findings for example from congenital blindness would constitute clear and direct evidence for abstract representations. The finding that congenitally blind individuals react to happy speech sounds by smiling (Arias et al., 2021) provides evidence that production of facial expressions does not require learning. However, by itself this does not constitute evidence for abstract representations. Nor does it show that such abstract representations need to play a crucial role in triggering facial expressions when a congenitally blind individual is exposed to smiles in speech. Indeed, production of smiles in reaction to "hearing" smiles can be explained parsimoniously by auditory-motor associations. Such an explanation does not require any crucial appeal to high order abstract representations. Undoubtedly, the many ways in which the brain processes information input from the different sensory systems is likely to involve also abstract layers of representations, depending or not on language. But their explanatory value is dependent on task settings and stimulus context.

Univariate analysis

Although our goal was to characterize neural responses with MVPA techniques, for the sake of comparisons with the literature, we also briefly discuss our univariate results. How do these results compare to findings and meta-analyses in the literature? In fact, there are no previous studies that used comparable materials (four emotion categories, three stimulus types, two modalities) and a different modality centered task as done here. The studies that did include bodies used only neutral actions, not whole body emotion expressions (Dricu and Fruhholz, 2016) except for one study comparing face and body expression videos by Kret et al. (2011a). Only the study by Peelen et al. used faces, bodies, and voices, but with a very different task as we discuss below (Peelen et al., 2010).

Compared to the literature, the findings of the univariate analysis present correspondences as well as differences. A previous study (Kret et al., 2011a) with face and body videos used only neutral, fear and anger expression and a visual oddball task. They reported that EBA and STS show increased activity to threatening body expressions and FG responds equally to emotional faces and bodies. For the latter, higher activity was found in cuneus, fusiform gyrus, EBA, tempo-parietal junction, superior parietal lobe, as well in as the thalamus while the amygdala was more active for facial than for bodily expressions, but independently of the facial emotion. Here we replicate that result for faces and bodies and found highly significant clusters with differential mean activation across stimulus types in primary and higher-order auditory and visual regions, as well as in motor, pre-motor and dorsal/superior parietal cortex (Supplementary Figure S1). Regions sensitive to stimulus category were not only found in primary visual and auditory cortex as expected but also in motor, pre-motor and dorsal/superior parietal cortex consistent with the findings in Kret et al. (2011a). To summarize, this univariate analysis including three stimulus types and four emotion categories replicates some main findings about brain areas involved, respectively, in face, body and voice expressions.

Multivariate analysis

The goal of our multivariate approach was to reveal the areas that contribute most strongly to an accurate distinction between the modalities and the stimulus emotion. Our MVPA searchlight analysis results show that stimulus modality can be decoded from the early sensory cortices and that emotion can be decoded in STG for voice stimuli with relatively high accuracy. In STS, cingulate and angular gyrus emotion could be decoded for face and body stimuli but only with low accuracies and lenient thresholding at the group level. On the other hand, we could not clearly identify supramodal emotion regions, defined by voxel patterns where emotion could be decoded and that would show very similar voxel patterns for the same emotion in the different modalities. This indicates that the brain responds to facial, body and vocal emotion expression in a sensory specific fashion. Thus, the overall direction pointed to by our results seems to be that that being exposed to emotional stimuli (that are not task relevant and while performing a task requiring attention to the other modality than that in which the stimulus is presented) is associated with brain activity that shows both an emotion specific and a stimulus and modality specific pattern.

ROI analysis

To follow up on the whole-brain analysis we performed a detailed and specific analysis of several ROIs. For the ROIs based on the

localizer scans (early visual areas as well as FFA and EBA) stimulus type could be decoded and these results are consistent with the MVPA searchlight analysis. The A1 ROI showed above chance emotion decoding (from all stimuli or within a specific stimulus type/session). However, this region also displayed strong stimulus type decoding with no evidence of supramodal representations. Additionally, a strong effect of emotion is seen in the RDM plots in Figure 2; however, a correlational structure relating to emotion is not clearly visible within the stimulus type/session blocks. These results, together with the searchlight results, lead us to reject the hypothesis that the human brain has stimulus modality or type invariant representations of basic emotions.

Modality specific emotion representations

Two previous MVPA studies addressed partly similar issues investigated in this study using faces, bodies and voices (Peelen et al., 2010) or bodies and voices and MVPA (Whitehead and Armony, 2019). The first study reported medial prefrontal cortex (MPFC) and posterior superior temporal cortex as the two areas hosting abstract supramodal emotion representations. These two areas are not found in our MVPA searchlight analysis. To understand the present result, it is important to remember that in the above studies participants were instructed to label the perceived emotional expressions. One motivation was that explicit judgments would increase activity in brain regions involved in social cognition and mental state attribution (Peelen et al., 2010). In contrast, the motivation of the present study was to approximate naturalistic perception conditions where people often act before and independently of tagging a label on their experience. Our design and task were intended to promote spontaneous non-focused processes of the target stimuli and did not promote amodal conceptual processing of the emotion content. It is likely that using an explicit recognition task would have activated higher level representations, e.g., orbitofrontal cortex, posterior STS, prefrontal cortex and posterior cingulate cortex that would then feed back to lower level representations and modulate these toward more abstract representations (Schirmer and Adolphs, 2017). Note that no amygdala activity was reported in that study. The second study using passive listening or viewing of still bodies and comparing fear and neutral expressions also concludes about a distributed network of cortical and subcortical regions responsive to fear in the two stimulus types they used (Whitehead and Armony, 2019). Of interest is their finding concerning the amygdalae and fear processing. While in their study this is found across stimulus type for body and voice, the classification accuracy when restricted to the amygdalae was not significantly above chance. They concluded that fear processing by the amygdalae heavily relies on contribution of a distributed network of cortical and subcortical structures.

Our findings suggest a novel perspective on the role of the different sensory systems and the different stimulus categories that convey affective signals in daily life. Paying attention to sensory specificity of affective signals may reflect better the role of emotions as seen from an evolutionary perspective and it is compatible with an ecological and context sensitive approach to brain organization (Cisek and Kalaska, 2010; Mobbs et al., 2018; de Gelder and Poyo Solanas, 2021). For comparison, a similar approach not to emotion concepts but to cognitive concepts was argued by Barsalou et al. (2003). This distributed organization of emotion representation may be more akin to what is at stake in the daily experience of affective signals and how they are flexibly processed for the benefit of ongoing action and interaction in a broader perspective of emotions as states of action readiness (Frijda, 2004).

Our results are relevant for two longstanding debates in the literature, one on the nature and existence of abstract emotion representations and basic categories and the other on processes of multisensory integration. Concerning the first one, our results have implications for the debate on the existence of basic emotions (Ekman, 2016). Interestingly, modality specificity has rarely been considered as part of the issue as the basic emotion debate largely focusses on facial expressions. The present results might be viewed as evidence in favor of the view that basic emotions traditionally understood as specific representations of a small number of emotions with an identifiable brain correlate (Ekman, 2016) simply do not exist but that these are cognitive-linguistic constructions (Russell, 2003). On the one hand, our results are consistent with critiques of basic emotions theories and meta-analysis (Lindquist et al., 2012) as we find no evidence for representations of emotions in general or specific emotions within or across modality and stimuli. Affective information processing thus appears not organized as categorically, neither by conceptual emotion category nor by modality, as was long assumed. Emotion representation, more so even than object representation, may possibly be sensory specific or idiosyncratic (Peelen and Downing, 2017) and neural representations may reflect the circumstances under which specific types of signals are most useful or relevant rather than abstract category membership. This pragmatic perspective is consistent with the notion that emotions are closely linked to action and stresses the need for more detailed ethological behavior investigations (de Gelder, 2016).

Additionally, the notion that supramodal representations of basic emotions are the pillars of emotion processing in the brain and are the basis allow of smooth translation and convergence between the different sensory modalities is not fully supported by the literature. First, since the original proposal by Ekman (1992) and the constructivist alternative argued by Russell (2003) and most recently Lewis et al. (2010) and Barrett (2017), the notion of a set of basic emotions with discrete brain correlates continues to generate controversy (Kragel and LaBar, 2016; Saarimaki et al., 2016). Second, detailed meta-analyses of crossmodal and multisensory studies, whether they are reviewing the findings about each separate modality or the results of crossmodal studies (Dricu and Fruhholz, 2016; Schirmer and Adolphs, 2017), provide a mixed picture. Furthermore, these meta-analyses also show that several methodological obstacles stand in the way of valid comparisons across studies. That is, taking into account the role of task (incidental perception, passive perception, and explicit evaluation of emotional expression) and the use of appropriate control stimuli limits the number of studies that can validly be compared. Third, findings from studies that pay attention to individual differences and to clinical aspects reveal individual differences in sensory salience and dominance in clinical populations, for example in autism and schizophrenia. For example Karle et al. (2018) report an alteration in the balance of cerebral voice and face processing systems and attenuated face-*vs*-voice bias in emotionally competent individuals. This is reflected in cortical activity differences as well as in higher voice-sensitivity in the left amygdala. Finally, even granting the existence of abstract supramodal representations—presumably in higher cognitive brain regions—it is unclear how they relate to earlier stages of affective processing where

the voice, the face and the body information are processed by different sensory systems comprising distinct cortical and subcortical structures. Based on previous literature general, supramodal or "abstract" representations might have been expected in brain regions such as the orbitofrontal and anterior cingulate cortex. But as noted above, these are most often reported in studies asking participants for explicit recognition and decisions on emotion categories. The modality-specific activations that were can thus not be compared with activations for abstract categories but they are interesting by virtue of their horizontal differences between each other.

It is important to make a clear distinction between supramodal perception and multisensory integration. Our study did not focus on multisensory perception, but our findings may have implications for theories of multisensory integration by challenging a strict hierarchical model. Studies reaching beyond facial expressions have primarily been motivated how the same emotion as defined by the facial expression may be communicated by different stimulus types. Our group has initiated studies on multi-stimulus and multi-modal perception and found rapid and automatic influence of one type of expression on another [face and voice (de Gelder et al., 1999); face and body (Meeren et al., 2005); face and scene (Righart and de Gelder, 2008; Van den Stock et al., 2013); body and scene (Van den Stock et al., 2014); auditory voice and tactile perception (de Borst and de Gelder, 2017)]. These original studies and subsequent ones (Müller et al., 2012) investigated the impact of one modality on the other and targeted the area(s) where different signals converge. For example, Müller et al. (2012) report posterior STS as the site of convergence of auditory and visual input systems and by implication, as the site of multisensory integration. Different affective expression signals may have horizontal and context sensitive links rather that connections that presuppose abstract emotion representations.

Limitations

Our motivation to include three stimulus categories led to some limitations of the current design because two separate scanning sessions were required to have the desired number of stimulus repetitions. To avoid that the comparison of representations of stimuli from two different sessions was biased by a session effect, we did not include any results that referred to differences or commonalities of stimuli from different sessions (e.g., bodies vs. faces). Another possible limitation of our study is the relatively small sample but this is compensated for by the use of very sensitive methods (MVPA and crossvalidation). Furthermore, a familiar difficulty in investigating the processing of high-order emotion perception is the relation between low-level stimulus properties (in terms of spatial and temporal statistics) and higher order emotion categories. Conversely, human detection of emotion in visual or auditory samples might be based on low-level spatio-temporal properties, and matching samples for these properties might result in unnatural appearing stimuli. To remain with the characteristics derived from the expression production we used the vocalizations as they were produced together with the face and body expressions. As they were not controlled for low-level acoustic features across emotions, our results from the decoding of emotion from the voice stimuli may partly reflect these differences. But a proper control for low level features in turn requires a better understanding of the relative (in)dependence between lower and higher-level features. Presumably bottom-up and top-down interactions determine the course of affect processing as seen for visual features of whole body expressions (Vaessen et al., 2019; Poyo Solanas et al., 2020). An analysis of low-level stimulus characteristics (see Supplementary Figure S3) did not reveal strong correlations between emotion category and features. Conversely, this analysis revealed that within category (possibly due to different actors) and between emotion category variances were similar.

Conclusion

Our results show that the brain correlates of emotional signals from the body, the face of the voice are specific for the modality as well as for the specific stimulus. These findings underscore the importance of considering the specific contribution of each modality and each type of affective signal rather than only their higher order amodal convergence possibly related to explicit recognition task demands. We suggest that future research may investigate the differences between the emotion signals and how they are complementary as a function of the context of action and not only at abstract, amodal similarity. Another source of representational variability that would need to be addressed is whether under natural conditions, the sensory modality carrying emotion information has its own preferred functionality such that, e.g., fear would more effectively conveyed by the face, anger by the body and happiness by the voice. If so, brain representation of emotions would be characterized by specific emotion, modality and spatial context combinations and behavioral relevance (Downar et al., 2001, 2002). These are highly relevant considerations for a future neuroethologically grounded research program that should start from detailed behavioral observations of how face, body, and voice expressions function in naturalistic contexts.

Data availability statement

The raw data supporting the conclusions of this article will be made available by the authors, without undue reservation.

Ethics statement

The studies involving human participants were reviewed and approved by FPN-Maastricht University. The ethics committee waived the requirement of written informed consent for participation.

Author contributions

MV, KV, and BD analysis, writing, editing. All authors contributed to the article and approved the submitted version.

Funding

This work was supported by the European Research Council ERC Synergy grant (Grant agreement 856495; Relevance), the Future and Emerging Technologies (FET) Proactive Program H2020-EU.1.2.2 (Grant agreement 824160; EnTimeMent), the

Industrial Leadership Program H2020-EU.1.2.2 (Grant agreement 825079; MindSpaces), and the Horizon 2020 Programme H2020-FETPROACT430 2020–2 (grant 101017884 GuestXR).

Acknowledgments

We thank R. Watson for stimulus preparation and data collection.

Conflict of interest

The authors declare that the research was conducted in the absence of any commercial or financial relationships that could be construed as a potential conflict of interest.

Publisher's note

Supplementary material

The Supplementary material for this article can be found online at: https://www.frontiersin.org/articles/10.3389/fnins.2023.1132088/full#supplementary-material

References

Arias, P., Bellmann, C., and Aucouturier, J. J. (2021). Facial mimicry in the congenitally blind. *Curr. Biol.* 31, R1112–R1114. doi: 10.1016/j.cub.2021.08.059

Barrett, L. F. (2017). *How emotions are made: The secret life of the brain*. New York: Houghton Mifflin Harcourt.

Barsalou, L. W., Simmons, W. K., Barbey, A. K., and Wilson, C. D. (2003). Grounding conceptual knowledge in modality-specific systems. *Trends Cogn. Sci.* 7, 84–91. doi: 10.1016/S1364-6613(02)00029-3

Benjamini, Y., and Hochberg, Y. (1995). Controlling the false discovery rate: a practical and powerful approach to multiple testing. *J. R. Stat. Soc. Ser. B (Methodological)* 57, 289–300.

Campanella, S., and Belin, P. (2007). Integrating face and voice in person perception. *Trends Cogn. Sci.* 11, 535–543. doi: 10.1016/j.tics.2007.10.001

Cisek, P., and Kalaska, J. F. (2010). Neural mechanisms for interacting with a world full of action choices. *Annu. Rev. Neurosci.* 33, 269–298. doi: 10.1146/annurev.neuro.051508.135409

de Borst, A. W., and de Gelder, B. (2017). fMRI-based multivariate pattern analyses reveal imagery modality and imagery content specific representations in primary somatosensory, motor and auditory cortices. *Cereb. Cortex* 27, 3994–4009. doi: 10.1093/cercor/bhw211

de Borst, A. W., Sanchez-Vives, M. V., Slater, M., and de Gelder, B. (2020). First-person virtual embodiment modulates the cortical network that encodes the bodily self and its surrounding space during the experience of domestic violence. *eNeuro* 7, ENEURO.0263–ENEU19.2019. doi: 10.1523/ENEURO.0263-19.2019

de Gelder, B. (2016). "Emotional body perception in the wild" in *Handbook of emotions*. eds. L. F. Barrett, M. Lewis and J. M. Haviland-Jones. *4th* ed (New York, NY: Guilford Press Publications), 483–494.

de Gelder, B., Bocker, K. B., Tuomainen, J., Hensen, M., and Vroomen, J. (1999). The combined perception of emotion from voice and face: early interaction revealed by human electric brain responses. *Neurosci. Lett.* 260, 133–136. doi: 10.1016/S0304-3940(98)00963-X

De Gelder, B., Hortensius, R., and Tamietto, M. (2012). Attention and awareness each influence amygdala activity for dynamic bodily expressions—a short review. *Front. Integr. Neurosci.* 6:54. doi: 10.3389/fnint.2012.00054

de Gelder, B., and Poyo Solanas, M. (2021). A computational neuroethology perspective on body and expression perception. *Trends Cogn. Sci.* 25, 744–756.

De Gelder, B., Snyder, J., Greve, D., Gerard, G., and Hadjikhani, N. (2004). Fear fosters flight: a mechanism for fear contagion when perceiving emotion expressed by a whole body. *Proc. Natl. Acad. Sci.* 101, 16701–16706. doi: 10.1073/pnas.0407042101

Downar, J., Crawley, A. P., Mikulis, D. J., and Davis, K. D. (2001). The effect of task relevance on the cortical response to changes in visual and auditory stimuli: an event-related fMRI study. *NeuroImage* 14, 1256–1267. doi: 10.1006/nimg.2001.0946

Downar, J., Crawley, A. P., Mikulis, D. J., and Davis, K. D. (2002). A cortical network sensitive to stimulus salience in a neutral behavioral context across multiple sensory modalities. *J. Neurophysiol.* 87, 615–620. doi: 10.1152/jn.00636.2001

Dricu, M., and Fruhholz, S. (2016). Perceiving emotional expressions in others: activation likelihood estimation meta-analyses of explicit evaluation, passive perception and incidental perception of emotions. *Neurosci. Biobehav. Rev.* 71, 810–828. doi: 10.1016/j.neubiorev.2016.10.020

Eickhoff, S. B., Paus, T., Caspers, S., Grosbras, M.-H., Evans, A. C., Zilles, K., et al. (2007). Assignment of functional activations to probabilistic cytoarchitectonic areas revisited. *NeuroImage* 36, 511–521. doi: 10.1016/j.neuroimage.2007.03.060

Ekman, P. (1992). An argument for basic emotions. *Cognit. Emot.* 6, 169–200. doi: 10.1080/02699939208411068

Ekman, P. (2016). What scientists who study emotion agree about. *Perspect. Psychol. Sci.* 11, 31–34. doi: 10.1177/1745691615596992

Ekman, P., and Cordaro, D. (2011). What is meant by calling emotions basic. *Emot. Rev.* 3, 364–370. doi: 10.1177/1754073911410740

Frijda, N. H. (1987). Emotion, cognitive structure, and action tendency. *Cognit. Emot.* 1, 115–143. doi: 10.1080/02699938708408043

Frijda, N. H. (2004). *Emotions and action*. Feelings and emotions: The Amsterdam symposium, pp. 158–173, doi: 10.1017/CBO9780511806582.010

Gerdes, A. B., Wieser, M. J., and Alpers, G. W. (2014). Emotional pictures and sounds: a review of multimodal interactions of emotion cues in multiple domains. *Front. Psychol.* 5:1351. doi: 10.3389/fpsyg.2014.01351

Hausfeld, L., De Martino, F., Bonte, M., and Formisano, E. (2012). Pattern analysis of EEG responses to speech and voice: influence of feature grouping. *NeuroImage* 59, 3641–3651. doi: 10.1016/j.neuroimage.2011.11.056

Hausfeld, L., Valente, G., and Formisano, E. (2014). Multiclass fMRI data decoding and visualization using supervised self-organizing maps. *NeuroImage* 96, 54–66. doi: 10.1016/j.neuroimage.2014.02.006

Karle, K. N., Ethofer, T., Jacob, H., Bruck, C., Erb, M., Lotze, M., et al. (2018). Neurobiological correlates of emotional intelligence in voice and face perception networks. *Soc. Cogn. Affect. Neurosci.* 13, 233–244. doi: 10.1093/scan/nsy001

Klasen, M., Kenworthy, C. A., Mathiak, K. A., Kircher, T. T., and Mathiak, K. (2011). Supramodal representation of emotions. *J. Neurosci.* 31, 13635–13643. doi: 10.1523/JNEUROSCI.2833-11.2011

Kragel, P. A., and LaBar, K. S. (2016). Decoding the nature of emotion in the brain. *Trends Cogn. Sci.* 20, 444–455. doi: 10.1016/j.tics.2016.03.011

Kret, M. E., Pichon, S., Grezes, J., and de Gelder, B. (2011a). Similarities and differences in perceiving threat from dynamic faces and bodies. An fMRI study. *Neuroimage* 54, 1755–1762. doi: 10.1016/j.neuroimage.2010.08.012

Kret, M. E., Pichon, S., Grèzes, J., and De Gelder, B. (2011b). Men fear other men most: gender specific brain activations in perceiving threat from dynamic faces and bodies–an fMRI study. *Front. Psychol.* 2:3. doi: 10.3389/fpsyg.2011.00003

Kriegeskorte, N., Mur, M., Ruff, D. A., Kiani, R., Bodurka, J., Esteky, H., et al. (2008). Matching categorical object representations in inferior temporal cortex of man and monkey. *Neuron* 60, 1126–1141. doi: 10.1016/j.neuron.2008.10.043

Lee, K. H., and Siegle, G. J. (2012). Common and distinct brain networks underlying explicit emotional evaluation: a meta-analytic study. *Soc. Cogn. Affect. Neurosci.* 7, 521–534. doi: 10.1093/scan/nsp001

Lewis, M., Haviland-Jones, J. M., and Barrett, L. F. (2010). *Handbook of emotions*. New York: Guilford Press.

Lindquist, K. A., Wager, T. D., Kober, H., Bliss-Moreau, E., and Barrett, L. F. (2012). The brain basis of emotion: a meta-analytic review. *Behav. Brain Sci.* 35, 121–143. doi: 10.1017/S0140525X11000446

Marrazzo, G., Vaessen, M., and de Gelder, B. (2020). The dynamics of body category and emotion processing in high-level visual, prefrontal and parietal cortex. *bioRxiv*. doi: 10.1101/2020.07.14.202515

Meeren, H. K., van Heijnsbergen, C. C., and de Gelder, B. (2005). Rapid perceptual integration of facial expression and emotional body language. *Proc. Natl. Acad. Sci. U. S. A.* 102, 16518–16523. doi: 10.1073/pnas.0507650102

Mobbs, D., Trimmer, P. C., Blumstein, D. T., and Dayan, P. (2018). Foraging for foundations in decision neuroscience: insights from ethology. *Nat. Rev. Neurosci.* 19, 419–427. doi: 10.1038/s41583-018-0010-7

Müller, V. I., Cieslik, E. C., Turetsky, B. I., and Eickhoff, S. B. (2012). Crossmodal interactions in audiovisual emotion processing. *NeuroImage* 60, 553–561. doi: 10.1016/j.neuroimage.2011.12.007

Ontivero-Ortega, M., Lage-Castellanos, A., Valente, G., Goebel, R., and Valdes-Sosa, M. (2017). Fast Gaussian naive Bayes for searchlight classification analysis. *NeuroImage* 163, 471–479. doi: 10.1016/j.neuroimage.2017.09.001

Peelen, M. V., Atkinson, A. P., and Vuilleumier, P. (2010). Supramodal representations of perceived emotions in the human brain. *J. Neurosci.* 30, 10127–10134. doi: 10.1523/JNEUROSCI.2161-10.2010

Peelen, M. V., and Downing, P. E. (2017). Category selectivity in human visual cortex: beyond visual object recognition. *Neuropsychologia* 105, 177–183. doi: 10.1016/j.neuropsychologia.2017.03.033

Penny, W. D., Friston, K. J., Ashburner, J. T., Kiebel, S. J., and Nichols, T. E. (2011). *Statistical parametric mapping: The analysis of functional brain images*. Amsterdam: Elsevier Ltd. (2007).

Poyo Solanas, M., Vaessen, M., and de Gelder, B. (2020). Computation-based feature representation of body expressions in the human brain. *Cerebral Cortex* 30, 6376–6390. doi: 10.1093/cercor/bhaa196

Righart, R., and de Gelder, B. (2008). Rapid influence of emotional scenes on encoding of facial expressions: an ERP study. *Soc. Cogn. Affect. Neurosci.* 3, 270–278. doi: 10.1093/scan/nsn021

Rolls, E. T. (2014) *Emotion and decision-making explained*. Oxford University Press: Oxford.

Rolls, E. T. (2019). The orbitofrontal cortex and emotion in health and disease, including depression. *Neuropsychologia* 128, 14–43. doi: 10.1016/j.neuropsychologia.2017.09.021

Rolls, E. T., Critchley, H. D., Browning, A. S., and Inoue, K. (2006). Face-selective and auditory neurons in the primate orbitofrontal cortex. *Exp. Brain Res.* 170, 74–87. doi: 10.1007/s00221-005-0191-y

Russell, J. A. (2003). Core affect and the psychological construction of emotion. *Psychol. Rev.* 110, 145–172. doi: 10.1037/0033-295X.110.1.145

Saarimaki, H., Gotsopoulos, A., Jaaskelainen, I. P., Lampinen, J., Vuilleumier, P., Hari, R., et al. (2016). Discrete neural signatures of basic emotions. *Cereb. Cortex* 26, 2563–2573. doi: 10.1093/cercor/bhv086

Schirmer, A., and Adolphs, R. (2017). Emotion perception from face, voice, and touch: comparisons and convergence. *Trends Cogn. Sci.* 21, 216–228. doi: 10.1016/j.tics.2017.01.001

Tamietto, M., and De Gelder, B. (2010). Neural bases of the non-conscious perception of emotional signals. *Nat. Rev. Neurosci.* 11, 697–709. doi: 10.1038/nrn2889

Vaessen, M. J., Abassi, E., Mancini, M., Camurri, A., and de Gelder, B. (2019). Computational feature analysis of body movements reveals hierarchical brain organization. *Cereb. Cortex* 29, 3551–3560. doi: 10.1093/cercor/bhy228

Van de Riet, W. A., Grèzes, J., and de Gelder, B. (2009). Specific and common brain regions involved in the perception of faces and bodies and the representation of their emotional expressions. *Soc. Neurosci.* 4, 101–120. doi: 10.1080/17470910701865367

Van den Stock, J., Vandenbulcke, M., Sinke, C. B., and de Gelder, B. (2014). Affective scenes influence fear perception of individual body expressions. *Hum. Brain Mapp.* 35, 492–502. doi: 10.1002/hbm.22195

Van den Stock, J., Vandenbulcke, M., Sinke, C. B., Goebel, R., and de Gelder, B. (2013). How affective information from faces and scenes interacts in the brain. *Soc. Cogn. Affect. Neurosci.* 9, 1481–1488. doi: 10.1093/scan/nst138

Vroomen, J., Driver, J., and De Gelder, B. (2001). Is cross-modal integration of emotional expressions independent of attentional resources? *Cogn. Affect. Behav. Neurosci.* 1, 382–387. doi: 10.3758/CABN.1.4.382

Warrier, C., Wong, P., Penhune, V., Zatorre, R., Parrish, T., Abrams, D., et al. (2009). Relating structure to function: Heschl's gyrus and acoustic processing. *J. Neurosci.* 29, 61–69. doi: 10.1523/JNEUROSCI.3489-08.2009

Whitehead, J. C., and Armony, J. L. (2019). Multivariate fMRI pattern analysis of fear perception across modalities. *Eur. J. Neurosci.* 49, 1552–1563. doi: 10.1111/ejn.14322

Winston, J. S., O'Doherty, J., and Dolan, R. J. (2003). Common and distinct neural responses during direct and incidental processing of multiple facial emotions. *NeuroImage* 20, 84–97. doi: 10.1016/S1053-8119(03)00303-3

Zhan, M., Goebel, R., and de Gelder, B. (2018). Ventral and dorsal pathways relate differently to visual awareness of body postures under continuous flash suppression. *eNeuro* 5, ENEURO.0285–ENEU17.2017. doi: 10.1523/ENEURO.0285-17.2017

Frontiers in Neuroscience

Provides a holistic understanding of brain function from genes to behavior

Part of the most cited neuroscience journal series which explores the brain - from the new eras of causation and anatomical neurosciences to neuroeconomics and neuroenergetics.

Discover the latest Research Topics

See more →

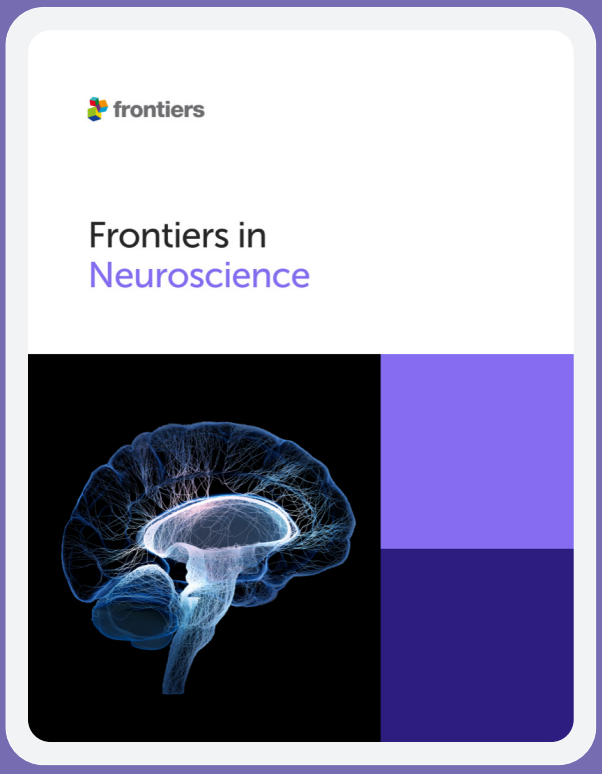

Frontiers

Avenue du Tribunal-Fédéral 34
1005 Lausanne, Switzerland
frontiersin.org

Contact us

+41 (0)21 510 17 00
frontiersin.org/about/contact